

RENDICONTI *Online*
della
Società Geologica Italiana

Volume 31 - Luglio 2014

**Climatic and Biotic Events of the Paleogene 2014
CBEP 2014**



Selected short notes and abstracts
Ferrara, Italy, July 1-6 2014

edited by: **G. R. Dickens & V. Luciani**



ROMA
SOCIETÀ GEOLOGICA ITALIANA
2014
www.socgeol.it

RENDICONTI *Online della Società Geologica Italiana*, è un periodico quadrimestrale della Società Geologica Italiana. Esce nei mesi di Dicembre, Aprile ed Agosto.

The RENDICONTI Online della Società Geologica Italiana is a journal of the Italian Geological Society. It is published every four months in December, April and August.

Direttore responsabile e Redattore (*Editor-in-Chief*): Domenico CALCATERRA (Napoli).

Responsabili editoriali (*Editorial Managers*): Alessandro ZUCCARI (SGI - Roma), Fabio Massimo PETTI (SGI - Roma).

Comitato di redazione (Associate Editors):

Alessandra ASCIONE (Napoli), Domenico COSENTINO (Roma TRE - Roma), Corrado CENCETTI (Perugia), Gianfranco CIANCETTI (Pavia), Massimo CIVITA (Torino), Piero FARABOLLINI (Camerino), Fabrizio GALLUZZO (ISPRA - Roma), Massimo MATTEI (Roma TRE - Roma), Carmelo MONACO (Catania), Paolo MOZZI (Padova), Mariano PARENTE (Napoli), Dario SLEJKO (OGS - Trieste), Iole SPALLA (Milano).

La **SOCIETÀ GEOLOGICA ITALIANA** fu fondata il 29 settembre 1881, eretta ad Ente Morale con Regio Decreto del 17 Ottobre 1885. La Segreteria è ospitata dal Dipartimento di Scienze della Terra della Sapienza, Università di Roma, Piazzale Aldo Moro, 5 - 00185 Roma, Italy.

The **SOCIETÀ GEOLOGICA ITALIANA** was founded in Bologna on September 29th, 1881. It was recognized as non-profit corporation with the Royal Decree of October 17th, 1885. The secretary office is hosted by the Dipartimento di Scienze della Terra of the Sapienza University, Piazzale Aldo Moro, 5 - 00185 Roma, Italy.

Contatti (*Contacts*): Tel. +39-06-4959-390; Fax +39-06-4991-4154; e-mail: info@socgeol.it

Sito web (*Society Web Site*): www.socgeol.it

Codice Fiscale (*Income Tax Number*): 80258790585; Conto corrente postale (*Postal giro account*): 350009.

CONSIGLIO DIRETTIVO 2014 (*Council Members for 2014*):

Carlo DOGLIONI - *President*, Alessandro ZUCCARI - *General Secretary*, Marco PETITTA - *Treasurer*, Elisabetta ERBA, Domenico CALCATERRA (*EiC of the ROL*), Piero CASERO, Paolo CONTI, Domenico COSENTINO, Stefano DALLA, David GOVONI, Carmelo MONACO, Fabio Massimo PETTI, Sandro CONTICELLI (*EiC of the IJG - BSGI*).

REVISORI DEI CONTI 2014 (*Financial Auditors 2014*):

Luca ALDEGA, Eugenio CARMINATI, Fabio TRIPPETTA

SEZIONI DELLA SOCIETÀ GEOLOGICA ITALIANA (*Italian Geological Society Sections*):

Marine Geology: Francesco CHIOCCI - *Chair*

Planetary Geology: Gian Gabriele ORI - *Chair*

Hydrogeology: Giovanni BARROCU - *Chair*

Carbonate Geology: Gloria CIARAPICA, Antonio PRATURLON - *Chairs*

Geo-informatics: Chiara D'AMBROGI - *Chair*

Structural Geology: Giovanni CAPPONI - *Chair*

Young Geologists: Ester TIGANO - *Chair*

Environmental Geology: Leo ADAMOLI - *Chair*

Himalayan Geology: Rodolfo CAROSI - *Chair*

GeoSed: Simonetta CIRILLI - *Chair*

History of Geosciences: Alessio ARGENTIERI, Marco PANTALONI - *Chairs*

Geoethics and Geological Culture: Silvia PEPPOLONI - *Chair*

La Società Geologica Italiana è affiliata alla European Geosciences Union (EGU).

The Società Geologica Italiana is affiliated to the European Geosciences Union (EGU).

QUOTA ASSOCIATIVA 2014 (*Association Fees 2014*): socio sostenitore (*supporter fellow*) € 100, socio ordinario (*ordinary fellow*) € 93; socio senior (*senior fellow*) € 68, socio junior (*junior fellow*) € 68; studente (*student*) € 36; Istituzioni (*Institutions*) € 300.

Iscrizione alla pagina (*Subscription at*): http://www.socgeol.it/284/quota_sociale.html or at

http://www.socgeol.it/285/pagamento_tramite_carta_di_credito.html

La **Società Geologica Italiana** detiene il copyright degli articoli, dei dati, delle figure e di tutto il materiale pubblicato.

Papers, data, figures, maps and any other material published are covered by the copyright own by the Società Geologica Italiana.

DISCLAIMER: The Società Geologica Italiana, the Editors (Chief, Associates), and the Publisher are not responsible for the ideas, opinions, and contents of the papers published; the authors of each paper are responsible for the ideas, opinions and contents published.

La Società Geologica Italiana, i curatori scientifici (Chief, Associates), e la Casa Editrice non sono responsabili delle opinioni espresse e delle affermazioni pubblicate negli articoli: l'autore/i è/sono il/i solo/i responsabile/i.

RENDICONTI *Online*
della
Società Geologica Italiana

Volume 31 - Luglio 2014

**Climatic and Biotic Events of the Paleogene 2014
CBEP 2014**

Selected short notes and abstracts
Ferrara, Italy, July 1-6 2014

edited by: G. R. Dickens & V. Luciani



ROMA
SOCIETÀ GEOLOGICA ITALIANA
2014
www.socgeol.it

Climatic and Biotic Events of the Paleogene 2014 CBEP 2014

July, 1-6, 2014, Ferrara, Italy

CONVENORS

Valeria Luciani (University of Ferrara, Italy) & Gerald Dickens (Rice University, Houston, Texas, USA)

SCIENTIFIC COMMITTEE

Jan Backman (Department of Geological Sciences, Stockholm University, Sweden)
William Clyde (Department of Earth Sciences, University of New Hampshire, Durham, NH USA)
Christopher Hollis (Institute of Geological and Nuclear Sciences, Lower Hutt, New Zealand)
Matthew Huber (Purdue Climate Change Research Center, Purdue University, USA)
Ursula Röhl (MARUM - Centre for Marine Environmental Sciences, University of Bremen, Germany)
Appy Sluijs (Department of Earth Sciences, Utrecht University, Netherlands)
Ellen Thomas (Department of Geology and Geophysics, Yale University, New Haven, CT USA)
Bridget Wade (University College London, UCL, UK)
Paul Wilson (Ocean & Earth Science National Oceanography Centre, University of Southampton, UK)
Scott Wing and Richard Barclay (Smithsonian Institution, National Museum of Natural History, Washington, DC USA)

ORGANISING COMMITTEE

Valeria Luciani, Department of Physics and Earth Sciences, Ferrara University, Italy
Gerald Dickens, Rice University, Houston, Texas, USA
Renato Posenato, Department of Physics and Earth Sciences, Ferrara University, Italy
Davide Bassi, Department of Physics and Earth Sciences, Ferrara University, Italy
Claudia Agnini, Department of Geosciences, Padova University, Italy
Luca Capraro, Department of Geosciences, Padova University, Italy
Eliana Fornaciari, Department of Geosciences, Padova University, Italy
Luca Giusberti, Department of Geosciences, Padova University, Italy
Cesare Andrea Papazzoni, Department of Chemical and Geological Sciences, University of Modena and Reggio Emilia, Italy
Massimo Verde, Department of Physics and Earth Sciences, Ferrara University, Italy
Michele Gambetti, Department of Physics and Earth Sciences, Ferrara University, Italy
Alberto Gianoli, INFN Ferrara, Italy

Con il patrocinio del



PROVINCIA
DI FERRARA



UNIVERSITÀ
DEGLI STUDI
DI FERRARA
- EX LABORE FRUCTUS -



Con il patrocinio

dell'Università degli Studi di Modena e
Reggio Emilia



UNIVERSITÀ
DEGLI STUDI
DI PADOVA



ISPRA



National Research Council of Italy



BNL
GRUPPO BNP PARIBAS

Contents

SHORT NOTES

Dickens G.R. & Luciani V. - CBEP 2014: preface and dedication (doi: 10.3301/ROL.2014.15).....	1
Abels H.A., Wang C., Lauretano V., Bowen G.J., Karssenberg D., Ziegler M., Li G., van den Berg P.F., van Broekhuizen S., Hopman T., Laks J., Adriaens R., Clyde W.C., Elsen J., Kraus M.J., Sluijs A., Vandenberghe N., Lourens L.J., Gingerich P.D. - Terrestrial sedimentary archives of episodes of greenhouse warming in ancient river floodplain deposits of the Bighorn Basin, Wyoming (doi: 10.3301/ROL.2014.16).....	3
Adatte T., Khozyem H., Spangenberg J.E., Samant B., Keller G. - Response of terrestrial environment to the Paleocene-Eocene Thermal Maximum (PETM), new insights from India and NE Spain (doi: 10.3301/ROL.2014.17).....	5
Agnini C., Costa A. - Calcareous nannofossil changes across the Middle Eocene Climatic Optimum from IODP Site U1410 (NW Atlantic): Preliminary results (doi: 10.3301/ROL.2014.18)	7
Agnini C., Fornaciari E., Raffi I., Catanzariti R., Pälke H., Backman J., Rio D. - Low to middle latitude Paleogene calcareous nannofossil biozonation and biochronology (doi: 10.3301/ROL.2014.19)	9
Agnini C., Kulhanek D.K., Shepherd C.L. - Calcareous nannofossil response to climatic changes in the early to middle Eocene (doi: 10.3301/ROL.2014.20).....	11
Armstrong McKay D., Toby T., Wilson P.A. - Investigating the evolution of the late Palaeogene carbon cycle using biogeochemical modelling and analysis (doi: 10.3301/ROL.2014.21).....	13
Arreguín-Rodríguez G.J., Alegret L., Thomas E. - Response of benthic foraminiferal assemblages to early Eocene hyperthermal events (doi: 10.3301/ROL.2014.22).....	15
Arreguín-Rodríguez G.J., Alegret L. - Are agglutinated benthic foraminifera affected by CaCO ₃ dissolution? Experiments across the Paleocene-Eocene boundary (doi: 10.3301/ROL.2014.23)	17
Baczynski A. A., McInerney F.A., Wing S.L., the BBCP Science Team -Alkane PETM records from the Bighorn Basin, Wyoming: A core-outcrop comparison (doi: 10.3301/ROL.2014.24).....	19
Badger M.P.S., Singarayer J.S., Valdes P.J., Pancost R.D. - Three dimensional coupled model approaches to terrestrial methane cycling during Paleogene greenhouse climates (doi: 10.3301/ROL.2014.25).....	21
Barclay R.S., Wing S.L. - Increasing atmospheric CO ₂ prior to the Paleocene-Eocene Thermal Maximum inferred from stomata of <i>Ginkgo adiantoides</i> , Bighorn Basin, Wyoming, USA (doi: 10.3301/ROL.2014.26).....	23
Benjamini C., Pugliese N. - Reinstatement of the marginal marine carbonate platform in the earliest Terziary at Duino, Trieste Karst (doi: 10.3301/ROL.2014.27).....	25
Bhatia R., Wade B.S., Müller W., Evans D., Thornalley D.J.R., Opdyke B.N. - Geochemical signals in Eocene planktonic foraminifera (doi: 10.3301/ROL.2014.28)	27
Bijl P., Sijp W. - Is there a causal link between early Eocene opening of the Tasmanian Gateway and the onset of Eocene cooling? (doi: 10.3301/ROL.2014.29)	29
Bijl P., Sluijs A., Schouten S., Dickens G.R., Hollis C.J., Zeebe R.E., Zachos J.C., Stocchi P., Brinkhuis H. - Significant continental ice volumes on mid-Paleocene Antarctica? Latitudinal temperature gradients, sea level change and the carbon cycle (doi: 10.3301/ROL.2014.30)	31

Bordiga M., Henderiks J. - Variations in calcareous nannofossil assemblages during the Eocene-Oligocene transition at mid-latitude: Walvis Ridge ODP Site 1263 (Atlantic Ocean) (doi: 10.3301/ROL.2014.31).....	33
Bornemann A., Möbius I., Friedrich O., Wilson P.A., Liebrand D. - The end of the Paleogene – A new surface-water temperature record for the Oligocene-Miocene Transition from the western Atlantic (IODP Site U1405) (doi: 10.3301/ROL.2014.32).....	35
Boscolo Galazzo F., Thomas E., Pagani M., Warren C., Giusberti L., Luciani V. - Warming, pelagic food webs and deep-sea biota during the Middle Eocene Climatic Optimum in the SE Atlantic (ODP Site 1263) (doi: 10.3301/ROL.2014.33).....	36
Cameron A.J., Sexton P.F., Anand P., Fehr M.A., Scher H.D. - Strengthening of North Atlantic deep water production from the Norwegian-Greenland Sea at onset of the Eocene cooling trend (doi: 10.3301/ROL.2014.34).....	38
Chew A. - Mammal faunal response to the ETM2 and H2 hyperthermals (doi: 10.3301/ROL.2014.35)....	40
Clyde W.C., Gingerich P.D., Wing S.L., the BBCP Science Team - Bighorn Basin Coring Project (BBCP): An IODP-Style Continental Coring Project Investigating Early Paleogene Hyperthermals (doi: 10.3301/ROL.2014.36)	42
Ćorić S. - Climatic and environmental changes in the Paratethys during Oligocene traced by changes in calcareous nannoplankton assemblages (Molasse Basin, Austria and Kamchia Depression, Bulgaria) (doi: 10.3301/ROL.2014.37)	44
Ćorić S., Benić J. - First evidence of the Paleogene age of the Bosnian Flysch Unit (Dinarides, Bosnia and Herzegovina) (doi: 10.3301/ROL.2014.38)	46
Coxall H., Lear C., Backman J., O'Regan M., Huck C., van De Flierdt T., Sliwinska K.K., Zachos J.C. - Strengthening of North Atlantic deep-water production pre-dates onset of Antarctic glaciation (doi: 10.3301/ROL.2014.39).....	48
Dallanave E., Bachtadse V., Agnini C., Muttoni G., Hollis C.J., Hines B.R., Morgans H.E.G., Strong C.P., Tauxe L., Crampton J.S. - Early-middle Eocene magneto-biochronology of the Southern Pacific Ocean: new data from the South Island of New Zealand (doi: 10.3301/ROL.2014.40).....	50
D'Ambrosia A.R., Clyde W.C., Fricke H.C., Gingerich P.D. - Repetitive mammalian dwarfism associated with early Eocene carbon cycle perturbations (doi: 10.3301/ROL.2014.41)	52
Dawson A., Grimes S., Ellis M., Duller R., Watkinson M., Stokes M., Leng M.J. - Initial paleohydrological observations from the Paleocene-Eocene boundary at Esplugafreda and Berganuy in northern Spain (doi: 10.3301/ROL.2014.42).....	54
Deprez A., Jehle S., Bornemann A., Speijer R.P. - Stable isotope and benthic foraminiferal records of the Latest Danian Event at ODP Site 1262 (Walvis Ridge) (doi: 10.3301/ROL.2014.43).....	56
Deprez A., Tesseur S., Stassen P., D'haenens S., Steurbaut E., King C., Claeys P. Speijer R.P. - Benthic foraminiferal and isotopic patterns during the Early Eocene Climatic Optimum (Aktulagay section, Kazakhstan) (doi: 10.3301/ROL.2014.44).....	58
D'haenens S., Bornemann A., Speijer R.P. - Deep-sea benthic foraminiferal turnovers in the early Eocene: The role of the PETM and ETM2 (doi: 10.3301/ROL.2014.45).....	60
Dickens G.R., Lee C.A., CIA Operatives - Continental - island arc fluctuations through time and the Eocene transition from a greenhouse to an icehouse world (doi: 10.3301/ROL.2014.46)	62

Dinarès-Turell J., Westerhold T., Pujalte V., Röhl U., Kroon D. - Astronomical calibration of the Danian Stage (Early Paleocene) revisited: settling chronologies across the Atlantic and Pacific Oceans (doi: 10.3301/ROL.2014.47).....	64
D'Onofrio R., Luciani V., Giusberti L., Fornaciari E., Sprovieri M. - Tethyan planktic foraminiferal record of the early Eocene hyperthermal events ETM2, H2 and I1 (Terche section, northeastern Italy) (doi: 10.3301/ROL.2014.48).....	66
Dupuis C., Quesnel F. & Baele J.-M. - PETM related paleoweathering on the southern margins of the North Sea Basin. Examples from the Mons Basin (Belgium) and the Dieppe-Hampshire Basin (Normandy, France) (doi: 10.3301/ROL.2014.49).....	68
Edgar K.M., Hull P.M. - Spatial variability of environmental change and the magnitude of biotic responses of planktic foraminifera across the PETM (doi: 10.3301/ROL.2014.50).....	70
Evans D., Müller W., Erez J., Renema W., Wade B.S., Ziegler M. - Quantitative ocean temperatures from foraminifera Mg/Ca over the Eocene-Oligocene transition (doi: 10.3301/ROL.2014.51).....	71
Fenner J. - First find of a late Paleocene biraphid diatom: implications for models of diatom evolution (doi: 10.3301/ROL.2014.52)	73
Fenton I.S., Pearson P.N., Dunkley-Jones T., Purvis A. - Onset of Eocene diversity gradients in macroperforate planktonic foraminifera (doi: 10.3301/ROL.2014.53).....	75
Fioroni C., Villa G., Persico D. - Middle Eocene-Lower Oligocene biostratigraphy and paleoceanography of the Western Equatorial Indian Ocean based on Calcareous Nannofossils, ODP Site 711 (doi: 10.3301/ROL.2014.54)	76
Frieling J., Gebhardt H., Adekeye O.A., Akande S.O., Reichart G.-J., Middelburg J.J., Schouten S., Sluijs A. - The Paleocene-Eocene Thermal Maximum: temperature and ecology in the tropics (doi: 10.3301/ROL.2014.55).....	78
Frisone V., Pisera A., Preto N. - Siliceous sponges (Porifera: Hexactinellida, Demospongiae) from Chiampo Valley (Eocene, Lessini Mts, northern Italy): taxonomy, taphonomy and paleoecology (doi: 10.3301/ROL.2014.56)	79
Galeotti S., Moretti M. - Orbital Forcing of Early Eocene dissolution events and Carbon Isotope Excursions from the Contessa Road-Bottaccione composite section (Gubbio, central Italy) (doi: 10.3301/ROL.2014.57).....	81
Ghirardi J., Jacob J., Huguet A., Bauer H., Le Milbeau C., Chateaufneuf J.-J., Di Giovanni C., Quesnel F. - A unique high resolution lacustrine record of climate and vegetation changes during the EOT. The CDB1 core, Rennes Basin, France (doi: 10.3301/ROL.2014.58).....	83
Gladenkov Yu. B. - Biotic evolution in the North Pacific shelf zones during the Paleogene (doi: 10.3301/ROL.2014.59).....	85
Gladenkov A. Yu. – New observation of the recent data on Eocene diatoms from Kamchatka region, Russian Far East (doi: 10.3301/ROL.2014.60).....	87
Greene S.E., Ridgwell A., Schmidt D.N., Kirtland Turner S., Pälike H., Thomas E. - Long-Term Behavior of the Carbonate Compensation Depth Across Early Paleogene Warming (doi: 10.3301/ROL.2014.61).....	89
Greenop R., Foster G.L., Wilson P.A., Sossian S.M., Lear C.H. - The Relationship between ice volume and CO ₂ across the Oligocene-Miocene boundary (doi: 10.3301/ROL.2014.62).....	91
Griira C., Karoui-Yaakoub N., Mtimet M.-S., Guesmi W. - Biostratigraphy of the Lutetian/Bartonian Boundary in the North of Tunisia (doi: 10.3301/ROL.2014.63)	93

Harrington G.J., Jardine P.E., Wing S.L., BBCP Science Team - Bighorn Basin Coring Project (BBCP): Pollen floral changes and organic matter from core – outcrop comparisons through the PETM (doi: 10.3301/ROL.2014.64).....	95
Heilmann-Clausen C. - Possible varves in the PETM interval in Denmark (doi: 10.3301/ROL.2014.65)..	97
Heilmann-Clausen C., Schultz B.P., Beyer C., Friis H., Schoon P: L., Tegner C. - New evidence for NE Atlantic pre-PETM volcanism (doi: 10.3301/ROL.2014.66)	99
Henehan M.J., Edgar K.M., Foster G.L., Pearson P.A., Anagnostou E., Hull P.M. - Using boron isotopes to characterise past carbon cycle perturbations: the case of the MECO (doi: 10.3301/ROL.2014.67).....	101
Hernitz Kucenjak M., Premec Fucek V., Huber B.T., Wade B.S. - The test size and abundance variations in planktonic foraminifera <i>Chiloguembelina cubensis</i> and <i>C. ototara</i> as response to climatic events in Oligocene (doi: 10.3301/ROL.2014.68).....	103
Hofmann C.C., Egger H. - Fossil <i>Laurelia</i> pollen (Atherospermataceae) from lower Eocene sediments of the Krappfeld (Austria) (doi: 10.3301/ROL.2014.69)	105
Hofmann C.C., King C. - New LM and SEM investigations of pollen and spores from the Brixton drillcores (lowermost Eocene, England) (doi: 10.3301/ROL.2014.70)	107
Hollis C.J., Pascher K.M., Hines B.R., Littler K., Kulhanek D.K., Strong C.P., Zachos J.C., Eggins S.M., Phillips A. - Was the Early Eocene ocean unbearably warm or are the proxies unbelievably wrong? (doi: 10.3301/ROL.2014.71).....	109
Hooker J.J. - Faunal succession, local correlation and isotopes push the Mammalian Dispersal Event in NW Europe into the cooler latest Paleocene (doi: 10.3301/ROL.2014.72).....	111
Huck C.E., van de Flierdt T., Bohaty S.M., Hammond S. - Seawater neodymium isotope record of Antarctic climate instability during the termination of the Early Eocene Greenhouse (doi: 10.3301/ROL.2014.73).....	113
Hull P.M., Sexton P.F., Norris R.D., Wilson P. A., Blum P., Agnini C., Boulila S., Bown P.R., Coxall H., Friedrich O., Greenop R., Kirtland Turner S., Kordesch W.E.C., Liebrand D., Matsui H., Moriya K., Nishi H., Opdyke B.N., Pälike H., Penman D., Röhl U., Smith R., Westerhold T., Yamamoto Y., Zachos J.C. - Resolving Eocene time and palaeoceanography in exceptional detail: an update on IODP Expedition 342, Newfoundland Ridge (doi: 10.3301/ROL.2014.74).....	115
Iakovleva A.I., Quesnel F., Fléhoc C., Dupuis C. - Rejuvenating the Paris Basin stratigraphy using “lost” drillings: the $\delta^{13}\text{C}_{\text{org}}$ calibration of Upper Thanetian to Lower Ypresian dinocyst events succession (doi: 10.3301/ROL.2014.75)	117
Jaramillo C., Cardenas A. - Expansion of Neotropical Forests during Paleogene Global Warming (doi: 10.3301/ROL.2014.76).....	119
Jehle S., Bornemann A., Deprez A., Speijer R.P. - Paleoceanographic reconstruction of the Latest Danian Event at ODP Site 1210 (Shatsky Rise, Pacific Ocean) (doi: 10.3301/ROL.2014.77)	120
Jennions S.M., Thomas E., Schmidt D.N., Ridgwell A., Lunt D.J. - Eocene Thermal Maximum 2: benthic ecosystems and ocean circulation in the SE Atlantic (doi: 10.3301/ROL.2014.78)	121
Khozyem H., Adatte T., Spangenberg J.E., Aziz Tantawy A., Keller G. - Toward a better understanding of Paleocene-Eocene Thermal Maximum: A multidisciplinary record from Dababiya GSSP, Luxor, Egypt (doi: 10.3301/ROL.2014.79).....	123
King C. - A high-resolution record of depositional sequences in the PETM in the southern North Sea Basin (doi: 10.3301/ROL.2014.80)	125

Kirtland Turner S., Greene S.E., Ridgwell A. - An Earth system model evaluation of carbon emissions across Paleocene hyperthermals vs. the PETM (doi: 10.3301/ROL.2014.81).....	127
Kirtland Turner S., Sexton P.F., Charles C.D., Norris R.D. - Regularity of Palaeogene hyperthermals inconsistent with a temperature threshold for carbon release (doi: 10.3301/ROL.2014.82).....	128
Kordesch W.E.C., Bohaty S.M., Pälike H., Westerhold T., Röhl U., Edgar K.M., Wilson P.A. - Carbonate dissolution in the deep equatorial Atlantic during the Middle Eocene Climatic Optimum (doi: 10.3301/ROL.2014.83)	129
Kordesch W.E.C., Bohaty S.M., Pälike H., Edgar K.M., Wilson P.A. - Evidence for the magnetochron C19r hyperthermal event in the northwest Atlantic Ocean: IODP Exp32 Site U1408 (doi: 10.3301/ROL.2014.84).....	130
Krishnan S., Huber M., Pagani M. - Compilation of hydrogen isotopic compositions of leaf wax biomarker records across the Paleocene-Eocene Thermal Maximum (doi: 10.3301/ROL.2014.85)....	131
Kunzmann L., Kvaček Z., Teodoridis V., Moraweck K. - Tracing terrestrial palaeoclimatic changes - vegetation dynamics of riparian forest in central Europe during late Palaeogene (doi: 10.3301/ROL.2014.86).....	133
Lauretano V., Zachos J.C., Lourens L.J. - High-resolution benthic stable isotope records from ODP Site 1263 in the Southern Atlantic encompassing early Eocene warming events (doi: 10.3301/ROL.2014.87).....	135
Lear C.H., Wilson P.A., Liebrand D. - The Oligocene-Miocene Transient Glaciation: Insights from IODP Expedition 342 (doi: 10.3301/ROL.2014.88).....	137
Lee D.E., Fordyce R.E., Conran J., Reichgelt T., Fox B., Kennedy E.M. - Biological stability during maximum marine transgression: the Paleogene – Neogene transition in New Zealand (doi: 10.3301/ROL.2014.89).....	139
Leighton A.D., Hart M.B., Smart C.W., Hampton M.J., Leng M. - Possible hyperthermal events (Dan-C2 and Lower 29n) in the lowermost Paleocene of the Brazos River area, Texas (doi: 10.3301/ROL.2014.90).....	141
Little K., Leng M., Agnini C., Zachos J.C., Westerhold T., Röhl U. - A new age model for the late Paleocene at ODP Site 1263, Walvis Ridge: new stable isotope and calcareous nannofossil data (doi: 10.3301/ROL.2014.91)	143
Luciani V., Giusberti L., Fornaciari E., Rio D., D’Onofrio R., Backman J. - Deterioration of symbiont-bearing morozovellid ecology (planktic foraminifera) habitat recorded within the Early Eocene Climatic Optimum: evidence from the Tethys and sub-tropical Atlantic Ocean (doi: 10.3301/ROL.2014.92).....	145
Manners H.R., Grimes S.T., Sutton P.A., Dunkley-Jones T., Pancost R.D., Leng M.J., Jardine P., Domingo L., Hart M.B., Lopez-Martinez N. - A Multi-Proxy Study of the PETM at the Zumaia Section, northern Spain (doi: 10.3301/ROL.2014.93).....	147
Miniati F., Monechi S., Cappelli C. - The Late Danian Event at Site 1209: a rapid diversification of calcareous nannofossils (doi: 10.3301/ROL.2014.94).....	149
Moebius I., Friedrich O., Edgar K.M., Sexton P.F. - Global increase in export productivity during the Middle Eocene Climatic Optimum (MECO)? (doi: 10.3301/ROL.2014.95).....	151
Moraweck K., Grein M., Konrad W., Kovar-Eder J., Kunzmann L., Kvaček J., Neinhuis C., Roth-Nebelsick A., Streubig M., Traiser C. - How does leaf morphology reflect palaeoclimate conditions? A quantitative approach tracing terrestrial climate conditions during the Palaeogene (doi: 10.3301/ROL.2014.96)	153

Newsam C., Bown P.R. - Calcareous nannoplankton response at the culmination of the Paleogene greenhouse world (doi: 10.3301/ROL.2014.97).....	155
Opdyke B.N., Haiblen A.M., Roberts A.P., Wilson P.A. - High-resolution paleotemperature record of the surface ocean from the Eocene-Oligocene boundary of the South Australian Coast (doi: 10.3301/ROL.2014.98).....	157
Ortiz S., Payros A., Millán I., Arostegui J., Orue-Etxebarria X., Apellaniz E. - The Early Eocene Climatic Optimum: chronological constraints and environmental impact at the North Iberian continental margin (doi: 10.3301/ROL.2014.99).....	159
Orue-Etxebarria X., Payros A., Caballero Estibaliz Apellaniz, F., Pujalte V., Ortiz S. - <i>Morozovella gorrondatxensis</i> vs <i>Morozovella crater</i> : taxonomy and biostratigraphic significance (doi: 10.3301/ROL.2014.100).....	161
Papazzoni C.A., Vescogni A., Bosellini F., Giusberti L., Roghi G., Dominici S. - First evidences of coral bioconstructions in the Monte Postale succession (Lower Eocene of Lessini Mts., Veneto, northern Italy) (doi: 10.3301/ROL.2014.101).....	163
Papazzoni C.A., Moretti A., Luciani V., Fornaciari E., Giusberti L. - The Varignano section (Trento Province, northern Italy): a chance to correlate shallow benthic zones and calcareous plankton zones near the Bartonian–Priabonian boundary (doi: 10.3301/ROL.2014.102).....	165
Pascher K.M., Hollis C.J., McKay R.M., Cortese G. - Southern Ocean endemism evident in Late Eocene radiolarian assemblages, DSDP Site 277, Campbell Plateau (New Zealand) (doi: 10.3301/ROL.2014.103).....	167
Payros A., Martinez-Braceras N. - Astronomically driven short-term climate change, a factor controlling Eocene turbidite accumulation (doi: 10.3301/ROL.2014.104).....	169
Pearson P.N., John E.H., Wilson J.D., Ridgwell A. - Testing the metabolic hypothesis: temperature-dependent carbon cycling in the Eocene oceans (doi: 10.3301/ROL.2014.105).....	171
Penman D. E., Hönisch B., Thomas E., Zeebe R.E., Clay Kelly D., Zachos J.C. - Boron proxy constraints on the magnitude of surface ocean acidification during the Paleocene-Eocene Thermal Maximum (doi: 10.3301/ROL.2014.106).....	173
Plink-Björklund P., Birgeneier L., Jones E. - Extremely bad early Eocene weather: Evidence for extreme precipitation from rived deposits (doi: 10.3301/ROL.2014.107).....	175
Pujalte V., Baceta J.I., Schmitz B. - Input of coarse-grained siliciclastics into the Pyrenean Basin during the PETM (1): overview (doi: 10.3301/ROL.2014.108).....	177
Pujalte V., Robador A., Payros A., Samsó J.M. - Input of coarse-grained siliciclastics into the Pyrenean Basin during the PETM (2): a river-dominated fan delta within a carbonate platform system (doi: 10.3301/ROL.2014.109).....	179
Pujalte V., Orue-Etxebarria X., Apellaniz E., Caballero F., Monechi S., Ortiz S., Schmitz B. - A prospective Early Late Paleocene event (ELPE) from the expanded Río Gor hemipelagic section (Betic Cordillera, southern Spain): foraminifera, nannofossil and isotopic data (doi: 10.3301/ROL.2014.110).....	181
Quesnel F., Storme J.-Y., Roche E., Iakovleva A., Missiaen P., Smith T., Bourdillon C., Baele J.-M., Yans J., Schnyder J., Iacumin P., Fléhoc C., Dupuis C. - An unexpected record of the PETM in terrestrial and organic sediments of Avesnois, between the Paris and Belgian Basins, NW Europe (doi: 10.3301/ROL.2014.111).....	183

Robinson M.M., Self-Trail J.M., Wandless G.A., Willard D.A. - A Paleocene Pre-onset Carbon Isotope Excursion Recorded in the Shallow Marine Environment of Southern Maryland (USA) (doi: 10.3301/ROL.2014.112).....	185
Robson B.E., Collinson M.E., Riegel W., Wilde V., Scott A.C., Pancost R.D. - A record of fire through the Early Eocene (doi: 10.3301/ROL.2014.113)	187
Rohrssen M., Charteris A., Inglis G.N., Grogan D., Pancost R.D., Whiteside J.H. - An organic geochemical investigation of organic matter sources and carbon cycling within Eocene Lake Uinta, Parachute Creek Member, Green River Formation, Uinta Basin (doi: 10.3301/ROL.2014.114).....	189
Scher H. - Stacking PEAT; A stacked Nd isotope record for the Paleogene equatorial Pacific (doi: 10.3301/ROL.2014.115).....	191
Scher H.D. - Deep water composition and water mass mixing in the Paleogene North Atlantic; Results from the Newfoundland ridges (doi: 10.3301/ROL.2014.116).....	193
Self-Trail J.M., Robinson M.M., Willard D.A., Bralower T.J., Edwards L.E., Powars D.S., Wandless G.A., Freeman K.H., Denis E. - Comparison between two middle to outer neritic PETM sections: South Dover Bridge and Mattawoman Creek Billingsley Road cores, Mid-Atlantic Coastal Plain, USA (doi: 10.3301/ROL.2014.117)	195
Shepherd C.L., Kulhanek D.K., Hollis C.J. - Eocene nannofossil biostratigraphy of the mid-Waipara river section, Canterbury Basin, New Zealand: preliminary results (doi: 10.3301/ROL.2014.118).....	197
Sheward R.M., Gibbs S.J., Bown P.R., Poulton A.J., Daniels C.J., Higgins D., Wilson P.A. - Cell geometry records the physiological responses of coccolithophores to Paleogene climate change (doi: 10.3301/ROL.2014.119).....	199
Slotnick B.S., Dickens G.R., Hollis C.J., Crampton J.S., Strong C.P., Zachos J.C. - Extending lithologic and stable carbon isotope records at Mead Stream (New Zealand) through the Middle Eocene (doi: 10.3301/ROL.2014.120).....	201
Smith R.E., Röhl U., Westerhold T., Bohaty S.M., Wilson P.A. - A Sub-orbital climate variability in the Late Oligocene North Atlantic Ocean (doi: 10.3301/ROL.2014.121).....	203
Snell K.E., Fricke H.C., Clyde W.C., Eiler J.M. - Large temperature changes on land during Early Eocene hyperthermals (doi: 10.3301/ROL.2014.122).....	204
Speijer R.P. - Scrutinizing data on climatic and biotic events of the Paleogene (doi: 10.3301/ROL.2014.123).....	206
Spray J.F., Wilson P.A., Bohaty S.M., Bailey I. - Possible evidence of ice-rafting in the North Atlantic across the Eocene-Oligocene Transition: Preliminary findings from the Newfoundland Margin (doi: 10.3301/ROL.2014.124).....	208
Stassen P., Speijer R.P., Devleeschouwer X., Abels H.A., King C., Willems W., Steurbaut E. - Eocene hyperthermals in the North Sea Basin: a Belgian Ypresian perspective (doi: 10.3301/ROL.2014.25)	209
Stocchi P., Galeotti S., Ladant J.-B., Gasson E., DeConto R.M., Pollard D., Rugenstein M., Vermeersen B.L.A., Brinkhuis H. - Placement and fluctuations of the Antarctic Ice Sheet across the Eocene-Oligocene transition (doi: 10.3301/ROL.2014.126)	211
Stoykova K. - The Paleocene-Eocene transition in Bulgaria: inference from calcareous nannofossils (doi: 10.3301/ROL.2014.127)	213
Thomas D.J. - Early Paleogene Pacific Deep-water Lead Isotope Variations – Implications for the Evolution of Water Mass Composition (doi: 10.3301/ROL.2014.128).....	215

Vanhove D., Speijer R.P., Steurbaut E., Claeys P., Ivany L. - Temperature, seasonality and salinity history of the early Eocene North Sea Basin inferred from fish otoliths and mollusks (doi: 10.3301/ROL.2014.129).....	217
Vellekoop J., Smit J., Esmeray S., Miller K.G., Browning J.V., Van De Schootbrugge B., Sinnighe-Damsté J.S.; Brinkhuis H. - Unravelling volcanism and impact related environmental change in the latest Maastrichtian and early Danian (doi: 10.3301/ROL.2014.130).....	219
Villa G., Fioroni C., Persico D., Roberts A.P., Florindo F. - Antarctic glacial history and Southern Ocean productivity during the Middle Eocene - Late Oligocene (doi: 10.3301/ROL.2014.131).....	221
Vonk R. - Ypresian isopod crustaceans from Monte Bolca and Monte Postale (Italy) (doi: 10.3301/ROL.2014.132).....	223
Westerhold T., Röhl U., Zachos J.C., Dinarès-Turell J. - Status and perspectives integrating marine and terrestrial archives (doi: 10.3301/ROL.2014.133).....	225
Woelders L., Sluijs A., Bijl P. - Climate and oceanography of the Tasmanian Gateway during the Middle Eocene Climatic Optimum (MECO) (doi: 10.3301/ROL.2014.134).....	226
Woelders L., Speijer R., Claeys P. - Benthic foraminiferal, sea level and climate change across the Cretaceous/Paleogene boundary at Brazos River, Texas (doi: 10.3301/ROL.2014.135).....	228
Yans J., Kocsis L., Gheerbrant E., Amaghazaz M., Bouya B., Cappetta H., Iacumin P., Mouflih M., Selloum O., Sen S., Noiret C., Storme J.-Y. - Chemostratigraphy ($\delta^{13}\text{C}_{\text{org}}$, $\delta^{13}\text{C}_{\text{inorg}}$, $\delta^{18}\text{O}_{\text{PO}_4}$) of the phosphate series from the Ouled Abdoun Basin, Morocco: constraints and significance for earliest known African placental mammals (doi: 10.3301/ROL.2014.136).....	230
Zachos J.C. - Paleogene Climate, Biota, and the Carbon Cycle: Progress and Promise (doi: 10.3301/ROL.2014.137).....	232
Zhang Q., Xu X., Willems H., Ding L., Liu X., Hinrichs K.-U. - Stepped carbon isotope excursion during the Paleocene-Eocene Thermal Maximum triggered initially by volcanic CO ₂ emission (doi: 10.3301/ROL.2014.138).....	234
Zhou X., Thomas E., Rickaby R.E.M., Winguth A., Lu Z. - I/CA in Planktic Foraminifera: Evidence for upper ocean deoxygenation during the Paleocene/Eocene Thermal Maximum (doi: 10.3301/ROL.2014.139).....	236

CBEP 2014: preface and dedication

Gerald R. Dickens ^(a) & Valeria Luciani ^(b)

^(a) Department of Earth Sciences, Rice University, Houston, TX, 77005, USA. E-mail: jerry@rice.edu

^(b) University of Ferrara, Dipartimento di Fisica e Scienze della Terra, Ferrara, Italy

KEY WORDS: Paleocene, Eocene, climate, fossils, earth systems.

Surrounding you, brick-by-brick, is an amazing stratigraphic record – a complex history of wealth and poverty, peace and violence, public revolts and exceptional ideas. We did not choose Castello Estense for Climatic and Biotic Events of the Paleogene (CBEP) this year because of its raw beauty and famous architecture; rather, this remarkable castle very much expresses the essence of the early Paleogene. Begun in 1385 as a medieval castle, it was heavily modified during the Renaissance. Along the way, disruptive events occurred, including a major fire in 1544, a takeover by the pope in 1598, allied bombing in 1944, and an earthquake in 2012. There is also the scope of time, intriguing people, and jargon: to fully appreciate Castello Estense, one needs to know about contemporaneous happenings in Europe, prominent families and artisans, and things like corbels, ravelins and scalcos.

CBEP 2014 arrives at a curious moment, a silver anniversary following the first such meeting (Albuquerque, 1989; Table 1). While vigorous debates then raged about the “bookends” (the K/Pg and E/O boundaries), our community suspected the intervening time might also be interesting and special. After all, the early Paleogene was a transition from a “greenhouse world” to an “icehouse world”, when major turnovers in biota on land and in the ocean occurred, and when stable isotope records show major variations. However, very little presented in 1989 would predict the realm of current topics and debates regarding the early Paleogene, which now revolve around general movements and specific events, all correlated in increasing detail across space and time, and all juxtaposed with a society interested in global warming. In 1989, our view of a castle was that of a fortified building; there were limited foundations in global biogeochemistry; there were minimal beams crossing climate and evolution; there were no windows of discussion regarding *Apectodinium* and neodymium; there were no disruptive events such as the PETM, EECO, MECO, H1/ETM-2, and a growing number of poorly-defined “hyperthermals” and acronyms; certainly, few thought key aspects of the Paleogene would play a role in

discussions of future climate change, and nobody presented the idea that past changes in the hydrological cycle seriously impact the sedimentary record.

Upon given the opportunity to co-chair CBEP 2014, we asked numerous colleagues three questions “What are you working on?” “What do you think are cool and exciting problems?” “What about organizing the meeting on key topics?” From these queries, 10 thematic sessions arrived easily, although without certainty these were the best or most appropriate. We also supposed, given our rapidly and continually evolving field, colleagues would submit abstracts on emerging topics, so probably we should add at least two “catch-all” sessions (which deservedly required Italian names). To hold the meeting within the fantastic walls of Castello Estense – and to link all together – we also had to adhere to governing time constraints. From these considerations, the meeting format (Table 2) and following volume emerged.

We welcome you, as a reader, to Castello Estense, either directly now and very real, or indirectly in the future and imaginary, so you can ponder the architecture, consider the enclosed abstracts, and think deeply about the early Paleogene. None of us who read this come here by chance. We are part of a wonderful renaissance, where we are not only deciphering ancient history but also rewriting scientific understanding on how our world works.

Table 1: List of CBEP Meetings

- 1989 Albuquerque (USA)
- 1996 Zaragoza (Spain)
- 1998 Paris (France)
- 1999 Göteborg (Sweden)
- 2001 Powell (USA)
- 2003 Luxor (Egypt)
- 2006 Bilbao (Spain)
- 2009 Wellington (New Zealand)
- 2011 Salzburg (Austria)
- 2014 Ferrara (Italy)

Table 2: Sessions at CBEP 2014

- Early Cenozoic climate and carbon cycling
- Biological evolution in the Late Cretaceous and Paleogene
- Refining and linking Paleogene records from the land to the deep sea
- Ricco buffet di Paleogene
- New Paleogene records from new Paleogene drilling
- A different ocean, atmosphere and geosphere during the Paleogene
- Comparing and contrasting the effects of late Paleocene early Eocene hyperthermals with implications for the Anthropocene
- Mercato aperto del Paleogene (speciale dell'anno: A hydrological cycle on steroids)
- Surviving in an Eocene world (the unbearable warmth of being)
- New insights from new proxies pertinent to the Paleogene World
- Early Paleogene near Bookend 1: MECO and the Late Eocene
- Early Paleogene near Bookend 2: The Early Paleocene and pre- cursor hyperthermal events?

DEDICATION

This abstract volume is dedicated to Robert W.O'B. Knox, who was an instrumental individual in our Paleogene community and at previous CBEP Meetings. A memorial meeting in tribute to Robert's career was held in Nottingham, England, March 2014. One can appreciate the contributions of Robert, especially regarding Paleogene stratigraphy, by reading the contents of this meeting:

Yorkshire Geological Society, Circular 585;

<http://www.yorksgeolsoc.org.uk/Circulars/585.pdf>.



Fig.1 – Robert Knox (middle) carefully contemplating an explanation by Robert Speijer regarding the Danian at Zumaia (northern Spain). We can only guess the first Robert is thinking about the initiation of climatic and biotic events of the Paleogene. (Photo courtesy of Claus Heilmann-Clausen).

Terrestrial sedimentary archives of episodes of greenhouse warming in ancient river floodplain deposits of the Bighorn Basin, Wyoming

Hemmo A. Abels^(a), Chaowen Wang^(a,b), Vittoria Lauretano^(a), Gabriel J. Bowen^(c), Derek Karssenberg^(d), Martin Ziegler^(a,e), Gaojun Li^(f), Peter F. van den Berg^(g), Sjors van Broekhuizen^(a), Tarek Hopman^(a), Jelmer Laks^(a), Rieko Adriaens^(h), William C. Clyde⁽ⁱ⁾, Jan Elsen^(b), Mary J. Kraus^(k), Appy Sluijs^(a), Noël Vandenberghe^(h), Lucas J. Lourens^(a) & Philip D. Gingerich^(k)

^(a) Dept. Earth Sciences, Utrecht Univ., Budapestlaan 4, 3584 CD, Utrecht, Netherlands. E-mail: h.a.abels@uu.nl

^(b) State Key Lab. Biogeology and Environm. Geology, China Univ. of Geosciences, Wuhan 430074, China

^(c) Geology & Geophysics, Univ. Utah, 115 S 1460 E, Salt Lake City, USA

^(d) Dept. Physical Geography, Utrecht Univ., Netherlands

^(e) Dept. Earth Sciences, ETH Zürich, CH-8092 Zürich, Switzerland

^(f) MOE Key Laboratory of Surficial Geochemistry, Department of Earth Sciences, Nanjing University, Nanjing 210093, China,

^(g) Enres International, Euclideslaan 201, 3584 BS, Utrecht, Netherlands

^(h) Dept. Geology, Leuven Univ., Leuven, Belgium

⁽ⁱ⁾ Dept. Earth Sciences, Univ. New Hampshire, Durham, New Hampshire 03824, USA

^(j) Dept. Geology, Univ. Colorado, Boulder, CO, USA

^(k) Dept. Earth and Environmental Sciences, Univ. Michigan, Ann Arbor, Michigan 48109, USA

Document type: Short note.

Manuscript history: received 15 May 2014; accepted 30 May 2014; editorial responsibility and handling by Gerald R. Dickens & Valeria Luciani.

KEY WORDS: Astronomical forcing, Bighorn Basin, Eocene, fluvial sediments, greenhouse warming, hyperthermals, sedimentary geology, terrestrial environments.

The Bighorn Basin of northwestern Wyoming provides hundreds of meters of excellently exposed river floodplain strata of Paleocene and early Eocene age. Records of the Paleocene-Eocene Thermal Maximum (PETM), the largest greenhouse-warming episode in this interval of time, were recovered soon after their discovery in deep marine sediments. This has allowed intensive study of the major impact this greenhouse warming event had on continental interior climate, flora and fauna, and river dynamics (e.g. McInerney & Wing, 2011). Recently, records of four successive, smaller, transient greenhouse warming events in the early Eocene - ETM2/H1/Elmo, H2, I1, and I2 - were located in the fluvial rock record of the basin (Abels et al., 2012). These events are now under study to clarify whether they were comparable to the PETM in terms of impact of climate, sedimentary processes, and biotas. Recently developed and improved proxies that reconstruct precipitation and temperature are crucial. Further, sedimentary cyclicity related to climate change induced by astronomical cycles enables much better resolved age models that shed light on rates of change during the hyperthermal events and also in the long rock record between events.

Global warming and its impact on river floodplain environments are both of major concern for human society. Using geological examples is a way to understand the causes and consequences of climate change and its impact on fluvial systems. The best fossil analogues for current carbon injection into the atmosphere are transient early Eocene (~56-50 million years ago) global warming events known as hyperthermals.

Bighorn Basin sediments

The Bighorn Basin is an intermontane basin that originated

during the Laramide orogeny. Thick piles of fluvial strata are now exposed at the surface and study of these reveals the history of fluvial sedimentation and ancient climate, and of floras and faunas that inhabited the basin in Paleocene and early Eocene times (Fig. 1). Meandering rivers brought water and sediment from surrounding mountain ranges to fill accommodation space generated by tectonic subsidence. The sediments were deposited at rates between 30-35 cm/kyr (Abels et al., 2013). They are composed of thick sheet-sandstone bodies representing ancient channel belts and a dominance of mudrocks representing fluvial overbank deposits and strata deposited by avulsion of river channels.

Astronomical forcing of sedimentation

Sedimentary cycles are present in the floodplain strata and consists of reddish mudrocks representing strongly-developed paleosols that formed on overbank sediments and alternate with pale-colored heterolithic sand- and mudstones deposited during phases of river avulsion when channels chose a new course on adjacent floodplains (Kraus, 1996). The overbank-avulsion cycles have an average thickness of ~7 meters in multiple sections of different age and geographic position (Abels et al., 2013). Sedimentation rates calculated by different means point to a 17-26-kyr duration for the cycles in line with the climatic precession cycle with a ~21-kyr duration (Abels et al., 2013).

Astronomical age models

Paleosols are regarded as geologic time lines in the fluvial strata. Tracing of individual paleosols shows that stratigraphic thicknesses between them can vary by as much as a factor of two between sections spaced several kilometers apart. This stratigraphic variability is caused by paleotopographic irregularities by occasional flooding or local river avulsion. Astronomical age models use the astronomical duration of sedimentary cyclicity to calculate the duration of sedimentation at relatively high resolution (Abdul Aziz et al., 2008). The thickness variability between sites implies that astronomical



Fig.1 – View to northeast of early Eocene river floodplain outcrops of the McCullough Peaks in the northern Bighorn Basin, Wyoming (USA). The succession on the photo belongs to Wasatchian mammal stages Wa2 to Wa5. Thicker pale bands represent channel belt sheet sandstone bodies. Red colors represent overbank mudrocks on which paleosols developed. Note that pale-red alternations at the top of the outcrops in sunlight in the center of the photo represent 5-10 m thick red overbank – pale avulsion-related sedimentary cyclicality likely driven by 21-kyr precession cycles of climate change (Abels et al. 2013). Outcrops there are approximately 5 km from the viewpoint at the top of the McCullough Peaks and are part of the Deer Creek Amphitheater section of Abels et al. (2013). The Elmo or ETM2 event is located in stratigraphy right above those outcrops, a little farther to the southeast (right on the photo).

age models should not be based on one-dimensional records of sedimentation in these fluvial strata.

Greenhouse warming episodes

High sedimentation rates and lack of carbonate dissolution make the sedimentary record of the Bighorn Basin very suitable to use for astronomical age models for these events (Abdul Aziz et al., 2008; Abels et al., 2012). Below the scale of precession-forced overbank-avulsion cycles, sedimentation rates are however not constant. One precession cycle consists of a slowly sedimented interval, the fine overbank sediments on which one, multiple, or cumulative paleosols developed, and a rapidly sedimented interval, the river avulsion-related heterolithic sediments on which only weak pedogenesis may have occurred (Kraus, 1996; Abels et al., 2013). The distinct sedimentation rates of these packages limit age models to at best 21-kyr resolution, unless sedimentation rates are inferred individually for the different styles of sedimentation.

Reconstructions of fluvial environments

Temperature and precipitation proxies reconstruct climate change for continental interiors across greenhouse warming episodes and for background climate (Kraus et al., 2013). This is needed to understand causes of large changes in fluvial sedimentation (Foreman et al., 2013) and, also of precession-related sedimentary cyclicality. How did climate change to cause overbank-avulsion sedimentary cyclicality? To solve such questions, an integrated approach is needed that uses data from sedimentology, paleontology, integrated stratigraphy, and proxy reconstructions, to test hypotheses derived from model

experiments of climate and fluvial architecture. The Bighorn Basin sedimentary record clearly has not yet revealed all its secrets, despite a long history of scientific investigation, and much of the variability in its thick fluvial rock record remains to be understood.

REFERENCES

- Abdul Aziz H., Hilgen F.J., van Lwijk G.M., Sluijs A., Kraus M.J., Pares J.M. & Gingerich P.D. (2008) - Astronomical climate control on paleosol stacking patterns in the upper Paleocene-lower Eocene Willwood Formation, Bighorn Basin, Wyoming. *Geology*, 36, 531–534.
- Abels H.A., Clyde W.C., Gingerich P.D., Hilgen F.J., Fricke H. C., Bowen G.J. & Lourens L.J. (2012) - Terrestrial carbon isotope excursions and biotic change during Palaeogene hyperthermals. *Nature Geosci.*, 5, 326-329.
- Abels H.A., Kraus M.J. & Gingerich P.D. (2013) - Precession-scale cyclicality in the lower Eocene fluvial Willwood Formation of the Bighorn Basin, Wyoming (USA). *Sedimentology*, 60, 1467-1483.
- Foreman B.Z. (2013) - Climate-driven generation of a fluvial sheet sand body at the Paleocene-Eocene boundary in northwest Wyoming (USA). *Basin Res.*, 25, 1-17.
- Kraus M.J. (1996) - Avulsion deposits in lower Eocene alluvial rocks, Bighorn Basin, Wyoming. *J. Sed. Res.*, 66, 354–363.
- Kraus M.J. et al. (2013) - Paleohydrologic response to continental warming during the Paleocene–Eocene Thermal Maximum, Bighorn Basin, Wyoming. *Palaeo3*, 370, 196-208.
- McInerney F.A. & Wing S.L. (2011) - The Paleocene-Eocene Thermal Maximum: A perturbation of carbon cycle, climate, and biosphere with implications for the future. *Annu. Rev. Earth Planet. Sci.*, 39, 489-516.

Response of terrestrial environment to the Paleocene-Eocene Thermal Maximum (PETM), new insights from India and NE Spain

Thierry Adatte ^(a), Hassan Khozyem ^(a,b), Jorge E. Spangenberg ^(c), Bandana Samant ^(d) & Gerta Keller ^(e)

^(a) Institute of Earth Sciences, University of Lausanne, Switzerland. E-mail: thierry.adatte@unil.ch

^(b) Department of Geology, Faculty of Sciences, Aswan University, Aswan, Egypt

^(c) Institute of Earth Surface Dynamics, University of Lausanne, Switzerland

^(d) Postgraduate Department of Geology, RTM Nagpur University, Nagpur, 440001, India

^(e) Department of Geosciences, Princeton University, Guyot Hall, Princeton, NJ 08544, USA

Document type: Short note.

Manuscript history: received 15 May 2014; accepted 30 May 2014; editorial responsibility and handling by Gerald R. Dickens & Valeria Luciani.

KEY WORDS: Geochemistry, ETM2, India, Paleoclimate PETM, Spain.

The late Paleocene - Early Eocene boundary (56Ma) is marked by the warmest climate period of the Cenozoic, known as the Paleocene-Eocene Thermal Maximum (PETM). Most notably, the culprit behind it was a massive injection of heat-trapping greenhouse gases into the atmosphere and oceans, comparable in volume to what our persistent burning of fossil fuels could deliver in coming centuries. The response of the oceanic and continental environments to the PETM is different. Many factors might control the response of the environments to the PETM such as paleogeography, paleotopography, paleoenvironment, and paleodepth. Herein, we present two different examples from terrestrial environment, their correlation with the marine record and their response to the PETM warming.

In northwestern India, the establishment of wetland conditions and related thick lignite accumulations reflect the response of the continental environments to the PETM. This continental climatic shift towards more humid conditions led to migration modern mammals northward following the migration of the climatic belts. What remains uncertain is the timing and tempo of this mammal migration event and whether it originated in Asia or more specifically out of India. Biostratigraphy and carbon isotope analyses in three lignite mines located in NW India reveal the presence of both PETM and ETM2 organic carbon isotope negative excursions and demonstrate that modern mammals appeared in India after the PETM. Relative ages of this mammal event based bio-chemo- and paleomagnetic stratigraphy support a migration path originating from Asia into Europe and North America, followed by later migration from Asia into India.

In contrast, at Esplugafreda, north-eastern Spain, the terrestrial environment reacted differently; increased weathering due to enhanced runoff led to the formation thick paleosol accumulation enriched with carbonate nodules (Microcodium like) suggesting a coeval semi-arid climate (Retallack, 2001). High-resolution $\delta^{13}\text{C}$ and $\delta^{18}\text{O}$ analyses of

two types of calcareous paleosol nodules reveal two distinct negative excursions. The lower $\delta^{13}\text{C}$ negative excursion represents the PETM with an abrupt onset due to an unconformity. The upper gradual $\delta^{13}\text{C}$ excursion represents the Eocene thermal maximum 2 (ETM2). The $\delta^{13}\text{C}_{\text{org}}$ data recorded slightly heavy values at the PETM possibly due to oxidation of organic matter and/or deposition in an open soil system formed under more humid conditions where $\delta^{13}\text{C}$ values reflect mixed CO_2 sources (atmospheric and oxidation of ancient organic matter). The $\delta^{13}\text{C}_{\text{org}}$ linked to the ETM2 records more negative values, which could be related to a

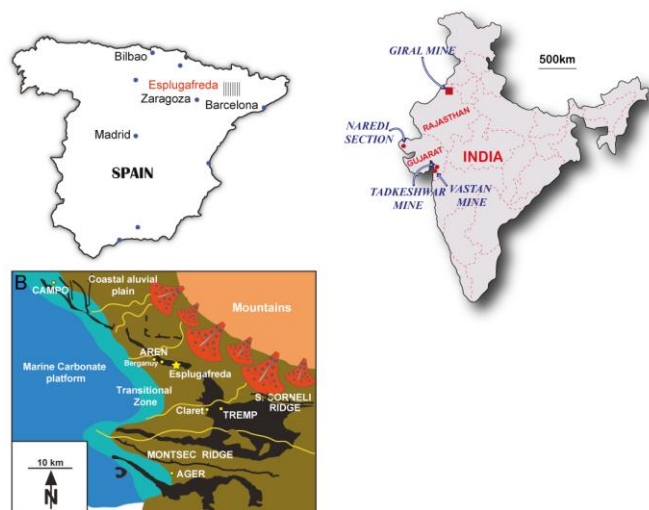


Fig. 1 – Location of the studied sections (Esplugafreda, Spain; Vastav and Tadkeshwar Naredi and Giral Mine, India). Paleogeographic map with location of the Esplugafreda section.

closed soil system under more arid conditions.

A rapid +8°C increase in the lower part of the section corresponds to the Paleocene-Eocene Thermal Maximum (PETM) in accordance with existing regional records of marine and terrestrial environments. A gradual increase from 6 to 8°C in the upper part of the section appears to be related to the Eocene Thermal Maximum 2 (ETM2). The well-known Claret

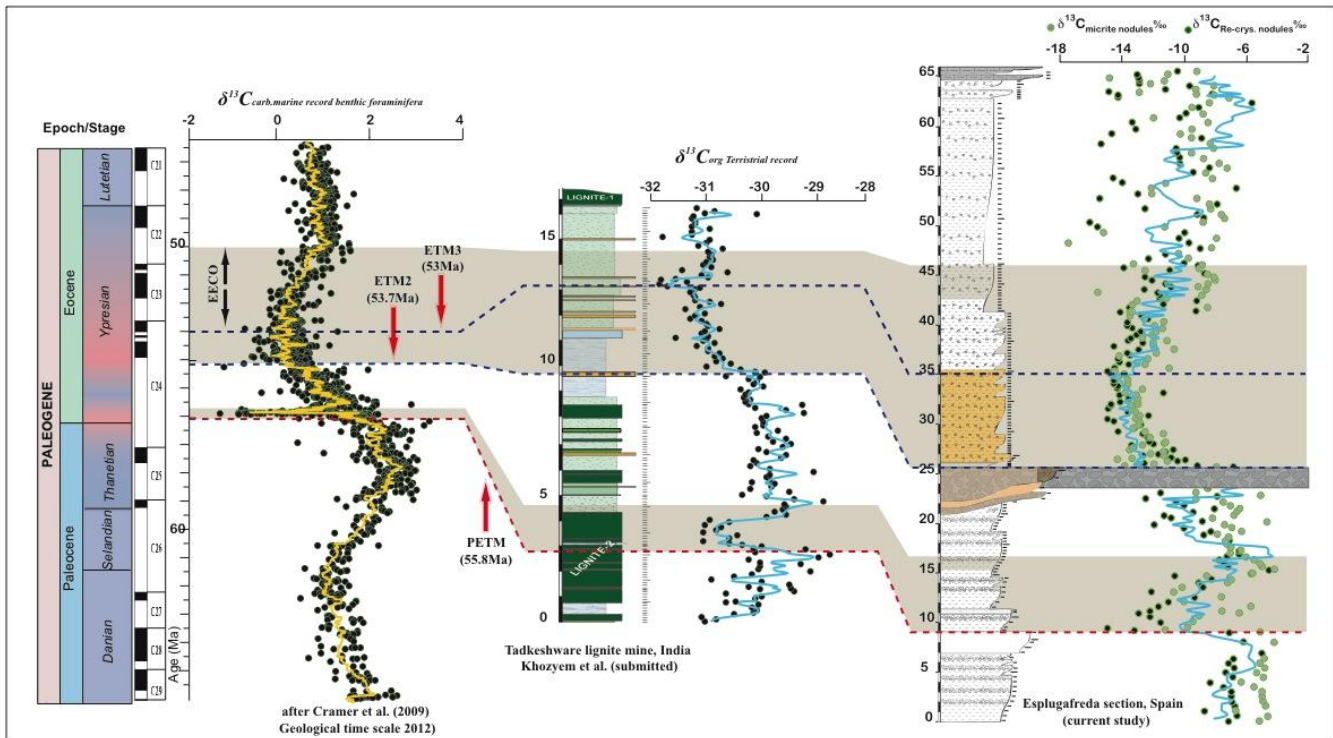


Fig.2 – Correlation of the terrestrial Esplugafreda $\delta^{13}\text{C}_{\text{carb}}$ (Micrite nodules and recrystallized N) with terrestrial organic carbon isotope from Takeswar, India and the marine isotopic record (Zachos et al., 2001; Cramer et al., 2009). Note that ages are recalibrated using the GTS 2012.

conglomerate, previously thought to represent an extreme climatic event in the Pyrenees linked to the PETM, occurred therefore between these two climate events and about 10m above the top of the PETM excursion and is therefore not related to the PETM. Soil and sediments at Esplugafreda area linked to two different weathering processes. During the PETM sediments are enriched with kaolinite from a detrital source due to denudation from the adjacent areas. The paleosols and sediments associated with the ETM2 event formed under semiarid conditions with weak chemical weathering producing high smectite. In contrast, the increased kaolinite content during the PETM reflects increasing precipitation and enhanced erosion of older kaolinite-rich soils and sediments.

REFERENCES

- Cramer B.S., Toggweiler J.R., Wright J.D., Katz M.E. & Miller K.G. (2009) - Ocean overturning since the Late Cretaceous: Inferences from a new benthic foraminiferal isotope compilation. *Paleoceanography* 24, PA4216. doi:10.1029/2008PA001683.
- Retallack G.J., Smith R.M.H. & Ward P.D. (2003) - Vertebrate extinction across the Permian-Triassic boundary in Karoo Basin, South Africa: *Geol. Soc. Am. Bull.*, 115, 1133–1152, doi:10.1130/B25215.1
- Zachos J.C., Pagani M., Sloan L., Thomas E. & Billups, K. (2001). - Trends, rhythms, and aberrations in global climate 65 Ma to present. *Science*, 292, 686–693.

Calcareous nannofossil changes across the Middle Eocene Climatic Optimum from IODP Site U1410 (NW Atlantic): Preliminary results

Claudia Agnini ^(a,b) & Alice Costa ^(a)

^(a) Dipartimento di Geoscienze, Università di Padova, Via G. Gradenigo, 6, 35131, Padova, Italy. E-mail: claudia.agnini@unipd.it

^(b) Department of Geological Sciences, Stockholm University, SE-106 91 Stockholm, Sweden

Document type: Short note.

Manuscript history: received 15 May 2014; accepted 30 May 2014; editorial responsibility and handling by Gerald R. Dickens & Valeria Luciani.

KEY WORDS: calcareous nannofossils, IODP Site U1410, MECO, NW Atlantic.

Overall, sites drilled during Integrated Ocean Drilling Program Expedition 342 recovered Paleogene sedimentary sequences with unusually high deposition rates across a wide range of water depths (Sites U1403– U1411; Norris et al. 2012; 2014). The drilling area is located in the NW Atlantic ocean and can be subdivided into two sub-areas: The J-Anomaly Ridge and the Southeast Newfoundland Ridge (SENR; Fig.1).

Here we present preliminary data on the response of calcareous nannofossils to the Middle Eocene Climatic Optimum (MECO; Bohaty & Zachos, 2003; Bohaty et al., 2009) at Site U1410.

The MECO is a global, relatively long-lasting (ca. 500kyr), warming event occurred at ca 40 Ma that suddenly interrupts and temporary inverts the long-term cooling through the Eocene (Sexton et al. 2006; Bohaty et al., 2009).

Just few data are available on the response of calcareous phytoplankton to this profound change in climate conditions. Actually, calcareous nannofossils are an excellent proxy resource with a number of taxa showing distinct responses to paleoenvironmental change, including to temperature and paleofertility. (e.g.; Toffanin et al., 2011).

In order to further assess the magnitude and world-wide spreading of changes recorded in calcareous nannofossils during the MECO, we have performed quantitative highly resolved calcareous nannofossil assemblage counts.

These results provide at least two kinds of information:

- We improve the bio-magnetostratigraphic framework available for this time interval at Site U1410. This is gained refining shipboard biostratigraphic that are then integrated with magnetostratigraphic results.

- We present a high-resolution study of calcareous nannofossil assemblages. This approach evidences for appearances (Base = B) and disappearances (Top = T) of several species (e.g., B *Dictyococcites bisectus*, B *Sphenolithus obtusus*, T *Sphenolithus furcatolithoides* and T *Sphenolithus spiniger*) as well as important changes in the relative abundance of taxa around the MECO.

Though our results from ODP Site U1410 seem to be in agreement with other low-middle latitude data, some inconsistencies are found if data available from high latitude ODP sites are compared with those from low-middle latitudes (Villa et al., 2008). This indicates that some calcareous nannofossil biohorizons are likely diachronous if low- middle and high latitudes data are compared one to each other (Agnini et al., in press) suggesting that strong paleotemperature gradients are already well developed at that time.

The next and perhaps more interesting step of this research will be to integrate these paleontological data with $\delta^{18}\text{O}$ and $\delta^{13}\text{C}$ records, which might highlight possible relationships, if any, between modifications observed in calcareous nannoflora and changes in geochemical proxies.

REFERENCES

- Agnini C., Fornaciari E., Raffi, I., Catanzariti, R., Pälke, H., Backman J. & Rio D. (in press) - Biozonation and biochronology of Paleogene calcareous nannofossils from low and middle latitudes. *Newsl. Stratigr.*
- Bohaty S.M. & Zachos J.C. (2003) - Significant Southern Ocean warming event in the late middle Eocene. *Geology*, 31(11);1017–1020.
- Bohaty S.M., Zachos J.C., Florindo F. & Delaney M.L. (2009) - Coupled greenhouse warming and deep-sea acidification in the middle Eocene. *Paleoceanography*, 24(2), PA2207.
- Sexton P.F., Wilson P.A. & Norris R.D. (2006) - Testing the Cenozoic multisite composite $\delta^{18}\text{O}$ and $\delta^{13}\text{C}$ curves: New monospecific Eocene records from a single locality, Demerara Rise (Ocean Drilling Program Leg 207), *Paleoceanography*, 21, PA2019.
- Norris R.D., Wilson P.A., Blum P., Fehr A., Agnini C., Bornemann A., Boulila S., Bown P.R., Cournede C., Friedrich O., Kumar Ghosh A., Hollis C.J., Hull P.M., Jo K., Junium C.K., Kaneko M., Liebrand D., Lippert P.C., Liu Z., Matsui H., Moriya K., Nishi H., Opdyke B.N., Penman D.E., Romans B., Scher H.D., Sexton, P.H., Takagi H., Kirtland Turner S., Whiteside J.H., Yamaguchi T. & Yamamoto Y. (2012) - Paleogene Newfoundland sediment drifts. IODP Prel. Rept., 342. doi:10.2204/iodp.pr.342.2012.

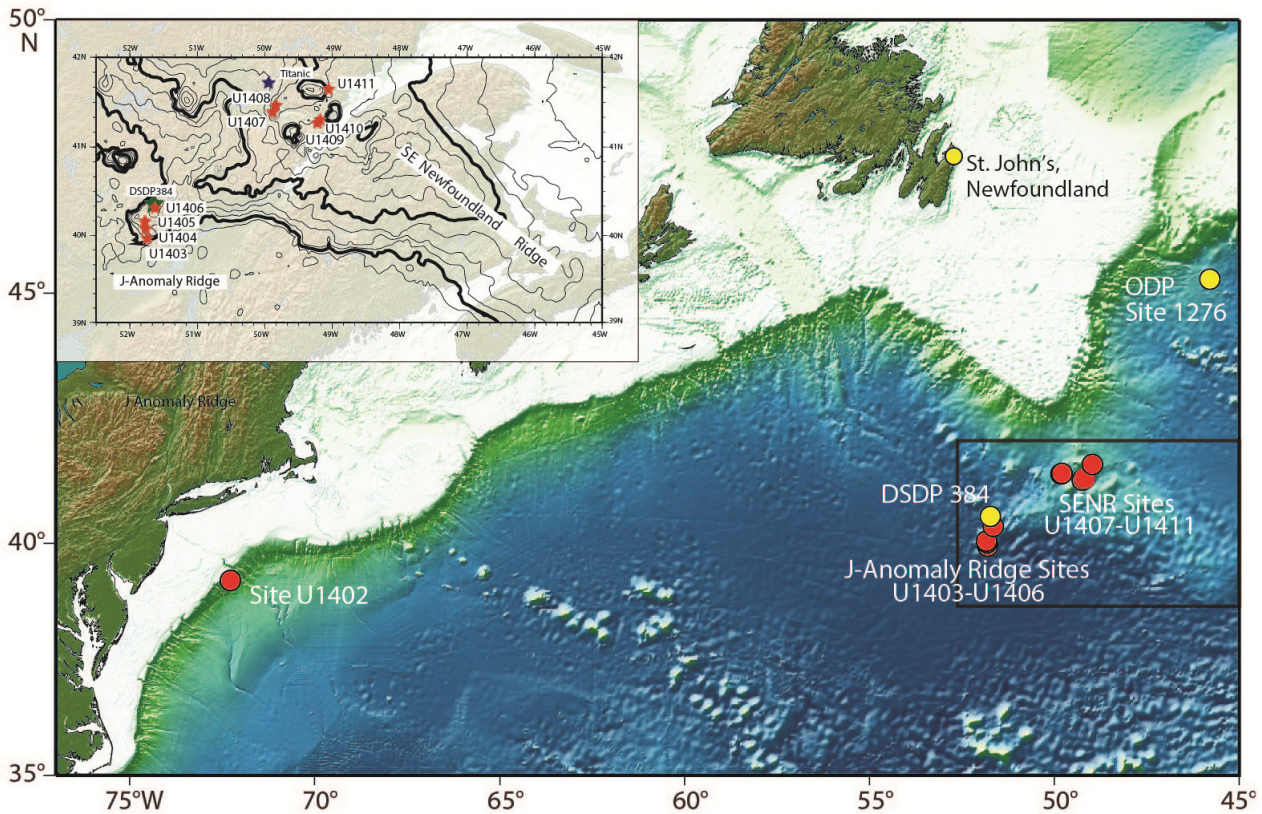


Fig.1 – Operational area of Expedition 342 (modified after Norris et al., 2014).

Norris R.D., Wilson P.A., Blum P., Fehr A., Agnini C., Bornemann A., Boulila S., Bown P.R., Cournede C., Friedrich O., Ghosh A.K., Hollis C.J., Hull P.M., Jo K., Junium C.K., Kaneko M., Liebrand D., Lippert P.C., Liu Z., Matsui H., Moriya K., Nishi H., Opdyke B.N., Penman D.E., Romans B., Scher H.D., Sexton P.H., Takagi H., Kirtland Turner, S.K., Whiteside J.H., Yamaguchi T. & Yamamoto Y. (2014) - Proc. IODP, 342: College Station, TX (Integrated Ocean Drilling Program). doi:10.2204/iodp.proc.342.2014.

Toffanin F., Agnini C., Fornaciari E., Rio D., Giusberti L., Luciani V., Spofforth D.J.A., & Pälke H. (2011) - Changes in calcareous nannofossil assemblages during the Middle Eocene Climatic Optimum: clues from the central-western Tethys (Alano section, NE Italy). *Mar. Micropaleontol.*, 81, 22-31.

Villa G., Fioroni C., Pea L., Bohaty S.M. & Persico D. (2008) - Middle Eocene–late Oligocene climate variability: Calcareous nannofossil response at Kerguelen Plateau, Site 748. *Mar. Micropaleontol.*, 69 (2008) 173–192.

Low to middle latitude Paleogene calcareous nannofossil biozonation and biochronology

Claudia Agnini ^(a), Eliana Fornaciari ^(a), Isabella Raffi ^(b), Rita Catanzariti ^(c), Heiko Pälike ^(d), Jan Backman ^(e) & Domenico Rio ^(a)

^(a)Dipartimento di Geoscienze, Università degli Studi di Padova, via G. Gradenigo 6, 35131 Padova, Italy. E-mail: claudia.agnini@unipd.it

^(b)Dipartimento di Ingegneria e Geologia (InGeo) – CeRSGeo, Università degli Studi “G. d’Annunzio” Chieti-Pescara, via dei Vestini 31, 66013 Chieti-Pescara, Italy

^(c)Istituto di Geoscienze e Georisorse, CNR-Pisa, Via G. Moruzzi, 1– 56124 Pisa, Italy

^(d)Center for Marine Environmental Sciences (MARUM), Bremen University, Leobener 8 Strasse, Bremen, 28359, Germany

^(e)Department of Geological Sciences, Stockholm University, SE-106 91 Stockholm, Sweden

Document type: Short note.

Manuscript history: received 15 May 2014; accepted 30 May 2014; editorial responsibility and handling by Gerald R. Dickens & Valeria Luciani.

KEY WORDS: biochronology, biozonation, calcareous nannofossils, Paleogene.

We have recently published a calcareous nannofossil biozonation for the Paleogene Period (Agnini et al., in press). This scheme is derived from the biostratigraphic methodologies and data we have generated over nearly three decades. Both DSDP/ODP Sites and on-land sections located in the Atlantic and Pacific Oceans and Tethyan regions are analyzed by means of semi-quantitative counting methods to describe the abundance pattern of each biostratigraphically useful calcareous nannofossil taxon.

The new biozonal scheme still partly relies on Martini’s and Okada & Bukry’s biozonations (Martini, 1971; Okada & Bukry, 1980). This in turn implies that we utilize reliable biohorizons previously used by classical biozonal schemes as well as new promising bioevents.

We describe four different types of biohorizons (Base = B; Base common = Bc; T = Top; Top common = Tc), which serve to define five different types of biozones: Base Zone (BZ), Top Zone (TZ), Taxon Range Zone (TRZ), Concurrent Range Zone (CRZ) and Partial Range Zone (PRZ).

The biozone code system used makes reference to that employed in the recent revision of Cenozoic planktonic foraminifera biostratigraphy (Wade et al. 2011), and consists of a code letter to identify the microfossil group (CN = Calcareous Nannofossils), a code letter for each series (P = Paleocene, E = Eocene, O = Oligocene) and a number for each biozone, starting from the base (= biozone 1) of the series.

The biozonation is subdivided into a total of thirty-eight Paleogene biozones:

-11 Paleocene Biozones (CNP1 to CNP11)

-21 Eocene Biozones (CNE1 to CNE21)

-11 Oligocene Biozones (CNO1 to CNO6)

This new Paleogene biozonation has an average duration of

1.1 Myr per biozone, ranging from 0.9 Myr in the Paleocene, to 1.0 Myr in the Eocene, and 1.8 Myr in the Oligocene.

Age estimations for calcareous nannofossils are also provided and they are based on both magnetostratigraphic and astronomically-tuned cyclostratigraphic data (Cande & Kent, 1995, Pälike et al., 2006).

REFERENCES

- Agnini C., Fornaciari E., Raffi, I., Catanzariti, R., Pälike, H., Backman J. & Rio D. (in press) - Biozonation and biochronology of Paleogene calcareous nannofossils from low and middle latitudes. *Newsl. Stratigr.*
- Cande S.C. & Kent D.V. (1995) - Revised calibration of the geomagnetic polarity time scale for the Late Cretaceous and Cenozoic. *J. Geophys. Res.*, 100 (B4), 6093-6096. doi:10.1029/94JB03098.
- Martini E. (1971) - Standard Tertiary and Quaternary calcareous nannoplankton zonation. In: Farinacci, A. (Ed.), *Proceedings 2nd International Conference Planktonic Microfossils Roma: Rome (Ed. Tecnosci.)* 2, 739-785.
- Okada H. & Bukry D. (1980) - Supplementary modification and introduction of code numbers to the low-latitude coccolith biostratigraphic zonation (Bukry, 1973; 1975). *Mar. Micropaleont.*, 5, 321-325.
- Pälike H., Norris R.D., Herrle J.O., Wilson P.A., Coxall H.K., Lear C.H., Shackleton N.J., Tripathi A.K. & Wade B.S. (2006) - The heartbeat of the Oligocene climate system. *Science*, 314, 1894-1898. doi:10.1126/science.1133822.
- Wade B.S., Pearson P.N., Berggren W.A. & Pälike H. (2011) - Review and revision of Cenozoic tropical planktonic foraminiferal biostratigraphy and calibration to the geomagnetic polarity and astronomical time scale. *Earth-Sci. Rev.*, 104, 111-142. doi:10.1016/j.earscirev.2010.09.003.

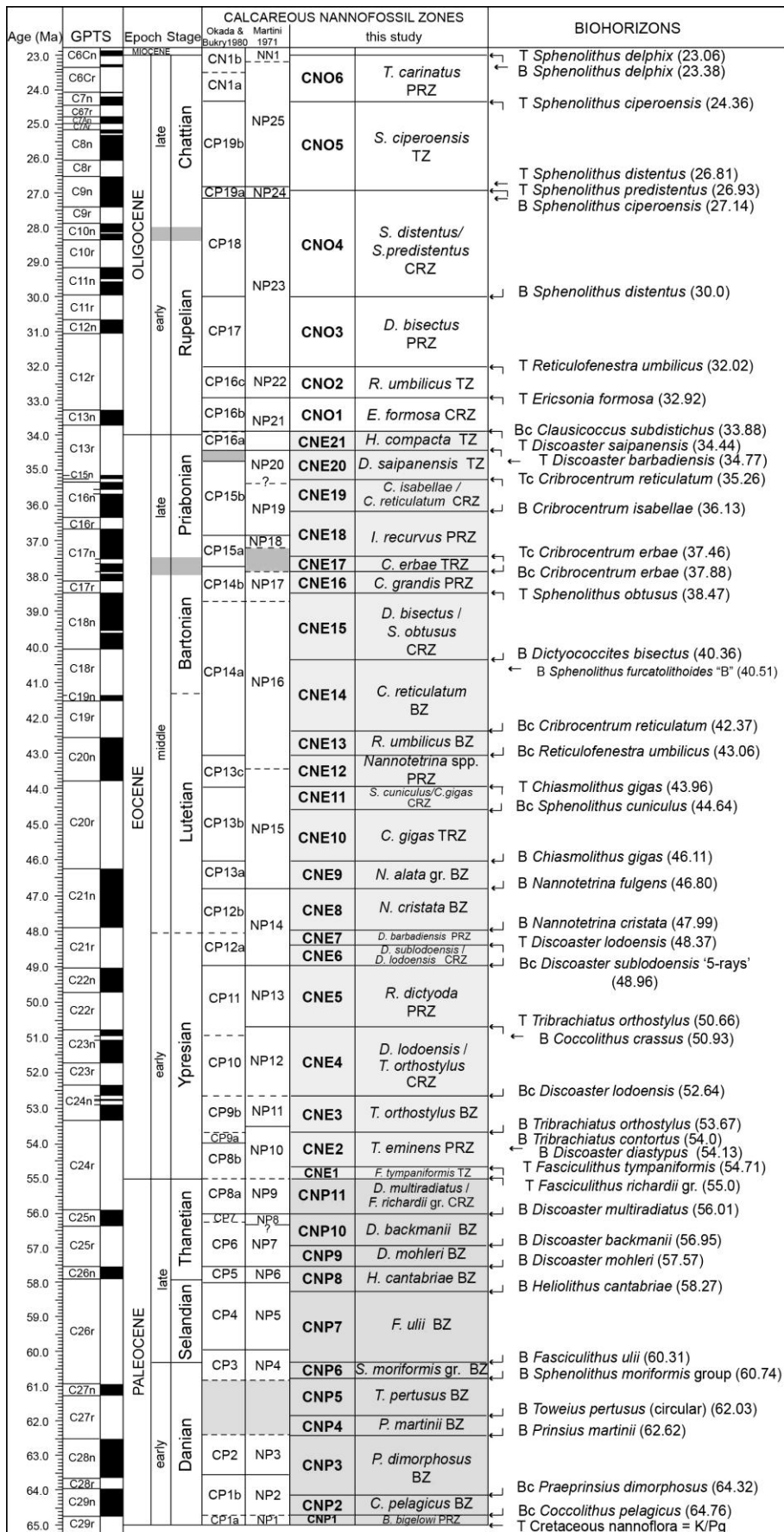


Fig.1 – Paleogene calcareous nannofossil biozonal scheme (modified after Agnini et al., in press).

Calcareous nannofossil response to climatic changes in the early to middle Eocene

Claudia Agnini ^(a), Denise K. Kulhanek ^(b) & Claire L. Shepherd ^(c,d)

^(a) Dipartimento di Geoscienze, Università di Padova, Via G. Gradenigo, 6, 35131, Padova, Italy. E-mail: claudia.agnini@unipd.it

^(b) Integrated Ocean Drilling Program, Texas A&M University, 1000 Discovery Drive, College Station, TX 77845-9547, United States

^(c) School of Geography, Environment and Earth Sciences, Victoria University of Wellington, PO Box 600, Wellington 6140, New Zealand

^(d) GNS Science, 1 Fairway Drive, Avalon 5010, Lower Hutt, New Zealand

Document type: Short note.

Manuscript history: received 15 May 2014; accepted 30 May 2014; editorial responsibility and handling by Gerald R. Dickens & Valeria Luciani.

KEY WORDS: biostratigraphy, calcareous nannofossils, Eocene, paleoecology

The Eocene was a time of incredible changes, being the bridge between greenhouse and icehouse worlds (e.g., Zachos et al., 2001; Cramer et al., 2009). Prominent long- and short-term climate events causing profound perturbations of the physical environment occurred in this interval and played a fundamental role in biosphere evolution.

During the late Paleocene to early Eocene interval, the Earth's climate experienced a long-term warming trend culminating with the so-called Early Eocene Climatic Optimum (EECO), when the maximum temperatures of the entire Cenozoic are recorded. From this point on, a cooling trend observed in proxies for sea temperature is accompanied by a decline in $p\text{CO}_2$ (Lear et al., 2000; Zachos et al., 2001; Pagani et al., 2005; Bijl et al., 2009; Hollis et al., 2012). In addition to this long-term trend, the Paleogene record also reveals the presence of short-lived episodes of global climate change (e.g. the Paleocene Eocene Thermal Maximum, PETM). These events have been the focus of much discussion and study in the last 20 years because they are considered to be, in part at least, analogues of the ongoing global warming.

Associated to these changes of the Earth's climate, the carbon cycling also records long-term (10^5 - 10^6 year scales) trends and short-term (10^3 - 10^4 year scales) transient variations in the exogenic carbon pool (Zachos et al., 2001; Cramer et al., 2009).

An essential prerequisite to understand the mode and tempo as well as the cause and consequences of the Paleogene Earth's climate evolution is the creation of a firm chronologic framework that needs the most updated and highly resolved bio-magnetostratigraphic datasets to be constructed. Calcareous plankton in general and calcareous nannofossils in particular have proved to be extremely useful both in biostratigraphy and paleoecology. Calcareous nannoplankton have been one of the main primary producers in the oceans since Mesozoic, when they first appeared (Bown et al., 2004). They are usually abundant in the geological record, have a widespread

distribution and show a rapid evolution. These are all hallmarks for good biostratigraphic and paleoecologic tools.

Recently, Agnini et al. (in press) have proposed a new calcareous nannofossil biozonal scheme. This is the first step to comprehensively examine how this microfossil group has evolved through the Paleogene time.

The next step will be to integrate high-resolution paleoclimatic proxies, such as $\delta^{18}\text{O}$ and $\delta^{13}\text{C}$ (and others), with paleontological data from different sites/sections with the aim to highlight spatial and/or temporal relationships between global changes in the physical environments and modifications of calcareous nannofossil assemblages.

Available data suggest that the early Eocene was a unique time because of the subdued latitudinal gradients. Most calcareous nannofossil taxa, even "warm" taxa, appear to have thrived in high latitudes and thus support evidence from geochemical proxies for polar amplification of temperature during periods of pronounced global warmth (e.g. Bijl et al., 2009; Hollis et al., 2012). Something changed in the late early Eocene when high latitudes started to become a distinct paleobiogeographic domain. During this time, calcareous nannofossil assemblages went through a fundamental change with the first appearance of taxa that are dominant in the modern ocean (*Reticulofenestra*, *Dictyococcites*; Agnini et al., 2006) and the progressive disappearance of "warm" taxa from high-latitudes.

We still lack a full understanding of how geosphere and biosphere interact, especially during times of profound alteration of global background conditions (e.g., hyperthermals such as the PETM). An indispensable tool to understanding this interaction is the correlation and comparison of high-resolution quantitative microfossil datasets from different depositional settings and geographic locations.

REFERENCES

Agnini C., Muttoni G., Kent D.V. & Rio D. (2006) - Eocene biostratigraphy and magnetic stratigraphy from Possagno, Italy: The calcareous nannofossil response to climate variability. *Earth Planet. Sci. Lett.*, 241, 815- 830.

- Agnini C., Fornaciari E., Raffi I., Catanzariti R., Pälike H., Backman J. & Rio D., in press. Biozonation and biochronology of Paleogene calcareous nannofossils from low and middle latitudes. *Newsl. Stratigr.*
- Bijl P.K., Schouten S., Sluijs A., Reichart G.-J., Zachos J.C. & Brinkhuis H. (2009) - Early Palaeogene temperature evolution of the southwest Pacific Ocean. *Nature*, 461, 776-779.
- Bown P.R., Lees J.A. & Young, J.R. (2004) - Calcareous nannoplankton evolution and diversity through time. In: Thierstein H.R & Young J.R. (eds.), *Coccolithophores - From molecular processes to global impact*, Springer, Berlin, 481-508.
- Cramer B.S., Toggweiler J.R., Wright J.D., Katz M. E. & Miller K.G. (2009) - Ocean overturning since the Late Cretaceous: Inferences from a new benthic foraminiferal isotope compilation. *Paleoceanography*, 24, PA4216.
- Hollis C.J., Taylor K.W.T., Handley L., Pancost R.D., Huber M., Creech J., Hines, B.R., Crouch E.M., Morgans H.E.G., Crampton J.S., Gibbs S., Pearson P. & Zachos J.C. (2012) - Early Paleogene temperature history of the Southwest Pacific Ocean: reconciling proxies and models. *Earth Planet. Sci. Lett.*, 349-350, 53-66.
- Lear C.H., Elderfield H. & Wilson P.A. (2000) - Cenozoic Deep-Sea Temperatures and Global Ice Volumes from Mg/Ca in Benthic Foraminiferal Calcite. *Science*, 287, 269-272.
- Pagani M., Zachos J.C., Freeman K.H., Tipple B. & Bohaty S.M. (2005) - Marked Decline in Atmospheric Carbon Dioxide Concentrations During the Paleogene. *Science*, 309, 600-603.
- Zachos J.C., Pagani M., Sloan L., Thomas E. & Billups K. (2001) - Trends, rhythms and aberrations in global climate 65 Ma to present. *Science*, 292, 686-693.

Investigating the evolution of the late Palaeogene carbon cycle using biogeochemical modelling and analysis

David Armstrong M^cKay ^(a), Toby Tyrrell ^(a) & Paul A. Wilson ^(a)

^(a) Ocean and Earth Science, University of Southampton, National Oceanography Centre Southampton, European Way, Southampton, England, United Kingdom, SO14 3ZY.

E-mail: D.Armstrong-Mckay@noc.soton.ac.uk

Document type: Short note.

Manuscript history: received 15 May 2014; accepted 30 May 2014; editorial responsibility and handling by Gerald R. Dickens & Valeria Luciani.

KEY WORDS: Eocene-Oligocene Transition, Biogeochemical modelling, Carbonate Compensation Depth, Carbon cycle, late Palaeogene

During the late Palaeogene the Earth's climate shifted from a 'Greenhouse' to 'Icehouse' state, with a major episode of Antarctic glaciation and global cooling occurring at the Eocene-Oligocene Transition (EOT) ~34 million years ago. As illustrated in Figure 1, palaeorecords indicate that during the late Eocene global temperatures were high enough to prevent significant ice sheet formation, atmospheric CO₂ was above ~750 ppm and the carbonate compensation depth (CCD) fluctuated between ~3.5 and 4.0 km and features significant carbonate accumulation events, whereas in the Oligocene global temperatures were low enough for large ice sheets to remain stable on Antarctica, atmospheric CO₂ concentrations fell below 750 ppm and the CCD stabilised at about 4.5 km (Beerling & Royer, 2011; Zachos et al., 2008; Pälike et al., 2012). Across the EOT itself these palaeorecords reveal two steps of rapid cooling and ice growth across the EOT along with a temporary ~1 ‰ positive excursion in benthic δ¹³C and a permanent ~500 m deepening of the CCD (Lear et al., 2008; Coxall and Wilson, 2011). Although the global cooling and the glaciation of the Antarctic across the EOT is likely to be the result of a climate threshold response to the falling concentration of atmospheric CO₂, the processes that drove the EOT carbon cycle perturbation and the longer term trends in the CCD and δ¹³C palaeorecords are debated. Investigating how the carbon cycle changed during the late Palaeogene is therefore crucial in understanding the differences between the Palaeogene and the Neogene Earth system.

Several different hypotheses have been advanced as to what drove the EOT carbon cycle perturbation. Previous biogeochemical modelling has demonstrated that a shift in carbonate burial from shallow shelf seas to deep ocean basins as a result of falling sea-level results in the required permanent CCD deepening and a temporary increase in δ¹³C (Merico et al., 2008). However, other studies have suggested that sea-level did not fall enough to cause the observed CCD deepening through this mechanism, and instead suggest that increased

ocean mixing could deepen the CCD through deep ocean ventilation while the benthic δ¹³C perturbation was driven by increased organic carbon burial (Zachos and Kump, 2005; Miller et al., 2009). Another hypothesis is that an increase in the ocean calcium ion concentration due to increased Antarctic weathering resulted in an increase in CaCO₃ burial and thus a deepening of the CCD (Rea and Lyle, 2005). Furthermore, the growth of permafrost and methane hydrate coverage due to pre-EOT cooling (DeConto et al., 2012) and the subsequent impact of Antarctic ice sheet growth on these potentially large stores of carbon could also have had a significant impact on the late Palaeogene carbon cycle, but this impact has not yet been fully investigated or quantified.

To investigate the relative importance of the different processes proposed to drive the EOT carbon cycle perturbation we use model simulations to determine the magnitude of change necessary for each process to reproduce the observed patterns in the benthic δ¹³C and CCD palaeorecords and then evaluate the feasibility of these scenarios. We use the biogeochemical box model first used by Merico et al. (2008) which comprises of a simple 3-box global ocean and 1-box atmosphere and includes all the major fluxes and processes in the carbon, phosphorus and silica cycles, including the carbonate system, air-sea gas exchange, the organic matter pump, CO₂ drawdown by silicate weathering, calcium carbonate formation and cycling, and carbon isotopes. We investigate the following hypothesised causes of the EOT carbon cycle perturbation: 1) increased ocean ventilation, 2) a global shift from shallow to deep ocean carbonate burial, 3) permafrost soil carbon inventory changes, 4) increased ocean calcium ion concentration, and 5) decreased rain ratio of carbonate to organic carbon export. We will present the full results of this modelling at the Climatic and Biotic Events of the Paleogene 2014 meeting.

We will also present the preliminary results of further numerical analysis of the link between changes in sea level and the CCD over the Cenozoic. This analysis will quantify the impact of the shelf-basin fractionation of carbonate burial on the CCD and indicate what other drivers of CCD change are required during the Cenozoic, which will in turn further reveal

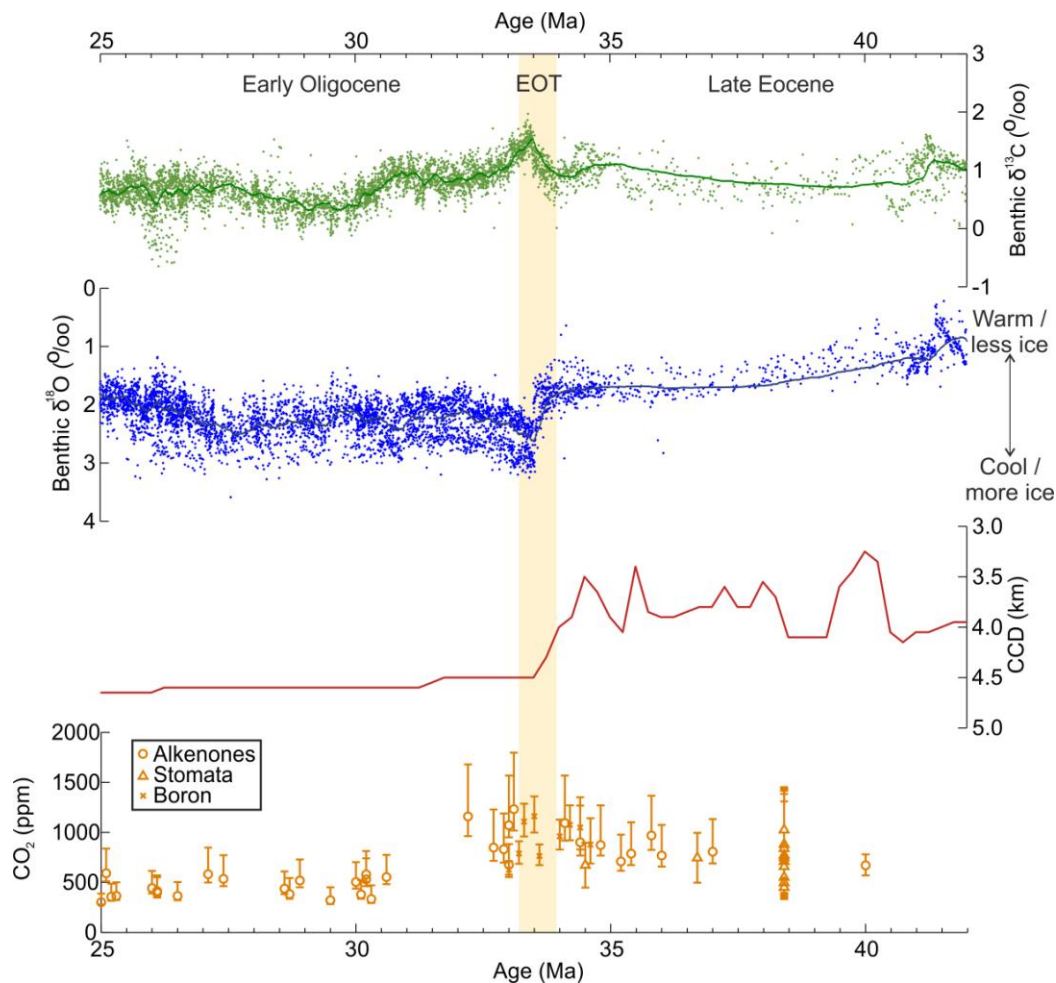


Fig.1 – Palaeorecords between 25 and 42 Ma illustrating the benthic $\delta^{13}\text{C}$ perturbation at the EOT and the shifts in baseline benthic $\delta^{18}\text{O}$ (Zachos et al, 2008), CCD (Pälike et al, 2012) and atmospheric CO_2 (Beerling & Royer, 2011) between the Late Eocene and the Early Oligocene. The yellow bar illustrates the duration of the EOT, the 100-point moving averages of the benthic $\delta^{13}\text{C}$ and $\delta^{18}\text{O}$ data are plotted as thick lines in the top two panels and the method of atmospheric CO_2 reconstruction and the associated error bars are shown in the bottom panel.

the differences in the state of the carbon cycle between the Palaeogene and Neogene. In particular we will attempt to address the key question of why the EOT appears to be a fairly unique event during the Cenozoic and why other sea-level fluctuations and changes in ocean dynamics did not also result in CCD deepening as significant and as permanent as at the EOT.

REFERENCES

- Beerling D.J. & Royer D.L. (2011) - Convergent Cenozoic CO_2 history. *Nat. Geosci.* 4, 418–420.
- Coxall H.K. & Wilson P.A. (2011) - Early Oligocene glaciation and productivity in the eastern equatorial Pacific: Insights into global carbon cycling. *Paleoceanography*, 26, PA2221, 1–18.
- DeConto R.M., Galeotti S., Pagani M., Tracy D., Schaefer K., Zhang T., Pollard D. & Beerling D.J. (2012) - Past extreme warming events linked to massive carbon release from thawing permafrost. *Nature*, 484, 7392, 87–91.
- Lear C.H., Bailey T.R., Pearson P.N., Coxall H.K. & Rosenthal Y. (2008) - Cooling and ice growth across the Eocene-Oligocene transition. *Geology*, 36, 3, 251.
- Merico A., Tyrrell T. & Wilson P.A. (2008) - Eocene/Oligocene ocean de-acidification linked to Antarctic glaciation by sea-level fall. *Nature*, 452, 7190, 979–82.
- Miller K.G., Wright J.D., Katz M.E., Wade B.S., Browning J.V. & Cramer B.S. (2009) - Climate threshold at the Eocene-Oligocene transition: Antarctic ice sheet influence on ocean circulation. In: *The Late Eocene Earth—Hothouse, Icehouse, and Impacts: Geological Society of America Special Paper 452*. The Geological Society of America, Boulder, CO.
- Pälike H., Lyle M.W., Nishi H. et al. (2012) - A Cenozoic record of the equatorial Pacific carbonate compensation depth. *Nature*, 488, 7413, 609–614.
- Rea D.K. & Lyle M.W. (2005) - Paleogene calcite compensation depth in the eastern subtropical Pacific: Answers and questions. *Paleoceanography*, 20, PA1012.
- Zachos J. & Kump L. (2005) - Carbon cycle feedbacks and the initiation of Antarctic glaciation in the earliest Oligocene. *Global and Planetary Change*, 47, 1, 51–66.
- Zachos J.C., Dickens G.R. & Zeebe R.E. (2008) - An early Cenozoic perspective on greenhouse warming and carbon-cycle dynamics. *Nature*, 451, 279–83.

Response of benthic foraminiferal assemblages to early Eocene hyperthermal events

Gabriela de Jesús Arreguín-Rodríguez ^(a), Laia Alegret ^(a,b) & Ellen Thomas ^(c,d)

^(a) Departamento de Ciencias de la Tierra, Universidad de Zaragoza, Pedro Cerbuna, 12, 50009, Zaragoza, Spain. E-mail: gjarreguin@gmail.com

^(b) IUCA, Universidad de Zaragoza, Zaragoza, Spain

^(c) Department of Geology and Geophysics, Yale University, New Haven CT, USA

^(d) Department of Earth and Environment Sciences, Wesleyan University, Middletown CT, USA

Document type: Short note.

Manuscript history: received 15 May 2014; accepted 30 May 2014; editorial responsibility and handling by Gerald R. Dickens & Valeria Luciani.

KEY WORDS: benthic foraminifera, environmental reconstruction, hyperthermal events.

The early-middle Paleogene was characterized by a globally warm climate, on which short-lived extreme-warming events (hyperthermals) were superimposed (Thomas & Zachos, 2000). The most extreme hyperthermal was the Paleocene-Eocene Thermal Maximum (PETM, 55.8 Ma). The combination of global warming, a negative carbon isotope excursion (CIE), and carbonate dissolution in the deep-sea indicates that hyperthermals were associated with large inputs of ¹³C-depleted carbon into the ocean-atmosphere system. During hyperthermals, the intensity of continental weathering and the activity of the hydrological cycle increased, and global ecosystems were perturbed. Early Eocene hyperthermals were seemingly similar to the PETM, but of lesser magnitude. This includes changes in benthic foraminifera, which were not as severe as the extinction that occurred during the PETM (Thomas, 2007). In order to understand the response of benthic foraminifera to hyperthermal events of different magnitude and in different settings, we analyzed lower Eocene assemblages at North Atlantic DSDP Site 550, and equatorial Pacific ODP Site 865.

Lower Eocene sediments from DSDP Site 550 (Porcupine Abyssal Plain) consist of brownish and grayish marly nannofossil chalk deposited at a present water depth of >4400 m (paleodepth ~3800 m; Greene et al., 2014), with highly variable carbonate content (30-60%, Graciansky et al., 1985). Eocene Thermal Maximum-2 (ETM2, or H1 or Elmo, 53.7 Ma) and the H2 event (53.6 Ma) are represented at this site. At ODP Site 865 on Allison Guyot, pale yellow-white foraminiferal-nannofossil ooze and chalk were deposited at a present water depth of 1518 m (paleodepth ~1300-1500 m; Bralower et al., 1995), with high carbonate content (92-98%, Sager et al., 1993). Eocene Thermal Maximum-3 (ETM3, X or K event, 52.5 Ma) is recognized at Site 865, which occurred 1.2 and 1.1 My after the ETM2 and H2 respectively; however, these events are not represented at Site 865, probably due to the low sedimentation rates.

At Site 550, assemblages are diverse (Fisher- α values = 11-20; 38 to 57 species per sample) and dominated by calcareous taxa (>90-96% of the assemblages) except in intervals of carbonate dissolution. They consist of mixed infaunal and epifaunal morphogroups, with epifaunal taxa (e.g., *Abyssamina poagi*, *Nuttallides truempyi*, *Cibicidoides micrus*, *Gyroidinoides depressus*, *Osangularia* sp.) making up 35-61% of the assemblages. Bolivinids (mainly *Bolivinooides decoratus*) dominate among infaunal morphogroups, with common occurrence of other infaunal taxa such as *Globocassidulina subglobosa*, *Oridorsalis umbonatus*, *Pullenia jarvisi*, *Quadriformina profunda*, *Tappanina selmensis* and *Turrilina brevispira*. Cylindrical uniserial taxa and buliminids are scarce throughout the studied interval, making up less than 5% of the assemblages. Diversity of the assemblages decreased during ETM2 and H2, although not to below background values. Very few benthic foraminifera were found within the interval of ETM2, although samples from its lower and upper part contain abundant foraminifera and provide information on the assemblage turnover across this event. Both hyperthermal events display a similar faunal turnover, with decreased percentages of *B. decoratus*, *N. truempyi*, *C. micrus* and *Q. profunda*, and increased relative abundance of *Gl. subglobosa* and *G. depressus*. The agglutinated species *Repmanina charoides*, *Glomospirella* sp., and the calcareous *Pyramidina rudita* peak in abundance during both events, but data from ETM2 may not be representative because of the small number of specimens.

The co-occurrence of mixed assemblages and the high relative abundance of *N. truempyi* suggest meso-oligotrophic conditions at the seafloor during the early Eocene. The decrease in relative abundance of bolivinids during the ETM2 and H2 events may indicate a weaker supply of labile and an increased input of refractory organic matter. The nutrient supply to the seafloor may have been sufficient to sustain both infaunal and epifaunal niches, with some taxa (e.g., *Repmanina charoides* and *Glomospirella* sp.) taking advantage of the enhanced input of refractory organic matter (Arreguín-Rodríguez et al., 2013), whereas *Gl. subglobosa* may indicate well-oxygenated bottom waters (Martins et al., 2007).

At Site 865, assemblages are diverse (Fisher- α values = 9-23; 32-58 species per sample) and dominated by calcareous taxa (>90% of the assemblages). The percentage of infaunal morphogroups is unusually high (51-89%), dominated by cylindrical uniserial taxa (mainly stilostomellids) and with common buliminids. *N. truempyi* dominates among epifaunal taxa, with common *Cibicidoides* spp., *Hanzawaia ammophila* and *N. umbonifera*. Diversity and heterogeneity of the assemblages slightly decreased during ETM3, recovering immediately after the event. The percentage of *O. umbonatus* and *A. aragonensis* increased, and the percentage of bolivinids slightly decreased during ETM3. Cylindrical uniserial taxa, bolivinids, buliminids, *Gl. subglobosa*, *N. umbonifera*, *P. rudita* and *Cibicidoides* spp. peaked immediately after the event. The high relative abundance of *N. truempyi* at Site 865 points to oligotrophic seafloor conditions. Little is known about the ecology of the extinct cylindrical taxa, but the abundant stilostomellids at this site may reflect the interaction between food supply and current activity over the top of Allison guyot. The increased abundance of *A. aragonensis* during ETM3 is interpreted as opportunistic proliferation during hyperthermals, as at other locations. Assemblage changes immediately after the ETM3 include a sharp decrease in %*N. truempyi* and peak abundance of stilostomellids, *P. rudita* and *Gl. subglobosa* suggest an enhanced food supply to the seafloor. The increased abundance of *P. rudita*, a species most common at intermediate paleodepths (Tjalsma & Lohmann, 1983), is consistent with an enhanced food supply to the seafloor. The peak abundance of *N. umbonifera* (up to >6%) and of agglutinated taxa (up to >7%) in the same interval may suggest slightly corrosive bottom waters. Higher CaCO₃ saturation in the pore waters might account for the high abundance of infaunal taxa, although we found no evidence for dissolution of epifaunal calcareous tests.

Study of three hyperthermal events at Sites 865 and 550 allowed us to identify species-specific responses:

- *Gl. subglobosa* and *P. rudita* increased in relative abundance across the studied hyperthermal events.
- *N. truempyi* and bolivinids decreased in abundance.
- *A. aragonensis* peaked during ETM3 at Site 865, as across other hyperthermal events (e.g., PETM) at other locations, but is very rare at Site 550, probably due to the greater paleodepth.
- *R. charoides* and *Glomospirella* spp. peaked across the ETM2 and H2 events at Site 550, as at many other locations in the NE Atlantic and Tethys Oceans across the PETM (Arreguín-Rodríguez et al., 2013), but have not been recorded at Site 865. This may be related to the paleogeographical location of this site, far from continental

margins and slopes and with a small input of refractory organic matter, consistent with the scarcity of bolivinids at Site 865.

Further analyses of benthic foraminiferal assemblages should be integrated in multi-disciplinary studies to evaluate the species-specific response of benthic taxa to hyperthermal events, and their relation to different paleoenvironmental parameters.

REFERENCES

- Arreguín-Rodríguez G.J., Alegret L. & Ortiz S. (2013) - *Glomospira acme* during the Paleocene-Eocene Thermal Maximum: response to CaCO₃ dissolution or to ecological forces? *J. Foramin. Res.*, 43, 40-54.
- Bralower T.J., Zachos J.C., Thomas E., Parrow M., Paull C.K., Kelly D.C., Premoli Silva I., Sliter W.V. & Lohmann, K.C. (1995) - Late Paleocene to Eocene paleoceanography of the equatorial Pacific Ocean: stable isotopes recorded at Ocean Drilling Program Site 865, Allison Guyot. *Paleoceanography*, 10, 841-865.
- de Graciansky P.C., Poag C.W., et al. (1985) - Initial reports Deep Sea Drilling Project 80: Washington D.C., U.S. Government Printing Office.
- Greene S.E., Ridgwell A.J., Kirtland Turner S., Schmidt D.N., Pälike H. & Thomas E. (2014) - Long-term stability of the carbonate compensation depth across the Late Paleocene-Early Eocene warming trend. In: Goldschmidt Conference 2014, Abstract volume, June 8-13, Sacramento, CA.
- Martins V., Dubert J., Jouanneau J.M., Webber O., Ferreira E., Patinha C., Alveirinho J.M. & Rocha F. (2007) - A multiproxy approach of the Holocene evolution of shelf-slope circulation on the NW Iberian Continental Shelf. *Mar. Geol.*, 239, 1-18.
- Sager W.W., Winterer E.L., Firth J.V. et al. (1993) - Site 865. In: Sager, W.W., Winterer, E.L., Firth, J.V., et al. *Proceedings of the Ocean Drilling Program, Initial Reports*, 143, 111-180.
- Thomas E. (2007) - Cenozoic mass extinctions in the deep sea: What perturbs the largest habitat on Earth? In: Monechi, S., Coccioni, R. & Rampino, M.R. (eds.), *Large ecosystem perturbations: causes and consequences*. Geological Society of America Special Paper, 424, 1-23.
- Thomas E. & Zachos J.C. (2000) - Was the late Paleocene thermal maximum a unique event? *Geologiska Föreningens i Stockholm Föreläsningar*, 122, 169-170.
- Tjalsma R.C. & Lohmann G.P. (1983) - Paleocene-Eocene bathyal and abyssal benthic foraminifera from the Atlantic Ocean. *Micropaleontology Special Publication*, 4, 89 pp.

Are agglutinated benthic foraminifera affected by CaCO₃ dissolution? Experiments across the Paleocene-Eocene boundary

Gabriela de Jesús Arreguín-Rodríguez ^(a) & Laia Alegret ^(a,b)

^(a) Departamento de Ciencias de la Tierra, Universidad de Zaragoza, Pedro Cerbuna, 12, 50009, Zaragoza, Spain. E-mail: gjarreguin@gmail.com

^(b) IUCA, Universidad de Zaragoza, Zaragoza, Spain

Document type: Short note.

Manuscript history: received 15 May 2014; accepted 30 May 2014; editorial responsibility and handling by Gerald R. Dickens & Valeria Luciani.

KEY WORDS: Agglutinated foraminifera, CaCO₃ dissolution, extinction, Paleocene-Eocene.

Ocean acidification has been invoked as one of the potential mechanisms that may have triggered the extinction of up to 50% of deep-sea benthic foraminiferal species during the Paleocene Eocene Thermal Maximum, PETM (Thomas, 2007; Alegret et al., 2009). Shoaling of the carbonate compensation depth & lysocline led to widespread but heterogeneous CaCO₃ dissolution in deep-sea sediments, with only a small decrease in CaCO₃ content in some basins (e.g., Zeebe & Zachos, 2007). In contrast, benthic foraminiferal extinction was global.

Regardless of this controversy, one may argue that CaCO₃ dissolution clearly affected benthic foraminifera with calcareous tests (although many calcareous species did not go extinct across the PETM; Alegret et al., 2009; 2010). As for agglutinated benthic foraminifera, some of which went extinct while others did not, the question remains: what were their shells made of? Some species may have agglutinated calcareous particles, and these were affected by CaCO₃ dissolution. Others may have produced calcareous cement (as opposed to organic cement) to agglutinate particles, whatever their composition. In addition, diagenesis may have played a major role during fossilization, modifying the mineralogical composition of the cement and/or the agglutinated particles.

In order to assess the susceptibility of fossil agglutinated benthic foraminiferal shells to CaCO₃ dissolution, we carried out dissolution experiments on several agglutinated species (>100 µm) from the Zumaia section (Spain), including species that went extinct during the PETM, species that locally disappeared and others that survived across the event (Alegret et al., 2009). The specimens were exposed to acetic acid (CH₃COOH; pH=3.5) during several time intervals (e.g., 30 min, 2.5 hrs., 24 hrs, etc.) depending on their response, reaching up to >5300 hours for a single specimen (Fig. 1). The preservation state of the tests was checked at different times during the experiments, assigning numerical values based on the absolute preservation scale (APS) proposed by Nguyen et al. (2009). This scale considers the degree of destruction of the

test: the 8 value refers to intact specimens, value 4 indicates that 55-70% of the test is preserved, and number 1 corresponds to the complete dissolution and disintegration of the test.

The results of the experiments show that most of the species that were not susceptible or only slightly susceptible to dissolution survived across the PETM, as expected (Fig. 1). Taxa that went extinct or locally disappeared across the PETM showed medium to high susceptibility (Fig. 1), showing that most of them have calcareous cement and/or calcareous particles in their fossil shells. However, some extinct species (*Dorothia cylindracea*) or species that locally disappeared at Zumaia (*Spiroplectammina spectabilis*, *Haplophragmoides walteri*) show low susceptibility to dissolution (high APS values), suggesting that CaCO₃ dissolution was not the only environmental parameter that perturbed the benthic habitat, as it does not account for the disappearance of species with high APS values.

Marked differences in reaction time of taxa affected by dissolution were also observed. Some species reached very low APS indices during the first 2.5 hours of acid exposure, while other taxa displayed a more gradual corrosion of their tests (Fig. 1). This may be related to the size, wall thickness and/or amount of cement in the test, with juvenile specimens reacting faster than adult ones (e.g., *Clavulinoides*; Fig. 1). Additionally, diagenetic replacement of the test may have influenced reaction velocity in our experiments. For instance, the cement of *Remesella varians* is calcareous but it is frequently silicified (Loeblich & Tappan, 1988). Furthermore, *D. cylindracea* forms its test by agglutinating calcareous particles (Loeblich & Tappan, 1988), but its APS index is high. It is suggested that mineralogical replacement of the test during diagenesis, or the characteristic protein coating of this species (Loeblich & Tappan, 1988), may have protected it from dissolution in our experiments.

In conclusion, our results demonstrate that most of the agglutinated benthic foraminifera with low susceptibility to dissolution survived across the PETM. Nonetheless, the fact that some species that went extinct or locally disappeared are resistant to dissolution suggests that other factors may have perturbed the benthic assemblages.

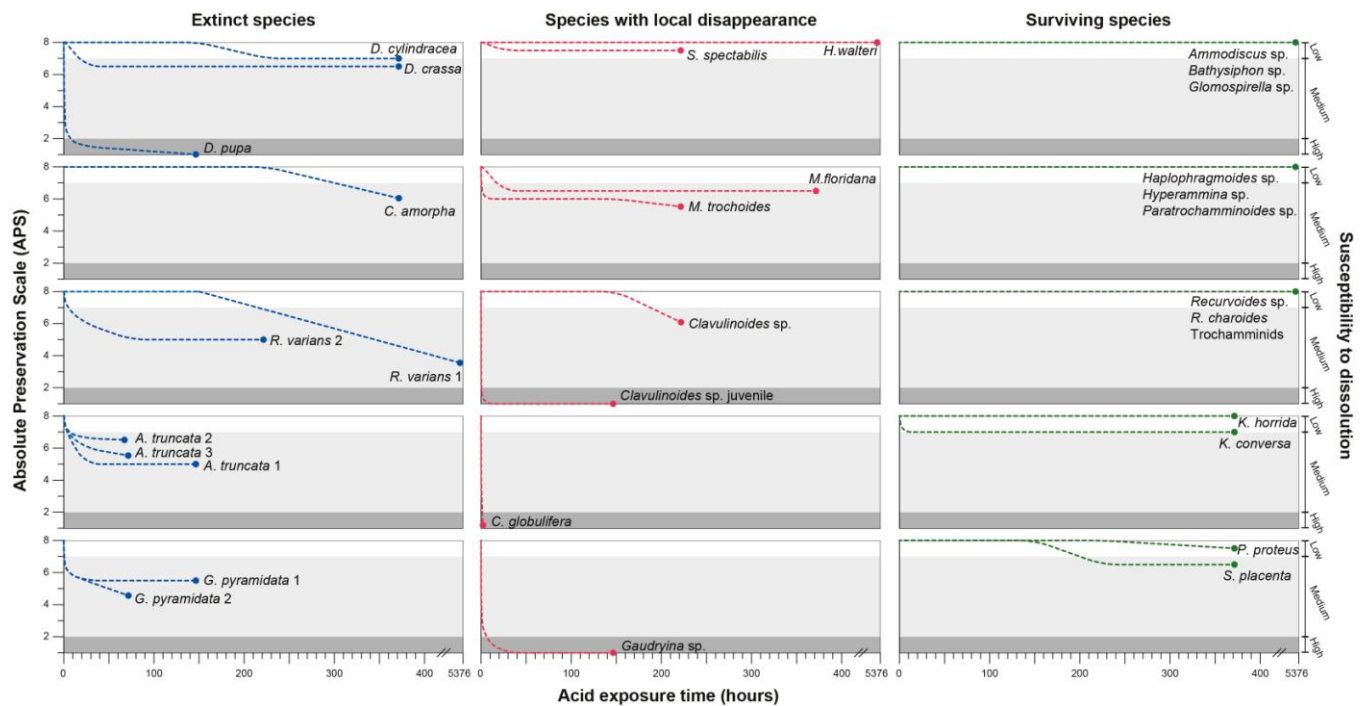


Fig.1 – Absolute Preservation Scale (APS) showing the exposure time to acetic acid. The Y axis (right) shows the susceptibility degree based on APS values (high susceptibility = APS 1-2, medium susceptibility = APS 2-7 and low susceptibility = APS 7-8).

REFERENCES

- Alegret L., Ortiz S., Orue-Etxebarria X., Bernaola G., Baceta J.I., Monechi S., Apellaniz E. & Pujalte V. (2009) - The Paleocene-Eocene Thermal Maximum: New data on microfossil turnover at Zumaia section, Spain. *Palaios*, 24, 318-328.
- Alegret L., Ortiz S., Arenillas I. & Molina E. (2010) - What happens when the ocean is overheated? The foraminiferal response across the Paleocene-Eocene Thermal Maximum at the Alamedilla section (Spain). *Geol. Soc. Am. Bull.*, 122 (9/10), 1616-1624.
- Loeblich A.R. & Tappan H. (1988) - Foraminifera genera and their classification. Van Nostrand Reinhold Company Inc., New York, 970 pp.
- Nguyen T.M.P., Petrizzo M.R. & Speijer R.P. (2009) - Experimental dissolution of a fossil foraminiferal assemblage (Paleocene-Eocene Thermal Maximum, Dababiya, Egypt): Implications for paleoenvironmental reconstructions. *Mar. Micropaleont.*, 73, 241-258.
- Thomas E. (2007) - Cenozoic mass extinctions in the deep sea: what disturbs the largest habitat on Earth? In: Monechi, S., Coccioni, R. & Rampino, M. (eds.), *Large ecosystems perturbations: causes and consequences*. Geological Society of America Special Paper, 424, 1-24.
- Zeebe R.E. & Zachos J.C. (2007) - Reversed deep-sea carbonate ion basin gradient during Paleocene–Eocene thermal maximum. *Paleoceanography*, 22, PA3201, doi: 10.1029/2006PA001395.

***n*-Alkane PETM records from the Bighorn Basin, Wyoming: A core-outcrop comparison**

Allison A. Baczynski ^(a), Francesca A. McInerney ^(b), Scott L. Wing ^(c) & the BBCP Science Team ^(d)

^(a) Department of Earth and Planetary Sciences, Northwestern University, Evanston, IL 60208. E-mail: allie.baczynski@gmail.com

^(b) Sprigg Geobiology Centre, Environment Institute and School of Earth and Environmental Sciences, University of Adelaide, Adelaide, SA 5005, Australia

^(c) Department of Paleobiology, Smithsonian Institution National Museum of Natural History, NHB MRC 121 P.O. Box 37012, Washington, DC 20013

^(d) Bighorn Basin Coring Project Science Team – See <http://earth.unh.edu/clyde/team.shtml> for full list

Document type: Short note.

Manuscript history: received 15 May 2014; accepted 30 May 2014; editorial responsibility and handling by Gerald R. Dickens & Valeria Luciani.

KEY WORDS: Bighorn Basin, carbon isotopes, Continental Scientific Drilling, Eocene, *n*-alkanes, organic carbon, Paleocene, PETM.

The Bighorn Basin Coring Project (BBCP) drilled two over-lapping cores at three locations in the Bighorn Basin, Wyoming (Basin Substation, Polecat Bench, and Gilmore Hill) during the summer of 2011. The Bighorn Basin preserves an unusually complete continental stratigraphic record of early Paleogene floodplain strata and has been the site of extensive paleontological, sedimentological, and geochemical research. The drill sites targeted three early Paleogene extreme global warming events, known as hyperthermals, in an effort to better understand how the earth system responds to rapid perturbations to the global carbon cycle. These complete (>98% core recovery), unweathered cores represent the first terrestrial sedimentary cores through early Paleogene hyperthermals and will allow us to produce integrated proxy records at unprecedented stratigraphic resolution. Here we present initial *n*-alkane results from the Basin Substation site in the eastern Bighorn Basin, which targeted the Paleocene-Eocene Thermal Maximum (PETM), the largest and best-studied Paleogene hyperthermal.

High molecular weight, odd-carbon numbered *n*-alkanes, biomarkers indicative of vascular plants, have been extracted and isolated from 114 samples from Basin Substation core 1B. Only 51 samples contain measureable quantities of *n*-alkanes, and *n*-alkane preservation varies strongly with lithology (Fig. 1). Carbonaceous shale and laminated mudstone have higher abundances of *n*-alkanes than massive mudstone, siltstone, and sandstone lithologies. Relative *n*-alkane abundance and $\delta^{13}\text{C}$ values from carbonaceous shales in the Basin Substation core were compared to carbonaceous shales exposed in nearby outcrop exposures to assess the impact of recent weathering on *n*-alkane preservation in outcrop exposures. Gas chromatograph peak areas (corrected for injection ratio and mass of sediment extracted) of *n*-alkanes in core samples are, on average, 60 times greater than in outcrop samples (Clyde et al., 2013). Although biomarkers are better preserved in the Basin Substation core than in corresponding outcrop samples, organic matter preservation is still poor in most core samples.

n-Alkane concentrations decrease rapidly at the onset of the PETM and remain low through the body of the PETM, such that *n*-alkane concentrations in most samples were too low (<100 ng) for stable carbon isotope analyses. *n*-Alkane $\delta^{13}\text{C}$ ratios of ten core samples have been measured.

A working stratigraphic position of the PETM (~90 to ~50 MCD) was established using distinctive marker beds and biostratigraphic data, projected from surface outcrops (Baczynski et al., 2014). All core *n*-alkane $\delta^{13}\text{C}$ ratios are located below or above this interval and exhibit non-excursion $\delta^{13}\text{C}$ values. Core *n*-alkane $\delta^{13}\text{C}$ values are similar to outcrop *n*-alkane $\delta^{13}\text{C}$ values both before and after the PETM. We have not yet acquired $\delta^{13}\text{C}$ measurements within the PETM interval, but we predict that the PETM $\delta^{13}\text{C}$ core *n*-alkane values would also be similar to outcrop values. The PETM interval coincides with the highest average chain length (ACL) of *n*-alkanes. Similar to outcrop studies, ACL increases from 28.2 to 29.4 during the PETM, perhaps indicating a plant community change or a physiological response to climate change. Similar response of ACL and *n*-alkane $\delta^{13}\text{C}$ values in outcrop and core samples suggests that *n*-alkanes are reliably preserving PETM climate conditions even in more oxidized outcrop sediments (Baczynski et al., 2012).

PETM conditions in the Bighorn Basin were far from ideal for organic matter preservation, perhaps due to high temperature and elevated organic matter decay rates, and even unweathered core material from Basin Substation does not preserve an abundance of organic microfossils or biomarkers. ACL currently appears to be one of the best proxies for identifying the PETM in the core. Advanced instrumentation for compound-specific carbon isotope analysis of small samples (<100 ng) will be required to produce a higher-resolution *n*-alkane $\delta^{13}\text{C}$ curve across the PETM for the Basin Substation core.

REFERENCES

- Baczynski A.A., McInerney F.A., Wing S. L. & the BBCP Science Team (2012) - Preliminary *n*-alkane results from Basin Substation, BBCP, American Geophysical Union Annual Fall Meeting, Abstract PP11B-2011.

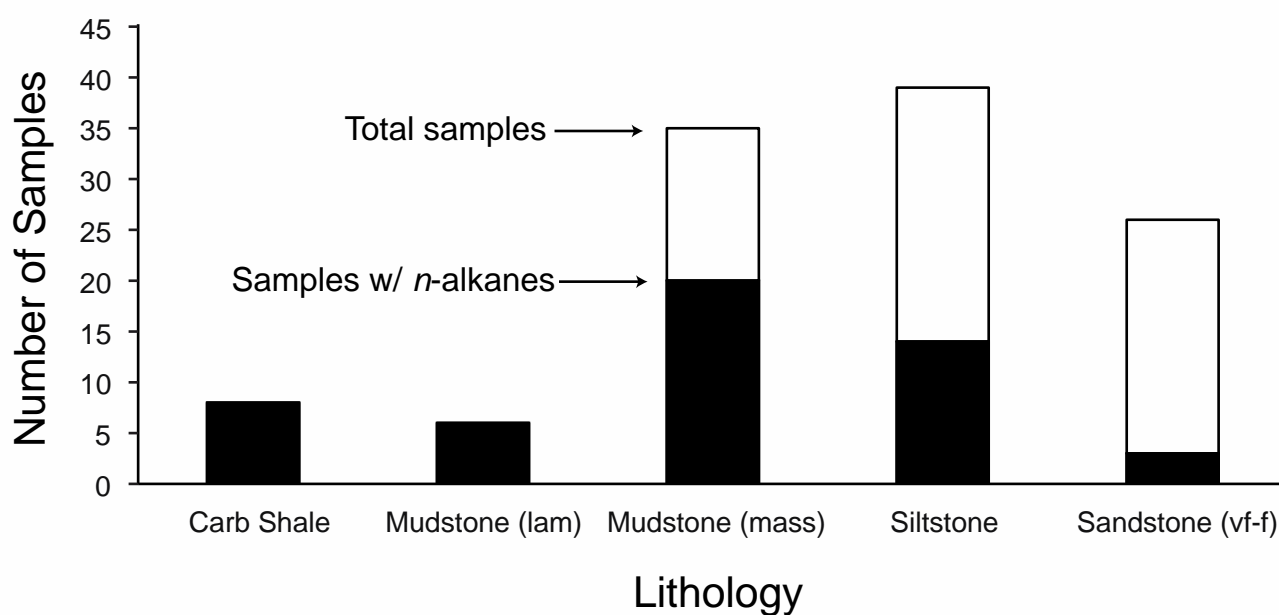


Fig.1 – Basin Substation core 1B organic geochemical samples separated by lithology: carbonaceous shale, mudstone (laminated), mudstone (massive), siltstone, sandstone (very fine-fine). Solid black fill represents number of samples that contain measurable n-alkanes.

Baczynski A.A., Barclay R.S., Bowen G.J., Denis E.H., Freeman C., Clyde W.C., Gingerich P.D., Wing S.L., Röh, U., Westerhold T., K.H., Harrington G.J., Jardine P.E., Maibauer B., McInerney F.A. & Wing S.L. (2014) - Effects of the Paleocene-Eocene Thermal Maximum on terrestrial plants and carbon storage, 10th North American Paleontological Convention, Florida Museum of Natural History, Abstract Book, Paleontological Society, 131.

Bowen G., Johnson K., Baczynski A.A., Diefendor, A., McInerney F., Schnurrenberger D., Noren A., Brady K., & the BBCP Science Team. (2013) - Bighorn Basin Coring Project (BBCP): a continental perspective on early Paleogene hyperthermals. *Scientific Drilling*, 16, 21-31, doi:10.5194/sd-16-21-2013.

Three dimensional coupled model approaches to terrestrial methane cycling during Paleogene greenhouse climates

Marcus P.S. Badger ^(a,b,c), Joy S. Singarayer ^(d), Paul J. Valdes ^(a,b,c) & Richard D. Pancost ^(b,c)

^(a) Bristol Research Initiative for the Dynamic Global Environment, School of Geography, University of Bristol, University Road, Bristol, BS8 1SS UK E-mail: marcus.badger@bristol.ac.uk

^(b) Organic Geochemistry Unit, School of Chemistry, University of Bristol, Cantock's Close, Bristol, BS8 1TS, UK

^(c) The Cabot Institute, University of Bristol, UK

^(d) Department of Meteorology, University of Reading, Earley Gate, PO Box 243, Reading, RG6 6BB, UK

Document type: Short note.

Manuscript history: received 15 May 2014; accepted 30 May 2014; editorial responsibility and handling by Gerald R. Dickens & Valeria Luciani.

KEY WORDS: HadCM3L, Paleogene, STOCHEM, SDGVM, terrestrial methane.

The biogeochemical cycling of methane presents a major challenge for paleoclimate scientists, although this critical greenhouse gas (GHG) has a forcing potential to drive significant changes in Earth System processes, and there are no proxy methods for reconstructing its ancient atmospheric concentration. This is especially important because biogenic methane emissions are controlled by environmental conditions, such as temperature and precipitation, and methane has significant power as a positive or negative feedback on global climate change. Understanding how methane emissions and cycling acted in the high $p\text{CO}_2$ greenhouse worlds of the Paleogene potentially bridges the gap between our understanding of other, better (although arguably still poorly-)

constrained GHGs and global temperature.

The recent application of advanced three dimensional global modelling strategies to the problem of Eocene trace GHG concentrations has begun to show how important these may be in high- CO_2 worlds (Valdes et al., 2005; Singarayer et al, 2011; Beerling et al, 2011), suggesting that as much as 2.7 °C of global warming may be contributed by increased trace GHGs.

This approach couples the unified Hadley Centre climate model (HadCM3L) with Sheffield Dynamic Global Vegetation Model (SDGVM; Beerling and Woodward, 2001) to simulate trace gas emissions, and the atmospheric chemistry model STOCHEM (Stevenson et al., 2005) to simulate the concentration of methane and ozone in the troposphere (fig. 1). Here we present initial results of a project to extend and develop the results of these earlier works, with revised and improved biogeochemistry and vegetation models, and broader

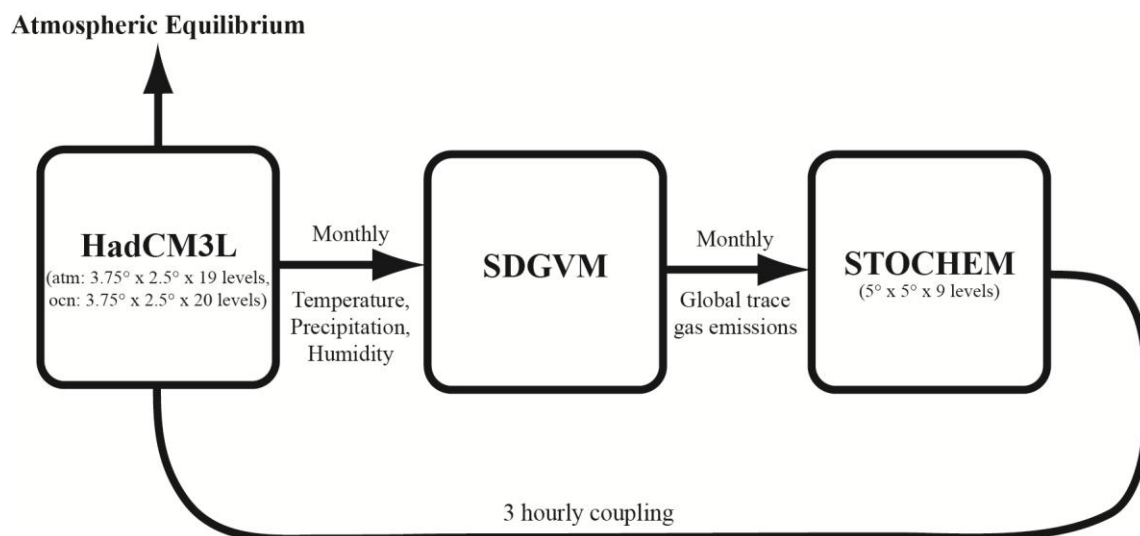


Fig.1 – Schematic of modelling approach.

consideration of boundary and initial conditions. These new results will be compared to indirect proxy methods to determine Paleogene methane emissions using lipid biomarker carbon isotopes in Eocene wetland settings (preserved as lignites) to probe past methanogenic and methanotrophic populations and constrain ancient methane emissions in high-CO₂ worlds.

REFERENCES

- Beerling D.J. & Woodward F.I. (2001) - *Vegetation and the Terrestrial Carbon Cycle. Modelling the First 400 Million Years*. Cambridge University Press, Cambridge.
- Beerling D.J., Fox A., Stevenson D.S. & Valdes P.J. (2011) – Enhanced chemistry-climate feedbacks in past greenhouse worlds. *P. Natl. Acad. Sci. USA*, 108, 9770-9775.
- Valdes P.J., Beerling D.J. & Johnson C.E. (2005) - The ice age methane budget. *Geophys. Res. Lett.*, 32, L02704.
- Singarayer J.S., Valdes P.J., Friedlingstein P., Nelson S. & Beerling D.J. (2011) - Late Holocene methane rise caused by orbitally controlled increase in tropical sources. *Nature*, 470, 82-85.
- Stevenson D., Doherty R., Sanderson M., Johnson C., Collins B. & Derwent D. (2005) - Impacts of climate change and variability on tropospheric ozone and its precursors. *Faraday Discuss.*, 130, 41-57.

Increasing atmospheric CO₂ prior to the Paleocene-Eocene Thermal Maximum inferred from stomata of *Ginkgo adiantoides*, Bighorn Basin, Wyoming, USA

Richard S. Barclay ^(a) & Scott L. Wing ^(a)

^(a) Paleobiology Department, Smithsonian Institution, National Museum of Natural History, 10th & Constitution, Washington, D.C., 20560-0121, USA. E-mail: barclay.rich@gmail.com

Document type: Short note.

Manuscript history: received 15 May 2014; accepted 30 May 2014; editorial responsibility and handling by Gerald R. Dickens & Valeria Luciani.

KEY WORDS: Bighorn Basin, carbon dioxide, climate-sensitivity, cuticle, deep-time climate change, paleobotany, stomatal index proxy.

The Paleocene-Eocene Thermal Maximum (PETM) was a geologically brief interval of intense global warming 56 million years ago. Multiple proxies suggest a temperature increase of 5-8 °C within ~20ka (Wing et al., 2005). It is arguably the best geologic analog for anthropogenic carbon emissions. The PETM is marked by a ~4-6‰ negative carbon isotope excursion (CIE) and extensive marine carbonate dissolution (Zachos et al., 2005), which together are powerful evidence for a massive addition of isotopically light carbon to the oceans and atmosphere. In spite of broad agreement that the PETM reflects a large carbon cycle perturbation, atmospheric concentrations of CO₂ (*p*CO₂) during the event are not well constrained (Schubert & Jahren, 2013).

In this study we reconstructed *p*CO₂ across the Paleocene/Eocene boundary using the stomatal index proxy. Stomatal index is the number of gas-exchange pores (stomata) on a leaf divided by the number of epidermal cells, both counted in a standard area and expressed as a percentage. An inverse relationship between stomatal index and *p*CO₂ is expected because plants lose water as well as gain CO₂ through their stomata, a process regulated by a genetic mechanism that balances the cost and the benefit by adjusting stomatal index (Woodward, 1987). Terrestrial sections in the Bighorn Basin, Wyoming, contain macrofossil plants with cuticle immediately bracketing the PETM, as well as dispersed plant cuticle from within the body of the CIE (Wing & Curran, 2013). These fossils allow for the first stomatal-based reconstruction of *p*CO₂ near the Paleocene-Eocene boundary. Cuticle-bearing fossils are used to determine both the relative timing of *p*CO₂ changes and to estimate the magnitude of *p*CO₂ shifts in relation to the CIE that defines the PETM.

Several studies have measured the relationship between *p*CO₂ and stomatal index in the living species *Ginkgo biloba* (Retallack, 2001; Royer et al., 2001; Royer, 2003). The largest and most widely cited calibration of stomatal index and *p*CO₂

in *Ginkgo biloba* (Royer et al., 2001) shows a strongly linear decrease of stomatal index as *p*CO₂ increases from 290 to 370 ppm, then a near asymptote as *p*CO₂ increases to higher values. There are, however, significant problems with previous calibrations. Either the data are sparse and don't include plants that grew in *p*CO₂ conditions above 370 ppm (Retallack, 2001), or counts of stomata and epidermal cells were made using multiple techniques for preparing and imaging the leaf epidermis (Royer et al., 2001), which could lead to inconsistency. Therefore we have generated a new dataset examining the relationship of stomatal index vs. *p*CO₂ in *Ginkgo biloba* (Fig. 1). Leaves were collected from herbarium sheets and living individuals from 1877 to 2013, macerated into lower and upper cuticles using hexavalent chromium. The internal view of the lower epidermis was imaged with an environmental SEM and seven intercostal areas were counted per leaf. This dataset covers a range of *p*CO₂ from 290 to 429 ppm and shows the expected decline in stomatal index with increasing *p*CO₂, but the slope is shallower than previously reported, with an r-squared value typical of biological datasets.

Applying the newly constructed calibration curve from *Ginkgo biloba* to the fossils of the nearly identical species *Ginkgo adiantoides* from the late Paleocene and early Eocene suggests at least a doubling of *p*CO₂ prior to the major CIE that defines the PETM. In the late Paleocene, reconstructed *p*CO₂ levels were ~300 ppm, a concentration maintained for at least 200ka, and potentially for 1Ma prior to the PETM (Royer et al., 2001). During the 150ka interval immediately prior to the CIE, inferred *p*CO₂ rose to as much as 700 ppm, and remained at least as high as 600 ppm following the rapid-recovery interval at the end of the CIE.

All evidence collected to date suggests a long-term rise in both *p*CO₂ and temperature, accompanied by drying of soils (Kraus et al., 2013) prior to the prominent CIE at the onset of the PETM. The *p*CO₂ doubling coincides in part with a ~5°C temperature increase during the "pre-warming" interval prior to the CIE, documented from δ¹⁸O in mammalian tooth enamel (Secord et al., 2010) and from fossil leaves in the Bighorn Basin. The ~5°C temperature increase with an approximate

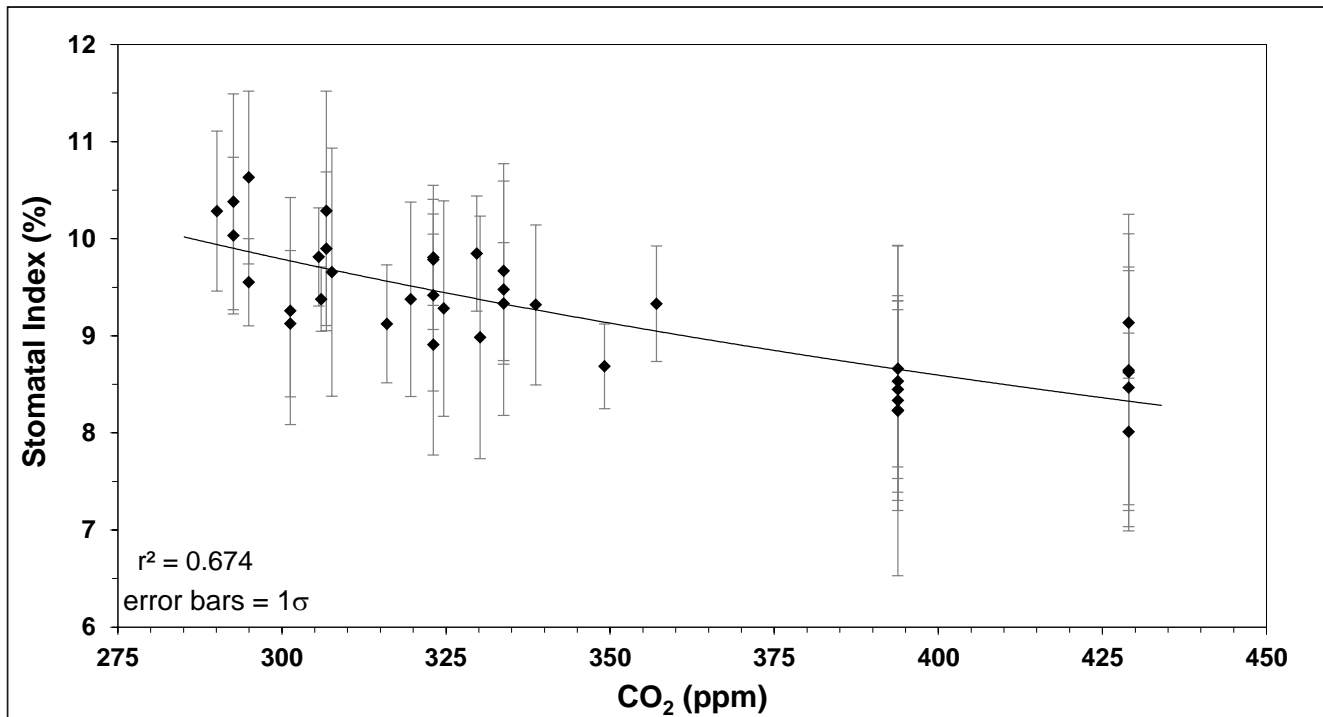


Fig.1 – Calibration dataset of extant *Ginkgo biloba* applied to fossil specimens of the nearly identical species *Ginkgo adiantoides* to estimate paleo- $p\text{CO}_2$. Figure combines historical samples from 1877 to 2013 (290 to 395 ppm) with samples from individual trees living in elevated CO_2 conditions of Washington D.C. (429 ppm). Seven stomatal index counts were made per leaf on SEM images, viewed from the interior of the lower epidermis after maceration using an aqueous solution of hexavalent chromium. Samples figured are mean values for each of 38 individual leaves, from 20 different years.

doubling of $p\text{CO}_2$, is consistent with previous estimates of full Earth-system temperature sensitivity to $p\text{CO}_2$ doublings. Presumably the source for CO_2 released prior to the CIE did not significantly alter the isotopic value of atmospheric CO_2 , and thus did not produce a significant isotope shift. This is explainable with submarine volcanism because CO_2 produced from this reservoir is relatively enriched in ^{13}C compared to other carbon sources. As suggested previously by multiple authors, warming prior to the CIE may have triggered the release of carbon from a source highly depleted in ^{13}C at the onset of the PETM.

REFERENCES

- Kraus M.J., McNerney F.A., Wing S.L., Secord R., Baczynski A.A. & Bloch J.I. (2013) - Paleohydrologic response to continental warming during the Paleocene–Eocene Thermal Maximum, Bighorn Basin, Wyoming. *Palaeogeogr. Palaeoclimatol., Palaeoecol.*, 370, 196-208.
- Retallack G.J. (2001) - A 300-million year record of atmospheric carbon dioxide from fossil plant cuticles. *Nature*, 411, 287-290.
- Royer D.L., (2003) - Estimating latest Cretaceous and Tertiary atmospheric CO_2 from stomatal indices, in Wing, S. L., Gingerich, P. D., Schmitz, B., and Thomas, E., eds., *Causes and consequences of globally warm climates in the Early Paleogene*, Geological Society of America Special Paper 369, Boulder, Colorado, 79-93.
- Royer D.L., Wing S.L., Beerling D.J., Jolley D W., Koch P.L., Hickey L.J. & Berner R.A. (2001) - Paleobotanical evidence for near present-day levels of atmospheric CO_2 during part of the Tertiary. *Science*, 292, 2310-2313.
- Schubert B.A. & Jahren A.H. (2013) - Reconciliation of marine and terrestrial carbon isotope excursions based on changing atmospheric CO_2 levels. *Nat. Commun.*, 4, 1653, 1-6.
- Secord R., Gingerich P.D., Lohmann K.C. & MacLeod, K.G. (2010) - Continental warming preceding the Palaeocene–Eocene thermal maximum. *Nature*, 467, 955-958.
- Wing S.L. & Currano, E.D. (2013) - The response of plants to five degrees of global warming. *American Journal of Botany*, 100, 1234-1254.
- Wing S.L., Harrington G.J., Smith F.A., Bloch J.I., Boyer D.M. & Freeman K.H. (2005) - Transient floral change and rapid global warming at the Paleocene-Eocene boundary. *Science*, 310, 993-996.
- Woodward F.I. (1987) - Stomatal numbers are sensitive to increases in CO_2 from preindustrial levels. *Nature*, 327, 6123, 617-618.
- Zachos J.C., Rohl U., Schellenberg S.A., Sluijs A., Hodell D.A., Kelly D.C., Thomas E., Nicolo M., Raffi I., Lourens L.J., McCarren H. & Kroon D. (2005) - Rapid acidification of the ocean during the Paleocene-Eocene thermal maximum. *Science*, 308, 5728, 1611-1615.

Reinstatement of the marginal marine carbonate platform in the earliest Tertiary at Duino, Trieste Karst

Chaim Benjamini ^(a) & Nevio Pugliese ^(b)

^(a) Department of Geological and Environmental Sciences, Ben Gurion University of the Negev, POB 653, Beer Sheva 84120 Israel, email chaim@bgu.ac.il

^(b) Department of Mathematics and Geosciences, University of Trieste, via Weiss 2, 34127 Trieste, Italy.

Document type: Short note.

Manuscript history: received 15 May 2014; accepted 30 May 2014; editorial responsibility and handling by Gerald R. Dickens & Valeria Luciani.

KEY WORDS: carbonate system, foraminifera, hypohaline, K-Pg, microbialites, Trieste Karst.

Limestones of fresh water origin have been reported beneath the foraminiferal limestones dated SBZ 1 (Serra-Kiel et al., 1998) of the earliest Tertiary on the Karst platform of northwestern Italy and Slovenia. A short 1.3 m section of these limestones at Duino in the Trieste Karst (Ciliberto et al., 1982; Cucchi et al., 1987) was here examined. In this short section, three 30-50 cm - thick shallowing-upwards cycles were found, each composed of three successive facies-sets.

A background dark limestone lithofacies was found to be composed of wackestone with small planktonic and benthic foraminifera, ostracods and thin-shelled mollusks. These beds, around 50 cm in thickness, are topped by a few centimeters of a bindstone, in fact a packstone and grainstone bound by microbialitic filaments. The grains are predominantly thin-walled miliolid, hyaline rotaliid and agglutinated benthic foraminifera, with the thick-walled form *Kayseriella decastroi*. The third successive facies-set is a superposed macroscopic columnar stromatolite that is in fact an earliest diagenetic overprinting of the two other contemporaneous facies sets. Autochthonous living components include the *Microcodium*-secreting organism (Košir, 2004) and attached foraminifera. Conversion to the stromatolitic morphology was accompanied by diagenetic modifications of the substrates - walls of serpulids and miliolid foraminifera were converted to a reddish aphanitic micrite, rotaliid foraminifera are well preserved, and trochoform bilocular foraminifera are preserved as sparry molds. Gypsum or anhydrite replaced by calcite is present in one sample.

These facies-sets represent a three-component shallowing-upwards succession that commenced with offshore subtidal wackestones, followed abruptly by nearshore, minor grainstones bound by microbialites. Fresh-water influx led to replacement by a hypohaline, vegetated marsh environment with high organic load. The small (ca. 60 cm) thickness of the complete cycle represents an accommodation response to sea level fluctuation consistent with extreme condensation.

The contrast between styles of carbonate accumulation of the latest Cretaceous is remarkable. Progradational nearshore biogenic buildups and thick bioclastic grainstones of the Cretaceous pass offshore to thick aggradational outer shelf wackestones of suspended rudist debris, and pelagic chalk (Carannante et al., 2008). The rapid accommodational potential of the Cretaceous, in which sea level fluctuations are hardly noticeable, were replaced in the earliest Tertiary by a three-component cyclic forcing due to slow response of the carbonate system to environmental change. In the wake of the extinctions, a severely suppressed, depleted carbonate system was dominated by default microbial carbonates. Fresh-water influx unimpeded by a barrier system, created a hypohaline surface layer extending well offshore. A dearth of consumers meant that the organic input from land that was utilized in the Cretaceous mesotrophic system, caused organic overload and eutrophication in the early Tertiary. Underlying carbonate aquifers in the Karst island system ensured the high levels of HCO_3^- necessary for secretion and preservation of carbonate tests under such conditions.

As the paleoenvironments of the K-Pg aftermath appear to have been unchanged across the K-Pg level, the earliest Tertiary repopulation included generalist or opportunist survivors of Cretaceous origin that did not play an important role in the previous carbonate system. Opportunists have mechanisms in place for repopulating sterile environments rapidly due to their reproductive capacity, and their potential for considerable genetic diversity as a continuous survival mechanism is inherent (Pugliese et al., 2000). However, this potential is in fact a kind of specialization, utilized primarily for survival under stressed conditions, and they are routinely replaced in an unstressed world by specialist competitors. Generalist and opportunist foraminifera, calcareous algae, non-rudist bivalves, corals and stromatolitic microbialites that played this role were those found above the K-Pg level in the Karst region (Ogorolec et al., 2007; Tunis et al., 2011). Generally, their presence is clear, immediate, locally abundant but unremarkable, they diversify little in the aftermath, and did not participate in development of carbonate export capacity.

Bivalve molluscs are common in the recovery succession, but potential repopulators had long since been squeezed-out

ecologically by the successful rudists, and no candidate for filling any niche beyond opportunist settling was present. Corals survived but failed to thrive following the K-Pg; apparently the globally warm calcite ocean was wrong for them, and they remained in their relatively cryptic niches until Late Eocene cooling. Larger foraminifera of the early Tertiary required some 4 Myr until they were able to produce carbonate in any significant quantity; this is a period of time similar to that required by orbitoid foraminifera to re-evolve following the end-Cenomanian crisis (Hottinger, 1987; Carannante, 1998; Pomar & Hallock, 2008).

A pathway for evolution of the Early Tertiary rotaliid and miliolid-dominated larger foraminiferal assemblages may be found in adaptation of species from siliciclastic coastlines to the HCO_3^- -rich marsh environments. Benthic foraminifera of clastic depositional systems would have been relatively tolerant of fresh-water input. Clastic coastlines occurred at this time above the slopes that sourced the flysch deposits of the Alpine orogenic zones. In the Karst region, mostly epifaunal hyaline rotaliids, thin-walled miliolids, and agglutinants, often typical of generalist faunas of siliciclastic sandy substrates, were the forms that repopulated the carbonate environments of the nearshore zone. Could these have ultimately diversified to become the main carbonate producers of the Early Tertiary?

REFERENCES

- Carannante G., Cherchi A., Graziano R., Ruberti D. & Simone L. (2008) - Post-Turonian rudist-bearing limestones of the Peri-Tethyan region: evolution of the sedimentary patterns and lithofacies in the context of global versus regional controls. In: Lukasik, J., Simo, A. (eds), Controls on Carbonate Platform and Reef Development, SEPM Spec. Publ., Tulsa, 89, 255-270.
- Ciliberto B.M., Pirini Radrizzani C. & Pugliese N. (1982) - La piattaforma carbonatica al passaggio Cretacico-Terziario nell'area di Duino (Carso Triestino). *Geologica Romana*, 21, 849-857.
- Cocchi F., Pirini Radrizzani C. & Pugliese N. (1987) - The carbonate stratigraphic sequence of the Karst of Trieste (Italy). *Mem. Soc. Geol. It.*, 40, 35-44.
- Drobne K., Ogorelec B., Pleničar M., Barattolo F., Turnšek D. & Zucchi-Stofa M.L. (1987) - The Dolenja vas section, a transition from Cretaceous to Palaeocene in the NW Dinarides, Yugoslavia. *Mem. Soc. Geol. It.*, 40, 73-84.
- Hottinger L. (1987) - Conditions for generating carbonate platforms. *Mem. Soc. Geol. It.*, 40, 265-271.
- Košir A. (2004) - Microcodium revisited: Root calcification products of terrestrial plants on carbonate-rich substrates. *J. Sediment. Petrol.*, 74, 845-857.
- Ogorelec B., Dolenc T. & Drobne K. (2007) - Cretaceous-Tertiary boundary problem on shallow carbonate platform: Carbon and oxygen excursions, biota and microfacies at the K/T boundary sections Dolenja Vas and Sopada in SW Slovenia, Adria CP. *Palaeogeogr. Palaeoclimatol. Palaeoecology*, 255, 64-76.
- Pomar L. & Hallock P. (2008) - Carbonate factories: A conundrum in sedimentary geology. *Earth-Sci. Rev.*, 87, 134-169.
- Pugliese N., Arbulli D., Caffau M. & Drobne K. (2000) - Strategia di vita nel biota daniano (SBZ 1) del Carso Triestino (Italia), In: Crisi biologiche, radiazioni adattative e dinamica delle piattaforme carbonatiche, *Accad. Naz. Sci. Lett. Arti di Modena, Collana di Studi*, 21, 215-220.
- Serra-Kiel J., Hottinger L., Caus E., Drobne K., Ferrandez C., Jauhri A.K., Less G., Pavlovec R., Pignatti J., Samsó J.M., Schaub H., Sirel E., Strougo A., Tambareau Y., Tosquella, J. & Zakrevskaya E. (1998) - Larger foraminiferal biostratigraphy of the Tethyan Paleocene and Eocene. *Bull. Soc. Géol. France*, 169, 281-299.
- Tunis G., Pugliese N., Jurkovšek B., Ogorelec B., Drobne K., Riccamboni R. & Tewari V.C. (2011) - Microbialites as Markers of Biotic and Abiotic Events in the Karst District, Slovenia and Italy, In: *Stromatolites: Interaction of Microbes with Sediments Cellular Origin, Life in Extreme Habitats and Astrobiology*, 18, 251-272, doi: 10.1007/978-94-007-0397-1_11.

Geochemical signals in Eocene planktonic foraminifera

Rehemat Bhatia^(a), Bridget S. Wade^(a), Wolfgang Müller^(b), David Evans^(b), David J.R. Thornalley^(c) & Bradley N. Opdyke^(d)

^(a) Department of Earth Sciences, University College London, London, WC1E 6BT, UK. E-mail: rehemat.bhatia.13@ucl.ac.uk

^(b) Department of Earth Sciences, Royal Holloway University of London, Egham, TW20 0EX, UK

^(c) Department of Geography, University College London, London, WC1E 6BT, UK

^(d) Research School of Earth Sciences, The Australian National University, Canberra 0200, Australia

Document type: Short note.

Manuscript history: received 15 May 2014; accepted 30 May 2014; editorial responsibility and handling by Gerald R. Dickens & Valeria Luciani.

KEY WORDS: Eocene, geochemistry, LA-ICPMS, Mg/Ca, palaeoecology, planktonic foraminifera.

The stable isotope and trace element geochemistry of planktonic foraminifera can be utilised to determine palaeoceanographic conditions. Carbon isotopes ($\delta^{13}\text{C}$) have been proposed as a proxy for photosymbiotic activity, and oxygen isotope data ($\delta^{18}\text{O}$) can be used to infer palaeotemperatures and seawater $\delta^{18}\text{O}$ related to changes in global ice volume. Trace element signatures have been suggested to be proxies for many palaeoceanographic conditions, including planktonic foraminiferal Mg/Ca for sea surface temperatures (SST), B/Ca for seawater pH and Cd/Ca for nutrient content, from which ocean circulation may be inferred. However, different species have different geochemical offsets, which occur due to varying depth habitats and the presence of photosymbionts. Therefore, when working on deep-time material, it is important to constrain the palaeobiology of extinct species in order to improve our understanding of palaeoceanographic conditions and the validity of the proxy signals obtained.

The palaeoecology and photosymbiotic associations of many Cenozoic planktonic foraminifera species have not been determined; this can be constrained using trace element and stable isotope multispecies analysis. The data obtained using these analyses can help identify and interpret the causes of the effect of vital effects on foraminiferal geochemistry. Accurate deep-time Mg/Ca palaeothermometry is further complicated as a result of both the poorly known secular variation of the Mg/Ca ratio of seawater (Broecker & Yu, 2011) and the non-linear control exerted by seawater Mg/Ca on the Mg-distribution coefficient variation with changing Mg/Ca_{sw} (Evans & Müller, 2012).

Oxygen isotope data from well preserved planktonic foraminifera imply that tropical sea surface temperatures during the Eocene were similar or slightly higher than present day (Pearson et al., 2007), whilst palaeoclimate models and some TEX₈₆ calibrations suggest temperatures 5-10°C higher (Heinemann et al., 2009, Kim et al., 2010, Tindall et al., 2010).

Eocene sediments of calcareous marls and glauconitic silty clays with porcellanitic interbeds were recovered from Ocean Drilling Program Leg 174AX at Bass River, New Jersey, USA (39°36'42"N, 74°26'12"W) (Fig. 1) (Miller et al., 1998). This study focuses on the interval from 39.8 – 55.4 Ma, covering a time of dramatic climatic change from peak warmth during the early Eocene climatic optimum and subsequent temperature decline. The sediments contain extremely well preserved, glassy planktonic foraminifera. Assemblages from the middle Eocene sediments are extremely diverse; species include *Hantkenina mexicana*, *Acarinina praetopilensis*, *Subbotina hagni* and *Morozovelloides lehneri* allowing for multispecies geochemical analyses to reconstruct marine temperatures and carbon isotope gradients.

Trace element/Ca ratios of individual chambers of various species of surface and deep dwelling planktonic foraminifera (*Pseudohastigerina wilcoxensis*, *Acarinina pseudotopilensis*, *Acarinina praetopilensis* and *Parasubbotina inaequispira*) were obtained by slow depth profiling, utilising laser ablation inductively coupled mass spectrometry (LA-ICPMS) as an analytical technique capable of achieving ultimate (sub-)µm spatial resolution. This has the advantage over other analysis methods because LA-ICPMS is less destructive, therefore the same samples can be used for scanning electron microscope and stable isotope analysis. Diagenesis can also be assessed on a sub-µm scale and it is also possible to resolve intra and inter test heterogeneity, since specific test areas/chambers can be analysed separately.

Here we present initial results and discuss the implications. Data obtained in this study will be useful to compare to other sites of exceptional preservation e.g. Tanzania, and will be valuable in resolving sea surface temperature and latitudinal gradients during the Eocene.

REFERENCES

- Broecker W. & Yu J. (2011) - What do we know about the evolution of Mg to Ca ratios in seawater? *Paleoceanography*, 26 (3), PA3203.

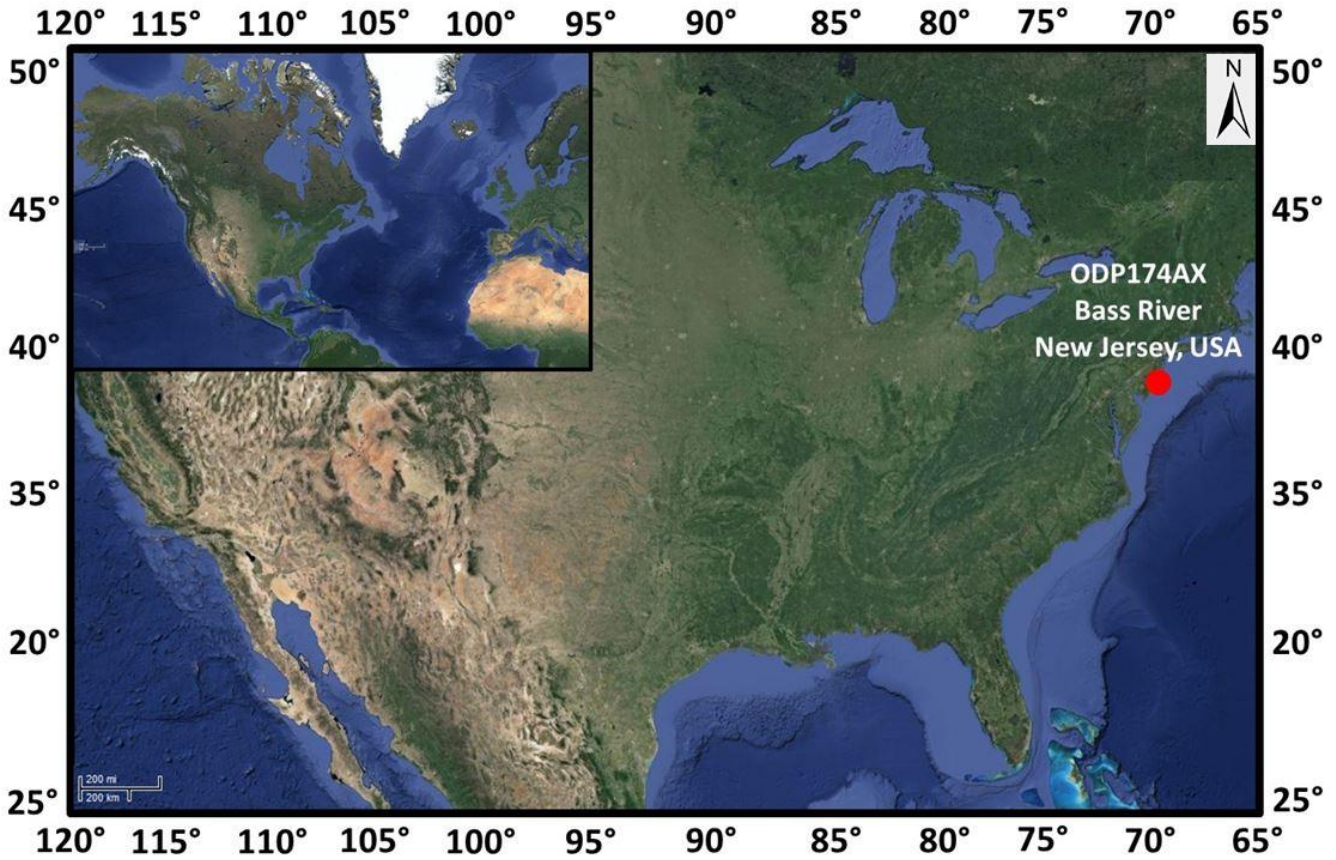


Fig.1 - Location map: Ocean Drilling Program Leg 174AX.

Evans D. & Müller W. (2012) - Deep time foraminifera Mg/Ca paleothermometry: Nonlinear correction for secular change in seawater Mg/Ca. *Paleoceanography*, 27, PA4205.

Heinemann M., Jungclaus J.H. & Marotzke J. (2009) - Warm Paleocene/Eocene climate as simulated in ECHAM5/MPI-OM. *Clim. Past.*, 5, 785–802

Kim J.H., van der Meer J., Schouten S., Helmke P., Willmott V., Sangiorgi F., Koç N., Hopmans E.C. & Damsté J.S.S. (2010) - New indices and calibrations derived from the distribution of crenarchaeal isoprenoid tetraether lipids: Implications for past sea surface temperature reconstructions. *Geochim. Cosmochim. Ac.*, 4, 152-164.

Miller, K.G. Sugarman, P.J., Browning, J.V., Olsson, R.K., Pekar, S.F., Reilly, T.J., Cramer, B.S., Aubry, M.-P.,

Lawrence, R.P., Curran, J., Stewart, M., Metzger, J.M., Uptegrove, J., Bukry, D., Burckle, L.H., Wright, J.D., Feigenson, M.D., Brenner, G.J., & Dalton, R.F., (1998) - Bass River site. In Miller, K.G., Sugarman, P.J., Browning, J.V., et al., *Proc. ODP, Init. Repts., 174AX: College Station, TX (Ocean Drilling Program)*, 5–43.

Pearson P.N., van Dongen B.E., Nicholas C.J., Pancost R.D., Schouten S., Singano J.M. & Wade B.S. (2007) - Stable warm tropical climate through the Eocene epoch. *Geology*, 35 (3), 211-214.

Tindall J., Flecker R., Valdes P., Schmidt D.N., Markwick P. & Harris J. (2010) - Modelling the oxygen isotope distribution of ancient seawater using a coupled ocean-atmosphere GCM: Implications for reconstructing early Eocene climate. *Earth Planet. Sci. Lett.*, 292, 265–273.

Is there a causal link between early Eocene opening of the Tasmanian Gateway and the onset of Eocene cooling?

Peter Bijl ^(a), Willem Sijp ^(b)

^(a) Department of Earth Sciences, Faculty of Geosciences, Utrecht, Netherlands. Email: p.k.bijl@uu.nl

^(b) ARC Centre of Excellence for Climate System Science, University of New South Wales, Sydney, NSW 2052, Australia

Document type: Short note.

Manuscript history: received 15 May 2014; accepted 30 May 2014; editorial responsibility and handling by Gerald R. Dickens & Valeria Luciani.

KEYWORDS: Eocene, Southern Ocean, Tasmanian Gateway, Drake Passage, paleoceanography, dinoflagellate cysts, numerical modeling.

The early Eocene is an interval in the Earth's climatic history with extremely warm climates, which most notably manifests itself in high latitudes (e.g., Bijl et al., 2009; Pross et al., 2012). This warmth culminates in the Early Eocene Climatic Optimum (EECO), 52-50 million years ago (Zachos et al., 2008). Following the EECO, Antarctic and the Southern Ocean began to cool, ultimately to temperatures that support the development of a large continental ice sheet on Antarctica around 33.5 Ma (Zachos et al., 2008). Initially it was hypothesized that the opening of critical Southern Ocean Gateways, Drake Passage and the Tasmanian Gateway controlled the Eocene climatic evolution (e.g., Kennett, 1977). Of these gateways, at least the Tasmanian Gateway was mostly closed in the early Eocene (Bijl et al., 2013), which prevented an isolating circumpolar ocean circulation. In turn it was hypothesized that the absence of such a circumpolar connection created the opportunity of a much stronger poleward oceanic heat transport (Kennett, 1977). This in turn would have led to warmer polar regions; a deep convection of warm water explains the warmer intermediate water temperatures seen in deep-sea oxygen isotope records (Zachos et al., 2008). Opposition to this hypothesis came from numerical models (e.g., Sloan and Rea, 1996) suggesting that closed Southern Ocean gateways would not result in increased poleward heat transport (Huber et al., 2004), and the timing of opening of the Southern Ocean Gateways did not coincide with the onset of Antarctic glaciation (Stickley et al., 2004), and thus could not have been the primary force factor. Instead, the increase in proxy data for Cenozoic greenhouse gases (notably CO₂) showed coherent patterns with the intermediate-water temperature evolution of the Eocene (Zachos et al., 2008), and numerical ice sheet models could reproduce the buildup of an Antarctic ice sheet by only decreasing atmospheric CO₂ (DeConto and Pollard, 2003). This laid the foundation of the hypothesis that the decline of atmospheric CO₂ during the Eocene was the primary force for the Eocene climatic evolution (Zachos et al., 2008). However, the greenhouse-gas hypothesis cannot explain why polar regions

cool during the middle Eocene while tropical regions seem to show stable warm temperatures over the same time interval. The absence of tropical Eocene cooling however heavily hinges on the record from Tanzania, with no representation of other oceanic basins (Pearson et al., 2007; Bijl et al., 2009). With only atmospheric CO₂ as forcing, the cooling should have been much more uniform over the Earth.

As an additional factor, we here first establish a more robust inventory of the Eocene tropical paleotemperature evolution through some new middle Eocene TEX⁸⁶ records from the Equatorial Atlantic Ocean, to conclude that the absence of equatorial cooling in the middle Eocene is not confined to the Indian Ocean only. Subsequently we investigate the role of an as yet unnoticed early phase of opening of the Tasmanian Gateway, and its potential role in contributing to the greenhouse gas decline to fully explain the regional patterns of climate change during the middle Eocene. We have found evidence for an early phase of Tasmanian Gateway opening around 50 Ma, through investigation of dinocyst biogeographic patterns from sediment cores from across the gateway (Bijl et al., 2013). These biogeographic patterns were subsequently simulated in different gateway scenarios using passive tracer experiments in an ocean circulation model. Also, we reconstructed the onset of surface water and terrestrial cooling terminating the EECO with use of organic biomarker- and terrestrial palynomorph-derived paleotemperature estimates at the same sedimentary archives. We investigate the causality of cooling and opening of the Gateway through comparative model simulations with different Gateway scenarios. This combined model-data approach yields a robust insight into the possible climatic consequences of the early opening of the Tasmanian Gateway, and the implications to the Eocene climatic evolution of Antarctica.

REFERENCES

- Bijl, P. K., Schouten, S., Brinkhuis, H., Sluijs, A., Reichert, G.-J., Zachos, J. C. (2009) - Early Palaeogene Temperature Evolution of the Southwest Pacific Ocean. *Nature*. 461, 776-779.

- Bijl, P. K., Schouten, S., Brinkhuis, H., Sluijs, A., Reichart, G.-J., Zachos, J. C. (2009) - Early Palaeogene Temperature Evolution of the Southwest Pacific Ocean. *Nature*. 461, 776-779.
- Bijl, P.K., Bendle, J.A., Bohaty, S. M., Pross, J., Schouten, S., Tauxe, L., Stickley, C. E., McKay, R. M., Röhl, U., Olney, M., Sluijs, A., Escutia, C., Brinkhuis, H. and Expedition 318 Scientists (2013) - Eocene cooling linked to early flow across the Tasmanian Gateway. *Proceedings of the National Academy of Sciences* 110(24) 9645-9650.
- DeConto, R. M., and D. Pollard (2003) - Rapid Cenozoic glaciation of Antarctica induced by declining atmospheric CO₂. *Nature*, 421, 245-249.
- Huber, M., Brinkhuis, H., Stickley, C. E., Döös, K., Sluijs, A., Warnaar, J., Schellenberg, S. A., Williams, G. L. (2004) - Eocene circulation of the Southern Ocean: Was Antarctica kept warm by subtropical waters? *Paleoceanography*. 19, 4026.
- Kennett, J. P. (1977) - Cenozoic evolution of Antarctic glaciations, the circum-Antarctic ocean and their impact on global paleoceanography, *J. Geophys. Res.*, 82, 3843–3860.
- Pearson, P. N., van Dongen, B. E., Nicholas, C. J., Pancost, R. D., Schouten, S., Singano, J. M., and Wade, B. S. (2007) - Stable warm tropical climate through the Eocene Epoch, *Geology*, 35, 211–214.
- Pross, J., Contreras, L., Bijl, P. K., Greenwood, D. R., Bohaty, S. M., Schouten, S., Bendle, J. A., Röhl, U., Tauxe, L., Raine, I., Huck, C. E., van de Flierdt, T., Jamieson, S. S. R., Stickley, C. E., van de Schootbrugge, B., Escutia, C., Brinkhuis, H., Expedition 318 Scientists (2013) - Persistent near-tropical warmth on the Antarctic continent during the early Eocene epoch. *Nature* 488, 73-77.
- Sloan, L. C., and D. K. Rea (1996) - Atmospheric carbon dioxide and early Eocene climate: A general circulation modeling sensitivity study, *Palaeogeogr. Palaeoclimatol. Palaeoecol.*, 119, 275–292.
- Stickley, C. E., Brinkhuis, H., Schellenberg, S. A., Sluijs, A., Röhl, U., Fuller, M., Grauert, M., Huber, M., Warnaar, J., Williams, G. L. (2004) - Timing and nature of the deepening of the Tasmanian Gateway. *Paleoceanography* 19, 4027.
- Zachos, J. C., Dickens, G. R., Zeebe, R. E. (2008) - An early Cenozoic perspective on greenhouse warming and carbon-cycle dynamics. *Nature* 451, 279-283.

Significant continental ice volumes on mid-Paleocene Antarctica? Latitudinal temperature gradients, sea level change and the carbon cycle

Peter Bijl ^(a), Appy Sluijs ^(a), Stefan Schouten ^(b), Gerald R. Dickens ^(c), Chris J. Hollis ^(d), Richard E. Zeebe ^(e),
James C. Zachos ^(f) Paolo Stocchi ^(b) & Henk Brinkhuis ^(a,b)

^(a) Utrecht University, Department of Earth Sciences, Faculty of Geosciences, Utrecht, Netherlands. Email: p.k.bijl@uu.nl

^(b) NIOZ Royal Netherlands Institute for Sea Research, Texel, the Netherlands

^(c) Rice University, Houston, TX, USA

^(d) GNS Science, Lower Hutt, New Zealand

^(e) University of Hawaii, Honolulu, USA

^(f) UCSC, Santa Cruz, CA, USA

Document type: Short note.

Manuscript history: received 15 May 2014; accepted 30 May 2014; editorial responsibility and handling by Gerald R. Dickens & Valeria Luciani.

KEYWORDS: continental ice volume, dinoflagellate cysts, Paleocene, temperature gradients, sea level.

Long-term global climatic cooling since the mid-Cretaceous (95 million years ago; Mega annum; Ma) culminated in the establishment of major continental ice sheets on Antarctica (by ~34 Ma) and on the Northern Hemisphere (by ~2.6 Ma). This general cooling trend was interrupted by several episodes of long-term (multi-million year) warming, of which the most prominent is that of the late Paleocene to early Eocene (60- 50 Ma). Many studies have shown temperate to tropical conditions in polar latitudes of both hemispheres at that time. Critically, the pole-to-equator temperature gradient was unexpectedly small. The inconsistency between these field data and the numerical models set up to reconstruct hothouse climates indicates that we do not fully understand the forcings behind and the dynamics of these 'hothouse' climates. The Early Paleogene is generally conceived as ice-free, except for the some polar glaciers towards the end of the Eocene. However, a remarkably cold episode of early Paleogene climate is often neglected: the mid-Paleocene (61-58 Ma). Paleotemperature reconstructions using organic biomarker proxies from the South Pacific Ocean (ODP Site 1172, but also New Zealand) revealed cold conditions during the mid-Paleocene (~61-57 Ma), in fact as cold as those for the early Oligocene at the same location, when massive ice sheets have appeared on the Antarctic continent. In our presentation, we will attempt to convince the audience that the early Paleogene was largely ice-free, and that first Cenozoic ice did not appear around the late Eocene, but at the mid-Paleocene, after which it disappeared towards the Paleocene Eocene boundary. Whereas the Eocene-Oligocene cooling resulted in a quasi-stable Antarctic glaciation, the suspected mid-Paleocene glaciations, were followed by ~6 million years of global warming. The project is an ongoing 4-year postdoctoral research. We will show preliminary results and a review of existing data that suggest the presence of substantial glaciers

on Paleocene Antarctica. We will be guided through our statements by addressing the following research questions:

1) How much cooler was the mid-Paleocene than the early Eocene 'hothouse'? Sea and land surface temperature reconstructions (notably from organic biomarker proxies for paleotemperature) reveal temperature distribution over the globe. The resulting Paleocene meridional temperature gradient will be compared to that of the early Eocene 'hothouse', the middle Eocene 'doubthouse' and the early Oligocene 'icehouse'. This data will comprise the foundation for estimating continental ice volume and climate sensitivity to CO₂ forcing during late Paleocene – early Eocene warming.

2) Was there a significant mid-Paleocene Antarctic ice sheet? If cold Southern Ocean SSTs are a prerequisite for Antarctic continental ice sheets to develop, there is potential for the presence of considerably large ice caps in the mid-Paleocene. Unfortunately there are not many Paleocene records around Antarctica to directly assess the presence of physical evidence for continental ice. We therefore rely on far-field indirect evidence. Many lithostratigraphic studies on the Paleocene show a consistent unconformity around the mid-Paleocene in sections all over the world, which is followed by a sea level rise during the late Paleocene. However, the biostratigraphic constraints thus far do not allow for a detailed chronostratigraphic correlation of these unconformities, and do not assess the dynamics of sea level change at that time. With studying dinoflagellate cyst assemblages in these sections, we not only provide a more detailed stratigraphic constraints on the duration of the unconformities, but also the dinocyst assemblages can reveal a lot on shelf environmental dynamics around the mid-Paleocene, including sea level dynamics.

With our preliminary data, we already see a remarkable time-equivalence of unconformities around the world in the mid-Paleocene indeed suggestive of some major sea level fall.

3) What role did the global carbon cycle play in the Paleocene cooling and the reversal into massive warming?

This part of our project has not started yet, but is intended to obtain more physical evidence for the carbon cycle dynamics of the Paleocene as reconstructed through carbon cycle box modeling.

The combined research efforts with all collaborators will

provide an answer to the questions how cold the mid-Paleocene really was and why the climate did not shift towards sustained glaciation but instead reversed to hothouse conditions during the Eocene. The first results of the project will be presented, as well as an outlook for future research.

Variations in calcareous nannofossil assemblages during the Eocene-Oligocene transition at mid-latitude: Walvis Ridge ODP Site 1263 (Atlantic Ocean)

Manuela Bordiga ^(a) & Jorijntje Henderiks ^(a)

(a) Department of Earth Sciences, University of Uppsala, Villavägen, 16, 752 36, Uppsala, Sweden. E-mail: manuela.bordiga@geo.uu.se

Document type: Short note.

Manuscript history: received 15 May 2014; accepted 30 May 2014; editorial responsibility and handling by Gerald R. Dickens & Valeria Luciani.

KEY WORDS: calcareous nannofossils, Eocene-Oligocene transition, mid-latitude, Principal Component Analysis, Walvis Ridge, ODP Site 1263.

This study aims to unravel the relationships between the variations recorded in the calcareous nannofossil assemblages and the climatic shifts that occurred during the Eocene/Oligocene transition (EOT). The transition from a warm world with high atmospheric CO₂ concentrations (pCO₂) during the Eocene to the development of Antarctic ice sheets and lower pCO₂ in the Oligocene, most likely also affected the oceanic phytoplankton.

ODP Site 1263 (27°11.160'S and 1°34.620'E, Walvis Ridge, Atlantic Ocean) was selected because it is located in a mid-latitude zone and it was located well above the lysocline also during the late Eocene. The calcareous nannofossil content of 113 samples is here analysed in detail. The sampling is at high resolution (every 10 cm) across the EOT and it decreases for the intervals above and below the boundary. The number of coccoliths per gram of sediment (N g⁻¹) is evaluated together with the relative abundances of all the identified species. The log-transformed percentages are processed using PAST (Hammer et al., 2001) to perform Principal Component Analysis (PCA). The results from the PCA are compared with independent foraminifera-derived geochemical data from the same site: planktic and benthic foraminiferal stable carbon isotope ratios (δ¹³C; Riesselman et al., 2007) and planktic foraminiferal Mg/Ca (Peck et al., 2010), as indicators of paleoproductivity and paleotemperature, respectively.

At Site 1263, calcareous nannofossils are abundant and have moderate to good preservation, even if the discoasterids' group shows strong signs of overgrowth. The PCA retains two principal components that, respectively, hold 30% and 14% of the total variance. Principal component 1 (PC1) is negatively loaded with *Cyclicargolithus* spp. and *Lanternithus minutus* and positively with *Dictyococcites bisectus*, *Dictyococcites stavensis*, *Discoaster* and large-sized reticulofenestrads (i.e., *Reticulofenestra umbilicus*, *R. scrippsae* and *R. samodurovii*). No apparent relationships are identifiable among the loading

species and the other independent data. But the PC1 curve corresponds well with the total coccolith abundance data (N g⁻¹): both record a decrease at the EOT boundary. PC1 has another clear relationship with the variations in coccoliths' size along the studied interval. Small-medium sized species have negative loadings on PC1, while large sized species have positive loadings. Mean cell sizes, estimated from mean coccolith size for the main species and expressed in mean volume to surface area ratio (V:SA) (*cf.* Henderiks & Pagani, 2008) corroborate this observation. The V:SA ratios were higher during the late Eocene and started decreasing across the EOT. Henderiks & Pagani (2008) documented a similar decrease in reticulofenestrads sizes from the late Eocene to the early Oligocene, largely corresponding to trends in alkenone-based pCO₂ estimates. They hypothesized that large coccolithophores proliferated in conditions of high pCO₂ and CO_{2(aq)} during the late Eocene, while small-sized species became more competitive when pCO₂ decreased during the Oligocene. Our high-resolution study confirms a distinct decrease of V:SA estimates across the EOT, supporting the hypothesis that larger species are more affected than the smaller ones by the transition from a "greenhouse" and an "icehouse" climate. This is also confirmed by the absolute abundance of the small-medium sized *Cyclicargolithus* spp. which is not recording intense variations along the entire succession; on the contrary the large *Reticulofenestra* and the *Dictyococcites* group show an abrupt decrease in abundance across the EOT.

Our coccolith dissolution index (given by the ratio between entire and fragmented coccoliths) confirms that preferential dissolution of small species did not bias the PC1 and V:SA results, as intervals of increased dissolution did not necessarily correspond to large V:SA. The only exception is represented by the interval at ~90-90.3 mcd (meters composite depth) where a high dissolution peak corresponds to an increase in mean size.

Principal component 2 (PC2) is negatively loaded by the holococcolith *Lanternithus minutus*, while the positive loadings are represented by *Coccolithus pelagicus* and *Sphenolithus* spp. We compared PC2 with the Δδ¹³C_{Planktic-Benthic} data, indicative of

paleoproductivity as suggested by Sarnthein & Winn (1990). Even if data are not available for the interval below 96 mcd (during late Eocene), overall, lower paleoproductivity corresponds to negative loadings on PC2, and vice versa. Studies on modern phytoplankton have confirmed that the holococcolith-bearing life stages, such as *Lanternithus minutus*, proliferate in oligotrophic conditions (e.g. Winter et al., 1994). Thus we infer that PC2 reflects a lower productivity during the late Eocene, and that both the PC1 and $\Delta\delta^{13}\text{C}_{\text{P-B}}$ curves show a higher productivity signal at the onset of Oi-1. Paleoproductivity subsequently decreased and remained relatively constant from the Oi-1 upwards. It is possible that a major instability during the onset of Oi-1 favoured upwelling and thus primary productivity in this area. During the Oi-1 a more stable system, related also to the onset of North Atlantic Deep Water (NADW) production in the early Oligocene (Via & Thomas, 2006), may have allowed the proliferation of more oligotrophic taxa, including holococcoliths. However, the increase in productivity at the Oi-1 onset is not reflected in the absolute coccolith abundance. The increased paleoproductivity at the EOT is usually evidenced also by the ecological diversity (Shannon index, H), which tends to decrease above the EOT boundary. At Site 1263 the H-index records a slight decrease across the EOT, but not as pronounced as at low- and high latitudinal sites in Tanzania (Dunkley Jones et al., 2008) and the southern Atlantic Ocean (Persico & Villa, 1996), respectively.

No information about fluctuations in sea surface temperature (SST) was derived from the PCA. It is possible that this mid-latitude had a stronger affiliation with tropical SST stability than with the SST cooling trend recorded in high latitudes after the EOT. This is also confirmed by the planktonic foraminifera Mg/Ca data recording no significant change (Peck et al., 2010). Instead, at Site 1263, the global decrease in the pCO₂ typical of the Eocene-Oligocene transition appears reflected by the coccolith and cell size variations, as represented in PC1, confirming the competitive disadvantages of large-celled species in the Oligocene "icehouse". The loss in large reticulofenestrids, however, was not compensated by other taxa, explaining a sustained decrease in total coccolith abundance at this site since the EOT.

REFERENCES

- Dunkley Jones T., Bown P.R., Pearson P.N., Wade B.S., Coxall H.K. & Lear C.H. (2008) - Major shifts in calcareous phytoplankton assemblages through the Eocene-Oligocene transition of Tanzania and their implications for low-latitude primary production. *Paleoceanography*, 23, doi:10.1029/2008PA001640.
- Hammer Ø., Harper D.A.T. & Ryan P.D. (2001) - PAST: paleontological statistics software package for education and data analysis. *Paleontologia Electronica*, 4, 9pp.
- Henderiks J. & Pagani M. (2008) - Coccolithophore cell size and Paleogene decline in atmospheric CO₂. *Earth Planet. Sci. Lett.*, 269, 576-584.
- Peck V.L., Yu J., Kender S. & Riesselman C.R. (2007) - Shifting ocean carbonate chemistry during the Eocene-Oligocene climate transition: implications for deep-ocean Mg/Ca paleothermometry. *Paleoceanography*, 25, doi:10.1029/2009PA001906.
- Persico D. & Villa G. (2006) - Eocene-Oligocene calcareous nannofossils from Maud Rise and Kerguelen Plateau (Antarctica): paleoecological and paleoceanographic implications. *Mar. Micropaleontol.*, 52, 153-179.
- Riesselman C.R., Dunbar R.B., Mucciarone D.A. & Kitasei S.S. (2007) - High resolution stable isotope and carbonate variability during the early Oligocene climate transition: Walvis Ridge (ODP Site 1263). U.S. Geological Survey and the national Academies, USGS OF-2007-1047, Short Research Paper 095, doi:10.3133/of2007-1047.srp095.
- Sarnthein M. & Winn K. (1990) - Reconstruction of low and middle latitude export productivity, 30,000 years BP to present: implication for global carbon reservoir. In: Schlesinger M.E., (Ed.), *Climate-Ocean Interaction*, Kluwer Academic Publishers, pp. 319-342.
- Via R.K. & Thomas D.J. (2006) - Evolution of Atlantic thermohaline circulation: Early Oligocene onset of deep-water production in the North Atlantic. *Geology*, 34, 441-444.
- Winter A., Jordan R.W. & Roth P.H. (1994) - Biogeography of living coccolithophores in ocean waters. In: *Coccolithophores*, Winter A. & Siesser W.G. (Eds.), 161-177 pp.

The end of the Paleogene – A new surface-water temperature record for the Oligocene-Miocene Transition from the western Atlantic (IODP Site U1405)

André Bornemann ^(a), Iris Möbius ^(b,c), Oliver Friedrich ^(b,c), Paul A. Wilson ^(d) & Diederik Liebrand ^(d)

^(a) Bundesanstalt für Geowissenschaften und Rohstoffe, Hannover, Germany. E-mail: andre.bornemann@bgr.de

^(b) Institut für Geowissenschaften, Universität Heidelberg, Germany

^(c) Institut für Geowissenschaften, Johann Wolfgang Goethe-Universität Frankfurt, Germany

^(d) National Oceanography Centre, Southampton, University of Southampton, UK.

Document type: Abstract.

Manuscript history: received 15 May 2014; accepted 30 May 2014; editorial responsibility and handling by Gerald R. Dickens & Valeria Luciani.

KEY WORDS Mg/Ca, Miocene–Oligocene Transition, planktic foraminifera, stable isotopes, temperature.

The Oligocene represents an early stage of the Cenozoic icehouse world and is characterized by a high variability in the $\delta^{18}\text{O}$ of deep-sea benthic foraminifera and high-amplitude sea-level fluctuations probably related to southern hemisphere ice sheet instability. This variability culminates in a major glaciation event during the earliest Miocene ~23 Million years ago (Mi-1 event). High-quality data sets based of well-preserved planktic foraminifera across the Mi-1 event are scarce and limited to the low-latitudes and southern hemisphere. During IODP Expedition 342 expanded sequences covering the Oligocene to early Miocene transition have been drilled at J-Anomaly Ridge off Newfoundland. These sediments contain exceptionally well-preserved calcareous microfossils and are characterized by high sedimentation rates.

Pristinely preserved, “glassy” planktic foraminiferal tests were analyzed at a resolution of ≈ 20 kyrs to unravel the long-term climate evolution during the magnetochron interval C6AAr.2n/C6AAr.3r to C6Cn.3n/C6Cr across the Oligocene-Miocene Transition. To achieve this goal, a dual-proxy approach ($\delta^{18}\text{O}$, Mg/Ca) has been employed to estimate sea-surface and thermocline temperatures based predominantly on *Globigerinoides primordius* and *Catapsydrax dissimilis*, respectively. This approach allows for the reconstruction of North Atlantic surface ocean response to the Mi-1 event and how it has been influenced by global climate dynamics. First results show a very high variability in $\delta^{18}\text{O}$ and Mg/Ca for both mixed-layer and thermocline dwelling taxa pointing towards highly variable climatic and oceanographic conditions in the northwestern Atlantic. Both habitats record a distinct shift to heavier $\delta^{18}\text{O}$ and lower Mg/Ca values across the Mi-1 event, implying decreasing temperatures.

Warming, pelagic food webs and deep-sea biota during the Middle Eocene Climatic Optimum in the SE Atlantic (ODP Site 1263)

Flavia Boscolo Galazzo ^(a), Ellen Thomas ^(b,c), Mark Pagani ^(b), Courtney Warren ^(b), Luca Giusberti ^(a) & Valeria Luciani ^(d)

^(a) Department of Geosciences, University of Padova, Via Gradenigo 6, 35131, Padova, Italy. E-mail: flavia.boscologalazzo@studenti.unipd.it

^(b) Department of Geology and Geophysics, Yale University, 210 Whitney Ave, New Haven CT 0651, USA

^(c) Department of Earth and Environmental Sciences, Wesleyan University, Middletown, CT 06459, USA

^(d) Department of Physics and Earth Sciences, University of Ferrara, Via G. Saragat 1, 44121, Ferrara, Italy

Document type: Short note.

Manuscript history: received 15 May 2014; accepted 30 May 2014; editorial responsibility and handling by Gerald R. Dickens & Valeria Luciani.

KEY WORDS: global warming, foraminifera, MECO, organic matter recycling, Thaumarchaeota.

During the Middle Eocene Climatic Optimum (MECO), at about 40 Ma, oceanic temperature steadily increased by up to 4-5°C globally. MECO stands out as a transient but prolonged (~400 kyr) interval of warming interrupting the long term cooling starting in the early middle Eocene. The duration and pattern of warming across MECO, combined with the absence of a globally well-defined, coeval negative carbon isotope excursion (CIE) challenge our understanding of this warming event. Triggering mechanisms and carbon cycle feedbacks which may have fueled warming and $p\text{CO}_2$ rise during MECO are poorly understood.

We investigated the biotic response to MECO at Site 1263 (South-Eastern Atlantic), which has a continuous record not affected by carbonate dissolution (Bohaty et al., 2009), and well constrained middle-upper Eocene biostratigraphy (Fornaciari et al., 2010). We used coupled analysis of micropaleontological, stable isotope and biomarker (GDGTs) proxies across MECO, so we could reconstruct sea surface temperatures (SST) and biotic changes throughout the water column.

The benthic foraminiferal accumulation rate (BFAR), the coarse fraction and fine fraction accumulation rates (CFAR; FFAR) were used as proxies for benthic, planktic foraminiferal and nannoplankton productivity, and combined with taxonomic and quantitative analysis of benthic foraminiferal assemblages in the $\geq 63 \mu\text{m}$ size fraction.

Benthic foraminiferal assemblages contain significant percentages (>15%) of *Nuttallides umbonifera* and phytodetritus-exploiting taxa (PET) such as *Epistominella exigua*, *E. vitrea* and *Alabama weddellensis*, with the cumulative abundance of PET peaking close to 30%. *N. umbonifera* and the PET are extant, and globally widespread in the deep-sea. The relative abundance of *N. umbonifera* and PET markedly increased after the early Oligocene and during the Neogene (e.g., Thomas, 2007), and they are considered indicators of typical “Ice-house” conditions, living in cold,

carbonate-corrosive bottom waters (*N. umbonifera*), at intense seasonality (PET). PET and *N. umbonifera* have been reported in benthic foraminiferal oceanic assemblages since at least the early Eocene (Thomas, 1989; D’haenens et al., 2012; Ortiz and Thomas, 2012), but such high relative abundances in the middle Eocene have not been documented before. Our data, combined with previous studies, indicate that *N. umbonifera* and PET were gradually gaining abundance locally to regionally throughout the Eocene, in parallel with the gradual cooling trend leading to the onset of the “Ice-house” world by the earliest Oligocene.

TEX₈₆ indicates a gradual, 4-5°C SST increase across MECO, followed by an abrupt cooling to pre-event temperatures after peak warming. Deep waters cooled to a similar degree.

FFAR remained unchanged throughout the studied period. In contrast, BFAR and CFAR gradually decreased across MECO, with lowest accumulation rates during peak-MECO warming. All major components (>5%) of the benthic foraminiferal assemblage decreased in accumulation rate during MECO, while epifaunal taxa and specifically *N. umbonifera* and PET show the sharpest decline. Despite changes in relative abundance, the faunal composition remained unchanged throughout the studied interval, without appearance/disappearance of taxa.

Biomarkers analyses indicate a significant increase in abundance of the Archeal group Thaumarchaeota across MECO, coinciding with the strongly decreasing foraminiferal accumulation rates. Thaumarchaeota are ammonia-oxidizing chemoautotrophs, thought to be the most important nitrifiers in the ocean. Their increase across MECO suggests increased remineralization rates of organic matter in the water column, leading to greater amounts of ammonia available for Thaumarchaeota uptake, in agreement with observations that warming enhances organisms’ metabolic rates and the transfer of organic matter between trophic levels (O’Connor et al., 2009; Ma et al., 2014). The decrease in BFAR during MECO warming, indicates a progressive reduction in the amount of organic matter arriving at the sea-floor in an already food-limited environment. The parallel decrease in CFAR indicates

a reduction in heterotroph planktic foraminiferal productivity, while FFAR indicates unchanged nannoplankton (i.e., autotroph) production. The reduction of planktic foraminiferal production and BFAR suggests heterotroph starvation, and increased recycling of organic matter in the water column, as an effect of warmth-enhanced metabolism in poorly productive waters. Photosynthetic rates are less responsive to warming (O'Connor et al., 2009), and may have been limited by nutrients limitation.

Together these data suggest that increased temperature during MECO was the main factor affecting marine biota at Site 1263, through a cascade effect on pelagic food webs and the transfer of organic carbon to the sea-floor.

REFERENCES

- Bohaty S.M., Zachos J.C., Florindo F. & Delaney M.L. (2009) - Coupled greenhouse warming and deep-sea acidification in the Middle Eocene. *Paleoceanography*, 24, PA2207.
- D'Haenens S., Bornemann A., Stassen P. & Spejer R.P. (2012) - Multiple early Eocene benthic foraminiferal assemblage and $\delta^{13}\text{C}$ fluctuations at DSDP Site 401 (Bay of Biscay-NE Atlantic). *Mar. Micropaleontol.*, 88-89, 15-35.
- Fornaciari E., Agnini C., Catanzariti R., Rio D., Bolla E.M. & Valvasoni E. (2010) - Mid-Latitude calcareous nannofossil biostratigraphy and biochronology across the middle to late Eocene transition. *Stratigraphy*, 7(4), 229-264.
- Ma Z., Gray E., Thomas E., Murphy B., Zachos J. C. & Paytan A. (2014) - Carbon sequestration during the Paleocene-Eocene Thermal maximum by an efficient biological pump. *Nat. Geosci.*, 7, 382-388.
- Ortiz S. & Thomas E. (2012) - Deep-sea turnover during the Ypresian-Lutetian transition, the inception of the Cenozoic global cooling trend. 34th IGC World Congress, Brisbane, Australia, 5-10 August 2012.
- O'Connor M., Piehler M.F., Leech D.M., Anton A. & Bruno J.F. (2009) - Warming and resource availability shift food web structure and metabolism. *Plos Biology*, 7(8), 1-6.
- Thomas E. (1989) - Development of Cenozoic deep-sea benthic foraminiferal faunas in Antarctic waters. *Geological Society London Special Publication*, 47, 283-296.
- Thomas E. (2007) - Cenozoic mass extinctions in the deep sea: What perturbs the largest habitat on Earth? In: Monechi, S., Coccioni, R., and Rampino, M.R., (Eds.). *Large Ecosystem Perturbations: Causes and Consequences*. Geological Society of America Special Paper, 424, 1-23.

Strengthening of North Atlantic deep water production from the Norwegian-Greenland Sea at onset of the Eocene cooling trend

Adele J. Cameron ^(a), Philip F. Sexton ^(a), Pallavi Anand ^(a), Manuela A. Fehr ^(a,b) & Howie D. Scher ^(c)

^(a) Department of Earth Sciences, Open University, Walton Hall, Milton Keynes, MK7 6AA, UK. E-mail: Adele.Cameron@open.ac.uk

^(b) Now at Institute for Mineralogy and Petrology, Clausiusstrasse 25, ETH Zürich, CH-8092 Zürich, Switzerland

^(c) Department of Earth and Ocean Sciences, University of South Carolina, Columbia, SC 29208, USA

Document type: Short note.

Manuscript history: received 15 May 2014; accepted 30 May 2014; editorial responsibility and handling by Gerald R. Dickens & Valeria Luciani.

KEY WORDS: deep-water formation, Eocene, fish teeth, Neodymium, North Atlantic, ocean circulation.

The meridional overturning circulation (MOC) is a planetary-scale oceanic flow that is of direct importance to the climate system because it transports heat, salt and nutrients to high latitudes and regulates the exchange of CO₂ with the atmosphere. The MOC is strongly influenced by the large temperature gradient between the warm equator and the cold polar regions, something that was largely absent (Bijl et al. 2009) during the acute global warmth of the early Eocene (Sexton et al. 2006; Zachos et al. 2008; Pross et al. 2012). It is currently poorly understood how ocean circulation may have operated without such a strong temperature gradient, and specifically, there is little existing geological data with which to determine whether an Atlantic MOC even existed during this warmth.

Here, we investigate changes in ocean circulation and water mass geometry in the North Atlantic throughout the early to middle Eocene using the neodymium isotopic signature of fossil fish teeth from three IODP drill sites. We utilise expanded and continuous sequences from two sites in the North west Atlantic spanning the early to middle Eocene recently recovered on IODP Exp. 342 that are located on the South East Newfoundland Ridge, directly in the flow path of today's Deep Western Boundary Current. We also present data from a third site (ODP Site 647), situated further north at the mouth of the Labrador Sea.

Neodymium isotopes act as a geochemical tracer of deep-water masses because the ¹⁴³Nd/¹⁴⁴Nd ratio (ϵ Nd) of water masses shows distinct isotopic patterns related to different sources of weathering inputs from surrounding continental rocks (Goldstein & Hemming 2003). We find that, through the early Eocene (~50.5 Myr ago), lower abyssal and mid-abyssal waters at Newfoundland consistently registered ϵ Nd values around -10, very similar to published ϵ Nd from the southern Atlantic (Walvis Ridge) (Via & Thomas 2006). However, contemporaneous early Eocene ϵ Nd from Site 647 at the mouth of the Labrador Sea reveal much lower values (by 1 to 2 ϵ Nd units), characteristic of a signature partially derived from the ancient unradiogenic source rocks surrounding the Labrador

Sea. We then find a major change in North Atlantic water mass compositions at the early to middle Eocene transition (~ 47.5 Myr ago) where abyssal waters at Newfoundland and those at the mouth of the Labrador Sea show large and rapid ~1.5 unit ϵ Nd excursions in opposite directions so that their ϵ Nd values converge. This ϵ Nd convergence occurs concurrently with the onset of sediment drift formation at Newfoundland (Expedition 342 Scientists, 2012) and is best explained by a sudden strengthening in deep water export from the Norwegian-Greenland Sea that overwhelmed the distinctive negative ϵ Nd signature of waters sourced from the Labrador Sea. Our findings suggest that deep water export from the Norwegian-Greenland Sea intensified at the start of the Cenozoic cooling trend but may not have penetrated as far south as the southern Atlantic until the middle Oligocene (Via & Thomas 2006).

REFERENCES

- Bijl P.K., Schouten S., Sluijs A., Reichert G.-J., Zachos J.C. & Brinkhuis H. (2009) - Early Palaeogene temperature evolution of the southwest Pacific Ocean. *Nature*, 461(7265), 776–779.
- Expedition 342 Scientists (2012) - Paleogene Newfoundland sediment drifts. IODP Prel. Rept., 342. doi:10.2204/iodp.pr.342.2012
- Goldstein S.L. & Hemming S.R. (2003) - Long-lived Isotopic Tracers in Oceanography. *Paleoceanography and Ice Sheet Dynamics*. *Earth*, 6, 453–489.
- Pross J., Contreras L., Bijl P.K., Greenwood D.R., Bohaty S.M., Schouten S., Bendle J.A., Röhl U., Tauxe L., Raine J.I., Huck C.E., van de Flierdt T., Jamieson S.S.R., Stickley C.E., van de Schootbrugge B., Escutia C., Brinkhuis H. & IODP Expedition 318 Scientists (2012) - Persistent near-tropical warmth on the Antarctic continent during the early Eocene epoch. *Nature*, 488(7409), 73–77.
- Sexton P.F., Wilson P.A. & Norris R.D. (2006) - Testing the Cenozoic multisite composite $\delta^{18}\text{O}$ and $\delta^{13}\text{C}$ curves: new monospecific Eocene records from a single locality, Demerara Rise (Ocean Drilling Program Leg 207). *Paleoceanography*, 21, 1–17.

Via R.K. & Thomas D.J. (2006) - Evolution of Atlantic thermohaline circulation: Early Oligocene onset of deep-water production in the North Atlantic. *Geology*, 34(6), 441-446.

Zachos, J.C., Dickens G.R. & Zeebe R.E. (2008) - An early Cenozoic perspective on greenhouse warming and carbon-cycle dynamics. *Nature*, 451, 279-283.

Mammal faunal response to the ETM2 and H2 hyperthermals

Amy Chew ^(a)

^(a) Department of Anatomy, Western University of Health Sciences, 309 E 2nd St, Pomona, CA, USA. E-mail: achew@westernu.edu

Document type: Short note.

Manuscript history: received 15 May 2014; accepted 30 May 2014; editorial responsibility and handling by Gerald R. Dickens & Valeria Luciani.

KEY WORDS: Bighorn Basin, Eocene, mammals, terrestrial paleoecology, Wasatchian.

Multiple perturbations in marine isotope records indicate that global climate warmed rapidly (~10-20 ka) several times during the early Eocene. The largest of these ‘hyperthermals’ is the Paleocene/Eocene Thermal Maximum (PETM), which has been identified on land and to which mammalian response has been thoroughly documented. Two smaller hyperthermals, Eocene Thermal Maximum 2 (ETM2=H1) and H2, occurred ~2 ma after the PETM, but their effects on terrestrial ecosystems are currently unknown. The carbon isotope excursions (CIEs) of ETM2 and H2 have been located in paleosol carbonate nodules from the McCullough Peaks area of the Bighorn Basin, Wyoming (Abels et al., 2012). The levels of these CIEs can be extrapolated to the Fifteenmile Creek (FC) stratigraphic section in the central part of the Bighorn Basin, where a dense, highly-resolved, well-documented mammal record chronicles the Wa-0 fauna that existed during the PETM and ~3 ma of subsequent faunal evolution. The FC record is ideal for high-resolution, multi-parameter paleoecological analysis to test faunal response to ETM2 and H2.

More than 30,000 mammal specimens (124 species) were previously collected (1975-2010) from 410 fossil localities tied to ~200 m (>1 ma) of the FC section around Biohorizon B, a major faunal event that precedes ETM2 by ~60 ka (Abels et al., 2012). Numeric ages were assigned to the FC section between three tie points and the levels of ETM2 and H2 were predicted (at ~410-420m and ~430-440 m, respectively) by compressing the McCullough Peaks carbon isotope record by 68% between common event levels (Fig 1A). Four series of the shortest possible (5-8 m), equal-time (~30~50 ka) data bins were created through an exhaustive search. The binned data were standardized by an iterative, re-sampling algorithm. Relative body size was approximated by the natural-log transformed occlusal surface area of complete lower first molars. Rates of species first and last appearances (F, L), alpha (α) and beta (β) richness, and ‘inclusive abundance’ (A) and inverse dominance (D) indices were calculated as in previous work (Chew, 2009; Chew and Oheim, 2013) with some modifications. *Gamma richness* (γ) = $\alpha + \beta$. *Evenness* (E) = $A + D$. *Diversity* (D) = $\gamma +$

E. *Turnover* (T) = F + L. Parameter values for each bin were assigned to all meter levels within that bin and averaged by meter level across all bins.

Log-likelihood G ratios of the D and T parameters indicate three peaks in biotic change (~371-393 m, ~406-417 m and 439-447 m, Fig. 1A). This analysis significantly refines previous work (Chew, 2009) based on 18-23 m (~100 ka) specimen data bins, in which Biohorizon B was thought to be ~40 m thick (370-410 m, ~240 ka). This analysis demonstrates two distinct events within that 40-meter zone, separated by ~13 m (~80 ka) of pre-event parameter values. The lowest peak contains the distinctive biostratigraphic events conventionally referred to Biohorizon B. The middle and upper peaks are referred to here as biohorizons C and D, which correspond closely (within <10 m) with the predicted levels of the ETM2 and H2 CIEs. Biohorizons C and D differ substantially from Biohorizon B as follows: 1) their T peaks consist of equal proportions of F and L versus 76% F at Biohorizon B, and 2) their D peaks are almost entirely related to jumps in β and D (temporarily decreased dominance of assemblages by the two most common lineages) versus increases in α and A (evenness of the majority of species abundances) at Biohorizon B. Major differences in faunal change at the biohorizons compared with that at Wa-0 (response to the PETM) include (Fig. 1B): 1) the magnitude of change is greatest at Wa-0, intermediate at Biohorizon B and smallest at biohorizons C and D, and 2) at Wa-0 no species increase in size compared to preceding close relatives or intraspecific populations (Secord et al., 2012), whereas ~12% of species at the biohorizons increase in relative size.

There are several indications that biohorizons C and D represent faunal responsiveness to ETM2 and H2. 1) Biohorizons C and D correspond closely to the predicted levels of the ETM2 and H2 CIEs. 2) Biohorizons C and D most closely resemble each other in all aspects of faunal change described here, the simplest explanation for which is a similar trigger. 3) Faunal change at biohorizons C and D is broadly similar to that at Wa-0, including comparably structured turnover, standing richness gains and decreases in body size, which may be under-reported at the biohorizons by an additional ~25% in Fig. 1B. 4) The magnitude of faunal change at biohorizons C and D is ~33% and ~47%, respectively,

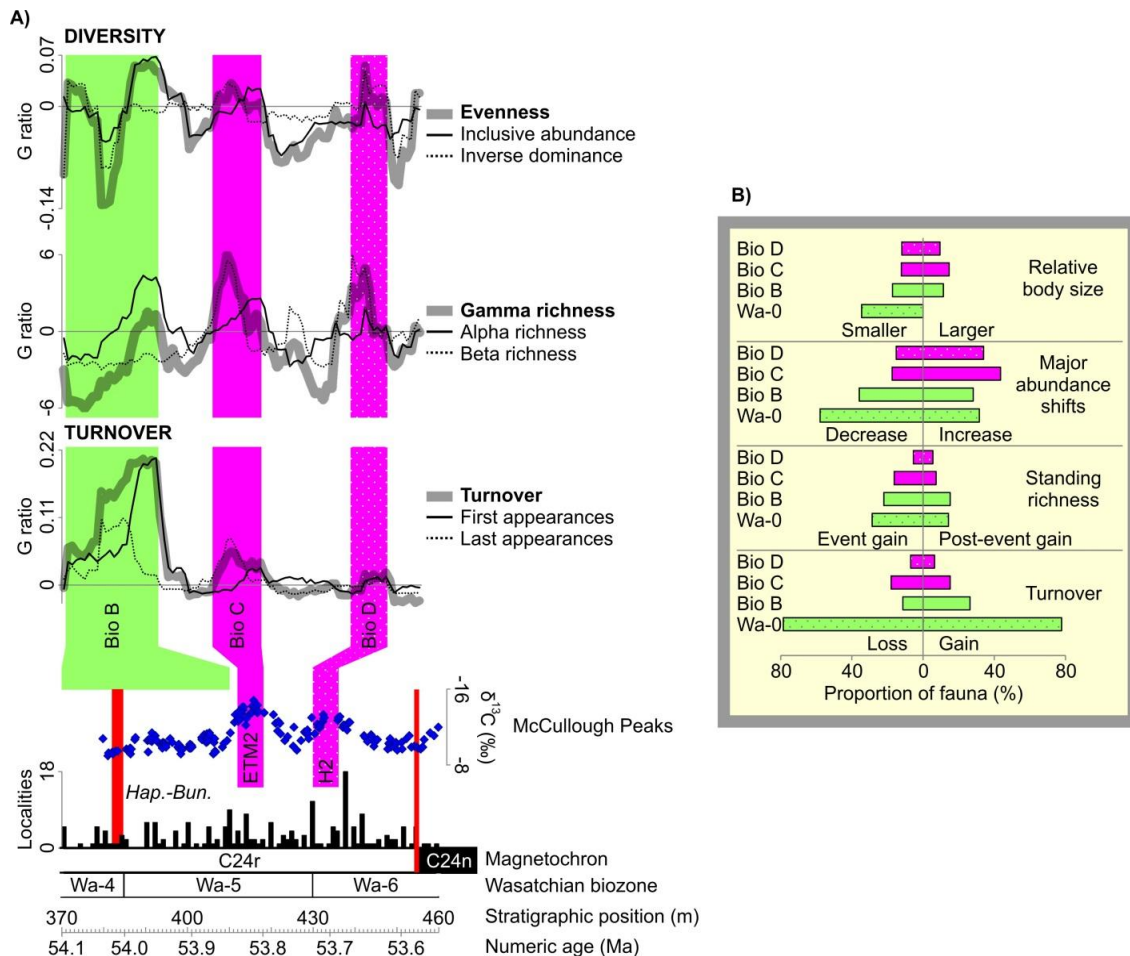


Fig.1 – Results of high-resolution multi-parameter paleoecological analysis and comparison with faunal change at the Paleocene-Eocene Thermal Maximum (Wa-0). **A)** Fossil localities from the Fifteenmile Creek (FC), central Bighorn Basin, Wyoming, USA. Interpolated numeric ages, early Eocene (Wasatchian North American Land Mammal Age) biozones, and paleomagnetic chrons are provided. The levels of ETM2 and H2 are predicted in the FC section by linearly compressing the Upper Dear Creek carbon isotope record (Abels et al., 2012) by 68% between the C24r-C24n geomagnetic shift (thin red line) and the last appearance of the condylarth *Haplomyilus*/first appearance of the artiodactyl *Bunophorus* (thick red line). Biohorizon B is a faunal event that was previously described. Log-likelihood G ratios of diversity parameters were binned, standardized specimen data (resolution ~30–50 ka) use randomized parameter sequences for expected values. **B)** Turnover: the proportion of species prior to the event that disappear versus the proportion of species within the event that are new. Standing richness: temporary range-through richness gains within each event versus lasting gains (~55–200 ka) after each event. Major abundance shifts: the proportion of species that range-through each event that decrease or increase in relative abundance by >50%. Relative body size: the proportion of species in each event that are smaller or larger than close relatives or intraspecific populations, as documented by Secord et al. (2012) for Wa-0 and as >3% change in natural-log transformed lower first molar surface area for the biohorizon assemblages.

smaller than at Wa-0 (except for turnover but the scale of magnitude of turnover between biohorizons C and D is consistent). This is proportional to the magnitude of the PETM, ETM2 and H2 CIEs, which is probably proportional to the magnitude of climate and environmental change (Abels et al., 2012). Similar scaling of biotic response in marine plankton at ETM2 and H2 has also been observed.

The major differences between Wa-0 and biohorizons C and D probably reflect different conditions at the start of the hyperthermals. The substantial differences between Biohorizon B and biohorizons C and D probably reflect different ecological processes. It has been speculated that Biohorizon B was also related to warming. If so, these results suggest a potential threshold response to warming at a different (probably lower) rate or a combination of factors, in contrast with a direct, linear response to rapid warming at Wa-0, ETM2 and H2.

REFERENCES

- Abels H.A., Clyde W.C., Gingerich P.D., Hilgen F.J., Fricke H.C., Bowen G.J. & Lourens L.J. (2012) - Terrestrial carbon isotope excursions and biotic change during Paleogene hyperthermals. *Nature Geosci.*, 5(5), 326–329.
- Chew A.E. (2009) - Paleoecology of the Early Eocene Willwood mammal fauna from the central Bighorn Basin, Wyoming. *Paleobiol.*, 35(1), 13–32.
- Chew A.E. & Oheim K.B. (2013) - Diversity and climate change in the middle-late Wasatchian (early Eocene) Willwood Formation, central Bighorn Basin, Wyoming. *Palaeo., Palaeo., Palaeo.*, 369, 67–78.
- Secord R., Bloch J.I., Chester S.G.B., Boyer D.M., Wood A.R., Wing S.L., Kraus M.J., McInerney F.A. & Krigbaum J. (2012) - Evolution of the earliest horses driven by climate change in the Paleocene-Eocene Thermal Maximum. *Science*, 335(6071), 959–962.

Bighorn Basin Coring Project (BBCP): An IODP-Style Continental Coring Project Investigating Early Paleogene Hyperthermals

William C. Clyde ^(a), Philip D. Gingerich ^(b), Scott L. Wing ^(c) & the BBCP Science Team ^(d)

^(a) Department of Earth Sciences, University of New Hampshire, Durham, NH 03824. E-mail: will.clyde@unh.edu

^(b) Department of Earth and Environmental Sciences, University of Michigan, 2534 CC Little Building, Ann Arbor, MI 48109

^(c) Department of Paleobiology, Smithsonian Institution National Museum of Natural History, NHB MRC 121 P.O. Box 37012, Washington, DC 20013

^(d) Bighorn Basin Coring Project Science Team – See <http://earth.unh.edu/clyde/team.shtml> for complete list

Document type: Short note.

Manuscript history: received 15 May 2014; accepted 30 May 2014; editorial responsibility and handling by Gerald R. Dickens & Valeria Luciani

KEY WORDS: Bighorn Basin, Continental Scientific Drilling, Eocene, Paleocene, PETM.

The Bighorn Basin of northwestern Wyoming (USA) preserves one of the thickest and most complete stratigraphic records of the early Paleogene period on Earth and its outcrops and fossils have been studied in detail for over a century. High-resolution proxy records like those typical of IODP projects, however, are difficult to develop using outcrops because of ubiquitous surface weathering, incomplete exposures, and the imprecision of measuring surface stratigraphic sections. During the summer of 2011, the Bighorn Basin Coring Project (BBCP) recovered over 900m of overlapping core from 3 different sites in late Paleocene to early Eocene Bighorn Basin fluvial deposits. These cores can be correlated to nearby surface sections which provide important additional paleontological and sedimentological information. By integrating core and outcrop records in this way, it is possible to combine information that is only available from outcrop records (e.g. macrofossils) with proxy records that have temporal resolution similar to (or in some cases higher than) comparable records from deep sea cores.

The BBCP cores are being used to investigate the Paleocene–Eocene Thermal Maximum (PETM) and Eocene Thermal Maximum 2 (ETM2) hyperthermal events to better understand what caused them, reveal the various biogeochemical and ecological feedbacks that operated during them, and measure their precise impact on continental sedimentary and biological systems. All of the drill sites were characterized by greater than 98% core recovery and most drilling was carried out without fluid additives, showing that continuous coring of continental smectitic deposits like these can be achieved with little risk of contamination to molecular biomarkers. Cores were processed (and are currently archived) in the Bremen Core Repository where the BBCP science team carried out IODP-like data collection and sampling protocols. Previous investigations of outcrops near the BBCP drill sites allow detailed evaluation of the effects of weathering on common proxy methods. Studies of lithofacies, organic

geochemistry, stable isotope geochemistry, calibrated XRF core scanning, paleomagnetism, and palynology are underway and will represent the highest resolution and most integrated proxy records of the PETM from a continental setting yet known. An extensive outreach program is in place to capitalize on the educational value associated with the Bighorn Basin's unusually complete record of Phanerozoic earth history.

Initial results show (1) the weathered horizon extends to as much as 30m below the surface (Clyde et al., 2013), (2) variations in magnetic susceptibility within the cores record an interplay between grain size and pedogenesis (Clyde et al., 2013), (3) there is an abrupt decline in organic carbon preservation at the beginning of the PETM that extends for whole body of CIE (Baczynski et al., 2014), and (4) the existence of a pronounced negative $\delta^{13}\text{C}$ excursion immediately prior to the onset of the PETM (Maibauer et al., 2012).

ACKNOWLEDGMENTS

This project is funded by NSF collaborative grants 0958821, 0958717, 0958975, 0958904, 1261312, 0958951, 0958583, and by the Deutsche Forschungsgemeinschaft (DFG).

REFERENCES

- Maibauer B.J., Bowen G.J., Srinivasaraghavan V., VanDeVelde J.H., Wing S.L., Gingerich P.D., Clyde W.C. & BBCP Science Team (2012) - High-resolution, high-fidelity carbon isotope stratigraphy of the Paleocene-Eocene Thermal Maximum in northern Wyoming from cores recovered by the Bighorn Basin Coring Project, American Geophysical Union Annual Fall Meeting, Abstract PP34A-02.
- Baczynski A.A., Barclay R.S., Bowen G.J., Denis E.H., Freeman K.H., Harrington G.J., Jardine P.E., Maibauer B., McInerney F.A. & Wing S.L. (2014) - Effects of the Paleocene-Eocene Thermal Maximum on terrestrial plants and carbon storage, 10th North American Paleontological Convention, Florida Museum of Natural History, Abstract Book, Paleontological Society, p. 131.

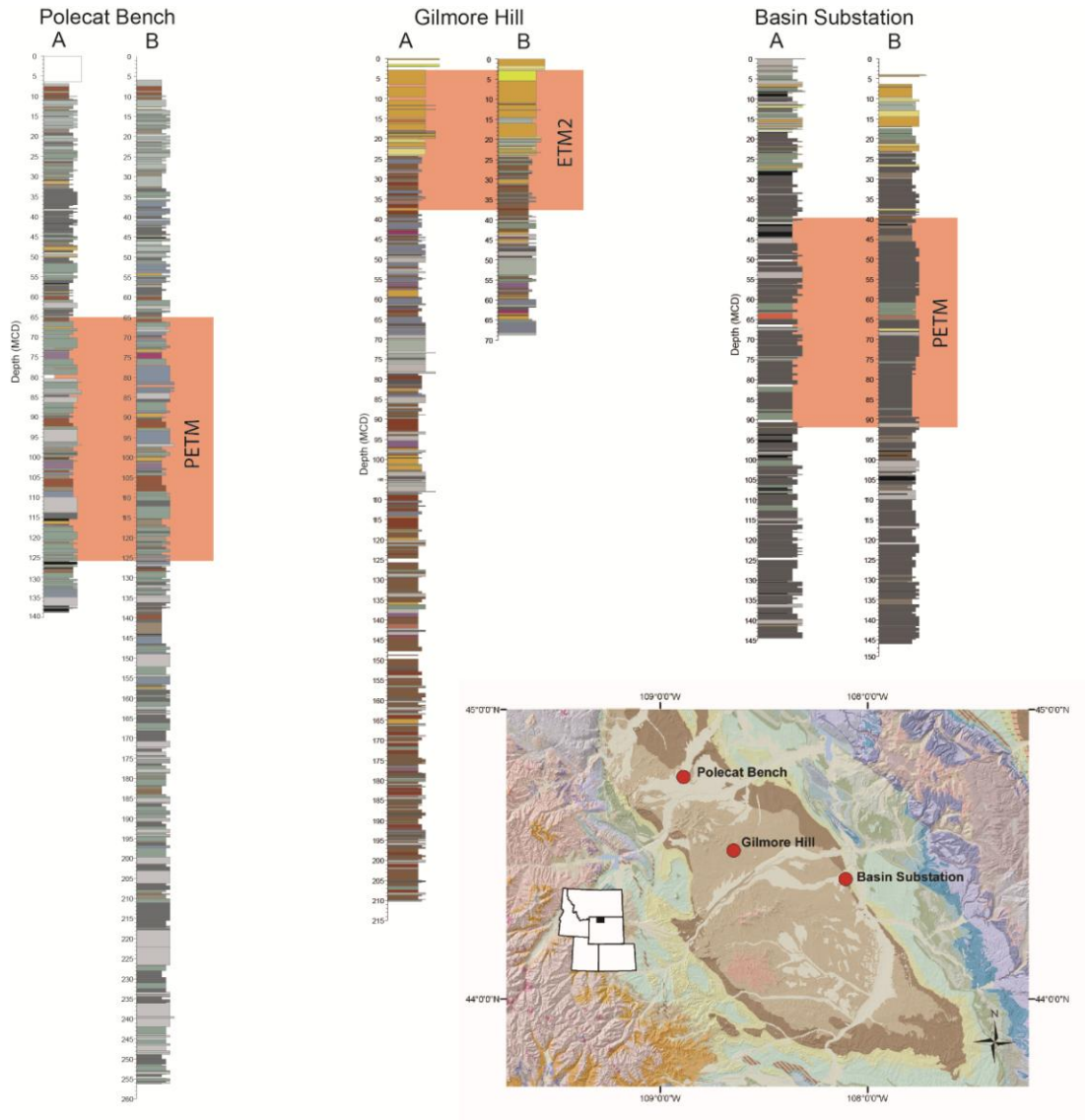


Fig.1 – Summary lithostratigraphic logs of the BBCP cores. Core was recovered from two overlapping drill holes at each of three sites in the basin (Polecat Bench, Gilmore Hill, and Basin Substation). Stratigraphic intervals of the targeted hyperthermals are highlighted by red shading (PETM for Polecat Bench and Basin Substation, ETM2 for Gilmore Hill).

Clyde W.C., Gingerich P.D., Wing S.L., Röhl U., Westerhold T., Bowen G., Johnson K., Baczynski A.A., Diefendorf A., McInerney F., Schnurrenberger D., Noren A., Brady K. &

the BBCP Science Team. (2013) - Bighorn Basin Coring Project (BBCP): a continental perspective on early Paleogene hyperthermals. *Scientific Drilling* 16, 21-31, doi:10.5194/sd-16-21-2013.

Climatic and environmental changes in the Paratethys during Oligocene traced by changes in calcareous nannoplankton assemblages (Molasse Basin, Austria and Kamchia Depression, Bulgaria)

Stjepan Čorić^(a)

^(a) Department of Sedimentology, Geological Survey of Austria, Neulinggasse 38, A-1030 Vienna, Austria. E-mail: stjepan.coric@geologie.ac.at

Document type: Short note.

Manuscript history: received 15 May 2014; accepted 30 May 2014; editorial responsibility and handling by Gerald R. Dickens & Valeria Luciani.

KEY WORDS: calcareous nannoplankton, Kamchia Basin, Molasse Basin, Oligocene, palaeoecology, Paratethys, stratigraphy.

Deep marine succession in the Austrian part of the Molasse Basin (the Central Paratethys) was analyzed on calcareous nannoplankton to precise the stratigraphical position of investigated cores. Variations in nannoplankton assemblages were used to trace palaeoecologic and palaeogeographic changes during the early/middle Oligocene.

The Eggerding Formation, typically about 45 m thick, forms part of the deep marine Oligocene succession in the Molasse Basin, which comprises from bottom to top the Schöneck (formerly “Fish Shale”), Dynow (“Bright Marlstone”), Eggerding (“Banded Marl”) and Zupfing formations (“Rupelian Marl”).

Additionally, the sediments of the Eggerding Formation and the lower part of the Zupfing Formation have been studied using core and cutting samples and a multidisciplinary approach involving core description, geochemistry and palynology (Sachsenhofer et al. 2010). The studied interval overlies the Dynow Formation dated as lower/middle nannoplankton Zone NP23 (middle Rupelian; Martini, 1971). Apart from zonal markers, bio-events caused by paleogeographical and paleoecological changes are important for the stratigraphic subdivision of Oligocene sediments in the Central Paratethys.

The Dynow Formation and the lower part of the Eggerding Formation have been deposited during nannoplankton Zone NP 23 corresponding to middle Rupelian, whereas the base of the Zupfing Formation was deposited during NP 24 (Rupelian to Chattian). The predominantly non-calcareous Šitborice Member of the Menilitic Formation in the western Carpathian Foreland Basin (NE Vienna) overlies the Dynow Marlstone and is about 40 m thick (Picha & Stranik, 2005). It is considered a time-equivalent to the Eggerding Formation and the lowermost Zupfing Formation. Among five low-diversity assemblages in the Šitborice Member, Bubik (1991) recognized an assemblage with a high dominance of *Cyclicargolithus floridanus*.

This horizon is placed into upper NP23 to lower NP24. High percentages of *C. floridanus*, *Reticulofenestra bisecta*, *R. ornata* and *Sphenolithus moriformis*, occurred during the upper NP23 and NP24, indicate a coeval bio-event caused by warmer climate during this part of the Oligocene.

The Eggerding Formation deposited in near-shore environments contains several sand layers. In contrast, the Eggerding Formation deposited along the northern slope is generally poor in sand (Sachsenhofer et al., 2010). Its lower part consists of dark grey laminated shaly marlstone with white bands rich in coccolithophorides. The Eggerding Formation is overlain by the Zupfing Formation, consisting of clay-marls up to 450 m thick.

Similar changes of palaeoecological conditions mainly caused by isolation and reopening of the Paratethys during Oligocene were documented in the Eastern Paratethys (Kamchia Depression, Western Black Sea) in investigated core and cutting samples from four offshore wells (Sachsenhofer et al., 2009).

Nannoplankton analyses were restricted to the Avren Formation (Eocene/lowermost Oligocene), Russlar Formation (Oligocene) and Galata Formation (Miocene) respectively. Russlar Formation calcareous nannoplankton has been detected in the lower part of unit II and in the upper part of unit IV. Assemblages of lower part of unit II are characterized by blooms of endemic nannoplankton with common *Reticulofenestra ornata*, and regular *Reticulofenestra lockeri*, *Pontosphaera multipora*, *P. pax* and *P. fibula*. Rare specimen of small reticulofenestrids, *Braarudosphaera bigelowii*, *Reticulofenestra daviesii*, and *R. umbilica* are restricted to a few samples.

Blooms of endemic calcareous nannoplankton with *Reticulofenestra ornata*, *Pontosphaera pax*, and *P. fibula* characterize the lowermost part of NP23 (lower Solenovian). Mono- and duospecific assemblages of endemic nannoplankton were observed on many localities in the Central and Eastern Paratethys and have been related to high productivity caused by high nutrient input and decreased salinity. Rare nanofossils with *Reticulofenestra lockeri* and *Pontosphaera desueta*,

which occur in upper part of Unit IV allows the attribution of this interval to the NP24/25 (upper Solenovian/Kalmykian).

Dysoxic to anoxic conditions together with meso-to euhaline salinities prevailed during deposition of the Ruslar Formation. Within this frame, relatively high oxygen contents occurred during early Solenovian times (NP23), when bright marls were deposited in a sea with reduced salinity ("Solenovian event"; lower part of Unit II). Brackish surface water favoured nannoplankton blooms with endemic *Reticulofenestra ornata* co-occurring with *P. pax* and *P. fibula*

REFERENCES

- Bubik M. (1991) - Low diversity calcareous nannoplankton assemblages from the Oligocene Sitborice Member of the Menilitic Formation (West Carpathians, Czechoslovakia) from Bystrice nad Olsi. In: B. Hamrsmid and J. Young (eds.), Proceedings of the 4th INA Conference, Prague 1991, Nannoplankton Research, Vol. II: Tertiary Biostratigraphy and Paleoecology; Quaternary coccoliths, Prague, pp. 223-246.
- Martini E. (1971) - Standard Tertiary and Quaternary calcareous nannoplankton zonation. In: A. Farinacci (ed.), Proceedings of the II Planktonic Conference. Edizioni Tecnoscienza, Roma, 739-785.
- Picha F. J. & Stranik Z. (2005) - Late Cretaceous to early Miocene deposits of the Carpathian foreland basin in southern Moravia. International Journal Earth Sciences, 88, 475-495
- Sachsenhofer R.F., Leitner B., Linze, H.-G.R., Bechtel A., Ćorić S., Reinhard Gratzner R., Reischenbacher D. & Soliman A. (2010) - Deposition, Erosion and Hydrocarbon Source Potential of the Oligocene Eggerding Formation (Molasse Basin, Austria). Austrian J. Earth Sci., 103/1, 76 – 99.
- Sachsenhofer R. F., Stummer B., Georgiev G., Dellmour R., Bechtel A., Gratzner R. & Ćorić S. (2009) - Depositional environment and hydrocarbon source potential of the Oligocene Ruslar Formation (Kamchia Depression; Western Black Sea). Marine and Petroleum Geology, 26, 57–84.

First evidence of the Palaeogene age of the Bosnian Flysch Unit (Dinarides, Bosnia and Herzegovina)

Stjepan Ćorić^(a) & Josip Benić^(b)

^(a) Department of Sedimentology, Geological Survey of Austria, Neulinggasse 38, A-1030 Vienna, Austria. E-mail: stjepan.coric@gmail.com

^(b) Faculty of science, University of Zagreb, Horvatovac 102A, 10000 Zagreb, Croatia.

Document type: Short note.

Manuscript history: received 15 May 2014; accepted 30 May 2014; editorial responsibility and handling by Gerald R. Dickens & Valeria Luciani.

KEY WORDS: Bosnian Flysch, calcareous nannoplankton, Dinarides, Palaeocene, stratigraphy.

Pre Karst and Bosnian Flysch Unit tectonically belong to the Dinarides, spreading from Croatia in the northwest to Serbia and Montenegro in the southeast (Fig. 1). The main part of Bosnia Flysch Unit however is placed in Bosnia and Herzegovina. This tectonic unit is sandwiched between the High Karst Unit of the External Dinaridic Platform in the south and the Dinaride Ophiolite Zone in the north. It forms an about 3000m thick stack of intensely folded rocks, comprising two formations: Ugar Fm. and Vranduk Fm. Investigations of calcareous nanofossils (Mikes et al., 2008) documented a Late Cretaceous age for the Ugar Fm. and Latest Jurassic-Early Cretaceous age for the Vranduk Fm.

Sedimentation of the Flysch started during the latest Jurassic and became progressively younger in the more external parts (Schmid et al. 2008). The age of this unit is generally and traditionally regarded as the Upper Cretaceous, according to sheets of Geological map (OGK, Osnovna Geološka Karta; 1:100.000).

The investigated area is situated in Western Bosnia, NE of the city of Jajce, locality Donji Bospelj (Fig. 1). During prospecting for bauxite in this area, a detailed geological mapping and intensive drill campaign were performed.

Stratigraphic investigation of calcareous nannoplankton was performed on 20 samples from the Donji Bospelj - Daljevac flysch section and borehole DB2. Standard methods were used for the preparation of smear slides, which were analysed under the microscope in normal and cross-polarized light at x1000 magnification. All investigated samples yielded generally well preserved calcareous nanofossil assemblages allowing stratigraphic attribution of this part of the Bosnian Flysch succession.

Calcareous are abundant in this Upper Cretaceous assemblage, but are moderately preserved nannoplankton. The occurrence of *Micula prinsii* in the assemblage including *Arkhangelskiella cymbiformis*, *Arkhangelskiella*

maastrichtiana, *Eiffellithus gorkae*, *Micua decussata*, *Micula murus*, *Placozygus fibuliformis*, *Prediscosphaera cretacea* etc., allows attribution to the uppermost Maastrichtian Subzone UC20d (Burnett, 1998). Accumulation of Palaeocene sediments from Danian to Thanetian was documented by the nannoplankton Zones NP1-NP9 (Martini, 1971). Nannoplankton Zone NP1 was documented by the occurrence of *Biantholithus sparsus* in the assemblage with high percentage of *Thoracosphaera* spp. The assemblage of Zone NP2 is characterised by a large amount of *Coccolithus pelagicus* co-occurring together with: *Braarudosphaera bigelowii*, *Cruciplacolithus tenuis*, *Ericsonia subpertusa*, *Markalius inversus*, *Placozygus sigmoides* etc. Nannoplankton Zones NP3-NP8 contain zone markers: *Chiasmolithus danicus*, *Ellipsolithus macellus*, *Fasciculithus tympaniformis*, *Heliolithus kleinpellii* and *Heliolithus riedelii*. Stratigraphically youngest sediments contain calcareous nannoplankton with *Discoaster multiradiatus*, *D. lenticularis*, *D. delicatus* and can be attributed to the NP9 (uppermost Palaeocene; Thanetian).

Beside Palaeocene sediments occurring in the High Karst Unit in North Bosnia (covering Ophiolitic Units), this is the very first documentation of sediments in this part of Dinarides.

REFERENCES

- Burnett, J. A., Gallagher, L. T. & Hampton, M. J. (1998) - Upper Cretaceous. In P. R. Bown, ed., *Calcareous Nanofossil Biostratigraphy*. British Micropalaeontological Society Publication Series. Vol. c. London: Chapman and Hall, 133-199.
- Martini E. (1971) - Standard Tertiary and Quaternary calcareous nannoplankton zonation. - *Proceedings of the II Planktonic Conference*, (Ed. Tecnoscienza), Roma, 739-785.
- Mikes, T., Christ, D., Petri, R., Dunkl, I., Frei, D., Báldi-Beke, M., Reitner, J., Wemmer, K., Hrvatović, H. & von Eynatten, H. (2008) - Provenance of the Bosnian Flysch. *Swiss J. Geosci.* 101 (2008) Supplement 1, 31-54.

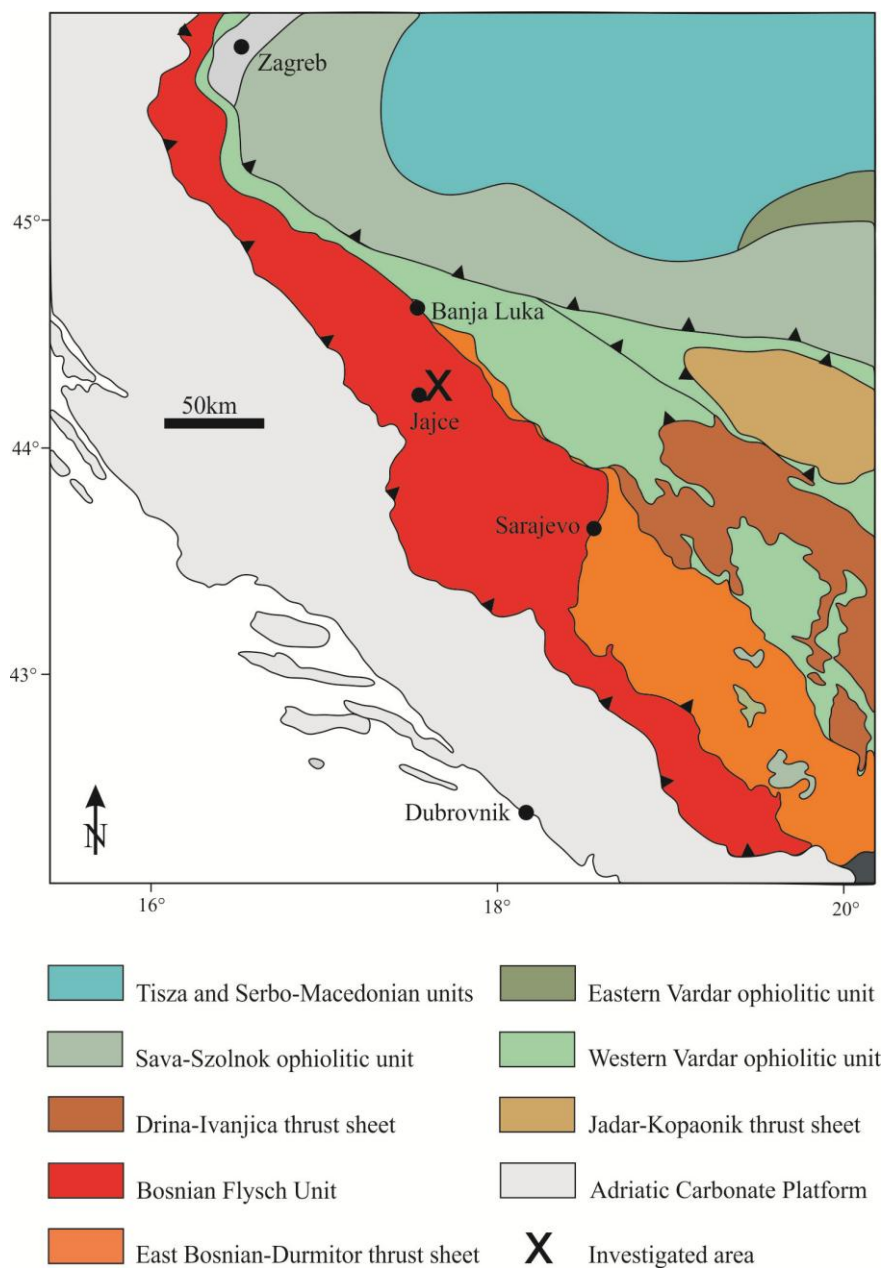


Fig. 1 - Bosnian Flysch and major structural units of Dinarides (after Schmid et al. 2008; Mikes et al. 2008)

Osnovna Geološka Karta SFRJ: Geological maps of former Yugoslavia, 1: 100.000, Beograd, Savezni Geoloski Zavod.

Schmid, S.M., Bernoulli, D., Fügenschuh, B., Matenco, L., Schefer, S., Schuster, R., Tischler, M. & Ustaszewski, K.

(2008) – The Alpine-Carpathian-Dinaridic orogenic system: correlation and evolution of tectonic units. *Swiss J. Geosci.* 101, 139 – 183.

Strengthening of North Atlantic deep-water production pre-dates onset of Antarctic glaciation

Helen Coxall ^(a), Caroline Lear ^(b), Jan Backman ^(a), Matt O'Regan ^(a), Claire Huck ^(c), Tina van De Flierdt ^(c), Kasia K. Sliwinska ^(d,e) & James C. Zachos ^(f)

^(a) Department of Geological Sciences, Stockholm University, SE-106 91 Stockholm, Sweden. E-mail: helen.coxall@geo.su.se

^(b) School of Earth, Ocean and Planetary Sciences, Cardiff University, Main Building, Park Place, Cardiff CF10 3YE, UK

^(c) Department of Earth Science and Engineering, Imperial College London, South Kensington Campus, London SW7 2AZ, UK

^(d) Geological Survey of Denmark and Greenland, GEUS, Øster Voldgade 10, DK-13, Copenhagen K, Denmark

^(e) NIOZ Royal Netherlands Institute for Sea Research, Department of Marine Organic Biogeochemistry, P.O. Box 59, 1790 AB Den Burg, Texel, The Netherlands

^(f) Earth Sciences Department, University of California, Santa Cruz, CA 95064, USA

Document type: Short note.

Manuscript history: received 15 May 2014; accepted 30 May 2014; editorial responsibility and handling by Gerald R. Dickens & Valeria Luciani.

KEY WORDS: benthic foraminifera, deep water circulation, Early Oligocene, Late Eocene, North Atlantic.

This document is a template created with Microsoft Word version Global ocean circulation is today dominated by the northern transport of warm salty surface water in the North Atlantic and sinking of cool dense water in high latitude Southern Ocean and North Atlantic basins. The Atlantic component of this system, known as the Atlantic Meridional Overturning Circulation (AMOC), plays a prominent role in a range of climatically relevant processes, redistributing heat, salt, carbon, nutrients and moisture across latitudes and connects the Atlantic, Pacific and Indian Oceans via the 'global conveyor' system (Broecker, 1991; de Boer et al., 2008). Episodes of pronounced climate change in the late Cenozoic, including extensive northern hemisphere glaciations, involved shifts between 'deep' (vigorous) and 'shallow' (weak) versions of the AMOC with corresponding decreases and increases in deep water production in the southern hemisphere (Broecker, 1998; Toggweiler et al., 2006). Such changes are well studied on Pleistocene glacial-interglacial timescales, however, the early history of the AMOC and its role surrounding major climatic tipping points in the early Cenozoic climate is uncertain.

A variety of sedimentary and geochemical evidence indicate that the initial evolution of the AMOC and the transition to a bipolar mode of deep-water circulation, involving significant production and export of North Atlantic deep water into the global conveyor, occurred close to the Eocene-Oligocene boundary (E/O) but the precise timing and relation to Early Oligocene Antarctic glaciation remains unconstrained. A significant obstacle to resolving these questions is that most high latitude North Atlantic deep sea drill sites spanning the E/O interval are (i) interrupted by hiatuses attributed to increased circulation and glacioeustatic sea-level fall associated with Antarctic ice-sheet growth (Miller et al., 1991), or (ii) lack fossilized sea-floor living (benthic)

foraminifera, suitable for deep sea geochemical proxy reconstructions. Consequently, existing evidence for North Atlantic Eocene-Oligocene deep-water circulation is indirect (hiatuses and drifts), down stream of potential sites of downwelling and often poorly constrained in time. In this study we present the first detailed multi proxy record of Late Eocene-Early Oligocene bottom water conditions in the high latitude North Atlantic from southern Labrador Sea ODP Site 647. Drilled in 1985 during ODP Leg 105 (Srivastava et al., 1987), this remains the northernmost (53°N) Atlantic carbonate-bearing deep sea sequence spanning the E/O interval, uniquely capturing deep ocean conditions in a vastly understudied and climatically sensitive corner of the Atlantic. Subsidence modeling of Site 647, accounting for effects of sedimentation and porosity loss during burial, eustatic sea level changes and

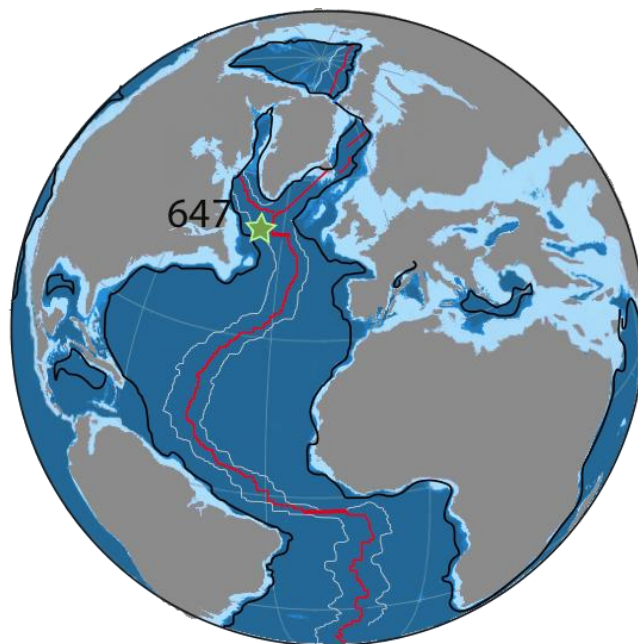


Fig. 1 – Paleogeographic setting of ODP Site 647 34 Ma.

sediment loading on the crust, show that Site 647 remained in bathyal water depths (3200-3500) throughout the late Eocene and early Oligocene.

Previous investigations using material from this site (Arthur et al., 1989) suggested that Eocene foraminifera stable isotope signals were compromised by early diagenetic processes. However, we show that the foraminifera preserved in Site 647 hemipelagic clays are exceptionally well preserved, show no evidence for significant alteration or appreciable change in preservation down core, and record very unusual bottom water conditions in the Late Eocene greenhouse North Atlantic.

Our new Site 647 stable isotope records show that during the Late Eocene (37-34 Ma) Site 647 benthic $\delta^{18}\text{O}$ is notably lighter than all other Atlantic sites by 1-2 ‰ indicating a considerably warmer or fresher deep-water mass occupying the southern Labrador Sea at this time. The occurrence of authigenic carbonates (siderite and rhodochrosite) in sediments, high concentrations of the redox sensitive trace metals Fe and Mn in benthic foraminiferal calcite, combined with a dominance of agglutinated over calcareous foraminifera (Miller et al., 1982; Ortiz & Kaminski, 2012), indicates restricted bottom water circulation, with low oxygen content, high organic carbon supply and/or low pH. Site 647 benthic $\delta^{18}\text{O}$ values gradually increased from approximately 36 Ma, in parallel with the gradual disappearance of Fe and Mn rich minerals, exit of agglutinated benthic foraminifera-dominated assemblages and an increase in calcareous species. Significantly, Site 647 benthic $\delta^{18}\text{O}$ converges on to the typical Atlantic and Pacific benthic $\delta^{18}\text{O}$ trend approximately 400 thousand years prior to the onset of E/O Antarctica glaciation. We suggest that this pattern documents the progressive ventilation of the southern Labrador Sea to bathyal depths (<2000-3000 m) and critical connection of the North Atlantic into a global deep conveyor system caused by onset of deep water production in the high latitude North Atlantic region, most likely sourced from the Norwegian-Greenland Seas in response to a critical deepening of the Greenland-Scotland Ridge.

Fossil fish teeth from Site 647 record a distinctly northern hemisphere Nd character throughout the Late Eocene to Early Oligocene suggesting bottom water from a North Atlantic or possibly Tethys source. The similarity in Nd isotopic composition of potential areas of North Atlantic deepwater production (excluding the Labrador Sea) mean that there is no appreciable change in Nd during the studied interval, although there is an indication of increased variability from ~34.5 Myrs ago. This is attributed to times of increased fluxes of unradiogenic Nd from the surrounding continents to the North Atlantic basin. The appearance of northern character Nd signature in South Atlantic sediments close to the E/O boundary found previously (Via & Thomas, 2006) records the initial export of North Atlantic sourced deep waters across the

equator, representing an early step in the development of a globally significant AMOC.

Our results provide the first direct geochemical evidence defining sluggish circulation and/or only weak overturning in the high latitude North Atlantic during the Late Eocene and to show that the fundamental switch in circulation mode predates Antarctic glaciation. Connection of the North Atlantic into the global thermohaline circulation to form a proto- AMOC could have played a role in driving Late Eocene global cooling and Eocene-Oligocene Antarctic glaciation through changes in heat and nutrient transport affecting the Southern Oceans.

REFERENCES

- Arthur M.A., Dean W.E., Zachos, J.C., Kaminski M., Hagerty Rieg S. & Elmstrom K (1989) - Geochemical expression of early diagenesis in middle Eocene-lower Oligocene pelagic sediments in the southern Labrador Sea, Site 647, ODP Leg 105. In Srivastava, S.P., Arthur, M.A., Clement, B. et al. (eds.), Proc. of the ODP, Sci. Res., Volume 105: College Station, TX, ODP, 111-135.
- Broecker W.S (1991) - The great ocean conveyor: Oceanography, The Changing Arctic Ocean, Special Issue on the International Polar Year (2007–2009), 4,79–89.
- Broecker W.S. (1998) - Paleoocean circulation during the last deglaciation: A bipolar seesaw?. *Paleoceanography*, 13, 119-121.
- de Boer A.M., Toggweiler J.R. & Sigman D.M. (2008) - Atlantic dominance of the meridional overturning circulation. *J. Phys. Oceanogr.*, 8, 435-450.
- Miller K.G., Gradstein F.M. & Berggren W. A (1982) - Late Cretaceous to Early Tertiary agglutinated benthic foraminifera in the Labrador Sea. *Micropaleont.*, 28, 1-30.
- Miller K.G., Wright J. & Fairbanks R. (1991) - Unlocking the icehouse: Oligocene-Miocene oxygen isotopes, eustasy and margin erosion. *J. Geophys. Res.*, 96, 6829-6848.
- Ortiz S. & Kaminski, M. (2012) - Record of deep-sea benthic elongate-cylindrical foraminifera across the Eocene-Oligocene transition in the North Atlantic Ocean (ODP Hole 647A). *JFR*, 42, 345-368.
- Srivastav, S.P., Arthur M., Clement B. et al. (1987) - Proc. of the ODP, Initial Reports, Volume 105: College Station, TX, ODP.
- Toggweiler J.R., Russell J.L. & Carson S.R. (2006) - Midlatitude westerlies, atmospheric CO₂ and climate change during the ice ages. *Paleoceanography*, 21, PA2005.
- Via R.K., & Thomas D.J. (2006) - Evolution of Atlantic thermohaline circulation: Early Oligocene onset of deep-water production in the North Atlantic. *Geology*, 34, 441–444.

Early–middle Eocene magneto-biochronology of the Southern Pacific Ocean: new data from the South Island of New Zealand

Edoardo Dallanave ^(a), Valerian Bachtadse ^(a), Claudia Agnini ^(b), Giovanni Muttoni ^(c), Christopher J. Hollis ^(d), Benjamin R. Hines ^(d), Hugh E.G. Morgans ^(d), C. Percy Strong ^(d), Lisa Tauxe ^(e) & James S. Crampton ^(d)

^(a) Department of Earth and Environmental Sciences, Ludwig-Maximilians University, Theresienstrasse 41, 80333 München, Germany. E-mail: dallanave@geophysik.uni-muenchen.de

^(b) Department of Geosciences, University of Padova, via G. Gradenigo 6, 35131 Padova, Italy

^(c) Department of Earth Sciences, University of Milan, via Mangiagalli 34, 25133 Milano, Italy

^(d) Department of Paleontology, GNS Science, PB 30368, Lower Hutt 5040, New Zealand

^(e) Scripps Institution of Oceanography, UCSD, 9500 Gilman Drive, La Jolla, California, 92093-0220, USA

Document type: Short note.

Manuscript history: received 15 May 2014; accepted 30 May 2014; editorial responsibility and handling by Gerald R. Dickens & Valeria Luciani.

KEYWORDS: Early–middle Eocene, EECO, Magneto-biostratigraphy, MECO, Southern Ocean, Sedimentation rates.

The Eocene epoch records the transition from the warmest Earth's climate conditions of the Cenozoic era (i.e., the early Eocene climatic optimum –EECO–, ~52–50 Ma; e.g., Zachos et al., 2001) to the icehouse world, and the first permanent emplacement of the south polar ice sheet. To understand the nature and causes of global climatic change during this time period, it is critical to have well-dated sedimentary records at key representative sites across the planet. Great advances have been made in the last few years in understanding the paleoclimate history of the southwestern Pacific Ocean (e.g., Bijl et al., 2013; Hollis et al., 2012 and reference therein), but precise correlations between sites and global events remain uncertain. In many cases, this is due to poor preservation of calcareous plankton fossil assemblages (e.g. calcareous nannofossils), diachroneity of index species, and a lack of a extended and continuous magnetic polarity reversals record.

Here we present the uppermost Paleocene–middle Eocene magneto-biostratigraphy from the mid-Waipara River and the Mead Stream marine sections, which crop out on South Island, New Zealand (Fig. 1a). These sections represent an important archive of paleoceanographic changes that occurred in southern Pacific high-latitudes (50–60°S) during the early Paleogene. The parts of interest in these two sections span from the Paleocene–Eocene boundary, within magnetic polarity Chron C24r, to Chron C18n.1n (~56–39 Ma of GTS12, Gradstein et al., 2012; Fig. 1b). At mid-Waipara (~51.5–47 Ma), we used the magnetic polarity chronology to calibrate ages of several dinoflagellate cyst (dinocyst) and benthic foraminiferal

bioevents. These data provide the first magnetostratigraphically-calibrated age of 48.88 Ma for the base of the New Zealand Heretaungan stage (latest early Eocene). Using our age model, we calibrate the sea temperature proxy data available from mid-Waipara section (Hollis et al., 2012), integrating the dataset with coeval Southern Ocean records (Bijl et al., 2013) using dinocyst biostratigraphy-based correlation (Fig. 1c).

At Mead Stream, the magnetic polarity stratigraphy has been integrated with calcareous nannofossils and planktic foraminiferal biostratigraphy. The section spans from calcareous nannofossil Zone NP9a to Zone NP17 (CNP11–CNE15 following a recently revised Paleogene zonation; Agnini et al., in press) and from the Ypresian to Bartonian stages (Waipawan to the Bartonian following the New Zealand stages; Fig. 1b). The ages of calcareous nannofossil biohorizons are consistent with low to mid latitude data from the literature, indicating that during the early–middle Eocene the low–mid latitude calcareous nannofossil biogeographic province extended at least to ~50–55°S in the South Pacific. We also found that two intervals of relatively high sedimentation rates, derived by increased input of smectite-rich sediment (Morris, 1987), occurred during the EECO and during the transient climate warming culminating with the middle Eocene climatic optimum (MECO; 40.5 Ma; Fig. 1c). This correlation indicates that times with warmer climates are characterized by high rates of precipitation and erosion (see also Slotnick et al., 2012), associated with enhanced chemical weathering, as revealed by the presence of smectite in the sediments (Fagel, 2007). This mechanism controls the consumption of the atmospheric CO₂ through the weathering of silicate minerals on land, buffering the long-term climate variations of the Earth (Walker et al., 1981).

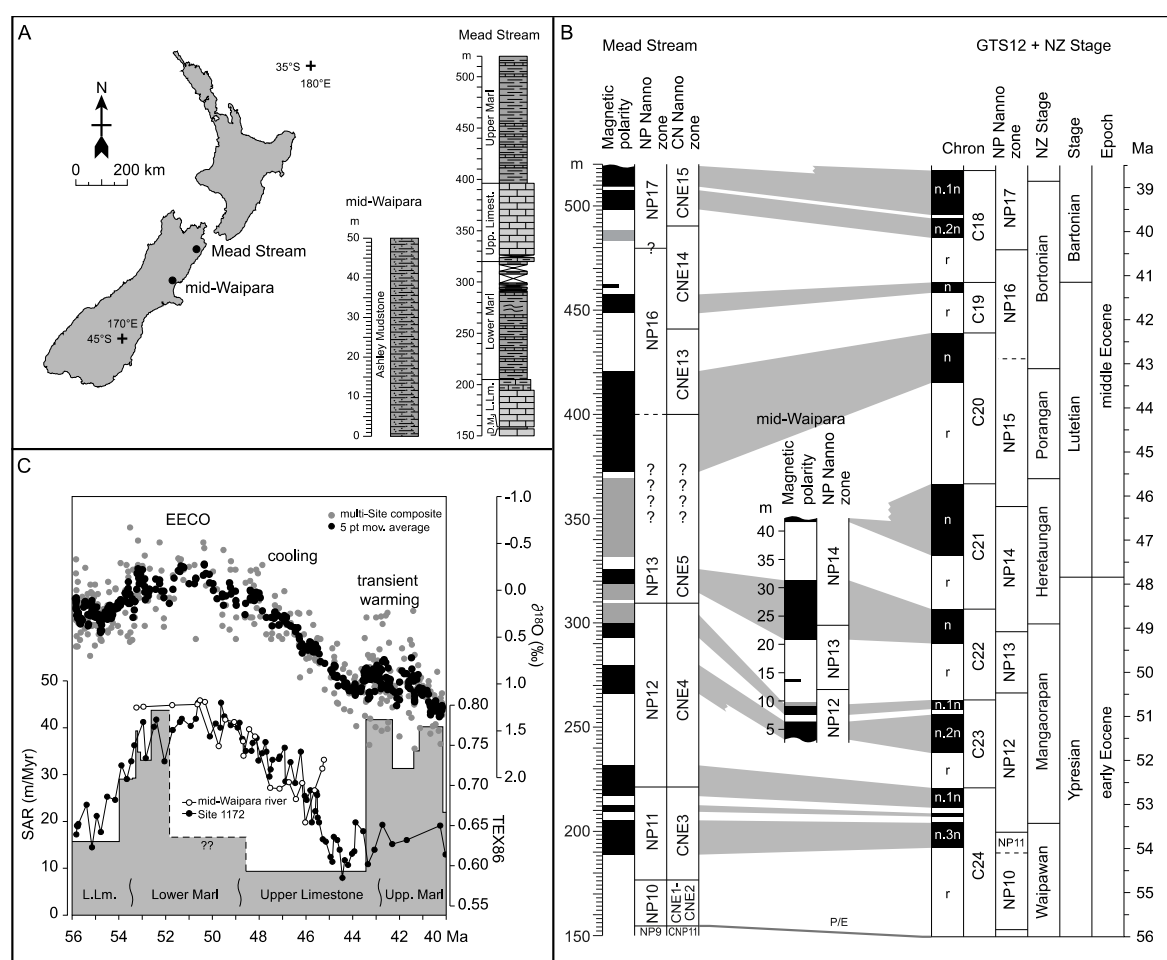


Fig.1 – A) Location and stratigraphy of the mid-Waipara and the Mead Stream sections (D.M.= Dee Marl; L. Lm.= Lower Limestone). B) Magnetostratigraphic correlation of the Mead Stream and the mid-Waipara sections with the GTS12 time scale (Gradstein et al., 2012). C) Sediment accumulation rates (SAR; gray area) compared with the paleoclimate proxy TEX₈₆ record from ODP Site 1172 and from the mid-Waipara River section as well as with the benthic oxygen isotope ($\delta^{18}\text{O}$) records of Zachos et al. (2001; global ocean).

REFERENCES

- Agnini C., Fornaciari E., Raffi I., Catanzariti R., Pälke H., Backman J. & Rio, D. (in press) - Biozonation and biochronology of Paleogene calcareous nannofossils from low and middle latitudes. *Newsletters Stratigr.*
- Bijl P.K., Bendle J.A.P., Bohaty S.M., Pross J., Schouten S., Tauxe L., Stickley C.E., McKay R.M., Röhl U., Olney M., Sluijs A., Escutia C. & Brinkhuis H. (2013) - Eocene cooling linked to early flow across the Tasmanian Gateway. *Proc. Natl. Acad. Sci. U. S. A.*, 110, 9645-9650.
- Fagel N. (2007) - Clay Minerals, Deep Circulation and Climate. In: Hillaire-Marcel C. & De Vernal A. (Eds.), *Developments in Marine Geology*, 1, 139-184, Elsevier, doi:10.1016/S1572-5480(07)01009-3.
- Gradstein F.M., Ogg J.G., Schmitz M.D. & Ogg G.M. (2012) - *The Geologic Time Scale 2012*. Elsevier.
- Hollis C.J., Taylor K.W.R., Handley L., Pancost R.D., Huber M., Creech J.B., Hines B.R., Crouch E.M., Morgans H.E.G., Crampton J.S., Gibbs S.J., Pearson P.N. & Zachos J.C. (2012) - Early Paleogene temperature history of the Southwest Pacific Ocean: Reconciling proxies and models. *Earth Planet. Sci. Lett.*, 349-350, 53-66.
- Morris J. C. (1987) - *The stratigraphy of the Amuri Limestone Group, east Marlborough, New Zealand*. University of Canterbury. PhD Thesis.
- Ogg J. & Smith A. (2012) - The geomagnetic polarity time scale. In: Gradstein F.M., Ogg J.G., Schmitz M.D. & Ogg G.M. (Eds.), *The Geologic Time Scale 2012*, Elsevier, 85-113.
- Slotnick B.S., Dickens G.R., Nicolo M.J., Hollis C.J., Crampton J.S., Zachos J.C. & Sluijs A. (2012) - Large-Amplitude Variations in Carbon Cycling and Terrestrial Weathering during the Latest Paleocene and Earliest Eocene: The Record at Mead Stream, New Zealand. *J. Geol.*, 120(5), 487505, doi:10.1086/666743.
- Zachos J.C., Pagani M., Sloan L., Thomas E. & Billups K. (2001) - Trends, rhythms, and aberrations in global climate 65 Ma to present. *Science* 292, 686-693.
- Walker J.C.G., Hays P.B., & Kasting J.F. (1981) - A negative feedback mechanism for the long-term stabilization of Earth's surface temperature. *J. Geophys. Res.*, 86(C10), 9776-9782.

Repetitive mammalian dwarfism associated with early Eocene carbon cycle perturbations

Abigail R. D'Ambrosia^(a), William C. Clyde^(a), Henry C. Fricke^(b) & Philip D. Gingerich^(c)

^(a) Dept. of Earth Sciences, University of New Hampshire, Durham, NH 03824, USA . E-mail: adambrosia@gmail.com

^(b) Dept. of Geology, Colorado College, Colorado Springs, CO 80903, USA

^(c) Dept. of Earth and Environmental Sciences, University of Michigan, Ann Arbor, MI 48109, USA

Document type: Short note.

Manuscript history: received 15 May 2014; accepted 30 May 2014; editorial responsibility and handling by Gerald R. Dickens & Valeria Luciani.

KEY WORDS: CIE, dwarfism, Eocene, ETM2, global warming, hyperthermal, PETM.

The geologic record of the early Paleogene is characterized by evidence of several successive carbon isotope excursions (CIE), associated with extreme bouts of global warming (Zachos et al., 2001; Stap et al., 2009). The largest of these events is known as the Paleocene-Eocene Thermal Maximum (PETM), and has been found in both marine and terrestrial records globally around 56 million years ago (Zachos et al., 2010). Additionally, the PETM has been found to coincide with fossil evidence of mammalian dwarfism from the Bighorn Basin of Wyoming (Clyde and Gingerich, 1998). Previous studies have suggested that dwarfism is an evolutionary response to increased global temperatures and/or high levels of atmospheric CO₂ (Gingerich, 2003; Gardner et al., 2011). Understanding the relationship between mammalian dwarfism and these ancient global warming events is useful for predicting effects of warming on modern mammalian taxa.

One method for understanding the relationship between atmospheric temperature, CO₂ concentration, and mammal body size is to evaluate these variables across multiple CIEs. However, records of CIEs other than the PETM have previously only been found in the marine realm. Recent geochemical analyses of paleosol carbonates within the Bighorn Basin have identified two successive smaller-magnitude CIEs, known as ETM2 and H2 (Abels et al., 2012), located in the stratigraphic record roughly two million years after the PETM.

To investigate whether mammalian dwarfism was a common occurrence associated with these younger CIEs, mammal teeth fossils were collected directly from stratigraphic sections within the Bighorn Basin, known to encompass ETM2 and H2 through geochemical analysis. Referred to as Gilmore Hill and White Temple, these sections are found within the McCullough Peaks region of the basin, and have been stratigraphically correlated to each other through the tracing of distinct marker beds as well as high-resolution carbon isotope

analyses of paleosol carbonates. Because tooth size is highly correlated to adult body size in mammals (Gingerich et al., 1982; Legendre, 1986), body size was tracked across the associated CIEs by measuring the total crown area (length multiplied by width) of lower molars. Carbon and oxygen isotope ratios of enamel from these same teeth will be used to directly track their relationship with the associated CIE (carbon), as well as atmospheric temperatures (oxygen).

Hyracotherium, one of the most commonly sampled mammalian lineages of the Bighorn Basin, exhibited the most distinct change in mean body size across ETM2. This particular mammalian equid lineage dwarfed in size ~19% from pre-ETM2 to mid-ETM2 records, coinciding with a -3.8‰ CIE. Following the peak CIE, *Hyracotherium* rebounded to its pre-ETM2 body size (when carbon isotope ratios returned to background values). These results are comparable to the PETM (-5.9‰ CIE), where the same lineage of equids decreases in body size by ~30% in records spanning the beginning of the PETM to the middle of the PETM (Secord et al., 2012). Similar patterns are also observed in *Diacodexis* (an artiodactyl) and *Cantius* (a primate), which decrease in body size by 22% and 7.7%, respectively, going into the middle of ETM2 (figure 1). Our results suggest that mammalian dwarfism is a common evolutionary response to rising levels of atmospheric CO₂ and/or increasing temperatures, and may even scale in relationship to the magnitude of a CIE.

ACKNOWLEDGMENTS

This project is funded by NSF collaborative grant 0958821.

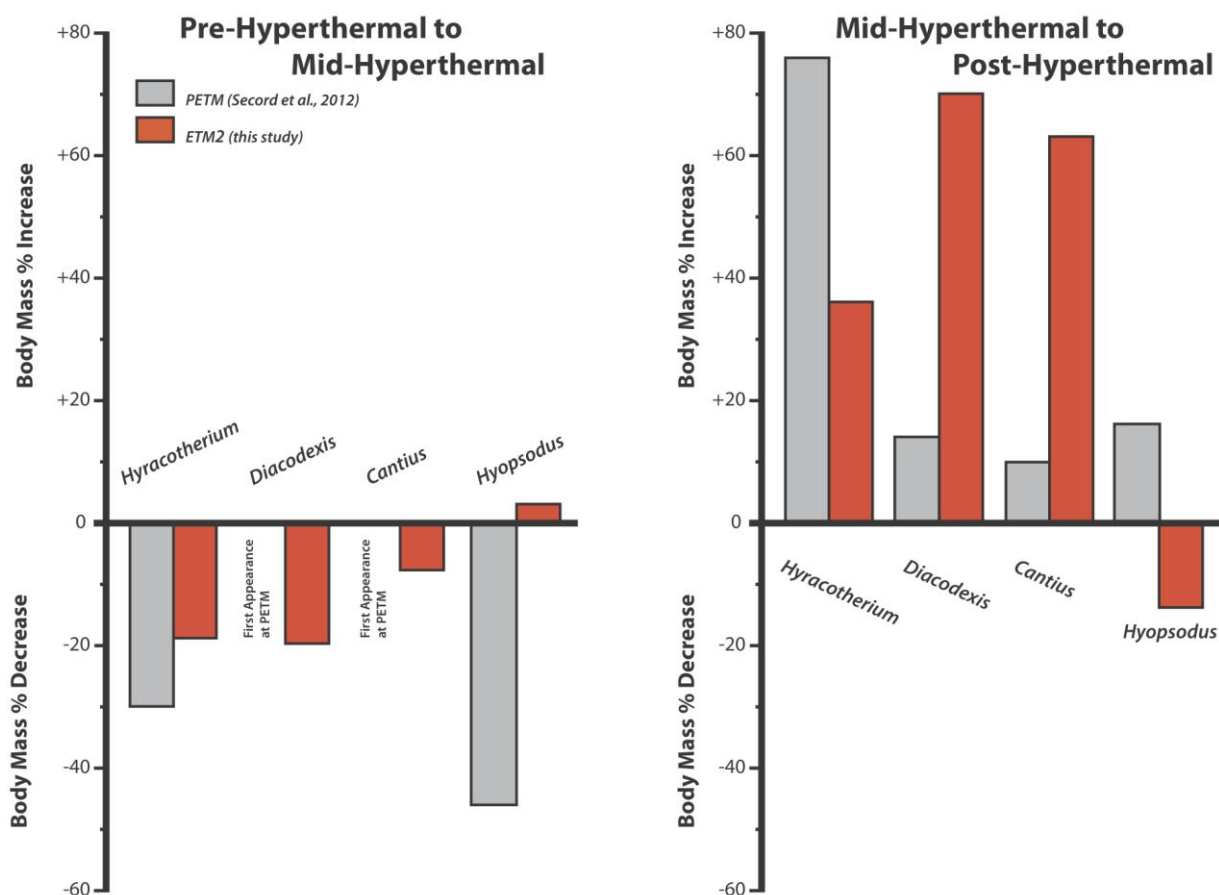


Fig.1 – Mammalian body size data for PETM (grey) and ETM2 (orange) lineages going into a CIE (left), and during the recovery of a CIE (right). Y-axes represent body size increase or decrease. Note that all lineages aside from *Hyopsodus* follow a similar dwarfism trend going into a CIE, followed by a rebound in body size in post-CIE records. Data for PETM come from Secord et al. (2012).

REFERENCES

- Abels H.A., Clyde W.C., Gingerich P. D., Hilgen F.J., Fricke H.C., Bowen G.J. & Lourens L. J. (2012) - Terrestrial carbon isotope excursions and biotic change during Paleogene hyperthermals. *Nature Geosci.*, 5, 326-329.
- Clyde W.C. & Gingerich P.D. (1998) - Mammalian community response to the latest Paleocene thermal maximum: an isotaphonomic study in the northern Bighorn Basin, Wyoming. *Geology*, 26, 1011-1014.
- Gardner J.L., Peters A., Kearney M.R., Joseph L. & Heinsohn R. (2011) - Declining body size: a third universal response to warming?. *Trends ecol. Evol.*, 26(6), 285-291.
- Gingerich P.D., Smith B.H., & Rosenberg K. (1982) - Allometric scaling in the dentition of primates and prediction of body weight from tooth size in fossils. *Am. J. Phys. Anthropol.*, 58(1), 81-100.
- Gingerich P.D. (2003) - Mammalian responses to climate change at the Paleocene-Eocene boundary: Polecat Bench record in the northern Bighorn Basin, Wyoming. *Special Papers-Geological Society of America*, 463-478.
- Legendre S. (1986) - Analysis of mammalian communities from the late Eocene and Oligocene of southern France. *Palaeovertebrata* 16, 191-212.
- Secord R., Bloch J.I., Chester S.G.B., Boyer D.M., Wood A.R., Wing S.L., Kraus M.J., McInerney F.A. & Krigbaum J. (2012) - Evolution of the earliest horses driven by climate change in the Paleocene–Eocene Thermal Maximum. *Science*, 335, 959–962.
- Stap L., Sluijs A., Thomas E. & Lourens L.J. (2009) - Patterns and magnitude of deep sea carbonate dissolution during Eocene Thermal Maximum 2 and H2, Walvis Ridge, southeastern Atlantic Ocean. *Paleoceanography*, 24(1), PA1211.
- Zachos J.C., Pagani M., Sloan L.C., Thomas E., & Billups K. (2001) - Trends, rhythms, and aberrations in global climate 65 Ma to present. *Science*, 292(5517), 686-693.
- Zachos J.C., McCarren H., Murphy B., Röhl U., & Westerhold, T. (2010) - Tempo and scale of late Paleocene and early Eocene carbon isotope cycles: Implications for the origin of hyperthermals. *Earth Planet. Sci. Lett.*, 299(1), 242-249.

Initial paleohydrological observations from the Paleocene-Eocene boundary at Esplugafreda and Berganuy in northern Spain

Alex Dawson ^(a), Stephen Grimes ^(a), Michael Ellis ^(b), Robert Duller ^(c), Matthew Watkinson ^(a), Martin Stokes ^(a), Melanie J. Leng ^(b)

^(a) School of Geography, Earth and Environmental Sciences, Plymouth University, UK. Email: alex.dawson@plymouth.ac.uk

^(b) British Geological Survey, Environmental Science Centre, Nottingham, UK

^(c) School of Environmental Sciences, University of Liverpool, Liverpool, UK

Document type: Short note.

Manuscript history: received 15 May 2014; accepted 30 May 2014; editorial responsibility and handling by Gerald R. Dickens & Valeria Luciani.

KEY WORDS: Berganuy, Carbon Isotope Excursion (CIE), climate, Esplugafreda, palaeopedology, palaeohydrology, Paleocene-Eocene Thermal Maximum (PETM).

The Paleocene Eocene Thermal Maximum (PETM) was a relatively short-lived (ca. 200kyr) climatic event characterized by the release of large amounts of ¹³C-depleted carbon and subsequent global warming (ca. 5-8°C; Sluijs et al., 2006). Despite the scientific attention the PETM has received, some contentious issues still remain regarding the response of the coupled climate-hydrological system.

Recent high resolution analyses of marine sediments from the North Sea and New Jersey shelf suggest an enhancement of the hydrological signal that may have occurred prior to the PETM (Sluijs et al., 2007a; Kender et al., 2012; John et al., 2008), which could be indicative of a more complex onset of carbon release. These records, however, come from relatively distal marine cores, such that signals related to terrestrial inputs are likely to be muted.

A test of this precursory phase in terrestrial successions is therefore required. This study builds on a plethora of high resolution delta ¹³C_{TOC}, ¹⁸O and clay records from the best-exposed PETM terrestrial successions ('Garumnian' or Tremp Group) in Europe at Esplugafreda and Berganuy in northern Spain (Schmitz & Pujalte, 2003; Schmitz & Pujalte, 2007; Domingo et al., 2009; Manners et al., 2013). Of particular importance within these sections is the presence of the Claret Conglomerate (CC), a laterally extensive conglomerate unit, representing a formative braid-plain that covered at least 500km². The coincidence of this unit with the Carbon Isotope Excursion (CIE) led Schmitz & Pujalte, (2007) to interpret this unit as the geomorphological and sedimentary response to an intensification of the hydrological cycle at the PETM (Schmitz & Pujalte, 2007). This study aims to capture and assess the associated hydrological changes that may have occurred prior to the CC and the onset of the PETM.

Here we present initial palaeohydrological observations from the Tremp Group, using qualitative and semi-quantitative techniques in palaeopedology to characterise the climatic

conditions existing prior to/during and post the PETM. A similar methodology was used to characterise paleosol development in late Paleocene-Eocene sediments in the Bighorn Basin, Wyoming, USA. This study demonstrated that palaeosols can be used to date and infer changes in sedimentary environments, induced by cyclical (Milankovitch) changes in climate (Aziz et al., 2008; Kraus et al., 2013). Therefore, palaeosol-based proxies have the potential to be amongst the most powerful tools for reconstructing the response and timing of terrestrial environments to climate change at the Spanish PETM sections.

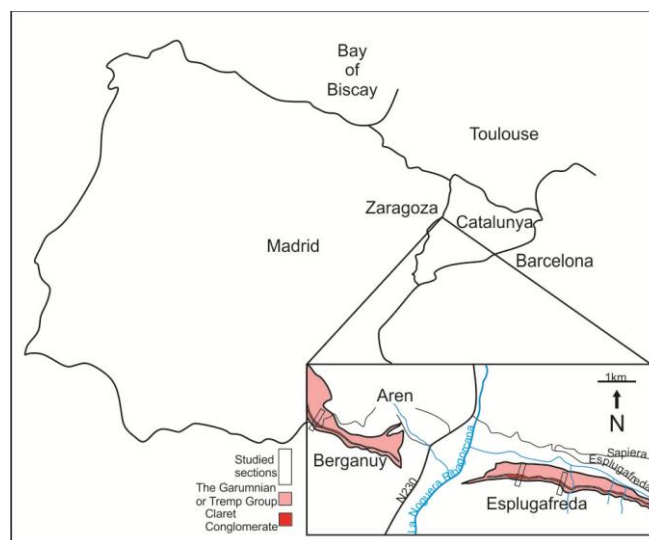


Fig.1 Map of Spain, showing the location of the Esplugafreda and Berganuy sections.

A new ¹³C_{TOC} profile from the Esplugafreda section reconfirms a temporal lag between the CIE and the deposition of the CC (Manners et al., 2013). Furthermore a detailed pedofacies analysis at Esplugafreda and Berganuy shows changes in soil colour from red (indicative of well drained, well oxidized conditions) towards grey/purple colours (moderate to poorly drained reducing conditions) ~17m before the CC and ~16m before CIE. A distinct yellow paleosol

horizon occurs above the CC and CIE, attributed to moderately drained conditions. Post the yellow interval sees a return to high chroma matrix colours. These features suggest a shift to wetter more poorly drained conditions pre and during the PETM, before partly recovering to pre PETM conditions. Pedofacies analysis also displays that there is a shift in the type of palaeosols present from compound and composite type profiles to cumulate type profiles, which has implications for sedimentation rates during the PETM.

In summary our initial observations in palaeopedology show a distinct shift in pedofacies relationships, pedogenic CaCO₃ formation and palaeosol colour before, during and post the onset of the CIE. This supports previous interpretations that changes in hydrology occurred prior to the onset of the CIE at Esplugafreda and Berganuy.

REFERENCES

- Aziz H.A., Hilgen F.J., van Luijk G.M., Sluijs A., Kraus M.J., Pares J.M. & Gingerich P.D. (2008) - Astronomical climate control on palaeosol stacking patterns in the upper Paleocene-lower Eocene Willwood Formation, Bighorn Basin, Wyoming. *Geology*, 36(7), 531-534.
- Domingo L., López-Martínez N., Leng M.J. & Grimes S.T. (2009) - The Paleocene-Eocene Thermal Maximum record in the organic matter of the Claret and Tendrúy continental sections (South Central Pyrenees, Lleida, Spain). *Earth Planet. Sc. Lett.*, 281 (3-4), 226-237.
- Kraus M.J., McInerney F.A., Wing S.L., Secord R., Baczynski A.A. & Bloch, J.I (2013) - Paleohydrologic response to continental warming during the Paleocene-Eocene Thermal Maximum, Bighorn Basin, Wyoming. *Palaeogeogr., Palaeoclimatol., Palaeoecol.*, 370, 196-208.
- Cédric M.J., Steven M.B., Zachos J.C., Sluijs A., Gibbs S.J., Brinkhuis H. & Bralower T.J. (2008) - North American continental margin records of the Paleocene-Eocene thermal maximum: Implications for global carbon and hydrological cycling. *Paleoceanography*, 23(2), PA 2217.
- Manners H.R., Grimes S.T., Sutton P.A., Domingo L., Leng M.J. Twitchett R.J., Hart M.B., Dunkley-Jones, T., Pancost R.D., Duller R. & Lopez-Martinez N. (2013) - Magnitude and profile of organic carbon isotope records from the Paleocene-Eocene Thermal Maximum: Evidence from northern Spain. *Earth Planet. Sc. Lett.*, 376, 220-230.
- Schmitz B. & Pujalte V. (2003) - Sea-level, humidity, and land-erosion records across the initial Eocene thermal maximum from a continental-marine transect in northern Spain. *Geology*, 31(8), 689-692.
- Schmitz B. & Pujalte V. (2007) - Abrupt increase in seasonal extreme precipitation at the Paleocene-Eocene boundary. *Geology*, 35, 215-218.
- Sluijs A., Schouten, S., Pagani M., Woltering M., Brinkhuis H., Damsté J.S.S., Dickens G.R., Huber M., Reichart G.-J., Stein R., Matthiessen J., Lourens L.J., Pedentchouk N., Backman J., Moran K., Clemens S., Cronin T., Eynaud F., Gattacceca J., Jakobsson M., Jordan R., Kaminski M., King J., Koc N., Martinez N.C., McInroy D., Moore Jr. T.C., O'Regan M., Onodera J., Pälike H., Rea B., Rio D., Sakamoto T., Smith D.C., St John K.E.K., Suto I., Suzuki N., Takahashi K., Watanabe M. & Yamamoto M. (2006) - Subtropical Arctic Ocean temperatures during the Palaeocene/Eocene Thermal Maximum. *Nature*, 441, 610-13.
- Sluijs A., Brinkhuis H., Schouten S., Bohaty S.M., John C.M., Zachos J.C., Reichart G.-J., Sinninghe Damsté J.S., Crouch E.M. & Dickens G.R. (2007) - Environmental precursors to rapid light carbon injection at the Paleocene/Eocene boundary. *Nature*, 450, 1218-1221.

Stable isotope and benthic foraminiferal records of the Latest Danian Event at ODP Site 1262 (Walvis Ridge)

Arne Depez (a), Sofie Jehle (b), André Bornemann(b,c) & Robert P. Speijer(a)

(a) Department of Earth and Environmental Sciences, KU Leuven, Celestijnenlaan 200E, 3001 Leuven, Belgium. E-mail: arne.depez@ees.kuleuven.be

(b) Institut für Geophysik und Geologie, Universität Leipzig, Talstr. 35, 04103 Leipzig, Germany

(c) Bundesanstalt für Geowissenschaften und Rohstoffe, Stillweg 2, 30655 Hannover, Germany

Document type: Short note.

Manuscript history: received 15 May 2014; accepted 30 May 2014; editorial responsibility and handling by Gerald R. Dickens & Valeria Luciani.

KEY WORDS: benthic foraminifera, hyperthermal, Latest Danian Event, Paleocene, stable isotope, Walvis Ridge

Superimposed on the warm greenhouse climate of the early Paleogene, several transient climate events, e.g. the Latest Danian Event (LDE, 61.8 Ma), the Paleocene-Eocene Thermal Maximum (PETM, 56 Ma) and Eocene Thermal Maximum 2 (ETM2, 54 Ma) were observed. Of these, the Paleocene-Eocene Thermal Maximum (PETM; c. 56 Ma) is the most

extreme and best studied example. The LDE (or Top Chron 27n Event) is characterized by a >1 ‰ negative benthic foraminiferal CIE in various sections in Egypt, which has been correlated to $\delta^{13}\text{C}$ shifts of ~ 0.7 ‰ in Zumaia (Spain), Wombat Plateau (ODP 761B, Indian Ocean) and Shatsky Rise (ODP 1209, Pacific Ocean) (Bornemann et al., 2009; Westerhold et al., 2011). Westerhold et al. (2011) calculated a distinct 2°C bottom water temperature rise during this event at ODP Site 1209 (Shatsky Rise), suggesting a hyperthermal nature for this

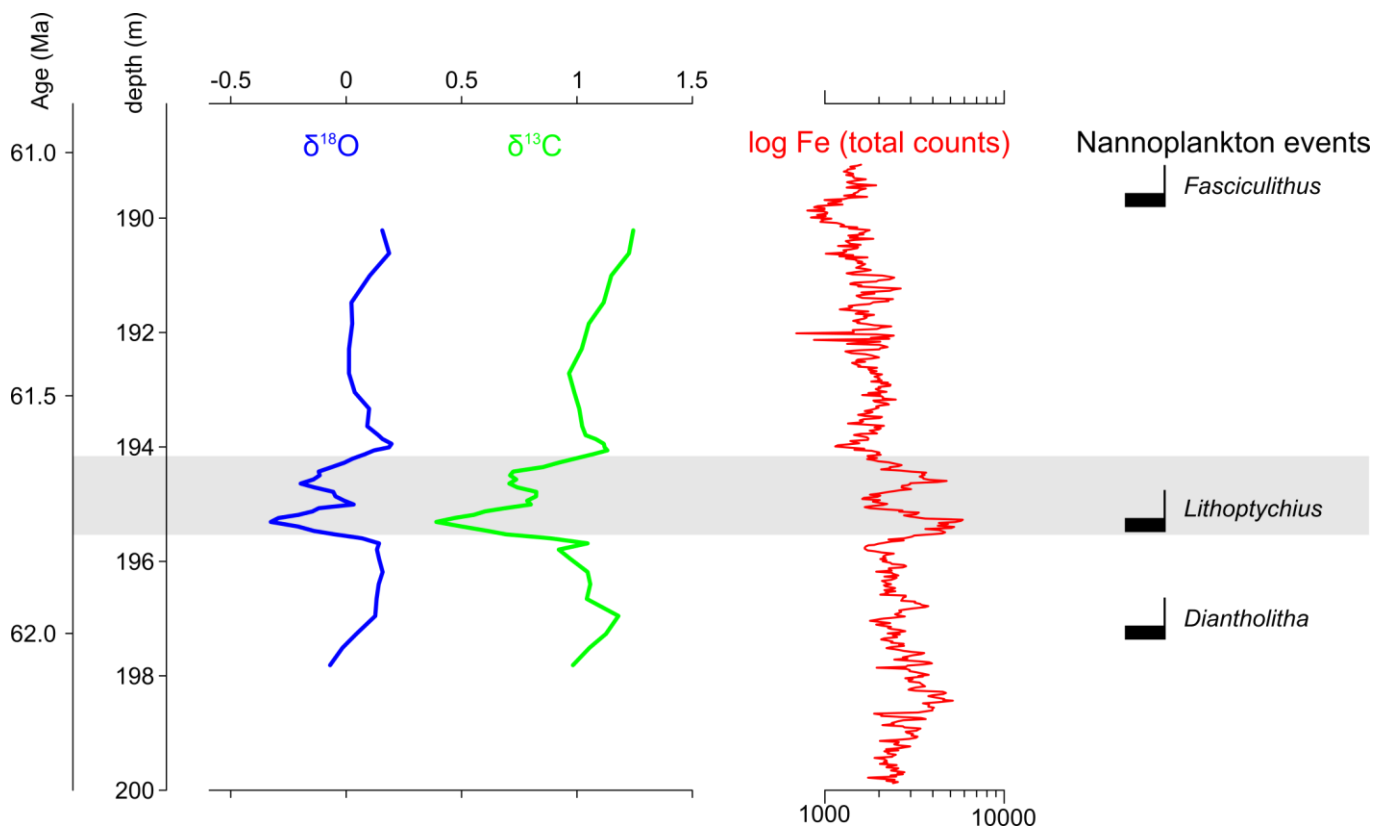


Fig.1 – ODP Site 1262 (Walvis Ridge) benthic foraminiferal isotope patterns, presented as a running 5-point average, together with XRF Fe core scanning data (Westerhold et al., 2008) and Nannoplankton first occurrences (Monechi et al., 2013). The thickness of the nannoplankton indicators indicates the sample resolution. The vertical scale is given in depth (mcd) and ages according to option 1 by Westerhold et al. (2008). The grey interval marks the negative carbon isotope excursion.

event.

On the Egyptian shelf, absence of benthic fauna, enrichment of redox-sensitive trace elements and lamination demonstrate the development of anoxic conditions at the onset of the LDE. As the sea-floor oxygenation improved, an opportunistic inner-middle neritic *Neoeponides duwi* assemblage occurred, after which the outer neritic-bathyal benthic fauna recovered (Schulte et al., 2013).

Studies on calcareous nannofossils show that the LDE coincides with the first radiation of fasciculithids, and relative abundance changes suggest warmer sea surface waters and more eutrophic conditions (Monechi et al., 2013). Deep-sea benthic foraminiferal assemblages have not been studied so far.

Here we show the first results of benthic foraminiferal faunal and isotope patterns related to the LDE at Walvis Ridge (ODP Site 1262, Southern Atlantic Ocean, paleodepth c. 3000 m). The percentage of planktic foraminifera is c. 99.5 % before and during the early part of the event, lowering slightly to c. 99.0 % during the second part. This indicates good carbonate preservation throughout the section.

Stable isotope analysis on single-species samples of the benthic foraminifer *Nuttallides truempyi* shows a ~ 0.9 ‰ $\delta^{13}\text{C}$ shift at ~ 61.8 Ma (adopting the “option 1” age model by Westerhold et al., 2008). Lowest values are measured at ~ 61.75 Ma. The $\delta^{13}\text{C}$ shift coincides with the first occurrence of the nannoplankton genus *Lithoptychius* (Monechi et al., 2013) and the first Fe peak as revealed by the XRF core scanning data (Westerhold et al., 2008). A concurrent ~ 0.8 ‰ $\delta^{18}\text{O}$ excursion, indicating a $\sim 3^\circ\text{C}$ temperature rise, shows a larger temperature rise at Walvis Ridge than at Shatsky Rise (Pacific Ocean, Northern Hemisphere).

The $\delta^{13}\text{C}$ recovers to reach a transient plateau at 0.75 ‰ during the second Fe peak (from ~ 61.7 to 61.6 Ma), coinciding with a second negative $\delta^{18}\text{O}$ excursion of 0.7 ‰. Both the $\delta^{18}\text{O}$ and Fe show a peak at 61.65 Ma. Also ODP Site 1209 (Shatsky Rise) data shows these double Fe, $\delta^{18}\text{O}$ and $\delta^{13}\text{C}$ peaks with roughly 100 kyr in between (Westerhold et al., 2011). This is a feature that the LDE shares with some early Eocene hyperthermals, like ETM-2/H1-H2 and I1-I2 (Zachos et al., 2010), and might point to a common origin with the early Eocene hyperthermals. At Gebel Qreiya the LDE may be characterized by two brief periods of anoxia and enhanced organic matter flux, separated by a period when oxygenation at the seafloor improved (Schulte et al., 2013). These two periods might correspond to both isotope excursions, although detailed correlation is currently not possible.

The Walvis Ridge samples show a highly diverse assemblage of benthic foraminifera with an abundance of ~ 20 % of *Gyroidinoides* spp. and lower relative abundances of *Epistominella* spp., *Cibicidoides* spp., *Quadrinorina* spp. and *Nuttallides truempyi*. The preliminary faunal data from

below, in and above the LDE interval as marked by the isotope record seem to show no distinct faunal trend. This is in contrast to data from ODP Site 1210 (Shatsky Rise), where data at low resolution show dominance of *Bolivina* spp. within the LDE interval and dominance of *Tappanina selmensis* afterwards (Deprez, unpublished data). The seeming lack of faunal response at Walvis Ridge is unexpected, given that the benthic foraminiferal isotope excursions at Walvis Ridge are larger than at Shatsky Rise.

The LDE hyperthermal event shows a double negative isotope excursion, with two peaks about 100 kyr apart. These isotope excursions can be correlated to isotope excursions in the Pacific Ocean (Shatsky Rise), and might be represented by two periods of anoxia in Gebel Qreiya (Egypt). Although the isotope excursions are slightly more prominent at Walvis Ridge than at Shatsky Rise, the benthic fauna seems unaffected during the LDE at Walvis Ridge.

REFERENCES

- Bornemann A., Schulte P., Sprong J., Steurbaut E., Youssef M. & Speijer R.P. (2009) - Latest Danian carbon isotope anomaly and associated environmental change in the southern Tethys (Nile Basin, Egypt). *J. Geol. Soc. London*, 166, 6, 1135-1142.
- Monechi S., Reale V., Bernaola G. & Balestra B. (2013) - The Danian/Selandian boundary at Site 1262 (South Atlantic) and in the Tethyan region: Biomagnetostratigraphy, evolutionary trends in fasciculiths and environmental effects of the Latest Danian Event. *Mar. Micropaleontol.*, 98, 28-40.
- Schulte P., Schwark L., Stassen P., Kouwenhoven T.J., Bornemann A. & Speijer R.P. (2013) - Black shale formation during the Latest Danian Event and the Paleocene-Eocene Thermal Maximum in central Egypt: Two of a kind? *Palaeogeogr. Palaeoclimatol. Palaeoecology*, 371, 9-25.
- Westerhold T., Röhl U., Raffi I., Fornaciari E., Monechi S., Reale V., Bowles J. & Evans H.F. (2008) - Astronomical calibration of the Paleocene time. *Palaeogeogr. Palaeoclimatol. Palaeoecol.*, 257, 4, 377-403.
- Westerhold T., Röhl U., Donner B., McCarren H.K. & Zachos J.C. (2011) - A complete high-resolution Paleocene benthic stable isotope record for the central Pacific (ODP Site 1209). *Paleoceanography*, 26, 2, PA2216.
- Zachos J.C., McCarren H., Murphy B., Röhl U. & Westerhold T. (2010) - Tempo and scale of late Paleocene and early Eocene carbon isotope cycles: Implications for the origin of hyperthermals. *Earth Planet. Sci. Lett.*, 299, 1-2, 242-249.

Benthic foraminiferal and isotopic patterns during the Early Eocene Climatic Optimum (Aktulagay section, Kazakhstan)

Arne Deprez ^(a), Steven Tesseur ^(a), Peter Stassen ^(a), Simon D'haenens ^(a), Etienne Steurbaut ^(a,b), Christopher King ^(c),
Philippe Claeys ^(d) & Robert P. Speijer ^(a)

^(a) Department of Earth and Environmental Sciences, KU Leuven, Celestijnenlaan 200E, B-3001 Leuven, Belgium E-mail: arne.deprez@ees.kuleuven.be

^(b) Department of Paleontology, Royal Belgian Institute of Natural Sciences, Vautierstraat 29, B-1000 Brussels, Belgium

^(c) 316A Park Rd., Bridport DT6 5DA, United Kingdom

^(d) Earth System Science, Vrije Universiteit Brussel, Pleinlaan 2, B-1050 Brussels, Belgium.

Document type: Short note.

Manuscript history: received 15 May 2014; accepted 30 May 2014; editorial responsibility and handling by Gerald R. Dickens & Valeria Luciani.

KEY WORDS: benthic foraminifera, Eocene, Kazakhstan, oxygen deficiency, paleoecology, stable isotope, trophic conditions

The early Eocene is characterized by long-term global warming culminating in the Early Eocene Climatic Optimum (EECO; Zachos et al., 2001; 2008). During this time interval, of which previously only the Paleocene Eocene Thermal Maximum was intensively studied, the Peri-Tethys was connected to the Arctic and Atlantic Oceans by north-south and east-west trending seaways (Akhmetiev, 2011). The Aktulagay section in Kazakhstan provides an expanded record of the middle Ypresian (NP11-13, ~54-50 Ma; King et al., 2013), including the EECO. It features a correlatable series of sapropel beds, observed throughout the Peri-Tethys (Oberhänsli and Beniamovskii, 2000). In order to unravel paleoenvironmental changes, we carried out quantitative faunal studies and stable isotopic (C, O) investigations on excellently preserved foraminiferal assemblages.

The period from 54 to 53 Ma (NP11 to lower NP12; Alashen Formation) is characterized by a diverse assemblage of deep outer neritic benthic foraminifera, with common *Pulsiphonina prima* and *Paralabamina lunata*. Coupled negative carbon and oxygen isotope excursions point to hyperthermals occurring during this time interval, but these are not evident from the faunal or sedimentological record. The initially (54 Ma) well-ventilated oligo- to meso-trophic sea floor conditions gradually change to more eutrophic and oxygen-limited. This gradual onset culminates in permanent stratification in the sapropel-bearing unit at 53-52 Ma (middle NP12; Aktulagay B1 unit), with the dominance of *Anomalinoidea acutus* and *Bulimina aksuatica*. The absence of ostracods and abundance of hematitic concretions are consistent with this interpretation. Rising $\delta^{13}\text{C}_{\text{endobenthic}}$ indicates migration of endobenthic species to the sediment-water interface, indicating oxygen limitation during deposition of the Aktulagay B1 unit. Benthic foraminiferal assemblages dominated by *Epistominella minuta* at ~52-50 Ma (top NP12-NP13; Aktulagay B2 unit) indicate a highly seasonal food

supply and episodic disruption of stratification. Dinoflagellate blooms and *Acarinina* isotope values at 20.25 m indicate lower salinity (lower $\delta^{18}\text{O}$) and higher productivity (higher $\delta^{13}\text{C}$), possibly due to riverine input. This coincides with the peak of the EECO, as indicated by its position close to the base of NP13 and rising $\delta^{13}\text{C}_{\text{foram}}$ values.

The long-term change from oligo-mesotrophic (Alashen Formation) to more eutrophic (Aktulagay B2 unit) coincides with a transition from a paratropical to a monsoonal (seasonal) climate, based on land vegetation changes (Akhmetiev & Beniamovskii, 2009). This climate change is linked to the formation of a land barrier in the Pripyat strait.

Although it is tempting to link the observed patterns to climate change, we cannot currently exclude that changing paleogeography and variable connections between the Peri-Tethys and the Tethys, Atlantic and the Arctic Oceans largely determined the long-term period of dysoxia and anoxia during deposition of the sapropel beds at the Peri-Tethyan seafloor.

REFERENCES

- Akhmetiev M.A. (2011) - Problems of Paleogene stratigraphy and paleogeography in the middle latitudes of Eurasia. *Russ. Geol. Geophys.*, 52, 10, 1075-1091, doi:10.1016/j.rgg.2011.09.004.
- Akhmetiev M.A. & Beniamovskii V.N. (2009) - Paleogene floral assemblages around epicontinental seas and straits in Northern Central Eurasia: proxies for climatic and paleogeographic evolution. *Geol. Acta*, 7, 1-2, 297-309, doi:10.1344/105.000000278.
- King C., Iakovleva A.I., Steurbaut E., Heilmann-Clausen C. & Ward D.J. (2013) - The Aktulagay section, west Kazakhstan: a key site for northern mid-latitude Early Eocene stratigraphy. *Stratigraphy*, 10, 171-209.
- Oberhänsli H. & Beniamovskii V.N. (2000) - Dysoxic bottom water events in the Peri-Tethys during the late Ypresian: A result of changes in the evaporation/precipitation balance in adjacent continental regions. *GFF*, 122, 1, 121-123.

- Zachos J.C., Pagani M., Sloan L.C., Thomas E. & Billups K. (2001) - Trends, rhythms and aberrations in global climate 65 Ma to present. *Science*, 292, 686–693, doi:10.1126/science.1059412.
- Zachos J.C, Dickens G.R. & Zeebe R.E. (2008) - An early Cenozoic perspective on greenhouse warming and carbon-cycle dynamics. *Nature*, 451, 279-283, doi:10.1038/nature06588.

Deep-sea benthic foraminiferal turnovers in the early Eocene: The role of the PETM and ETM2

Simon D'haenens ^(a), André Bornemann ^(b,c) & Robert P. Speijer ^(a)

^(a) Department of Earth and Environmental Sciences, KU Leuven, Belgium. E-mail: simon.dhaenens@ees.kuleuven.be

^(b) Institut für geophysik und Geologie, Universität Leipzig, Germany

^(c) Bundesanstalt für Geowissenschaften und Rohstoffe, Hannover, Germany

Document type: Short note.

Manuscript history: received 15 May 2014; accepted 30 May 2014; editorial responsibility and handling by Gerald R. Dickens & Valeria Luciani.

KEY WORDS: benthic foraminifera, deep-sea, ETM2, hyperthermal, PETM, taxonomy

Throughout the Cenozoic, deep-sea benthic foraminiferal communities have faced many periods of environmental turmoil. Three major, yet relatively gradual faunal turnovers occurred during the Eocene-Oligocene, middle Miocene and middle Pleistocene - all periods of pronounced cooling and increases in polar ice volume. In contrast, the Paleocene-Eocene Thermal Maximum (PETM; ~56 Ma) - a transient global warming event or hyperthermal - is characterized by a rapid extinction of 30-50% of all deep-sea benthic foraminiferal species (Thomas, 1998; 2007). So far, the exact cause(s) of this severe extinction event that devastated bathyal and abyssal faunas is not known. It is likely that a change in food-web structure, affected by high temperatures, a decrease in the oxygenation state of the oceans, calcite undersaturation, primary productivity or ocean current circulation changes played an important role in the benthic foraminiferal extinction (BFE) and in the establishment of the opportunistic fauna that characterizes the PETM itself (Thomas, 1998, 2007).

Historically, the earliest Eocene benthic foraminiferal associations were considered as a transitional fauna, recovering from the BFE and gradually recolonizing vacant niches and habitats. This transition from a Cretaceous-Paleocene *Velasco-type* fauna into a typical Eocene *Barbados-type* fauna appeared to be characterized by the gradual appearance of new taxa (Tjalsma & Lohmann, 1983; Berggren & Miller, 1989).

With the discovery of several Eocene hyperthermals similar to the PETM (e.g. Eocene Thermal Maximum 2; ETM2; ~53.7 Ma), the question arises of what role these events played in the development of early Eocene benthic communities. For instance, how did the impoverished benthic fauna cope with the environmental perturbations associated with these successive and smaller Eocene hyperthermals on short time scales? Did it become more or less sensitive to climatic and oceanographic changes? One can also wonder what the effects were on longer time scales. Did early Eocene hyperthermals hamper or stimulate recolonization of the benthic realm, and if so, in what way?

To answer these questions, we generated detailed

quantitative benthic foraminiferal (>63 µm) data from two Deep Sea Drilling Project (DSDP) sites from the Bay of Biscay, NE Atlantic Ocean. The studied interval from bathyal DSDP Site 401 (~2 km paleodepth) ranges from NP9 to NP12 (~3 My) including the PETM and ETM2, while the studied material from abyssal DSDP Site 550 (~4 km paleodepth) encompasses a ~800 kyr interval including ETM2 and H2.

At DSDP Site 401, we observe the loss of typical Paleocene taxa (e.g. *Gavelinella beccariiiformis*, *Eponides hillebrandti* and *Bolivinoidea delicatulus*) at the onset of the well-expressed PETM (Bornemann *et al.*, 2014), clearly demonstrating the abrupt nature of the BFE. However, the extinction rate is only about 20%, which is considerably lower than reported elsewhere (Thomas, 1998). Typical excursion taxa such as *Nuttallides umbonifera*, *Tappanina selmensis* and various abyssaminids dominate the core of the PETM, but are rapidly replaced by a relatively stable benthic association composed of *Epistominella minuta*, *Globocassidulina subglobosa* and various buliminids ranging up to ETM2 (D'haenens *et al.*, 2012; *in prep.*). Following ETM2, the loss of buliminids and a minor but significant shift towards a *Cibicidoides*-dominated fauna illustrates the sudden transition towards a post-ETM2 benthic foraminiferal association (D'haenens *et al.*, 2012). At the deeper DSDP Site 550, we also document a stable post-PETM benthic fauna dominated by abyssal taxa such as *Bolivinoidea crenulata*, *Quadrimorphina profunda*, *N. truempyi*, *G. subglobosa* and *Gyroidinoides* spp. Similar to Site 401, a significant faunal transition occurs across ETM2, with the reduction of several taxa (*Q. profunda*, *Gyroidinoides* spp. and *G. subglobosa*) and the relative increase of others (*Anomalinoidea* spp., *N. umbonifera* and *C. ungerianus*). The interval right after ETM2 is also characterized by the first occurrence of several taxa (e.g. *Pullenia quinqueloba*, *Buliminella grata*) that are known to persist throughout the Eocene (Fig. 1). Although of much lower resolution and using a different size fraction, data from nearby DSDP Site 549 corroborate these patterns (Reynolds, 1992).

Our results suggest that bathyal and abyssal NE Atlantic post-PETM benthic associations were all stable up to ETM2, despite their slightly different composition. Furthermore, we

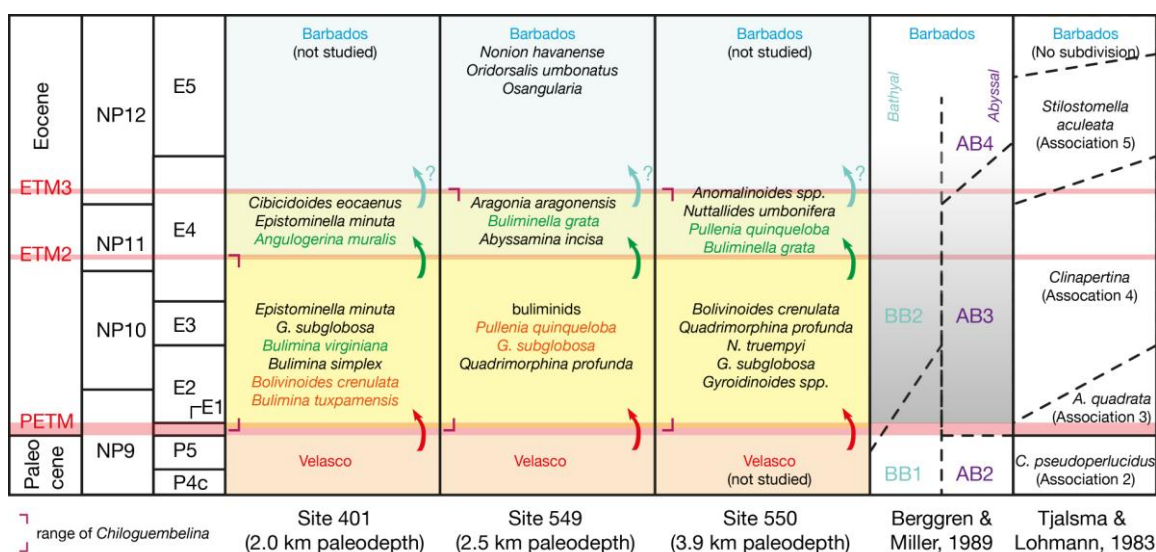


Fig. 1 – Scheme of latest Paleocene to early Eocene benthic foraminiferal associations in the NE Atlantic (DSDP sites 401, 549 and 550). Across the PETM, site-specific (i.e. bathymetry-dependent) and stable early Eocene faunas replace the lost *Velasco-type* fauna. Another (minor) turnover, as indicated by the arrows, occurs across ETM2, resulting in new stable associations. Orange species names represent taxa that (virtually) disappear during the subsequent turnover, while green species names are taxa that have their lowest occurrence. Bathyal (BB)/abyssal (AB) zonations by Berggren & Miller (1989) and numbered benthic associations by Tjalsma & Lohmann (1983). The AB3/AB4 or *S. aculeata* association may correspond to an ETM3-related faunal turnover (teal arrows). Note that excursion assemblages (PETM, ETM2, ETM3) are not presented in this figure. Also note the lowest occurrence of the planktic foraminiferal genus *Chiloguembelina* at the onset of the PETM and its highest occurrence at ETM2 (401) or ETM3 (549 & 550).

show that a minor benthic turnover takes place contemporaneous with ETM2, independent of bathymetry. As such, this particular hyperthermal event appears to play a significant role in the development of Eocene benthic foraminiferal communities. One can argue that this particular transition is only limited to the NE Atlantic and has no significance on the global evolution of deep-sea faunas. Indeed, large and persistent environmental changes have been documented for the interval between the PETM, ETM2 and ETM3 in the Bay of Biscay (Bornemann *et al.*, 2014; D'haenens *et al.*, 2014) and there is no doubt that the benthic assemblages reflect them. Nevertheless, we note that global benthic foraminiferal data show similar patterns (e.g. Thomas, 1990; unpublished data; Stassen *et al.*, 2012).

The historical view of a post-PETM transitional fauna that gradually recolonizes vacant niches and slowly evolves into a *Barbados-type* Eocene fauna may actually not be so accurate. Instead, based on our observations, we tentatively conclude that post-PETM faunas may have been in a relative state of stability ('stasis'), only to be kick-started into other stable states by subsequent early Eocene hyperthermals such as the ETM2 and ETM3 (Fig. 1). What impact other Eocene events (i.e. EECO-related hyperthermals, MECO, CAEs) had on long-term benthic ecosystem evolution, remains to be explored.

REFERENCES

- Berggren W.A. & Miller K.G. (1989) - Cenozoic bathyal and abyssal calcareous benthic foraminiferal zonation. *Micropal.* 35 (4), 308-320.
- Bornemann A., Norris R.D., Lyman J.A., D'haenens S., Groeneveld J., Röhl U., Farley K.A. & Speijer R.P. (2014) - Persistent environmental change after the Paleocene-Eocene Thermal Maximum in the eastern North Atlantic. *Earth. Planet. Sci. Lett.*, 394, 70-81.
- D'haenens S., Bornemann A., Stassen P. & Speijer, R.P. (2012) - Multiple early Eocene benthic foraminiferal assemblage and $\delta^{13}\text{C}$ fluctuations at DSDP Site 401 (Bay of Biscay – NE Atlantic). *Mar. Micropaleont.*, 88-89, 15-35.
- D'haenens S., Bornemann A., Claeys P., Steurbaut E., Röhl U. & Speijer R.P. (2014) - A transient deep-sea circulation switch during Eocene Thermal Maximum 2. *Paleoceanography*, doi: 10.1002/2013PA002567.
- Reynolds L.E. (1992) - Faunal change in benthic foraminifera at the Paleocene/Eocene boundary, DSDP Site 549. Unpublished Master of Science Thesis, Orono: University of Maine, 130 pp.
- Stassen P., Steurbaut E., Morsi A.-M.M., Schulte P. & Speijer R.P. (2012) - Biotic impact of Eocene Thermal Maximum 2 in a shelf setting (Dababiya, Egypt). *Austrian J. Earth Sci.*, 105 (1), 154-160.
- Tjalsma R.C. & Lohmann G.P. (1983) – Paleocene-Eocene bathyal and abyssal benthic foraminifera from the Atlantic Ocean. *Micropal. Spec. Pub.* 4, 1-90.
- Thomas, E. (1990) - Cretaceous through Neogene deep-sea benthic foraminifera (Maud Rise, Weddell Sea, Antarctica). In: Barker, P.F. & Kennett, J.P. (Eds.), *Proc. of the Ocean Drilling Program, Sci. Res.*, 113 (35). Ocean Drilling Program, College Station, TX, 571-594.
- Thomas, E. (1998) - Biogeography of the late Paleocene benthic foraminiferal extinction. In: Aubry, M.-P., Lucas, S.G. & Berggren, W.A. (eds.), *Late Paleocene-Early Eocene Biotic and Climatic Events in the Marine and Terrestrial Records*. Columbia University Press, New York, 214-243.
- Thomas E. (2007) – Cenozoic mass extinctions: What perturbs the largest habitat on Earth? In: Monechi, S., Coccioni, R. & Rampino M.R. (eds.), *Large Ecosystem Perturbations: Causes and Consequences*. Geological Society of America Special Paper, 424, 1-23.

Continental - island arc fluctuations through time and the Eocene transition from a greenhouse to an icehouse world

Gerald R. Dickens ^(a), Cin-ty A. Lee ^(a) & CIA Operatives ^(b)

^(a) Department of Earth Sciences, Rice University, Houston, 77005, Texas, USA. E-mail: jerry@rice.edu

^(b) Individuals working on aspects of the continental-island arc (CIA) hypothesis, including Jaime D. Barnes, Rajdeep Dasgupta, Jade Star Lackey, Adrian Lenardic, Tapio Schneider, Michael M. Tice, and Richard Zeebe

Document type: Short note.

Manuscript history: received 15 May 2014; accepted 30 May 2014; editorial responsibility and handling by Gerald R. Dickens & Valeria Luciani.

KEY WORDS: Cenozoic, volcanism, carbon cycling.

Earth's surface temperature follows its radiative energy balance, which principally depends on solar insolation, albedo, and atmospheric composition, particularly $p\text{CO}_2$. Atmospheric $p\text{CO}_2$ is governed by exchange of C with other reservoirs of the exogenic C cycle (ocean and biosphere), with the endogenic C cycle (crust and mantle), and possibly one or more organic carbon capacitors. On moderate time scales, certainly >0.1 Myr, the exogenic system can be considered a single entity, with a mass of C dictated by inputs and outputs to and from external reservoirs. Volcanism and metamorphism release CO_2 , weathering produces HCO_3^- , and deposition of organic matter and carbonate sequesters CH_2O and CaCO_3 (Berner, 1994; Kerrick, 2001; Ridgwell and Zeebe, 2005). True global carbon cycling occurs on even longer time scales (>10 Myr), whereby subduction of oceanic lithosphere transfers C into the deep Earth, and volcanism returns C to the atmosphere.

If long-term sources and sinks to the exogenic C cycle were balanced, atmospheric $p\text{CO}_2$, averaged over millions of years, would remain relatively constant, and for the most part, so should Earth's surface temperature, excepting changes in insolation and albedo. This has not been the case over much of Earth's history, as perhaps most obvious from records of the Paleogene. Earth's surface temperature and very likely $p\text{CO}_2$ were much higher in the "greenhouse world" of the Cretaceous and early Paleogene (>50 Ma) than in the "icehouse world" of the late Paleogene (<35 Ma) to present-day (e.g., Zachos et al., 2008). Clearly, inputs and outputs to the exogenic C cycle have changed over long time intervals. The overarching question is "why?", and the subsidiary question pertinent to the Paleogene is "and how come the transition from greenhouse to icehouse conditions began at ~ 50 Ma?"

To understand early Paleogene C cycling and climate change, a series of papers have focused on the idea of an "organic carbon capacitor" (e.g., Kurtz et al., 2003; DeConto et al., 2010; Komar et al., 2013). This would be one or more reservoirs in the shallow geosphere (e.g., methane in marine sediment, peat or permafrost on land) that store and release massive amounts of C over time. While the existence of an

organic capacitor can explain some perplexing observations, such as long-term and short-term variations in $\delta^{13}\text{C}$ and deep sea carbonate accumulation, and perhaps even relationships between the timing and magnitude of "hyperthermal events", such a capacitor cannot explain the full magnitude of temperature change nor why it would grow and decay over time.

Past variations in $p\text{CO}_2$ often are ascribed to changes in C fluxes through the amount of volcanism. For example, and of direct relevance to the Early Paleogene, there is a recurring idea to explain broad changes in C cycling through enhanced North Atlantic volcanism. All along, however, perhaps the most striking change in Paleogene tectonics and the mode of volcanism generally has been overlooked.

Based on compilations of geologic maps, and known tectonic changes, there is a major switch from continental arc to island arc volcanism around 50 Ma. Continental arcs (e.g., Andean style volcanism) were longer in the Cretaceous to early Paleogene than in the mid-Cenozoic. Notably, Cretaceous–Paleogene continental arc batholiths occur (1) along the entire North American Cordillera, from southern Alaska through western North America and into Mexico, (2) in the South American Cordillera, extending from Columbia to southern Chile, (3) along the southern margin of Eurasia extending from eastern Turkey through southern Tibet and into present-day southeast Asia, and (4) along the eastern part of Eurasia, extending from southern China through Korea, Japan, and eastern Siberia. The total length of these Cretaceous–early Paleogene continental arcs was $\sim 33,000 \pm 3000$ km, which is $\sim 63\%$ of the present length of all subduction zones (52,000 km), or $\sim 200\%$ greater than the length of present continental arcs, which include the Andes, Mexico, Cascades, Alaska, Kamchatka, and Sumatra ($<16,500$ km or $\sim 30\%$ that of current subduction zones). The present-day configuration of subduction zones was largely defined ca. 50 Ma with the termination of continental arcs in southern and eastern Eurasia and in western North America and the initiation of widespread intraoceanic subduction and associated island arcs in the western Pacific, extending from Izu-Bonin-Mariana to Fiji and the Tonga-Kermadec convergent margins (Stern et al., 2012).

There is a key implication of this tectonic reorganization.

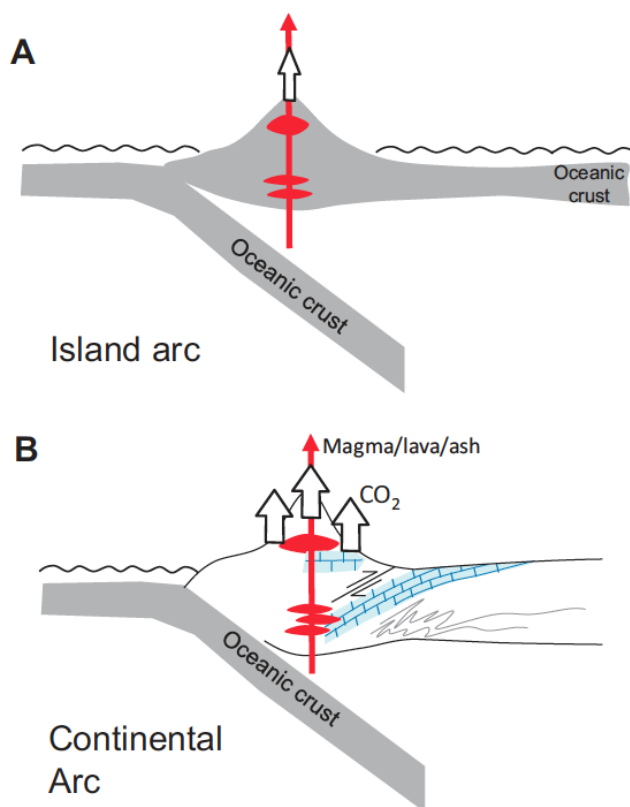


Figure 1. The difference between island arc and continental arc volcanism. (A) Island arcs are formed at intraoceanic subduction zones with little to no carbonates in the overlying crust. (B) Continental arcs are formed along active continental margins where magma can intrude through ancient carbonate on the overlying crust. This can lead to magmatically assisted decarbonation of crustal carbonates and much higher fluxes of CO_2 .

Continental arcs are built through continental crust, whereas island arcs are built on oceanic lithosphere. Given the abundance of carbonate production and preservation along continental margins, the switch from continental arc to island arc volcanism almost necessarily means that far more magma intersected and reacted with pre-existing carbonate during the Cretaceous and early Paleogene compared to the Neogene and present-day. Interactions between magma and limestone at present-day generate the lion's share of volcanic C emissions to the atmosphere. Consequently, we argue that long-term variations in climate and carbon cycling were related to changes in the relative abundance of continental arc and island arc volcanism. We elaborate on this idea here, originally presented by Lee et al. (2013), and try to mesh this with the notion of an organic carbon capacitor.

REFERENCES

- Berner R.A. (1994) - GEOCARB II: A revised model of atmospheric CO_2 over Phanerozoic time: *American Journal of Science*, 294, 56–91.
- DeConto R.M., Galeotti S., Pagani M., Tracy D., Schaefer K., Zhang T., Pollard D. & Beerling D.J. (2012) - Past extreme warming events linked to massive carbon release from thawing permafrost. *Nature*, 484, 87–92.
- Kerrick D.M. & Connolly J.A.D. (2001) - Metamorphic devolatilization of subducted marine sediments and transport of volatiles into the Earth's mantle: *Nature*, 411, 293–296.
- Komar N., Zeebe R.E. & Dickens G.R. (2013) - Understanding long-term carbon cycle trends: The late Paleocene through the early Eocene. *Paleoceanography*, 28, 650–662.
- Kurtz A.C., Kump L.R., Arthur M.A., Zachos J.C. & Paytan A. (2003) - Early Cenozoic decoupling of the global carbon and sulfur cycles. *Paleoceanography*, 18, 1090, doi:10.1029/2003PA000908.
- Lee C.T., Shen B., Slotnick B.S., Liao K., Dickens G.R., Yokoyama Y., Lenardic A., Dasgupta R., Jellinek M., Lackey J.S., Schneider T. & Tice M.M. (2013) - Continental arc-island arc fluctuations, growth of crustal carbonates, and long-term climate change. *Geosphere*, 9, 21–36.
- Ridgwell A., and R.E. Zeebe (2005) - The role of the global carbonate cycle in the regulation and evolution of the Earth system: *Earth and Planetary Science Letters*, 234, 299–315
- Stern R.J., Reagan M., O. Ishizuka, Y. Ohara, & S. Whattam (2012) - To understand subduction initiation, study forearc crust: To understand forearc crust, study ophiolites. *Lithosphere*, 4, 469–483.
- Zachos J.C., Dickens G.R. & Zeebe R.E. (2008) - Cenozoic climate and carbon cycling. *Nature*, 451, 279–283.

Astronomical calibration of the Danian Stage (Early Paleocene) revisited: settling chronologies across the Atlantic and Pacific Oceans

Jaume Dinarès-Turell ^(a), Thomas Westerhold ^(b), Victoriano Pujalte ^(c), Ursula Röhl ^(b) & Dick Kroon ^(d)

^(a) Istituto Nazionale di Geofisica e Vulcanologia, Via di Vigna Murata 605, I-00143, Rome, Italy. E-mail: jaume.dinares@ingv.it

^(b) MARUM - Center for Marine Environmental Sciences, Univ. of Bremen, Leobener Strasse, D-28359 Bremen, Germany

^(c) Department of Stratigraphy and Paleontology, University of the Basque Country, UPV/EHU, PO Box 644, E-48080 Bilbao, Spain

^(d) School of GeoSciences, Grant Institute, Univ. of Edinburgh, King's Buildings, West Mains Rd., Edinburgh, EH9 3JW, UK

KEY WORDS: cyclostratigraphy, magnetostratigraphy, ODP, orbital tuning.

The astronomical time scale for the Paleocene is hampered by some uncertainties including discrepant number of 405-kyr eccentricity related cycles and correlation schemes among key records being proposed by different authors (Westerhold et al., 2008; Kuiper et al., 2008; Hilgen et al., 2010). Here we present a new Danian correlation framework resolved at the ~100-kyr short-eccentricity level between the land-based Zumaia and Sopelana hemipelagic sections from the Basque Basin and deep-sea records drilled during ODP Legs 198 (Shatsky Rise, North Pacific) and 208 (Walvis Ridge, South Atlantic) that reconciles both the magnetostratigraphy and the short and long-eccentricity cycle patterns among the records and, hence, improves synchronicity of events. The correlation has been aided by composite images from ODP cores and a new whole-rock $\delta^{13}\text{C}$ isotope record at Zumaia while its original magnetostratigraphy (Dinarès-Turell et al., 2003; 2010) is reinforced by new data from Sopelana. Notably, we challenge the correlation of the Pacific Sites 1209–1210 that were offset by as much as one 405-kyr cycle in previous interpretations (i.e., the *Fasciculithus* spp. LO, which approximates the Danian–Selandian (D–S) boundary, and the “Top chron C27n” climatic event were at odds between oceans in the interpretation of Hilgen et al. (2010). It is found that the Danian consists of 11 (and not 10) consecutive 405-kyr eccentricity cycles.

The new consistent stratigraphic framework enables accurate estimates to be made of ages for magnetostratigraphic boundaries, bioevents, and sedimentation rates. Low sedimentation rates appear common in all records in the mid-Danian interval along the upper part of chron C28n, including conspicuous condensed intervals in some of the oceanic records that in the past have hampered the proper identification of cycles. The new chronological framework, spanning a duration of about 4.5 My, allows assessing the role of orbital forcing on the paleoclimatic variability as registered by the related isotope records. It appears clear that there exists a

periodic beat at the 100-ky and 405-kyr eccentricity cycles impressed in the record. The phase relationship between the benthic isotope record and eccentricity is similar to patterns documented for the Oligocene and Miocene, as indicated by others, confirming the role of orbital forcing as the pace maker for paleoclimatic variability on Milankovitch time scales. The preferred tuning to the La2011 orbital solution provides astronomically calibrated ages of 66.022 ± 0.040 Ma and 61.607 ± 0.040 Ma for the (D–S) and Cretaceous–Paleogene (K–Pg) boundaries respectively. Finally, we envisage that the Zumaia section, which already hosts the Selandian GSSP, could serve as the global Danian stratotype.

REFERENCES

- Dinarès-Turell J., Baceta J.I., Pujalte V., Orue-Etxebarria X., Bernaola G. & Lorito S. (2003) - Untangling the Palaeocene climatic rhythm: an astronomically calibrated Early Palaeocene magnetostratigraphy and biostratigraphy at Zumaia (Basque basin, northern Spain). *Earth Planet. Sci. Lett.*, 216, 483–500.
- Dinarès-Turell J., Stoykova K., Baceta J.I., Ivanov M. & Pujalte V. (2010) - High-resolution intra- and interbasinal correlation of the Danian–Selandian transition (Early Paleocene): The Bjala section (Bulgaria) and the Selandian GSSP at Zumaia (Spain). *Palaeogeogr. Palaeoclimatol. Palaeoecol.*, 297, 511–533.
- Hilgen F.J., Kuiper K.F. & Lourens L.J. (2010) - Evaluation of the astronomical time scale for the Paleocene and earliest Eocene. *Earth Planet. Sci. Lett.*, 300, 139–151.
- Kuiper K.F., Deino A., Hilgen F.J., Krijgsman W., Renne P.R. & Wijbrans J.R. (2008) - Synchronizing rock clocks of Earth history. *Science* 320, 500–504. doi: 10.1126/science.1154339.
- Westerhold T., Röhl, U. Raffi, I. Fornaciari, E. Monechi, S. Reale V., Bowles J. & Evans, H.F. (2008) - Astronomical calibration of the Paleocene time. *Palaeogeogr. Palaeoclimatol. Palaeoecol.*, 257, 377–403.

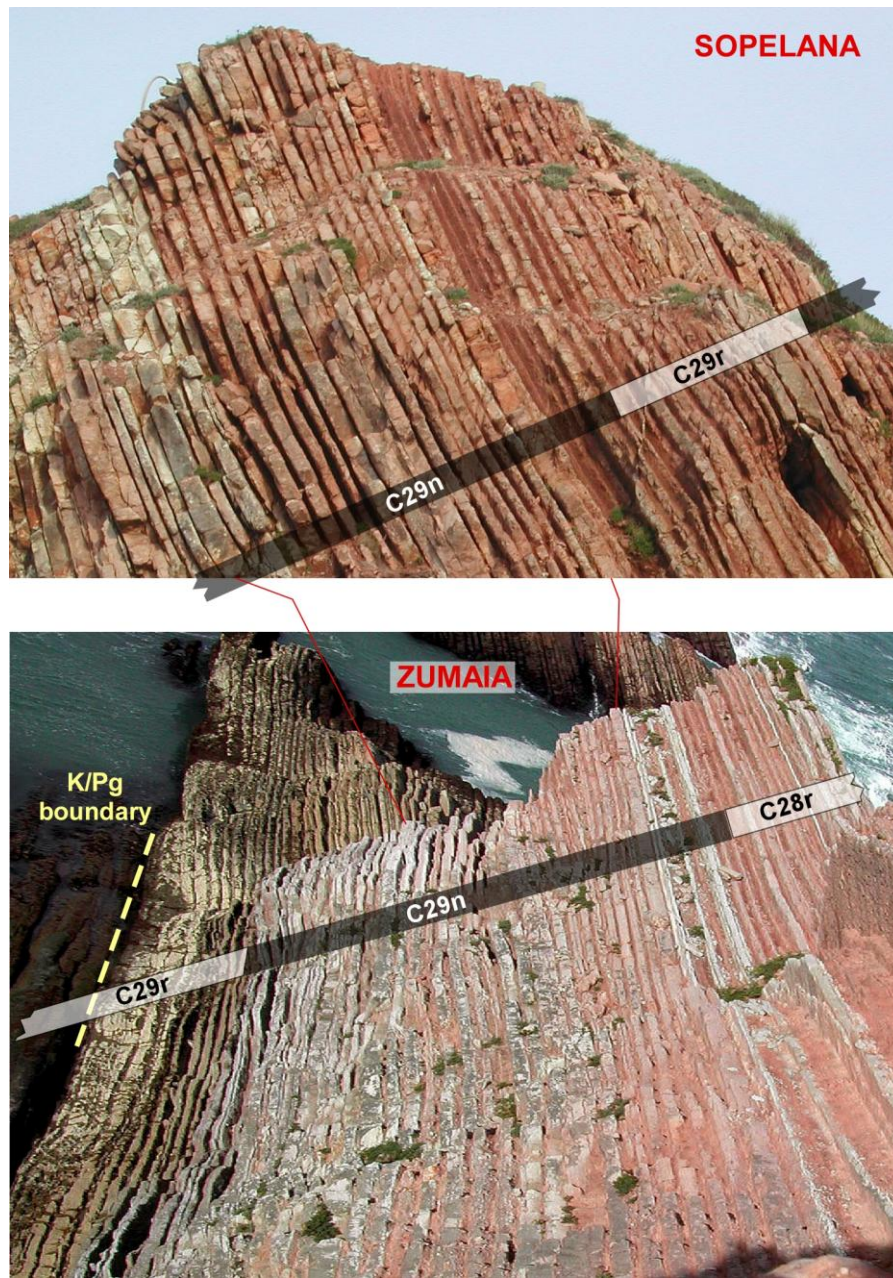


Fig.1 – Field photographs of the lower Danian succession at Sopedana and Zumaia outcrops.

Tethyan planktic foraminiferal record of the early Eocene hyperthermal events ETM2, H2 and I1 (Terche section, northeastern Italy)

Roberta D'Onofrio ^(a), Valeria Luciani ^(a) Luca Giusberti ^(b), Eliana Fornaciari ^(b) & Mario Sprovieri ^(c)

^(a) University of Ferrara, Dipartimento di Fisica e Scienze della Terra, Ferrara, Italy. E-mail: roberta.donofrio@unife.it

^(b) University of Padova, Dipartimento di Geoscienze, Padova, Italy

^(c) Institute for Coastal Marine Environment (IAMC), CNR, Campobello di Mazzara, Italy

Document type: Short note.

Manuscript history: received 15 May 2014; accepted 30 May 2014; editorial responsibility and handling by Gerald R. Dickens & Valeria Luciani.

KEY WORDS: Early Eocene hyperthermals, ETM2, H2, I1, planktic foraminifera, northeastern Italy, Tethyan setting

The early Paleogene climate variability is characterized by long-term warming which culminated at the Early Eocene Climatic Optimum, EECO (~49 Ma) and was followed by a cooling trend that ultimately led to the emplacement of a stable ice sheet on Antarctica (e.g., Zachos et al., 2001). Superimposed on the long-term Paleocene-early Eocene warming trend, several transient episodes of extreme warming, the so-called hyperthermals (e.g. Lourens et al., 2005; Nicolo et al., 2007), have been recognized in addition to the well-know Paleocene-Eocene Thermal Maximum (PETM; ~ 55.5 Ma; e.g. Zachos et al., 2008). To the present, perturbations produced by hyperthermals are rather well documented in terms of isotopic variations whereas their influence on the biota is still largely unexplored.

The Terche section, located in the Venetian Pre-Alps of northeastern Italy, is an expanded upper Paleocene-lower Eocene succession deposited in a bathyal setting of a continental margin of the central-western Tethys. This section contains three well-exposed and expanded marly-clay units (MUs) corresponding to intervals of negative carbon isotope excursions (CIEs). Calcareous plankton biostratigraphy allow us to correlate them to hyperthermal events ETM2 (or H1; ~53.7 Ma), H2 (~53.6 Ma) and I1 (~53.3 Ma). The recorded $\delta^{13}\text{C}$ excursions are in-line with values from the literature for H2 and I1 but the ETM2 negative shift is considerably smaller and most probably affected by diagenetic or laboratory bias.

Quantitative analysis of planktic foraminiferal genera (>63 μm fraction) shows marked changes closely related to the CIEs and to the MUs, consisting of a pronounced increase in abundance of warm-indices acarininids (up to 68% for ETM2) and a parallel marked decline in subbotinids abundance. The MUs are also associated with an increase of the eutrophic radiolarians. This record shows similarities with the PETM response in the nearby Forada section and with smaller magnitude changes such as those documented for the X-event (ETM3) at the Farra section, located in the same area (Luciani

et al., 2007; Agnini et al., 2009). These observations suggest abrupt and transient episodes of environmental perturbations that resulted in improved eutrophication of the sea-surface waters coupled with intense warmth. The increased surface-water eutrophication during hyperthermals was forced by strengthening of the hydrological cycle and increased weathering, as a consequence of an expanded greenhouse effect that improved nutrient availability in the surface waters. These conditions favoured the acarininids, able to temporarily colonize warmer deeper and nutrient-richer waters previously occupied by subbotinids. The highly specialized, warm-indices morozovellids, that should largely share the surface-water habitat with acarininids, do not show significant changes except for a temporary but substantial increase in abundance at the initial portion of the MU corresponding to ETM2 (up to 61%) and, to a lesser extent, to I1 (up to 45%). We hypothesize that the first phase of warming favoured morozovellids until the enhanced hydrological cycle increased eutrophic conditions, detrimental for morozovellids but better tolerated by acarininids.

It must be noted that calcareous plankton variations during the hyperthermals in a deep-water setting could be affected by selective dissolution susceptibility due to the lysocline rise associated to these events. The planktic foraminiferal fragmentation index (F-index), which can give indications about the degree of carbonate dissolution (Hancock & Dickens, 2005), shows very low values in correspondence to the MUs of the Terche section when compared with those observed in other sections of the Belluno Basin across the PETM and X-event. This indicates that planktic foraminiferal record, not significantly biased by taphonomic effects, reflects genuine modifications of the assemblages. The marked decrease of carbonate content within MUs can be thus largely attributed to dilution rather than dissolution. The coarse fraction values (CF), which give indications on planktic foraminiferal productivity in pelagic sediments not significantly affected by dissolution (Hancock & Dickens, 2005), slightly decrease across the MUs. We interpret this change as mainly related to dilution, produced by enhanced terrigenous sediments, rather than to a decrease in planktic foraminiferal productivity. The

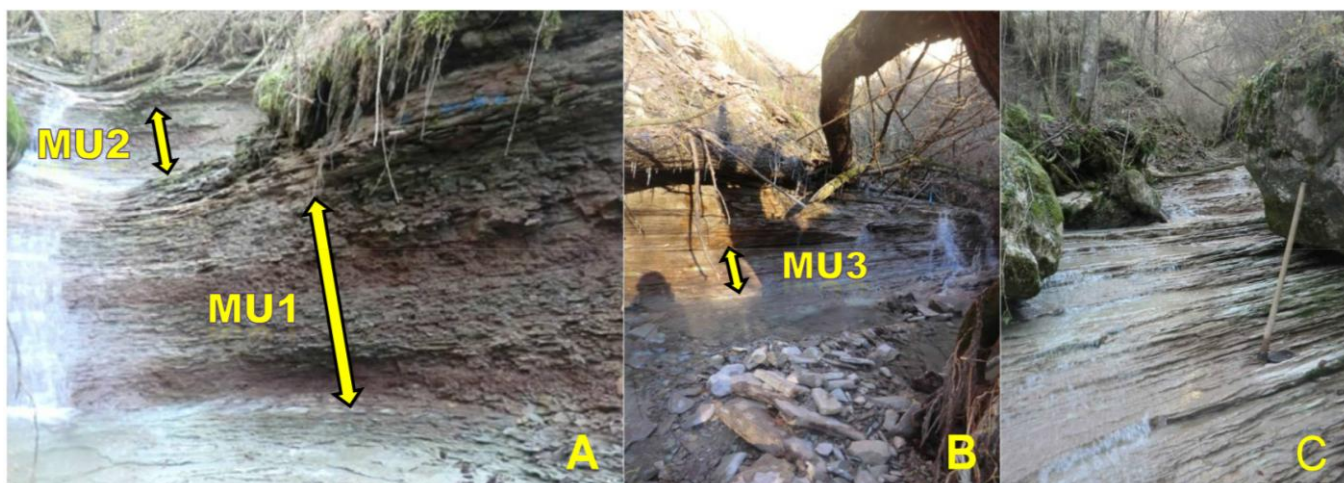


Fig.1 – Overviews of the Terche section located in the Venetian Pre-Alps (northeastern Italy): A) Marly units MU1 and MU2, which correspond respectively to the hyperthermal events ETM2 and H2; B) Marly unit MU3, which corresponds to the hyperthermal event I1; C) Markedly cyclical Ypresian Scaglia Rossa below the Marly Unit MU1.

strong decline in the abundance of subbotinids across the MUs was probably balanced by the marked increase of the muricate warm-indices, thus total planktic foraminiferal productivity could have remained approximately unchanged. The observation that the CF and carbonate content curves show very similar trends in correspondence to the MUs seems to support this hypothesis.

REFERENCES

- Agnini C., Macri P., Backman J., Brinkhuis H., Fornaciari E., Giusberti L., Luciani V., Rio D., Sluijs A. & Speranza F. (2009) - An early Eocene carbon cycle perturbation at similar to 52.5 Ma in the Southern Alps: Chronology and biotic response. *Paleoceanography*, 24; 2209.
- Hancock H.J.L. & Dickens G.R. (2005) - Carbonate dissolution episodes in Paleocene and Eocene sediment, Shatsky Rise, west-central Pacific. In: Bralower T.J., Premoli Silva I., Malone M.J. (eds), *Proceedings of ODP, science results, 198* [Online]. Available from World Wide Web: http://www-odp.tamu.edu/publications/198_SR/116/116.htm.
- Lourens L.J., Sluijs A., Kroon D., Zachos J.C., Thomas E., Rohll U., Bowels J. & Raffi I. (2005) – Astronomical pacing of late Palaeocene to early Eocene global warming events. *Nature*, 435, 1083-1087.
- Luciani V., Giusberti L., Agnini C., Backman J., Fornaciari E. & Rio D. (2007) - The Paleocene-Eocene thermal maximum as recorded by Tethyan planktonic foraminifera in the Forada section (northern Italy). *Mar. Micropaleontol.*, 64, 189–214.
- Nicolo M.J., Dickens G.R., Hollis C.J. & Zachos J.C. (2007) - Multiple early Eocene hyperthermals: their sedimentary expression on the New Zealand continental margin and in the deep sea. *Geology*, 35, 699–702.
- Zachos J.C., Pagani M., Sloan L., Thomas E. & Billups K. (2001) - Trends, rhythms, and aberrations in global climate 65 Ma to present. *Science*, 292, 686–693.
- Zachos J.C., Dickens G.R. & Zeebe R.E. (2008) - An early Cenozoic perspective on green house warming and carbon-cycle dynamics. *Nature*, 451, 279-283.

PETM related paleoweathering on the southern margins of the North Sea Basin. Examples from the Mons Basin (Belgium) and the Dieppe-Hampshire Basin (Normandy, France)

Christian Dupuis ^(a), Florence Quesnel ^(b, c) & Jean-Marc Baele ^(a)

^(a) Geology and Applied Geology, Faculty of Engineering, University of Mons, 20, Place du Parc, 7000, Mons, Belgium. E-mail: Christian.DUPOUIS@umons.ac.be

^(b) BRGM (French Geological Survey), DGR/GAT, 1, Av. Cl. Guillemin, BP 36009, 45060 – Orléans Cedex 2, France

^(c) UMR 7327 of the CNRS/INSU, Orléans University & BRGM, 1A, rue de la Férollerie, 45071 Orléans, France

Document type: Short note.

Manuscript history: received 15 May 2014; accepted 30 May 2014; editorial responsibility and handling by Gerald R. Dickens & Valeria Luciani.

KEY WORDS: Dieppe-Hampshire Basin, onshore outliers (Varengueville, Normandy, France), Mons Basin (Carnières, Belgium), NW Europe, paleoweathering, PETM, Quartzitic silcrete, Sparnacian.

At the very end of the Paleocene, NW Europe experienced an abrupt sea-level drop which resulted in the spreading of terrestrial environments over the southern margins of the North Sea Basin (Dupuis et al. 2011). River systems invaded all the area and cut down pre-existing Thanetian beds. Subsequent transgression filled the incised channels with a sequence of fluvial, then floodplain or palustrine to lacustrine and marsh pond deposits. The transgression gradually flooded low-lying and/or subsiding areas with lagoonal (brackish) and shallow marine beds. This succession, historically referred to as “Sparnacian” facies, recorded the Carbone Isotope Excursion (CIE) and the *Apectodinium* acme, which mark the base of the Eocene series and the PETM. Both events constitute good complementary stratigraphic markers supporting precise correlation between distant sections and derived high time resolution paleogeographic reconstructions. Since the XIXth Century, the Eocene is known to be a period of silicification in NW Europe (Heren, 1910; Thiry et al. 1983). Due to extensive pre-existing Thanetian sandy deposits, silicified sandstones, well known as ‘grès landéniens’ are particularly frequent. As they essentially have a quartzitic texture, the name “quartzitic silcretes” (QS) is recommended here for their designation. Hereafter, silicification is shown to be linked to alteration processes closely related to the latest Paleocene regional uplift and the PETM climatic/hydrologic perturbations, two major events of the P-E boundary. QS appear to be the prominent products of this earliest Eocene paleoweathering. As a coveted building material, QS are known since Neolithic times as they were extensively used in megalithic monuments. Their extraction lasted until the beginning of the XXth Century in numerous historical extraction centres (Heren, 1910), which constitute a rich and accurate source of information together with the regional geological literature (Dupuis, 1979). Field work and geological mapping completed the data collection together with relevant BRGM geological maps where QS remnants are often mapped as “erratics” (Dupuis & Kuntz, 1971; Quesnel, 1997; Quesnel et al., 2009). Obviously a special attention was paid to sections in which QS can be studied *in situ* and of which prominent results are reported here

(Dupuis & Steurbaut, 1987). Main occurrences concentrate upon classic structural highs (Dupuis, 1979). Such a superimposition of the QS distribution with long-term upheaval trending structures suggests that their development was influenced by the P-E uplift rejuvenation of regional ancient structures (Dupuis, 1979; 2011). The size of QS concretions may vary between a few decimetres up to several metres. Their overall shape is generally quite irregular, rather frequently tabular, sometimes more or less conical or cylindrical. Their surface is frequently complicated by protuberances and hollows depicting a complex multiphase growth. They often exhibit a mammillated, botryoidal or custard-like external morphology evocating the coalescence of several distinct smallest concretions. Occasionally elongated tubular structures resembling thick folded draperies may be interpreted as the result of a silica cementation driven by flowing water. Studying the internal structure clearly suggests accretion of successive generations of silicified sandstone. Occurrences of *in situ* QS are scarce. Two of them, which are located at the extremities of the study area, are here examined: the Normandy cliffs at Varengueville and Sotteville (onshore outcrops of the Dieppe-Hampshire Basin) to the west and the Carnières quarry (eastern Mons Basin) to the east. In the Varengueville outcrops the P-E succession consists in a twofold transgressive sequence. QS occupy the basal sand of the first sequence –the only considered here– which lies in large fluvial channels cutting down the Upper Cretaceous Chalk. Above it, in ascending order, are lying fresh-water limestone, marls and lignite complex (L1). Subsequent deposits consist in two sets of an alternation of clay, silt and coquina beds of probable tidal origin (Ailly Mb) separated by a lignite complex (L2). All these beds constitute the Sparnacian facies. They are capped by a marine glauconitic clay (Craquelins Mb) in which the transgressive trend culminates. The lignite complex L1 bears the CIE onset which marks the P-E boundary. The *Apectodinium* acme was essentially identified from the very top of the L1 complex up to the top of the Ailly Mb and is interpreted as relevant to the PETM. QS developed in bleached parts of the fluvial sand that were originally calcareous, pyritic and clayey, and locally rich in reworked flint debris and ‘rognons’. Weathered and original sands are separated by a cm-thick front of iron oxides and gypsum-cemented sand revealing acidification as a major process of the bleaching. In addition,

geopetal cappings on sparse flints point up to the migration of fine-grained material as another process contributing to the bleaching of the sand (Dupuis & Steurbaut, 1987). In the Carnières quarry, the P-E succession exhibits two contrasting parts. At the base, Thanetian sands rest on the strongly decalcified Coniacian (Saint-Vaast Chalk). The upper part, which is predominantly clayey and silty, dark and glauconiferous, belongs to the so-called "Morlanwelz Argilite" of Ypresian *s.s.* age. The Thanetian sands are divided into two units: the lower consists in glauconiferous bioturbated sands (Grandglise Mb) and the upper is made of poorly glauconiferous stratified sands. The Morlanwelz Argilite clearly lies unconformably on the Thanetian sands with a gravel lag and sparse small pebbles-rich channels at its base. Beneath the unconformity, a large volume of the sands is altered into Fe-Mn oxides stained sands, black to reddish in colour. The altered sand mass has diffuse boundaries and its shape is a grossly curved strip some metres thick. A QS concretion more than two metres in height occupies its central part. Laterally, a narrow graben postdating alteration and predating the Ypresian *s.s.* transgression cuts the weathered zone. It is filled with a succession of sandy clay and sand, which are also partly weathered. These deposits exhibit plenty of Ophiomorpha-type burrows indicating a brackish or shallow marine deposition. The weathered/bleached sand masse with QS concretion and the brackish sediments, sandwiched between the Thanetian Sands and Ypresian *s.s.* sediments, are in the stratigraphic position of the Sparnacian interval and then may have formed during the PETM. In both cases, QS developed only in bleached sands. This means that weathering was a necessary preliminary step allowing silica cementation of the sands. Indeed, it is well known that the "cleanness" of a sand favours its cementation (see for example Heald and Larese, 1974). In the Varengeville cliffs, the sand filling the channels is calcareous, pyritic, slightly silty and clayey. Bleaching this material needs acidification and the removal of the clay and silt fractions. The weathering front contains poecilitic gypsum crystals showing that groundwater carried once sulphuric acid. In addition, illuviation features (silanes) and silty geopetal cappings on gravels also point up to an intense percolation of water transporting fines grains through the sand. In the Carnières quarry, the bleaching of the sands needs hydrolysis of the glauconite and again the washing out of the fine-grained materials. A similar acidification process is suspected as being responsible for the destabilisation of the glauconite with, in particular, the liberation of iron and other cations from the silicates. Such an acidification is also supported by evidence of smectite to kaolinite transformation across the weathering profile. Illuviation ribbons (enriched in Mn-Fe oxides) superimposed over strata and clay/silt capping on burrows also suggest that the downward migration of small particles substantially contributed to the bleaching of the sand.

It can be postulated that QS formation requires an adequate sandy substrate to be cemented by silica. During Sparnacian times, efficient bleaching processes seem to have been very active and efficient enough to weather different kinds of sands, to wash out the fine fractions, to dissolve carbonate and to

hydrolyse silicates. Specific minerals present in the substratum or/and in the near-contemporaneous terrestrial environment probably have played a significant role for example in delivering acidified water, but other determinant parameters must be invoked too. Clearly, groundwaters have played the major role both in the weathering "preparation" of the sand and in transporting enough silica to build the QS concretions. This surely means that huge quantities of groundwater were circulating at that time in the permeable sands. This suggests that the reliefs created by the Upper Paleocene uplift together with the subsequent PETM-related perturbations of the hydrologic cycle may have boosted the groundwater circulation and must be regarded as responsible of the effects unravelled in the studied area, leading to the regional Quartzitic Silcrete development.

REFERENCES

- Cayeux L. (1906) – Structures et origine des grès du Tertiaire parisien. Mém. Serv. Carte géol. Fr., (Études des gîtes minéraux de la France), 161p.
- Dupuis C. & Kuntz G., (1972) - Carte géologique d'Amiens à 1/50 000ème - 46, Editions du B.R.G.M.
- Dupuis C. (1979) - Esquisse paléogéographique du nord et du nord-ouest du Bassin de Paris au Paléocène et à l'Eocène inférieur. Incidences structurales. C.R. Acad. Sc. Paris, t. 288, D, 1587-1590.
- Dupuis C. et Steurbaut E. (1987) - Altérites, sables marins (NP8, NP9), silicification et stromatolites dans le Paléocène supérieur entre Criel et le Cap d'Ailly (Haute-Normandie). Ann. Soc. Géol. Nord, CV, 233-242.
- Dupuis C., Quesnel P., Iakovleva A.I., Storme J.Y., Yans J. & Magioncalda R. (2011) – Sea level changes in the Paleocene-Eocene interval in the NW France: Evidence of two major drops encompassing the PETM. In: Egger H. (ed.), CBEP 2011, Conference Program and Abstracts, 5-8 June 2011, Salzburg, Austria. Berichte der Geologischen Bundesanstalt, 85, 68.
- Heald M.T. & Larese R.E. (1974) – Influence of coatings on quartz cementation. J. sedim. Petrology, 44, 4, 1269-1274.
- Heren, E. 1910 – Histoire du grès et de la gresserie en Picardie et particulièrement dans le département de la Somme. Mém. Soc. Antiquaires de Picardie. T. XXXVI, 327-642.
- Quesnel F., (1997) – Cartographie numérique en géologie de surface- Application aux altérites à silex de l'ouest du Bassin de Paris. Thèse Doctorat Géologie, Univ. Rouen, Documents du BRGM, Orléans, 263, 428 p.
- Quesnel F., Dupuis C., Yans J., Ricordel-Prognon C., Rad S., Storme J.-Y., Barbier F., Roche E., Bourdillon C. & Smith T. (2009) - Reconstructing the Late Paleocene-Early Eocene continental paleosurface in and around the Paris Basin: new insights for paleogeographic, geodynamic and climatic studies. In: Crouch, E.M., Strong, C.P., Hollis, C.J., (Eds). Climatic and Biotic Events of the Paleogene (CBEP 2009), extended abstracts, GNS Science Miscellaneous Series, 18, 102-106.
- Thiry M., Delaunay A., Dewolf Y., Dupuis C., Ménéillet F., Pellerin J. & Rasplus L. (1983) – Les périodes de silicification au Cénozoïque dans le Bassin de Paris. Bull. Soc. géol. Fr., 25, 1, 31-40.

Spatial variability of environmental change and the magnitude of biotic responses of planktic foraminifera across the PETM

Kirsty M. Edgar ^(a,b) & Pincelli M. Hull ^(c)

^(a) School of Earth Sciences, University of Bristol, Bristol, BS8 1RJ, UK. E-mail: kirsty.edgar@bristol.ac.uk

^(b) The Cabot Institute, University of Bristol, UK

^(c) Yale University, Geology and Geophysics, New Haven, CT 06511, USA

Document type: Abstract.

Manuscript history: received 15 May 2014; accepted 30 May 2014; editorial responsibility and handling by Gerald R. Dickens & Valeria Luciani.

KEY WORDS: biotic sensitivity, PETM, planktic foraminifera, tropics.

Tropical taxa are adapted to relatively uniform and narrow environmental niches and often live at or close to their environmental and/or physiological limits. These taxa may therefore be relatively more sensitive to anthropogenic climate change than those from the temperate or polar regions.

Here we test this hypothesis by assessing the planktic foraminiferal response to the largest of the known transient Paleogene global warming events, the Paleocene Eocene Thermal Maximum (PETM). During the PETM (~56 million years ago), global sea surface temperatures increased by ~5–6°C with the largest temperature change (up to 8°C) recorded at the poles and the smallest (<2°C) in the tropics (e.g., synthesis by Dunkley-Jones et al., 2013).

We compiled published planktic foraminiferal assemblage records from multiple deep-sea and shelf sites that span the PETM, updated species concepts for consistency with the Paleogene Planktonic Foraminiferal Working Group (Olsson et al., 1999; Pearson et al., 2006) and placed all of the sites onto a common age-scale. We then applied a range of biotic metrics to assess individual through community level changes across

this event. We constrain for the first time the spatial variability in the magnitude and mode of planktic foraminiferal response to environmental change across the PETM. Ultimately, these records allow us to determine if tropical communities really are more sensitive to environmental change than their polar counterparts despite the disparity in the magnitude of environmental change that these communities experienced.

REFERENCES

- Dunkley Jones T., Lunt D.L., Schmidt D.N., Ridgwell A., Sluijs A., Valdes P.J. & Maslin M. (2013) - Climate model and proxy data constraints on ocean warming across the Paleocene-Eocene Thermal Maximum, *Earth-Sci. Rev.*, 125 123–145.
- Olsson R.K., Berggren W.A., Hemleben C. & Huber B.T. (1999): Atlas of Paleocene planktonic foraminifera. *Smithsonian Contributions to Paleobiology*, 85, 252p.
- Pearson P.N., Olsson R.K., Hemleben C., Huber B.T. & Berggren W.A. (2006) - Atlas of Eocene Planktonic Foraminifera, *Cushman Foundation Special Publication*, 41: Allen Press, Lawrence, Kansas, 513p.

Quantitative ocean temperatures from foraminifera Mg/Ca over the Eocene-Oligocene transition

David Evans ^(a), Wolfgang Müller ^(a), Jonathan Erez ^(b), Willem Renema ^(c), Bridget S.Wade ^(d) & Martin Ziegler ^(e)

^(a) Department of Earth Sciences, Royal Holloway University of London, TW20 0EX, UK E-mail: david.evans.2007@rhul.ac.uk

^(b) Earth Science Institute, The Hebrew University of Jerusalem, Israel

^(c) Naturalis Biodiversity Center, Leiden, The Netherlands

^(d) Department of Earth Sciences, UCL, WC1E 6BT, UK

^(e) ETH Zürich, Switzerland

Document type: Short note.

Manuscript history: received 15 May 2014; accepted 30 May 2014; editorial responsibility and handling by Gerald R. Dickens & Valeria Luciani.

KEY WORDS: clumped isotopes, EOT, foraminifera, laser-ablation ICPMS, Mg/Ca, seawater chemistry.

Foraminifera Mg/Ca is an extensively studied palaeothermometer which provides a significant proportion of the available quantitative ocean temperatures in the recent geological past. However, before the Pleistocene the application of this proxy is complicated by uncertainties regarding the Mg/Ca ratio of seawater which exerts a control on test Mg/Ca of similar magnitude to temperature (Evans & Müller, 2012). There are two major current limitations preventing the application of Mg/Ca palaeothermometry in deep-time which we address here: (1) Detailed secular variation in Paleogene seawater Mg/Ca is poorly constrained although the majority of model and proxy data suggests a 2-3× rise from ~2 to 5.2 mol/mol over the last ~40 Ma (see e.g. Coggon *et al.*, 2010), and (2) there are no published seawater-test Mg/Ca calibrations for any species of widely utilized foraminifera. After showing how these present limitations can be overcome, we apply our new calibrations to well-preserved planktic foraminifera spanning the Eocene-Oligocene transition (EOT) from St. Stephens Quarry, Alabama (Wade *et al.*, 2012) and Shubuta, Mississippi.

A new method for reconstructing seawater chemistry

In order to form the basis for new seawater Mg-Sr-Ba/Ca reconstructions, we calibrated the relationship between Mg/Ca-temperature and test-seawater Mg/Ca in the large benthic foraminifera *Operculina ammonoides*, the nearest living relative of the abundant Eocene genus *Nummulites*. Laser-ablation ICPMS measurements (Müller *et al.*, 2009) of calcein and barium labelled, laboratory-cultured foraminifera demonstrate a nonlinear (quadratic) relationship between seawater-test Mg/Ca. LA-ICPMS analyses of exceptionally-preserved fossil *Nummulites*, which demonstrably incorporate Mg in an equivalent manner to *Operculina* (Evans *et al.*, 2013), enable these culture-derived equations to be solved for Eocene seawater Mg/Ca whilst simultaneously providing an estimate of tropical seasonality. The sensitivity of nummulitid Mg

incorporation to temperature is much smaller than that typical of planktic species (~2 cf. 9%), which means that uncertainties in the palaeotemperature of the fossil locations from which these specimens are derived translate into small errors in calculated seawater Mg/Ca, typically ±0.2 mol/mol. Seasonality reconstructions are possible because these foraminifera have a longevity of >6 months, enabling seasonal shifts in proxy trace element incorporation to be assessed (Evans & Müller, 2013). Using this methodology, we reconstruct the alkali earth chemistry of seawater for the EOT, based on early Oligocene *Nummulites* from Mississippi. The development of Mg/Ca data and calibrations from these foraminifera for the purposes of seawater chemistry reconstruction is simplified by the fact that there are no significant secondary controls on Mg incorporation in these large benthic species: salinity, growth rate and saturation state effects are smaller than analytical error (see also Toyofuku *et al.*, 2000).

Globigerinoides ruber test-seawater Mg/Ca

To investigate the control exerted by seawater chemistry variations on planktic foraminifera, we calibrated the relationship between test-seawater Mg/Ca, and evaluated the similarity of Mg/Ca-temperature dependence at seawater Mg/Ca = 5 compared to 3, a ratio similar to that suggested by late-Paleogene/early Neogene reconstructions (Rausch *et al.*, 2013). New chambers precipitated under controlled laboratory conditions following plankton tow collection in the Red Sea were labelled using a ¹³⁵Ba seawater spike which can in turn unequivocally be identified by LA-ICPMS. These culture calibrations also show a quadratic dependence of test Mg incorporation on seawater Mg/Ca, and a reduction in the exponential constant of the Mg/Ca-temperature calibration with decreasing seawater Mg/Ca.

EOT foraminifera Mg/Ca-derived palaeotemperatures

Using the relationship between test-seawater Mg/Ca derived from *G. ruber* and an EOT seawater Mg/Ca reconstruction derived from LBF enables us to produce more accurate deep-time Mg/Ca-derived SST, and forms the basis of the easy application of this proxy globally for the Eocene-

Oligocene transition, or any time for which seawater Mg/Ca is precisely known. Our measurements, derived from LA-ICPMS depth profiles of individual chambers of *Turborotalia ampliapertura* and *Hantkenina alabamensis*, show the extent to which EOT cooling impacted the US Gulf, with the caveat that it is assumed that multi-species Mg/Ca-temperature and our test-seawater calibrations are broadly applicable to non-extant planktic foraminifera.

REFERENCES

- Coggon R.M, Teagle D.A.H., Smith-Duque C.E., Alt J. C. & Cooper M. J. (2010) – Reconstructing past seawater Mg/Ca and Sr/Ca from mid-ocean ridge flank calcium carbonate veins. *Science*, 327, 1114-1117.
- Evans D. & Müller W. (2012) - Deep-time foraminifera Mg/Ca thermometry: Nonlinear correction for secular change in seawater Mg/Ca. *Paleoceanography*, 27, PA4205.
- Evans D. & Müller W. (2013) – LA-ICPMS imaging of complex discontinuous carbonates: An example using large benthic foraminifera. *J. Anal. Atom. Spectrom.*, 28, 1039-1044.
- Evans D., Müller W., Oron S. & Renema W. (2013) - Eocene seasonality and seawater alkaline earth reconstruction using shallow-dwelling large benthic foraminifera. *Earth Planet. Sci. Lett.*, 381, 104-115.
- Müller W., Shelley M., Miller P. & Broude S. (2009) – Initial performance metrics of a custom-designed ArF excimer LA-ICPMS system coupled to a two-volume laser-ablation cell. *J. Anal. Atom. Spectrom.*, 24, 209-214.
- Rausch S., Böhm F., Bach W., Klügel A., Eisenhauer A. (2013) – Calcium carbonate veins in ocean crust record a threefold increase of seawater Mg/Ca in the past 30 million years. *Earth Planet. Sci. Lett.*, 362, 215-224.
- Toyofuku T., Kitazato H., Kawahat, H., Tsuchiya M. & Nohara M. (2000) – Evaluation of Mg/Ca thermometry in foraminifera: Comparison of experimental results and measurements in nature. *Paleoceanography*, 14, 456-464.
- Wade B.S., Houben A.J.P., Quaijtaal, W., Schouten S., Rosenthal Y., Miller K.G., Katz M.E., Wrigth J.D & Brinkhuis H. (2012) - Multiproxy record of abrupt sea-surface cooling across the Eocene-Oligocene transition in the Gulf of Mexico. *Geology*, 40, 159-162.

First find of a late Paleocene biraphid diatom: implications for models of diatom evolution

Juliane Fenner ^(*)

^(*) Federal Institute of Geosciences and Resources, Subdepartment B 1.4 Marine Resources, Stilleweg 2, D 30655 Hannover, Germany. E-mail: juliane.fenner@bgr.de

Document type: Short note.

Manuscript history: received 15 May 2014; accepted 30 May 2014; editorial responsibility and handling by Gerald R. Dickens & Valeria Luciani.

KEY WORDS: diatom evolution, *Haslea*, Paleocene, Pennales.

Since the early days of diatom studies it is known that pennate diatoms evolved later than centric diatoms. While finds of valves of Centrales are known from sediments as old as Early Jurassic (Rothpletz, 1896), the oldest valves of araphid pennate diatoms are reported from the late Cretaceous, and the oldest finds of valves of raphid pennate diatoms are from the Early Eocene. On the other hand molecular clock calculations based on nuclear DNA suggest an older age for the origin of raphid diatoms. Kooistra & Medlin (1996) calculated that raphid diatoms evolved within the late Cretaceous.

The here presented find of a number of specimens of valves and frustules of a new *Haslea* species, *Haslea antiqua* in deep sea sediment of ODP Hole 1121B in the Southwest Pacific at the foot of the Campbell Plateau (water depth 4499 m) extends the known record of hard parts of biraphid pennate diatoms into the lower part of the Late Paleocene (Calcareous Nannofossil Zone NP5).

Haslea species are pennate species, which already have a rather complex raphe system. It is a tongue- and groove type raphe. In *Haslea antiqua* the tongue is rail-shaped, and for most of the length of the raphe it is firmly locked into the groove part of the raphe embracing it. In addition the raphe structure is stabilized on the inside of the valve by a thickened rib along the groove side of the raphe as well as by simple fibulae across the raphe slit near the apices.

The basic valve construction is a two-layered architecture. The inner layer being a meshwork of orthogonally arranged bars, a two-dimensional silica bar lattice ("Rippengitter"-type construction of Kramer and Lange-Bertalot, 1986), which is the

bearing construction of each valve. Its bars running in apical direction and the piers positioned on them carry the upper layer of the valve, which consists of longitudinal strips.

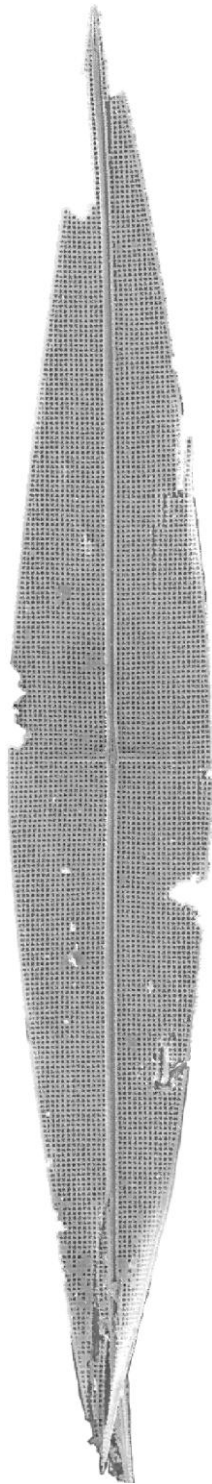
In the sample of deep sea ooze, in which *Haslea antiqua* occurs, species occur, which were displaced from a coastal marine environment by e.g. either a storm or tsunami. This suggests that also the valves and frustules of *H. antiqua* probably were displaced from near-shore environments into the deep sea sediments in which they now are found.

Considering that Pre-Miocene raphid diatoms predominantly lived in shallow water benthic habitats, and that with increasing sediment age the effects of diagenesis become stronger the find of such relatively well preserved raphid diatoms in Paleocene sediments is a fortunate situation.

The relatively complex construction of the tongue- and groove-type raphe of *Haslea antiqua* implies that definitely finds of biraphid pennate diatoms of even higher age can be expected in the future. And in this way this find of a biraphid pennate diatom species supports the trend indicated by the calculations based on molecular sequencing and assuming constant rates of evolution.

REFERENCES

- Rothpletz A. (1896) - Über die Fytsch-Fucoiden und einige andere fossile Algen, sowie über liassische Diatomeen führende Hornschwämme. Zeitschrift der Deutschen Geologischen Gesellschaft, 48, 854-915.
- Kooistra W.H.C.F. & Medlin L.K. (1996) - Evolution of the diatoms (Bacillariophyta) IV. A reconstruction of their age from small subunit rRNA coding regions and the fossil record. Mol. Phylogenet. Evol., 6(3), 391-407.



—20 μm —

Fig.1 – *Haslea antiqua*, internal view of valve showing the construction of the inner valve layer with an orthogonal pattern of bars and a narrow sternum with raphe slit.

Onset of Eocene diversity gradients in macroperforate planktonic foraminifera

Isabel S. Fenton ^(a,b), Paul N. Pearson ^(c), Tom Dunkley-Jones ^(d) & Andy Purvis ^(a,b)

^(a) Department of Life Sciences, Natural History Museum, Cromwell Road, London SW7 5BD, UK. Email: isabel.fenton@nhm.ac.uk

^(b) Department of Life Sciences, Silwood Park Campus, Imperial College London, Ascot, Berkshire SL5 7PY, UK

^(c) School of Earth and Ocean Sciences, Cardiff University, Cardiff CF10 3YE, UK

^(d) School of Geography, Earth and Environmental Sciences, University of Birmingham, Edgbaston, Birmingham B15 2TT, UK

Document type: Short note.

Manuscript history: received 15 May 2014; accepted 30 May 2014; editorial responsibility and handling by Gerald R. Dickens & Valeria Luciani.

KEYWORDS: Eocene, functional diversity, latitudinal diversity gradient, planktonic foraminifera, phylogenetic diversity, species richness.

The latitudinal diversity gradient (LDG) – whereby species richness within a taxon is highest at low latitudes – is one of the most widespread patterns in macroecology, being found in almost all habitats, regions and clades whether terrestrial or marine. Many explanations have been put forward to explain the LDG, invoking different mixtures of present environmental conditions and Earth history as causal factors, but a general consensus is lacking. Incorporating fossil data into studies of the LDG can provide insight into how it has changed through time, giving the potential to separate out some of these explanations.

The macroperforate planktonic foraminifera offer a model system for the study of how the LDG originated. They have a widespread distribution with species inhabiting a broad range of latitudes across all the major oceans. They are abundant in the water column, and on death their calcareous tests are deposited on the ocean floor, providing an excellent fossil record. Aze et al. (2011) produced a phylogeny of macroperforate planktonic foraminifera through the Cenozoic and collated information on some aspects of their ecology.

This combination of factors allows us to investigate the LDG both in the present day and through geological history to determine whether it, and its causes, has changed through time.

The global cooling through the Eocene allows us to test the primacy of environment as an explanation of the LDG. Large scale biological changes are known to have occurred through this time period (Bown, 2005; Pearson et al., 2008). However it is unclear what drove those changes and whether there was feedback between the biological diversity and the changing climate. Investigating the nature of the diversity changes in the macroperforate planktonic foraminifera provides insight into the importance of temperature, or other factors, as long-term drivers of global diversity patterns.

This study uses a collated global dataset of macroperforate planktonic foraminiferal occurrences throughout the Eocene and Oligocene. These records were obtained from a number of

sources including DSDP, ODP and IODP reports as well as literature searches. Geographic coordinates were converted to palaeocoordinates. The latest taxonomy was used to update old taxonomic names. The reported ages were also checked using the latest age models.

This dataset was used to investigate how a range of diversity measures, including phylogenetic and functional diversity, have changed through time. These different aspects of diversity can provide insight into the possible causes of the observed changes in diversity beyond what is possible from just measuring species richness.

Palaeoenvironmental data were used to identify possible drivers of these changes. Using a similar dataset for the Recent, we have been able to assess how well current environmental associations can predict past diversity patterns. Strong correlations are observed between species richness and these variables. The results of this study can then be compared to the Eocene diversity patterns to determine whether the variables affecting global diversity have changed through geological time.

Preliminary results suggest that temperature, which is the most important driver of diversity in the Recent, was also a strong driver of diversity through the Eocene global cooling.

REFERENCES

- Aze T., Ezard T.H.G., Purvis A., Coxall H.K., Stewart D.R.M., Wade B.S. & Pearson P.N. (2011) - A phylogeny of Cenozoic macroperforate planktonic foraminifera from fossil data. *Biol. Rev.*, 86, 900-927.
- Berling D.J. & Royer D L. (2011) - Convergent Cenozoic CO₂ history. *Nat. Geosci.*, 4(7), 418-420.
- Bown P.R. (2005) - Calcareous nannoplankton evolution: A tale of two oceans. *Micropaleontol.*, 51(4), 299-308.
- Pearson P.N., McMillan I.K., Wade B.S., Dunkley-Jones T., Coxall H.K., Bown P.R. & Lear C.H. (2008) - Extinction and environmental change across the Eocene-Oligocene boundary in Tanzania. *Geology*, 36(2), 179-182.

Middle Eocene–Lower Oligocene biostratigraphy and paleoceanography of the Western Equatorial Indian Ocean based on Calcareous Nannofossils, ODP Site 711

Chiara Fioroni ^(a), Giuliana Villa ^(b) & Davide Persico ^(b)

^(a) Università degli Studi di Modena e Reggio Emilia, Dipartimento di Scienze Chimiche e Geologiche, L.go S. Eufemia, 19, 41100 Modena, Italy. E-mail: chiara.fioroni@unimore.it

^(b) Università degli Studi di Parma, Dipartimento di Fisica e Scienze della Terra, Parco Area delle Scienze, 157 a, 78, 43124 Parma, Italy

Document type: Short note.

Manuscript history: received 15 May 2014; accepted 30 May 2014; editorial responsibility and handling by Gerald R. Dickens & Valeria Luciani.

KEY WORDS: biostratigraphy, Eocene, nannofossils, Oligocene, paleoceanography, paleoecology.

New quantitative analyses of Middle Eocene to Lower Oligocene Calcareous Nannofossils from ODP Site 711 (western equatorial Indian Ocean) allowed to improve the biostratigraphic resolution by proposing new bioevents in addition to the recent studies from low and mid latitudes. Comparison of biostratigraphic data with magnetostratigraphy (Saviani et al., 2013) enabled to establish an accurate time control at Site 711 for the investigated interval, and to infer paleoceanographic implications.

Thirty bioevents throughout ~11 Ma have been discussed and provide an increased biostratigraphic resolution for low latitudes and some represent alternative markers (Fig.1). This is the case of *Criboecium erbae*, that seems to be a promising biohorizon as an alternative event for the base of Zone NP18 (Martini, 1971), usually defined by the Lowest Occurrence (LO) of *Chiasmolithus oamaruensis*. In fact, this latter species is very rare at low to middle latitudes, thus the *C. erbae* Acme Beginning (AB) could be of essential importance for the definition of the Priabonian GSSP (Agnini et al., 2011), and our results confirm the reproducibility of this event also at equatorial Indian paleolatitudes.

Also several sphenoliths, very abundant at this low latitude site, provide many appreciable biohorizons, such as the Highest occurrence (HO) of *S. kempfi*, the LOs and HOs of *S. runus*, *S. strigosus*, and *S. obtusus*, the HOs of *S. spiniger* and *S. furcatholithoides*, the LO of *S. akropodus*, leading to increase the biostratigraphic resolution for the Middle -Late Eocene.

Additional discussion is devoted to the variation in abundance of selected nannofossil taxa as response to paleoenvironmental changes. The investigated interval includes the long-term cooling trend that leads to the Oligocene glacial state (Oi-1, Miller et al., 1991) following the Middle Eocene Climatic Optimum (MECO). The relationship between CCD fluctuations, ocean acidity variations, $p\text{CO}_2$ concentrations, and

ultimately climate, are matter of discussion (Coxall & Wilson, 2011) and the study of calcareous nannofossils have been proved to be an excellent tool to add information on paleoclimate variations (Villa et al., 2013). Our data show that the Nannofossil total abundance, expressed as Number/mm², considerably decreases in an interval about 3m thick corresponding to an interval of low CaCO₃ content, indicating a shoaling of the CCD (Peterson & Backman, 1990). This interval is almost barren in nannofossils and the only taxa present are the rare dissolution-resistant *Discoaster* spp. and *Cyclicargolithus floridanus*. The age of the interval deprived of CaCO₃ is dated to ~39.5-39.1 Ma by means of the correlation with the magnetostratigraphy and the MAR data. Previously, Bohaty et al. (2009) locate this interval as coinciding to the peak of the MECO at 40.1 Ma. Therefore, not being the oxygen isotopes data available from Site 711, we could suppose that the dissolution event is not strictly tied to the MECO interval, or, less plausibly, that the peak of the MECO is younger (39.5 Ma) in the equatorial Indian Ocean.

Also, we document a shift of the nannofossil assemblage, starting before the inception of the Eocene – Oligocene Transition (EOT), at about 34.5-34.1 Ma, evidenced by an increase in eutrophic species and a decrease in oligotrophic-warm-water taxa. The general trend of the selected taxa shows a decrease in *Discoaster* and *Criboecium reticulatum*, usually considered warm and oligotrophic water taxa, and a concurrent increase in eutrophic *Reticulofenestra daviesii*, *Cyclicargolithus floridanus*, *Sphenolithus predistentus* and *Helicosphaera* spp., just before the beginning of the EOT. This turnover highlights an early response of nannofossil assemblage to paleoceanographic and climatic changes of the EOT (~34-33.5 Ma), here interpreted as a shift toward increased nutrient availability in the surface waters of the equatorial Indian Ocean. This increase could be related to the Late Eocene glacial event (Katz et al., 2008), precluding the EOT, which would have favoured a sea level drop and, in turn, a runoff increase and eventually ocean eutrophication.

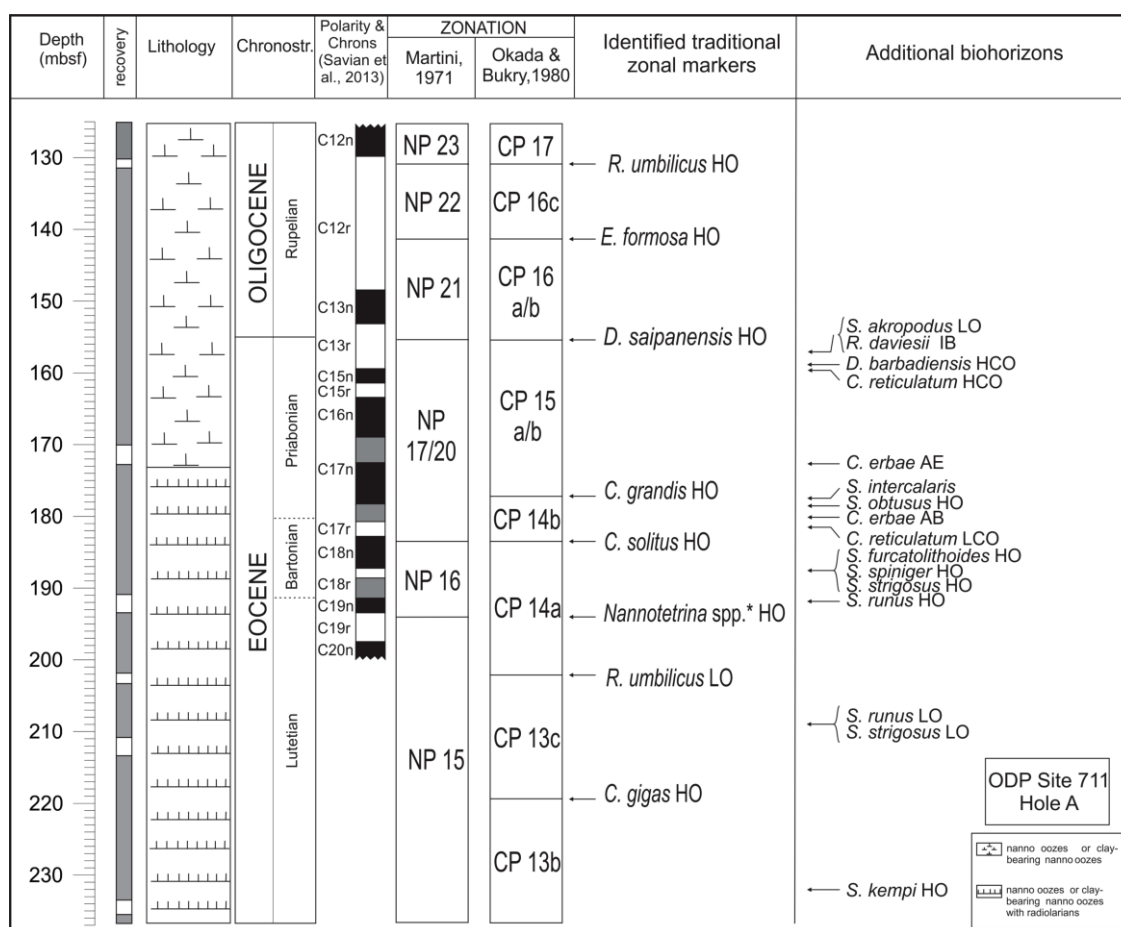


Fig.1 – Calcareous Nannofossil biostratigraphic summary of the middle Eocene-lower Oligocene at Site 711 plotted against depth and magnetostratigraphy. Simplified lithology is from Backman and Duncan (1988).

REFERENCES

Agnini C., Fornaciari E., Giusberti L., Grandesso P., Lanci L., Luciani V., Muttoni G., Pälike H., Rio D., Spofforth D.J.A. & Stefani C. (2011) - Integrated biomagnetostratigraphy of the Alano section (NE Italy): A proposal for defining the middle-late Eocene boundary. *Geol. Soc. Am. Bull.*, 123, 841–872, doi:10.1130/B30158.1.

Bohaty S.M., Zachos J.C., Florindo F. & Delaney M. L. (2009) - Coupled greenhouse warming and deep-sea acidification in the middle Eocene. *Paleoceanography*, 24, PA2207, doi:10.1029/2008PA001676.

Coxall H.K., & Wilson P.A. (2011) - Early Oligocene glaciation and productivity in the eastern equatorial Pacific: Insights into global carbon cycling. *Paleoceanography*, 26, PA2221, doi:10.1029/2010PA002021.

Katz M.E., Miller K.G., Wright J.D., Wade B.S., Browning J.V, Cramer B.S. & Rosenthal Y., (2008) - Stepwise transition from the Eocene greenhouse to the Oligocene icehouse. *Nat. Geosci.*, 1, 329–334, doi:10.1038/ngeo179.

Martini E. (1971) - Standard Tertiary and Quaternary calcareous nannoplankton zonation. In: Farinacci, A. (Eds.), *Proc. 2nd Int. Conf. Planktonic Microfossils*, Roma, 2, 739-785.

Miller K.G., Wright J.D. & Fairbanks R.G. (1991) - Unlocking the Ice House: Oligocene-Miocene Oxygen Isotopes, Eustasy, and Margin Erosion. *Journal Geophys. Res.*, 96, 6829-6848.

Peterson L.C. & Backman J. (1990) - Late Cenozoic carbonate accumulation and the history of the carbonate compensation depth in the western equatorial Indian Ocean. In: Duncan, R.A., Backman J., Peterson L., C. et al. (1990) - *Proc. ODP Progr., Sci Results*, 115: College Station, TX (Ocean Drilling Program).

Saviani J. F., Jovane L., Bohaty S.M. & Wilson P.A. (2013) - Middle Eocene to early Oligocene magnetostratigraphy of ODP Hole 711A (Leg 115), western equatorial Indian Ocean. *Geol. Soc. London, Spec. Publ.* v.373, doi: 10.1144/SP373.16.

Villa G., Fioroni C., Persico D., Roberts A.R. & Florindo F. (2013) - Middle Eocene to Late Oligocene Antarctic glaciation/deglaciation and Southern Ocean productivity. *Paleoceanography*, 29(3), 223-237, doi: 10.1002/2013PA002518

The Paleocene – Eocene Thermal Maximum: temperature and ecology in the tropics

Joost Frieling ^(a), Holger Gebhardt, ^(b), Olujide A. Adekeye ^(c), Samuel. O. Akande ^(c), Gert-Jan Reichart ^(a,d),
Jack J. Middelburg ^(a), Stephan Schouten, S. ^(a,d) & Appy Sluijs ^(a)

^(a) Department of Earth Sciences, Utrecht University, Budapestlaan, 4, 3584CD, Utrecht, Netherlands. E-mail: j.frieling1@uu.nl

^(b) Geologische Bundesanstalt, Neulinggasse 38, A 1030 Wien, Austria

^(c) Department of Geology and Mineral Sciences, University of Ilorin, P.M.B. 1515, Kwara State, Nigeria

^(d) NIOZ Royal Netherlands Institute for Sea Research, 1790AB Den Burg, Texel, The Netherlands

Document type: Abstract.

Manuscript history: received 15 May 2014; accepted 30 May 2014; editorial responsibility and handling by Gerald R. Dickens & Valeria Luciani.

KEY WORDS: $\delta^{18}\text{O}$, dinoflagellates, Mg/Ca, PETM, tropics, TEX_{86} .

Various records across the Paleocene – Eocene Thermal Maximum (PETM) have established approximately 5 °C of additional surface and deep ocean warming (Dunkley Jones et al., 2013), superimposed on the already warm latest Paleocene. The PETM is further characterized by a global negative stable carbon isotope excursion (CIE), poleward migration of thermophilic biota (Sluijs et al., 2006), ocean acidification (Zachos et al., 2005), increased weathering, photic zone euxinia and intensified hydrological cycle. Reconstructed temperatures for the PETM in mid and high-latitudes regularly exceed modern open marine tropical temperatures (Zachos et al., 2006; Sluijs et al., 2011). Constraints on absolute tropical temperatures are, however, limited.

We studied the PETM in a sediment section from the Nigerian sector of the Dahomey Basin, deposited on the shelf near the equator. We estimate sea surface temperatures by paired analyses of TEX_{86} , and Mg/Ca and $\delta^{18}\text{O}$ of foraminifera from the Shagamu Quarry (Gebhardt et al., 2011). These show Paleocene temperatures of ~33 °C and SSTs rose by 4 °C during the PETM based on $\text{TEX}_{86}^{\text{H}}$ (Kim et al., 2010). During the PETM, intermittent photic zone euxinia developed based on the presence of the biomarker isorenieratane. Interestingly, during peak warmth, dinoflagellate cyst abundances and diversity are remarkably low.

From our new data and evidence from modern dinoflagellate experiments, we conclude that thermal stress was the main driver for this observation. We derive that endothermal and most ectothermal nektonic and planktonic marine eukaryotic organisms could not have lived in the surface waters in this part of the tropics during the PETM.

REFERENCES

Dunkley-Jones T., Lunt D.J., Schmidt D.N., Ridgwell A., Sluijs A., Valdes P.J. & Maslin M. (2013) - Climate model

and proxy data constraints on ocean warming across the Paleocene–Eocene Thermal Maximum. *Earth Sci. Rev.* 125, 123-144.

Gebhardt H., Adekeye O.A. & Akande S.O. (2011) - Late Paleocene to Initial Eocene Thermal Maximum (IETM) Foraminiferal Biostratigraphy and Paleocology of the Dahomey Basin, Southwestern Nigeria. *Jb. Geol. B.-A.*, 150, 3-4, 407-419.

Kim J.-H., van der Meer J., Schouten S., Helmke P., Willmott V., Sangiorgi F., Koc N., Hopmans E.C. & Sinninghe Damsté J.S. (2010) - New indices and calibrations derived from the distribution of crenarchaeal isoprenoid tetraether lipids: Implications for past sea surface temperature reconstructions. *Geochim. Cosmochim. Acta*, 74, 4639-4654.

Sluijs A., Schouten S., Pagani M., Woltering M., Brinkhuis H., Sinninghe Damsté J.S., Dickens G.R., Huber M., Reichart G.-J., Stein R., Matthiessen J., Lourens L.J., Pedentchouk N., Backman J., Moran K. & the Expedition 302 Scientists. (2006) - Subtropical Arctic Ocean temperatures during the Palaeocene/Eocene thermal maximum. *Nature* 441, 610-613.

Sluijs A., Bijl P.K., Schouten S., Rohl U., Reichart G.-J. & Brinkhuis H. (2011) - Southern ocean warming, sea level and hydrological change during the Paleocene-Eocene thermal maximum. *Clim. Past.*, 7, 47-61.

Zachos J.C., Rohl U., Schellenberg S.A., Sluijs A., Hodell D.A., Kelly D.C., Thomas E., Nicolo M., Raffi I., Lourens L.J., McCarren H. & Kroon D. (2005) - Rapid Acidification of the Ocean during the Paleocene-Eocene Thermal Maximum. *Science*, 308, 1611- 1615.

Zachos J.C., Schouten S., Bohaty S.M., Quattlebaum T., Sluijs A., Brinkhuis H., Gibbs S.J. & Bralower T.J. (2006) - Extreme warming of mid-latitude coastal ocean during the Paleocene-Eocene Thermal Maximum: Inferences from TEX_{86} and isotope data. *Geology*, 34, 737-740.

Siliceous sponges (Porifera: Hexactinellida, Demospongiae) from Chiampo Valley (Eocene, Lessini Mts, northern Italy): taxonomy, taphonomy and paleoecology

Viviana Frisone ^(a,b), Andrzej Pisera ^(c) & Nereo Preto ^(b)

^(a) Museo di Archeologia e Scienze Naturali "G. Zannato". 17, Piazza Marconi. 36075 Montecchio Maggiore (Vicenza). Italy. E-mail: museo.scienze@comune.montecchio-maggiore.vi.it

^(b) Università degli Studi di Padova, Dipartimento di Geoscienze. 6, via Gradenigo. 35131 Padova. Italy

^(c) Institute of Paleobiology. Polish Academy of Science. 51/55, Twarda. 00-818 Warszawa. Poland

Document type: Short note.

Manuscript history: received 15 May 2014; accepted 30 May 2014; editorial responsibility and handling by Gerald R. Dickens & Valeria Luciani.

KEY WORDS: Eocene, Italy, Hexactinellida, lithistid Demospongiae, siliceous sponges.

The fossil record of sponges is a very old one, beginning in the Precambrian, but rather incomplete. In order to achieve a better understanding of the evolution of sponges and the role they played in marine ecosystems, it is important to document their diversity through time (Pisera, 2006).

Eocene faunas that preserve siliceous sponge body fossils are known only from five areas worldwide: N Spain, S France, SW Australia, New Zealand and E USA (Frisone, 2014). We studied the taxonomy, taphonomy and paleoecology of an early Lutetian three-dimensionally preserved sponge fauna from Chiampo Valley (E Lessini Mts, northern Italy). Only preliminary publications exist so far about the fauna (Menin, 1972; Visentin, 1994; Matteucci & Russo, 2005). The material comes from a horizon of tuffites. The study area belongs to the Veneto Volcanic Province (VVP), identified by principally mafic and ultramafic rocks erupted during the Paleocene–Oligocene, mainly in submarine environments. Several magmatic pulses occurred separated by periods of magmatic inactivity during which marine sedimentation took place (e.g. Barbieri et al., 1982; Barbieri et al., 1991).

The material studied consists of more than 900 sponge body fossils (fig. 1) housed in Italian public museums. The fauna from Chiampo Valley shows a high diversity (32 taxa), and is dominated by siliceous sponges with a solid skeleton (Hexactinellida, lithistid demosponges). 10 new species and 2 new genera are proposed (Frisone, Pisera, Preto, in preparation). 15 taxa (47%) belong to class Hexactinellida, with 1 species (3%) belonging to order Lyssacosida, 7 Hexactinosida (22%), 7 Lychniscosida (22%). 17 taxa belong to Demospongiae (53%) with 16 lithistids (50%) and 1 Dictyoceratida (3%).

Of 22 genera described (excluding the 2 new genera), 14 are in common with a typical Cretaceous fauna of NW Germany (e.g. Schrammen, 1910; 1912). On the other hand the number of genera in common with other Eocene faunas is quite

low, ranging from 1 to 5. The present study extends the stratigraphic range of the genera *Camerospongia*, *Toulminia*, and *Bolidium* to the Eocene; previously their last appearance was Cretaceous..

There are 3 genera, i.e. *Stauractinella*, *Laocoetis* and *Ventriculites* that have roots in the Jurassic (Kaesler, 2004). Five genera are extant and live in a rather deep-water environment (Hooper & Van Soest, 2002).

The associated fauna consists mainly of smaller (benthic and planktonic) and larger foraminifera (e.g. Miliolidae, Rotalidae, *Nummulites*, *Discocyclina*). There are also crustaceans (decapods and ostracods), echinoids, bryozoans, mollusks (gastropods, especially pteropods, rare cephalopods, and bivalves), red algae and rare corals. The sponges from Chiampo show often basal discs or encrust other sponges, shells, nummulites, and unpreserved organisms (probably dissolved during diagenesis or originally organic in nature), indicating hard substrate colonization. Tuber-like or root-like basal structures were also documented alongside encrusting bases. The former type of attachment indicates anchoring in soft sediment. The presence of different modes of attachment in the Chiampo sponge fauna suggests heterogeneous bottom surface conditions.

In this study we documented also the presence of sponge clusters composed mainly of hexactinellid sponges. Together with the evidence of some taxa at various ontogenetic stages, the presence of delicate encrusting bases and the fact that sponges were reported in one site only, we assume that the sponge fauna is essentially *in situ*.

Study of thin sections has proved that both spicules and cement are calcite sparite. Pyrite framboids are common, peloidal micrite is often present and it is fluorescent. The sediment around sponges is a tuffite with arenaceous grain size, composed of rounded volcanic fragments, calcareous bioclasts, and calcitic cement. The volcanic clasts are strongly altered, with palagonitized glass in vesicles. The precipitation of pyrite and peloidal micrite could be induced by the presence of sulfate reducing bacteria.



Fig.1 – 3-D models of Chiampo fossil sponges (photo: S. Castelli).

CONCLUSIONS

1. The fauna from Chiampo Valley shows a high diversity (32 taxa), and is dominated by siliceous sponges with solid skeletons (Hexactinellida, lithistid demosponges). The fauna has a Cretaceous character. Ten new species and two new genera are proposed.
2. The original siliceous skeletons of the sponges were dissolved and replaced by molds in calcite sparite. Peloidal micrite, possibly of microbial origin, is ubiquitous.
3. Sponges colonized a mixed substrate, eventually forming clusters. The sponge fauna is essentially *in situ* and inhabited the middle-distal portion of a carbonate ramp.

REFERENCES

- Barbieri G., De Zanche V., Medizza F. & Sedeà, R. (1982) - Considerazioni sul vulcanismo terziario del Veneto occidentale e del Trentino meridionale. *Rend. Soc. Geol. It.*, 4, 267–270.
- Barbieri G., De Zanche V. & Sedeà R. (1991) - Vulcanismo paleogenico ed evoluzione del semigraben Alpone-Agno (Monti Lessini). *Rend. Soc. Geol. It.*, 14, 5-12.
- Frisone V. (2014) - Eocene siliceous sponges (Porifera: Hexactinellida, Demospongiae) from Eastern Lessini Mountains (northern Italy). Unpublished Ph.D. thesis, University of Padova, 132 pp.
- Hooper J.N.A. & Van Soest R.W.M. (eds) (2002) - *Systema Porifera: a guide to the classification of Sponges*. Kluwer Academic/Plenum Publishers, New York. 1–1101, 1102–1706 pp.
- Kaesler R.L. (ed.) (2004) - *Treatise on Invertebrate Paleontology, part E (revised), Porifera. Volume 3*. The Geological Society of America, Boulder, Colo., and the University of Kansas, Lawrence, 903 pp.
- Matteucci R. & Russo A. (2005) - The Middle Eocene siliceous sponges from Val di Chiampo (Lessini Mountains, northern Italy), *Annali dell'Università di Ferrara, Sezione Museologia Scientifica e Naturalistica. Volume speciale*. 51-62.
- Menin A. (1972) - Silicosponge dell'Eocene medio della Valle del Chiampo (M. Lessini, Vicenza). *Annali dell'Università di Ferrara (nuova serie), Scienze Geologiche e Paleontologiche*, 5, 63-69.
- Pisera A. (2006) - Palaeontology of sponges — a review, *Canadian J. of Zoology*, 84(2), 242-261.
- Schrammen A. (1910) - Die Kieselspongien der oberen Kreide von Nordwestdeutschland, I, Tetraxonia, Monaxonia und Silicea incertae sedis. *Palaeontographica, Supplement 5*, 1-175.
- Schrammen A. (1912) - Die Kieselspongien der oberen Kreide von Nordwestdeutschland, II, Triaxonia (Hexactinellida), *Palaeontographica, Supplement 5*, 176-385.
- Visentin M. (1994) Segnalazione di una spongiofauna eocenica nella Valle del Chiampo (Lessini orientali, Vicenza), *Lavori – Società Veneziana di Scienze Naturali*, 19, 229-230.

Orbital Forcing of Early Eocene dissolution events and Carbon Isotope Excursions from the Contessa Road-Bottaccione composite section (Gubbio, central Italy)

Simone Galeotti ^(a) & Matteo Moretti ^(a)

^(a) Department of Earth, Life and Environmental Sciences, University of Urbino, Campus Scientifico 'E. Mattei', 61029, Urbino, Italy. E-mail: simone.galeotti@uniurb.it

Document type: Short note.

Manuscript history: received 15 May 2014; accepted 30 May 2014; editorial responsibility and handling by Gerald R. Dickens & Valeria Luciani.

KEY WORDS: Eocene, Gubbio, hyperthermals, orbital forcing.

A continuous record of the Early Eocene (~56-49 Million years ago; Ma), is preserved in the Scaglia Rossa pelagic red limestones of the Umbria–Marche succession from central Italy (Alvarez et al., 1977; Lowrie et al., 1982). Bio-magnetostratigraphic calibration of the Bottaccione and Contessa-Road outcrops in the Gubbio area allows assembling a continuous and undisturbed composite section spanning the entire Paleocene to the middle Eocene. Spectral analysis of a high-resolution geochemical record spanning the Paleocene Eocene Thermal Maximum (PETM, at ~56 Ma) to the Early Eocene Thermal Maximum 3 (ETM3, at ~53 Ma) has shown that the Lower Eocene weight percent (wt.%) CaCO₃ record at Contessa Road is intimately linked to orbital cycles of eccentricity (Galeotti et al., 2010).

Changes in the thickness of individual eccentricity cycles indicate that CaCO₃-depleted intervals are relatively condensed in the lower Eocene Scaglia Rossa, suggesting that carbonate dissolution is the main cause of changes in wt.% CaCO₃ and sedimentation rate (Galeotti et al., 2010). Lower proportions of planktonic foraminifera (more sensitive to dissolution than benthic species) and higher proportions of agglutinating specimens (more resistant to dissolution than calcareous hyaline forms) in benthic foraminiferal assemblages within clay-rich layers provide further evidence for dissolution as a driving mechanism for the observed cyclicity. Similar to observed in oceanic successions (e.g., Lourens et al., 2005, Westerhold et al., 2007) lower wt.% CaCO₃ intervals corresponding to dissolution events, are associated with increased insolation and arguably warmer global temperatures. Filters of the orbitally forced components in the geochemical records provide evidence that hyperthermals ETM2 and ETM3 (H1 and K of Cramer et al., 2003, respectively) are larger expressions of a continuum of dissolution horizons during the Early Eocene (Galeotti et al., 2010).

In this work we have complemented the record of the Contessa-Road with new wt.% CaCO₃ data spanning the base of magnetochron C23n to the base of C22n (~52 to ~49 Ma) derived from the Bottaccione section. The composite record,

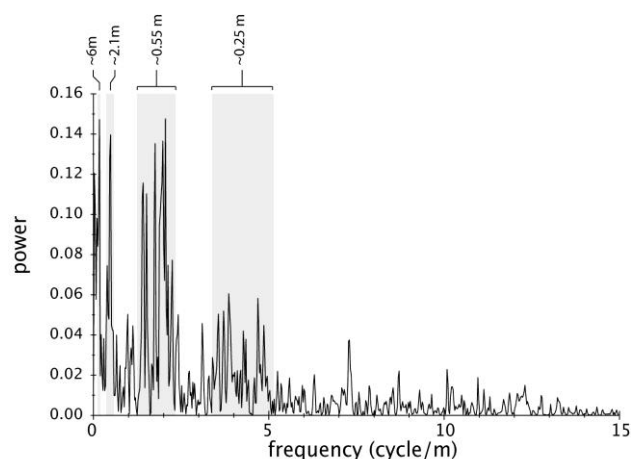


Fig.1 – Fourier power spectra of wt.% CaCO₃ from the composite Contessa Road-Bottaccione section calculated in the depth domain by the AnalySeries program (Paillard et al., 1996). The numbers at the spectral peaks denote the period in metres.

therefore, spans the PETM to well above the Early Eocene Climatic Optimum (EECO), with a sampling resolution of 3 cm corresponding to ~6 kyr in the time domain based on the average sedimentation rate (0.5 cm/kyr) of the lower Eocene Scaglia Rossa (Galeotti et al., 2010).

Spectral analysis of the obtained composite record carried out in the depth domain (i.e., before tuning) shows that the continuum of dissolution intervals – including the well known hyperthermal events ETM2 and ETM3 – is dominated by periodic components with spectral peaks at frequencies of ~4 cycles/m, ~1.9 cycles/m, ~0.48 cycle/m and ~0.17 cycles/m corresponding to periods of ~0.25 m, ~0.55 m, ~2.1 m and ~6 m, respectively (Fig. 1). Based on an average sedimentation rate of ~0.5 cm/kyr, these periodic components can be ascribed to the 41 kyr obliquity (0.25 m), the 100 kyr- (0.55m) and 400 kyr (2.1 m) eccentricity, and to a ~1.2.Myr component resembling the long-term modulation of obliquity.

Filtering of these periodic components together with an evolutive spectral analysis of the wt.% CaCO₃ indicates that the frequency and magnitude of dissolution events through

time is controlled by long-term modulations of orbital parameters, including long eccentricity (400 kyr) and a 1.2 million year modulation. Notably, the highest frequency of dissolution events – at the orbital scale – is observed across magnetochron C23n, which corresponds to the long-term warm peak of the EECO. This provides an observational basis to validate theoretical models predicting a threshold effect resulting from orbital forcing superimposed on gradually changing mean global boundary conditions (Lunt et al., 2011; DeConto et al., 2012). For ~1 Myr across the EECO, in fact, each short eccentricity maximum was effective in triggering the mechanism(s) responsible for carbonate dissolution, in spite of the absence of major Carbon Isotope Excursions across the same interval (Zachos et al., 2008).

The observation of a 1.2 million year beat (long-term modulation of obliquity) together with the evidence for enhanced obliquity (41 kyr) across the 1.2 My maxima corresponding to ETM2, ETM3 and the onset of the 1 Myr-long dissolution interval of the EECO, suggests that high latitude feedbacks to orbital forcing played a role in the emplacement of the hyperthermals.

REFERENCES

- Alvarez W., Arthur M.A., Fischer A.G., Lowrie W., Napoleone G., Premoli Silva I. & Roggenthen W.M. (1977) - Upper Cretaceous-Paleocene magnetic stratigraphy at Gubbio, Italy V. Type section for the Late Cretaceous-Paleocene geomagnetic reversal time scale. *Geol. Soc. Am. Bull.*, 88, 383-389.
- Cramer B.S., Wright J.D., Kent D.V., Aubry M.-P. (2003) - Orbital climate forcing of $\delta^{13}\text{C}$ excursions in the late Paleocene–early Eocene (chrons C24n–C25n). *Paleoceanography*, 18, 21-1, 10.1029/2003PA000909.
- DeConto R.M., Galeotti S., Pagani M., Tracy D., Schaefer K., Zhang T., Pollard D., Beerling D.J. (2012) - Past extreme warming events linked to massive carbon release from thawing permafrost. *Nature*, 484, 87-91.
- Galeotti S., Krishnan S., Pagani M., Lanci L., Gaudio A., Zachos J.C., Monechi S., Morelli G. & Lourens L. (2010) - Orbital chronology of Early Eocene hyperthermals from the Contessa Road section, central Italy: *Earth Planet. Sci. Lett.*, 290, 192-200.
- Lourens L.J., Sluijs A., Kroon D., Zachos J.C., Thomas E., Rohl U., Bowles J. & Raffi, I. (2005) - Astronomical pacing of late Palaeocene to early Eocene global warming events. *Nature*, 435, 1083-1087.
- Lowrie W., Alvarez W., Napoleone G., Perch-Nielsen K., Premoli Silva I. & Toumarkine M. (1982) - Paleogene magnetic stratigraphy in Umbrian pelagic carbonate rocks: the Contessa sections, Gubbio. *Geol. Soc. Am. Bull.*, 93, 414-432.
- Lunt D.J., Ridgwell A., Sluijs A., Zachos J.C., Hunter S. & Haywood A. (2011) - A model for orbital pacing of methane hydrate destabilization during the Palaeogene. *Nature Geosci.*, 4, 775-778.
- Paillard D., Labeyrie L. & Yiou P. (1996) - Macintosh program performs time-series analysis. *Eos Trans. AGU* 77, 379.
- Westerhold, T., Rohl, U., Laskar, J., Raffi, I., Bowles, J., Lourens L.J. & Zachos J.C. (2007) - On the duration of magnetochrons C24r and C25n and the timing of early Eocene global warming events: Implications from the Ocean Drilling Program Leg 208 Walvis Ridge depth transect. *Paleoceanography*, 22, PA2201, doi:10.1029/2006PA001322.
- Zachos J.C., Dickens G.R. & Zeebe R.E. (2008) - An early Cenozoic perspective on greenhouse warming and carbon-cycle dynamics. *Nature*, 451(17), 279-283.

A unique high resolution lacustrine record of climate and vegetation changes during the EOT. The CDB1 core, Rennes Basin, France

Julie Ghirardi ^(a,b), Jérémy Jacob ^(a), Arnaud Huguet ^(c), Hugues Bauer ^(b), Claude Le Milbeau ^(a), Jean-Jacques Chateaufneuf ^(d), Christian Di Giovanni ^(a) & Florence Quesnel ^(a,b)

^(a) Institut des Sciences de la Terre d'Orléans, ISTO, UMR 7327 du CNRS/INSU, Université d'Orléans, BRGM, 1A rue de la Fêrolierie, 45071 Orléans, France. E-mail:

julie.ghirardi@univ-orleans.fr

^(b) BRGM (French Geological Survey), Georessources Division, 45060 Orléans Cedex 2, France

^(c) CNRS/UPMC UMR 7619 METIS, 75005 Paris, France

^(d) 8 quai du Châtelet, 45000-Orléans, France

Document type: Short note.

Manuscript history: received 15 May 2014; accepted 30 May 2014; editorial responsibility and handling by Gerald R. Dickens & Valeria Luciani.

KEY WORDS: biomarkers, climate, Eocene-Oligocene transition, vegetation.

The transition between Eocene and Oligocene (EOT) is known as one of the major climatic change of the Paleogene. This climatic transition is marked by the shift from a greenhouse to an icehouse climatic mode. Although the effect of climate change on terrestrial setting correspond to major changes in plant and animal communities (the well-known “Grande Coupure”, Stehlin, 1910), most of studies are realized on marine successions in which several side-effects were identified (stepwise cooling, faunistic turnover, deepening of the CCD, eg. Coxall et al., 2005). Although more sensitive to climate changes, terrestrial settings suffer from the lack of continuous and well calibrated sections. Recently, the BRGM (French Geological Survey) has conducted a fully-cored deep drilling (CDB1) in the Cenozoic Rennes Basin. A continuous organic matter and clay rich lacustrine record encompasses the EOT as shown by palynology (Bauer et al., in prep.) and confirmed by magnetostratigraphy (Dupont-Nivet et al., 2013).

In order to decipher the climatic evolution during the EOT and its impacts on ecosystems, we have performed a full palynological study accompanied by the analysis of molecular biomarkers and of their isotopic composition. After extraction and separation of lipids, quantification of branched Glycerol Dialkyl Glycerol Tetraethers (GDGTs) was achieved by liquid chromatography coupled to mass spectrometry, whereas other lipids were identified and quantified by gas chromatography coupled to mass spectrometry. Additionally, the δD of vascular plants leaf-wax *n*-alkanes (with 27, 29 and 31 carbon atoms) was determined by gas chromatography coupled to isotope ratio mass spectrometry.

Indices calculated from branched GDGT concentrations in 50 samples allowed us estimating the evolution of mean annual air temperature based on two calibrations developed in recent soils (Peterse et al., 2012 and Weijers et al., 2007).

The paleohydrological reconstruction relies on the δD of *n*-

alkanes determined for 50 samples and on their Average Chain Length (ACL, Eglinton and Hamilton, 1967). δD of *n*-alkanes depends on hydrological parameters such as temperature at precipitation site, precipitation amount and evapotranspiration (Gleixner and Mügler, 2007; Sachse et al., 2006). ACL is used to decipher vascular plant adaptation to relative humidity: the longer the chain, the better vascular plants are adapted to dry conditions.

The two temperature records obtained from GDGTs show the same evolution, marked by two cooling trends: one during the late Early Priabonian and a second during the Early Rupelian. Conversely, two warming intervals are observed during the Early Priabonian and the Late Priabonian (EOT).

The ACL values vary between 26 and 28. From the Late Priabonian and the Early Rupelian, recurrent ACL variations indicate changes in relative humidity. One of these variations occurs during the EOT and shows the transition from humid to dry conditions. This interpretation is supported by the most negative *n*-alkanes δD values recorded during the Late Priabonian to the Early Rupelian that either indicate high precipitation rates or lower evaporation rates. Then, and as for ACL, δD values increase after the EOT, showing the sudden settlement of dryer conditions.

How did these climatic changes impact the environment, especially the vegetation? The evolution of vegetation is unraveled through specific biomarkers of ferns (farnenes), gymnosperms (diterpenes) and angiosperms (triterpenes ketones) and compared to spores and pollen data. From the Late Eocene to the Early Oligocene, spores and pollen counts delineate an increase in mesothermal species compared to megathermal species.

In detail, we observe an increase in coniferous species from the Late Priabonian to the Rupelian that is classically interpreted as the result of the installation of a cool and dry climate. These evolutions are in agreement with temperature evolutions deduced from branched GDGTs and also with the global cooling that is characteristic for this transition. However, diterpenes evolution is different from that of

gymnosperm pollen since they are as abundant during the Eocene as during the Oligocene, except for a peak of concentrations recorded during the early Late Priabonian.

As for gymnosperms, fern and angiosperm biomarkers do not show any global trend in concentration but high frequency changes from the Late Eocene to the Early Oligocene. Remarkably, these high frequency changes in vascular plants are consistent with the rhythm of ACL values. Thus, the evolution of continental ecosystems during the Priabonian and Rupelian appears paced by changes in relative humidity.

REFERENCES

- Bauer H., Saint-Marc P., Châteauneuf J.-J., Bourdillon C. & Guillocheau F. (in prep.) - New insights on the Armorican geology: contribution of the CDB1 deep borehole (Rennes Basin, France). To be submitted to *C.R. Geoscience*.
- Coxall H.K., Wilson P.A., Palike H., Lear C.H. & Backman J. (2005) - Rapid stepwise onset of Antarctic glaciation and deeper calcite compensation in the Pacific Ocean. *Nature*, 433, 5-57.
- Dupont-Nivet G., Lin F., Bauer H., Guillocheau F., Ghirardi J. & Quesnel F. (2013) - La transition Eocène-Oligocène identifiée par magnétostratigraphie dans le bassin continental de Rennes. 14^{ème} congrès français de sédimentologie, 4-8 nov. 2013.
- Eglinton G. & Hamilton R.J. (1967) - Leaf Epicuticular Waxes. *Science*, 156, 1322-1335.
- Gleixner G. & Mügler I. (2007) - Compound specific hydrogen isotope ratios of biomarkers: Tracing climatic changes in the past, In: Dawson T. & Siegwolf R. (Eds.), *Stable Isotopes as Indicators of Environmental Change*, 249-267.
- Peterse F., van der Meer J., Schouten S., Weijers J.W.H., Fierer N., Jackson R.B., Kim J.-H. & Sinninghe Damsté J.S. (2012) - Revised calibration of the MBT-CBT paleotemperature proxy based on branched tetraether membrane lipids in surface soils. *Geochim. Cosmochim. Acta*, 96, 215-229. doi:10.1016/j.gca.2012.08.011
- Sachse D., Radke J. & Gleixner G. (2006) - δD values of individual n-alkanes from terrestrial plants along a climatic gradient - Implications for the sedimentary biomarker record. *Org. Geochem.*, 37, 469-483. doi: 10.1016/j.orggeochem.2005.12.003
- Stehlin H.G. (1910) - Remarques sur les faunes de Mammifères des couches éocènes et oligocènes du Bassin de Paris. *Bull. Soc. Geol. Fr.*, 9, 488-520.
- Weijers J.W.H., Schouten S., van den Donker J.C., Hopmans E.C. & Sinninghe Damsté J.S. (2007) - Environmental controls on bacterial tetraether membrane lipid distribution in soils. *Geochim. Cosmochim. Ac.*, 71, 703-713. doi: 10.1016/j.gca.2006.10.003.

Biotic evolution in the North Pacific shelf zones during the Paleogene

Yury B. Gladenkov ^(a)

(a) Geological Institute of Russian Academy of Sciences, Pyzhevskii per., 7, 119017, Moscow, Russia. E-mail: gladenkov@ginras.ru

Document type: Short note.

Manuscript history: received 15 May 2014; accepted 30 May 2014; editorial responsibility and handling by Gerald R. Dickens & Valeria Luciani.

KEY WORDS: biotic evolution, climatic fluctuations, migrations of marine biota, North Pacific, Paleogene, shelves.

1. Paleogene deposits of the North Pacific are still poorly known. Few data from deep-water drilling are available (besides for the Aleutian and Kommandor islands regions). The main source of information is from sections of the ocean-continent transition zone. There are a series of key sections mostly in Eastern Kamchatka and the Koryak Upland, which allow for a Paleogene correlation scheme to be constructed for the region. In spite of the difficulty of investigating Paleogene strata because of their great thickness, occurrences of coarse clastics, etc., we can outline real stage boundaries based on biostratigraphic evidence and paleomagnetic zones. The North Pacific Paleogene is composed of two distinguishable parts, i.e., Paleocene-Eocene (mudstones, siltstones) and Oligocene (mudstones, diatomites). The Paleocene-Eocene part is characterized by planktonic foraminifers. Owing to their presence, the warm-water zonation can be used there. So, according to V. Beniamovsky (Volobueva et al., 1994), in Eastern Kamchatka (the Il'pinsky and Kamchatsky Mys peninsulas) seven Paleocene and Eocene regional zones can be established basing on characteristic biomarkers (*Globigerina nana*, *Globorotalia wilcoxensis*, *Pseudohastigerina wilcoxensis*, *Globigerina boweri*, *Globigerapsis index*, *Globigerina praebulloides*, *Globigerapsis tropicalis*). The lowest Paleogene deposits contain widespread benthic foraminifers (*Rzehakina kakyeica*, *Rzehakina epigone-Bolivinopsis spectrabilis*, *Glomospira corona-Silicosigmoilina californica*, *Cibicides praeventratumidus-Bulimina minnseni*). In the Oligocene part, four diatom zones (*Rhizosolenia oligocaenica*, *Rocella vigilans*, *Cavitatus rectus*, and *Rocella gelida* zones) can be distinguished in the Komandorsky islands and Il'pinsky Peninsula (Gladenkov, 2007). The biostratigraphic data are supplemented by paleomagnetic markers (Minyuk, 2004) and radiometric dates for some horizons. This enables us to construct a real Paleogene scale for the region.

These materials are of great significance for dating benthic assemblages which are commonly used for subdivision of sedimentary strata and geological mapping (Gladenkov, 2004).

Based on benthic associations, seven to nine Paleogene horizons (or regiostages) have been established in Kamchatka (two of them in Oligocene deposits).

2. Some paleogeographic conclusions can be inferred from the biostratigraphic data.

a) In the Paleogene period the North Pacific was a "semiclosed" basin because the Bering Strait opened in the terminal Miocene-early Pliocene only. The region was connected with other basins in the south via the Tethyan passage.

b) During Paleocene-Eocene time the climate was generally paratropic (a greenhouse type) with certain fluctuations and a warming peak in the early Eocene. In the Oligocene it changed to a glacial type climate (appearance of ice-draft debris, glendonites, and siliceous rocks).

c) In Oligocene time a boreal type of biota was formed. The North Pacific was isolated from the North Atlantic because, on the one hand, the Tethyan Ocean was closed (and biotic interTethyan migrations ceased) and, on the other hand, the tropical belt became an insuperable climatic barrier for boreal forms confined to the middle and high latitudes. Consequently, before the Bering Strait opened, the two boreal biotas of the North Pacific and North Atlantic developed in isolation and in parallel. This allowed the appearance of specific endemic species. Only after the Bering Strait was opened was biotic exchange between these regions possible via the Arctic.

In 2013 new data were published on Paleogene sections of Northern Kamchatka, which enlightened a problem of the Paleocene-Eocene boundary in the region (Gladenkov et al., 2013). The boundary is finely marked by appearance of a great number of tropical forms, both mollusks and foraminifera.

REFERENCES

Gladenkov A.Yu. (2007) - Late Cenozoic detailed stratigraphy and marine ecosystems of the North Pacific region (based on diatoms). GEOS Publishers, Moscow, 296 pp. (in Russian).

- Gladenkov Yu.B. (2004) - Biosphere Stratigraphy (stratigraphic problems in the early XXI century). GEOS Publishers, Moscow, 120 pp. (in Russian).
- Gladenkov Yu.B., Sinel'nikova V.N., Beniamovsky V.N. & Fregatova N.A. (2013) - Stratigraphy of the marine Paleocene and Lower Eocene in West Kamchatka (paleontological characteristic, paleogeographic environments). GEOKART, GEOS Publishers, Moscow, 160 pp. (in Russian).
- Minyuk P.S. (2004) - Magnetostratigraphy of Cenozoic of the North-East of Russia. NEISRI FEB RAS, Magadan, 198 pp. (in Russian).
- Volobueva V.I., Gladenkov Yu.B., Beniamovsky V.N., Vitukhin D.I., Minyuk P.S., Muzylev N.G., Oleinik A.E., Sinel'nikova V.N., Sokolova Z.Sh., Titova L.V., Fregatova N.A. & Shiraya O.A. (1994) - Marine Paleogene key section in the northern Far East (Il'pinsky Peninsula). Part 1. Stratigraphy. NEISRI FEB RAS, Magadan, 64 pp. (in Russian).

New observations on Eocene diatoms from the Kamchatka region, Russian Far East

Andrey Yu. Gladenkov ^(*)

^(*) Geological Institute of Russian Academy of Sciences, Pyzhevskii per., 7, 119017, Moscow, Russia. E-mail: agladenkov@iran.ru

Document type: Short note.

Manuscript history: received 15 May 2014; accepted 30 May 2014; editorial responsibility and handling by Gerald R. Dickens & Valeria Luciani.

KEY WORDS: Eocene, increased diatom productivity, Kamchatka region, marine diatoms.

Fossil diatoms occur widely in onshore and near-shore upper Cenozoic stratigraphic sequences of the Kamchatka region, Russian Far East, and are the primary biostratigraphic tool for the precise dating and correlation of marine sediments in this area. The current high-resolution North Pacific diatom zonation with numerous biohorizons based on datum levels is used here for the detailed subdivision, dating and correlation of Oligocene to Quaternary marine deposits. However, Eocene diatom assemblages from the Kamchatka region are less well studied than the younger floras, and successions of Eocene assemblages of different age are not yet well documented. In many respects, this is due to the fact that Eocene stratigraphic sections yielding preserved fossil diatoms are more limited and not complete.

Until recently, data on Eocene diatoms from the region were quite poor. Rare finds of diatoms (referred as a rule to the middle Eocene) were known only from a few localities lacking direct correlation with carbonate plankton or magnetostratigraphy. In general, the diatoms were found in rare and isolated samples derived from onshore sections. The exact age and correlation of these assemblages is still unclear. Their age estimate was inferred mainly from available data on other paleontological groups, primarily mollusks and benthic foraminifera. In addition, these diatom assemblages lack marker forms of oceanic plankton that are used for zonal subdivision in other regions. Along with a certain endemism, this hampers the exact dating of enclosed sediments. As a result, diatom stratigraphy of the Eocene was largely tentative in Kamchatka because of the lack of good correlation to the geological time scale. However, new materials on the Eocene marine diatoms from the Kamchatka region were accumulated during the last decade. Among the most important are the following.

Rich and well-preserved Eocene diatom assemblages have been documented from dredge samples off southeast Kamchatka (Tsoy, 2003) (Fig. 1). The studied flora yields oceanic planktic species including *Triceratium kanayae*, *Tr. inconspicuum* var. *trilobata*, *Praecymatosira*

monomembranaceae, *Rylandsia conniventa* typical of the Eocene from different regions. The presence of these pelagic elements allows recognition of three middle Eocene diatom assemblages, one late Eocene assemblage, and their correlation with diatom zones of the Norwegian Sea, low latitudes and California (Tsoy, 2003).

Eocene diatoms have been also found recently from the Paleogene stratigraphic key section of northeast Kamchatka on the Il'pinskii Peninsula, west coast of the Bering Sea (Gladenkov, 2012, 2013) (Fig. 1). Until recently, the section was considered barren of fossil diatoms. However, new sampling made it possible to discover remains of diatoms from the Paleogene sediments. Collection of concretions was critical, as diatoms were absent in the enclosing matrix as shown by previous studies. Sampling the concretions was done because in some cases diatoms are present in fine sediment within concretions and are thereby protected from mechanical and chemical abrasion in the course of sedimentation or during fossilization and catagenesis. As a result, the first data on the Eocene diatoms from the Il'pinskii Peninsula stratigraphic section were obtained. Planktic taxa including *Triceratium inconspicuum* var. *trilobata*, *Pyxilla gracilis*, and *Riedelia borealis* are typical of the studied marine neritic diatom assemblage. The occurrence of these species implies a middle Eocene age for the studied sediments, which is in agreement with the Lutetian age determined using planktic foraminifera. These are the first finds of Eocene diatoms in the northwest Pacific having such correlation with calcareous plankton.

Data on Eocene diatoms from west Kamchatka (the Sea of Okhotsk-side) were essentially absent. That is why materials obtained recently on Paleogene diatoms from the hole drilled off southwest Kamchatka (Fig. 1) are of interest (Gladenkov, unpublished data). The presence of *Costopyxis* cf. *broschii*, *Triceratium brachiatum*, *Tr. inconspicuum* var. *trilobata*, *Cestodiscus trochus*, *Anuloplicata ornata* and *Pyxilla* cf. *gracilis* are typical of the studied marine diatom assemblage. The co-occurrence of these planktic elements may imply a middle Eocene age for the studied sediments. This is the first record of biostratigraphically-important planktic Eocene diatoms from the Sea of Okhotsk province.

The obtained data are quite important for an elaboration of detailed biostratigraphic subdivisions based on siliceous

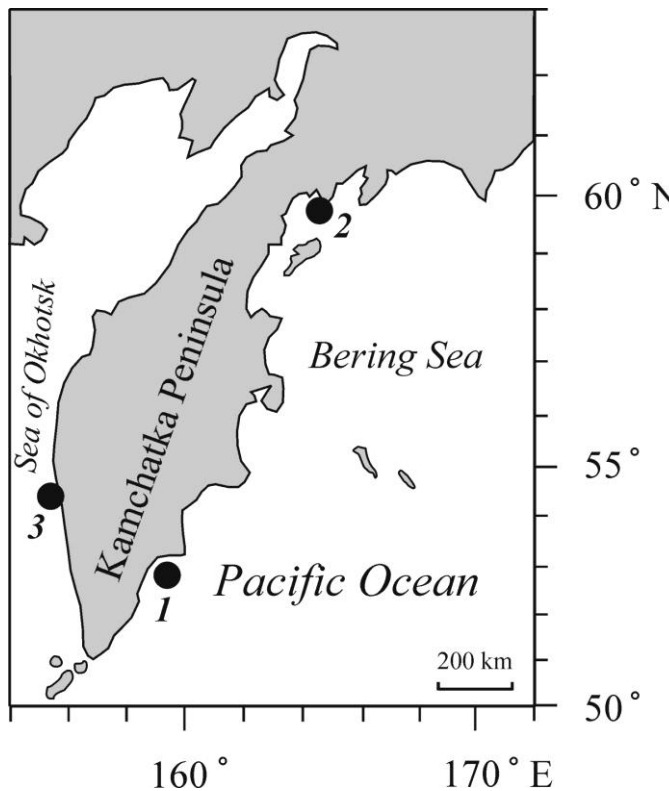


Fig. 1 – Locations of stratigraphic sections (black circles) in the Kamchatka region where Eocene marine diatom assemblages are documented, including biochronologically important oceanic planktic species.

- 1 – The Kronotskii Bay, off southeast Kamchatka;
 2 – The Il'pinskii Peninsula, northeast Kamchatka;
 3 – Off southwest Kamchatka

microfossils, and contribute to regional correlations of the Eocene strata in Kamchatka. The finding of middle Eocene diatom assemblages in other sections of the North Pacific, along with the absence of Paleocene and early Eocene assemblages, probably indicates a beginning of relatively wide distribution of diatoms in the peripheral basins in the North

Pacific in the middle Eocene. At approximately that time, a relative widening of diatom distribution and their increased productivity owing to paleoclimatic and paleoceanographic changes and reorganization of oceanic circulation are recorded in the World Ocean (Barron & Baldauf, 1989; Baldauf & Barron, 1990).

ACKNOWLEDGEMENTS

This work was supported by project no. 13-05-00115 of Russian Foundation for Basic Research and Program no. 28 of the Presidium of Russian Academy of Sciences.

REFERENCES

- Baldauf, J.G. & Barron, J.A. (1990) - Evolution of biosiliceous sedimentation patterns - Eocene through Quaternary: paleoceanographic response to polar cooling. In: Bleil U. & Thiede J. (eds.), *Geological History of the Polar Oceans: Arctic versus Antarctic*. Kluwer Academic Publisher, 575-607.
- Barron, J.A. & Baldauf J.G. (1989) - Tertiary cooling steps and paleoproductivity as reflected by diatoms and biosiliceous sediments. In: Berger W.H., Smetacek V.S. & Wefer G. (eds.), *Productivity of the Ocean: Present and Past*. Wiley-Interscience, 341-354.
- Gladenkov, A.Yu. (2012) - Middle Eocene diatoms from the marine Paleogene stratigraphic key section of northeast Kamchatka. *Austrian J. Earth Sci.*, 105/1, 72-76.
- Gladenkov, A.Yu. (2013) - First finds of Eocene diatoms in the marine Paleogene reference section in the Il'pinskii Peninsula, northeastern Kamchatka. *Stratigraphy and Geological Correlation*, 21, 96-106.
- Tsoy, I.B. (2003) - Eocene diatoms and silicoflagellates from the Kronotskii Bay deposits (East Kamchatka). *Stratigraphy and Geological Correlation*, 11, 376-390.

Long-Term Behavior of the Carbonate Compensation Depth Across Early Paleogene Warming

Sarah E. Greene ^(a), Andy Ridgwell ^(a), Daniela N. Schmidt ^(b), Sandra Kirtland Turner ^(a), Heiko Pälike ^(c) & Ellen Thomas ^(d)

^(a) School of Geographical Sciences, University of Bristol, University Road, BS8 1SS, Bristol, United Kingdom. E-mail: sarah.greene@bristol.ac.uk

^(b) School of Earth Sciences, University of Bristol, Bristol, United Kingdom

^(c) MARUM—Center for Marine Environmental Sciences, University of Bremen, Bremen, Germany

^(d) Department of Geology and Geophysics, Yale University, New Haven, CT, USA

Document type: Short note.

Manuscript history: received 15 May 2014; accepted 30 May 2014; editorial responsibility and handling by Gerald R. Dickens & Valeria Luciani.

KEY WORDS: Carbonate Compensation Depth, Early Eocene, Late Paleocene, long-term climate Change, lysocline.

The depth below which ocean sediments are virtually carbonate free is termed the carbonate compensation depth (CCD). Over geological timescales the CCD is thought to reflect mean climate state via the requirement that carbonate burial balance weathering inputs to the ocean (Ridgwell and Zeebe, 2005). So long as weathering is responsive to atmospheric $p\text{CO}_2$ (Bernier and Caldeira, 1997), then the steady-state behavior of carbonate compensation should, in turn, reflect long-term atmospheric $p\text{CO}_2$.

We test this relationship between CCD behavior and mean climate state by reconstructing the CCD for the late Paleocene to early Eocene (~58 to ~50 Ma). This interval hosts a ~4°C increase in deep sea temperatures, one of the most dramatic long-term deep sea temperature increases in the Cenozoic (Cramer et al., 2009). In addition, late Paleocene to early Eocene benthic $\delta^{13}\text{C}$ records show a pronounced trend towards more depleted values. Together, the carbon and oxygen isotopic trends across this interval may represent an increase in atmospheric $p\text{CO}_2$ (Komar et al., 2013) and thus the late Paleocene – early Eocene presents an excellent test case for the link between CCD behavior and climate.

Using carbonate content from nearly 80 sites drilled through the DSDP/ODP/IODP programs, we reconstruct the behavior of the CCD for three timeslices – the late Paleocene, the early Eocene, and the peak warmth of the early Eocene climate optimum. (We exclude from our reconstruction the interval surrounding the rapid, non-steady state CCD perturbation at the Paleocene-Eocene thermal maximum).

Across the late Paleocene to early Eocene, the CCD is at least ~3500m-4000m deep. Moreover, the position of the CCD is indistinguishable between the three timeslices. The observed CCD stability implies that over long timescales, the position of the CCD may be unresponsive to warming (and potentially unresponsive to major changes in atmospheric CO_2 /weathering as well).

Using the Earth system model cGENIE, we observe that higher $p\text{CO}_2$ does not greatly deepen the modeled CCD. The excess weathering triggered by higher $p\text{CO}_2$ in cGENIE is compensated for by increased carbonate burial above the CCD, leaving the position of the CCD relatively unchanged, a cGENIE feature noted by other authors (Pälike et al., 2012). The pattern of carbonate compensation observed at higher $p\text{CO}_2$ in cGENIE results from changes in the response of sedimentary carbonate content to porewater dissolution and organic carbon remineralization in an ocean with higher dissolved inorganic carbon content. The net result is that in a higher $p\text{CO}_2$ simulation, dissolution at the lysocline is reduced while dissolution at the CCD is enhanced. We suggest that this mechanism could explain the observed long-term stability of the CCD across the late Paleocene – early Eocene.

REFERENCES

- Berner R.A. & Caldeira, K. (1997) - The need for mass balance and feedback in the geochemical carbon cycle. *Geology*, 25, 955-956.
- Cramer B.S., Toggweiler J.R., Wright J.D., Katz M.E. & Miller K.G. (2009) - Ocean overturning since the Late Cretaceous: Inferences from a new benthic foraminiferal isotope compilation. *Paleoceanography*, 24(4), PA4216.
- Komar N., Zeebe R.E. & Dickens G.R. (2013) - Understanding long-term carbon cycle trends: The late Paleocene through the early Eocene. *Paleoceanography*, 28 (4), 650–662.
- Pälike H., Lyle M.W., Nishi H., Raffi I., Ridgwell A., Gamage K., Klaus A., Acton G.D., Anderson L., Backman J., Baldauf J.G., Beltran C., Bohaty S.M., Bown P.R., Busch W.H., Channell J.E.T., Chun C.O.J., Delaney M.L., Dewang P., Dunkley Jones T., Edgar K.M., Evans H.F., Fitch P., Foster G.L., Gussone N., Hasegawa H., Hathorne E.C., Hayashi H., Herrle J.O., Holbourn A.E.L., Hovan S.A., Hyeong K., Iijima K., Ito T., Kamikuri S.-I., Kimoto K., Kuroda J., Leon-Rodriguez L., Malinverno A., Moore T.C., Murphy B., Murphy D.P., Nakamura H., Ogane K., Ohneiser C., Richter C., Robinson R.S., Rohling E.J., Romero O.E., Sawada K., Scher H.D., Schneider L., Sluijs

A., Takata H., Tian J., Tsujimoto A., Wade B.S., Westerhold T., Wilkens R.H., Williams T., Wilson P.A., Yamamoto Y., Yamamoto S., Yamazaki T. & Zeebe R.E. (2012) - A Cenozoic record of the equatorial Pacific

carbonate compensation depth. *Nature*, 488, 609-614.

Ridgwell A. & Zeebe R.E. (2005) - The role of the global carbonate cycle in the regulation and evolution of the Earth system. *Earth Planet. Sci. Lett.*, 234, 299-315.

The Relationship between ice volume and CO₂ across the Oligocene-Miocene boundary

Rosanna Greenop ^(a), Gavin L. Foster ^(a), Paul A. Wilson ^(a), Sindia M. Sosdian ^(b) & Caroline H. Lear ^(b)

^(a) School of Ocean and Earth Science, National Oceanography Centre Southampton, University of Southampton Waterfront Campus, European Way, Southampton, SO14 3ZH, UK.

E-mail: r.greenop@noc.soton.ac.uk

^(b) School of Earth and Ocean Sciences, Cardiff University, Main Building, Park Place, Cardiff, CF10 3AT, UK.

Document type: Short note.

Manuscript history: received 15 May 2014; accepted 30 May 2014; editorial responsibility and handling by Gerald R. Dickens & Valeria Luciani.

KEY WORDS: Boron isotopes, CO₂, hysteresis, Mi-1 glaciation, Oligocene-Miocene boundary

The results of coupled climate-ice sheet model experiments suggest that once grown, large ice sheets on East Antarctica are inherently stable as a result of powerful hysteresis effects, requiring high levels of greenhouse gas forcing (CO₂ ~1000 ppm) to initiate deglaciation (Pollard and DeConto 2005). Yet a growing body of evidence suggests that a dynamic ice sheet existed on Antarctica during certain intervals of the comparatively low CO₂ regime of the Neogene and late Paleogene (Cook et al., 2013; Passchier et al., 2011; Pälike et al., 2006). A good time interval to investigate this problem further is the Mi-1 glaciation, ~ 23 Ma, which is evident in the oxygen isotope record as a two-step positive, transient excursion in benthic $\delta^{18}\text{O}$ of approximately 1‰ (Liebrand et al., 2011; Pälike et al., 2006). The glaciation is associated with an ice volume change of ~ 50 m (s.l.e) and bottom water cooling of ~ 2°C (Mawbey and Lear 2013). While it is not possible to discount the involvement of Northern Hemisphere ice in contributing to the amplitude of the Mi-1 glaciation, it has been shown at least some of the ice volume change occurred on Antarctica (Naish et al., 2001).

The controls on the timing of the Mi-1 glaciation are still uncertain. It has long been known orbital forcing is an important factor and the Mi-1 glaciation coincides with low obliquity, associated with the 1.2 Myr modulation of the Earth's orbit and axial tilt (node of obliquity), as well as reduced amplitude eccentricity (400 kyr long eccentricity cycle), both of which reduce seasonal extremes and increase the chances that winter snowfall accumulation will survive summer ablation (Zachos et al., 2001; Pälike et al., 2006). However, the coincidence of a node in obliquity with low amplitude eccentricity is not unique to the Oligocene-Miocene boundary. Indeed, the amplitude of the previous node in obliquity at 24.4 Ma is more extreme than that associated with the Oligocene-Miocene boundary. A further mystery relates to the mechanism by which the hysteresis inherent in the Antarctic ice sheet was overcome during the deglaciation phase

of the event. Consequently other factor(s) are also needed in order to explain the climate perturbation. Changes in the carbon cycle have been cited as a possible secondary factor influencing the timing and nature of the Mi-1 glaciation (Mawbey and Lear 2013; Zachos et al., 1997).

To better understand the timing and causes of the Mi-1 glaciation we present a high-resolution boron isotope based CO₂ record between 22 and 24 Myrs from Site 926 This site is currently located in a region where surface waters are close to equilibrium with the atmosphere with respect to CO₂ and has successfully been used to produce boron isotope records during other Miocene time intervals (Foster et al. 2012). Some preliminary $\delta^{11}\text{B}$ data from Exp. 342 Site 1406 across the Oligocene-Miocene boundary will also be presented. We will examine the role of CO₂ in controlling the stability of the East Antarctic ice sheet across the Oligocene-Miocene boundary. We will also determine the extent to which ice sheet hysteresis is evident during the growth and deglaciation phases of the Mi-1 glaciation.

REFERENCES

- Cook C.P., van de Flierdt T., Williams T.J., Hemming S.R., Iwai M., Kobayashi M., Jimenez-Espejo F.J., Escutia C., Tauxe L., Sugisaki S., Lopez Galindo A., Patterson M.O., Riesselman C., Sangiorgi F., Pierce E.L., Brinkhuis H. & IODP Expedition 318 Scientists (2013) - Dynamic behaviour of the East Antarctic ice sheet during Pliocene warmth. *Nature Geosci.*, 6(9), 765-769.
- Foster G.L., Lear C.H. & Rae J. (2012) - The evolution of $p\text{CO}_2$, ice volume and climate during the middle Miocene. *Earth Planet. Sci. Lett.*, 341-344: 243-254.
- Liebrand D., Lourens L.J., Hodell D.A., de Boer B., van de Wal R.S.W. & Pälike H. (2011) - Antarctic ice sheet and oceanographic response to eccentricity forcing during the early Miocene. *Clim. Past*, 7, 869-880.
- Mawbey E.M. & Lear C.H. (2013) - Carbon cycle feedbacks during the Oligocene-Miocene transient glaciation. *Geology*, 41, 963-966

- Naish T.R., Woolfe K.J., Barrett P.J., Wilson G.S., Atkins C., Bohaty S.M., Bückler C.J., Claps M., Davey F.J., Dunbar G.B., Dunn A.G., Fielding C.R., Florindo F., Hannah M.J., Harwood D.M., Henrys S.A., Krissek L.A., Lavelle M., van der Meer J., McIntosh W.C., Niessen F., Passchier S., Powell R.D., Roberts A.P., Sagnotti L., Scherer R.P., Strong C.P., Talarico, F., Verosub K.L., Villa G., Watkins D.K., Webb P.-N. & WonikT. (2001) - Orbitally induced oscillations in the East Antarctic ice sheet at the Oligocene/Miocene boundary. *Nature*, 413(6857), 719-723.
- Pälike H., Norris R.D., Herrle J.O., Wilson P.A., Coxall H.K., Lear C.H., Shackleton N.J., Tripathi A.K. & Wade B.S. (2006), The Heartbeat of the Oligocene Climate System. *Science*, 314(5807), 1894-1898.
- Passchier S., Browne, G., Field, B., Fielding, C. R., Krissek, L. A., Panter, K., Pekar, S. F. & Team, A.-S. S. (2011) - Early and middle Miocene Antarctic glacial history from the sedimentary facies distribution in the AND-2A drill hole, Ross Sea, Antarctica: *Geol. Soc. Am. Bull.*, 123(11-12) 2352-2365.
- Pollard D. & DeConto R. M. (2005) - Hysteresis in Cenozoic Antarctic ice-sheet variations. *Global Planet. Change*, 45(1-3), 9-21.
- Zachos J.C., Flower B.P & Paul H. (1997) - Orbitally paced climate oscillations across the Oligocene/Miocene boundary. *Nature*, 388(6642), 567-570.
- Zachos J.C., Shackleton N.J., Revenaugh J.S., Pälike H. & Flower B.P. (2001) - Climate response to orbital forcing across the Oligocene-Miocene boundary. *Science*, 292, 274-278.

Biostratigraphy of the Lutetian/Bartonian Boundary in the North of Tunisia

Chaima Grira ^(a), Narjess Karoui-Yaakoub ^(a,b), Moncef-Saïd Mtimet ^(a) & Wafa Guesmi ^(a)

^(a) Université de Carthage, Faculté des Sciences de Bizerte, Département des Sciences de la Terre. Jarzouna, Bizerte, 7021, Tunisie. E-mail : grirachaima@yahoo.fr

^(b) Unité de recherche : Pétrologie sédimentaire et cristalline, Université de Tunis El Manar, Tunisie

Document type: Short note.

Manuscript history: received 15 May 2014; accepted 30 May 2014; editorial responsibility and handling by Gerald R. Dickens & Valeria Luciani.

KEY WORDS: Lutetian/Bartonian boundary, planktonic foraminifera, Tunisia.

The Saouaf section is located in the Center-North of Tunisia in the geological map of Enfidha, about 70 kms from Tunis (Fig. 1A). The accessibility is excellent and the access of the section is free. The section is thick about forty meters and has a well exposed Eocene series of the Souar Formation (Burolet, 1956; Ben Ismail, 1994). The sedimentation is continuous, with no detected hiatus and the sampling is done every meter (Fig. 1B). The micropaleontologic study reveals the abundance and the diversity of well-preserved foraminifera (Fig. 1C). At the bottom, the section begins with two meters of hard brown-yellow marls covered by four meters of green-yellow marls. These levels contain a well preserved association of planktonic foraminifera mainly composed of *Igorina broedermanni*; *Acarinina praetopilensis*; *Acarinina bullbrookii*; *Subbotina crociapertura*; *Morozovelloides coronatus*; *Morozovella crater* and *Guembelitroides nuttali*. The presence of the species *Guembelitroides nuttali* with the absence of *Morozovella aragonensis* marks the *Acarinina topilensis* zone (E10) (Pearson et al., 2006; Wade et al., 2011, Vanderberghe et al., 2012).

Above there is an unity composed of grey marls thick about 27 meters, revealing the extinction of *Guembelitroides nuttali* at the base and the apparition of new species of planktonic foraminifera: *Acarinina rohri*; *Acarinina topilensis*; *Acarinina medizzai*; *Hantkenina lehneri*; *Hantkenina australis*; *Parasubbotina pseudowilsoni*; *Subbotina linaperta*; *Pseudohastegerina micra*; *Morozovelloides lehneri*; *Morozovelloides crassatus*; *Hantkenina dumblei*; *Globigerinatheka index*. This unity corresponds to the *Morozovelloides lehneri* zone (E11).

Ten meters above, there are grey marls, rich in oxide iron and contain in the middle, a calcareous bed, rich in lamellibranch. The association of the planktonic foraminifera contains especially at the base, the index *Orbulinoides*

beckmanni. We note also a presence of *Acarinina collactea*; *Acarinina praetopilensis*; *Subbotina crociapertura*; *Subbotina hagni*; *Parasubbotina wilsoni*; *Dipsidripella danvillensis*; *Globigerinatheka mexicana*; *Globigerinatheka euganea*; *Globorotaloides quadrocameratus*; *Hantkenina australis*; *Hantkenina lehneri*; *Hantkenina dumblei*; *Hantkenina compressa*.

The lower occurrence of *Orbulinoides beckmanni* indicates the base of the E12 zone, which corresponds to the Lutetian/Bartonian boundary (Pearson et al., 2006; Wade et al., 2011).

Above, there is a marly series including a glauconitic and phosphatic level thick about 20cm. At the base, we note the extinction of *Orbulinoides beckmanni* and the lower part of *Morozovelloides crassatus* zone (E13).

REFERENCES

- Ben Ismail K. (1994) - Mise au point sur l'âge des formations Metlaoui et Souar en Tunisie. Notes du service Géologique de Tunisie, 60, 59-87.
- Burolet P.F. (1956) - Contribution à l'étude stratigraphique de la Tunisie centrale. Ann. Mines Géol. Tunis, 18, 350p.
- Pearson P.N., Olsson R.K., Huber B.T., Hemleben C. & Berggren W.A. (Eds.) (2006) - Atlas of Eocene Planktonic Foraminifera. Cushman Foundation Special Publication No. 41, 514 p.
- Vanderberghe N., Hilgen F.J., Speijer R.P., Ogg J.G., Gradstein F.M., Hammer O., Hollis C.J. & Hooker J.J. (2012) - The Paleogene Period. In: Gradstein, F., Ogg, J.G., Schmitz, M.D., Ogg, G.M. (Eds.), 2012. The Geologic Time Scale, 855-921, Elsevier, Amsterdam.
- Wade B.S., Pearson P.N., Berggren W.A. & Pälike H. (2011) - Review and revision of Cenozoic tropical planktonic foraminiferal biostratigraphy and calibration to the geomagnetic polarity and astronomical time scale. Earth-Sci. Rev., 104, 111-142.

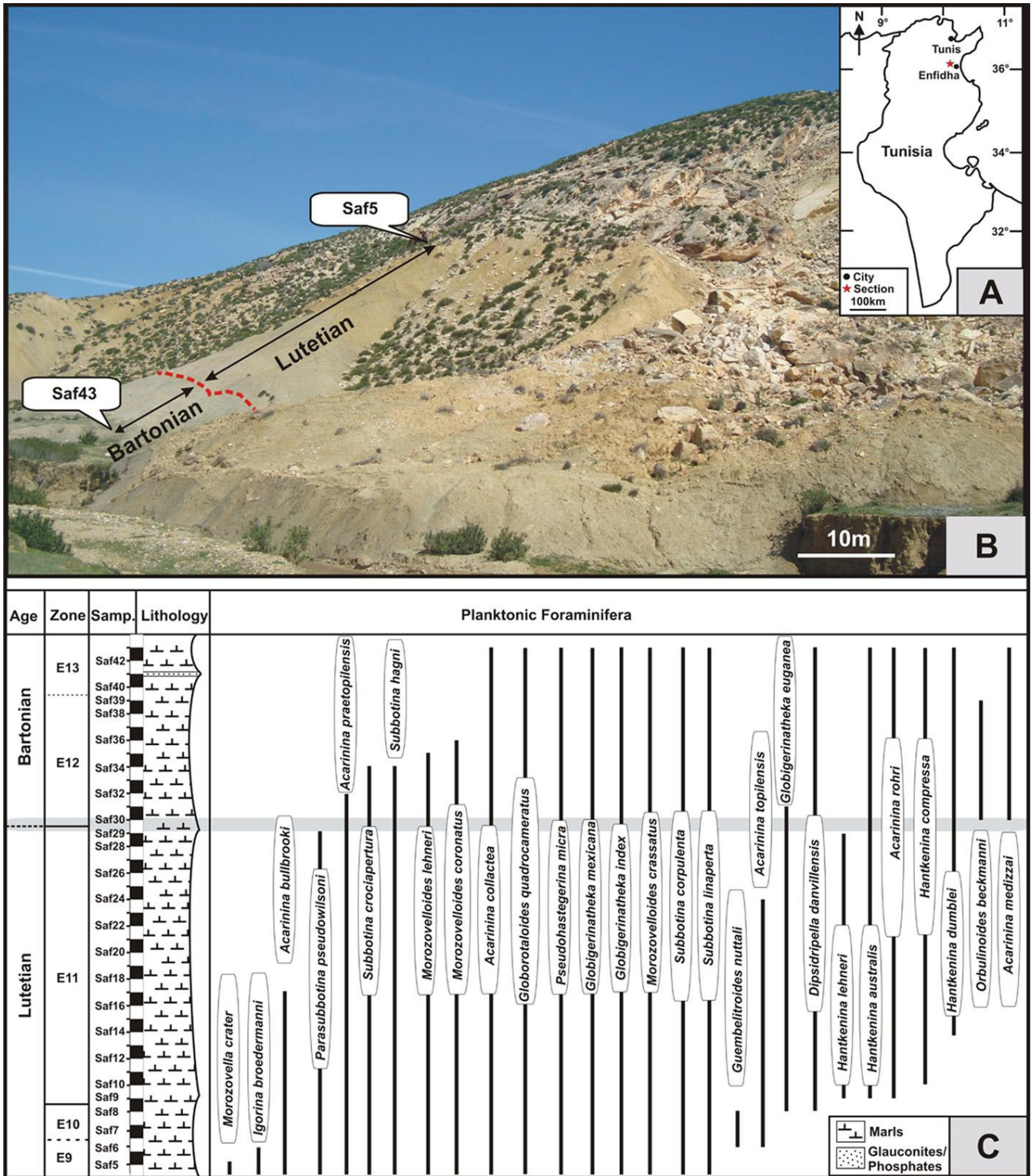


Fig.1 – A) Location map of the Saouaf section, B) Panoramic view of the Saouaf section, C) Planktonic Foraminifera distribution.

Bighorn Basin Coring Project (BBCP): Pollen floral changes and organic matter from core - outcrop comparisons through the PETM

Guy J. Harrington ^(a,b), Phillip E. Jardine ^(c) & Scott L. Wing ^(d), and the BBCP Science Team ^(e)

^(a) Earth Sciences, GEES, University of Birmingham, Birmingham, B15 2TT, UK. E-mail: g.j.harrington@bham.ac.uk

^(b) British Geological Survey, Keyworth, Nottingham, NG15 2GG, UK

^(c) Palaeoenvironmental Change Research Group, Department of Environment Earth & Ecosystems, The Open University, Walton Hall, Milton Keynes, MK7 6AA, UK

^(d) Department of Paleobiology, National Museum of Natural History, Smithsonian Institution, NHB MRC 121, P.O.Box 37012, Washington, DC 20013, USA

^(e) Bighorn Basin Coring Project Science Team – See <http://earth.unh.edu/clyde/team.shtml> for full list

Document type: Short note.

Manuscript history: received 15 May 2014; accepted 30 May 2014; editorial responsibility and handling by Gerald R. Dickens & Valeria Luciani.

KEY WORDS: Bighorn Basin, continental scientific drilling, Eocene, Paleocene, palynology, PETM.

The early Palaeogene hyperthermals provide an unprecedented opportunity to investigate the biotic responses to rapid and transient global warming events. As part of the Bighorn Basin Coring Project (BBCP), we have analyzed 182 sporomorph (pollen and spore) samples from three newly cored sites in the Bighorn Basin of Wyoming (Clyde et al., 2013). Two sites, Basin Substation (121 samples) and Polecat Bench (41 samples), contain the Paleocene-Eocene Thermal Maximum (PETM, ETM1), and one early Eocene site, Gilmore Hill (20 samples), contains the ELMO (ETM2) event. These datasets augment palynological and macrofossil collections taken from outcrop (Wing & Harrington, 2001; Wing & Currano, 2013)

Here, we report on the Basin Substation section (BSN), because it is more organic rich, has demonstrated higher sporomorph recovery potential than the other two sites, and is the main focus of complementary geochemical analyses (Maibauer et al., 2012). Below 90 m core depth sporomorph concentrations are typically 1000 – 10 000 grains/gram, but between 90 and 60 m these decline to <100 grains/gram, before rising again to levels similar to those seen at the base of the core. Illustrations of typical organic matter found in a pre-PETM sample and one from the PETM is presented in fig. 1. Correlation between marker beds in the core and those at outcrop suggests that this zone of low recovery corresponds closely to the position of the PETM. Prior to this interval, the sporomorph assemblage is dominated by the gymnosperms *Cupressacites hiatipites* (*Metasequoia* or *Glyptostrobus*) and bisaccate pollen (Pinaceae), and the angiosperm taxa *Polyatriopollenites vermontensis* (Juglandaceae), *Caryapollenites* spp. (hickory, Juglandaceae), and *Alnipollenites* spp. (alder, Betulaceae). However, samples are heterogeneous in terms of the dominant taxon, with different taxa having the highest relative abundance in different samples. The sampling resolution in the core greatly exceeds that

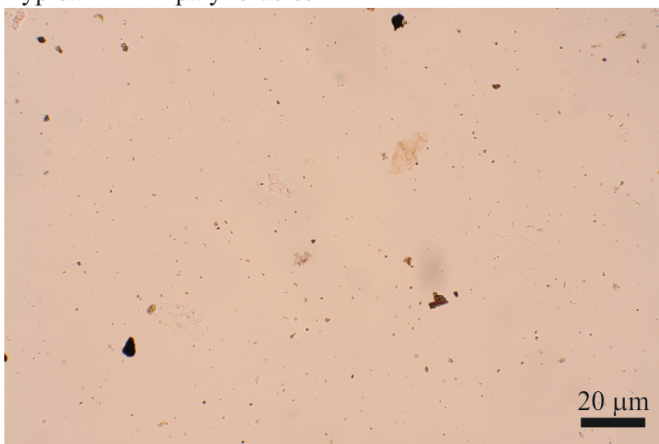
possible from outcrop-generated collection of samples. In the upper part of the core, the assemblage is similar to that in the lower part, but with a more consistent dominance of gymnosperm taxa, and with the addition of Eocene marker taxa *Intratropollenites instructus* and *Celtis* spp. (hackberry) (fig.1). These both have their first appearance in the body of the PETM, just above the zone of low sporomorph recovery.

Correlation with outcrop samples taken from macrofloral localities in the PETM (Wing & Currano, 2013) together with previously published data (Wing & Harrington, 2001; Wing et al., 2005) indicate that the mid-part of the PETM is noted by the first occurrence of *Celtis*. However outcrops primarily represent channel fill deposits rather than the floodplains and soils of BSN and have reasonable yields of pollen and spores. These indicate floral turnover akin to that of the megafloreal record and show the arrival during the inception of the PETM of classic Eocene marker taxa of lower latitude areas such as *Brosipollis* (Burseraceae), and *Retistephanocolporites* that has previously only been observed in Mississippi (Harrington, 2003). The important marker taxon *Platycarya* appears in the recovery of the PETM and is mirrored also at this level in the megafloreal (Wing & Currano, 2013). The recovery period of the PETM is noted by the return into the pollen flora of typical late Paleocene – early Eocene taxa. The PETM is also noted in core and outcrop by presence of reworked late Cretaceous palynomorphs including dinoflagellate cysts (such as *Oligosphaeridium* spp. and *Dinogymnium* sp.) and spores.

Despite poor record of pollen recovery from paleosols during the PETM, our results indicate that coring provides recovery of palynomorphs in lithologies outside of the PETM that previously have not yielded fossil pollen and spores. Hence, our records of vegetation in the late Paleocene and early Eocene from BSN are of unrivalled high- temporal resolution. A decrease in sporomorph preservation is linked to environmental change during the PETM event that affected preferentially soils and floodplain environments. Channel fills and wetter substrates of the floodplain appear less impacted as evidenced by the yields in the outcrop data. Results also indicate floral turnover not only across the Paleocene-Eocene

Celtis sp.

Typical PETM palynofacies



Typical Paleocene palynofacies

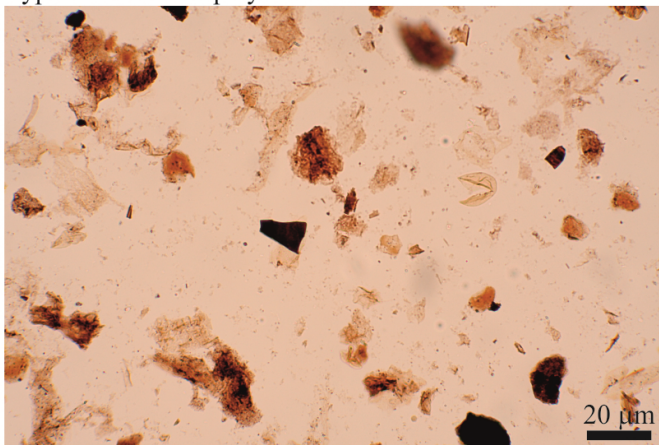


Fig.1 – A) An example of *Celtis* pollen that first occurs in the body of the PETM from both the BSN core (this specimen) and also from outcrop samples. Scale bar represents 10 microns. B,C) Palynofacies from the Paleocene and PETM from the BSN core. In this case PETM organic matter is sparse and represented by reworked material, rare palynomorphs and resistant wood. In the Paleocene the organic matter is very well preserved in most lithologies, that are also represented during the PETM, and incorporates a spectrum of plant material and palynomorphs.

transition but also discrete changes within the event including the transient presence of some taxa (e.g. *Brosipollis*) and the permanent arrival into the region of others (e.g. *Celtis*, and *Platycarya*).

REFERENCES

- Clyde W.C., Gingerich P.D., Wing S.L., Röhl U., Westerhold T., Bowen G., Johnson K., Baczynski A.A., Diefendorf A., McInerney F., Schnurrenberger D., Noren A., Brady K., & the BBCP Science Team. (2013) - Bighorn Basin Coring Project (BBCP): a continental perspective on early Paleogene hyperthermals. *Scientific Drilling* 16, 21-31, doi:10.5194/sd-16-21-2013.
- Harrington G.J. (2003) – Wasatchian (early Eocene) pollen floras from the Red Hot Truck Stop, Mississippi, USA. *Palaeontology*, 46, 725-738.
- Maibauer, B.J., Bowen, G.J., Srinivasaraghavan, V., VanDeVelde, J H., Wing, S L., Gingerich, P.D., Clyde, W.C., & BBCP Science Team (2012) - High-resolution, high-fidelity carbon isotope stratigraphy of the Paleocene-Eocene Thermal Maximum in northern Wyoming from cores recovered by the Bighorn Basin Coring Project, American Geophysical Union Annual Fall Meeting, Abstract PP34A-02.
- Wing S.L. & Currano E.D. (2013) – Plant responses to a global greenhouse event 56 million years ago. *Am. J. Bot.*, 100, 1234-1254.
- Wing S.L. & Harrington G.J. (2001) – Floral response to rapid warming in the earliest Eocene and implications for concurrent faunal change. *Paleobiology*, 27, 539-563.
- Wing S.L., Harrington G.J., Smith F.A., Bloch J.I., Boyer D.M., & Freeman K.H. (2005) – Transient floral change and rapid global warming at the Paleocene-Eocene boundary. *Science*, 310, 993-996.

Possible varves in the PETM interval in Denmark

Claus Heilmann-Clausen ^(*)

(*) Department of Geoscience, Aarhus University, Høegh-Guldbergs Gade 2, 8000 Aarhus C, Denmark. E-mail: claus.heilmann@geo.au.dk

Document type: Short note.

Manuscript history: received 15 May 2014; accepted 30 May 2014; editorial responsibility and handling by Gerald R. Dickens & Valeria Luciani.

KEY WORDS: annual layering, Denmark, North Sea Basin, PETM, varve.

The PETM is represented in Denmark by an up to 15 m thick laminated clay unit, the Stolleklint Clay of the Ølst Formation (Heilmann-Clausen & Schmitz, 2000). The Stolleklint Clay was deposited in the Danish Subbasin of the paleo-North Sea at water depths probably exceeding 100 m (Heilmann-Clausen, 2006). It represents an offshore facies and resembles the Sele Formation from the central part of the North Sea.

The clay pit at Hinge, south of Randers (coordinates 56° 22' 45" N, 10° 03' 06" E) currently exposes most of the PETM-interval, although the strata are tectonized by Quaternary glaciers.

High resolution photographs of hand-specimens prepared for XRF scanning from different levels of the PETM-interval at Hinge reveal three types of layerings, 1) intervals with well-preserved, presumed varves, 2) intervals with thicker, blurred laminae, and 3) intervals with small scale slumping and erosion.

Intervals with well-preserved, presumed varves

Most of the presumed varves are around 0.25 mm thick. They are seen in the samples as couplets, each consisting of a grey clay lamina and a thinner, nearly black, more pyritic clay lamina (Fig. 1). The couplets occur in series of up to 8 consecutive grey/black couplets and appear undisturbed by bioturbation. Rather similar-looking couplets have been illustrated from the PETM-interval in a core from the central North Sea (Kender et al., 2012).

The preservation of such delicate lamination implies absence of a benthic fauna and microfauna, and anoxic sea-floor conditions. The preservation also depends on absence of turbulence and erosion.

Intervals with blurred lamination

The intervals with less distinct lamination are up to 1-2 cm thick. Barely discernible, ghost-like remnants of couplets, as described above, are seen in major parts of these intervals. Sporadic, small presumed burrows are present at some levels.

The bottom water was apparently, temporarily, sufficiently oxygenated to maintain a sparse fauna of microorganisms which have partly or wholly obliterated the presumed varve-couplets. Sediments with indistinct lamination are typically formed under conditions with less than 0.1 ml oxygen/l in the bottom water according to Savrda & Bottjer (1991), who termed this facies the Quasi-anaerobic Biofacies.

Consecutive series of until at least 28 couplets (both well preserved and ghost-like) are present in the samples (Fig. 1).

Intervals with small scale slumping and erosion

A few 1 mm-4 cm thick intervals of disturbed bedding suggest minor events of slumping. At other levels interruption of laminae indicate small scale erosional events, possibly caused by currents.

If a varve-thickness of 0.25 mm is representative for the sedimentation rate in the entire 15 m of PETM sediments in the Hinge clay pit, the Stolleklint Clay at this site represents 60.000 years of sedimentation, i.e. a third or less of the total duration of the PETM.

The missing time-recovery may be explained by periods of small-scale erosion and by undetected intervals of non-sedimentation. Furthermore, the abrupt upper boundary of the Stolleklint Clay is associated with a coprolithic and glauconitic thin layer indicating an unconformity.

The cyclicity registered by the approximately 0.25 mm thick couplets in the PETM sediment at Hinge is presumed to represent annual variation in sediment input.

REFERENCES

- Heilmann-Clausen C. (2006) - Chapter 10. Koralrev og lerhav (excl. Danian). In: Larsen E. (ed.), *Naturen i Danmark, Geologien*. Gyldendal, Copenhagen 181-186 & 191-226.
- Heilmann-Clausen C. & Schmitz B. (2000) - The late Paleocene thermal maximum $\delta^{13}\text{C}$ excursion in Denmark? *GFF*, 122, 70.

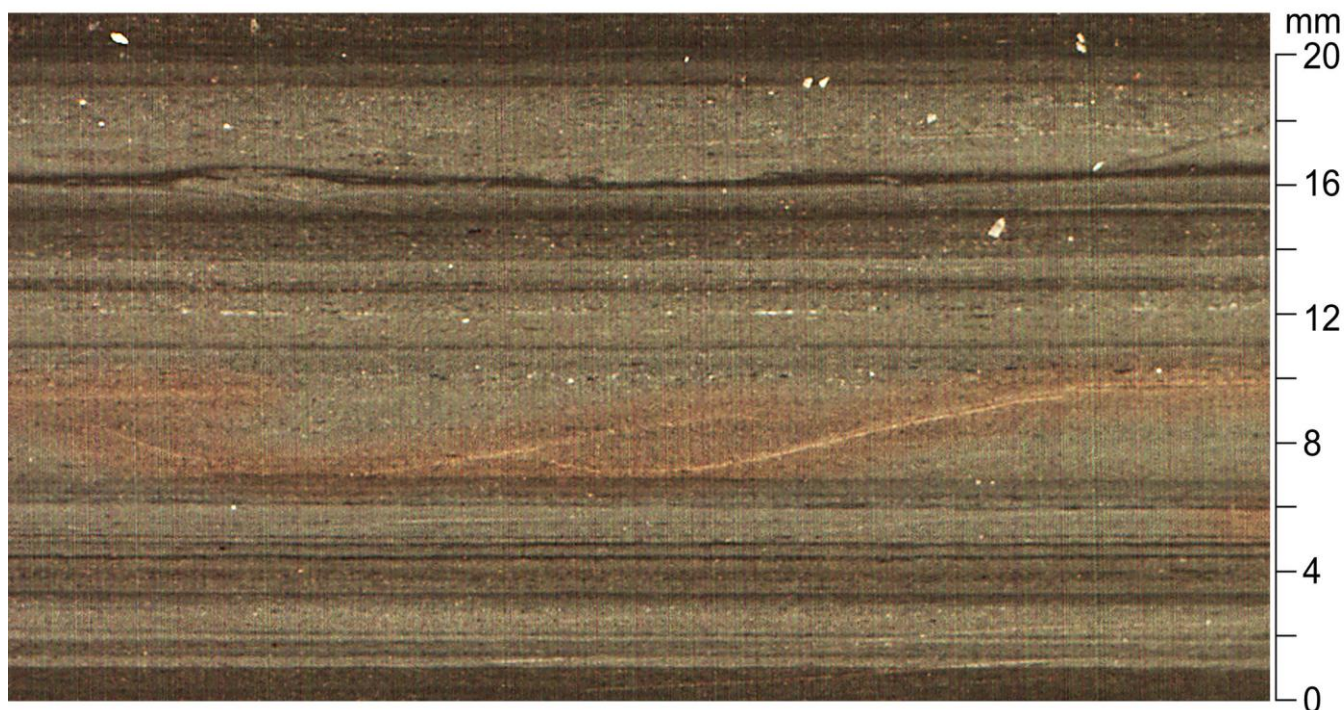


Fig. 1 – A 21 mm thick vertical section of PETM-sediment from Hinge clay pit. Twenty-eight consecutive, mainly well-preserved light-dark couplets are present in the interval 0-6.7 mm. Blurred lamination is seen in the interval 6.7-13 mm. Disturbed bedding is present at 16.5 mm, and well-preserved couplets are present at 19-21 mm.

Kender S., Stephenson M.H., Riding J.B., Leng M.J., Knox R.W. O'B, Peck V.L., Kendrick C.P., Ellis M.A., Vane C.H. & Jamieson R (2012) - Marine and terrestrial environmental changes in NW Europe preceding carbon release at the Paleocene-Eocene transition. *Earth Planet. Sci. Lett.*, 353-354, 108-120.

Savrda C.E. & Bottjer D.J. (1991) - Oxygen-related biofacies in marine strata: an overview and update. In: Tyson R.V. & Pearson T.H. (eds.), *Modern and Ancient Continental Shelf Anoxia*, Geological Society Special Publication no. 58. Geological Society of London, 201-219.

New evidence for NE Atlantic pre-PETM volcanism

Claus Heilmann-Clausen ^(a), Bo Pagh Schultz ^(b), Claus Beyer ^(c), Henrik Friis ^(a), Petra L. Schoon ^(d) & Christian Tegner ^(a)

^(a) Department of Geoscience, Aarhus University, Høegh-Guldbergs Gade 2, 8000 Aarhus C, Denmark. E-mail: claus.heilmann@geo.au.dk

^(b) Muserum, Division of Natural History, Havnevej 14, 7800 Skive, Denmark

^(c) CB-Magneto, Nørregade 27, 8670 Låsby, Denmark

^(d) Department of Geology, Lund University, Sölvegatan 12, 22362 Lund, Sweden

Document type: Short note.

Manuscript history: received 15 May 2014; accepted 30 May 2014; editorial responsibility and handling by Gerald R. Dickens & Valeria Luciani.

KEY WORDS: anoxia, *Apectodinium*, ash layers, CIE, Denmark, density flow, North Sea Basin, PETM, volcanism.

A recently exposed section on the Fur island in Denmark spans the base of the Paleocene-Eocene Thermal Maximum (PETM). The section represents an offshore facies of the North Sea Basin. The base of the CIE of the PETM is established in the section by carbon isotope analysis of TOC and of a specific biomarker for marine Thaumarchaeota (Schoon et al., 2013).

Several lithologic features in this section indicate major environmental change coinciding with the beginning of the PETM. The most important of these features are two quadruple volcanic ash layers occurring immediately below a thin density flow deposit (see below). The lowest sample showing the $\delta^{13}\text{C}$ excursion is taken just above this density flow deposit.

The total thickness of these pre-PETM ash layers is ca. 10 cm and the ash layers must therefore represent an important episode of NE Atlantic Paleogene volcanism. They are followed by two thin ash layers occurring a few centimeters above the base of the CIE. The pre-PETM ash layers are older than the previously known, and well studied, ash layers of the NE Atlantic volcanism, the so-called positive and negative numbered ash series of Bøggild (1918). The main part of the Bøggild ash series occurs in post-PETM sediments (Pedersen et al., 2011). No other ash layers are known from the underlying Upper Paleocene sediments (Østerrende Clay and Holmehus Formation) in this or other previously studied Danish sections.

The occurrence of ash layers prior to the onset of the CIE lends support to previous suggestions that NE Atlantic volcanism was a trigger of the global warming of the PETM (e.g. Svensen et al., 2004).

In the Fur section, sea-floor conditions changed from oxic (indicated by bioturbation and absence of lamination) to anoxic (indicated by a fine lamination) immediately above the upper quadruple ash layer, i.e., within sample resolution simultaneous with the start of the CIE. Previous observations suggest a similar shift to anoxic bottom waters in the offshore settings of the entire North Sea Basin at the beginning of the PETM (Refe). Organic geochemistry of the Fur section indicates that the euxinia at this site reached the photic zone during the entire PETM (Schoon et al., in review).

The lowermost 5 cm of the PETM section is a small density flow deposit witnessing transient sea-floor instability right at the onset of the PETM. The density flow may have been triggered by an increased sediment load, as there is evidence for an increased sedimentation rate during the PETM in the Danish Subbasin (CH-C unpublished data). This is the only observation of a density flow in Danish onshore sections of the entire Upper Paleocene and Lower Eocene. It is noteworthy that sea-floor instability has previously been shown to coincide with the beginning of the PETM in the western North Atlantic (Katz et al., 1999). The local nature of the density flow in the Fur section may be due to a local sloping of the seafloor caused by movement in one of the nearby salt structures.

The dinoflagellate genus *Apectodinium* was probably favoured by warmth and high nutrient levels, and showed a global abundance peak in neritic environments during the PETM (Crouch et al., 2001). *Apectodinium* increases in the Fur section from less than 2% below, to ca. 50% within the density flow and in the overlying anoxic clay of the CIE (Stolleklint Clay of the Ølst Formation).

In summary, the new Fur section shows ash layers of a significant volcanic episode immediately below sediments from the PETM, supporting NE Atlantic volcanism as a trigger of the PETM. The base of the PETM is a local density flow deposit, which was probably caused by an increased sedimentation rate during the PETM. The bottom waters became anoxic and in the surface waters a bloom of *Apectodinium* began at the start of the PETM.

REFERENCES

- Bøggild O.B. (1918) - Den vulkanske Aske i Moleret. Danmarks Geologiske Undersøgelse II. Række, 38, 3-159.
- Crouch E.M., Heilmann-Clausen C., Brinkhuis H., Morgans H.E.G., Rogers K.M., Egger H. & Schmitz B. (2001) - Global dinoflagellate event associated with the late Paleocene thermal maximum. *Geology*, 29, 315-318.
- Katz M.E., Pak D.K., Dickens G.R. & Miller K.G. (1999) - The Source and Fate of Massive Carbon Input During the Latest Paleocene Thermal Maximum. *Science*, 286, 1531-1533.

Pedersen G.P. & 11 co-authors (2011) - Molerområdet geologi – sedimenter, fossiler, askelag og glacialtektonik. *Geologisk Tidsskrift* 2011, 41-135.

Schoon P.L. Heilmann-Clausen C., Schultz B.P., Sluijs A., Sinninghe Damsté J.S. & Schouten S. (2013) - Recognition of Early Eocene global carbon isotope excursions using

lipids of marine Thaumarchaeota. *Earth Planet. Sci. Lett.*, 373, 160-168.

Svensen H., Planke S., Malthe-Sorensen A. et al. (2004) - Release of methane from a volcanic basin as a mechanism for initial Eocene global warming. *Nature*, 429.

Using boron isotopes to characterise past carbon cycle perturbations: the case of the MECO

Michael J. Henehan ^(a), Kirsty M. Edgar ^(b), Gavin L. Foster ^(c), Paul A. Pearson ^(d), Eleni Anagnostou ^(c) & Pincelli M. Hull ^(a)

^(a) Department of Geology and Geophysics, Yale University, 210 Whitney Avenue, New Haven, CT-06511, USA. E-mail: Michael.Henehan@yale.edu

^(b) School of Earth Sciences, University of Bristol, Wills Memorial Building, Queen's Road, Bristol BS8 1RJ, UK

^(c) Ocean and Earth Science, University of Southampton, National Oceanography Centre, Southampton, European Way, Southampton SO14 3ZH, UK

^(d) School of Earth & Ocean Sciences, Cardiff University, Main Building, Park Place, Cardiff CF10 3AT, UK

Document type: Short note.

Manuscript history: received 15 May 2014; accepted 30 May 2014; editorial responsibility and handling by Gerald R. Dickens & Valeria Luciani.

KEY WORDS: boron isotopes CO₂, Eocene, MC-ICPMS, MECO, planktic foraminifera.

The Middle-Eocene Climatic Optimum (MECO) is an interval of global warming that occurred around 40 Ma, as evident from a number of marine sedimentary records (Bohaty & Zachos, 2003; Bohaty et al., 2009). However, the patterns of climate perturbation during the MECO event are strikingly dissimilar to those during other Palaeogene ‘hyperthermal’ events such as the PETM or ETM 2. Firstly, the MECO bucks a long-term cooling trend between the early Eocene and the Eocene-Oligocene transition, whereas other hyperthermals are superimposed on an underlying warming trend. In addition, the MECO does not coincide with any rapid negative excursion in marine $\delta^{13}\text{C}$, suggesting that methane clathrate release (such as has been suggested for the PETM; Dickens, 2003) is unlikely. The MECO is also unusual in the timescale of observed warming: whereas the PETM took place within < 150 kyr (Murphy et al., 2010), the MECO warmed at a much slower rate and was more prolonged, over >500 kyr (Edgar et al., 2010). Another curious feature of the MECO event is its ‘reverse sawtooth’ pattern in marine records, largely antithetical to other warming pulses (e.g. deglacials, PETM). In all, then, the MECO constitutes a somewhat puzzling anomaly that, if understood, could confer important insights into long-term climate drivers, climate sensitivity in greenhouse worlds, and timescales and capacities of biogeochemical ‘recovery’ mechanisms.

As with other warming events (e.g. PETM) the MECO is thought to have been caused by a transient rise in greenhouse gas concentrations. Both shoaling of the lysocline coincident with warming (Bohaty et al., 2009), and changes in the $\delta^{13}\text{C}$ of alkenones (Bijl et al., 2010) implicate CO₂ rise as a principal driver. However, some puzzles remain - most notably the mechanism through which the necessarily large quantities of CO₂ could be delivered to, and be retained in, the atmosphere over long timescales that should intuitively be tempered by changes in rates of silicate weathering. This ‘carbon cycle conundrum’ is further exacerbated by a dearth of empirical

evidence for enhanced volcanism or eustatic sea level rise as models would require (Sluijs et al., 2013). Finally, the mechanisms through which environmental conditions rapidly returned to pre-event values after a prolonged period of carbon cycle perturbation are still unclear.

One crucial objective for the palaeo-proxy community is to accurately and quantitatively reconstruct carbonate system changes across this event. The existing alkenone-based reconstruction (Bijl et al., 2010), while valuable, invokes drastic CO₂ rise of > 10,000 ppm in magnitude, and large fluctuations in CO₂ within the MECO on sub-eccentricity timescales that would likely necessitate very large reorganisations of ocean and terrestrial carbon reservoirs. This combination of large-scale variability in atmospheric CO₂ concentrations accompanied by relatively modest changes in global temperature records would imply very low climate sensitivity. Given the potential implications of such a finding, there is an acute need for these alkenone-based estimates to be corroborated by independent proxies.

Here, we detail ongoing efforts to reconstruct atmospheric CO₂ levels across this interval using boron isotopes in multiple species of planktic foraminifera, from multiple drill sites in the Atlantic and Pacific. Preliminary data suggest that there was indeed a drop in ocean pH coincident with MECO warming, which supports CO₂ rise during this interval. In absolute terms, $\delta^{11}\text{B}$ values are comparable to values seen at the PETM (Penman et al., 2014) and throughout the Eocene (Anagnostou et al., in prep.). We will discuss the significance of these values in terms of atmospheric CO₂ concentrations, bearing in mind uncertainty deriving from foraminiferal vital effects (e.g. Henehan et al., 2013) and the value of $\delta^{11}\text{B}_{\text{sw}}$ (Raitzsch & Hönisch, 2013). Most notably, these values seem incompatible with peak-MECO CO₂ estimates derived from alkenone $\delta^{13}\text{C}$, and imply lower absolute atmospheric CO₂ concentrations across the interval.

We discuss the importance of these findings, both in terms of untangling the mechanisms behind the onset of and recovery from the MECO event, and in terms of understanding Eocene greenhouse climate state and sensitivity. In addition, we discuss briefly the evidence for a potentially MECO-like

warming event in the latest Maastrichtian, and outline future research directions.

REFERENCES

- Bijl P.K., Houben A.J.P., Schouten S., Bohaty S.M., Sluijs A., Reichart G.-J., Sinninghe Damsté J.S. & Brinkhuis, H. (2010) - Transient Middle Eocene Atmospheric CO₂ and Temperature Variations. *Science*, 330 (6005), 819–21.
- Bohaty S.M. & Zachos J. C. (2003) - Significant Southern Ocean Warming Event in the Late Middle Eocene. *Geology*, 31 (11), 1017–1020.
- Bohaty S. M. Zachos J.C., Florindo F. & Delaney M.L. (2009) - Coupled Greenhouse Warming and Deep-Sea Acidification in the Middle Eocene. *Paleoceanography*, 24 (2), PA2207.
- Dickens G.R. (2003) - Rethinking the Global Carbon Cycle with a Large, Dynamic and Microbially Mediated Gas Hydrate Capacitor. *Earth Planet. Sci. Lett.*, 213 (3-4), 169–83.
- Edgar K.M., Wilson P.A., Sexton P.F., Gibbs S.J., Roberts A.P. & Norris R.D. (2010) - New Biostratigraphic, Magnetostratigraphic and Isotopic Insights into the Middle Eocene Climatic Optimum in Low Latitudes. *Palaeogeogr. Palaeoclimatol. Palaeoecol.*, 297 (3–4), 670–82.
- Henehan M.J., Rae J.W.B., Foster G.L., Erez J., Prentice K. C., Kucera M., Bostock H.C., Martínez-Botí M.A, J. Milton J.A., Wilson P.A, Marshall B.J. & Elliott T. (2013) - Calibration of the Boron Isotope Proxy in the Planktonic Foraminifera *Globigerinoides ruber* for Use in Palaeo-CO₂ Reconstruction. *Earth Planet. Sci. Lett.*, 364, 111–22.
- Murphy B.H., Farley K.A. & Zachos J. C. (2010) - An Extraterrestrial ³He-Based Timescale for the Paleocene–Eocene Thermal Maximum (PETM) from Walvis Ridge, IODP Site 1266. *Geochim. Cosmoch. Ac.*, 74(17), 5098–5108.
- Penman D.E., Hönisch B., Zeebe R.E., Thomas E. & Zachos J.C. (2014) - Rapid and Sustained Surface Ocean Acidification during the Paleocene-Eocene Thermal Maximum. *Paleoceanography*, 27, PA4210.
- Raitzsch M. & Hönisch, B. (2013) - Cenozoic Boron Isotope Variations in Benthic Foraminifers. *Geology*, 41 (5), 591–94.
- Sluijs A., Zeebe R.E., Bijl P.K. & Bohaty S.M. (2013) - A Middle Eocene Carbon Cycle Conundrum. *Nature Geosci.*, 6 (6), 429–34.

The test size and abundance variations in planktonic foraminifera *Chiloguembelina cubensis* and *C. ototara* as response to climatic events in the Oligocene

Morana Hernitz Kucenjak ^(a), Vlasta Premec Fucek ^(a), Brian T. Huber ^(b) & Bridget S. Wade ^(c)

^(a) INA-Industrija nafte d.d., BD E&P; Exploration Sector, E&P Research Laboratory Department, Loviniceva 4, 10 000 Zagreb, Croatia; Email morana.hernitz-kucenjak@ina.hr

^(b) Department of Paleobiology, Smithsonian Institution, 10th and Constitution Ave, Washington, DC 20560-0121, U.S.A

^(c) Department of Earth Sciences, University College London, Gower Street, London, WC1E 6BT, UK

Document type: Short note.

Manuscript history: received 15 May 2014; accepted 30 May 2014; editorial responsibility and handling by Gerald R. Dickens & Valeria Luciani.

KEY WORDS: Adriatic Sea, climatic events, planktonic foraminifera, Oligocene, size.

The rich and well-preserved planktonic foraminifera assemblages extracted from samples of deep sea exploration wells Istra more-3 and Istra more-4 in the northern Adriatic Sea (Fig. 1A), enabled the identification of all seven Oligocene biozones (from O1 to O7), according to a new biozonation (Wade et al., 2011). Biometric measurements were made on the tests of 20 specimens of *Chiloguembelina cubensis* and *C. ototara* recovered from the small sieve fraction (125-63 µm) of each sample. Abundance was also assessed through the Oligocene. The long-lived species *Chiloguembelina ototara* has its lowest occurrence (LO) in Eocene Zone E9, while the species *C. cubensis* occurs in the uppermost Eocene (Zone E16). *Chiloguembelina ototara* has highest occurrence (HO) at the base of the Zone O2 and *C. cubensis* has HO in the North Adriatic at the end of Zone O5. Both species show fluctuations in abundance (Fig. 1B).

C. ototara reached a peak in abundance immediately prior Eocene/Oligocene boundary and after that became rare and finally disappeared at the base of Zone O2. In contrast, *C. cubensis* was rare from its appearance in Zone E16, and in Zone O1 never reached more than 5% in the small size fraction. We recorded a peak in abundance of this species in upper Zone O2. A similar trend in abundance has been observed in the Umbria-Marche Basin in Italy (Coccióni et al., 2008) and in southern Spain (Alegret et al., 2008). Alegret et al. (2008) attributed the maximum abundance of *C. cubensis* at the end of Zone O2 to high primary production and eutrophic conditions. An increasing trend in heterohelicid abundance has also been reported from lower Oligocene sediments in the Atlantic Ocean (Beersma & Premoli Silva, 1989) and the Ontong Java Plateau (Resig, 1993). In Zone O3 *C. cubensis*

significantly drops in abundance (2,5%), whereas at the end of Zone O4 reaches almost 10%. This event is characterized as its highest common occurrence (HCO), and subsequently this species never reaches its previous abundance. In the Adriatic Sea in Zone O5 *C. cubensis* becomes rare and at the end of this zone it disappears. However, this species sporadically continues in very rare abundance up to the latest Oligocene at the low latitudes of Syria (Palmyra region; unpublished data) and in the equatorial western Pacific Ocean (Leckie et al., 1993).

Chiloguembelina ototara reaches a maximum size and abundance before the Eocene-Oligocene transition. During the time interval that spans the Eocene/Oligocene boundary glaciations (EOT 1, EOT 2, O1 1) the size and abundance of *C. ototara* are significantly reduced (Figs. 1B, 1D).

Chiloguembelina cubensis, with its first appearance in the latest Eocene Zone E16, shows slightly different trends (Fig 1C). The oldest specimens of this species were small but they increased in test size and abundance during lower Oligocene Zones O1 and O2, reaching a maximum in Zone O2. After that, their test size decreased to uppermost Zone O5 where they disappeared from mid-latitude regions.

The data obtained show that populations of *Chiloguembelina cubensis* and *C. ototara* were strongly affected by intensive climatic changes during the early and earliest late Oligocene. Both species reduced test size and abundance as a response to climate deterioration and unfavorable paleoceanographic conditions. The interpretation of Zone O2 as a period of a warmer interglacial climate, is consistent with high abundance of the turborotalids and subbotinids (especially *Turborotalia ampliapertura*), which are thought to prefer temperate to warm water (Pearson et al., 2006).

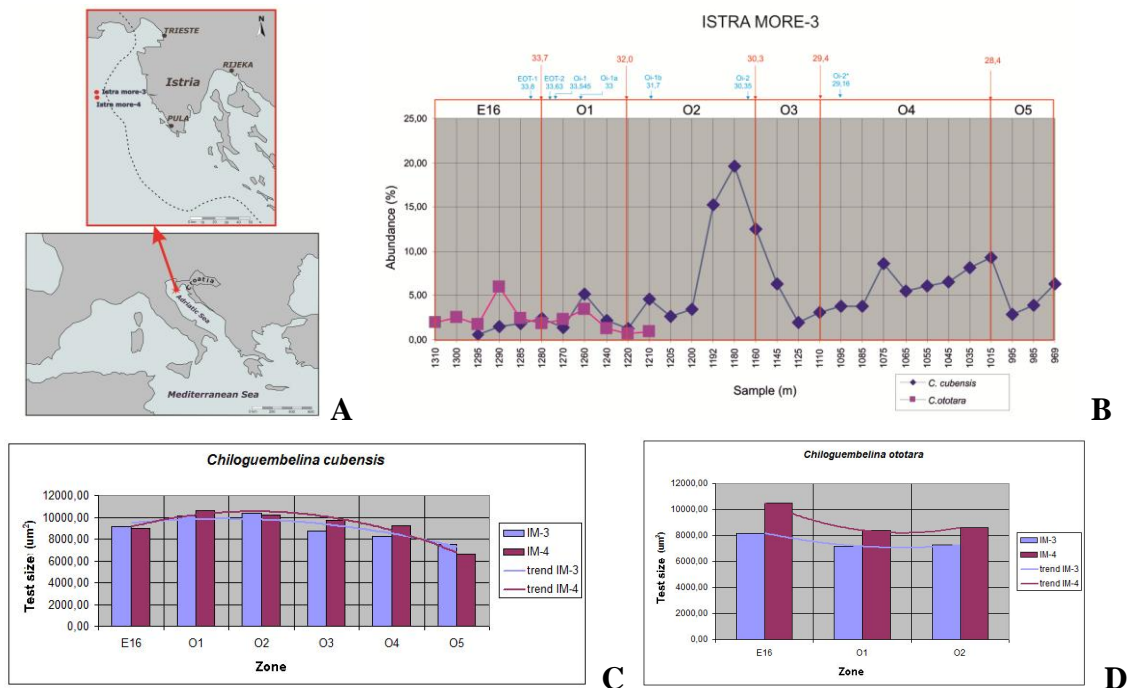


Fig.1 – A) Location map of exploration wells; B) Figure show the abundance of *Chiloguembelina cubensis* and *C. ototara* in Istra more -3 well and comparison biostratigraphic zones with the absolute age and glaciation events (after Pekar et al., 2002; Wade & Pälike, 2004; Katz et al., 2008, Miller et al., 2009; Coxal & Wilson, 2011; Wade et al., 2011); C) Test size of *Chiloguembelina cubensis* in Istra more-3 and Istra more-4; D) Test size of *Chiloguembelina ototara* in Istra more 3 and Istra more-4 well

REFERENCES

- Alegret L., Cruz L.E., Fenero R., Molina E., Ortiz S. & Thomas E. (2008) - Effects of the Oligocene climatic events on the foraminiferal record from Fuente Caldera section (Spain, western Tethys). *Palaeogeogr. Palaeoclimatol., Palaeoecol.*, 269, 94-102.
- Boersma A. & Premoli Silva I. (1989) - Atlantic Paleogene biserial heterohelicid foraminifera and oxygen minima. *Paleoceanography*, 4(3), 271-286.
- Coccioni R., Montanari A., Bellanca A., Bice D.M., Brinkhuis H., Church N., Deino A., Lirer F., Macalady A., Maiorano P., Marsili A., Mcdaniel A., Monechi S., Neri R., Nini C., Nocchi M., Pross P., Sagnotti L., Sprovieri M., Tateo F., Touchard Y., Van Simaey S. & Williams G. (2008) - Integrated stratigraphy of the Oligocene pelagic sequence in the Umbria-Marche basin (Northeastern Apennines, Italy): A potential Global Stratotype Section and Point (GSSP) for the Rupelian/Chattian boundary. *Geol. Soc. Am. Bull.*, 120(3/4), 487-511.
- Coxal H.K. & Willson P.A. (2011) - Early Oligocene glaciation and productivity in the eastern equatorial Pacific: Insights into global carbon cycling; *Palaeoceanography*, 26, PA2221.
- Katz M.E., Miller K.G., Wright J.D., Wade B.S., Browning J.V., Cramer B.S., & Rosental Y. (2008) - Stepwise transition from the Eocene greenhouse to the Oligocene icehouse. *Nature Geosci.*, 1, 329-333.
- Leckie R.M., Farnham C. & Schmidt M. G. (1993) - Oligocene planktonic foraminifer biostratigraphy of Hole 803D (Ontong, Java Plateau) and Hole 628A (little Bahama Bank), and comparison with the southern high latitudes. *Proceedings of the ODP, Sci. Res.*, 130, 113-136.
- Miller K.G., Wright J.D., Katz M.E., Wade B.S., Browning J.V., Cramer B.S. & Rosenthal Y. (2009) - Climate treshold at the Eocene-Oligocene transtion: Antarktic ice sheet influence on ocean circulation. In: Koeberl, C. & Montanari, A. (Eds.): *The Late Eocene Earth-Hothouse, Icehouse, and Impacts*. Geological Society of America Special Publication, 452, 169-178.
- Pearson P.N., Premec Fuček V. & Premoli Silva I. (2006) - Taxonomy, biostratigraphy and phylogeny of Eocene Turborotalia. U: Pearson, P. N., Olsson, R. K., Huber, B. T., Hemleben, C. & Berggren, W. A. (eds.): *Atlas of Eocene Planktonic Foraminifera*. The Cushman Foundation for Foraminiferal Research, Special Paper, 41, 433-460.
- Pekar S.F., Christie-Blick N., Kominz M.A. & Miller K.G. (2002) - Calibration between eustatic estimates from backstripping and oxygen isotopic records for the Oligocene. *Geology*, 30, 903-906.
- Resig J.M. (1993) - Cenozoic stratigraphy and paleoceanography of biserial planktonic foraminifers, Ontong Java Plateau. In: Berger, W. H., Kroenke, L. W., Mayer, L. A. et al., *Proceedings of the ODP, Scientific Results: ODP, College Station, TX*, 130, 231-244.
- Wade B.S. & Pälike H. (2004) - Oligocene climate dynamics. *Paleoceanography*, 19, 1-16.
- Wade B.S., Pearson P.N., Berggren W.A. & Pälike H. (2011) - Review and revision of Cenozoic planktonic foraminiferal biostratigraphy and calibration to the geomagnetic polarity and astronomical time scale. *Earth Sci. Rev.*, 104, 111-142.

Fossil *Laurelia* pollen (Atherospermataceae) from lower Eocene sediments of the Krappfeld (Austria)

Christa-Ch. Hofmann ^(a) & Hans Egger ^(b)

^(a) University of Vienna, Department of Palaeontology, Althanstrasse 14, 1090 Vienna, Austria. E-mail: christa.hofmann@univie.ac.at

^(b) Geological Survey of Austria, Neulinggasse 38, 1030 Vienna, Austria

Document type: Short note.

Manuscript history: received 15 May 2014; accepted 30 May 2014; editorial responsibility and handling by Gerald R. Dickens & Valeria Luciani.

KEY WORDS: Atherospermataceae pollen, Austria, EECO, *Laurelia*, palynology

Laurelia Juss (Atherospermataceae R. Br.) is today a disjunct genus in the southern hemisphere that consists of undergrowth trees inhabiting temperate moist forests of South America and New Zealand. Despite the fact that unequivocal Atherospermataceae fossils are still rare, they are known since the Upper Cretaceous from the southern hemisphere (Renner et al., 2000; Conran et al., 2013; Knight & Wilf, 2013). Here we present the first findings of *Laurelia* pollen in the northern hemisphere, from the lower Eocene of Krappfeld, in southern Austria.

The Krappfeld area is located in Carinthia, in southern Austria, and the now inaccessible section was exposed in the Pemberg Quarry, west of Klein St. Paul. The rocks represented the upper part of the Gosau Group, comprising Campanian (Pemberger Formation) to Middle Eocene sedimentary rocks. However, the Paleogene (Holzer Formation) rests with an erosional unconformity on the Campanian, interpreted to be the result of a major sea-level drop in the latest Paleocene (Egger et al., 2009). At the base of the Paleogene succession, the 8 m-thick terrestrial Holzer Formation is composed of soft red and green claystone, devoid of carbonate, and intercalated lenses of coaly clay and coal. The lenses of coaly clay are rich in terrestrial palynomorphs. Previously published surveys revealed highly diverse and well preserved palynofloras from the Krappfeld and the Pemberg quarry and suggested that the Holzer Formation was deposited during the EECO (Hofmann & Zetter, 2001; Zetter & Hofmann, 2001; Hofmann et al., 2012). A major transgression in the Ypresian (early Biochron NP12 – Egger et al., 2009) flooded the shelf and brought back marine conditions (black transgressive shales) and terrestrial pollen co-occurred with numerous marine dinoflagellates. The overlying Sittenberg Formation has a faunal assemblage indicative of the lower part of shallow benthic zone SBZ10, which has been correlated with calcareous nannoplankton zone NP12 (Serra-Kiel et al., 1998).

The pollen and spores were examined with LM and SEM and, when possible, assigned to botanical families and genera.

Overall, three different palynomorph-rich facies were identified: The first, at the base of the Holzer Formation, is characterized by abundant and diverse fern spores, lumps of fern spores (Schizaeales, *Leiotriletes* spp. and various Polypodiaceae s.l.), various Arecaceae (e.g., affiliated to extant *Elais* sp.), Myricaceae, and Juglandaceae. The second facies is from the black transgressive shale and characterized by the co-occurrence of marine dinoflagellates and terrestrial palynomorphs. More than 90% of the dinoflagellates are specimens of the peridinioid genus *Apectodinium* spp. and the terrestrial palynomorphs are abundant *Normapolles* s.l., *Nypa*, various Calamoideae palm pollen, and *Avicennia*. The third facies is composed of grey and dark grey clays and dominated by wind pollinated triporate taxa (e.g., *Normapolles* s.l., Myricaceae, Juglandaceae), with Calamoideae, other monosulcate palm taxa and numerous fern spores also present (Hofmann et al., 2012).

The Atherospermataceae pollen, which resembles most closely the genus *Laurelia*, has been encountered in low numbers in all samples and facies from the Holzer Formation, but until recently has been always misidentified as putable Arecaceae or Myricaceae pollen (Hofmann et al., submitted). The reason lies in the peculiar aperture type: Atherospermataceae pollen are composed of two hemispherical halves that are separated by a complete ring-like aperture or an incomplete ring-like aperture that acts as a zone of weakness so that the deposited fossil pollen have, therefore, tended to fall into two parts. Most fossil *Laurelia* pollen in the Krappfeld are preserved as rolled up individual halves and look like boat-shaped sulcate pollen grains of monocots or basal angiosperms; preservation of complete grains is rare. The presence of *Laurelia* pollen during the EECO in Austria supports the theory of Renner et al. (2000) that the taxon originated in western Gondwana and subsequently dispersed eastwards via Antarctica to reach New Zealand before the early Miocene (*Laurelia* leaf fossils of Conran et al., 2013), but also is a witness of a northward migration through Africa to reach southern Europe during the early Paleogene. During its northward migration, the plant must have adapted to warmer temperatures in order to grow under the early Eocene

“subtropical to tropical” climatic conditions and probably evolved into an understory tree where the environment was not so hot and more humid.

REFERENCES

- Conran J.G., Bannister J.M., Lee D.E. (2013) - Fruits and leaves with cuticle of *Laurelia otagoensis* sp. nov. (Atherospermataceae) from the early Miocene of Otago (New Zealand). *Alcheringa*, 37, 496-509.
- Egger H., Heilmann-Clausen C. & Schmitz B. (2009) - From shelf to abyss: Record of the Palaeocene/Eocene-boundary in the Eastern Alps (Austria). *Geol. Acta*, 7, 215-227.
- Hofmann Ch.-Ch. & Zetter R. (2001) - Palynological investigation of the Krappfeld area, Palaeocene/Eocene, Carinthia (Austria). *Palaeontographica Abt. B*, 259, 47-64.
- Hofmann Ch.-Ch., Pancost R., Ottner F., Egger H., Taylor K. & Zetter R. (2012) - Palynology Biomarker and Clay mineralogy of the Early Eocene Climate Optimum (EECO) in the transgressive Krappfeld succession (Eastern Alps, Austria). *Austrian J. Earth Sci.*, 105, 224-239.
- Hofmann Ch.-Ch., Egger H. & King C. (submitted) - LM and SEM investigations of pollen from PETM and EECO localities of Austria and Great Britain: New findings of Atherospermataceae, Annonaceae, Araceae and Arecaceae from the Lower Eocene. *Plant Syst. Evol.*
- Knight C.L. & Wilf P. (2013) - Rare leaf fossils of Monimiaceae and Atherospermataceae (Laurales) from the Eocene Patagonian rainforests and their biogeographic significance. *Palaeontologica Electronica*, 16, 3, 26A, pp. 39.
- Renner S.S., Foreman D.B. & Murray D. (2000) - Timing transantarctic disjunctions in the Atherospermataceae (Laurales): Evidence from coding and noncoding chloroplast sequences. *Syst. Biol.*, 49, 579-591.
- Serra-Kiel J., Hottinger L., Caus E., Drobne K., Ferrandez C., Jaurhi A.K., Less G., Pavlovec R. Pignatti J., Samsó J.M., Schaub H., Sirel E., Strougo A., Tambareau Y., Tosquella J. & Zakrevskaya E. (1998) - Larger foraminiferal biostratigraphy of the Tethyan Paleocene and Eocene. *Soc. Géol. France Bull.*, 169, 281-299.
- Zetter R., Hofmann Ch.-Ch. (2001) - New aspects of the palynoflora of the lowermost Eocene (Krappfeld Area, Carinthia). *Österreichische Akademie der Wissenschaften, Schriftenreihe der Erdwissenschaftlichen Kommission*, 12, 473-507.

New LM and SEM investigations of pollen and spores from the Brixton drillcores (lowermost Eocene, England)

Christa-Ch. Hofmann ^(a) & Chris King ^(b)

^(a) University of Vienna, Department of Palaeontology, Althanstrasse 14, 1090 Vienna, Austria. E-mail: christa.hofmann@univie.ac.at

^(b) 16A Park Road, Bridport, DT6 5DA, UK

Document type: Short note.

Manuscript history: received 15 May 2014; accepted 30 May 2014; editorial responsibility and handling by Gerald R. Dickens & Valeria Luciani.

KEY WORDS: England, lower Eocene, megathermal elements, palynology, SEM.

The samples for this study come from boreholes drilled in Brixton (SW London, England) that penetrated down through the lower part of the London Clay Formation, the underlying and interfingering Woolwich and Reading Formations and then the Upnor Formation. The Upnor Formation is a shallow marine sand-dominated unit, dated as NP9 (late Thanetian). The top is marked by a paleosol, marking emergence and probably indicating a hiatus. The overlying succession comprises the Lower Mottled Clay (Reading Formation), Lower Shelly Clay and Laminated Beds (Woolwich Formation), Upper Mottled Clay (Reading Formation) and Upper Shelly Clay (Woolwich Formation; Ellison & King, 2004). The Woolwich Formation comprises mainly low-energy marginal-marine environments, the Reading Formation non-marine coastal plain environments with intensive pedogenesis. These were deposited during the earliest Eocene PETM (Paleocene-Eocene Thermal Maximum). In the Brixton boreholes there is a sand unit (probably a fluvial channel) at the base of the Upper Mottled Clay, and in one borehole a sand-filled channel beneath the Upper Shelly Beds, directly overlying the Lower Shelly Clay. The carbon isotope excursion marking the base of the CIE and of the PETM (and base of the Eocene) has been identified elsewhere in London to lie near the base of the Lower Mottled Clay (Thiry et al., 1998). The start of the *Apectodinium* influx, which in marine and marginal-marine environments is co-extensive with the PETM is delayed in this area, due to the initial non-marine environment, and occurs within the PETM, at the base of the Lower Shelly Clay. The influx extends to the top of the Upper Shelly Clay (Collinson et al., 2009).

Palynology: All samples, except the terrestrial wetland facies of the Upper Mottled Beds (UMB, see below) are dominated by angiosperm pollen (eudicots and monocots). Gymnosperms (lumped bisaccates such as *Pinus*, *Cathaya*, *Picea*, *Abies*, and monosaccates such as *Tsuga*, *Sciadopitys*) are rare, and occur generally below 1 %, except in six samples (1,2% to max 4,8% lumped bisaccates). Gymnospermous

Cupressaceae/ Taxodiaceae pollen types occur frequently with up to 7,6 %. The most frequent and dominant angiosperm is *Platycarya* (2 taxa), followed by *Plicatopollis plicatus*, followed by *Platanus* and the Fagaceae *Eotriginobalanus* (three types) and *Lithocarpus/Castanea* (including under SEM two *Lithocarpus* species and an unknown small form of *Triginobalanus*), and Juglandalean *Engelhardia/Engelhardioid* types. The UMB are generally dominated by fern spore types (often in lumps, connected with sporangial tissues) and *Sparganium* (also occasionally in lumps) and show exceptionally low gymnosperm percentages. Animal-pollinated taxa also occur in lumps and therefore all the terrestrial samples are interpreted to be autochthonous to par-autochthonous. Of the 171 counted taxa, 61 (36%) are interpreted as megathermal (by botanical affiliation). There might be more, but many taxa cannot yet be affiliated to a family or genus, despite SEM investigation. 21 megathermal taxa occur more (21 times) or less (4 times) frequently from the Lower Mottled Beds to the Upper Shelly Beds: *Plicapollis*, Myristicaceae?, *Sideroxylon*-type, indet. Sapotaceae, Arecaceae, *Diospyros*, Anacardiaceae, *Zanthoxylon*, indet. Rutaceae, three Euphorbiaceae, *Aristogeitonia* type (Picrodendraceae), Mastixioid form, Nyssoid form, three “*Craigia*” types (Malvaceae), and *Reevesia* (Malvaceae). The most common megathermal elements are the Arecaceae and *Craigia*; all the other Sapotaceae, Anacardiaceae, Meliaceae, Rutaceae, Euphorbiaceae etc. occur only in very low percentages <1,5% and much lower.

An overview of taxa diversity in different beds shows the following pattern: Near the PETM, in the Lower Mottled Beds (LMB, 1 sample) altogether 65, including 23 (35%) megathermal taxa; channel sediments (CS, 3 samples) altogether 98, including 31 (32%) megathermal taxa; Lower Shelly Beds (LSB, 5 samples) altogether 100, including 30 (30%) megathermal taxa; Laminated Beds (LB, 2 samples) altogether 80, including 24 (30%) megathermal taxa; Sand Unit below upper Mottled Beds (SU, 2 samples) altogether 75, including 15 (20%) megathermal taxa; Upper Mottled Beds (UMB, 5 samples) altogether 108, including 36 (33%) megathermal taxa; Upper Shelly Beds (USB, 9 samples)

altogether 127, including 38 (30%) megathermal taxa. This shows a general increase in taxa diversity and amount of megathermal taxa up-stratigraphy, but shows also that the percentage of megathermal elements is highest near the PETM in the LMB. However, the younger beds become more and more diverse and eleven megathermal taxa first appear after the deposition of the LMB: *Lannea* type (Anacardiaceae, known from the PETM in St Pancraz and EECO of Krappfeld in Austria; Hofmann et al., 2011; Hofmann & Zetter, 2001), two Euphorbiaceae (*Cephalocroton*; and a type known from PETM of Pankraz), Myrtaceae (indet), two Icacinaceae, *Milletia* type (Leguminosae), Arecaceae (*Elaeis*-type, Calamoideae known from younger Eocene deposits and Bactridinae) and a trilete thin-walled fern spore, probably assignable to *Acrostichum*. These increases and first appearances might indicate the gradual warming climaxing in the EECO.

Noteworthy are the occurrences of yet unknown pollen of e.g., Apiaceae indet., Araliaceae indet., *Panax*, *Cephalocroton*, *Cornus*, *Diospyros*, *Parthenocissus*, *Thalictrum*, and *Viburnum*.

ACKNOWLEDGMENTS

This study was initiated by Robert Knox (British Geological Survey), who provided the samples. Robert Knox carried out extensive research on aspects of the Paleocene/Eocene boundary, in

the North Sea Basin and elsewhere, which was continuing at his death in 2013. We regret the loss of a valued colleague and friend.

REFERENCES

- Collinson, M.E., Steart, D.C., Harrington, G.J., Hooker, J.J., Scott, A.C., Allen, L.O., Glasspool, I.J. & Gibbons, S.J. (2009) - Palynological evidence of vegetation dynamics in response to palaeoenvironmental change across the onset of the Paleocene-Eocene Thermal Maximum at Cobham, southern England. *Grana*, 48, 38-66.
- Ellison, R.A. & King, C. (2004) - Chapter 4. Palaeogene: Paleocene. In: Ellison R.A., Woods M.A., Allen D.J., Forster A., Pharoah T.C. & King C. *Geology of London*. British Geological Survey, Keyworth, 22-43.
- Hofmann, Ch.-Ch. & Zetter, R. (2001) - Palynological investigation of the Krappfeld area, Palaeocene/Eocene, Carinthia (Austria). *Palaeontographica Abt. B* 259, 47-64.
- Hofmann Ch.-Ch., Mohamed O., Egger H. (2011) - A new terrestrial palynoflora from the Palaeocene/Eocene boundary in the northwestern Tethyan realm (St. Pankraz, Austria). *Rev. of Paleobot. Palynol.*, 166, 295-310.
- Thiry, M., Dupuis, C., Aubry, M.-P., Berggren, W.A., Ellison, R.A., Knox, R.W.O'B., Sinha, A. & Stott, L. (1998) - Tentative correlations between continental deposits of the argiles plastiques (Paris Basin) and Reading Beds (London Basin), based on chemostratigraphy. *Strata* 9, 125-129.

Was the Early Eocene ocean unbearably warm or are the proxies unbelievably wrong?

Christopher J. Hollis ^(a), Kristina M. Pascher ^(a,b), Benjamin R. Hines ^(b), Kate Littler ^(c,d), Denise K. Kulhanek ^(e), C. Percy Strong ^(a), James C. Zachos ^(c), Stephen M. Eggins ^(f) & Andy Phillips ^(a)

^(a) GNS Science, PO Box 30368, Lower Hutt 5040, New Zealand. E-mail: c.hollis@gns.cri.nz

^(b) Antarctic Research Centre, Victoria University Wellington, PO Box 600, Wellington 6140, New Zealand

^(c) Earth & Planetary Sciences, University of California – Santa Cruz, California 95060, USA

^(d) Camborne School of Mines, University of Exeter, Penryn Campus, Cornwall, TR10 9FE, UK

^(e) Integrated Ocean Drilling Program, Texas A&M University, TX 77845-9547, USA

^(f) Research School of Earth Sciences, The Australian National University, Canberra 0200, Australia

Document type: Short note.

Manuscript history: received 15 May 2014; accepted 30 May 2014; editorial responsibility and handling by Gerald R. Dickens & Valeria Luciani.

KEY WORDS: geochemistry, micropaleontology, paleobiogeography, paleoceanography, Paleogene, paleotemperature, radiolarians.

Geochemical proxies for sea temperature indicate that there were times in the Early Eocene (56-48 Ma) when warm-subtropical to tropical surface water masses extended into the polar oceans (Sluijs et al., 2006; Pross et al., 2012). If the proxies are to be believed, the Early Eocene oceans occasionally must have been unbearably warm for some groups of surface dwelling plankton. However, there is little evidence for high rates of species turnover amongst calcareous nannoplankton, planktonic foraminifera or radiolarians during this time (Norris et al., 2013). Instead, paleobiogeographic trends within these groups indicate the cosmopolitan taxa thrived through the Early Eocene and low-latitude taxa exhibited only modest poleward expansions in range.

Preliminary studies of Paleocene-Eocene radiolarian assemblages in the middle to high latitude SW Pacific (50-70°S paleolatitude) reveal the presence of three biogeographic species groups: tropical-subtropical, cosmopolitan and sub-polar/deep. Cosmopolitan taxa dominate assemblages from Middle Paleocene to Middle Eocene. Sub-polar/deep species are common at one site (ODP Site 1121, Campbell Plateau, 63°S) during a period of relatively cool conditions in the late middle and early Late Paleocene. The sub-polar/deep species group is widespread in the South Tasman Sea (65-70°S) from Late Eocene to Oligocene (DSDP Sites 277, 280, 281 and 283, ODP Site 1172). Definitively tropical-subtropical species (e.g. *Bekoma bidartensis*, *Phormocyrtis turgida*, *Theocorys? physella* s.s.) are only evident in small numbers within the Paleocene-Eocene thermal maximum (PETM) and overlying earliest Eocene at Mead Stream (53°S) (Fig. 1a).

Such modest increases in warm-water biogeographic indicators are difficult to reconcile with multi-proxy sea temperature estimates ($\delta^{18}\text{O}$, Mg/Ca and TEX₈₆) from sites south of Mead Stream which indicate that (a) warm subtropical to fully tropical surface waters bathed the region from the PETM to the Late Eocene (Bijl et al., 2009; Liu et al., 2009;

Hollis et al., 2012; Sluijs et al., 2011), and (b) both surface and seafloor temperatures warmed by 5°C during the PETM (Fig. 1b). In contrast, radiolarian paleobiogeography can be reconciled with modeled temperatures under high CO₂ Eocene boundary conditions (Hollis et al., 2012). We conclude that a variety of factors are responsible for a warm bias in temperature proxies: seasonal production and/or packaging of foraminifera and Archaea (Hollis et al., 2012); inaccuracies surrounding ocean chemistry and trace element partitioning in foraminiferal tests (Evans & Müller, 2012); the assumption of ice-free conditions for the early Paleogene. A simple correction to $\delta^{18}\text{O}$ -based temperature calculations, based on recently published evidence for Antarctic ice sheets in the Paleocene (Hollis et al., 2014), reduces PETM warming by 2°C. These preliminary results suggest that zonal heterogeneity in Eocene high-latitude SSTs may not be as pronounced as current proxy datasets imply (Douglas et al., 2014).

REFERENCES

- Bijl P.K., Schouten S., Sluijs A., Reichert G.-J., Zachos J.C. & Brinkhuis H. (2009) - Early Palaeogene temperature evolution of the southwest Pacific Ocean. *Nature*, 461, 776-779.
- Douglas P.M.J., Affek H.P., Ivany L.C., Houben A.J.P., Sijp W.P., Sluijs A., Schouten S. & Pagani M. (2014) - Pronounced zonal heterogeneity in Eocene southern high-latitude sea surface temperatures. *P. Natl. Acad. Sci. USA*, doi: 10.1073/pnas.1321441111
- Evans D. & Müller W. (2012) - Deep time foraminifera Mg/Ca paleothermometry: Nonlinear correction for secular change in seawater Mg/Ca. *Paleoceanography*, 27, A4205.
- Hollis C.J., Taylor K.W.T., Handley L., Pancost R.D., Huber M., Creech J., Hines, B.R., Crouch E.M., Morgans H.E.G., Crampton J.S., Gibbs S.J., Pearson P.N. & Zachos J.C. (2012) - Early Paleogene temperature history of the Southwest Pacific Ocean: reconciling proxies and models. *Earth Planet. Sci. Lett.*, 349-350, 53-66.

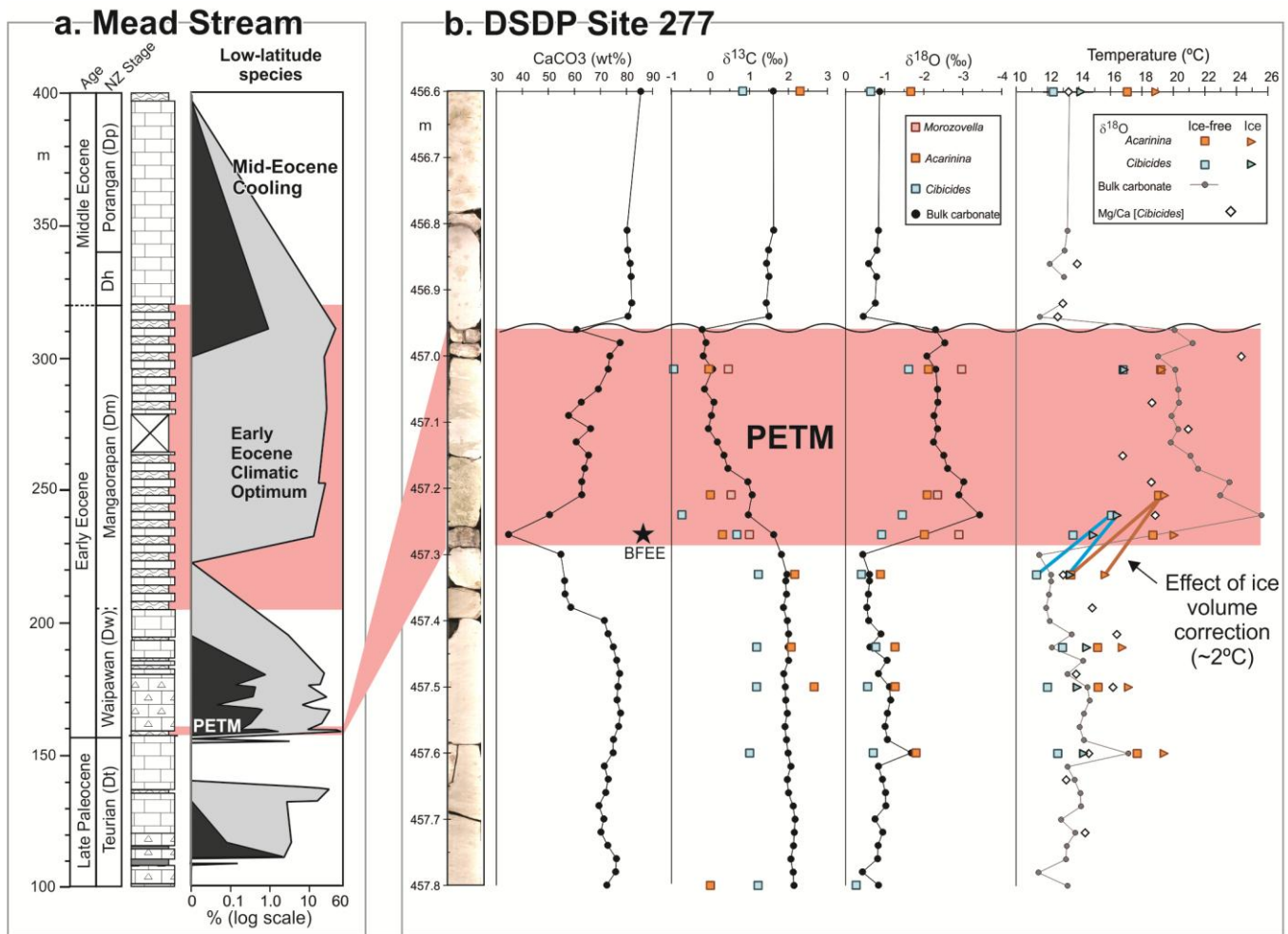


Fig.1 – (a) Distribution of low-latitude (Tropical/Subtropical, dark grey) and cosmopolitan (medium grey) radiolarians through the Paleocene-Eocene transition at Mead Stream, Dh = Heretaungan; (b) geochemical signature of the Paleocene-Eocene thermal maximum (PETM) at DSDP Site 277, showing % CaCO₃, bulk carbonate and foraminiferal $\delta^{13}\text{C}$ (see legend), bulk carbonate and foraminiferal $\delta^{18}\text{O}$ (ice-free), *Acarinina* and *Cibicides* $\delta^{18}\text{O}$ (ice-free and with an ice volume factor of 0.5‰ for $\delta^{18}\text{O} = -0.33\text{‰}$), and sea temperature estimates based on bulk carbonate $\delta^{18}\text{O}$ (ice-free), *Acarinina* and *Cibicides* $\delta^{18}\text{O}$ (ice-free and with an ice volume factor of 0.5‰ for $\delta^{18}\text{O} = -0.33\text{‰}$), and Mg/Ca ratio for *Cibicides* (Mg/Ca_{SW} = 4). Note that the bulk carbonate $\delta^{18}\text{O}$ excursion is inferred to be amplified by diagenetic factors: diagenesis decreases as clay content increases in the PETM and therefore Paleocene values reflect seafloor temperatures whereas PETM values are closer to sea surface temperatures. This implies that the temperature estimates derived from *Acarinina* are thermocline temperatures rather than the sea surface temperatures.

Hollis C.J., Tayler M.J.S., Andrew B., Taylor K.W., Lurcock P., Bijl P.K., Kulhanek D.K., Crouch E.M., Nelson C.S., Pancost R.D., Huber M., Wilson G.S., Ventura G.T., Crampton J.S., Schiøler P. & Phillips A. (2014) - Organic-rich sedimentation in the South Pacific Ocean associated with Late Paleocene climatic cooling. *Earth-Sci. Rev.*, 134, 81-97, doi.org/10.1016/j.earscirev.2014.03.006.

Liu Z., Pagani M., Zinniker D., DeConto R., Huber M., Brinkhuis H., Shah S.R., Leckie R.M. & Pearson A. (2009) - Global Cooling During the Eocene-Oligocene Climate Transition. *Science*, 323, 1187-1190.

Norris R.D., Turner, S.K., Hull P.M. & Ridgwell A. (2013) - Marine Ecosystem Responses to Cenozoic Global Change. *Science*, 341, 492-498.

Pross J., Contreras L., Bijl P.K., Greenwood D.R., Bohaty S.M., Schouten S., Bendle J.A., Röhl U., Tauxe L., Raine

J.I., Huck C.E., van de Flierdt T., Jamieson S.S.R., Stickley C.E., van de Schootbrugge B., Escutia C., Brinkhuis H. & IODP Expedition 318 Scientists. (2012) - Persistent near-tropical warmth on the Antarctic continent during the early Eocene epoch. *Nature* 488, 73-77.

Sluijs A., Bijl P.K., Schouten S., Röhl U., Reichert G.J. & Brinkhuis, H. (2011) - Southern ocean warming, sea level and hydrological change during the Paleocene-Eocene thermal maximum. *Clim. Past*, 7, 47-61.

Sluijs A., Schouten S., Pagani M., Woltering M., Brinkhuis H., Sinninghe Damste J.S., Dickens G.R., Huber M., Reichert G.-J., Stein R., Matthiessen J., Lourens L.J., Pedentchouk N., Backman J., Moran K. & Expedition 302 Scientists. (2006) - Subtropical Arctic Ocean temperatures during the Palaeocene/Eocene thermal maximum. *Nature*, 441, 610-613.

Faunal succession, local correlation and isotopes push the Mammalian Dispersal Event in NW Europe into the cooler latest Paleocene

Jerry J. Hooker ^(*)

^(*) Department of Earth Sciences, Natural History Museum, London SW7 5BD, UK. E-mail: j.hooker@nhm.ac.uk

Document type: Short note.

Manuscript history: received 15 May 2014; accepted 30 May 2014; editorial responsibility and handling by Gerald R. Dickens & Valeria Luciani.

KEY WORDS: biozone, CIE, dispersal, Eocene, PETM.

Most NW European latest Paleocene and earliest Eocene mammal faunas lack unequivocal evidence of stratigraphic order and, until recently, any direct link to the onset of the Paleocene-Eocene (P-E) carbon isotope excursion (CIE). Evolutionary grade using MP reference levels to resolve the first issue leads to circular arguments and poor time resolution. Previously, I used a parsimony analysis program (PAUP) to relate faunas through shared taxa (Hooker, 1996). Major faunal groupings were placed in biozones PE I-V, currently envisaged as ranging from the beginning of the Eocene till mid Ypresian. Incorporating newly found mammal faunas in a new analysis reinforces the status of zones PE I and PE II.

Recently, a small mammal fauna from Sotteville, France, was discovered 1.5m above CIE onset (Smith et al., 2011). According to estimated accumulation rates, this is probably equivalent to only a few thousand years into the Paleocene-Eocene Thermal Maximum (PETM). The fauna was placed in zone PE II, because of the presence of the marsupial *Peradectes* and the plesiadapiform *Arcius*, both unknown in PE I. If PE I pre-dates PE II, there is essentially no room within the earliest Eocene for PE I faunas. The PAUP results should reflect time, rather than geography or ecology, given that PE I-II geographical distributions overlap and ecological diversity between the two faunal zones is nearly identical (Hooker & Collinson, 2012). On the basis that PE I faunas pre-date the Sotteville fauna, they should also pre-date the P-E boundary and thus be latest Paleocene. Two other mammal sites, Rivecourt (France) and Dormaal (Belgium), also have carbon isotope records. That at Rivecourt has recently been shown to have pre-CIE values, making it (with MP6-surviving taxa) latest Paleocene (Smith et al., 2014). Dormaal, in contrast, is usually considered earliest Eocene, although carbon isotopes at the base of the Dormaal Member, the apparently indigenous source of the mammals, also have pre-CIE values (Grimes et al., 2006). PE II faunas all occur in the Woolwich, Mortemer, Soissonnais or Vaugirard formations, largely time equivalents

and virtually restricted to the PETM. PE I faunas occur in valley fills, incising marine Paleocene (NP8 or NP9). What overlies them is often uncertain. However, the PE I Le Quesnoy fauna occurs in channels at the base of the Soissonnais Formation (Nel et al., 1999). Numerous other similar incised valley fills, without mammal fossils, underlie the Woolwich, Reading, Mortemer or Soissonnais formations, their bases marking the Th4-5 sequence boundary. The French Cernay and Berru faunas (MP6) are accepted as Late Paleocene, although their exact dating has been disputed (Hooker & Millbank, 2001; Smith et al., 2014). Local correlation shows their host strata are lateral equivalents of the Bracheux Formation (NP9) (Laurain & Meyer, 1986), the base of whose equivalent in the London Basin, the Upnor Formation (NP9), is within Chron C25n (Ellison et al., 1996). The beginning of the Clarkforkian North American Land Mammal Age also lies within C25n (Butler et al., 1980), making Cernay and Berru earlier and PE I faunas later Clarkforkian equivalents.

Redating PE I mammal faunas as latest Paleocene means that the Mammalian Dispersal Event (MDE), originally thought to coincide throughout the Northern Hemisphere with the P-E boundary, occurred earlier in NW Europe. This has implications for some contested intercontinental dispersal directions. PE I primates (*Teilhardina*, *Cantius*), perissodactyls (*Cymbalophus*) and artiodactyls (*Diacodexis*) have their first appearances significantly earlier in Europe than in North America and thus dispersed westwards to that continent. The dating also implies that, although temperatures in the final stages of the Paleocene were cooler than in the PETM, high-latitude dispersal from North America to Europe took place at that time, e.g., *Coryphodon*, rodents and oxyaenid creodonts, all newcomers in PE I. However, it may not have been warm enough in Greenland to allow the primates, perissodactyls and artiodactyls to cross from Europe to North America or the peradectids and paromomyids to cross from North America to Europe until the PETM. Low sea-levels following the Th4-5 sequence boundary are likely to have played a major part in these events.

REFERENCES

- Butler R.F., Lindsey E.H. & Gingerich P.D. (1980) - Magnetic polarity stratigraphy and Paleocene-Eocene biostratigraphy of Polecat Bench, northwestern Wyoming. In: Gingerich P.D. (ed.), *Early Cenozoic Paleontology and Stratigraphy of the Bighorn Basin, Wyoming*. University of Michigan Papers on Paleontology, 24, 95-98.
- Ellison R.A., Ali J.R., Hine N.M. & Jolley D.W. (1996) - Recognition of Chron C25n in the upper Paleocene Upnor Formation of the London Basin, UK. In: Knox R.W.O'B., Corfield R.M. & Dunay R.E. (eds), *Correlation of the Early Paleogene in Northwest Europe*. Geological Society Special Publications, 101, 185-193.
- Grimes S.T., Yans J., Grassineau N., Bugler M., Steurbaut E. & Smith T. (2006) - The first stable isotope records from the Dormaal Sand Member and its earliest modern mammal fauna, Belgium. In: Caballero F., Apellaniz E., Baceta J.I., Bernaola G., Orue-Etxebarria X., Payros A. & Pujalte V. (eds), *Climate and Biota of the Early Paleogene 2006*. Volume of Abstracts, Bilbao, 55.
- Hooker J.J. (1996) - Mammalian biostratigraphy across the Paleocene-Eocene boundary in the Paris, London and Belgian basins. In: Knox R.W.O'B., Corfield R.M. & Dunay R.E. (eds), *Correlation of the Early Paleogene in Northwest Europe*. Geological Society Special Publications, 101, 205-218.
- Hooker J.J. & Collinson M.E. (2012) - Mammalian faunal turnover across the Paleocene-Eocene boundary in NW Europe: the roles of displacement, community evolution and environment. *Austrian Journal of Earth Sciences*, 105, 17-28.
- Hooker J.J. & Millbank C. (2001) - A Cernaysian mammal from the Upnor Formation (Late Paleocene, Herne Bay, UK) and its implications for correlation. *Proceedings of the Geologists' Association*, 125, 331-338.
- Laurain M. & Meyer R. (1986) - Stratigraphie et paléogéographie de la base du Paléogène champenois. *Géologie de la France*, 1986, 103-123.
- Nel A., Plöeg G. de, Dejoux J., Dutheil D., Franceschi D. de, Gheerbrant E., Godinot M., Hervet S., Menier J.-J., Augé M., Bignot G., Cavagnetto C., Duffaud S., Gaudant J., Hua S., Jossang A., Lapparent de Broin F. de, Pozzi J.-P., Paicheler J.-C., Beuchet F. & Rage J.-C. (1999) - Un gisement sparnacien exceptionnel à plantes, arthropodes et vertébrés (Éocène basal, MP7): Le Quesnoy (Oise, France). *Comptes Rendus hebdomadaires des Séances de l'Académie des Sciences, Paris (Sciences de la terre et des planètes)*, 329, 65-72.
- Smith T., Dupuis C., Folie A., Quesnel F., Storme J.-Y., Iacumin P., Riveline J., Missiaen P., Ladevèze S. & Yans J. (2011) - A new terrestrial vertebrate site just after the Paleocene-Eocene boundary in the Mortemer Formation of Upper Normandy, France. *Comptes Rendus Palevol*, 10, 11-20.
- Smith T., Quesnel F., Plöeg G. de, Franceschi D. de, Métais G., De Bast E., Solé F., Folie A., Boura A., Clause J., Dupuis C., Gagnaison C., Iakovleva A., Martin J., Maubert F., Prieur J., Roche E., Storme J.-Y., Thomas R., Tong H., Yans J. & Buffetaut E. (2014) - First Clarkforkian equivalent Land Mammal Age in the latest Paleocene basal Sparnacian facies of Europe: fauna, flora, palaeoenvironment and (bio)stratigraphy. *Plos One*, 9 (1), 1-19.

Seawater neodymium isotope record of Antarctic climate instability during the termination of the Early Eocene Greenhouse

Claire E. Huck ^(a), Tina van de Flierdt ^(a), Steven M. Bohaty ^(b) & Sam Hammond ^(c)

^(a) Imperial College London, London SW7 2AZ, UK. E-mail: c.huck10@imperial.ac.uk

^(b) Ocean and Earth Science, University of Southampton, Southampton SO14 3ZH, UK

^(c) The Open University, Walton Hall, Milton Keynes, MK7 6AA, UK

Document type: Short note.

Manuscript history: received 15 May 2014; accepted 30 May 2014; editorial responsibility and handling by Gerald R. Dickens & Valeria Luciani.

KEY WORDS: Antarctica, Early Eocene Climatic Optimum, Eocene, Neodymium, Oligocene, Southern Ocean.

The warmest climatic conditions of the entire Cenozoic occurred during the early Eocene—a time period that may provide important insight into the operation of the climate system under elevated atmospheric CO₂ levels. The termination of intense greenhouse conditions during the Early Eocene Climatic Optimum (EECO) at ~49 Ma, initiated a long-term decline in global temperatures, eventually leading to the abrupt development continental-scale glaciation on Antarctica at Eocene/Oligocene transition (EOT) (~34 Ma). Whether declining CO₂ levels (e.g., DeConto and Pollard, 2003) or thermal isolation of Antarctica due to the onset of circum-Antarctic circulation (e.g., Kennett, 1977) caused high-latitude cooling and ice-sheet expansion remains controversial. In order to better understand the relative roles of these forcing factors and mechanisms of Eocene climate change, it is necessary to further develop detailed paleoclimate records spanning the ‘cooling period’ between the early hyperthermal events and the EECO, and the rapid transition to full glaciation by the earliest Oligocene. Evidence from terrestrial (e.g., Contreras et al., 2013; Pross et al., 2012) and marine (e.g., Bijl et al., 2013) proxies indicate a much more variable climate during the early to mid-Eocene (~53 to 46 Ma) and provide insights into what may have preconditioned the Antarctic continent for the rapid change in environmental conditions that occurred at the EOT.

In this study, we present a new neodymium (Nd) isotope and rare earth element (REE) data set, extracted from fossil fish teeth and debris from seven Deep Sea Drilling Project (DSDP), Ocean Drilling Program (ODP), and Integrated Ocean Drilling Program (IODP) drill sites situated in the area around the Tasman Gateway in the Southern Ocean. We have targeted the early-to-middle Eocene interval (~53 to 45 Ma) at ODP Sites 1171 and 1172 (South Tasman Rise and East Tasman Plateau respectively), ODP Site 738 (Kerguelen Plateau), ODP Site 757 (Ninety East Ridge), DSDP Site 264 (Naturaliste Plateau) and DSDP Site 277 (Campbell Plateau), in conjunction with a longer term Eocene–Oligocene record

IODP Site U1356 (Wilkes Land margin of East Antarctica). The origin and robustness of the seawater signal preserved by the fossil fish teeth were examined using the REE data. Profiles from the four open ocean sites (277, 264, 757, 738) reveal negative cerium and positive yttrium anomalies, diagnostic of seawater origin, while the three margin sites (U1356, 1171, 1172) show features more characteristic of continental influence.

Compilation of Nd isotope records from our study sites reveals a number of important findings. Shallow sites on either side of the Tasman Gateway (ODP Site 1171 and IODP Site U1356) show a significant, transient excursion to more negative values between 49 and 48 Ma coincident with a recently proposed shallow opening of the Tasman Gateway (Bijl et al., 2013). Neodymium isotopic signatures of proximal shallow and deep-water masses in the southern Indian and Pacific are more positive than that observed at Site U1356, and increased influenced of either of these water masses cannot explain such an excursion. Analyses of bulk sediments at Sites 1171 and U1356, however, reveal that the respective on-land source regions are more negative than their seawater end members. These data combined with evidence for continental wide climate change at the end of the EECO (~49 Ma) suggest instead that a major perturbation to the hydrological cycle occurred at the termination of the EECO. Moreover, the cooling observed at the time we record our seawater Nd excursion may in fact be the result of a larger, previously undocumented climatic event originating on the Antarctic continent.

A study of the longer term seawater Nd isotopic composition at IODP Site U1356 shows that the average values do not change from the Eocene to the Oligocene, and are similar to modern-day bottom water in the Australo-Antarctic Basin and on the shelf off Adélie Land where bottom water formation takes place (e.g. van de Flierdt et al., 2006). Additionally, DSDP Site 277, located in the southwest Pacific Ocean, records Nd compositions that are also similar to modern values found at the same depth (~2000 m) in the Ross Sea (e.g., Rickli et al., 2014), pointing to active deep-water formation on the Antarctic margin. We therefore interpret

deep/bottom-water production in the Southern Ocean on the Antarctic shelves (i.e. off Adélie Land and in the Ross Sea) throughout the Eocene and Oligocene.

In summary, our data provide the first multi-site evidence of a large scale perturbation to the hydrological cycle on the Antarctic continent coinciding with the termination of the EECO. Our datasets also provide a new survey of Eocene seawater Nd end members in the Southern Ocean, which indicate active deep-water formation in the Southern Ocean during the Paleogene.

REFERENCES

- Bijl P.K., Bendle J.A., Bohaty S.M., Pross J., Schouten S., Tauxe L., Stickley C.E., Mckay R.M., Röhl U. & Olney M. (2013) - Eocene cooling linked to early flow across the Tasmanian gateway. *P. Natl. Acad. Sci. USA*, 110, 9645-9650.
- Contreras L., Pross J., Bijl P.K., Koutsodendris A., Raine J.I., van De Schootbrugge B. & Brinkhuis H. (2013) - Early to middle Eocene vegetation dynamics at the Wilkes Land margin (Antarctica). *Rev. Paleobot. Palynol.*, 197, 119-142.
- Deconto R.M. & Pollard D. (2003) - Rapid cenozoic glaciation of Antarctica induced by declining atmospheric CO₂. *Nature*, 421, 245-249.
- Kennett J.P. (1977) - Cenozoic evolution of Antarctic glaciation, circum-antarctic ocean, and their impact on global paleoceanography. *J. Geophys. Res. - Oc. Atm.*, 82, 3843-3860.
- Pross J., Contreras L., Bijl P.K., Greenwood D.R., Bohaty S.M., Schouten S., Bendle J.A., Röhl U., Tauxe L. & Raine J.I. (2012) - Persistent near-tropical warmth on the Antarctic continent during the early Eocene epoch. *Nature*, 488, 73-77.
- Rickli J., Gutjahr M., Vance D., Fischer-Gödde M., Hillenbrand C.-D. & Kuhn G. (2014) - Neodymium and hafnium boundary contributions to seawater along the West Antarctic continental margin. *Earth Planet. Sci. Lett.*, 394, 99-110.
- van De Flierdt T., Hemming S.R., Goldstein S.L. & Abouchami W. (2006) - Radiogenic isotope fingerprint of Wilkes Land-Adélie Coast bottom water in the circum-Antarctic ocean. *Geophys. Res. Lett.*, 33, L12606.

Resolving Eocene time and palaeoceanography in exceptional detail: an update on IODP Expedition 342, Newfoundland Ridge

Pincelli M. Hull^(a), Philip F. Sexton^(b), Richard D. Norris^(c), Paul A. Wilson^(d), Peter Blum^(e), Claudia Agnini^(f), Slah Boulila^(g), Paul R. Bown^(h), Helen Coxall⁽ⁱ⁾, Oliver Friedrich^(j), Rosanna Greenop^(k), Sandra Kirtland Turner^(l), Wendy E. C. Kordesch^(m), Diederik Liebrand⁽ⁿ⁾, Hiroki Matsui^(o), Kazuyoshi Moriya^(p), Hiroshi Nishi^(q), Bradley N. Opdyke^(r), Heiko Pälike^(s), Donald Penman^(t), Ursula Röhl^(u), Richard Smith^(v), Thomas Westerhold^(w), Yuhji Yamamoto^(x) & James C. Zachos^(y)

^(a) Department of Geology and Geophysics, Yale University, PO Box 208109, New Haven, CT, 06511, USA. E-mail: pincelli.hull@yale.edu

^(b) Department of Earth Sciences, The Open University, Milton Keynes, MK7 6AA, UK

^(c) Scripps Institution of Oceanography, University of California, San Diego, 9500 Gilman Drive, La Jolla, CA, 92093-0244, USA

^(d) School of Ocean & Earth Science, National Oceanography Centre, University of Southampton, European Way, Southampton, SO14 3ZH, UK

^(e) United States Implementing Organization, Integrated Ocean Drilling Program, Texas A&M University, 1000 Discovery Drive, College Station, TX, 77845, USA

^(f) Department of Geological Sciences, Stockholm University, Stockholm, SE-106 91, Sweden

^(g) Institut des Sciences de la Terre a Paris, Université Pierre et Marie Curie, 4 Place Jussieu, Paris, 75252, France

^(h) Department of Earth Sciences, University of College London, Gower Street, London, WC1E 6BT, UK

⁽ⁱ⁾ Institute of Earth Sciences, Ruprecht-Karls-Universität Heidelberg, Im Neuenheimer Feld 234, Heidelberg, D-69120, Germany

^(j) School of Earth Sciences, University of Bristol, University Road, Clifton, Bristol, BS8 1RJ, UK

^(k) Graduate School of Science, Tohoku University, Aramaki Aza Aoba 6-3, Aobaku, Sendai 980-8578, Japan

^(l) Department of Earth Sciences, Waseda University, 1-6-1 Nishiwaseda, Shinjuku-ku, Tokyo 169-8050, Japan

^(m) Center for Academic Resources and Archives, Tohoku University, Aramaki Aza Aoba 6-3, Aobaku, Sendai 980-8578, Japan

⁽ⁿ⁾ Department of Geology, Australian National University, Canberra, ACT 0200, Australia

^(o) MARUM Center for Marine Environmental Sciences, Universität Bremen, Leobener Str. D-28359 Bremen, Germany

^(p) Department of Earth and Planetary Sciences, University of California, Santa Cruz, CA, 95064, USA

^(q) Marine and Core Research Center, Kochi University, 8200 Monobe Nankoku-City, Kochi 783-8505, Japan

Document type: Short note.

Manuscript history: received 15 May 2014; accepted 30 May 2014; editorial responsibility and handling by Gerald R. Dickens & Valeria Luciani.

KEY WORDS: CCD, Eocene, cyclostratigraphy, Exp 342, hyperthermal, IODP, North Atlantic, palaeoceanography, time scale.

The Eocene greenhouse is a beguiling interval for those seeking to understand climate and carbon cycle processes in high atmospheric CO₂ worlds. In addition to higher-than-modern pCO₂, the Eocene features long-term shifts in boundary conditions, including secular cooling and the opening of oceanic gateways, and short-term perturbations, like hyperthermals and carbonate accumulation events (Zachos et al., 2008). In spite of much interest, there remain critical gaps in our understanding of these dynamics, in part because we lack a key tool –namely, a well constrained, anchored, astronomical time scale (Pälike and Hilgen, 2008). Accurate age models are central to investigations of Earth system dynamics as they provide the necessary framework for establishing the timing and spatial extent of events (e.g., Pälike and Hilgen, 2008; Westerhold et al., 2012; Expedition 342 Scientists 2012).

In the summer of 2012, Integrated Ocean Drilling Program (IODP) Expedition 342 set sail to the J-Anomaly and Newfoundland Ridges under Co-Chief Scientists Richard Norris and Paul Wilson and Staff Scientist Peter Blum with the hope of plugging this major gap in the Cenozoic astronomically calibrated timescale (Norris et al., 2011). In targeting the northern North Atlantic, the expedition also aimed to detail the palaeoceanographic history of a climatically

critical region. Palaeoceanographic targets of particular interest included reconstructing the carbonate saturation state of the northern North Atlantic, detailing the events leading up to and across the onset of Antarctic glaciation, and constraining hypotheses on the origin of Eocene hyperthermals and carbon cycle dynamics.

Expedition 342 was spectacularly successful in these aims, recovering expanded sections with often glassy foraminiferal preservation (Norris et al., 2014). The J-Anomaly and Newfoundland Ridges lie in the flow path of North Atlantic deep-water. As a result, the region is peppered with sediment drifts –or, contourites– built up as sediment swept from one region are deposited in the next. Many of the massive drifts in this corner of the North Atlantic are Plio-Pleistocene in age. Rarer are the older, acoustically transparent, plastered drifts drilled by Expedition 342, which range from Early-Middle Eocene to Miocene in age. Newfoundland drift formation appears to have begun in the early Middle Eocene (~47 Ma) (Norris et al., 2014). This timing coincides with the onset of drift formation in the northern Greenland-Scotland Ridge, Labrador Sea, and Northeast Atlantic and in the southern Blake, Hatteras, and Chesapeake drifts and the inferred spin up of earth North Atlantic deep-water formation (Mountain and Tucholke, 1985; Arthur et al., 1989; Hohbein et al., 2012; Norris et al., 2014). In Newfoundland sediments, the onset of drift formation brings a many fold (from <1 cm/kyr to ~2-10 cm/kyr) increase in sedimentation rates, a lithological

change from predominately oozes to predominantly nannofossil clays, a marked improvement in carbonate preservation, and the eventual loss of radiolarians from Eocene coarse fractions (Expedition 342 Scientists, 2012; Norris et al., 2014).

Over two kilometers of Eocene aged sediment were recovered from eight sites: U1403, U1407, U1408, U1409, U1408, U1409, U1410, and U1411 (Expedition 342 Scientists, 2012). Shipboard bio- and magneto-stratigraphy indicated that that, when spliced across sites, Expedition 342 cores spanned from the Palaeocene-Eocene Thermal Maximum continuously to and across the Eocene-Oligocene boundary (Norris et al. 2014). Key events like the Eocene Oligocene Transition (EOT), the Middle-Eocene Climatic Optimum (MECO), and carbonate accumulation events are recorded in rapidly accumulating sediments (~2-10 cm/kyr) with semi-glassy to glassy preservation throughout. Crucially, the expedition recovered complete sections across the notorious Eocene Gap – a middle Eocene interval typically characterized by hiatuses (Pälike and Hilgen 2008). In spanning the gap in four sites, these sediments provide a means to anchor floating early Palaeogene age models into a fixed Cenozoic time scale.

The construction of astronomical age models depends on resolving orbital cycles in sediments. To this end, the finding of significant cyclicity in orbital frequencies during the Middle Eocene using shipboard age models and measurements of color reflectance, is promising indeed. Eocene cores from Expedition 342 have subsequently been scanned with elemental-scanning techniques (i.e., X-ray fluorescence [XRF] core scanning) at the Bremen Core Repository at MARUM, the Gulf Coast Repository, and the Geological Collections at Scripps Institution of Oceanography through a massive coordinated effort. Fe and other elements have confirmed and improved shipboard splices and the presence of pronounced orbital cyclicity. With scanning efforts nearly complete, these records can now be used to derive an orbital age model.

An Expedition 342 megasplice was constructed shipboard from three primary sites –U1406, U1408, and U1409– in order to generate the first, highly resolved, single location benthic isotope record for the Eocene. For palaeoceanographic inference, single locale, benthic foraminiferal isotopic records are the gold standard, as they avoid problems of multisite comparisons including offsets in the isotopic composition of bottom waters and unrecognized time gaps. In addition, the often spectacular preservation and expanded sections offer the opportunity to directly track palaeoceanographic evolution from early Eocene warmth and hyperthermals across the oceanographic reorganization of the Early-Middle transition and through the long term cooling and Middle to Late Eocene dynamics. To generate a continuous, highly resolved benthic isotopic record, a consortium was formed to sample, process, and analyze the more than 8,000 samples spanning the 22-million years of the Eocene megasplice at a resolution of 2-5 thousand years.

Here we provide an update on the progress and discoveries to date from these Eocene cores, highlighting early results from across the consortia. With kilometers of cores XRF scanned,

>3500 samples washed, and ~400 stable isotopic measurements made, we are now in the position to present a first glimpse of what the exceptional Eocene resolution might bring. In particular, we will discuss early results on long-term trends in carbonate accumulation, lithology, % coarse fraction, and orbital cyclicity; key transitions like the Early-Middle transition; and perturbations including evidence for North Atlantic carbonate accumulation events.

REFERENCES

- Arthur M.A., Srivastava S.P., Kaminski M., Jarrard R. & Osler J. (1989) - Seismic stratigraphy and history of deep circulation and sediment drift development in Baffin Bay and the Labrador Sea. In Srivastava S.P., Arthur M.A., Clement B., et al. (eds.). Proc. ODP, Sci. Results, 105. Ocean Drilling Program, 957–988. doi:10.2973/odp.proc.sr.105.118.1989
- Hohbein M.W., Sexton P.F. & Cartwright J.A. (2012) - Onset of North Atlantic Deep Water production coincident with inception of the Cenozoic global cooling trend, *Geology*, 40, 255-258. doi: 10.1130/G32461.1
- Mountain G.S. & Tucholke B.E. (1985) - Mesozoic and Cenozoic geology of the U.S. Atlantic continental slope and rise. In Poag C.W. (Ed.), *Geologic Evolution of the United States Atlantic Margin*. Van Nostrand Reinhold, 293–341.
- Norris R.D., Wilson P.A. & Blum, P. (2011) - Paleogene Newfoundland sediment drifts. *IODP Sci. Prosp.*, 342. doi:10.2204/iodp.sp.342.2011
- Norris R.D., Wilson P.A., Blum P., Fehr A., Agnini C., Bornemann A., Boulila S., Bown P.R., Cournede C., Friedrich O., Kumar Ghosh A., Hollis C.J., Hull P.M., Jo K., Junium C.K., Kaneko M., Liebrand D., Lippert P.C., Liu Z., Matsui H., Moriya K., Nishi H., Opdyke B.N., Penman D.E., Romans B., Scher H.D., Sexton, P.H., Takagi H., Kirtland Turner S., Whiteside J.H., Yamaguchi T. & Yamamoto Y. (2012) - Paleogene Newfoundland sediment drifts. *IODP Prel. Rept.*, 342. doi:10.2204/iodp.pr.342.2012.
- Norris R.D., Wilson P.A., Blum P., Fehr A., Agnini C., Bornemann A., Boulila S., Bown P.R., Cournede C., Friedrich O., Ghosh A.K., Hollis C.J., Hull P.M., Jo K., Junium C.K., Kaneko M., Liebrand D., Lippert P.C., Liu Z., Matsui H., Moriya K., Nishi H., Opdyke B.N., Penman D.E., Romans B., Scher H.D., Sexton P.H., Takagi H., Kirtland Turner, S.K., Whiteside J.H., Yamaguchi T. & Yamamoto Y. (2014) - Proc. IODP, 342: College Station, TX (Integrated Ocean Drilling Program). doi: 10.2204/iodp.proc.342.2014
- Pälike H. & Hilgen F. (2008) - Rock clock synchronization. *Nature Geosci.*, 1, 282-282. doi: 10.1038/Ngeo197.
- Westerhold T., Röhl U. & Laskar J. (2012) -Time scale controversy: Accurate orbital calibration of the early Paleogene. *Geochem. Geophys. Geosyst.*, 13, Q06015, doi:10.1029/2012GC004096.
- Zachos J.C., Dickens G.R. & Zeebe R.E. (2008) - An early Cenozoic perspective on greenhouse warming and carbon-cycle dynamics. *Nature*, 451, 279-283. doi: 10.1038/Nature06588.

Rejuvenating the Paris Basin stratigraphy using “lost” drillings: the $\delta^{13}\text{C}_{\text{org}}$ calibration of Upper Thanetian to Lower Ypresian dinocyst events succession

Alina I. Iakovleva ^(a), Florence Quesnel ^(b,c), Christine Fléhoc ^(d) & Christian Dupuis ^(e)

^(a) Geological Institute, Russian Academy of Sciences, Pyzhevsky pereulok 7, 119017 Moscow, Russia. E-mail: alina.iakovleva@gmail.com

^(b) BRGM (French Geological Survey), Georesources Division, Land Use Geology Unit, 3, Avenue Cl. Guillemin, 45060 Orléans Cedex 2, France

^(c) UMR 7327 of the CNRS/INSU, Orléans University & BRGM, 1A, rue de la Férollerie, 45071 Orléans, France

^(d) BRGM (French Geological Survey), Laboratory Division, Isotopes Unit, 3, Avenue Cl. Guillemin, 45060 Orléans Cedex 2, France

^(e) Geology and Applied Geology, Faculty of Engineering, University of Mons, 20, Place du Parc, 7000 Mons, Belgium

Document type: Short note.

Manuscript history: received 15 May 2014; accepted 30 May 2014; editorial responsibility and handling by Gerald R. Dickens & Valeria Luciani.

KEY WORDS: *Apectodinium*-acme, CIE, $\delta^{13}\text{C}_{\text{org}}$, dinocysts, Paris Basin, PETM, “Sparnacian”, stratigraphy, Thanetian, Ypresian.

The Paris Basin represents an historical cradle of the Paleogene stratigraphy, where the notion of “Sparnacian” took shape in the Nineteenth century (Dollfus, 1880). Whereas Aubry et al. (2005) pointed on that the chronostratigraphic connotation of the “Sparnacian Stage”, sandwiched between the Thanetian and “Cuisian” marine sands, occurred to be controversial since its initial definition, modern studies of the Late Paleocene-Early Eocene interval revealed that the so-called “Sparnacian” deposits are not only often associated with the Paleocene-Eocene Thermal Maximum (PETM), but they are also diachronous across the Paris Basin. Hence the Sparnacian succession, represented by diverse and laterally variable, predominantly lagoonal and non-marine facies, is still insufficiently documented and needs an updated chronostratigraphic correlation with other Paleogene records worldwide. Although dinoflagellate cysts have been studied there since over 45 years (Châteauneuf & Gruas-Cavagnetto, 1968, 1978; Costa and Downie, 1976), no updated and revised dinoflagellate cysts distribution data are available yet, nor calibrated to more recent zonations (Powel et al., 1996) and to carbon isotope data.

Focusing on the high-resolution study of the “Sparnacian” deposits and their relationship with the PETM and its CIE events and processes, a number of new as well as some old drillings have been investigated in details palynologically and chemostratigraphically. The most expanded record of the Late Thanetian to Early Ypresian (*sensu* GTS 2012) here presented, including the Sparnacian facies, is preserved in the central part of the Paris Basin and has been deciphered thanks to the study of discrete samples of old drillings whose cores were lost: Le Tillet and Cuise-La-Motte.

In the Le Tillet core, $\delta^{13}\text{C}_{\text{org}}$ values fluctuate between -23 and -26‰ PDB in the Châlons-sur-Vesles and Bracheux Fms and lower part of the Mortemer Fm; they exhibit three maxima, the most positive one occurring in the lowest second half of the Le Tillet Sand Mb, which is more shelly and was deposited in

shallower marine conditions. From this maximum at -23‰ PDB, an upward regressive trend is recorded until estuarine followed by terrestrial lignitic sands (Rivecourt Sand Mb) characterized also by upward decreasing $\delta^{13}\text{C}_{\text{org}}$ values that reach -25.5 to -26.5‰ PDB.

According to our data, two successive NW European dinocyst zones of Thanetian age are recognized within the Châlons-sur-Vesles Fm (Le Tillet Sand Mb) from Le Tillet and Cuise La Motte cores: *Alisocysta margarita* and *Apectodinium hyperacanthum*. Dinocyst assemblages from the uppermost Thanetian (Bracheux Fm) may contain up to 30% of *Apectodinium* spp.

Above a terrestrial interval where the CIE onset is not clearly delineated in the top of Mortemer Fm or basal Soissonnais Fm from the Le Tillet core yet, the Muirancourt and Vauxbuin Mbs (Soissonnais Fm) reveal the most negative $\delta^{13}\text{C}_{\text{org}}$ values (-27 to -28‰ PDB). The part of the CIE interval present in the lagoonal units of the Soissonnais Fm shows also an extremely pronounced *Apectodinium* acme (65-98% of dinocyst assemblage), while it is less pronounced in the more open marine units of the Dieppe-Hampshire Basin, for example in the Sotteville-sur-Mer, Cap d’Ailly and Siège-Madame drillings (Iakovleva, unpublished). The PETM assemblages are characterized by a significant number of longer specimens of *Apectodinium parvum*, which could represent an ecological onshore substitute of species *Apectodinium augustum* in the Paris and Dieppe-Hampshire Basins. The uppermost part of the Sparnacian facies included in the CIE interval reveals a number of unusual Wetzelielloids previously known from the *Apectodinium augustum* Zone interval in the Turgay Passage (Iakovleva, unpublished).

The lowermost unit (postdating the PETM) of the Mont Notre Dame Fm (Sinceny Mb) in the Paris Basin contains a very distinctive dinocyst assemblages, characterized by *Biconidinium longissimum* acme combined with still abundant *Apectodinium* (up to 50%). Unknown from adjacent Belgian, London or Dieppe-Hampshire Basins, the *Biconidinium longissimum* acme event has now been recognized in a number of sites; it may reflect a local and extremely specific environment in the Paris Basin, and appears to be a possible

stratigraphic equivalent of the North Sea Basin *Glaphyrocysta ordinata* or *Deflandrea oebisfeldensis* Zones (Early Ypresian *sensu* GTS 2012). As in the Sinceny drilling (Quesnel et al., 2011) this interval is characterized by very homogeneous $\delta^{13}\text{C}_{\text{org}}$ values between -24 and -25‰ PDB in the Le Tillet core.

Overlying the Sinceny Mb in that core, the Laon Sand Mb exhibits more negative $\delta^{13}\text{C}_{\text{org}}$ values calibrated with the occurrence of *Wetzeliella astra/lobisca*. The overlying Cuise Sand Fm can be attributed to the *W. meckelfeldensis* Zone, as shown previously also by Châteauneuf and Gruas-Cavagnetto (1978). It exhibits constant then decreasing $\delta^{13}\text{C}_{\text{org}}$ values in the 'Sables d'Aizy', reaching a minimum at -27‰ PDB during an interval of 10 m, suggesting the record of the lower part of the EECO (or ETM2?) at the top of the 'Sables d'Aizy' and notably in the 'Horizon de Pierrefonds', just before a new upward increasing trend of the $\delta^{13}\text{C}_{\text{org}}$ values in the 'Argile de Laon' which belongs to the *Dracodinium varielongitudinum* Zone interval.

Our new isotopic data obtained from the Le Tillet core's discrete samples spanning 90 m of the Upper Thanetian to Lower Ypresian succession (including Sparnacian facies) delineate a curve comparable to the one compiled by Cramer et al. (2009) and reported in the GTS 2012. The data are then integrated to the other ones obtained with a higher resolution but lesser stratigraphic interval during the last years from the Paris and Belgian Basins, the Avesnois, and the eastern part of the Dieppe-Hampshire Basin; all of them enable to refine the high-resolution stratigraphic frame built from new drillings or exposures (Dupuis et al., 2011; Quesnel et al., 2011; Iakovleva et al., 2013; and unpublished data). Our study is the first attempt to make a first-order calibration between dinocyst and isotopic data from that interval (NP8 to NP12) in the shallow marine to lagoonal settings of the Paris and Dieppe-Hampshire Basins. It should be enlarged to similar depositional environments of the adjacent basins in order to provide high resolution bio- and chemo- stratigraphic frames, and then to correlate to the Arctic, North Sea and Atlantic records within deeper marine realms, the final objective being to decipher and compare in various and connected terrestrial to marine settings the impacts of the climatic events (among which a few hyperthermals) of the Early Paleogene, a critical episode of the Earth's history.

REFERENCES

- Aubry M.P., Thiry M., Dupuis Ch. & Berggren W.A. (2005) – The Sparnacian deposits of the Paris Basin: A lithostratigraphic classification. *Stratigraphy*, 2 (1), 65-100.
- Châteauneuf J.J. & Gruas-Cavagnetto C. (1968) – Etude palynologique du Paléogène de quatre sondages du bassin parisien (Chaignes, Montjavoult, Le Tillet, Ludes). *Mémoire du Bureau de Recherches Géologiques et Minières*, 59, 16-19.
- Châteauneuf J.J. & Gruas-Cavagnetto C. (1978) – Les zones de Wetzeliellaceae (Dinophyceae) du bassin de Paris. Comparaison et corrélations avec les zones du Paléogène des bassins du Nord-Ouest de l'Europe. *Mémoire du Bureau de Recherches Géologiques et Minières*, section 4 (2), 59-93.
- Costa L.I. & Downie C. (1976) – The distribution of the dinoflagellate *Wetzeliella* in the Paleocene of North-Western Europe. *Palaeontology*, 19, 591-614.
- Cramer B.S., Toggweiler J.R., Wright J.D., Katz M.E. & Miller K.G. (2009) – Ocean overturning since the Late Cretaceous: Inferences from a new benthic foraminiferal isotope compilation. *Paleoceanography*, 24, PA4216. Doi: 10.1029/2008PA001683
- Dollfus G. (1880) – Essai sur l'extension des terrains tertiaires dans le Bassin anglo-parisien. *Bulletin de la Société géologique de Normandie*, VI, 584-605.
- Dupuis Ch., Quesnel F., Iakovleva A.I., Storme J.Y., Yans J. & Magioncalda R. (2011) – Sea level changes in the Paleocene-Eocene interval in NW France: Evidence of two major drops encompassing the PETM. In: Egger H. (Ed.), *Climate and Biota of the Early Paleogene*, Conference Program and Abstracts, 5-8 June 2011, Salzburg, Austria. *Berichte der Geologischen Bundesanstalt*, 85, 68.
- Iakovleva A.I., Quesnel F., Dupuis Ch., Storme J.Y., Breillat N., Magioncalda R., Iacumin P., Flehoc Ch., Roche E., Smith Th., Baele J.M., Yans J. & De Coninck J. (2013) – New integrated high-resolution dinoflagellate cyst, litho- and chemo- stratigraphy from the Paris and Dieppe-Hampshire Basins «Sparnacian». *Ciências da Terra*, Volume Especial VII, International Congress on Stratigraphy, 1-7 July 2013, 22-23.
- Powell A.J., Brinkhuis H. & Bujak J.P. (1996) – Upper Paleocene – Lower Eocene dinoflagellate cyst sequence biostratigraphy of southeast England. In: KNOX R.W.O.B., CORFIELD R.M. & DUNAY R.S. (Eds.), *Correlation of the Early Paleogene in Northwest Europe*. Geological Society Special Publication 101, 145-183.
- Quesnel F., Storme J.Y., Iakovleva A.I., Roche E., Breillat N., André M., Baele J.M., Schnyder J., Yans J. & Dupuis Ch. (2011) – Unravelling the PETM record in the «Sparnacian» of NW Europe: new data from Sinceny, Paris Basin, France. In: Egger H. (ed.), *Climate and Biota of the Early Paleogene*, Conference Program and Abstracts, 5-8 June 2011, Salzburg, Austria. *Berichte der Geologischen Bundesanstalt*, 85, 135.

Expansion of Neotropical Forests during Paleogene Global Warming

Carlos Jaramillo ^(a) & Andres Cardenas ^(a)

^(a) Smithsonian Tropical Research Institute, Panamá. E-mail: jaramilloc@si.edu

Document type: Abstract.

Manuscript history: received 15 May 2014; accepted 30 May 2014; editorial responsibility and handling by Gerald R. Dickens & Valeria Luciani.

KEY WORDS: Amazonia, biome, Paleogene, plants.

There is concern over the future of the tropical rainforest (TRF) in the face of global warming. Will TRFs collapse? Expand? The fossil record can inform us about that.

Our compilation of 5,998 empirical estimates of temperature over the past 120 Ma indicates that tropics have warmed as much as 7°C during both the mid-Cretaceous and 3-5°C during the Paleogene. Empirical tropical temperatures are still much lower than those estimated from most paleoclimate modeling.

We analyzed the paleobotanical record (both pollen/spores and macrofossils) of South America during warming events of the Paleogene and found that:

1) TRF increased diversity and biomass as opposite to collapsing as it has been predicted before, suggesting that increases in temperature drives up origination rates. The actual mechanism linking temperature and origination is still unknown but we suggest that a rise in temperature would increase metabolic and growth rates as well as the degree of biotic interactions. Given that selection in warm environments is largely driven by biotic interactions, and that biotic interactions are stronger in a warmer climate, the shifting selective landscape may promote speciation by creating a more

intense search for a phenotypic optimum, therefore, enhancing origination. This process could also be enhanced by higher rates of molecular evolution that in turn provides the source of genetic novelties needed to increase rates of speciation;

2) TRF did not expand towards temperate latitudes of South America even though temperatures were appropriate for doing so, suggesting that solar insolation can be a strong constraint on the distribution of the tropical biome. Rather, a novel biome adapted to temperate latitudes with warm winters, developed south of the tropical zone. Only relicts of this biome remain in insolated areas of Chile nowadays. Previous models had assumed that TRF would expand towards higher latitudes reaching even the southern tip of South America. Empirical data show that this is not the case.

We also found a widespread use of the term "paratropical rainforest" in the literature. However, this term has been used to name a wide variety of biomes very different to the original meaning proposed by Wolfe in 1979 that defined "paratropical" as a biome with rainforest-like physiognomic characteristics and a closed multistratified canopy. We encourage the abandonment of this term.

We think identifying truly TRF in the fossil record is important because TRF has a unique set of physiognomic, nutrient, and biomass characteristics that strongly modify local and regional climate, and therefore may have a significant influence on modeled climate simulations.

Paleoceanographic reconstruction of the Latest Danian Event at ODP Site 1210 (Shatsky Rise, Pacific Ocean)

Sofie Jehle ^(a), André Bornemann ^(a,c), Arne Deprez ^(b) & Robert P. Speijer ^(b)

^(a) Institut für Geophysik und Geologie, Universität Leipzig, Talstr 35, 04103 Leipzig, Germany. Corresponding author: sofie.jehle@uni-leipzig.de

^(b) Department of Earth and Environmental Sciences, KU Leuven, Celestijnenlaan 200E, 3001 Heverlee, Belgium

^(c) Bundesanstalt für Geowissenschaften und Rohstoffe, Stilleweg 2, 30655 Hannover, Germany

Document type: Abstract.

Manuscript history: received 15 May 2014; accepted 30 May 2014; editorial responsibility and handling by Gerald R. Dickens & Valeria Luciani.

KEY WORDS: Latest Danian Event, Pacific Ocean, planktic foraminifera assemblage, Shatsky Rise Site 1210, stable isotopes

During the Paleocene the marine ecosystem was disturbed by several transient climate events, e.g. the Dan-C-2 (65.2 Ma), the Latest Danian Event (LDE, 61.75 Ma), the Early Late Paleocene Event (ELPE 58.9 Ma) and, most intensely studied, the Paleocene-Eocene Thermal Maximum (PETM, 56 Ma). So far the LDE (or “Top Chron 27n Event” according to Westerhold et al., 2011) has rarely been studied in the deep-sea and with respect to planktic foraminifera. The event is known from Zumaia/Spain, Bjala/Bulgaria, Egypt, Shatsky Rise and Walvis Ridge (e.g. Bornemann et al., 2009; Westerhold et al., 2011).

In deep-sea cores the LDE is usually characterized by two distinctive Fe peaks in XRF core scanning data, paralleled by high levels in magnetic susceptibility, and a prominent (~0.7 ‰) negative $\delta^{13}\text{C}$ excursion (CIE) in benthic foraminifera (Westerhold et al., 2008; 2011). Benthic foraminiferal $\delta^{18}\text{O}$ data from ODP Site 1209 suggest a bottom-water temperature rise of ~2°C accompanying the negative CIE. Thus, the LDE has been considered as a further potential Paleocene “hyperthermal”.

ODP Site 1210 at Shatsky Rise covers most of the Paleocene. Here we present new data of the biotic response (planktic foraminifera assemblages), carbonate preservation as well as $\delta^{18}\text{O}$ and $\delta^{13}\text{C}$ isotope signals of the surface, subsurface and benthic foraminifera covering a time span of about 800 kyr around the LDE.

Trends of both $\delta^{18}\text{O}$ and $\delta^{13}\text{C}$ of planktic and benthic foraminifera show negative shifts at the onset of the LDE. A 0.6 ‰ decrease within 100 ky in planktic oxygen isotope data suggest a temperature rise of ~3 to 3.5°C, whereas benthic foraminifera bottom water temperatures confirm a ~2°C rise from Site 1209. $\delta^{13}\text{C}$ changes are more abrupt and pronounced than $\delta^{18}\text{O}$ changes at the base of the LDE. Dissolution according to planktic foraminiferal fragmentation, P/B-ratios and coarse fraction can be considered to be minor during the LDE, but worsen of preservation has been observed about 300

kyr before and 350 kyr after the main event peak. This observation is consistent with a decrease in the total carbonate record, which drops by 10% from ~95%, while planktic foraminifera suffer a strong decrease in abundance. Planktic foraminiferal fauna shows distinct changes during the onset of the LDE, especially *Praemurica* spp., which disappear shortly before the event, whereas *Igorina albeari* increases from ‘few’ to ‘abundant’ within the first Fe LDE peak. *Morozovella angulata* follows a slow but constant rise, while *Morozovella praeangulata* shows the opposite pattern. Further, a $\delta^{13}\text{C}$ - $\delta^{18}\text{O}$ biplot shows distinct clusters of selected Paleocene benthic and planktic species, representing clearly different depth habitats.

REFERENCES

- Bornemann A., Schulte P., Sprong J., Steurbaut E., Youssef M., Speijer R.P. (2009) - Latest Danian carbon isotope anomaly and associated environmental change in the southern Tethys (Nile Basin, Egypt). *J. Geol. Soc. London*, 166, 1135-1142.
- Dinarès-Turell J., Pujalte V., Stoykova K., Baceta J.I. & Ivanov, M. (2012) - The Palaeocene “top chron C27n” transient greenhouse episode: evidence from marine pelagic Atlantic and peri-Tethyan sections. *Terra Nova* 24 (6), 477-486.
- Speijer R.P. 2003 - Danian–Selandian sea-level change and biotic excursion on the southern Tethyan margin (Egypt). In: Wing, S.L., Gingerich, P.D., Schmitz, B. & Thomas, E. (eds.) *Causes and Consequences of globally warm climates in the Early Paleogene*. Geological Society of America, Special Papers, 369, 275–290.
- Westerhold T., Röhl U., Raffi I., Fornaciari E., Monechi S., Reale V., Bowles J., Evans H.F. (2008) - Astronomical calibration of the Paleocene time. *Palaeogeogr. Palaeoclimatol. Palaeoecol.* 257, 377-403.
- Westerhold T., Röhl U., Donner B., McCarren H.K., Zachos J.C., 2011. A complete high-resolution Paleocene benthic stable isotope record for the central Pacific (ODP Site 1209). *Paleoceanography*, 26, PA2216.

Eocene Thermal Maximum 2: benthic ecosystems and ocean circulation in the SE Atlantic Ocean

Suzanne M. Jennions ^(a), Ellen Thomas ^(b,c), Daniela N. Schmidt ^(a), Andy Ridgwell ^(d) & Daniel J. Lunt ^(d)

^(a) School of Earth Sciences, University of Bristol, Bristol, BS8 1RJ, UK. E-mail: Suzanne.Jennions@bristol.ac.uk

^(b) Department of Geology and Geophysics, Yale University, New Haven, CT 06511, USA

^(c) Department of Earth & Environmental Sciences, Wesleyan University, Middletown, CT 06459, USA

^(d) School of Geographical Sciences, University of Bristol, Bristol, BS8 1SS, UK

Document type: Short note.

Manuscript history: received 15 May 2014; accepted 30 May 2014; editorial responsibility and handling by Gerald R. Dickens & Valeria Luciani.

KEY WORDS: benthic foraminifera, Eocene, hyperthermals, ocean circulation.

Anthropogenic carbon dioxide released into the ocean-atmosphere system is rapidly perturbing the global climate and carbon cycle with potential impacts including warming, increased intensity of the hydrological cycle and nutrient influx in the oceans, increased ocean stratification and decreased pelagic productivity, ocean acidification and increased hypoxia (e.g., Reid et al., 2009). Anticipating the short- and long-term response of species and ecosystems to multiple, potentially synergistic environmental parameters is challenging (Norris et al., 2013). Records of periods of past climate change may provide a detailed, quantifiable account of the biotic response to such changes (e.g., Hönisch et al., 2012). A series of global warming - carbon release events ('hyperthermals') super-imposed upon gradually rising global temperatures during the early Palaeogene (Thomas et al., 2002) make it possible to compare events of varying duration and amplitude, in order to assess ecosystem resilience, threshold effects, and differential impact on organisms. Eocene Thermal Maximum 2 (ETM2) occurred ~1.8 Myr after the Paleocene Eocene Thermal Maximum (PETM), and was, like the PETM, characterized by a prominent negative carbon isotope excursion (CIE) coupled with global warming and ocean acidification (Lourens et al., 2005). The PETM was linked to severe deep-sea benthic extinction, but little is known about benthic ecosystems during ETM2. We combined benthic foraminiferal and sedimentary records (CaCO₃%, accumulation rates, fragmentation) with published stable isotope data (Stap et al., 2009) for Southeast Atlantic (Walvis Ridge) Sites 1263 (1500 m paleodepth) and 1262 (3500 m paleodepth).

We conclude that ETM2 can be divided into three parts: a similar start and recovery period (0-40 and 55-100 ka), separated by an interval of peak warming (40-55 ka). Sedimentary records during the start and recovery intervals show the expected pattern of more severe dissolution and planktic foraminiferal fragmentation at the deeper site, but during the peak event, in contrast, dissolution was similar at both sites, suggesting that the lysocline shoaled independently of the CCD in response to ocean acidification. There were

more extreme negative excursions in bulk $\delta^{18}\text{O}$ and $\delta^{13}\text{C}$ at Site 1263 than at Site 1262 (Stap et al., 2009). Benthic foraminiferal diversity and accumulation rates decreased gradually at both sites during the starting period, but during peak ETM2 both declined much more precipitously and severely at the shallower Site 1263, leaving the sediment essentially barren of benthic foraminifera. Benthic assemblages just above and below the barren interval suggest low oxygen conditions in bottom and/or pore waters at Site 1263, not Site 1262. We rule out that changes in surface productivity at the two sites caused the differential effects in sediment and benthic biotic records during peak warming, because the sites are geographically close, with similar nannoplankton floras (Agnini et al., 2007; Raffi & de Bernardi, 2008). In addition, nannofossil evidence does not support a major change in productivity over Walvis Ridge (Dedert et al., 2012). Climate modeling experiments demonstrate that orbitally induced climate change may drive changing ocean circulation patterns after exceeding a temperature threshold, causing more pronounced warming at intermediate depths (Site 1263; Lunt et al., 2010). We infer that ocean warming crossed such a threshold during the starting phase of ETM2, which led to a change in ocean circulation during the peak phase, bringing warmer waters to intermediate depths (Site 1263). The differential warming at the two sites caused the more severe effects on benthos at the shallower site, probably by some combination of deoxygenation and warming, the latter increasing metabolic rates thus leading to a decrease in effective food supply. The drop in benthic populations of foraminifera may indicate a similar loss in population numbers of larger organisms, which may have led to a cessation of bioturbation, with potential effects on the sedimentological record of the event. Therefore we used a sediment model to test whether a strong reduction in bioturbational sediment mixing at the shallower Site 1263 can explain the more extreme excursion in bulk $\delta^{13}\text{C}$ and $\delta^{18}\text{O}$ values at the shallower Site 1263. We produced a qualitatively similar response, but cannot explain the magnitude of the Site 1263 peak excursion. We thus illustrate the potential role of ocean circulation changes in response to thresholds crossed during gradual warming in amplifying benthic environmental change and

driving temporary, but drastic loss of benthic biodiversity and abundance. An event of lesser magnitude does not simply lead to a ubiquitously smaller biotic response, but effects of increased atmospheric CO₂ can lead to ocean circulation change and other feedbacks, creating a complex picture of the influence of climate change on biota.

REFERENCES

- Agnini C., Fornaciari E., Raffi I., Rio D. Röhl U. & Westerhold T. (2007) - High-resolution nannofossil biochronology of middle Paleocene to early Eocene at ODP Site 1262: Implications for calcareous nannoplankton evolution. *Mar. Micropaleontol.*, 64, 215-248.
- Dedert M., Stoll H.M., Kroon D., Shimizu N., Kanamaru K. & Ziveri P. (2012) - Productivity response of calcareous nannoplankton to Eocene Thermal Maximum 2 (ETM2). *Clim. Past*, 8, 977-993.
- Hönisch B., Ridgwell A., Schmidt D.N., Thomas E., Gibbs S.J., Sluijs A., Zeebe R.E., Kump L., Martindale R.C., Greene S.E., Kiessling W., Ries J., Zachos J.C., Royer D.L., Barker S., Marchitto Jr T.M., Moyer R., Pelejero C., Ziveri P., Foster G.L., Williams B. (2012) - The geological record of ocean acidification. *Science*, 335 (6072), 1058-1063, doi: 10.1126/science.1208277.
- Lourens L., Sluijs A., Kroon D., Zachos J.C., Thomas E., Röhl U., Bowles J. & Raffi I. (2005) - Astronomical modulation of late Palaeocene to early Eocene global warming events. *Nature*, 435, 1083-1087
- Lunt D.J., Valdes, P.J., Jones T.D., Ridgwell A., Haywood M., Schmidt D.N., Marsh R. & Maslin M. (2010) - CO₂-driven ocean circulation changes as an amplifier of Paleocene-Eocene thermal maximum hydrate destabilization, *Geology*, 38, 875-878.
- Norris R.D., Turner S.K., Hull P.M. & Ridgwell, A. (2013) - Marine Ecosystem Responses to Cenozoic Global Change. *Science*, 341, 492-498.
- Raffi I. & De Bernardi B. (2008) - Response of calcareous nannofossils to the Paleocene-Eocene Thermal Maximum: Observations on composition, preservation and calcification in sediments from ODP Site 1263 (Walvis Ridge — SW Atlantic). *Mar. Micropaleontol.*, 69, 119-138.
- Reid P.C., Fischer A.C., Lewis-Brown E., Meredith M.P., Sparrow M., Andersson A.J., Antia A., Bates N.R., Bathmann U., Beaugrand G., Brix H., Dye S., Edwards M., Furevik T., Gangsto R., Hatun H., Hopcroft R.R., Kendall M., Kasten S., Keeling R., Le Quere C., Mackenzie F.T., Malin G., Mauritzen C., Olafsson J., Paull C., Rignot E., Shimada K., Vogt M., Wallace C., Wang Z.M. & Washington R. (2009) - Impacts of the Oceans on Climate Change. *Advances in Marine Biology*, 56, Elsevier Academic Press Inc, 1-150.
- Stap L., Lourens L., Sluijs A. & Thomas E. (2009) - Patterns and magnitude of deep sea carbonate dissolution during Eocene Thermal Maximum 2 and H2, Walvis Ridge, southeastern Atlantic Ocean. *Paleoceanography*, 24, PA1211
- Thomas E., Zachos J.C. & Bralower T.J. (2000) - Deep-Sea Environments on a Warm Earth: latest Paleocene - early Eocene. In: Huber B., MacLeod K. & Wing S.L. (Eds.) *Warm Climates in Earth History*, Cambridge University Press, 132-160.

Toward a better understanding of Paleocene-Eocene Thermal Maximum: A multidisciplinary record from Dababiya GSSP, Luxor, Egypt

Hassan Khozyem ^(a,b), Thierry Adatte ^(a), Jorge E. Spangenberg ^(c), Abdel Aziz Tantawy ^(b) & Gerta Keller ^(d)

^(a) Institute of Earth Sciences, University of Lausanne, Switzerland. E-mail: khozyem@gmail.com

^(b) Department of Geology, Faculty of Sciences, Aswan University, Aswan, Egypt

^(c) Institute of Earth Surface Dynamics, University of Lausanne, Switzerland

^(d) Department of Geosciences, Princeton University, Guyot Hall, Princeton, NJ 08544, USA

Document type: Short note.

Manuscript history: received 15 May 2014; accepted 30 May 2014; editorial responsibility and handling by Gerald R. Dickens & Valeria Luciani.

KEY WORDS: Dababiya GSSP, Egypt, Geochemical proxies, Luxor, PETM.

The Paleocene-Eocene thermal maximum (PETM) shows an extraordinary drop in both $\delta^{13}\text{C}_{\text{carb}}$ and $\delta^{13}\text{C}_{\text{org}}$ values, suggesting that a massive amount of ^{12}C -rich carbon dioxide was released into the atmosphere in a very short time (on the order of few hundred ky). The Dababiya GSSP (Luxor, Egypt) is thought to be the most complete known PETM section. The expanded sedimentary record of the Dababiya GSSP improves our understanding of the processes leading to the PETM events. Our multiproxy dataset, which includes geochemistry, mineralogy, micropaleontology and sedimentology, provided

the following crucial clues for the PETM interval at Dababiya GSSP (Fig. 1).

The Dababiya GSSP is deposited in the deepest part of an asymmetric submarine channel as indicated by the paleotopography, and absence of uppermost Paleocene and lowermost Eocene sediments from the Eastern section located 25m away from the main GSSP outcrop (Fig.1). At 50 m to the NW, the sediment beds thin out and finally disappear at about 150 m from the main GSSP outcrop. Thus, the Dababiya GSSP represents a localized expanded PETM sequence with a maximum extent of about 200m. At the GSSP, the Paleocene-Eocene boundary (PEB) coincides therefore with a sequence

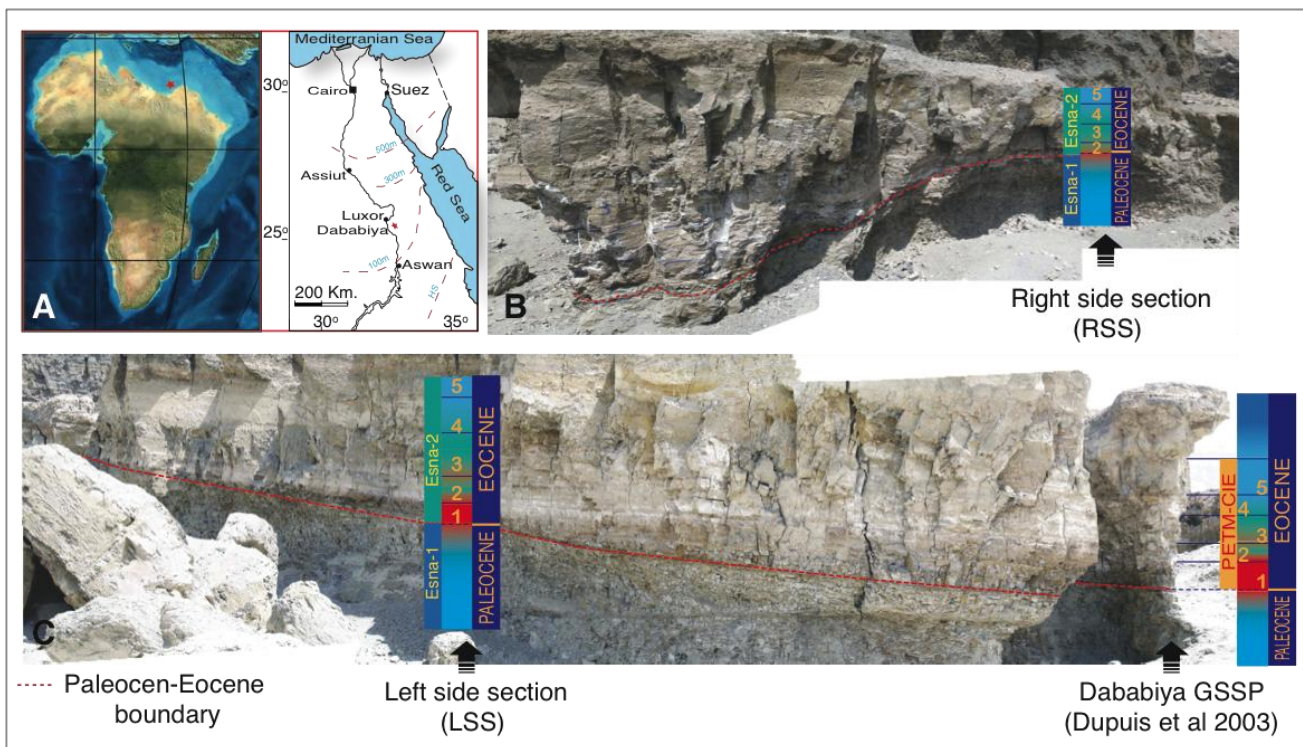


Fig.1 – A) Location of the Dababiya GSSP. B) and C): Field photographs show the lithology across the 25 m from the GSSP to the right side section (RSS) and the 50 m to the left side section (LSS). Note the sharp thinning out of the sedimentary units to the right and more gradual thinning out to the left of the GSSP marks a channel deposit.

boundary (SB) and erosional surface, which can be traced over hundreds of km.

$\delta^{13}\text{C}_{\text{Carb}}$ and $\delta^{13}\text{C}_{\text{Org}}$ profiles show gradual decrease during the latest Paleocene reaching the CIE-minimum above the SB. This interval represents the initiation of the PETM, and may be explained by the onset of the North Atlantic volcanism activity. The CIE- minimum in $\delta^{13}\text{C}_{\text{Carb}}$ coincides with the SB (base of bed 1), but $\delta^{13}\text{C}_{\text{Org}}$ minimum values are reached higher up in the top third of bed 2, which marks the onset of the recovery. The delayed recovery in $\delta^{13}\text{C}_{\text{Org}}$ may be due to variable rates of carbon cycling (e.g. continental silicate weathering, increased rate of organic carbon burial, and increased ocean productivity). Above the middle of bed 3, $\delta^{13}\text{C}_{\text{Carb}}$ and $\delta^{13}\text{C}_{\text{Org}}$ and the bulk rock composition return to background values observed below the PETM.

The Ce/Ce* shows two distinctive negative peaks located just

above the SB and in the middle part of bed 2 respectively.

The first peak is associated with strong dissolution and may be linked to chemical anoxia due to the release of methane and oxygen exhalation from the seawater. The second peak corresponds to an abrupt change in all redox parameters (V, U, Mo, Cd, etc.) associated with the maximum accumulation of organic matter. High U, Mo, V, Fe and abundant small sized (2–5 μm) pyrite framboids confirm that anoxic to euxinic conditions prevailed in the water column, which coincide with increased productivity sensitive elements (Cu, Ni, and Cd) suggesting high productivity in surface water. Above, phosphorus and barium tend to precipitate, as oxic conditions were re-installed. The recovery phase begins at the top of the second anoxia and marked by increase in P and Ba indicating the reestablishment of oxic conditions and ocean re-nitrification.

A high-resolution record of depositional sequences in the PETM in the southern North Sea Basin (NW Europe)

Chris King ^(*)

(*) 16A Park Road, Bridport, DT6 5DA, UK. E-mail: chrking@globalnet.co.uk

Document type: Short note.

Manuscript history: received 15 May 2014; accepted 30 May 2014; editorial responsibility and handling by Gerald R. Dickens & Valeria Luciani.

KEY WORDS: depositional sequences, marginal marine, North Sea Basin, PETM

The earliest Eocene is a critical period in earth history, with the brief but extreme PETM (Paleocene-Eocene Thermal Maximum) recording the highest global temperatures in the last 60 million years (e.g. Sluijs et al., 2007). This interval has been intensely researched in recent years, but most sections studied are either in marine sediment-starved environments (often partially or wholly dysoxic or anoxic) (e.g. the Paleocene/Eocene boundary GSSP at Dababaiya, Egypt), or in fully terrestrial environments (e.g. Bighorn Basin). These are environments insensitive to sea-level fluctuations.

Most studies agree on a sea-level rise at the onset of the PETM (e.g. Sluijs et al., 2008), but details of sea-level change within the PETM have been difficult to document, due to the factors cited above. Sections in inner neritic or marginal marine environments, more likely to be sensitive to sea-level fluctuations, are characteristically incomplete (e.g. in the US Gulf Coast: Sluijs et al., 2013).

The centre of the North Sea Basin (NW Europe) preserves a thick and apparently continuous record of sedimentation through the Paleocene/Eocene boundary (Kender et al., 2012), but in a dysoxic/anoxic marine environment. However on the southern margin of the North Sea Basin marginal-marine and coastal-plain sediments deposited during the PETM are represented in several discrete areas, including the London 'Basin', Hampshire 'Basin', Newhaven Outlier, Paris Basin, Varengeville Outlier (NW France) and NW Belgium (e.g. Aubry et al., 2005; Dupuis et al., 2011; Entwisle et al., 2013; Steurbaut et al., 2003). Here they form a readily recognisable package, generally 10-20 metres thick, between marine Thanetian and Ypresian sediments. Their distinctive facies and associated environmentally-related faunas led to their differentiation in the 19th century as a regional stage, the Sparnacian. The PETM has been identified in these areas isotopically, and through the identification of the corresponding *Apectodinium* dinoflagellate cyst influx (e.g. Steurbaut et al. 2003).

The term 'Sparnacian facies' can be usefully applied to their distinctive facies association, including channel-filling fluvial sands and gravels, pedogenised coastal plain overbank silts and clays, dark shelly lagoonal clays, estuarine channel sands, coastal plain lignites and (in the Paris Basin) freshwater limestones. Details of the succession in each area differ, and in the past each occurrence has often been interpreted as representing a discrete minor 'basin'. However it now seems probable that they represent deposition in a single wide southern embayment of the North Sea Basin, now disrupted by inter-Ypresian uplift and erosion (King, 2006).

Detailed correlation between these areas has not previously been carried out. This is due partly to their interpretation as separate depositional areas, and also to the assumption that in these marginal environments local environmental differences are likely to over-ride any regional features. However these environments are also very sensitive to sea-level fluctuations.

Detailed analysis has shown that three depositional sequences can be traced throughout this area, labelled SP1 - SP3. These were first differentiated in the London Basin (Knox, 1996) as Lmb-2 to Lmb-4; SP2 and SP3 correspond to sequences Y-A1a and Y-A1b differentiated in NW Belgium (Steurbaut *et al.*, 2003). These indicate that fluctuating sea-levels (either eustatic or resulting from regional tectonism) are the main controlling factor on the vertical facies-changes represented.

Four phases can be differentiated in each sequence (though not all phases are represented in all areas):

1. Deeply incised channels/channel complexes filled by mainly fluvial sediments. These are interpreted as incised valley fills, filled during the early TST, with their base marking the sequence boundary. These include the Erquelinnes sands (Mons Basin), Sables et Grès du Pays-de-Caux (Varengeville Outlier), sands at Rivecourt (Paris Basin) (all at the base of Sequence SP1), and Sables d'Auteuil (Paris Basin: base of Sequence SP3). These are generally relatively localised:
2. Sediment-starved coastal plain facies (lignites, freshwater limestones) (Calcaire de Mortemer, Lignites L1 & L2 (Varengeville Outlier); Cobham Lignite (London Basin) etc. These are interpreted as representing sediment starvation

during continued sea-level rise; they are less extensive than overlying phases.

3. Lagoonal clays and silts with brackish faunas, with sand-filled channels in some areas. These are widespread, including the Lower and Upper Shelly Clay (London Basin), Fausses Glaises (Paruis Basin) and most of the *Sables et Argiles a Ostracodes et Mollusques* (Varengeville Outlier). The base of this facies is interpreted as a brackish transgressive surface, and this phase as the late TST. In areas where phases 1 and 2 are unrepresented the basal surface forms a combined SB and TS. It is represented by a thalassinoid-burrowed surface in the London Basin and parts of the Paris Basin.

4. Pedogenised colour-mottled clays. These include the Lower and Upper Mottled Beds in the London Basin, the *Marnes a Rognons* and Limay Member in the Paris Basin. These are interpreted as representing aggradation and filling of accommodation space during the HST. In sequence 1 these terminate in a major calccrete in the London area and the Paris Basin, indicating a significant hiatus at this level ('mid-Lambeth hiatus': Entwisle et al., 2013).

The sequence boundary forming the base of SB1 is the MSLD1 surface of Dupuis et al. (2011). The base of the CIE is within sequence SP1. SP1 is unrepresented in NW Belgium, where the transgressive base of sequence SP2 overlies mid Thanetian sediments unconformably. There is an overall progressive increase in base-level at the maximum transgressive phase of these sequences, from coastal plain (SP1) to brackish (SP2) to brackish-marine (SP3). The base of the *Apectodinium* influx is at the transgressive surface of SP2, which is the earliest level with marine influence in this area. The lagoonal clays of SP3 include brackish-tolerant marine molluscs in all area, including the oyster *Ostrea bellovacina*, which confirms the regional correlation of these units.

The base of the sequence following SP3, post-dating the PETM, is the MSLD2 surface of Dupuis et al., (2011). This is a regional unconformity, probably tectonically enhanced (Knox, 1996). with the earliest overlying sediments again incised channel complexes, filled by estuarine sediments (Blackheath Formation etc.), followed by shallow marine glauconitic sands (Oldhaven Member of the London Basin), continuing the previous base-level trend.

This high-resolution record indicates repeated sea-level fluctuations in this area before, during and following the PETM. These may be eustatic, perhaps partly reflecting repeated injections of CO₂ into the atmosphere (Bains et al., 2003), or related to regional tectonism. Details of these fluctuations, and their calibration with the carbon isotope record, remain to be resolved, but they establish the southern North Sea Basin as a key area for interpreting the detail of the PETM.

REFERENCES

Aubry M.-P., Thiry M., Dupuis C. & Berggren W. A. (2005) - The Sparnacian deposits of the Paris Basin: A lithostratigraphic classification. *Stratigraphy*, 2, 65-100.

Bains S., Norris R.D., Corfield R.M., Bowen G.J., Gingerich P.D. & Koch P.L. (2003) - Marine & terrestrial linkages at the Paleocene- boundary. In: Wing S.L, Gingerich P.D., Schmitz B & Thomas E (Eds.) *Causes and Consequences of Globally Warm Climates in the Early Paleogene*. Geological Society of America Special Paper 369. Boulder, Colorado, USA, 1-9.

Dupuis C., Quesnel F., Iakovleva A., Storme J.-Y., Yans J. & Magioncalda R. (2011) - Sea level changes in the Paleocene-Eocene interval in NW France. Evidence of two major drops encompassing the PETM. *Berichte der Geologischen Bundesanstalt*, 85, 102.

Entwisle D.C., Hobbs P.R.N., Northmore K.J., Skipper J., Raines M.R., Self S.J., Ellison R.A. & Jones L.D. (2013) - *Engineering Geology of British Rocks and Soils - Lambeth Group*. British Geological Survey Open Report, OR/13/006, 316 pp.

Kender S., Stephenson M.H., Riding J.B., Leng M.J., Knox R. W. O'B., Peck V.L., Kendrick C.P., Ellis M.A., Vane C.H. & Jamieson R. (2012) - Marine and terrestrial environmental changes in NW Europe preceding carbon release at the Paleocene-Eocene transition. *Earth Planet. Sci. Lett.*, 353-354, 108-120.

King C. *Paleogene and Neogene: Uplift and a cooling climate* (2006) - In: Brenchley, P.J. & Rawson, P.F. (Eds.) *The Geology of England and Wales*. Second Edition. Geological Society, London, 395-427.

Knox R. W. O'B. (1996) - Tectonic controls on sequence development in the Palaeocene and earliest Eocene of southeast England: implications for North Sea stratigraphy. In: Hesselbo S.P. & Parkinson D.N. (Eds.) *Sequence Stratigraphy in British Geology*. Geological Society, London, Special Publications, 103, 209-230.

Sluijs A., Brinkhuis H., Crouch E. M., John C. M., Handley L., Munsterman D., Bohaty S., M., Zachos J. C., Reichert G.-J., Schouten S., Pancost R. D., Sinninghe Damste J. S., Welters N. L. D., Lotter A. F. & Dickens G. R. (2008) - Eustatic variations during the Paleocene-Eocene greenhouse world. *Paleoceanography*, 23, PA4216.

Sluijs A., Bowen G. J., Brinkhuis H., Lourens L. J. & Thomas E. (2007) - The Palaeocene-Eocene thermal maximum super greenhouse: biotic and geochemical signatures, age models and mechanisms of global change. In: Williams M., Haywood A.M., Gregory F.J. & Schmidt D.N. (Eds.), *Deep time perspectives on Climate Change: Marrying the Signal from Computer Models and Biological Proxies*, The Geological Society, London, 323-347..

Steurbaud E., Magioncalda R., Dupuis C., Van Simaey S., Roche E. & Roche M. (2003) - Palynology, paleoenvironments and organic carbon isotope evolution in lagoonal Paleocene-Eocene boundary settings in North Belgium. In: Wing S. L., Gingerich P. D., Schmitz B. & Thomas E. (Eds.), *Causes and consequences of Globally Warm Climates in the Early Paleogene*. Geological Society of America, Special Paper 369, 291-317.

An Earth system model evaluation of carbon emissions across Paleocene hyperthermals vs. the PETM

Sandra Kirtland Turner ^(a), Sarah E. Greene ^(a) & Andy Ridgwell ^(a)

^(a) School of Geographical Sciences, University of Bristol, Bristol BS8 1SS. E-mail: ggxsk@bristol.ac.uk

Document type: Abstract.

Manuscript history: received 15 May 2014; accepted 30 May 2014; editorial responsibility and handling by Gerald R. Dickens & Valeria Luciani.

KEY WORDS: carbon release, Earth system modeling, hyperthermals, Paleocene.

Increased resolution of deep-sea stable isotope records across the Paleocene epoch has led to the identification of multiple events with geochemical characteristics similar to records of the Paleocene-Eocene Thermal Maximum (PETM, ~56 Ma). Examples include the Dan-C2 event (~65.2 Ma) (Quillévéré et al., 2008), the Latest Danian or Top Chron 27 Event (~61.7 Ma) (Westerhold et al., 2008; Bornemann et al., 2009), and the Mid-Paleocene Biotic Event (~58.2) (Bernaola et al., 2007). Yet, without criteria for what defines a hyperthermal event, it remains unclear whether such events are driven by similar mechanisms to the PETM and/or smaller hyperthermals from the early Eocene like Eocene Thermal Maximums 2 and 3. Here we use the Earth system model cGENIE to test the idea that these events represent injections of isotopically depleted carbon to the oceans and calculate a range of possible carbon forcing scenarios using records of the $\delta^{13}\text{C}$ of bulk carbonate as constraints. In these experiments, modeled surface ocean dissolved inorganic carbon $\delta^{13}\text{C}$ is forced to follow the same trajectory as bulk carbonate $\delta^{13}\text{C}$ time series from each of three events – Dan-C2 (Quillévéré et al., 2008), Latest Danian Event (Quillévéré et al., 2002), and the Mid-Paleocene Biotic Event (Bernaola et al., 2007) – which is accomplished by adding and/or removing isotopically depleted dissolved inorganic carbon from the modeled surface ocean. We then compare the calculated forcing across each experiment with an equivalent PETM experiment using a bulk carbonate $\delta^{13}\text{C}$ record from ODP Site 690 (Bains et al, 1999). All experiments are run assuming the same initial steady state carbon cycle and climate conditions such that the analysis

demonstrates only the effect of the magnitude and shape of the $\delta^{13}\text{C}$ perturbation on the inferred carbon release.

REFERENCES

- Bains, S. Corfield, R.M., & Norris, R.D. (1999) - Mechanisms of climate warming at the end of the Paleocene. *Science*, 285, 724-727.
- Bernaola, G., Baceta J.I., Orue-Etxebarria X., Alegret L., Martín-Rubio M., Arostegui J. & Dinarès-Turell J. (2007) - Evidence of an abrupt environmental disruption during the mid-Paleocene biotic event (Zumaia section, western Pyrenees). *Geol. Soc. Am. Bull.*, 119, 785-795.
- Bornemann, A., Schulte P., Sprong J., Steurbaut E., Youssef M. & Speijer R.P. (2009) - Latest Danian carbon isotope anomaly and associated environmental change in the southern Tethys (Nile Basin, Egypt). *J. Geol. Soc. London*, 166, 1135-1142.
- Quillévéré F., Aubry M.-P., Norris R.D., & Berggren W.A. (2002) - Paleocene oceanography of the eastern subtropical Indian Ocean: An integrated magnetobiostratigraphic and stable isotope study of ODP Hole 761B (Wombat Plateau). *Palaeogeogr. Palaeoclimatol. Palaeoecol.*, 184, 371-405.
- Quillévéré F., Norris R.D., Kroon D., & Wilson P.A. (2008) - Transient ocean warming and shifts in carbon reservoirs during the early Danian. *Earth Planet. Sci. Lett.*, 265, 600-615.
- Westerhold T., Röhl U., Raffi I., Fornaciari E., Monechi S., Reale V., Bowles J., Evans H.F. (2008) - Astronomical calibration of the Paleocene time. *Palaeogeogr. Palaeoclimatol. Palaeoecol.*, 257, 377-403.

Regularity of Palaeogene hyperthermals inconsistent with a temperature threshold for carbon release

Sandra Kirtland Turner ^(a,b), Philip F. Sexton ^(c), Chris D. Charles ^(b) & Richard D. Norris ^(b)

^(a) School of Geographical Sciences, University of Bristol, Bristol, BS8 1SS, UK. E-mail: ggxsk@bristol.ac.uk.

^(b) Scripps Institution of Oceanography, UC San Diego, La Jolla, CA, 92093-0244, USA

^(c) Centre for Earth, Planetary, Space & Astronomical Research, The Open University, Milton Keynes, MK7 6AA, UK

Document type: Abstract.

Manuscript history: received 15 May 2014; accepted 30 May 2014; editorial responsibility and handling by Gerald R. Dickens & Valeria Luciani.

KEY WORDS: Carbon cycle instability, carbon reservoir size, Early Eocene climatic warmth, hyperthermals, thresholds for carbon release.

During the early Palaeogene Period, rapid greenhouse gas-fuelled warming events (Thomas and Zachos, 2000; Cramer et al., 2003; Lourens et al., 2005; Nicolo et al., 2007; Zachos et al., 2008; Zachos et al., 2010), termed hyperthermals (Thomas and Zachos, 2000), occurred during a ~6 million year (Myr)-long interval of progressive global warming culminating in the Early Eocene Climatic Optimum (EECO) (53 to 50 Myr ago) (Zachos et al., 2008). Hyperthermals leading into the EECO appear to decrease in size while increasing in frequency (Cramer et al., 2003; Nicolo et al., 2007; Zachos et al., 2010) — a pattern that has been explained by a thermodynamic threshold for carbon release and a decrease in the size of carbon reservoirs during times of extreme global warmth (Dickens, 2003; Lunt et al., 2011; DeConto et al., 2012; Komar et al., 2013). However, hypotheses that the size and volatility of carbon reservoirs may vary with global climate conditions have been difficult to test owing to the lack of continuous records throughout the EECO. Here we present a continuous ~4.2 Myr-long stable isotope record spanning the entire EECO that we combine with published records to create a 10 Myr-long high resolution composite record spanning peak Paleocene-Eocene greenhouse warmth. We find continuity in the size and frequency of carbon isotope excursions throughout the ~10 Myr-long onset, acme, and termination of the EECO. The existence of a regular series of hyperthermal events, even in the peak of the Eocene greenhouse climate, is inconsistent with progressive depletion of carbon reservoirs during extreme warmth and contradicts expectations for a thermodynamic threshold for carbon release. We also show that this persistent Eocene carbon cycle instability is strikingly similar in amplitude, frequency and phasing (with respect to orbital eccentricity) to that of the later Cenozoic, further emphasizing broad consistencies in the mode of carbon cycling across markedly different background climate regimes.

REFERENCES

- Cramer B.S., Wright J.D., Kent D.V. & Aubry M.-P. (2003) - Orbital climate forcing of delta C-13 excursions in the late Paleocene-early Eocene (chrons C24n-C25n). *Paleoceanography*, 18 (4), 1097, doi: 10.1029/2003 PA000909.
- DeConto R.M., Galeotti S., Pagani M., Tracy D., Schaefer K., Zhang T., Pollard D. & Beerling D.J. (2012) - Past extreme warming events linked to massive carbon release from thawing permafrost. *Nature*, 484 (7392), 87-91, doi:10.1038/nature10929.
- Dickens, G.R. (2003) Rethinking the global carbon cycle with a large, dynamic and microbially mediated gas hydrate capacitor. *Earth Planet. Sci. Lett.*, 213 (3-4), 169-183, doi:10.1016/S0012-821X(03)00325-X.
- Komar N., Zeebe R.E., & Dickens G.R. (2013) - Understanding long-term carbon cycle trends: The late Paleocene through the early Eocene. *Paleoceanography*, 28 (4), 650–662, doi: 10.1002/palo.20060.
- Lourens L.J., Sluijs A., Kroon D., Zachos J.C., Thomas E., Röhl U., Bowles J. & Raffi I. (2005) - Astronomical pacing of late Palaeocene to early Eocene global warming events. *Nature*, 435, 1083–1087, doi:10.1038/nature03814.
- Lunt D.J., Ridgwell A., Sluijs A., Zachos J.C., Hunter S. & Haywood A. (2011) - A model for orbital pacing of methane hydrate destabilization during the Palaeogene. *Nat. Geosci.*, 4 (11), 775-778, doi: 10.1038/ngeo1266.
- Nicolo M.J., Dickens G.R., Hollis C.J. & Zachos, J.C. (2007) - Multiple early Eocene hyperthermals: Their sedimentary expression on the New Zealand continental margin and in the deep sea. *Geology*, 35 (8), 699-702, doi: 10.1130/G23648A.1.
- Thomas E. & Zachos J.C. & Bralower T. J. (2000) - Deep sea environments on a warm earth. In Huber B., MacLeod K., & Wing S.L. (Eds.), *Warm Climates in Earth History*, (Cambridge Univ. Press, Cambridge), pp. 132-160.
- Zachos J.C., Dickens G.R. & Zeebe R.E. (2008) - An early Cenozoic perspective on greenhouse warming and carbon-cycle dynamics. *Nature*, 451, 279-283, doi: 10.1038/nature06588.
- Zachos J.C., McCarren H., Murphy B., Rohl U., & Westerhold T. (2010) - Tempo and scale of late Paleocene and early Eocene carbon isotope cycles: Implications for the origin of hyperthermals. *Earth Planet. Sci. Lett.*, 299, 242-249, doi: 10.1016/j.epsl.2010.09.004.

Carbonate dissolution in the deep equatorial Atlantic during the Middle Eocene Climatic Optimum

Wendy E. C. Kordesch ^(a), Steven M. Bohaty ^(a), Heiko Pälike ^(b), Thomas Westerhold ^(b), Ursula Röhl ^(b), Kirsty M. Edgar ^(c) & Paul A. Wilson ^(a)

^(a) Ocean and Earth Science, National Oceanography Centre, University of Southampton, SO14 3ZH, Southampton, UK. E-mail: wendy.kordesch@noc.soton.ac.uk

^(b) MARUM-Center for Marine Environmental Sciences, University of Bremen, 28359, Bremen, Germany

^(c) School of Earth Sciences, University of Bristol, BS8 1RJ, Bristol, UK

Document type: Abstract.

Manuscript history: received 15 May 2014; accepted 30 May 2014; editorial responsibility and handling by Gerald R. Dickens & Valeria Luciani.

KEY WORDS: benthic Foraminifera, carbonate accumulation, Middle Eocene Climatic Optimum, Site 929, stable isotopes, XRF.

Several major transient climate events disrupt the long-term cooling trend through the middle–late Eocene, most notably the rapid global warming of the Middle Eocene Climatic Optimum (MECO). The MECO (~500–750 kyr in duration) is characterized by a rise in atmospheric $p\text{CO}_2$ concentrations, gradual (~4°C) warming of both surface and deep waters, and prolonged carbonate dissolution in the deep ocean at ~40 Ma. A primary driving mechanism for abrupt warming during the MECO has not yet been identified and tested by comprehensive interrogation of middle Eocene geological datasets—a challenge that will require construction of a diverse set of high-resolution multi-proxy datasets from sites around the globe and carbon cycle modeling. The duration of warming (500+ kyr) and prolonged carbonate dissolution (>150 kyr) during the MECO suggests that prevailing theories for the origin of the MECO (e.g., a gradual increase in $p\text{CO}_2$ due to volcanic degassing) disagree with basic carbon cycle theory (Sluijs, et al. 2013).

The focus of this study is the history of the calcite compensation depth (CCD) in the Atlantic basin during the MECO at Ocean Drilling Program Site 929 and Deep Sea Drilling Project Site 523. ODP Site 929 is located in the tropical Atlantic Ocean (paleodepth: 4350 m) and provides new clues that may help disentangle mechanism(s) of carbon cycle change during the MECO. At this site, the MECO is identified within a condensed pelagic carbonate section (~2 m) and characterized by two or more dissolution layers. Across this interval, we have developed records of benthic foraminiferal stable isotopes ($\delta^{18}\text{O}$ and $\delta^{13}\text{C}$), X-ray fluorescence core scanning, carbonate content and an orbitally tuned age model spanning 39.3 to 42.2 Ma. These records reveal two distinct phases of carbonate dissolution during the MECO: initially carbonate content decreases to 0 wt.% and then increases to 30 wt.% before returning to 0 wt.%. Similar features are also observed at ODP Site 523 in the deep southern Atlantic (paleodepth: 3350 m). Together, ODP Site 929 and 523

records provide evidence for pulsed deep-ocean acidification during the MECO, which could be related to multiple carbon injections to the exogenic carbon cycle, short-term $p\text{CO}_2$ variation, carbonate compensation, and dynamic weathering feedbacks during the MECO.

At Site 929 we also find evidence of dissolution in conjunction with the magnetochron C19r hyperthermal event. It has been suggested that the C19r event is orbitally paced through long (2.4 myr) eccentricity cycle (Westerhold & Röhl, 2013). Previously observed only at nearby ODP Site 1260 (paleodepth: 2550 m; Edgar et al., 2007), our record at Site 929 provides evidence that this event may extend across the Atlantic basin.

Our findings are timely, given recent expeditions (e.g. IODP Expeditions 320 and 342) have targeted expanded middle Eocene sediment sequences and a number of high-resolution palaeoceanographic studies focused on this time interval are now underway. Our results provide a compelling new perspective on deep Atlantic dissolution during the MECO and C19r event and highlight the need to increase the fidelity and resolution of middle Eocene records to test the pervasiveness these transient events at sites around the globe.

REFERENCES

- Edgar K.M., Wilson P.A., Sexton P.F. & Suganama Y. (2007) - No extreme bipolar glaciation during the main Eocene calcite compensation shift. *Nature*, 448(7156), 908-911.
- Sluijs A., Zeebe R.E., Bijl P.K. & Bohaty S.M. (2013) - A middle Eocene carbon cycle conundrum. *Nature Geosci.*, 6(6), 429-434.
- Westerhold T. & Röhl U. (accepted 2013) - Orbital pacing of Eocene climate during the Middle Eocene climate optimum and the chron C19r event: missing link found in the tropical western Atlantic. *Geochem. Geophys. Geosyst.*, 14(11), 4811-4825.

Evidence for the magnetochron C19r hyperthermal event in the northwest Atlantic Ocean: IODP Exp. 342, Site U1408

Wendy E. C. Kordesch ^(a), Steven M. Bohaty ^(a), Heiko Pälike ^(b), Kirsty M. Edgar ^(c) & Paul A. Wilson ^(a)

^(a) Ocean and Earth Science, National Oceanography Centre, University of Southampton, SO14 3ZH, Southampton, UK. E-mail: wendy.kordesch@noc.soton.ac.uk

^(b) MARUM-Center for Marine Environmental Sciences, University of Bremen, 28359, Bremen, Germany

^(c) School of Earth Sciences, University of Bristol, BS8 1RJ, Bristol, UK

Document type: Abstract.

Manuscript history: received 15 May 2014; accepted 30 May 2014; editorial responsibility and handling by Gerald R. Dickens & Valeria Luciani.

KEY WORDS: C19r, Middle Eocene, Site U1408, Stable Isotopes.

The long-term global climate transition from Greenhouse to Icehouse conditions through the Eocene is characterized by a prolonged cooling trend through the middle and late Eocene punctuated by transient warming events, most notably global warming of the Middle Eocene Climate Optimum (MECO; ~40 Ma). Several short-lived (<200 kyr) events including the magnetochron C19r ‘hyperthermal’ event (~41.5 Ma) have also been identified (Edgar et al., 2007; Sexton et al., 2011). The C19r event was identified and studied in detail at ODP Site 1260 in the equatorial Atlantic, but a dissolution horizon at the peak of the event complicates accurate determination of its duration and magnitude (Edgar et al., 2007; Westerhold & Röhl, 2013) and it has yet to be identified elsewhere. Research within this interval of the middle Eocene has been particularly hindered by recovery of stratigraphically discontinuous sediments, poor preservation of carbonate microfossils and carbonate dissolution in most pelagic sections. Here, we utilize new deep-sea drillcores recovered during IODP Exp. 342 (Paleogene Newfoundland Sediment Drifts) in the northwestern Atlantic Ocean that targeted expanded sequences of Eocene clay-rich calcareous oozes excellent preservation of foraminifers. We present preliminary results through a late

middle Eocene time slice (~41.5 – 41.8 Ma) at Site U1408 (paleodepth: 2570 m; 41°26.3'N, 49°47.1'W) that confirms the presence of the C19r event in the northwest Atlantic using high-resolution (~2 kyr) records of foraminiferal stable isotopes ($\delta^{18}\text{O}$ and $\delta^{13}\text{C}$), coarse fraction (%), sediment color, and magnetic susceptibility. These datasets will allow us to better constrain changes in the magnitude, timing, and drivers of this little known event.

REFERENCES

- Edgar K.M., Wilson P.A., Sexton P.F. & Suganama Y. (2007) - No extreme bipolar glaciation during the main Eocene calcite compensation shift. *Nature*, 448(7156), 908-911.
- Sexton P.F., Norris R.D., Wilson P.A., Pälike H., Westerhold T., Röhl U., Bolton C. & Gibbs S.J. (2011) - Eocene global warming events driven by ventilation of oceanic dissolved organic carbon. *Nature*, 471(7338) 349-352.
- Westerhold T. & Röhl U. (2013) - Orbital pacing of Eocene climate during the Middle Eocene climate optimum and the chron C19r event: missing link found in the tropical western Atlantic. *Geochem. Geophys. Geosyst.*, 14(11), 4811-4825.

Compilation of hydrogen isotopic compositions of leaf wax biomarker records across the Paleocene-Eocene Thermal Maximum

Srinath Krishnan ^(a), Matthew Huber ^(b) & Mark Pagani ^(a)

^(a) Department of Geology and Geophysics, Yale University, PO Box 208109, New Haven, Connecticut 06520, USA. E-mail: srinath.krishnan@yale.edu

^(b) Institute for the Study of Earth, Oceans, and Space Morse Hall University of New Hampshire 8 College Road Durham, NH 03824-3525

Document type: Short note.

Manuscript history: received 15 May 2014; accepted 30 May 2014; editorial responsibility and handling by Gerald R. Dickens & Valeria Luciani.

KEY WORDS: biomarkers, hydrogen isotopes, PETM.

The late Paleocene/early Eocene (~57-50 Ma) time interval is characterized by substantial global and high-latitude warmth (Haq, 1981; Zachos et al., 2001). Additionally, it is interspersed with short periods of rapid greenhouse-gas induced warming events, known as hyperthermals (Cramer et al., 2003; Zachos et al., 2005). Warming estimates for the largest of these hyperthermals, the Paleocene Eocene Thermal Maximum (PETM; ~55Ma), suggest that global temperatures rose by ~5°C during the body of the event (Dunkley-Jones et al., 2013). Reconstructions of hydrological (evaporation & precipitation) changes during the PETM, however, have been more complex. One proxy that has recently been applied to evaluate these hydrological changes in the Big-Horn Basin, USA (Smith et al., 2007), Forada, Italy (Tippie et al., 2011), Tanzania (Handley et al., 2012), Venezuela (Jaramillo et al., 2012), and the Arctic (Pagani et al., 2006) is compound-specific hydrogen isotopic composition (D/H) of leaf-wax biomarker compounds. Traditionally, a simple Rayleigh distillation mechanism has been applied to interpret the changes in terms of poleward moisture transport. However, isotopic changes in n-alkane records can be complicated by local factors such as environmental and ecological changes, or biomarker integration and transport processes, which can substantially alter observed D/H compositions.

In this study, we present a compilation of existing D/H biomarker records for the PETM. All records are divided into five stages; late Paleocene, pre-CIE or the base of the CIE, peak CIE or the body of the PETM, recovery interval and post-PETM (Table 1). For preliminary evaluation, a constant apparent fractionation factor of 100‰ is used to convert $\delta D_{n-alkane}$ to $\delta D_{precipitation}$. A comparison of trends, direction, and magnitude of changes in these records are then used to broadly distinguish local and global changes in the hydrological cycle. Common features in the middle and high latitude δD records include D-enrichment at the base of the negative carbon isotope excursion (CIE) and D-depletion during peak warmth

of the PETM. This trend was initially observed at Lomonosov Ridge and was hypothesized to reflect reduced rainout during polar moisture transport due to a reduction in the meridional temperature gradient during greenhouse-gas induced warming (Pagani et al., 2006). Reduced D/H fractionation during moisture transport would theoretically result in greater D-enrichment of precipitation at the mid- and high-latitudes. Similar D/H trends observed for the second Eocene Thermal Maximum-2 (ETM2) from the same core at Lomonosov Ridge point to the validity of these trends as representative of high-latitude hydrological changes associated with the early Eocene hyperthermals (Krishnan et al., submitted). Biomarker reconstructions for the PETM at the Big-Horn Basin (Smith et al., 2007) and Forada, Italy (Tippie et al., 2011) sites also show similar, albeit smaller D-enrichments at the base of the CIE. However, it is clear that the D-enrichment is observed at the base of the CIE, prior to the peak warmth of the PETM.

In order to reevaluate this hypothesis, we simulate the Rayleigh distillation model with several combinations of low, middle and high-latitude temperatures to evaluate D/H isotopic changes for a wide range of global mean temperatures and meridional temperature gradients. Model-data comparisons are then used to express isotopic changes at each stage in terms of changes in meridional temperature gradients and global mean temperature. Results suggest that D-enrichment at the base of the CIE is coeval with reduced meridional temperature gradient and early high-latitude warming. Three mechanisms that could potentially drive high-latitude warming and hydrological changes that precede carbon input are discussed.

Existing modeling studies have so far struggled to replicate the “reduced meridional temperature gradients” observed during periods of high global warmth. However, for the early Eocene hyperthermals, this supposition is primarily driven by temperature records at the mid- and high-latitudes and therefore may be limited by proxy-related errors and/or the lack of a sufficient number of temperature records at the low-latitudes. Based on preliminary interpretations of D/H isotopic compilation in this study, we suggest that the meridional temperature gradient increased during the body of the PETM

and may be linked to a larger degree of warming at the low-latitudes than previously assumed. This study describes the utility of using coeval carbon and hydrogen isotopic compositions to reconstruct the temporal and spatial nature of

greenhouse-induced global warming for the PETM and provides important clues for understanding source and feedback mechanisms in the climate system.

Table 1- Compilation of $\delta D_{n\text{-alkane}}$ values for the late Paleocene, pre-CIE, and the body of the PETM from Venezuela (Jaramillo et al., 2010), Tanzania (Handley et al., 2012), Forada (Tipple et al., 2011), Cicogna (Krishnan et al., submitted), Big-Horn Basin, Wyoming (Smith et al., 2007), and Lomonosov Ridge, Arctic (Pagani et al., 2006).

Site	Approximate $\delta^2\text{H}_{n\text{-alkane}}$ for late Paleocene (‰)	Approximate $\delta^2\text{H}_{n\text{-alkane}}$ for pre-CIE (‰)	Approximate $\delta^2\text{H}_{n\text{-alkane}}$ during body of the CIE (‰)
Venezuela	-145	–	-170
Tanzania	-155	–	-140
Forada, Italy	-140	-130	-150
Cicogna, Italy	-125	–	-140
Big-Horn Basin, Wyoming	-190	-185	-200
Lomonosov Ridge, Arctic	-210	-160	-230

REFERENCES

- Cramer B.S., Wright J.D., Kent D.V. & Aubry M.-P. (2003) - Orbital climate forcing of $\delta^{13}\text{C}$ excursions in the late Paleocene – early Eocene (chrons C24n – C25n), *Paleoceanography*, 18 (4), 1097, doi:10.1029/2003PA000909.
- Dunkley Jones T., Lunt D.J., Schmidt D.N., Ridgwell A., Sluijs A., Valdes P.J. & Maslin M. (2013) - Climate model and proxy data constraints on ocean warming across the Paleocene–Eocene Thermal Maximum. *Earth-Sci. Rev.*, 125, 123-145.
- Handley L., O'halloran A., Pearson P.N., Hawkins E., Nicholas C.J., Schouten S., McMillan I.K. & Pancost R.D. (2012) - Changes in the hydrological cycle in tropical East Africa during the Paleocene–Eocene Thermal Maximum. *Palaeogeogr. Palaeoclimatol. Palaeoecol.* 329, 10-21.
- Haq B.U. (1981) - Paleogene paleoceanography: Early Cenozoic oceans revisited, pp. 71–82 *Oceanologica Acta*, Proceedings of the 26th International Geologic Congress, Geology of Ocean Symposium, Paris, July 7–17, 1980.
- Jaramillo C., Ochoa D., Contreras L., Pagani M., Carvajal-Ortiz H., Pratt L.M., Krishnan S., Cardona A., Romero M., Quiroz L., Rodriguez G., Rueda M.J., de la Parra F., Moran S., Green W., Bayona G., Montes C., Quintero O., Ramirez R., Mora G., Schouten S., Bermudez H., Navarrete R., Parra F., Alvarán M., Osorno J., Crowley J.L., Valencia V., Vervoort J. (2010) - Effects of rapid global warming at the Paleocene-Eocene boundary on neotropical vegetation. *Science*, 330, 957-961.
- Pagani M., Pedentchouk N., Huber M., Sluijs A., Schouten S., Brinkhuis H., Damste J.S.S., Dickens G.R. & the Expedition 302 Scientists (2006) - Arctic hydrology during global warming at the Palaeocene/Eocene Thermal Maximum. *Nature*, 442, 671-675.
- Smith F., Wing S. & Freeman K. (2007) - Magnitude of the carbon isotope excursion at the Paleocene-Eocene thermal maximum: The role of plant community change. *Earth Planet. Sci. Lett.*, 262, 50-65.
- Tipple B.J., Pagani M., Krishnan S., Dirghangi S.S., Galeotti S., Agnini C., Giusberti L. & Rio D. (2011) - Coupled high-resolution marine and terrestrial records of carbon and hydrologic cycles variations during the Paleocene-Eocene Thermal Maximum (PETM). *Earth Planet. Sci. Lett.*, 311, 82 - 92.
- Zachos J.C., Pagani M., Sloan L., Thomas E. & Billups K. (2001) - Trends, rhythms, and aberrations in global climate 65 Ma to present. *Science*, 292, 686–93.
- Zachos J.C., Röhl U., Schellenberg S.A., Sluijs A., Hodell D.A., Kelly D.C., Thomas E., Nicolo M., Raffi I., Lourens L.J., McCarren H. & Kroon D. (2005) - Rapid acidification of the ocean during the Paleocene-Eocene thermal maximum. *Science*, 308 (5728), 1611-1615.

Tracing terrestrial palaeoclimatic changes - vegetation dynamics of riparian forest in central Europe during late Palaeogene

Lutz Kunzmann ^(a), Zlatko Kvacek ^(b), Vasilis Teodoridis ^(c) & Karolin Moraweck ^(a)

^(a) Museum of Mineralogy and Geology, Senckenberg Natural History Collections Dresden, Königsbrücker Landstr., 159, 01109, Dresden, Germany. E-mail: Lutz.Kunzmann@senckenberg.de

^(b) Faculty of Science, Charles University in Prague, Albertov, 6, 128 43 Prague 2, Czech Republic

^(c) Department of Biology and Environmental Studies, Faculty of Education, Charles University in Prague, M.D. Rettigová, 4, 116 39 Prague 1, Czech Republic

Document type: Short note.

Manuscript history: received 15 May 2014; accepted 30 May 2014; editorial responsibility and handling by Gerald R. Dickens & Valeria Luciani.

KEY WORDS: central Europe, Eocene-Oligocene, fossil riparian forests, palaeobotany, palaeoclimate, vegetation change

Riparian environments are characterized by unstable conditions in terms of ground water level, immature soils, periodic flooding, accumulation of sediments and/or plant litter, and destructive processes accompanying rapid changes in local topography. Riparian vegetation, i.e. any vegetation unit that is affected by periodic flooding of meadows and waterlogging, is influenced by dynamics of running waters. In contrast to the mesic or zonal vegetation away from waterlogging, riparian vegetation is categorized as azonal or intrazonal. However, even riparian vegetation represents the respective vegetation and climate zone in its composition. Therefore it is possible to infer local and regional palaeoclimatic conditions based on plant fossils derived from riparian vegetation. Different types of riparian vegetation, although robust against habitat variations to a certain degree, are also quite sensitive to environmental changes including palaeoclimate.

Habitats in fluvial environments are sites where plant remains became fossilized in most cases, thus preserving primarily riparian vegetation. However, transitions to swamp forests in floodplains with almost permanent flooding and to pioneer vegetation in highly disturbed habitats within deltas, such as river banks, are also documented in fossil taphocoenoses recovered in fluvial facies types (Kunzmann & Walther, 2012).

Central Europe, namely central Germany and northern Bohemia, has an extensive fossil record of riparian vegetation traceable over a long time span. Here we focus on late Eocene to latest Oligocene plant assemblages covering the response to the Eocene-Oligocene turnover and the late Oligocene cooling. As we compare plant megafossils from similar environmental settings, i.e. riparian habitats, changes in species composition caused by immigrations and disappearance of species, are often directly linked to climatic variations.

A *Rhodomырthophyllum-Steinhauera* association with Lauraceae, Theaceae, Ericaceae and palms represents the late middle to late Eocene riparian vegetation in the Atlantic-Boreal province of central Europe. Contemporaneous zonal vegetation

is characterized as a notophyllous evergreen subtropical forest (Kvacek, 2010). Although main subtropical riparian and swamp elements persist until the Eocene-Oligocene turnover, gradual restructuring during the late Eocene is recorded (Kvacek et al., 2014). Among the new immigrants are thermophilous partly deciduous broad-leaved elements, such as *Platanus neptuni* and *Trigonobalanopsis rhamnoides*, and conifers, such as *Taxodium dubium* and *Glyptostrobus europaeus*. Appearance of new accessory Lauraceae, such as the *Laurophyllum (Ocotea) pseudoprinceps* and *Daphnogene cinnamomifolia* complexes are also detectable.

These thermophilous elements, as well as persistent *Eotrigonobalanus furcinervis*, are adaptive enough to withstand all Oligocene changes and thus survive at least until the Oligocene-Miocene boundary. However, Oligocene riparian forests are characterized as mixed broad-leaved vegetation types in which canopy-forming trees are mostly deciduous, e. g. *Populus* spp. in softwood associations and *Carpinus grandis*, *Acer* spp. and others in hardwood associations (e. g., Kunzmann, 2012; Fig. 1). These changes clearly mirror regional transitions from subtropical to warm-temperate vegetation. Later, *Liquidambar europaea* becomes predominant in riparian forests during the late Oligocene cooling phase. Respective zonal vegetation is identified as broad-leaved mixed mesophytic to broad-leaved deciduous (Mai & Walther, 1991, Teodoridis, 2010).

Based on these megafossil plant assemblages from fossil riparian environments, not only qualitative assumptions on palaeoclimatic changes are revealed, but also quantitative estimations and modelling are possible. Palaeoclimatic parameters are estimated by the Coexistence Approach (Mosbrugger and Utescher 1997) and/or CLAMP (Teodoridis et al., 2011, 2012, Kvacek, et al. 2014); palaeo-CO₂ concentrations in the atmosphere are calculated by gas exchange modelling (e.g., Grein et al., 2013).

ACKNOWLEDGEMENTS

We warmly thank the late Dieter Hans Mai and the late Harald Walther for fruitful scientific discussions and collaborations during the last decades. This work is supported by a grant to ZK from GA ČR (Grant Agency of the Czech Republic) 14-23108S.

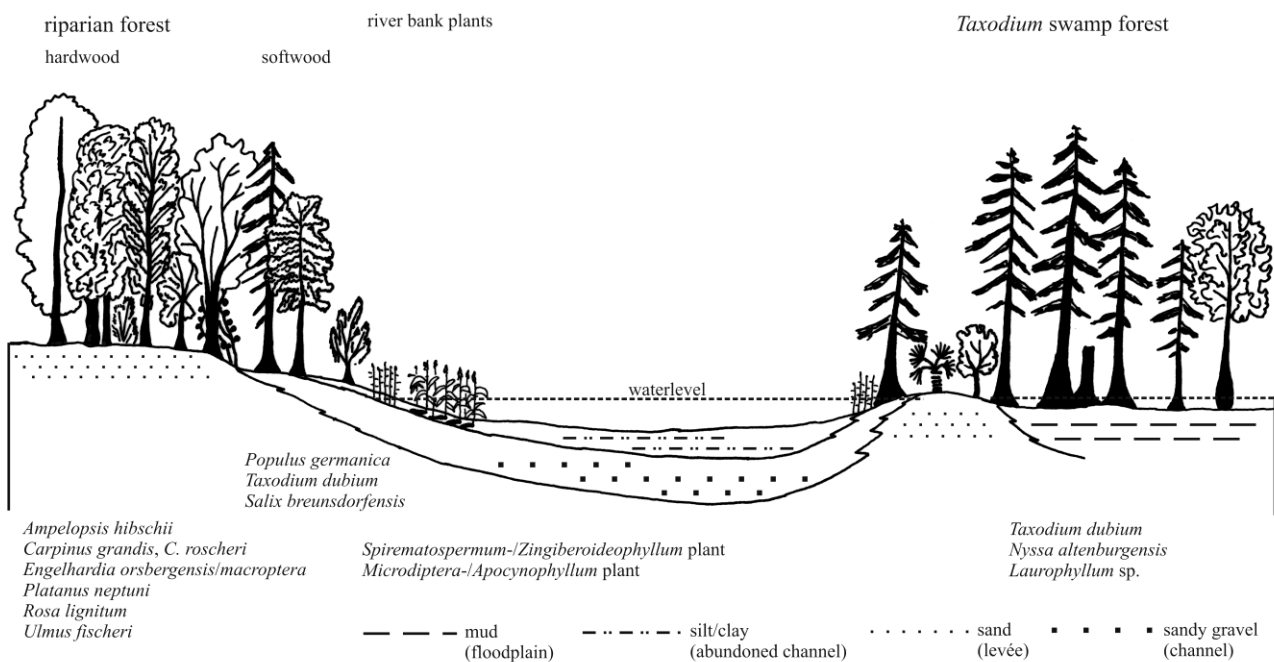


Fig.1 – Reconstruction of local intrazonal palaeovegetation and palaeoenvironment from the early Oligocene Weißelster Basin, central Germany, based on the fossil flora, sedimentological, taphonomic, and palaeoecological aspects (from Kunzmann 2012).

REFERENCES

- Grein M., Oehm C., Konrad W., Utescher T., Kunzmann L. & Roth-Nebelsick A. (2013) - Atmospheric CO₂ from the late Oligocene to early Miocene based on photosynthesis data and fossil leaf characteristics. *Palaeogeogr. palaeoclimatol. palaeoecol.*, 374, 41-51.
- Kunzmann L. (2012) - Early Oligocene plant taphocoenosis with mass occurrence of *Zingiberoideophyllum* (extinct Zingiberales) from central Germany. *Palaios*, 27, 765-778.
- Kunzmann L. & Walther H. (2012) - Early Oligocene plant taphocoenoses of the Haselbach megafloral complex and the reconstruction of palaeovegetation. *Palaeobiodiv. Palaeoenvir.*, 92(3), 295-307.
- Kvaček Z. (2010) – Forest flora and vegetation of the European early Palaeogene – a review. *Bull. Geosci.*, 85(1), 63-76.
- Kvaček Z., Teodoridis V., Mach K., Přikryl T. & Dvořák Z. (2014) - Tracing the Eocene–Oligocene transition: a case study from North Bohemia. *Bull. Geosci.*, 89(1), 21-66.
- Mai D.H. & Walther H. (1991) - Die oligozänen und untermiozänen Floren NW-Sachsens und des Bitterfelder Raumes. *Abh. Staatl. Mus. Mineral. Geol. Dresden*, 38, 1-230.
- Mosbrugger V. & Utescher T. (1997) - The coexistence approach – a method for quantitative reconstructions of Tertiary terrestrial palaeoclimate data using plant fossils. *Palaeogeogr. Palaeoclimatol. Palaeoecol.*, 134, 61–86.
- Teodoridis V. (2010) - The Integrated Plant Record vegetation analysis from the Most Basin (Czech Republic). *N. Jb. Geol. Paläont., Abh.*, 256(3), 303-316.
- Teodoridis V., Mazouch P., Spicer R.A., Uhl D. (2011) - Refining CLAMP – Investigations towards improving the Climate Leaf Analysis Multivariate Program. *Palaeogeogr. Palaeoclimatol. Palaeoecol.*, 299, 39-48.
- Teodoridis V., Kvaček Z., Zhu Hua, Mazouch P. (2012) - Environmental analysis of the mid-latitude European Eocene sites of plant macrofossils and their possible analogues in East Asia. *Palaeogeogr. Palaeoclimatol. Palaeoecol.*, 333-334, 40-58.

High-resolution benthic stable isotope records from ODP Site 1263 in the Southern Atlantic encompassing early Eocene warming events

Vittoria Lauretano ^(a), James C. Zachos ^(b) & Lucas J. Lourens ^(a)

^(a) Department of Earth Sciences, Faculty of Geosciences, Utrecht University, Budapestlaan 4, 3584 CD Utrecht, The Netherlands. E-mail: v.lauretano@uu.nl

^(b) Earth and Planetary Sciences Dept., University of California, Santa Cruz, CA 95064, USA

Document type: Short note.

Manuscript history: received 15 May 2014; accepted 30 May 2014; editorial responsibility and handling by Gerald R. Dickens & Valeria Luciani.

KEY WORDS: benthic stable isotopes, carbon cycle, Eocene hyperthermals, greenhouse warming.

From the late Paleocene to the early Eocene, the Earth's surface experienced a long-term warming trend that resulted in a temperature increase of at least 5°C in the deep ocean and that culminated in the Early Eocene Climatic Optimum (EECO). The long-term warming was punctuated by a series of short-lived global warming events known as “hyperthermals”, of which the Paleocene-Eocene Thermal Maximum (PETM) represents the most extreme example. At least two other short-term episodes have been identified as hyperthermals: the ETM2 (or Elmo event) at about 53.7 Myr and the ETM3 (or X-event) at about 52.5 Myr. These transient events are marked by prominent carbon isotope excursions (CIEs), recorded in marine and continental sedimentary sequences and were driven by fast and massive injections of ¹³C-depleted carbon into the ocean-atmosphere system leading to changes in global temperatures and carbon cycles, possibly triggered by a common orbital forcing mechanism (Lourens et al., 2005). Different sources and mechanisms have been proposed for the large release of carbon, including the release of methane by thermal dissociation of gas hydrates on the continental slopes (Dickens et al., 1995); the burning of extensive peat and coal deposits (Kurtz et al., 2003); the release of carbon from thawing of the permafrost soils at high latitudes in response to orbital forcing (DeConto et al., 2012) and the redistribution of ¹³C-depleted carbon within oceans, as proposed for the Early to Middle Eocene interval (Sexton et al., 2011).

Throughout the last decades, the occurrence of multiple events has been recognized globally but our understanding of their causes and mechanisms is still limited by the scarcity of well-resolved records covering this pivotal interval of the early Paleogene. New complete records are necessary to unravel whether these events share common sources and mechanisms. Also, the definition of a time framework is needed to locate the succession of these events on the long-term variations of the Early Eocene climate system.

Here, we present new high-resolution benthic stable isotope records of the Early Eocene from sediments recovered at ODP

Site 1263, (Walvis Ridge, SE Atlantic). This site represents the shallowest end-member of the 2-km depth transect recovered during ODP Leg 208 and its estimated paleodepth was about 1500 m. The new $\delta^{13}\text{C}$ and $\delta^{18}\text{O}$ records extend the previously published record of the benthic foraminiferal species *Nuttallides truempyi* across the ETM2/Elmo and H2 (Stap et al., 2010), confirming the presence of additional episodes of ¹³C-depleted carbon injection and warming. These transient events have been identified as the events I1 and I2, J and the ETM3 (or X-event). We discuss their CIEs and their response in $\delta^{18}\text{O}$, defining their timing, durations and paleoceanographic implications. Our records document the warming during the transient events as well as the long-term trend, from the ETM2, across the Early Eocene hyperthermal events, up to its culmination during the EECO.

The aim of this study is to investigate changes in carbon fluxes and deep-ocean temperatures during the Early Eocene warming events, exploring their timing, nature and possible mechanisms behind them. We construct an orbitally tuned age model, proposing two possible tuning options, depending on the available options for the age of the PETM (Westerhold et al., 2008). Spectral and wavelet analyses confirm that these events are paced by orbital forcing, specifically long and short eccentricity cycles. Moreover, we test the relationship between changes in the global carbon cycle and mutual responses in global temperatures by observing the covariance of benthic foraminiferal $\delta^{13}\text{C}$ and $\delta^{18}\text{O}$. The isotopic relationship across each event is used to assess whether the warming events share similar patterns and characteristics, thus implying analogous origins and sources. We investigate the warming related to the Early Eocene Climatic Optimum and its duration as inferred from the oxygen isotopes, while exploring responses and effects in the carbon cycle system.

REFERENCES

DeConto R.M., Galeotti S., Pagani M., Tracy D., Schaefer K., Zhang T., Pollard D. & Beerling D.J. (2012) - Past extreme warming events linked to massive carbon release from thawing permafrost. *Nature*, 484, 87-91.

- Dickens G.R., O'Neil J.R., Rea D.K. & Owen R.M. (1995) - Dissociation of Oceanic Methane Hydrate as a Cause of the Carbon-Isotope Excursion at the End of the Paleocene. *Paleoceanography*, 10 (6), 965-971.
- Kurtz A.C., Kump L.R., Arthur M.A., Zachos J.C. & Paytan A. (2003) - Early Cenozoic decoupling of the global carbon and sulfur cycles. *Paleoceanography*, 18, 1090.
- Lourens L.J., Sluijs A., Kroon D., Zachos J.C., Thomas E., Röhl U., Bowles J. & Raffi I. (2005) - Astronomical pacing of late Palaeocene to early eocene global warming events. *Nature*, 435, 1083-1087.
- Sexton P.F., Norris R.D., Wilson P. A., Palike H., Westerhold T., Röhl U., Bolton C.T. & Gibbs S.J. (2011) - Eocene global warming events driven by ventilation of oceanic dissolved organic carbon. *Nature*, 471, 349-353.
- Stap L., Lourens L.J., Thomas E., Sluijs A., Bohaty S.M. & Zachos J.C. (2010) - High-resolution deep-sea carbon and oxygen isotope records of Eocene Thermal Maximum 2 and H2. *Geology*, 38, 607-610.
- Westerhold T., Röhl U., Raffi I., Fornaciari E., Monechi S., Reale V., Bowles J. & Evans H.F. (2008) - Astronomical calibration of the Paleocene time. *Palaeogeogr. Palaeoclimatol. Palaeoecol.*, 257(4), 377-403.

The Oligocene-Miocene Transient Glaciation: Insights from IODP Expedition 342

Caroline H. Lear ^(a), Paul A. Wilson ^(b) & Diederik Liebrand ^(b)

^(a) School of Earth and Ocean Sciences, Cardiff University, Main Building, Park Place, Cardiff, CF10 3AT, UK. E-mail: learc@cf.ac.uk

^(b) School of Ocean and Earth Science, National Oceanography Centre Southampton, University of Southampton Waterfront Campus, European Way, Southampton, SO14 3ZH, UK

Document type: Short note.

Manuscript history: received 15 May 2014; accepted 30 May 2014; editorial responsibility and handling by Gerald R. Dickens & Valeria Luciani.

KEY WORDS: glaciation, hysteresis, Mg/Ca, temperature, Oligocene.

The high altitude of the upper surface of the East Antarctic ice sheet severely limits the potential for surface melt. Ice sheet models therefore require a large radiative forcing to melt the ice sheet from the top down, such that modeled CO₂ thresholds for ice melt are far higher than those for ice growth. The problem with this apparent hysteresis effect is that the geological record contains several convincing lines of evidence for major ice sheet growth and retreat in the past. There are four potential solutions to the “ice sheet hysteresis problem”. Firstly, the models may be overestimating the magnitude of hysteresis by incorrectly capturing ice sheet ablation processes. Secondly, proxy records may be providing inaccurate estimates of past ice sheet growth and decay. Thirdly, the degree and variability of past radiative forcing may have been underestimated. Fourthly, a significant component of the ice decay inferred from the geological records perhaps took place in less stable (e.g., Northern Hemisphere, West Antarctic) ice sheets.

The Oligocene-Miocene transient glaciation provides an excellent opportunity to examine the ice sheet hysteresis problem. Over approximately two short eccentricity cycles the Antarctic ice sheet is believed to have roughly doubled in size culminating in a brief interval termed “Mi-1” (Miller et al., 1991; Zachos et al., 2001; Lear et al., 2004; Pekar & DeConto, 2006; Liebrand et al., 2011; Mawbey & Lear, 2013). However, within another two short eccentricity cycles, global ice volume apparently returned to near background levels.

IODP Expedition 342 drilled three expanded Oligocene-Miocene boundary sections from a depth transect across J-Anomaly Ridge – Sites U1404, U1405 and U1406 (Expedition 342 Scientists, 2012; Figure 1). The shallowest of these sites (U1406, 3814 m) contains a magnetostratigraphy and relatively abundant foraminifera suitable for geochemical analysis. A preliminary age model places the Oligocene-Miocene boundary at approximately 80 m burial depth (Expedition 342 Scientists, 2012). The shallow burial depth and relatively clay-rich

lithology is consistent with the apparently excellent preservation of the Oligocene-Miocene foraminifera when viewed under binocular microscope. We further assessed the preservation of the benthic foraminifera present using scanning electron microscopy (Fig. 1). The presence of original wall structure and lack of secondary crystallites argues against significant diagenetic alteration. The high sedimentation rate coupled with the unusually enhanced foraminiferal preservation at Site U1406 therefore provides an excellent opportunity for a geochemical study of the Oligocene-Miocene transient glaciation event.

We analysed 50 benthic foraminiferal samples (*Cibicidoides mundulus*) for their oxygen ($\delta^{18}\text{O}$) and carbon ($\delta^{13}\text{C}$) isotopic composition. The transient excursion to higher $\delta^{18}\text{O}$ known as “Mi-1” is visible, with *C. mundulus* $\delta^{18}\text{O}$ reaching a maximum of 2‰ (VPDB) at this Site. Some intriguing differences between the stable isotope records from U1406 and other sites await refinement of the age model before further interpretation. We also analysed 100 shallow infaunal benthic foraminiferal samples (*O. umbonatus*) for their trace metal composition (Mg/Ca, Sr/Ca, Li/Ca, Al/Ca, U/Ca). Assuming minimal contribution from a carbonate ion effect (Mawbey and Lear, 2013), the *O. umbonatus* Mg/Ca record suggests bottom water temperature variations on the order of 3°C at U1406 during the Oligocene-Miocene boundary event. The bottom water temperature record is combined with the benthic $\delta^{18}\text{O}$ record to calculate relative changes in seawater $\delta^{18}\text{O}$ (δw). This preliminary δw record from Site U1406 is in very good agreement with that determined using samples from ODP Site 926 on Ceara Rise, (Mawbey & Lear, 2013).

IODP Site 1406 therefore provides an excellent opportunity to study both the onset and just as important, the termination of the Oligocene-Miocene transient glaciation. The high sedimentation rate will allow orbital variability (including precessional cycles) to be defined and the enhanced foraminiferal preservation will allow a more robust, quantitative assessment of ice volume variability, crucial for a rigorous testing of the “ice sheet hysteresis problem”.

during the Oligocene-Miocene transient glaciation.

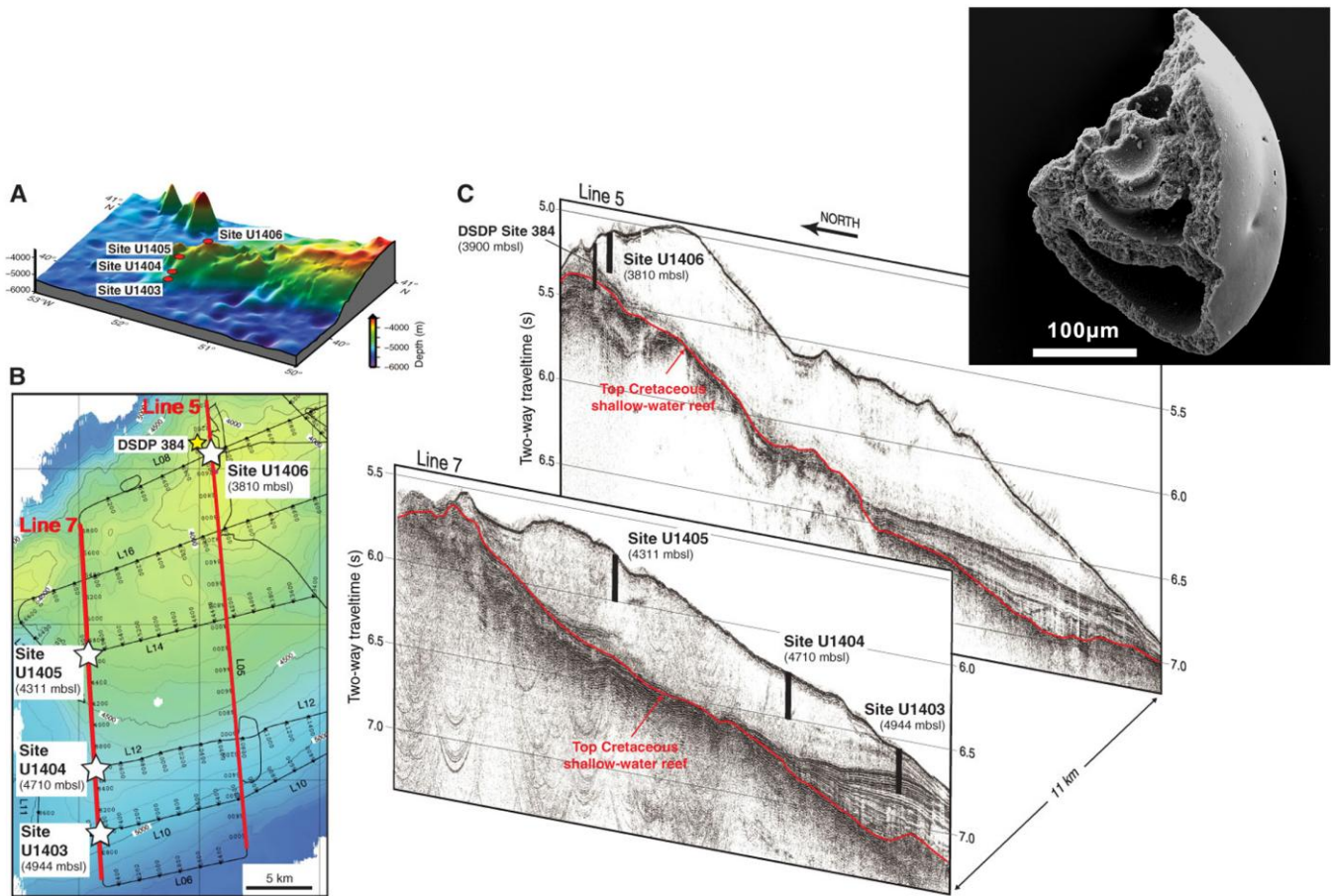


Fig.1 – Location of Oligocene-Miocene boundary sites recovered during IODP Expedition 342 (Expedition 342 Scientists, 2012). Inset: Scanning electron microscope image of benthic foraminifera *Oridorsalis umbonatus* from 1406A-8H-3W-98,100cm, showing wall structure.

REFERENCES

- Expedition 342 Scientists (2012) - Paleogene Newfoundland sediment drifts. IODP Prel. Rept., 342.
- Lear C.H., Rosenthal Y., Coxall H.K. & Wilson P.A. (2004) - Late Eocene to Early Miocene ice sheet dynamics and the global carbon cycle. *Paleoceanography*, 19, PA4015, doi:10.1029/2004PA001039.
- Liebrand D., Lourens L.J., Hodell D.A., de Boer B., van de Wal R.S.W. & Pälike H. (2011) - Antarctic ice sheet and oceanographic response to eccentricity forcing during the early Miocene. *Clim. Past*, 7, 869-880.
- Mawbey E.M. & Lear C.H. (2013) - Carbon cycle feedbacks *Geology*, 41, 963-966.
- Miller K.G., Wright J.D. & Fairbanks R.G. (1991) - Unlocking the ice house: Oligocene-Miocene oxygen isotopes, eustasy, and margin erosion. *J. Geophys. Res.*, 9, 6829-6848.
- Pekar S.F. & DeConto R.M. (2006) - High-resolution ice-volume estimates for the early Miocene: Evidence for a dynamic ice sheet in Antarctica. *Palaeogeogr. Palaeoclimatol. Palaeoecol.*, 231, 101-109.
- Zachos J.C., Shackleton N.J., Revenaugh J.S., Pälike H. & Flower B.P. (2001) - Climate response to orbital forcing across the Oligocene-Miocene boundary. *Science*, 292(5515), 274-278.

Biological stability during maximum marine transgression: the Paleogene - Neogene transition in New Zealand

Daphne E. Lee ^(a), R. Ewan Fordyce ^(a), John Conran ^(b), Tammo Reichgelt ^(a), Bethany Fox ^(c) & Elizabeth M. Kennedy ^(d)

^(a) Department of Geology, University of Otago, PO Box 56, Dunedin, New Zealand. E-mail: daphne.lee@otago.ac.nz

^(b) ACEBB & SGC, School of Earth and Environmental Sciences, The University of Adelaide, SA 5005, Australia

^(c) Department of Earth Sciences, University of Waikato, Private Bag 3105, Hamilton 3240, New Zealand

^(d) GNS Science, PO Box 30-368 Lower Hutt, New Zealand

Document type: Short note.

Manuscript history: received 15 May 2014; accepted 30 May 2014; editorial responsibility and handling by Gerald R. Dickens & Valeria Luciani.

KEY WORDS: Late Oligocene, marine invertebrates, marine vertebrates, paleoclimate, paleogeography, terrestrial flora, Zealandia.

Oligocene to earliest Miocene New Zealand (Zealandia) was an isolated archipelago situated in mid-latitudes (40–45°S) in the southwest Pacific, and well-placed to record changes in Southern Hemisphere climate. Further, Zealandia underwent major environmental changes across the Paleogene–Neogene transition, and has an exceptional fossil record for both terrestrial and marine ecosystems. We summarise the major changes in paleogeography and topography at the end of the Paleogene (Chattian and lower Aquitanian) and highlight notable characteristics and changes in the biota. Sites are mainly southern (Canterbury, Otago and Southland) where terrestrial, estuarine, and shallow marine environments of late Oligocene–earliest Miocene age are particularly well-represented, and macro- and microfossil assemblages have been well-studied. Fossils are preserved in lignites, lacustrine diatomites, estuarine mudstones, marine sandstones, greensands, and limestones.

Paleogeography and topography – New paleogeographic maps (Kamp et al., 2013) show the dramatic reduction in the land area of Zealandia through the Paleogene, from a substantial landmass about twice the area of modern New Zealand in the early Paleocene, to a series of islands occupying less than 10% of the present land area (about 25,000 km²) by the late Oligocene (a little larger than present-day New Caledonia). These islands were separated by extensive shallow seaways allowing considerable expansion of land area, and reconnections of islands, during sea level low-stands (Cooper & Cooper, 1995). At the beginning of the Paleogene, Zealandia had moderate relief, but through the Eocene and early Oligocene, a combination of crustal thinning and long-continued erosion reduced the overall land elevation to probably less than 500 m. By the late Oligocene, southern Zealandia comprised low-lying islands of exposed Paleozoic and Mesozoic basement terranes with a veneer of Cretaceous to Oligocene terrigenous and marine sediments.

Climate - Following long-term warming through the early Eocene and subsequent cooling through the later Eocene and early Oligocene, New Zealand seas experienced the Late Oligocene Warming Event (Zachos et al., 2001). Some marine invertebrate assemblages are of subtropical aspect. Quantitative terrestrial climate approximations derived from palynomorph data and leaf physiognomy suggest a humid subtropical climate at the Paleogene–Neogene transition (Reichgelt et al., 2013). There is evidence for a seasonal gradient in precipitation, possibly the effect of weakening oceanic influence on land during the summer months. This, combined with a seasonal light regime at mid-latitudes, would have created a marked contrast between summer and winter at this time, with mesic conditions in winter and possible drought in summer. Physical and magnetic properties data from high-resolution lake sediments indicate that longer-term climate variation in New Zealand was dominantly controlled by high-latitude (obliquity) signals, while shorter-term variation was dominated by tropical (ENSO-like) variation.

Terrestrial flora – There is compelling evidence both from the excellent palynomorph and more patchy macrofossil record to show that New Zealand was forested throughout the Paleogene. Well-preserved late Oligocene/earliest Miocene plant macrofossils in swamp and lake deposits reveal a diversity and provinciality of vegetation types. Forests were usually mixed, but were locally dominated by araucarians (*Agathis/Araucaria*), Nothofagaceae and/or Lauraceae. Conifers were extremely diverse, with at least 17 genera (e.g., *Dacrydium*, *Dacrycarpus*, *Halocarpus*, *Lagarostrobos*, *Microcachrys*, *Phyllocladus*, *Podocarpus/Prumnopitys*) and 30 distinct species: compared to the extant New Zealand diversity of 10 genera and 19 species (Jordan et al., 2011). Ferns were also diverse and included representatives of Cyatheaceae, Davalliaceae, Dennstaedtiaceae, Dicksoniaceae, Lycopodiaceae, Nephrolepidaceae, Osmundaceae, Pteridaceae, Psilotaceae and Polypodiaceae. The angiosperm flora included many monocots (?Amaryllidaceae, Anarthriaceae, Arecaceae, Asparagaceae, Asteliaceae, Pandanaceae, Typhaceae) and numerous dicots and basal angiosperms such as Aquifoliaceae,

Aralicaceae, Atherospermataceae, Casuarinaceae, Chloranthaceae, Cunoniaceae, Ericales, Euphorbiaceae, Lauraceae, Loranthaceae, Malvaceae, Monimiaceae, Myrsinaceae, Myrtaceae, Nothofagaceae (six species), Onagraceae, Proteaceae, Rutaceae, Sapindaceae, Strasburgeriaceae and Winteraceae. Many of the genera represented in the late Oligocene vanished from the New Zealand flora during late Miocene to Quaternary cooling.

Terrestrial fauna – In contrast to our expanding knowledge of the earliest Miocene biota (including numerous insects preserved in diatomite and amber) little is known about the late Oligocene terrestrial fauna, apart from freshwater mussels and fish remains (otoliths and rare skeletons).

Marine invertebrates – New Zealand has an excellent record of marine invertebrates through the Paleogene, particularly for molluscs (Beu & Maxwell, 1990). Late Oligocene Mollusca are extremely diverse, with, for example, 360 species of rarely-preserved shallow-water taxa at Cosy Dell (Lee et al., 2014). Other groups with high diversity at this site include arthropods, with >125 species of ostracod and 9 species of barnacle representing 7 families. A Hakataramea assemblage is comparable in diversity.

Marine vertebrates – Paleogene marine tetrapods from Zealandia include turtles, penguins and rarely other seabirds, and cetaceans (whales, dolphins). For the Oligocene, the Rupelian cetacean record is sparse in Zealandia and globally, probably because high-stand/ peak submergence facies generally preclude a dense record. Nevertheless, the latest Eocene–early Oligocene was a time of major radiation of crown Cetacea (Neoceti), driven by modernisation of ocean circulation and concurrent evolution of phytoplankton. Later Chattian cetaceans, especially from Hakataramea (Fordyce 2014), represent many earlier-evolving lineages in Zealandia: relict archaeocetes (Kekenodontidae); archaic toothed mysticetes including Mammalodontidae; dawn mysticetes – Eomysticetidae; archaic balaenid-like (right whale?) species; gulp-feeding baleen whales probably in the Balaenopteroidea, including *Mauicetus*; shark-toothed dolphins – Squalodontidae; waipatiids – Waipatiidae; archaic ocean dolphins – Delphinoidea; and putative Dalpiazinidae. Notable absences from the shelf-sequences of Zealandia include ancestral sperm whales and beaked whales, for which modern relatives are deep-diving pelagic forms. Chattian penguins include the giant *Kairuku* species, which probably foraged in deep waters remote from the Zealandia archipelago, and species of *Platydyptes* close to the start of the radiation of crown-penguins. The Paleogene-Neogene transition needs further research; the Aquitanian is a major gap in the global cetacean and penguin record.

Conclusions – In summary, the New Zealand record of climatic and biotic events at the Paleogene – Neogene transition is one of the most comprehensive available globally. Sea surface temperatures at Southern Hemisphere mid-latitudes remained marginally subtropical throughout the late Oligocene–early Miocene. Temperatures on land were similarly marginally subtropical, and rainfall was relatively

high, with strong seasonality. Annually laminated sediments in a 23 Ma maar lake indicate well-developed ENSO-like cycles.

The relative climatic and topographic stability in Zealandia through this period sustained a diverse forested terrestrial landscape and a complex marine biota. Importantly, a considerable decline in extent of terrestrial environments appears to have had little impact on the composition and diversity of biota.

REFERENCES

- Beu A.G. & Maxwell P.A. (1990) - Cenozoic Mollusca of New Zealand. NZ Geological Survey Paleontological Bulletin, 58, 1–518.
- Conran J.G., Mildenhall D.C., Lee D.E., Lindqvist J.K., Shepherd C., Beu A.G., Bannister J.M. & Stein J.K. (2014) - Subtropical rainforest vegetation from Cosy Dell, Southland: plant fossil evidence for Late Oligocene terrestrial ecosystems. NZ Journal of Geology and Geophysics, doi:10.1080/00288306.2014.888357.
- Cooper A. & Cooper R.A. (1995) - The Oligocene bottleneck and New Zealand biota: genetic record of a past environmental crisis. Proceedings of the Royal Society of London. Series B. Biological Sciences, 261, 293–302.
- Fordyce R.E. (2014) - A southern view of Oligocene marine tetrapods: Kokamu Greensand and Otekaike Limestone, Hakataramea Valley, New Zealand. Abstracts, Secondary Adaptations of Tetrapods to Life in the Water 7th triennial meeting, George Mason University, Virginia, June 2014.
- Jordan G.J., Carpenter R.J., Bannister J.M., Lee D.E., Mildenhall D.C. & Hill R.S. (2011) - High conifer diversity in Oligo-Miocene New Zealand. Australian Systematic Botany, 24, 121–136.
- Kamp P.J.J., Vincent K.A., Lucas K.R. & Tayler, M.J.S. (2013) - PMAP Series: A new paleoenvironment and paleogeography map set for understanding the New Zealand Cenozoic. In: Reid C.M. & Wandres A. (eds), Abstracts, Geosciences 2013 Conference, Christchurch, NZ. Geoscience Society of NZ Miscellaneous Publication, 136A, 52.
- Lee D.E., Lindqvist J.K., Beu A.G., Robinson J.H., Ayress M., Morgans H.E.G. & Stein J.K. (2014) - Geological setting and diverse fauna of a Late Oligocene rocky shore ecosystem, Cosy Dell, Southland. NZ Journal of Geology and Geophysics, doi:1080/00288306.2014.898666.
- Mildenhall D.C., Kennedy E.M., Lee D.E., Kaulfuss U., Bannister J.M., Fox B. & Conran J.G. (2014) - Palynology of the Early Miocene Foulden Maar, Otago, New Zealand: diversity following destruction. Review of Palaeobotany and Palynology, 204, 27–42.
- Reichgelt T., Kennedy E.M., Mildenhall D.C., Conran J.G., Greenwood D.R. & Lee D.E. (2013) - Quantitative palaeoclimate estimates for Early Miocene southern New Zealand: evidence from Foulden Maar. Palaeogeogr., Palaeoclimatol., Palaeoecol., 378, 36–44.
- Zachos J.C., Pagani M., Sloan L., Thomas E. & Billups K., (2001) - Trends, rhythms, and aberrations in global climate 65 Ma to present. Science, 292, 686–693.

Possible hyperthermal events (Dan-C2 and Lower 29n) in the lowermost Paleocene of the Brazos River area, Texas

Andrew D. Leighton^(a), Malcolm B. Hart^(a), Christopher W. Smart^(a), Matt Hampton^(b) & Melanie J. Leng^(c)

^(a) School of Geography, Earth & Environmental Sciences, Plymouth University, Drake Circus, Plymouth PL4 8AA, UK. E-mail: andrew.leighton@plymouth.ac.uk

^(b) Network Stratigraphic Consulting Ltd, Harvest House, Cranborne Road, Potters Bar, Hertfordshire EN6 3JF, UK

^(c) Department of Geology, University of Leicester, University Road, Leicester LE1 7RH, UK

Document type: Short note.

Manuscript history: received 15 May 2014; accepted 30 May 2014; editorial responsibility and handling by Gerald R. Dickens & Valeria Luciani.

KEY WORDS: Brazos River, foraminifera, hyperthermal events, Lower Paleocene, stable isotopes.

The Cretaceous/Paleogene boundary successions in Texas and Alabama record events relatively close to the Chicxulub impact site. Recent work in both areas has shown that there was a single ‘impact’ event that is coincident with the extinctions of planktic foraminifera and calcareous nannofossils, although the dinoflagellate cyst community was un-affected (Hart et al., 2012, 2013). The benthic foraminifera are little changed, with many taxa being found in both the Corsicana Mudstone Fm (uppermost Maastrichtian) and the Kincaid Mudstone Fm (lowermost Paleocene). In the sediments just above the erosive surface that marks the ‘impact’ event (and the K/Pg boundary following Molina et al., 2006) there are large benthic foraminifera, including nodosariids <1.5 mm in length and lenticulinids <1.5 mm in diameter. As *Lenticulina rotulata* Lamarck occurs throughout the succession, this taxon has been used for stable isotope analysis ($\delta^{18}\text{O}$ and $\delta^{13}\text{C}$) in a range of different size fractions. The results show both a variation in oxygen and carbon isotope values with size as well as a distinct cyclicity which, most likely, reflects astronomical tuning. It is possible, therefore, to use this cyclicity to determine the possible duration of zones P0 and P α (80–100 kys), and the timing of biotic recovery following the ‘impact’ event. The size of the stable isotope excursions (close to the base of zone P1a) is indicative of the Dan-C2 and the Lower 29n hyperthermal events, allowing direct correlation with the two other locations where these have been described: most notably in the Gubbio succession where there is also a good record of the magnetostratigraphy and biostratigraphy (Coccioni et al. 2010).

During the course of this work ADL and MBH re-discovered a section on the Brazos River (Texas) that had previously been described by Plummer (1926) but forgotten by later workers. This is located on the west bank of the Brazos River between the Darting Minnow and Cottonmouth creeks and has been described as River Bank South (Hart et al., 2012). Just above river level is the K/Pg boundary (‘Event Bed’) which is overlain by ~6 m of the Lower Paleocene (Hart et al.,

2012, fig. 3). Samples collected throughout this succession have been prepared for micropaleontological analysis, including foraminifera (benthic and planktic), ostracods, calcareous nannofossils and dinoflagellates cysts. Benthic foraminifera are both abundant and diverse throughout this succession. One of the most common species is *Lenticulina rotulata* Lamarck, an epifaunal/semi-infaunal species which has been used by other authors for stable isotope analysis from other K/Pg locations (e.g., Adatte et al., 2011).

Stable isotope analysis was performed on individual specimens from three different size fractions in order to assess the isotopic variation with specimen size and maturity. Specimens from the >500 μm , 500–250 μm and 250–150 μm size fractions were identified and checked to ensure no evident re-crystallization or chamber infilling. Approximately 15–100 mgm were required for isotope analysis. The stable isotope measurements were performed at the NERC Isotope Geosciences Laboratory (NIGL), British Geological Survey, Nottingham.

The cyclical appearance of the resulting $\delta^{13}\text{C}$ and $\delta^{18}\text{O}$ isotope signal is quite distinctive and appears to follow a Milanković frequency, indicative of a precession signal. In both sets of data ($\delta^{13}\text{C}$ and $\delta^{18}\text{O}$) there is a variable response in the >500 μm , 500–250 μm and 250–150 μm size fractions, with the greatest variation within the smallest (= more juvenile) specimens. The ontogenetic variation in stable isotope data from living benthic foraminifera has been described by Schumacher et al. (2010), with their data being comparable to the variation seen in our material. Schumacher et al. (2010) indicated that this variation in stable isotope data was the result of an in-faunal mode of life, with juveniles residing at a greater depth than the larger adults. Ishimura et al. (2012) have confirmed this variation, although they used the overall weight (i.e., calcification) of the specimens.

Key results of our research in the Gulf Coast are:

(1). The basal Paleocene, large, negative $\delta^{13}\text{C}$ excursion (Hart et al., 2005) is not evident, probably because the reworked spherule-rich bed and the sandstones of the ‘Event Bed’ represent a disturbed environment in which the stable isotope signal has been lost.

(2). The pattern of $\delta^{18}\text{O}$ and $\delta^{13}\text{C}$ excursions above the 'Event Bed' probably represents an orbital forcing. If this is a 21 kyr precession signal we can suggest that zone P0 represents ~30,000 years and that zone P α represents ~70,000 years. This would indicate that planktic foraminifera and calcareous nannofossils begin their recovery after 25–30 kyrs and that significant recovery is seen by zone P1a after 80–100 kyrs.

(3). The $\delta^{18}\text{O}$ excursion near the P α /P1a boundary may represent a short-lived <6°C temperature shift. This is coeval with the Dan-C2 or Lower 29n hyperthermal events of Coccioni et al. (2010) and the warming event 100 kyrs above the K/Pg boundary in the Boltsh Crater (Jolley et al., 2013).

REFERENCES

- Adatte, T., Keller, G. & Baum, G.R. (2011) - Age and origin of the Chicxulub impact and sandstone complex, Brazos River, Texas: evidence from lithostratigraphy and sedimentology. In: Keller, G. & Adatte, T. (eds.), *The end-Cretaceous mass extinction and the Chicxulub impact in Texas*. Society of Economic Paleontologists and Mineralogists, Special Publication, 100, 43-80.
- Coccioni, R., Frontalini, F., Bancalà, G., Fornaciari, E., Jovane, L. & Sprovieri, M. (2010) - The Dan-C2 hyperthermal event at Gubbio (Italy): global implications, environmental effects, and cause(s). *Earth Planet. Sci. Lett.*, 297, 298–305.
- Hart, M.B., Feist, S.E., Håkansson, E., Heinberg, C., Price, G.D., Leng, M.J. & Watkinson, M.P. (2005) - The Cretaceous-Paleogene boundary succession at Stevns Klint, Denmark: Foraminifers and stable isotope stratigraphy. *Palaeogeogr., Palaeoclimatol. Palaeoecol.*, 224, 6-26.
- Hart, M.B., Yancey, T.E., Leighton, A.D., Miller, B., Liu, C., Smart, C.W. & Twitchett, R.J. (2012) - The Cretaceous/Paleogene boundary on the Brazos River, Texas: New stratigraphic sections and revised interpretations. *Gulf Coast Association of Geological Societies Journal*, 1, 69-80.
- Hart, M.B., Harries, P.J. & Cárdenas, A.L. (2013) - The Cretaceous/Paleogene boundary events in the Gulf Coast: Comparisons between Alabama and Texas. *Gulf Coast Association of Geological Societies, Transactions*, 63, 235-255.
- Ishimura, T., Tsunogai, U., Hasegawa, S., Nakagawa, F., Oi, T., Kitazato, H., Suga, H. & Toyofuku, T. (2012) - Variation in stable carbon and oxygen isotopes of individual benthic foraminifera: tracers for quantifying the magnitude of isotopic disequilibrium. *Biogeosciences*, 9, 4353-4367.
- Jolley, D.W., Daly, R., Gilmour, I. & Kelley, S.P. 2013. Climatic oscillations stall vegetation recovery from K/Pg event devastation. *J. Geol. Soc. London*, 170, 477-482.
- Molina, E., Alegret, L., Arenillas, I., Arz, J.A., Gallala, N., Hardenbol, J., von Salis, K., Steurbaut, E., Vandenberghe, N. & D. Zaghbib-Turki, D. (2006) - The global boundary stratotype section and point for the base of the Danian Stage, Paleocene, Paleogene, "Tertiary", (Cenozoic) at El Kef, Tunisia – Original definition and revision. *Episodes*, 29, 263-278.
- Plummer, H. (1926) – Foraminifera of the Midway Formation in Texas. *University of Texas Bulletin*, 2644, 1-206.
- Schumacher, S., Jorissen, F.J., Mackensen, A., Gooday, A.J. & Pays, O. (2010) - Onogenetic effects on stable carbon and oxygen isotopes in tests of live (Rose Bengal stained) benthic foraminifera from the Pakistan continental margin. *Mar. Micropaleontol.*, 76, 92-103.

A new age model for the late Paleocene at ODP Site 1263, Walvis Ridge: new stable isotope and calcareous nannofossil data

Kate Littler ^(a), Melanie Leng ^(b), Claudia Agnini ^(c), James C. Zachos ^(d), Thomas Westerhold ^(e) & Ursula Röhl ^(e)

^(a) Camborne School of Mines, University of Exeter, Penryn Campus, Penryn, Cornwall, TR10 9FE, U.K. E-mail: k.littler@exeter.ac.uk

^(b) NERC Isotope Geosciences Laboratory, British Geological Survey, Nicker Hill, Keyworth, Nottingham, NG12 5GG, UK

^(c) Dipartimento di Geoscienze, Università degli Studi di Padova, Via Giovanni Gradenigo, 6 - I-35131, Padova, Italy

^(d) Department of Earth and Planetary Sciences, University of California Santa Cruz, 1156 High Street, Santa Cruz, CA 95064, USA

^(e) MARUM, University of Bremen, Leobener Strasse, 28359 Bremen, Germany

Document type: Short note.

Manuscript history: received 15 May 2014; accepted 30 May 2014; editorial responsibility and handling by Gerald R. Dickens & Valeria Luciani.

KEYWORDS: Age model, calcareous nannofossils, orbital tuning, Paleocene, South Atlantic, stable isotopes

ODP Site 1263 on Walvis Ridge is one of the shallowest Paleogene sites in the South Atlantic, with an estimated paleodepth of ~1500 m (ref). Here we present a new age model for the discontinuous late Paleocene sediments at Site 1263, based on new high-resolution bulk carbon isotope records, integrated with new calcareous nannofossil data. Through comparison with the orbitally-tuned bulk carbon isotope record at nearby ODP Site 1262 (ref), the existing high-resolution age model can be transferred to the shallower Site 1263 sediments. This will allow future geochemical, sedimentological and paleontological studies to be carried out, which will exploit the full potential of the ~2 km water column separation between the deep and shallow sites on the Walvis Ridge during this key interval of Earth's climate history.

At a current water depth of 2717 m, ODP Site 1263 is the shallowest of five sites on the Walvis Ridge, South Atlantic, drilled during ODP Expedition 208 (Zachos et al., 2004). Core recovered at this site by extended core barrel (XCB), from Holes 1263A–D, contain carbonate-rich sediments spanning the late Paleocene and early Eocene interval. The early Paleogene sediments at the deeper ODP Site 1262 (4759 m), recovered by hydrolic piston coring, have been extensively studied, with the generation of an orbitally-tuned age model (Westerhold et al., 2007, 2008), detailed calcareous nannofossil biostratigraphy (Agnini et al., 2007), and subsequent construction of both bulk (Zachos et al., 2010) and benthic high-resolution stable isotope records (Littler et al., in press). The Paleogene carbonate oozes at Site 1263 have thus far been investigated in less detail, owing in part to the non-continuous nature of the Paleocene core recovery. However, the excellent preservation of both planktic and benthic foraminifera, and other biogenic components such as fish teeth, in the Paleocene Site 1263 cores presents an opportunity to exploit the extensive paleodepth separation between Sites 1262 and 1263 to investigate climate, ocean circulation and carbon cycling in this

region. This new age model, therefore, is the foundation on which future geochemical studies will be built.

On the basis of new high-resolution bulk carbon isotope data from Holes 1263A and B, generated at the NERC Isotope Geosciences Laboratory (UK) and at the department of Earth and Planetary Sciences at the University of California at Santa Cruz (USA), we identify many of the eccentricity-paced A-D cycles known from the late Paleocene (Cramer et al., 2003; Zachos et al., 2010), including some of the larger 100 kyr-paced events associated with significant changes in bottom water temperature and the carbon cycle. The presence of these cycles at Site 1263 is further confirmed by the new high-resolution biostratigraphy, permitting the identification of calcareous nannofossil zones CP5 to CP8 (NP5 to NP9) in both Holes 1263A and 1263B.

REFERENCES

- Agnini C., Fornaciari E., Raffi I., Rio, D. Röhl U. & Westerhold T. (2007) - High-resolution nannofossil biochronology of middle Paleocene to early Eocene at ODP Site 1262: Implications for calcareous nannoplankton evolution. *Mar. Micropaleontol.* 64, 215–248.
- Cramer B.S., Wright J.D., Kent D.V. & Aubry M.P. (2003) - Orbital climate forcing of $\delta^{13}\text{C}$ excursions in the late Paleocene-early Eocene (chrons C24n-C25n). *Paleoceanography* 18 (4), 1097.
- Littler K., Röhl U., Westerhold T. & Zachos J.C. (in press) - A high-resolution benthic stable-isotope record for the South Atlantic: implications for orbital-scale changes in Late Paleocene–Early Eocene climate and carbon cycling. *Earth Planet. Sci. Lett.*
- Westerhold T., Röhl U., Laskar J., Raffi I., Bowles J., Lourens, L.J. & Zachos J.C. (2007) - On the duration of magnetochrons C24r and C25n and the timing of early Eocene global warming events: Implications from the Ocean Drilling Program Leg 208 Walvis Ridge depth transect. *Paleoceanography* 22, PA2201.

- Westerhold T., Röhl U., Raffi I., Fornaciari E., Monechi S., Reale V., Bowles J. & Evans H.F. (2008) - Astronomical calibration of the Paleocene time. *Palaeogeogr. Palaeoclimatol. Palaeoecol.*, 257, 377–403.
- Zachos J.C., Kroon D., Blum P. et al., (2004) - Proceedings of the Ocean Drilling Program, Initial Reports, Site 1263, 208, doi:10.2973/odp.proc.ir.208.104.2004.
- Zachos J.C., McCarren H., Murphy B., Röhl U. & Westerhold T. (2010) - Tempo and scale of late Paleocene and early Eocene carbon isotope cycles: Implications for the origin of hyperthermals. *Earth Planet. Sci. Lett.* 299, 242–249.

Deterioration of symbiont-bearing morozovellid (planktic foraminifera) habitat recorded within the Early Eocene Climatic Optimum: evidence from the Tethys and sub-tropical Atlantic Ocean

Valeria Luciani ^(a), Luca Giusberti ^(b), Eliana Fornaciari ^(b), Domenico Rio ^(b), Roberta D'Onofrio ^(a) & Jan Backman ^(c)

^(a) Dipartimento di Fisica e Scienze della Terra, University of Ferrara, Ferrara, Italy e-mail: lcu@unife.it

^(b) Dipartimento di Geoscienze, University of Padova, Padova, Italy

^(c) Department of Geology and Geochemistry, Stockholm University, SE-106 91 Stockholm, Sweden

Document type: Short note.

Manuscript history: received 15 May 2014; accepted 30 May 2014; editorial responsibility and handling by Gerald R. Dickens & Valeria Luciani.

KEY WORDS: Early Eocene Climatic Optimum (EECO), northeastern Italy, North Atlantic site, planktic foraminifera, Tethyan setting.

The early Paleogene section of Possagno (Venetian Prealps of northeastern Italy), deposited in a bathyal setting, provides an excellent magneto- and calcareous plankton stratigraphic record of the lower-middle Eocene transition as occurring in a marginal basin of the central-western Tethys (~55 to 46 Ma; Agnini et al., 2006; Luciani & Giusberti, 2014). This section therefore spans the time interval in which Earth's climate attained its warmest state of the Cenozoic, referred to as Early Eocene Climatic Optimum (EECO), when high-latitude sea surface temperatures increased by at least ~5°C (Zachos et al., 2001). The EECO peak warming represents a major turning point in the Cenozoic climate since it was followed by a long-term cooling, ultimately leading to the emplacement of a stable ice sheet on Antarctica (Zachos et al., 2001). Extremely high $p\text{CO}_2$ is considered to have played a primary control on the long-lasting EECO warmth. Superimposed to the long-term climate trend, short-lived (<200 kyr) peak-warming events, named hyperthermals, are recorded and related to major global carbon-cycle perturbations, the most extreme of which is the well-known Paleocene-Eocene Thermal Maximum (PETM).

Only a few studies have focused on paleoecological and evolutionary consequences of the EECO on planktic foraminifera. Within this group, the symbiont-bearing shallow-dwelling morozovellids and acarininids are of particular interest because they dominated the tropical and subtropical assemblages of early Paleogene oceans but almost completely disappeared ~38 Ma, near the Bartonian/Priabonian boundary. These forms, also known as muricates (muricae are conical pustules on the test wall), were indeed consistent calcifiers in the low-latitude early Paleogene oceans.

The Possagno section offers the exceptional opportunity to record the changes in relative abundance of this crucial component of the calcareous plankton across the EECO warmth and post-EECO climatic variability (Chron C24r to base Chron C20r, Zones E1 to lower E8; Luciani & Giusberti,

2014). A planktic foraminiferal response to the Paleogene maximum warmth appears evident because assemblages show significant variations that correlate with the pronounced $\delta^{13}\text{C}$ perturbation linked to the EECO. The dominance of the warm-water acarininids during the EECO can be interpreted as a consequence of the extreme warmth. In contrast, the significant reduction in abundance of morozovellids, which should share the warm, surface-water habitats with acarininids, is apparently contradictory. Dominance of acarininids, coupled with reduction in abundance of morozovellids, is a recurring feature within planktic foraminiferal assemblages across the PETM and ETM3 (or X) events, as recorded from Tethyan successions of northeastern Italy (Luciani et al., 2007; Agnini et al., 2009). The temporary decrease in morozovellid abundance during these hyperthermals was interpreted to reflect minor intolerance in this highly specialized group to the eutrophic conditions that were induced by the extreme warming events at the examined Tethyan successions. However, our analysis shows that the decline of morozovellids across the EECO is irreversible and cannot be explained by short- localised perturbations. The genus markedly drops in relative abundance from ~24% to ~5% and never recovers in northeastern Italy. The sub-tropical Atlantic Site 1051 shows the same dramatic demise (from ~40% to ~10%) across the EECO interval, recognized on the basis of magneto-biostratigraphic correlation. The differences in the relative proportions of morozovellids clearly indicate a morozovellid preference for an open-ocean setting. Our data demonstrate therefore that the profound climatic changes across the EECO signal a first dramatic step in the crisis of the early Paleogene symbiont-bearing group. Possible causes explaining the permanent deterioration of morozovellid habitat may include a crisis of the symbiosis processes, such as bleaching. We know the importance of photosymbiosis in extant species for foraminiferal test calcification and ecology and we assume similar requirements for fossil forms. One of the possible reasons for bleaching is the extremely high temperature evident during the EECO. A bleaching episode caused by global warming has been proposed to explain the second muricate

crisis, which occurred at the Middle Eocene Climatic Optimum, when large acariniids and *Morozovelloides* (*Morozovella* descendent genus) markedly declined (Luciani et al., 2010; Edgar et al., 2012). There is, however, scarce documentation on mechanisms responsible for bleaching and, besides the extreme warming, a number of other factors may have been involved. Other causes to explain the morozovellid crisis across the EECO may consist of complex interactions with other microfossil groups, such as radiolarians, diatoms or dinoflagellates, which may have been competitors in the use of the same algal-symbionts (radiolarians) or symbiont-providers, but we still need detailed comparisons of trends in other fossil groups to validate this hypothesis. Protracted intervals of weak water-column stratification and increased eutrophication are known as hostile conditions for the highly specialized oligotrophic morozovellids. These conditions are documented in several ocean sites by the recorded decline in the surface-benthic $\delta^{13}\text{C}$ gradient (Hilting et al., 2008) and are considered linked to turnovers in calcareous nannofossil assemblages (Schneider et al., 2011). Weakened thermal stratification with increased vertical mixing is predicted for many (although not all) oceanic areas during hyperthermals. The fact that the morozovellid collapse occurs in the EECO implies that a threshold, never reached before, was surpassed. The ecological effects of the event may have combined to produce conditions unfavourable for continued diversification of morozovellids but not harsh enough to cause their extinction. Because morozovellids, exhibit transient reduction in abundance during the hyperthermals preceding the EECO and the imprecise definition of this event, we are not able to pinpoint the exact turning point of the morozovellid decline, i.e. whether it began within the EECO, at one of the hyperthermal events just below the EECO or at the termination of the event.

The carbon-isotope curve in the interval following the EECO at Possagno shows several relatively small negative $\delta^{13}\text{C}$ excursions, thought to represent minor hyperthermals, most of which can be correlated with those recorded in the tropical Atlantic by Sexton et al. (2011). Although the $\delta^{13}\text{C}$ perturbations these possible hyperthermals at Possagno are small, they are associated with significant, short-lived changes in planktic foraminiferal communities that record distinct increases of the warm-water acariniids similar to those observed in the pre-EECO hyperthermals from Tethyan sections, thus implying a high susceptibility of planktic foraminifera to climate changes.

REFERENCES

- Agnini, C., Muttoni, G., Kent, D. V. & Rio, D. (2006) - Eocene biostratigraphy and magnetic stratigraphy from Possagno, Italy: the calcareous nannofossils response to climate variability: *Earth Planet. Sci. Lett.*, 241, 815–830.
- Agnini, C., Macrì, P., Backman, J., Brinkhuis, H., Fornaciari, F., Giusberti, L., Luciani, V., Rio, D., Sluijs, A. & Speranza, F. (2009) - An early Eocene carbon cycle perturbation at ~52.5 Ma in the Southern Alps: Chronology and biotic response. *Paleoceanography*, 24, PA2209, doi:10.1029/2008PA001649, 2009.
- Edgar, K.M., Bohaty, S.M., Gibbs, S.J., Sexton, P.F., Norris, R.D. & Wilson, P.A. (2012) - Symbiont 'bleaching' in planktic foraminifera during the Middle Eocene Climatic Optimum. *Geology*, 41, 15-18, doi:10.1130/G33388.1.
- Hilting, A.K., Kump, L.R. & Bralower, T.J. (2008) - Variations in the oceanic vertical carbon isotope gradient and their implications for the Paleocene–Eocene biological pump. *Paleoceanography*, 23, PA3222.
- Luciani, V., Giusberti, L., Agnini, C., Backman, J., Fornaciari, F. & Rio D. (2007) - The Paleocene–Eocene Thermal Maximum as recorded by Tethyan planktonic foraminifera in the Forada section (northern Italy), *Mar. Microplentol.*, 64, 189-214.
- Luciani, V., Giusberti, L., Agnini, C., Fornaciari, F., Rio, D., Spofforth, D.J.A., Pälike, H. (2010) - Ecological and evolutionary response of Tethyan planktonic foraminifera to the middle Eocene climatic optimum (MECO) from the Alano section (NE Italy). *Palaeogeogr. Palaeoclimatol. Palaeoecol.*, 292, 82-95.
- Luciani V. & Giusberti L. (2014) - Reassessment of the early–middle Eocene planktic foraminiferal biomagnetostratigraphy: new evidence from the Tethyan Possagno section (NE Italy) and Western North Atlantic Ocean ODP Site 1051. *J. Foram. Res.*, 44, 2, 187-201.
- Schneider, L.J. Bralower, T.J. & Kump, L.J. (2011) - Response of nannoplankton to early Eocene ocean de-stratification. *Palaeogeogr. Palaeoclimatol. Palaeoecol.*, 310, 152-162.
- Sexton, P.F., Norris, R.D., Wilson, P.A., Pälike, H., Westerhold, T., Röhl, U., Bolton, C. & Gibbs, S.J. (2011) - Eocene global warming events driven by ventilation of oceanic dissolved organic carbon. *Nature*, 471, 349-352.
- Zachos, J.C., Pagani, M., Sloan, L.C., Thomas, E. & Billups, K. (2001) - Trends, rhythms, and aberrations in global climate 65 Ma to Present. *Science*, 292, 686-693.

A Multi-Proxy Study of the PETM at the Zumaia Section, northern Spain

Hayley R. Manners^(a,b), Stephen T. Grimes^(a), Paul A. Sutton^(a), Tom Dunkley-Jones^(c), Richard D. Pancost^(d), Melanie J. Leng^(e), Phillip Jardine^(f), Laura Domingo^(g,h,i), Malcolm B. Hart^(a) & Nieves Lopez-Martinez^(j)

^(a) School of Geography, Earth & Environmental Sciences, Plymouth University, Drake Circus, Plymouth, Devon, PL4 8AA, UK. E-mail: hayley.manners@plymouth.ac.uk

^(b) School of Ocean and Earth Sciences, University of Southampton, National Oceanography Centre, Waterfront campus, Southampton, SO14 3ZH, UK

^(c) School of Geography, Earth and Environmental Sciences, University of Birmingham, Edgbaston, Birmingham, B15 2TT, UK

^(d) Organic Geochemistry Unit, The Cabot Institute, School of Chemistry, University of Bristol, Bristol, BS8 1TS, UK

^(e) NERC Isotope Geosciences Laboratory, British Geological Survey, Nottingham, NG12 5GG, UK

^(f) Palaeoenvironmental Change Research Group, Department of Environment, Earth & Ecosystems, The Open University, Walton Hall, Milton Keynes, MK7 6AA, UK

^(g) Departamento de Paleontología and ^(h) Departamento de Estratigrafía. Universidad Complutense de Madrid, 28040, Madrid, Spain

⁽ⁱ⁾ Departamento de Ingeniería Geológica. Universidad Politécnica de Madrid, 28003, Madrid, Spain

^(j) Earth and Planetary Sciences Department. University of California, Santa Cruz, CA 95064, USA

^(†) Deceased.

Document type: Short note.

Manuscript history: received 15 May 2014; accepted 30 May 2014; editorial responsibility and handling by Gerald R. Dickens & Valeria Luciani.

KEY WORDS: Carbon Isotope Excursion, *n*-alkanes, northern Spain, PETM.

The Paleocene - Eocene Thermal Maximum (PETM) is thought to be the most appropriate analogue of the Cenozoic for rapid injection of carbon into the global climate system, and provides insight into how the Earth system responds to rapid carbon cycle perturbations (Zachos et al., 2008). However, debate continues over the amount, source and mechanisms of carbon release.

Here, we report results for total organic carbon ($\delta^{13}\text{C}_{\text{TOC}}$), bulk carbonate ($\delta^{13}\text{C}_{\text{CARB}}$), and *n*-alkane ($\delta^{13}\text{C}_{n\text{-alkane}}$) $\delta^{13}\text{C}$ profiles across the PETM at the marine section of Zumaia, northern Spain (Fig. 1). This new data builds upon the work of Manners et al. (2013) and represents the first $\delta^{13}\text{C}_{n\text{-alkane}}$ record for this section along with the highest resolution $\delta^{13}\text{C}_{\text{CARB}}$ record, allowing comparison of terrestrial and marine carbon isotope excursions (CIEs) within one section. The bulk $\delta^{13}\text{C}_{\text{TOC}}$ profile records a CIE magnitude of 4.1‰, whilst the terrestrial $\delta^{13}\text{C}_{n\text{-alkane}}$ profile records 5.5‰ and the marine $\delta^{13}\text{C}_{\text{CARB}}$ values record 6.0‰. This demonstrates that no obvious difference is recorded in the $\delta^{13}\text{C}_{n\text{-alkane}}$ (terrestrial) and $\delta^{13}\text{C}_{\text{CARB}}$ (marine) CIE magnitudes at this site, contrary to observations reported between other widespread localities.

What is unusual about our new data is that a sharp ^{13}C -enrichment is recorded in both $\delta^{13}\text{C}_{n\text{-alkane}}$ and $\delta^{13}\text{C}_{\text{CARB}}$ values immediately following the onset of the CIE. This could be interpreted as reflecting a change in the terrestrial paleohydrological regime leading to the reworking of ancient, pre-CIE, carbon into the system, or it could reflect a two stage CIE onset caused by the pulsed release of ^{13}C -depleted carbon.

Furthermore, the initial onset of the CIE recorded in the $\delta^{13}\text{C}_{\text{TOC}}$, $\delta^{13}\text{C}_{\text{CARB}}$ and $\delta^{13}\text{C}_{n\text{-alkane}}$ records appear to be temporally offset from one another, with the $\delta^{13}\text{C}_{\text{CARB}}$ profile recording the earliest onset, and the $\delta^{13}\text{C}_{n\text{-alkane}}$ profile

recording the latest onset. This is suggested to reflect the long residence time of soil organic carbon, as previously described by Tipple et al. (2011).

Furthermore, the onset of the CIE as recorded by $\delta^{13}\text{C}_{\text{TOC}}$ and $\delta^{13}\text{C}_{n\text{-alkane}}$ data appears to occur after the start of deposition of the Siliciclastic Unit (SU). Previously, the onset of the CIE and deposition of the SU have been thought to be coincident (Schmitz et al., 2001), thus suggesting that the change in lithology is related to the PETM. Our new data may suggest evidence for an increased hydrological cycle during the period preceding the PETM, which in turn may have brought about sedimentological changes through deeper continental erosion.

Finally, palynological analysis was used to assess the extent of reworking and degradation, and also to determine the dominant terrestrial palynomorph types throughout the Zumaia section. At the current data resolution, no shift in the dominant vegetation from mixed gymnosperm/angiosperm to purely angiosperm flora was detected at this locality, although transport bias has to be taken into account in this interpretation.

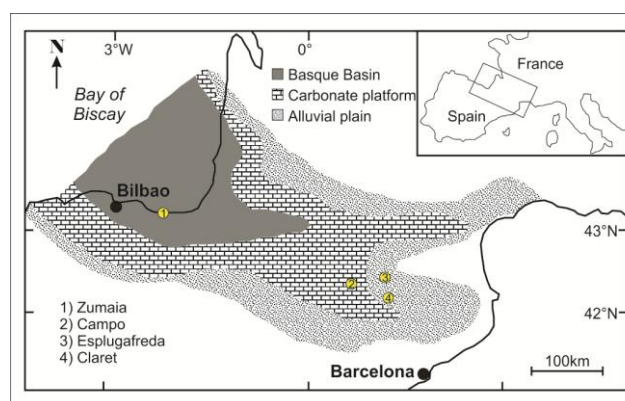


Fig. 1 – Palaeogeographic reconstruction and location map, redrawn from Schmitz and Pujalte (2003) illustrating the location of the Zumaia section and that of other important PETM sections in Northern Spain referred to in Manners et al. (2013).

REFERENCES

- Manners H. R., Grimes S.T., Sutton P.A., Domingo L., Leng M.J., Twitchett R.J., Hart M.B., Dunkley-Jones T., Pancost R.D., Duller R. & Lopez-Martinez N. (2013) - Magnitude and profile of organic carbon isotope records from the Paleocene–Eocene Thermal Maximum: Evidence from northern Spain. *Earth Planet. Sci. Lett.*, 376, 220-230.
- Schmitz B., Pujalte V. & Núñez-Betelu K. (2001) - Climate and sea-level perturbations during the Incipient Eocene Thermal Maximum: evidence from siliciclastic units in the Basque Basin (Ermua, Zumaia and Trabakua Pass), northern Spain. *Palaeogeogr. Palaeoclimatol. Palaeoecol.*, 165, 299-320.
- Schmitz B. & Pujalte V. (2003) - Sea-level, humidity, and land-erosion records across the initial Eocene thermal maximum from a continental-marine transect in northern Spain. *Geology*, 31, 689-692.
- Tipple B.J., Pagani M., Krishnan S., Dirghangi S.S., Galeotti S., Agnini C., Giusberti L. & Rio D. (2011) - Coupled high-resolution marine and terrestrial records of carbon and hydrologic cycles variations during the Palaeocene-Eocene Thermal Maximum (PETM). *Earth Planet. Sci. Lett.*, 311, 82 – 92.
- Zachos J.C., Dickens G.R. & Zeebe R.E. (2008) - An early Cenozoic perspective on greenhouse warming and carbon-cycle dynamics. *Nature* 451, 279-283.

The Late Danian Event at Site 1209: a rapid diversification of calcareous nannofossils

Francesco Miniati ^(a), Simonetta Monechi ^(a) & Carlotta Cappelli ^(a)

^(a) Dipartimento di Scienze della Terra, Università di Firenze, Via La Pira 4, I-50121 Firenze, Italy. E-mail: simonetta.monechi@unifi.it

Document type: Short note.

Manuscript history: received 15 May 2014; accepted 30 May 2014; editorial responsibility and handling by Gerald R. Dickens & Valeria Luciani.

KEY WORDS: calcareous nannofossils, Central Pacific, LDE hyperthermal, Paleocene.

Site 1209 (Shatsky Rise, Central Pacific) represents one of the most continuous and complete stratigraphic successions for the Paleocene. The presence of an astronomically calibrated magnetostratigraphy (Westerhold et al., 2008) and a complete carbonate and oxygen isotope record (Westerhold et al., 2011) make this site suitable for high resolution biostratigraphic and paleoclimatic studies.

The Paleocene is a time interval characterized by a long-term warming trend marked by some intervals of intense warming indicated as “hyperthermals”, associated with a negative carbon isotopic excursion (CIE). In addition to the well known PETM (Paleocene/Eocene Thermal Maximum), other lesser negative carbon isotopic excursions were recognized during the Danian.

The Late Danian Event (LDE) (Bornemann et al., 2009) was established for the first time in the Egyptian section of Qreiya and characterized by a negative shift in the $\delta^{13}\text{C}$ curve. This event was correlated with the CIE-DS1 of Zumaia (Arenillas et al. 2008) and the “Top Chron C27n event” of ODP Site 1209 (Westerhold et al., 2011). At ODP Site 1209 the LDE is marked by a double peak in carbon isotopes close to the top of C27n with an age of 61.75 Ma, a total duration of about 200Ka and a suggested 2°C warming of the deep ocean. The LDE has been also recognized with the characteristic double peak at Site 1262 (Walvis Ridge, South Atlantic).

The Danian is an interval of diversification in the calcareous nannoplankton assemblage with the appearance of new morphological structures and forms. In particular, fasciculiths and sphenoliths evolved in a short lapse of time and dominate the Paleocene. During the LDE several paleoenvironmental changes have been suggested. Monechi et al. 2013 have shown for Site 1262 how this event has influenced the calcareous nannofossil assemblages and the diffusion of fasciculiths; furthermore, the onset of LDE coincides with the beginning of the First Radiation of fasciculiths (occurrence of *Lithoptychius*).

The calcareous nannofossil content at Site 1209 has been investigated across the LDE in order to verify the previous correlation, to improve the biostratigraphy of Fuqua et al. 2008 and describe the ecological responses among fasciculiths and sphenoliths linked to these distinctive environmental perturbations.

The calcareous nannofossil studies have confirmed the correlation between the base of LDE and the beginning of the First Radiation (*Lithoptychius*), as observed at Site 1262, Zumaia and Qreiya sections, pointing to the global significance of this event. Quantitative analyses on *Diantholitha*, *Lithoptychius* and *Fasciculithus* have allowed the identification of a succession of numerous events and the evolutionary trends.

The LDE is characterized by the following features:

- a) a sharp increase in the abundance of *Diantholitha* that occurs shortly below the onset of the LDE.
- b) an increase in the species richness of fasciculiths, within the LDE
- c) the Lowest Continuous Occurrence of *Sphenolithus primus*

ACKNOWLEDGEMENTS

Funding for this research was provided by the Ministero dell'Istruzione dell'Università e della Ricerca (MIUR/PRIN 2011) and the University of Florence.

REFERENCES

- Arenillas I.J., Molina E., Ortiz S. & Schmitz B. (2008) - Foraminiferal and $\delta^{13}\text{C}$ isotopic event-stratigraphy across the Danian-Selandian transition at Zumaya (northern Spain): Chronostratigraphic implications. *Terra Nova*, 20(1), 38–44.
- Bornemann A., Schulte P., Sprong J., Steurbaut E., Youssef M. & Speijer R.P. (2009) - Latest Danian carbon isotope anomaly and associated environmental change in the southern Tethys (Nile Basin, Egypt). *J. Geol. Soc. London*, 166, 1135-1142.

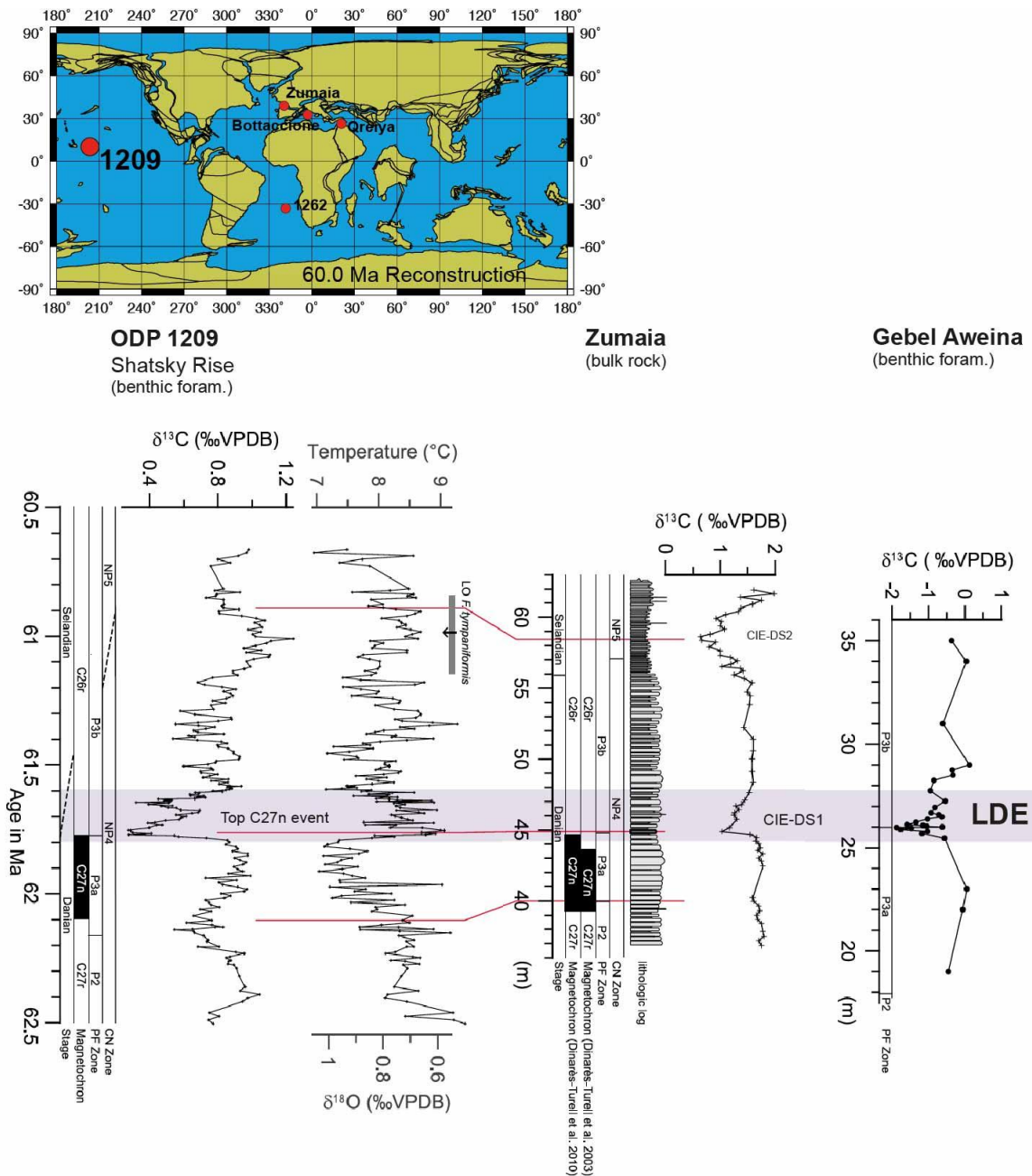


Fig.1 – (A) Paleogeographic reconstruction at 60.0Ma showing the location of ODP Site 1209 (Shatsky Rise, Central Pacific) and other sections, <http://www.ods.de/ods/services/paleomap/paleomap>. (B) Benthic foraminiferal $\delta^{13}\text{C}$ and $\delta^{18}\text{O}$ and stratigraphy from ODP Site 1209, Gebel Aweina in the Nile Basin (Egypt) and bulk rock $\delta^{13}\text{C}$ from Zumaia (Spain) across the Latest Danian Event (LDE). The pink shaded area represents the correlation between the LDE (Gebel Aweina) and the CIE-DS1 (Zumaia) and TopC27n event (ODP Site 1209). Modified from Westerhold et al. (2011).

Bralower, T. J., et al. (2002), Proceedings of the Ocean Drilling Program, Initial Reports, 198, U.S. Gov. Print. Off., Washington, D. C.

Fuqua L.M., Bralower T.J., Arthur M.A. & Patzkowsky M.E. (2008) - Evolution of calcareous nannoplankton and the recovery of marine food webs after the Cretaceous - Paleocene mass extinction. *Palaios*, 23, 185-194.

Monechi S., Reale V., Bernaola G. & Balestra B. (2013) - The Danian/Selandian boundary at Site 1262 (South Atlantic) and in the Tethyan region: Biomagnetostratigraphy, evolutionary trends in fasciculiths and environmental

effects of the Latest Danian Event. *Mar. Micropaleontol.*, 98, 28-40.

Westerhold T., Röhl U., Raffi I., Fornaciari E., Monechi S., Reale V., Bowles J. & Evans H.F. (2008) - Astronomical calibration of the Paleocene Time. *Palaeogeogr. Palaeoclimatol. Palaeoecol.*, 257, 377-403.

Westerhold T., Röhl U., Donner B., McCarren H.K. & Zachos J.C. (2011) - A complete high-resolution Paleocene benthic stable isotope record for the central Pacific (ODP Site 1209). *Paleoceanography*, 26, PA2216.

Global increase in export productivity during the Middle Eocene Climatic Optimum (MECO)?

Iris Moebius ^(a,b), Oliver Friedrich ^(a,b), Kirsty M. Edgar ^(c) & Phil F. Sexton ^(d)

^(a) Institute for Geosciences, Goethe-University Frankfurt, Altenhöferallee 1, 60438 Frankfurt, Germany. E-mail: moebius@em.uni-frankfurt.de

^(b) Institute for Geosciences, University Heidelberg, Im Neuenheimer Feld 234-236, 69120 Heidelberg, Germany

^(c) School of Earth Science, University of Bristol, Wills Memorial Building, Queen's Road, Bristol BS8 1RJ, UK

^(d) Centre for Earth, Planetary, Space & Astronomical Research, The Open University, Milton Keynes, MK7 6AA, UK

Document type: Short note.

Manuscript history: received 15 May 2014; accepted 30 May 2014; editorial responsibility and handling by Gerald R. Dickens & Valeria Luciani.

KEY WORDS: foraminifera, MECO, Middle Eocene Climatic Optimum, paleoproductivity.

The Middle Eocene Climatic Optimum (MECO, ~40 Ma) was a gradual, but short-living warming event in the midst of the long-term cooling trend of the Eocene (Bohaty and Zachos, 2003). It was characterized by a 3-6°C warming of global surface and bottom waters (Bohaty et al., 2009; Edgar et al., 2010) during the ~500 – 650 kyr period (Bohaty et al., 2009; Westerhold & Röhl, 2013) (Fig. 1A). The event culminated in a brief (50 kyr) peak-warming interval and subsequent rapid cooling where climate returned to pre-event conditions (e.g., Bohaty et al., 2009) (Fig. 1A). The MECO was also accompanied by a global shoaling of the CCD (Bohaty et al., 2009; Pälike et al., 2012), a proposed increase in atmospheric CO₂ (Bijl et al., 2010) and a small, positive δ¹³C excursion restricted to peak-warming (Bohaty et al., 2009) (Fig. 1B).

Here, we investigate ecological changes caused by the oceanic warming associated with the MECO and on the implications these findings have on regional and global export productivity and bottom-water oxygenation, as well as deep-water circulation patterns. Specifically, a study was performed on Ocean Drilling Program (ODP), Site 1051 in the subtropical North Atlantic off the coast of Florida, investigating benthic foraminiferal assemblages, benthic foraminiferal accumulation rates (BFAR) from the >125 μm size fraction and planktonic foraminiferal abundances (PFA) from the >300 μm size fraction. Carbonate contents and lightness values show that the sediments were not subject to significant dissolution in spite of the CCD shoaling (Fig. 1E)

Previous hyperthermals similar to the MECO (such as the Paleocene- Eocene Thermal Maximum, PETM) were subject to significant faunal changes associated with rapid warming and coupled changes in ocean chemistry (e.g., Thomas, 1998). However, at Site 1051 little change in the benthic foraminiferal species composition can be identified. Instead, two transient intervals of BFARs increasing by one order of magnitude and a substantial increase in PFAs can be observed associated with peak warming and ~300 kyr thereafter (~40.02 Ma and 39.66

Ma) (Fig. 1C and D). The first peak is accompanied by elevated abundances of radiolarians (Witkowski et al., 2014). This combined evidence indicates an increase in surface and bottom-water trophic state at this site, potentially associated with increased continental run-off associated with an enhanced hydrological cycle or enhanced upwelling.

To assess the global significance of these findings, we compared our results to previous studies to evaluate if the increase in trophic state at the termination and following the MECO was a regional effect, or if the signal was a more widespread or even global significance. Episodes of enhanced total organic carbon (TOC) content in marine sediments of the Tethys (Luciani et al., 2010; Spofforth et al., 2010) point to enhanced productivity in the Tethys, and even though a reasonable age model for this Site is missing, it appears that these episodes of increased TOC content may represent correlatable periods of strengthened productivity in the subtropical North Atlantic and the Tethys. Total organic carbon content is generally very low in the sediments of Site 1051, but the recorded increase in productivity (that would be associated with carbon burial) in different ocean basins during and slightly after the peak warming period tentatively implies that carbon burial may have been associated with the termination of the MECO. Additionally, benthic foraminiferal assemblage composition and siliceous microfossil content records from the Southern Ocean revealed an increase in surface and export productivity during the MECO (40.40 – 39.95 Ma; Moebius et al., in press; Witkowski et al., 2012), and a siliceous phytoplankton record from the South Atlantic also indicates an increase in trophic state some time during the MECO, although correlation is not possible due to an insufficient age model at this site (Renaudie et al., 2010).

Overall, our data show that the extent and rate of environmental change associated with the MECO varied greatly in different ocean basins and that the processes influencing bottom waters were subject to large latitudinal differences. Nevertheless, it appears that increases in primary and export productivity were a feature of the MECO in many shore and slope locations, but the extent and timing of these eutrophication events varied between the different ocean basins

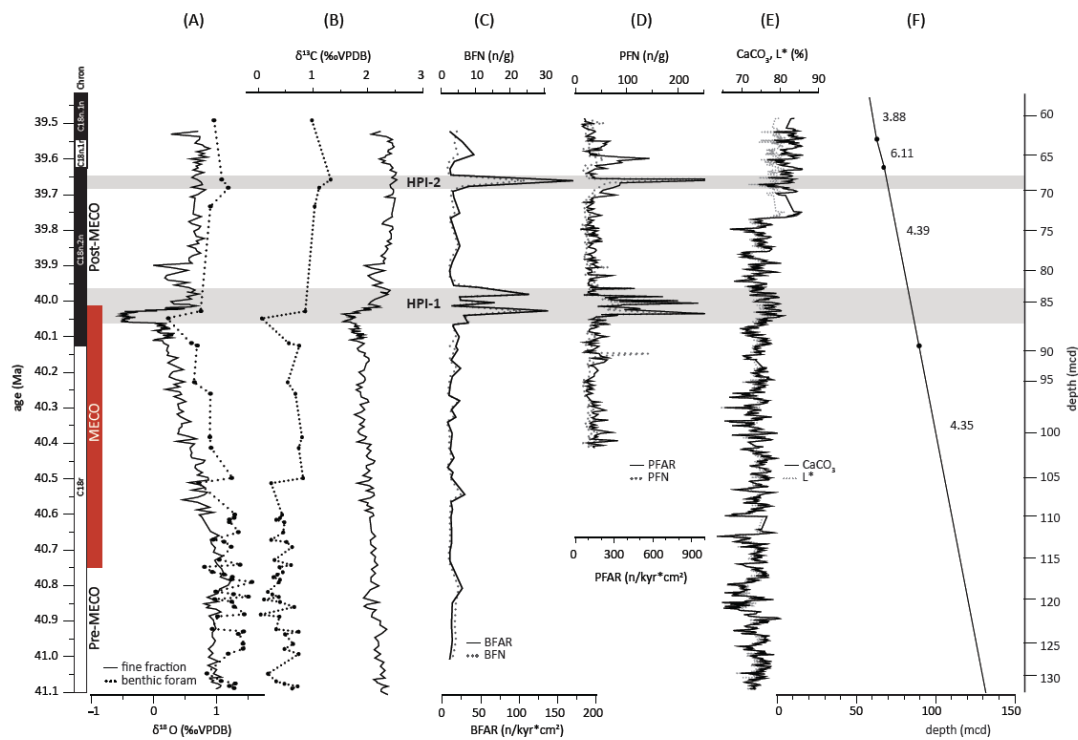


Fig.1 – Stable oxygen and carbon isotopes from (Bohaty et al., 2009; Edgar et al., 2010). (A, B), benthic and planktic foraminiferal accumulation rates and abundances (C, D), Carbonate concentration and lightness (L^*) of the sediment (E) and sedimentation rates (F).

and between the proxy's used to reconstruct paleo-productivity. This suggests that different microorganisms may have different thresholds and coping mechanisms for environmental change, complicating inter-proxy comparisons.

REFERENCES

- Bijl P.K., Houben A.J.P., Schouten S., Bohaty S.M., Sluijs A., Reichart G.-J., Sinninghe Damsté J.S. & Brinkhuis H. (2010) - Transient Middle Eocene Atmospheric CO_2 and Temperature Variations. *Science*, 330(6005), 819-821.
- Bohaty S.M. & Zachos J.C. (2003) - Significant Southern Ocean warming event in the late middle Eocene. *Geology*, 31(11), 1017.
- Bohaty S. M., Zachos J.C., Florindo F. & Delaney M.L. (2009) - Coupled greenhouse warming and deep-sea acidification in the middle Eocene. *Paleoceanography*, 24(2), PA2207.
- Edgar K.M., Wilson P.A., Sexton P.H., Gibbs S.J., Roberts A. & Norris R.D. (2010) - New biostratigraphic, magnetostratigraphic and isotopic insights into the Middle Eocene Climatic Optimum in low latitudes. *Palaeogeogr. Palaeoclimatol. Palaeoecol.*, 297, 670–682.
- Luciani V., Giusberti L., Agnini C., Fornaciari E., Rio D., Spofforth D.J.A. & Pälike H. (2010) - Ecological and evolutionary response of Tethyan planktonic foraminifera to the middle Eocene climatic optimum (MECO) from the Alano section (NE Italy). *Palaeogeogr. Palaeoclimatol. Palaeoecol.*, 292(1-2), 82-95.
- Moebius I., Friedrich O. & Scher H.D. (in press) - Changes in Southern Ocean bottom water environments associated with the Middle Eocene Climatic Optimum (MECO). *Palaeogeogr., Palaeoclimatol., Palaeoecol.*
- Pälike H. et al. (2012) - A Cenozoic record of the equatorial Pacific carbonate compensation depth. *Nature*, 488(7413), 609-614.
- Renaudie J., Danelian T., Saint Martin S., Le Callonnec L. & Tribouillard N. (2010), Siliceous phytoplankton response to a Middle Eocene warming event recorded in the tropical Atlantic (Demerara Rise, ODP Site 1260A). *Palaeogeogr., Palaeoclimatol., Palaeoecol.*, 286(3-4), 121-134.
- Spofforth D J.A., Agnini C., Pälike H., Rio, D., Fornaciari E., Giusberti L., Luciani V., Lanci L. & Muttoni G. (2010) - Organic carbon burial following the Middle Eocene Climatic Optimum in the central western Tethys. *Paleoceanography*, 25(3), PA3210.
- Thomas E. (1998) - Biogeography of the late Paleocene benthic foraminiferal extinction. In: Aubry M.-P., Lucas S. & Berggren W.A. (Eds.), *Late Paleocene-Early Eocene Climatic and Biotic Events in the Marine and Terrestrial Records*, 214-243, Columbia University Press, New York.
- Westerhold T. & Röhl U.(2013), Orbital pacing of Eocene climate during the Middle Eocene climate optimum and the chron C19r event – missing link found in the tropical western Atlantic. *Geochem. Geophys. Geosyst.*, 14(11), 4811–4825.
- Witkowski J., Bohaty S.M., McCartney K. & Harwood D.M: (2012) - Enhanced siliceous plankton productivity in response to middle Eocene warming at Southern Ocean ODP Sites 748 and 749 *Palaeogeogr. Palaeoclimatol. Palaeoecol.*, 326, 78-94.

How does leaf morphology reflect palaeoclimate conditions? A quantitative approach tracing terrestrial climate conditions during the Palaeogene

Karolin Moraweck ^(a), Michaela Grein ^(b), Wilfried Konrad ^(c), Johanna Kovar-Eder ^(d), Lutz Kunzmann ^(a), Jiří Kvaček ^(e),
Christoph Neinhuis ^(f), Anita Roth-Nebelsick ^(d), Madeleine Streubig ^(a) & Christopher Traiser ^(d)

^(a) Museum of Mineralogy and Geology, Senckenberg Natural History Collections Dresden, Königsbrücker Landstr. 159, 01109, Dresden, Germany. E-mail: karolin.moraweck@senckenberg.de

^(b) Department of Palaeontology, State Museum of Natural History, Rosenstein 1, 70191 Stuttgart, Germany

^(c) Department Natural History, Übersee-Museum Bremen, Bahnhofsplatz 13, 28195 Bremen, Germany

^(d) Department Palaeobiology, University of Tübingen, Hölderlinstr. 12, 72074 Tübingen, Germany

^(e) Department Palaeontology, Natural History Museum Prague, Cirkusová 1740, 193 00 Prague 9, Czech Republic

^(f) Institute of Botany, Technical University of Dresden, Zellescher Weg 20 b, 01069 Dresden, Germany

Document type: Short note.

Manuscript history: received 15 May 2014; accepted 30 May 2014; editorial responsibility and handling by Gerald R. Dickens & Valeria Luciani.

KEY WORDS: Climate Leaf Analysis Multivariate Program, CO₂, Coexistence Approach, Leaf Margin Analysis, leaf morphology, palaeoclimate, Palaeogene, Stomata.

The Palaeogene was a time of extraordinarily strong climate and environmental changes. During this period, the Earth's climate experienced a major global warming and subsequent cooling and shifting from more or less ice-free greenhouse conditions during the Paleocene/Eocene turnover towards substantial glaciation of Antarctica during the Oligocene (Zachos et al., 2001). In addition to changes in the floristic composition of plant assemblages (Mai, 1995), also morphological and anatomical adaptations (leaf size, stomatal parameters) through time give indication of distinct climatic and environmental changes (Wing & Greenwood, 1993).

To trace these changes we analyse plant assemblages from Palaeo-Europe that thrived under various environmental conditions (coastal and riparian habitats, volcanic sites, hinterland floras) covering the whole Palaeogene and early Neogene. To track morphometric and anatomical traits during times of vast environmental and climatic changes we used the following species that are characteristic elements of riparian palaeovegetation: *Rhodomyrtophyllum reticulosum*, a dominant evergreen subtropical species within the middle to late Eocene (Glinka and Walther 2003) and *Platanus neptuni*, representing an important thermophilous element of subtropical to temperate vegetation in Europe within the late Eocene up to the Oligocene-Miocene (Roth-Nebelsick et al., 2014).

During our studies we focused both on measuring morphometric traits (length/width-ratio, pairs of secondary veins per leaf size, length of the tertiary vein network per area) and anatomical traits (stomatal density, stomatal index) as well as on determining palaeoclimate conditions within different stratigraphic positions by using Leaf Margin Analysis, Climate Leaf Analysis Multivariate Program and the Coexistence Approach (Fig. 1). The aim is (1) to plot palaeoclimate

estimates (mainly MAT, seasonality in the distribution of precipitation) and shifts in leaf traits among different palaeoenvironmental conditions (e.g. coastal plain and hinterland floras) through time; (2) to compare them with commonly used climate reconstructions derived mainly by marine records and (3) to compare the estimates of each method with the focus on applicability to different environments. First palaeoclimatic results for the late Eocene until the Oligocene-Miocene turnover show no significant temperature trend (Grein et al., 2013, Moraweck et al., 2013,

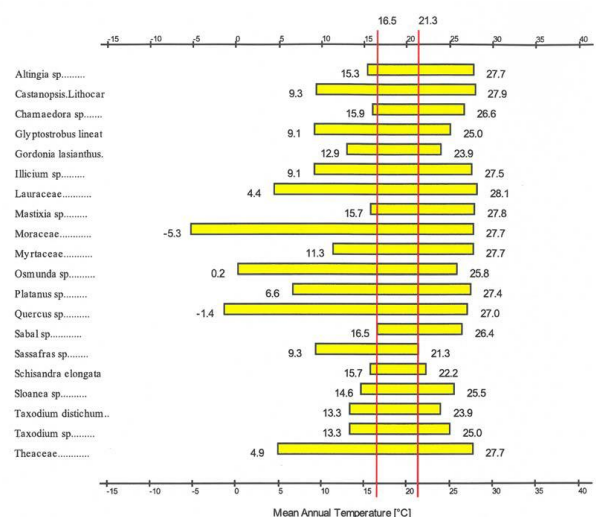


Fig. 1 – Mean annual temperature estimates, derived by CA for a typical flora of the Weissenluisen basin (from Moraweck et al. 2013).

Roth-Nebelsick et al., 2014).

In addition to the analysis of floral assemblages using leaf physiognomic methods and nearest living relatives, we also focused on tracing anatomical adaptations of the above mentioned taxa to track possible adaptation strategies on atmospheric pCO₂-changes (e.g. stomatal density, stomatal index). The contribution will focus on (1) the possibility of

coupling morphometric traits and stomatal parameters with climate conditions, (2) the results obtained by the quantitative palaeoclimate methods for a variety of sites within the Palaeogene; (3) on taphonomic biases due to different palaeoenvironments and thus (4) the applicability of different methods to derive palaeoclimatic evidences.

ACKNOWLEDGEMENTS

We kindly thank the VolkswagenStiftung for funding the project "Ecophysiological signals of plant fossils as indicators of climatic and atmospheric change during the Paleogene". For further information: <http://www.volkswagenstiftung.de/de/foerderung/personenundstruktur/en/forschung-in-museen/bewilligungen-2013.html>.

REFERENCES

- Glinka U. & Walther H. (2003) - *Rhodomyrtophyllum reticulosum* (ROSSM.) KNOBLOCH & Z. KVAČEK – ein bedeutendes eozänes Florenelement im Tertiär Mitteleuropas. Feddes Repertorium, 114, 30-55.
- Grein M., Oehm C., Konrad W., Utescher T., Kunzmann L. & Roth-Nebelsick A. (2013) - Atmospheric CO₂ from the late Oligocene to early Miocene based on photosynthesis data and fossil leaf characteristics. Palaeogeogr. Palaeoclimatol. Palaeoecol., 374, 41-51.
- Mai D.H. (1995) - Tertiäre Vegetationsgeschichte Europas. Springer, 1-691.
- Moraweck K., Kunzmann L. & Uhl D. (2013) - Palaeoclimate reconstruction within the upper Eocene in central Germany using fossil plants. EGU General Assembly Conference Abstracts, 15, 5851.
- Roth-Nebelsick A., Oehm C., Grein M., Utescher T., Kunzmann L., Friedrich J.-P. & Konrad W. (2014) - Stomatal parameters of *Platanus neptuni* leaf fossils: implications for atmospheric CO₂ during the Oligocene. Rev. of Palaeobot. Palyno., 206, 1-9.
- Wing S.L. & Greenwood D.R. (1993) - Fossils and fossil climate: the case for equable continental interiors in the Eocene. Philosophical Transactions of the Royal Society of London, Series B 341, 243-252.
- Zachos J.C., Pagani M., Sloan, L.C., Thomas E. & Billups K. (2001) - Trends, rhythms and aberrations in global climate 65 Ma to present. Science, 292, 686-693.

Calcareous nannoplankton response at the culmination of the Paleogene greenhouse world

Cherry Newsam^(a) & Paul R. Bown^(a)

(a) Department of Earth Sciences, University College London, Gower Street, London, United Kingdom. E-mail: cherry.newsam.11@ucl.ac.uk

Document type: Short note.

Manuscript history: received 15 May 2014; accepted 30 May 2014; editorial responsibility and handling by Gerald R. Dickens & Valeria Luciani.

KEY WORDS: calcareous nannoplankton, Eocene, Oligocene.

The Eocene-Oligocene transition (EOT) was a profound climatic interval marking the culmination of the long term Paleogene shift from a 'greenhouse' to an 'icehouse' world. The marine and terrestrial environments underwent physical, chemical and biological changes across half a million years, from 34 to 33.5 Ma (Coxall & Pearson, 2007). Significant global change in this interval is highlighted by prominent positive shifts in oxygen isotope ($\delta^{18}\text{O}$) records, which indicate stepped temperature change, signalling the start of the icehouse world (Coxall & Pearson, 2007; Miller et al., 2009). There is also evidence for the initiation and expansion of significant Antarctic ice sheets (Coxall et al., 2005) and coincident global sea level fall of approximately 80 m (Miller et al., 2009), >1 km deepening of the calcite compensation depth (CCD) (Coxall et al., 2005) and high levels of marine biotic disturbance, with elevated rates of plankton extinction and turnover during the EOT (Coxall & Pearson, 2007; Dunkley Jones et al., 2008; Pearson et al., 2008). The Eocene-Oligocene boundary, which lies within this transition, is marked by the extinction of the planktonic foraminifera family Hantkeninidae, and numerous extinctions in calcareous nannoplankton, planktonic foraminifera and radiolarians occur through the interval.

Calcareous nannoplankton, marine calcifying haptophyte algae, dominated the phytoplankton record of the early Paleogene and were highly diverse. Throughout the greenhouse to icehouse transition the calcareous nannoplankton underwent a significant diversity loss (Aubry, 1992; Bown et al., 2004) into the early Oligocene, coincident with a rise in diatoms. Previous work across the EOT rapid climatic shift has documented changes in the diversity and population composition of calcareous nannoplankton, identifying shifts in the assemblage structure to try to understand the cause for this diversity demise (Dunkley-Jones et al., 2008; Villa et al., 2008). Few high-resolution records exist across this key climatic event and none of note in the northern hemisphere. Here we therefore aim to document the calcareous

nannoplankton diversity and assemblage changes across the EOT dynamic interval at high resolution, from a northern hemisphere mid latitude site, in order to compile global records of calcareous nannoplankton during the EOT, and to build a greater understanding of how the calcareous nannoplankton responded to the palaeoceanographic/ palaeoclimatic changes at this time. Furthermore, our study sections were carefully targeted in order to deliver calcareous microfossil preservation of exceptional quality, a crucial prerequisite for the acquisition of high quality diversity and population data.

The sections used in this study are from IODP Expedition 342, Site U1411 located in the North Atlantic off the coast of Newfoundland on the Southeast Newfoundland Ridge. The site was drilled in 2012, in drift deposits located at approximately 41°37'N 48°60'W in the Northeast Atlantic and was a mid-depth site at approximately 2850 metres below sea level (mbsl) in the Eocene. The sedimentary sequence at this site had rapid accumulation rates reaching up to 3 cm/kyr at the EOT (Norris et al., 2014). The pelagic deep-sea sediments from Site U1411 are nanofossil ooze and clays with high quality carbonate preservation due to the site's position above the CCD and the high clay content. This has resulted in the exceptional preservation of calcareous microfossils akin to that seen in the hemipelagic sediments of the Paleogene Kilwa Group of coastal Tanzania (Bown et al., 2008; Norris et al., 2014). The exceptional preservation has been recognized under the light microscope and scanning electron microscope by the presence of fragile nannoplankton taxa, species maintaining fine details such as delicate grills across the central areas and ornamentation on spines, the presence of holococcoliths and the presence of intact coccospheres (see Fig. 1). Fragile planktonic foraminifera (e.g., *Hantkenina*) and glassy preservation are also documented from this site.

So far, 111 samples have been quantitatively and semi quantitatively analysed from Site U1411 across the EOT. The samples contain well-preserved, highly diverse calcareous nanofossil assemblages. The diversity records reflect the exceptional preservation at Site U1411 with very high species richness and the changes in assemblage structure throughout the EOT documented by the SHE analysis. The assemblages

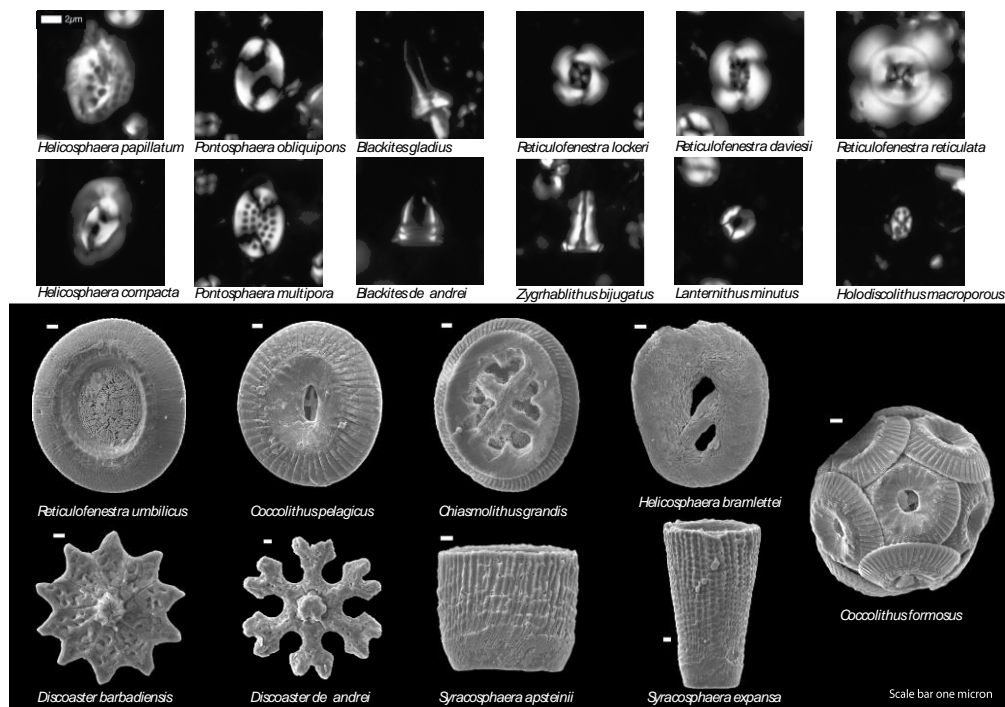


Fig.1 – Exceptional preservation of the calcareous nanofossils from IODP Expedition 342 shown in light microscope (upper images) and scanning electron microscope images (lower images).

are dominated by the reticulofenestrids, which comprise on average 80% of the assemblage. Simple abundance counts highlight key species last occurrences, such as, *Discoaster barbadensis*, *Discoaster saipanensis* and *Coccolithus formosus*, and acmes, *Clausicoccus subdistichus*, as well as major shifts in abundance patterns across this transition in high resolution. In order to examine the relationship between plankton evolution and the striking climatic change, taxa have been grouped relative to their temperature and nutrient preferences and palaeoenvironmental indices have been produced to identify shifts in key groups of taxa and to identify destabilisation in the assemblage structure due to the palaeoceanographic/palaeoclimatic perturbation through the two million year transition. The effects of both changing sea surface temperature and surface water productivity are seen in these nanoplankton assemblage changes.

REFERENCES

- Aubry M. (1992) - Late Paleogene calcareous nanoplankton evolution: A tale of climatic deterioration. In: Prothero, D. R. & Berggren, W. A. (Eds.) Eocene-Oligocene Climatic and Biotic Evolution. Princeton University Press, 272-309.
- Bown P.R., Lees J. A. & Young J. R. (2004) - Calcareous nanoplankton evolution and diversity. In: Thierstein, H. & Young, J. R. (Eds.) Coccolithophores – From molecular processes to global impact. Springer-Verlag, 481-508.
- Bown P.R., Dunkley-Jones T., Lees J.A., Pearson, P.N., Randell R., Coxall H. K., Mizzi J., Nicholas C., Karega A., Singano J. & Wade B.S. (2008) - A calcareous microfossil Konservat-Lagerstätte from the Paleogene Kilwa Group of coastal Tanzania. Geol. Soc. Am. Bull., 120, 3-12.
- Coxall H.K., Wilson P.A., Palike H., Lear C.H. & Backman J. (2005) - Rapid stepwise onset of Antarctic glaciation and deeper calcite compensation in the Pacific Ocean. Nature, 433, 53-57.
- Coxall H.K. & Pearson P.N. (2007) - The Eocene-Oligocene transition. In: Williams, M., Hayward, A., Gregory, J. & Schmidt, D. N. (Eds) Deep time perspectives on climate change: Marrying the signal from computer models and biological proxies. The Micropaleontological Society Special Publication, 351-388.
- Dunkley-Jones T., Bown, P.R., Pearson P.N., Wade, B.S., Coxall H.K. & Lear C.H. (2008) – Major shifts in calcareous phytoplankton assemblages through the Eocene-Oligocene transition of Tanzania and their implications for low-latitude primary production. Paleocyanography, 23, 4, 1-14.
- Miller K.G., Wright J.D., Katz M.E., Wade B.S., Browning J.V., Cramer B.S. & Rosenthal Y. (2009) - Climate threshold at the Eocene-Oligocene transition: Antarctic ice sheet influence on ocean circulation. The Geological Society of America Special Paper, 452, 169-178.
- Norris R.D., Wilson P.A., Blum P. & the Expedition 342 Scientists (2014) - Paleogene Newfoundland Sediment Drifts and MDHDS Test. Proceedings of the Integrated Ocean Drilling Program, 342.
- Pearson P.N., McMillan I.K., Wade B.S., Dunkley-Jones T., Coxall H.K., Bown P.R. & Lear C.H. (2008) - Extinction and environmental change across the Eocene-Oligocene boundary in Tanzania. Geology, 36, 2, 179-182.
- Villa G., Fioroni C., Pea L., Bohaty S.M. & Persico D. (2008) - Middle Eocene-late Oligocene climate variability: Calcareous nanofossil response at Kerguelen Plateau, Site 748. Mar. Micropaleontol., 69, 173-192.

High-resolution paleotemperature record of the surface ocean from the Eocene-Oligocene boundary of the South Australian Coast

Bradley N. Opdyke ^(a), Anna M. Haiblen ^(a) Andrew P. Roberts ^(a) & Paul A. Wilson ^(b)

^(a) The Australian National University, Research School of Earth Sciences, Canberra ACT 0200 Australia. E-mail: Bradley.Opdyke@anu.edu.au

^(b) Ocean & Earth Science, National Oceanography Centre, Southampton, European Way, Southampton, SO14 3ZH, UK

Document type: Short note.

Manuscript history: received 15 May 2014; accepted 30 May 2014; editorial responsibility and handling by Gerald R. Dickens & Valeria Luciani.

KEY WORDS: Antarctic Ice Sheet, Eocene-Oligocene boundary, Mg/Ca Temperature Proxy

Relatively well-preserved benthic foraminifera (*Cibicides cf. perforatus*) are found in clay-rich lithologies of the late Eocene Blanche Point Formation, which crops out along the coastline south of Adelaide, South Australia (shelf embayment, paleolatitude ~50°S; estimated paleo-water depth ~50 m). This stratigraphic section spans the Latest Eocene through to an Eocene-Oligocene unconformity. The polarity of Blanche Point Formation sediments is reversed up to the unconformity. Above the unconformity a normal polarity is recorded. The NP19/20-N21 boundary is identified at this location based on the last occurrence of the nannofossil *Discoaster saipanensis* in the Blanche Point Formation, 12.5m below the unconformity. The sedimentation rate is calculated to be 46 m/my. Analysis of the stable isotopic composition of *Cibicides cf. perforatus* suggests that the stratigraphic section includes glaciation ‘Step 1’ of the stable isotopic shift known to have occurred at the Eocene-Oligocene boundary (Coxall et al. 2005, Bohaty et al 2012). In the Blanche Point Formation, stable oxygen isotopes in *C. cf. perforatus* shift from a $\delta^{18}\text{O}$ value of -0.1‰ VPDB prior to ‘Step 1’ to 0.3‰ VPDB during ‘Step 1’, roughly equivalent to a 2°C drop in temperature if no ice volume change occurred. Mg/Ca data also indicate a temperature drop of just over 2°C early in ‘Step 1’. In the horizon immediately below the unconformity, a further decrease in Mg/Ca is observed, which suggests at least a further 2°C cooling. This temperature drop is not reflected in the stable isotopic results. These data represent the first detailed, high-latitude paleotemperature record from a shallow-water site of the latest Eocene in the Southern Ocean.

REFERENCES

Bohaty S.M., Zachos J.C. & Delaney M.L. (2012) - Foraminiferal Mg/Ca evidence for Southern Ocean cooling across the Eocene-Oligocene transition. *Earth Planet. Sci. Lett.*, 317, 251-61.

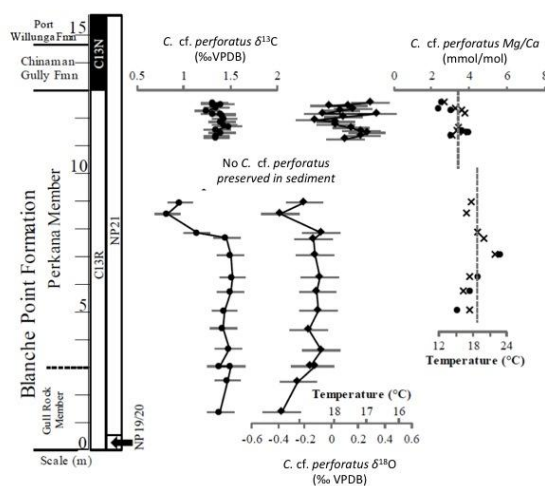


Fig.1 – Stratigraphy and geochemical data from the Blanche Point Formation. The latest Eocene *Cibicides cf. perforatus* stable isotopic and Mg/Ca results indicate pronounced surface water cooling, likely the beginning of ‘Step 1’ of Eocene-Oligocene transition. Error bars on the stable isotopic data are 95% confidence intervals. Temperature is calculated from $\delta^{18}\text{O}$ using the equation of Shakleton (1974). The value for $\delta^{18}\text{OSW}$ is taken from Zachos et al. (2001). A value of 0.64 is added to $\delta^{18}\text{O}$ results to correct *Cibicides* measurements to the *Uvigerina* scale (Mulitza et al. (2003). Mg/Ca was measured using LA-ICPMS. Crosses represent measurements obtained from chambers, dots represent measurements from test centers, on the umbilical side. The two dashed lines indicate the average Mg/Ca values for measurements prior to, and during, glaciation ‘Step 1.’ Mg/Ca temperature calculations are based on unpublished unpublished foraminifera culture experiments, conducted at Catalina Island and by Stephen Eggins (pers com).

Coxall H.K., Wilson P.A., Palike H., Lear C.H. & Backman J. (2005) - Rapid stepwise onset of Antarctic glaciation and deeper calcite compensation in the Pacific Ocean. *Nature*, 433, 7021, 53-7.

Mulitza S., Boltovskoy D., Donner B., Meggers H. Paul A. & Wefer G. (2003) - Temperature: delta O-18 relationships of planktonic foraminifera collected from surface waters. *Palaeogeogr. Palaeoclimatol. Palaeoecol.*, 202 (1-2), 143-52.

- Shackleton N.J. (1974) - Attainment of isotopic equilibrium between ocean water and the benthonic foraminifera genus *Uvigerina*: Isotopic changes in the ocean during the last glacia. *Colloques Internationaux du C.N.R.S.*, 219, 203-9.
- Waghorn D.B. (1989) - Middle Tertiary calcareous nanofossils from Aire District, Victoria - A comparison with equivalent assemblages in South Australia and New Zealand. *Mar. Micropaleontol.*, 14, 1-3, 237-255.
- Zachos J., Pagani M., Sloan L., Thomas E. & Billups K. (2001) - Trends, rhythms, and aberrations in global climate 65 Ma to present. *Science*, 292, 5517, 686-93.

The Early Eocene Climatic Optimum: chronological constraints and environmental impact at the North Iberian continental margin

Silvia Ortiz ^(a), Aitor Payros ^(b), Isabel Millán ^(c), Javier Arostegui ^(d), Xabier Orue-Etxebarria ^(b) & Estibaliz Apellaniz ^(b)

^(a) PetroStrat Ltd, Tan-y-Graig, Parc Caer Seion, Conwy, LL32 8FA, Wales, UK. E-mail: silvia.ortiz@petrostrat.com

^(b) Department of Stratigraphy and Paleontology, Faculty of Science and Technology, University of the Basque Country (UVP/EHU), B° Sarriena s/n, 48940 Leioa, Spain

^(c) Earth Sciences Department, Geological Institute, ETH Zürich, Sonneggstrasse 5, 8092 Zürich, Switzerland

^(d) Department of Mineralogy and Petrology, Faculty of Science and Technology, University of the Basque Country (UVP/EHU), B° Sarriena s/n, 48940 Leioa, Spain

Document type: Short note.

Manuscript history: received 15 May 2014; accepted 30 May 2014; editorial responsibility and handling by Gerald R. Dickens & Valeria Luciani.

KEY WORDS: EECO, foraminifera, mineralogy, North Iberian continental margin, paleoclimate, stable isotopes.

It has long been recognized that the early Paleogene represents the warmest period of the past 80 million years. There were no significant polar ice sheets, high-latitude seas and deep-sea waters were several degrees warmer than today, and latitudinal gradients were low (Shackleton & Boersma, 1981). This long-term warm phase peaked at the Early Eocene Climatic Optimum (EECO; 52 to 50 Ma) and was followed by a period of global cooling and ice cap growth, which peaked in the early Oligocene Glacial Maximum (Zachos et al., 2001). The EECO was linked to high atmospheric $p\text{CO}_2$ injected into the ocean-atmosphere system, and intense global warming, but its cause(s), timing and environmental impact had not been studied in detail to date.

New insights are provided from a sedimentological, stable isotope, mineralogical and micropaleontological study of a 1100 m-thick Lower-Middle Eocene deep-marine succession accumulated on the North Iberian continental paleomargin (Spain) (Fig. 1). The succession exposed at the Barinatxe and Gorrondatxe beaches (western Pyrenees, southeastern coast of the Bay of Biscay) is one of the most complete and expanded Eocene deep-sea sections in the world (Bernaola et al., 2006; Payros et al., 2006). The fact that the Global Stratotype Section and point (GSSP) for the base of the Lutetian Stage has recently been defined in this section (Molina et al., 2011) demonstrates its suitability for multidisciplinary stratigraphic studies. The EECO is represented by a 410 m-thick interval characterized by the scarcity of hemipelagic limestones, the abundance of dark marls, which record a reduction in carbonate content and an increase in kaolinite, and the occurrence of conspicuous red layers with a high siderite and pyrite content.

For the first time, a series of stratigraphically significant events frame the EECO. Based on this analysis, the EECO took place at biozones E5/P7-E6/P8 and NP12 and lasted for ~ 1.8 Myr. It is marked by a rapid 1.5‰ drop in $\delta^{13}\text{C}$, which records the addition of ^{13}C -depleted carbon into the ocean-atmosphere system. This process intensified the greenhouse effect and resulted in significant warming of the sea-surface, which is recorded by planktic foraminiferal assemblages. A hotter climate and a perennial rainfall regime strengthened the hydrological cycle and increased the supply of terrestrial organic matter and iron oxides into the sea. Eventually, these changes affected the deep-sea bottom, leading to post-mortem dissolution of calcareous microfossils and increased methanogenesis, which caused the formation of siderite and created conditions in which opportunistic foraminifera thrived.

Consumption of atmospheric CO_2 through silicate weathering processes favoured a subsequent gradual recovery. This culminated abruptly with a global cooling episode, which is locally recorded by an increase in high-latitude foraminifera and the accumulation of lowstand resedimentation deposits. Taking everything into account, findings indicate that the main driving force of the EECO was long-term variation in atmospheric $p\text{CO}_2$.

ACKNOWLEDGMENTS

This study is a contribution to Research Project CLG2011-23770 (Ministerio de Economía y Competitividad, Spanish Government) and Research Group of the Basque University System, Basque Government, IT-631-13.

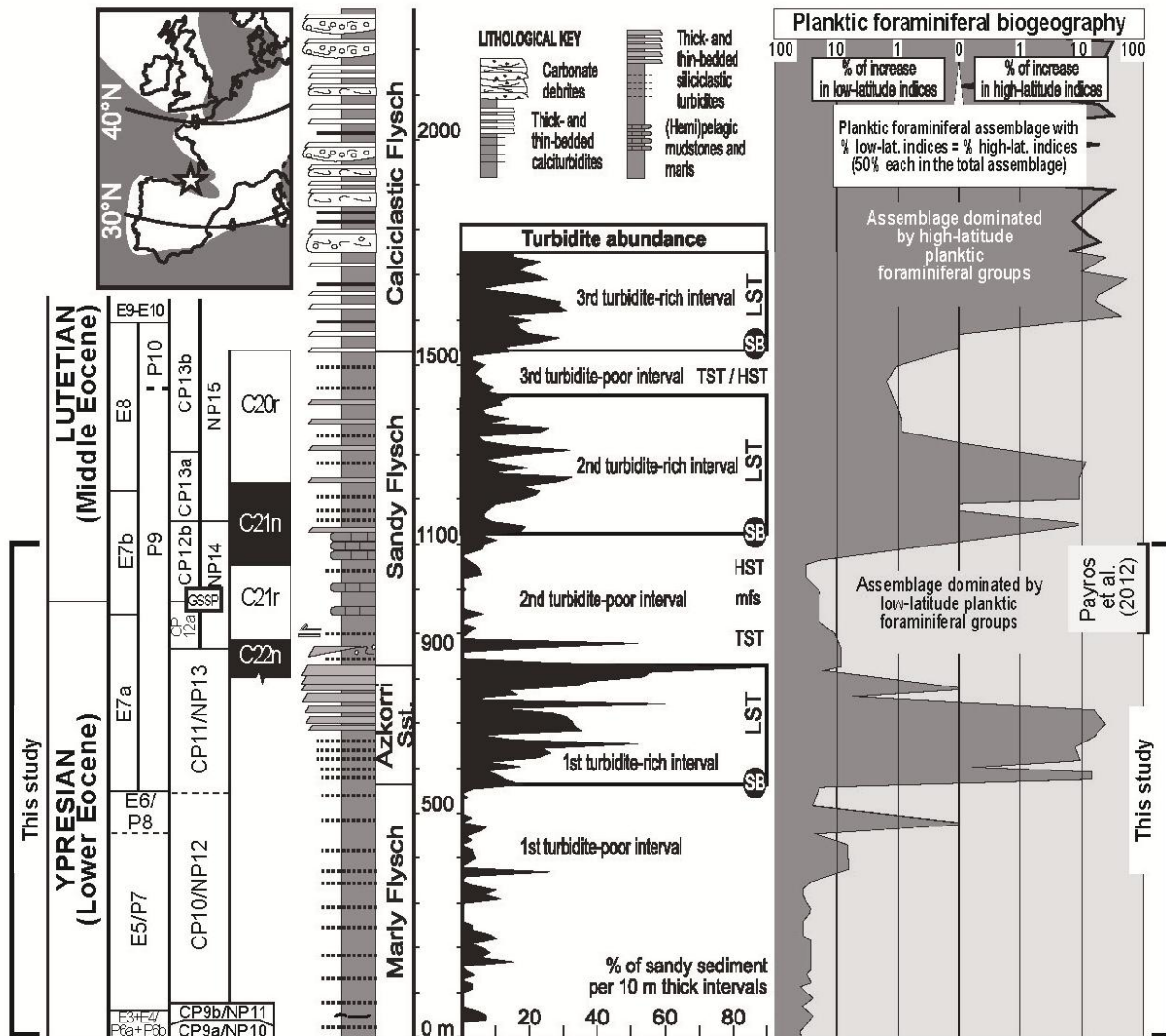


Fig.1 – Inset: paleogeographic location (white star) of the Barinatzte-Gorrondatxe area (white: land; grey: sea). Simplified lithology of the Eocene deep-marine succession in the Barinatzte-Gorrondatxe area, showing chronostratigraphy (planktic foraminiferal E and P scales; calcareous nannofossil CP and NP scales), distribution of turbidites, depositional sequences (SB: sequence boundary; LST: lowstand systems tract; TST: transgressive system tract; mfs: maximum flooding surface; HST: highstand systems tract), and planktic foraminiferal paleobiogeographic indices; based on Payros et al. (2006). The succession studied herein extends from 0 to 1100 m. GSSP: Global Stratotype Section and Point.

REFERENCES

- Bernaola G., Orue-Etxebarria X., Payros A., Dinarès-Turell J., Tosquella J., Apellaniz E. & Caballero F. (2006) - Biomagnetostratigraphic analysis of the Gorrondatxe section (Basque Country, Western Pyrenees): Its significance for the definition of the Ypresian/Lutetian boundary stratotype. *Neues Jahrb. Geol. P.-A.*, 241, 67-109.
- Molina E., Alegret L., Apellaniz E., Bernaola G., Caballero F., Dinarès-Turell J., Hardenbol J., Heilman-Clausen C., Larrasoana J.C., Luterbacher H., Monechi S., Ortiz S., Orue-Etxebarria X., Payros A., Pujalte V., Rodríguez-Tovar F.J., Tori F., Tosquella J. & Uchman A. (2011) - The Global Standard Stratotype-section and Point (GSSP) for the base of the Lutetian Stage at the Gorrondatxe section, Spain. *Episodes*, 34(2), 86-108.

- Shackleton N.J. & Boersma, A. (1981) - The climate of the Eocene ocean. *J. Geol. Soc. London*, 138, 153-157.
- Payros A., Orue-Etxebarria X. & Pujalte V. (2006) - Covarying sedimentary and biotic fluctuations in Lower – Middle Eocene Pyrenean deep-sea deposits: palaeoenvironmental implications. *Palaeogeogr. Palaeoclimatol. Palaeoecol.*, 234, 258-276.
- Payros A., Ortiz S., Alegret L., Orue-Etxebarria X., Apellaniz E. & Molina E. (2012) - An early Lutetian carbon-cycle perturbation: insights from the Gorrondatxe section (western Pyrenees, Bay of Biscay). *Paleoceanography*, 27, PA2213, doi: 10.1029/2012PA002300.
- Zachos J.C., Pagani M., Sloan L.C., Thomas E. & Billups K. (2001) - Trend, rhythms, and aberrations in global climate 65 Ma to present. *Science*, 292, 686-693.

Morozovella gorrondatxensis vs *Morozovella crater*: taxonomy and biostratigraphic significance

Xabier Orue-Etxebarria ^(a), Aitor Payros ^(a), Fernando Caballero ^(a), Estibaliz Apellaniz ^(a), Victoriano Pujalte ^(a) & Silvia Ortiz ^(b)

^(a) Dept. Stratigraphy and Paleontology, Faculty of Science and Technology, University of the Basque Country (UPV/EHU), Ap. 644, E48080 Bilbao, Spain- E-mail: xabi.orueetxebarria@ehu.es

^(b) PetroStrat Ltd, Tan-y-Graig, Parc Caer Seion, Conwy, LL32 8FA, Wales, UK

Document type: Short note.

Manuscript history: received 15 May 2014; accepted 30 May 2014; editorial responsibility and handling by Gerald R. Dickens & Valeria Luciani.

KEY WORDS: Eocene, Lutetian, planktonic foraminifera, *Morozovella*, biostratigraphy.

Morozovella gorrondatxensis was formally defined at the Gorrondatxe section (Biscay province, Basque Country, western Pyrenees) almost 30 years ago (Orue-Etxebarria, 1985). However, the species was not catalogued in the Atlas of Eocene Planktonic Foraminifera (Pearson et al., 2006), as it was included in synonymy with *Morozovella crater* (Hornibrook, 1958). In 2011, the ICS and the IUGS selected Gorrondatxe as the Global Stratotype Section and Point (GSSP) for the base of the Lutetian Stage due to its suitability for detailed, multidisciplinary stratigraphic studies (Molina et al., 2011). This recognition gives previous studies carried out in Gorrondatxe a renewed stratigraphic value. Accordingly, the taxonomic and biostratigraphic significance of *M. gorrondatxensis* has now been re-examined (Orue-Etxebarria et al., 2014).

Morozovella gorrondatxensis is characterized by a trochospiral, plano-convex test with a lobulate equatorial outline and an angular axial outline with well-developed muricocarina. Its spiral side is almost flat, but shows a small convexity in the first part of the spire. The umbilical side is highly convex. The test is composed of about 10 chambers arranged in two whorls, the last whorl showing 4½-5 chambers that rapidly increase in size. These chambers are imbricated on the spiral side, appear flattened and are tangentially wider than radially high; their sutures range from slightly curved to oblique. On the umbilical side, the chambers are triangular and slightly inflated, showing rounded umbilical rims; the intercameral sutures are radial and depressed. The umbilicus is relatively small, deep and open. The aperture is interiomarginal and in an umbilical-extraumbilical position. The diameter of the test ranges from 0.5 to 0.6 mm. The wall is finely perforate and its surface is generally smooth but rugose on the umbilical side.

When compared with *M. crater*, the characteristics of *M. gorrondatxensis* are distinct enough to be ascribed to a separate species. Firstly, the equatorial outline is more lobulate in *M.*

crater than in *M. gorrondatxensis*. Secondly, the umbilical side of *M. gorrondatxensis* is lower than that of *M. crater*, whereas the spiral side is more convex in the former. Thirdly, the umbilicus is smaller in *M. gorrondatxensis* than in *M. crater*, and has a less marked muricae on the circumumbilical collar. Finally, successive chambers in the last whorl of *M. gorrondatxensis* increase in size rapidly, whereas those of *M. crater*, being essentially equidimensional, increase in size gradually.

These differences clearly stand out in samples containing both species and show in fact that the characteristics of *M. gorrondatxensis* fall outside the morphological variability of *M. crater*. It must be acknowledged, however, that younger, more evolved specimens of *M. gorrondatxensis*, are slightly larger than the more primitive specimens, have a wider umbilicus, and their muricocarina is more prominent, therefore giving an appearance morphologically closer to *M. crater*. An evolution towards progressively bigger tests with more clearly marked ornamentation is common in most planktonic foraminiferal species. Interestingly, however, the stratigraphic range of *M. crater* does not reach the stratigraphic levels containing the fully evolved morphotype of *M. gorrondatxensis*, as the disappearance of *M. crater* overlapped with the appearance of *M. gorrondatxensis* in its most primitive form.

The lowest occurrence of *M. gorrondatxensis* in the Gorrondatxe section was found 115 m above the Lutetian GSSP, within the upper part of the standard planktonic foraminiferal Zone E7b; according to the age model developed by Payros et al. (2007) at Gorrondatxe, the lowest occurrence of *M. gorrondatxensis* can be dated at 46.6 Ma, being 1.2 myr younger than the Ypresian/Lutetian boundary and 1.1 myr older than the E7b/E8 zonal boundary. Given that *M. gorrondatxensis* is the planktonic foraminiferal species that first appears in the Lutetian deposits of the Gorrondatxe stratotype section, its lowest occurrence is a valuable event to approximate the position of the Ypresian/Lutetian boundary using planktonic foraminifera and could in fact provide greater

precision to the standard planktonic foraminiferal biostratigraphic scale around the Ypresian/Lutetian boundary.

In addition to its occurrence in its type area, *M. gorrondatxensis* has been found in coeval deposits from other Pyrenean basins and the Betic Cordillera (southern Spain); furthermore, a literature survey has shown that some morozovellids found in Austria (EU), the Cape Verde Islands (Atlantic Ocean), the Alabama coastal plain (USA) and Shatsky Rise (Pacific Ocean) show characteristics that fall within the morphological variability of *M. gorrondatxensis* (Orue-Etxebarria et al., 2014). In all of the Pyrenean basins, in the Cape Verde Islands and in the Austrian successions *M. gorrondatxensis* occurs at the same stratigraphic interval as in Gorrondatxe (Zones E7b and E8). However, in the Betic Cordillera the stratigraphic range of *M. gorrondatxensis* extends up to the middle part of the late Lutetian Zone E10. The longer stratigraphic range of *M. gorrondatxensis* in the Betic basins was probably related to the prevalence of warmer conditions in Tethyan low latitudes, whereas the Boreal basins became too cold for most morozovellids by late Lutetian times.

In conclusion, the occurrence of *M. gorrondatxensis* in different paleobiogeographic domains shows that it was not a regionally restricted endemic species. However, independent records from other areas worldwide would be required to determine whether *M. gorrondatxensis* was more globally distributed.

ACKNOWLEDGEMENTS

Research funded by the Spanish Government FEDER project CGL 2011-23770 and by the Basque Government project GIC07/122-IT-215-07.

REFERENCES

- Hornibrook N.B. (1958) - New Zealand Upper Cretaceous and Tertiary foraminiferal zones and some overseas correlations. *Micropaleontol.*, 4, 25-38.
- Molina E., Alegret L., Apellaniz E., Bernaola G., Caballero F., Dinarès-Turell J., Hardenbol J., Heilmann-Clausen C., Larrasoana J.C., Luterbacher H., Monechi S., Ortiz S., Orue-Etxebarria X., Payros A., Pujalte V., Rodríguez-Tovar F.J., Tori F., Tosquella J. & Uchman, A. (2011) - The Global Stratotype Section and Point (GSSP) for the base of the Lutetian Stage at the Gorrondatxe section, Spain. *Episodes*, 34, 86-108.
- Orue-Etxebarria X. (1985) - Descripción de dos nuevas especies de foraminíferos planctónicos en el Eoceno costero de la provincia de Bizkaia. *Revista Española de Micropaleontología*, 17, 467-477.
- Orue-Etxebarria X., Payros A., Caballero F., Apellaniz E., Pujalte V., & Ortiz S. (in press) - *Morozovella gorrondatxensis* (Orue-Etxebarria 1985) vs *M. crater* (Hornibrook 1958): taxonomy and significance for Early/Middle Eocene boundary biostratigraphy. *Stratigraphy*.
- Payros A., Bernaola G., Orue-Etxebarria X., Dinarès-Turell J., Tosquella J. & Apellaniz E. (2007) - Reassessment of the Early-Middle Eocene biomagnetostratigraphy based on evidence from the Gorrondatxe section (Basque Country, western Pyrenees). *Lethaia*, 40, 183-195.
- Pearson P.N., Olsson R.K., Huber B.T., Hemleben C. & Berggren W.A. (2006) - Atlas of Eocene Planktonic Foraminifera. *Cushman Foundation Special Publication*, 1, 514 pp.

First evidence of coral bioconstructions in the Monte Postale succession (Lower Eocene of Lessini Mts., Veneto, northern Italy)

Cesare Andrea Papazzoni ^(a), Alessandro Vescogni ^(a), Francesca Bosellini ^(a), Luca Giusberti ^(b),
Guido Roghi ^(c) & Stefano Dominici ^(d)

^(a) Dipartimento di Scienze Chimiche e Geologiche, Università di Modena e Reggio Emilia, Largo S. Eufemia, 19, 41121, Modena, Italy. E-mail: papazzoni@unimore.it

^(b) Dipartimento di Geoscienze, Università di Padova, Via Gradenigo, 6, 35131 Padova, Italy

^(c) Istituto di Geoscienze e Georisorse, CNR, Via Gradenigo, 6, 35131 Padova, Italy

^(d) Museo di Storia Naturale, Università di Firenze, Via La Pira, 4, 50121, Firenze, Italy

Document type: Short note.

Manuscript history: received 15 May 2014; accepted 30 May 2014; editorial responsibility and handling by Gerald R. Dickens & Valeria Luciani.

KEY WORDS *Alveolina*, Bolca Lagerstätten, coral reefs, dasycladacean algae, Eocene, northern Italy.

The world-famous *Fossil-Lagerstätten* of the Bolca area have long been interpreted (e.g., Sorbini, 1972) as deposited in a carbonate platform setting, within an intra-platform depression or basin, protected from the open-marine environment by some kind of threshold (Papazzoni & Trevisani, 2006; Schwark et al., 2009). The presence of corals, both in the Pesciara di Bolca site and in the nearby Monte Postale succession, suggests that the threshold may be formed by some kind of bioconstructed margin. Although the occurrence of a possible “reef” environment has been suggested by the composition of the fish fossil assemblage (Landini & Sorbini, 1996; Belwood, 1996; Bellwood et al., 2014), no direct observation of a preserved coral bioconstruction has ever been reported for the Bolca area.

The Monte Postale succession represents the most complete stratigraphic record of the area, tracing the depositional history before and after the deposition of the laminated limestones containing the fish fauna of the Bolca Lagerstätten. Considering that the last detailed study of the area dates from the beginning of the last century (Fabiani, 1914), a new survey was necessary to update the knowledge of both paleoecological and biostratigraphic aspects. During this survey, some massive limestone bodies were observed, and their *in situ* position within the stratigraphic succession was ascertained. They turned out to be small bioconstructions, a few metres thick, with abundant coral colonies in growth position or preserved as broken rubble. Detailed field mapping and facies analysis of several of these structures allowed the identification of a discontinuous belt along the northern side of the Monte Postale, and to recognize four different facies types:

- Facies A: Coral boundstone. It forms the bulk of the massive outcrops (Fig 1a, b). Dominant genera are *Goniopora*, *Stylophora*, *Actinacis*, *Goniastrea*, *Astrocoenia* and *Astreopora*, while *Stylocoenia*, *Siderastrea*, *Pachygyra*

and *Caulastrea* are subordinate. Corals are often encrusted by foraminifera and coralline red algae. A fine-grained micritic wackestone fills the small cavities among the colonies, associated also with a coarser *Alveolina* packstone. In both cases, fragments of dasycladacean green algae represent one of the most important bioclastic components.

- Facies B: Stratified *Alveolina* grainstone. This facies represents the sediment above and within Facies A (Fig 1a). Associated with the larger forams, coral fragments are also abundant.

- Facies C: Well-bedded, fine-grained packstone. These sediments onlap on the south-eastern side of the massive outcrops (Fig. 1b), and mainly contain small fragments of *Alveolina* and corals. The stratified packstone succession is sometimes interrupted by the presence of fine-grained, laminated strata, characterized by few fossil remains and a darker colour related to the abundant presence of organic matter.

- Facies D: *Nummulites* packstone. This facies crops out along the northern boundary of Facies A. *Nummulites* are also associated with *Alveolina* and abundant coral fragments.

The rich *Alveolina* assemblages of Facies A and B contain, among others, *Alveolina cremae*, *A. aff. croatica*, *A. decastroi*, *A. cf. dainellii*, and *A. distefanoi*, that date the depositional system to SBZ 11 (Middle Cuisian, Lower Eocene) of Serra-Kiel et al. (1998).

The preliminary interpretation of these four facies allows recognition of distinct paleoenvironments. The massive carbonates of Facies A, dominated by corals and associated with a remarkable amount of dasycladacean algae, indicate the presence of a wave-resistant structure, represented by a discontinuous alignment of small coral bioconstructions that developed in a very shallow-water environment, located within the upper part of the photic zone. This interpretation is also supported by the coalescence of these buildups with the sediments of Facies B, whose *Alveolina* grainstone also suggests deposition at some meters of depth. Hence, the paleoenvironment of Facies A and B may be interpreted as a

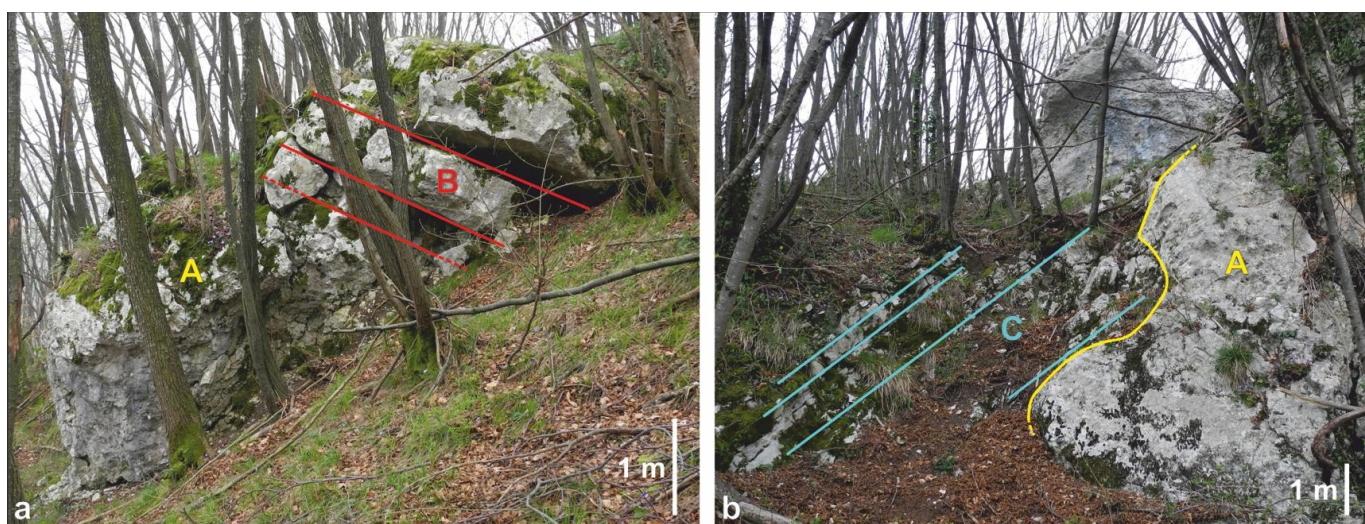


Fig.1 – a) Stratigraphic relationships between the massive boundstone of Facies A and the stratified packstone of Facies B; b) onlap of the bedded limestone of Facies C on a massive outcrop of Facies A.

belt of small patch reefs and sand bodies, delineating a threshold that created a protected lagoon extended towards the south-east. Facies C was deposited in this low-energy environment, and the presence within the fine-grained packstone strata of finely-laminated levels, also rich in organic matter, could indicate the occurrence of periodic dysoxic events during the evolution of the Monte Postale lagoon. Such events, if proven, might be related to the deposition of the laminated limestones that characterize the *Konservat-Lagerstätten* of the Pesciara di Bolca and Monte Postale. On the opposite side, along the northern boundary of the coral belt, sediments are mainly represented by the *Nummulites* packstone of Facies D, suggesting more open, normal marine conditions.

These results, although very preliminary, describe for the first time the coral-bioconstructed system that allowed the formation of one of the most important Eocene *Fossil-Lagerstätten* in the world. Moreover, some components of the reef biota, such as the abundant dasycladacean algae of Facies A, are indeed rare in the Eocene limestones of northern Italy and have never been previously reported from this area.

Research supported by grants PRIN 2010 “Past Excess CO₂ worlds: biota responses to extreme warmth and ocean acidification”.

REFERENCES

- Bellwood D.R. (1996) - The Eocene fishes of Monte Bolca: the earliest coral reef fish assemblage. *Coral Reefs*, 15 (1), 11-19.
- Bellwood D.R., Goatley C.H.R., Brandl S.J. & Bellwood O. (2014.) - Fifty million years of herbivory on coral reefs: fossils, fish and functional innovations. *Proc. R. Soc. B*, 281, 20133046.
- Fabiani R. (1914) - La serie stratigrafica del Monte Bolca e dei suoi dintorni. *Mem. Ist. Geol. R. Univ. Padova*, 2, 223-235.
- Landini W. & Sorbini L. (1996) - Ecological and trophic relationships of Eocene Monte Bolca (Pesciara) fish fauna. In: Cherchi, A. (Ed.), *Autecology of selected fossil organisms: Achievements and problems*. *Boll. Soc. Paleont. It., Spec. Vol. 3*, 105-112.
- Papazzoni C.A. & Trevisani E. (2006) - Facies analysis, palaeoenvironmental reconstruction, and biostratigraphy, of the “Pesciara di Bolca” (Verona, northern Italy): An early Eocene Fossil-Lagerstätte. *Palaeogeogr., Palaeoclimat., Palaeoecol.*, 242 (1-2), 21-35.
- Schwark L., Ferretti A., Papazzoni C.A. & Trevisani E. (2009) - Organic geochemistry and paleoenvironment of the Early Eocene “Pesciara di Bolca” Konservat-Lagerstätte, Italy. *Palaeogeogr., Palaeoclimat., Palaeoecol.*, 273 (3-4), 272-285.
- Serra-Kiel J., Hottinger L., Caus E., Drobne K., Ferrández C., Jauhri A.K., Less G., Pavlovec R., Pignatti J., Samsó J.M., Schaub H., Sirel E., Strougo A., Tambareau Y., Tosquella J. & Zakrevskaya E. (1998) - Larger foraminiferal biostratigraphy of the Tethyan Paleocene and Eocene. *Bull. Soc. Geol. Fr.*, 169, 281-299.
- Sorbini L. (1972) - I fossili di Bolca. *Museo Civico di Storia Naturale di Verona, Verona*, 133 pp.

The Varignano section (Trento Province, northern Italy): a chance to correlate shallow benthic zones and calcareous plankton zones near the Bartonian–Priabonian boundary

Cesare Andrea Papazzoni ^(a), Alessandra Moretti ^(a), Valeria Luciani ^(b), Eliana Fornaciari ^(c) & Luca Giusberti ^(c)

^(a) Dipartimento di Scienze Chimiche e Geologiche, Università di Modena e Reggio Emilia, Largo S. Eufemia, 19, 41121, Modena, Italy. E-mail: papazzoni@unimore.it

^(b) Dipartimento di Fisica e Scienze della Terra, Università di Ferrara, Polo Scientifico e Tecnologico – Blocco B Via Saragat 1, 44100, Ferrara, Italy

^(c) Dipartimento di Geoscienze, Università di Padova, Via Gradenigo, 6, 35131 Padova, Italy

Document type: Short note.

Manuscript history: received 15 May 2014; accepted 30 May 2014; editorial responsibility and handling by Gerald R. Dickens & Valeria Luciani.

KEY WORDS: biostratigraphy, calcareous nannoplankton, larger foraminifera, Middle–Upper Eocene, planktonic foraminifera, shallow benthic zones.

The GSSP for the base of the Priabonian stage has not yet been defined, but a candidate section has been recently proposed by Agnini et al. (2011) near Alano di Piave (Veneto region, northern Italy), some 50 km far from the historical stage stratotype of Priabona. The Alano section, deposited in a bathyal setting, has been investigated for the calcareous nannoplankton, planktonic foraminifera, as well as magnetostratigraphy. The ‘Tiziano bed’, a prominent lithological tuff layer whose base has been proposed for the base of the Priabonian (Agnini et al., 2011) is very close to different events, namely the *Cribozentrum erbae* acme (Fornaciari et al., 2010; Agnini et al., 2011), the extinction of morozovellids and large acariniids (Agnini et al., 2011; Wade et al., 2012), and the base of magnetochron C17n.1n (Vandenberghe et al., 2012).

Unfortunately, at Alano di Piave there is no way to directly correlate any of these events with the larger foraminifera shallow-water biozones, namely the Shallow Benthic Zones (SBZ) of Serra-Kiel et al. (1998). In the lower part of the Alano section, two coarse-grained bioclastic levels indeed contain larger foraminifera, but they both belong to the SBZ 17 (lower Bartonian). Moreover, these beds are at least 25 m below the extinction of muricate planktonic foraminifera, the lowest event that could approximate the base of the Priabonian.

However, a unique chance for a direct correlation between the SBZ and the calcareous plankton zones is provided by the Varignano section (Trento Province, northern Italy), which is 80 km west of Alano di Piave, deposited in a similar bathyal setting but with much more larger-foraminiferal bearing bioclastic levels (eleven sampled). The Varignano section was first studied by Luciani & Lucchi Garavello (1986) and recently re-sampled in its Middle–Upper Eocene part on a thickness of more than 25 m. The coarse-grained levels are

quite evenly distributed from base to top of this interval, intercalated with the hemipelagic sediments. In the lowermost part of the section, the second coarse-grained level cuts a sapropelic interval recording the post-MECO phase as in the Alano di Piave section (Luciani et al., 2010; Spofforth et al., 2010).

The Varignano section spans from E12 to the lower E14 zone according to the biozonation of Wade et al. (2011), and from MNP16Bc to MNP18 calcareous nannoplankton zones of Fornaciari et al. (2010). The event of extinction of morozovellids and large acariniids occurs in the upper third of the section, just between the eighth and the ninth coarse-grained bioclastic levels (counted from base to top). The *Cribozentrum erbae* acme has been detected between the ninth and the tenth coarse-grained bioclastic level and occurs, as in the Alano section above the morozovellids/acariniids extinction.

The lower part of the section is attributed to the SBZ 17 (lower Bartonian) for the presence of *Nummulites alponensis*, *N. millecaput*, and *Discocyclina discus adamsi*. The passage to the SBZ 18 (upper Bartonian), is considered sure with the first appearance of *Pellatispira* sp. (Fig. 1), even if this genus has not been reported since now from the very base of the biozone. *Pellatispira* appears between the seventh and the eighth coarse-grained bioclastic levels, so well below any of the planktonic events proposed in the literature for recognizing the base of the Priabonian.

This direct correlation raises the problem of the heterochrony between what is usually considered the base of the Priabonian in shallow-water settings (the appearance of *Nummulites fabianii*, or base of SBZ 19; see e.g. Serra-Kiel et al., 1998) and the same boundary in pelagic settings. This heterochrony has been alleged recently by Costa et al. (2013) in the Ebro Basin, northeastern Spain: they reported the NP19/20 starting within the SBZ 18, but the quality of their nannofossil record hampers reliable comparisons with the Varignano record.

Research supported by grants PRIN 2010 “Past Excess CO₂

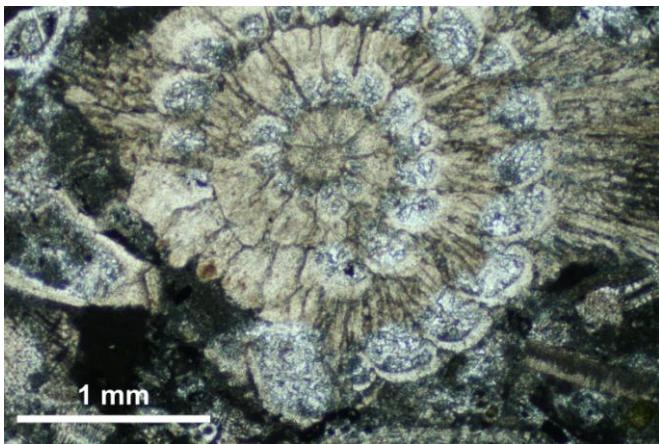


Fig.1 – *Pellatispira* sp., sample VAR 6, eighth coarse-grained level.

worlds: biota responses to extreme warmth and ocean acidification”.

REFERENCES

- Agnini C., Fornaciari E., Giusberti L., Grandesso P., Lanci L., Luciani V., Muttoni G., Pälike H., Rio D., Spofforth D.J.A. & Stefani C. (2011) - Integrated biomagnetostratigraphy of the Alano section (NE Italy): A proposal for defining the middle-late Eocene boundary. *Geol. Soc. America Bull.*, 123 (5-6), 841-872.
- Costa E., Garcés M., López-Blanco M., Serra-Kiel J., Bernaola G., Cabrera L. & Beamud E. (2013) - The Bartonian–Priabonian marine record of the eastern South Pyrenean foreland basin (NE Spain): a new calibration of the larger foraminifers and calcareous nannofossil biozonation. *Geol. Acta*, 11 (2), 177-193.
- Fornaciari E., Agnini C., Catanzariti R., Rio D., Bolla E.M. & Valvasoni E. (2010) - Mid-latitude calcareous nannofossil biostratigraphy and biochronology across the middle to late Eocene transition. *Stratigraphy* 7, 229-264.
- Luciani V. & Lucchi Garavello A.M. (1986) - Biostratigrafia del Paleogene pelagico del Bacino del Sarca (Trentino meridionale). *St. Trent. Sci. Nat., Acta Geol.*, 62, 19-70.
- Luciani V., Giusberti L., Agnini C., Fornaciari E., Rio D., Spofforth D.J.A. & Pälike H. (2010) - Ecological and evolutionary response of Tethyan planktonic foraminifera to the middle Eocene climatic optimum (MECO) from the Alano section (NE Italy). *Palaeogeogr. Palaeoclimatol. Palaeoecol.*, 292, 82-95.
- Serra-Kiel J., Hottinger L., Caus E., Drobne K., Ferrández C., Jauhari A.K., Less G., Pavlovec R., Pignatti J., Samsó J.M., Schaub H., Sirel E., Strougo A., Tambareau Y., Tosquella J. & Zakrevskaya E. (1998) - Larger foraminiferal biostratigraphy of the Tethyan Paleocene and Eocene. *Bull. Soc. Geol. Fr.*, 169, 281-299.
- Spofforth D.J.A., Agnini C., Pälike H., Rio D., Fornaciari E., Giusberti L., Luciani V., Lanci L. & Muttoni G. (2010) - Organic carbon burial following the middle Eocene climatic optimum in the central western Tethys. *Paleoceanography*, 25, PA3210.
- Vandenbergh N., Hilgen F.J. & Speijer R.P. (2012) - Chapter 28. The Paleogene Period. In: Gradstein F.M., Ogg J.G., Smith A.G. & Ogg G.M. (Eds.), *The Geologic Time Scale 2012*. Elsevier, 855-921.
- Wade B.S., Pearson P.N., Berggren W.A. & Pälike H. (2011) - Review and revision of Cenozoic tropical planktonic foraminiferal biostratigraphy and calibration to the geomagnetic polarity and astronomical time scale. *Earth Sci. Rev.*, 104, 111-142.
- Wade B.S., Premec Fucek V., Kamikuri S., Bartol M., Luciani V. & Pearson P.N. (2012) - Successive extinctions of muricate planktonic foraminifera (*Morozovelloides* and *Acarinina*) as a candidate for marking the base Priabonian. *Newsl. Strat.*, 45 (3), 245-262.

Southern Ocean endemism evident in Late Eocene radiolarian assemblages, DSDP Site 277, Campbell Plateau (New Zealand)

Kristina M. Pascher ^(a,b), Christopher J. Hollis ^(a), Robert M. McKay ^(b) & Giuseppe Cortese ^(a)

^(a) GNS Science, PO Box 30368, Lower Hutt 5040, New Zealand. Email: K.Pascher@gns.cri.nz

^(b) Victoria University Wellington, Antarctic Research Centre, PO Box 600, Wellington 6140, New Zealand

Document type: Short note.

Manuscript history: received 15 May 2014; accepted 30 May 2014; editorial responsibility and handling by Gerald R. Dickens & Valeria Luciani.

KEY WORDS: Campbell Plateau, Eocene, Eocene-Oligocene transition, faunal change, radiolaria, Southern Ocean, SW Pacific.

We studied Eocene radiolarian assemblages as a guide to oceanographic changes in the Southern Pacific through the Eocene and across the Eocene-Oligocene (E-O) transition (54-34 Ma ago). DSDP Site 277 (52°13.43'S; 166°11.48'E) offers a unique record of pelagic sedimentation in the Pacific sector of the Southern Ocean at ~65°S from late Paleocene to Oligocene times (Shackleton & Kennett, 1975; Hollis et al., 1997). In contrast to previous evidence for warm subtropical to tropical temperatures in this region during the Eocene (Liu et al., 2009; Bijl et al., 2010), Middle and Late Eocene radiolarian assemblages lack many low-latitude taxa and are comparable to other high-latitude assemblages. They are interpreted to be temperate water assemblages. A major change in assemblages occurs in the middle Late Eocene, with improved preservation, increased abundance and diversity and the appearance of taxa with strong Southern Ocean affinities, including the following endemic species: e.g. *Larcopyle hayesi*, *L. polyacantha*, *Spongopyle osculosa*, *Lithomelissa sphaerocephalis*, *L. gelasinus*, *Ceratocyrtis* sp., *Dictyophimus* cf. *archipilium*, *Lamprocyclas particollis*, and Antarctic morphotypes of *Aphetocyrtis gnomabax*, *A. rossi*, *Lophocyrtis aspera*, *L. keraspera* and *L. longiventer*. This change in radiolarian assemblages is associated with the first significant appearance of diatoms and silicoflagellates and occurs at the boundary between the Kaiatan and Runangan local New Zealand stages, dated at 36.4 Ma in the middle Late Eocene (226.1 mbsf). The radiolarian faunal change is linked to a positive shift on planktic $\delta^{18}\text{O}$ (Shackleton & Kennett, 1975) and a pronounced decline in the abundance of warm-water calcareous nannofossils (*Discoaster* spp.) (Hollis et al., 1997), suggesting that the radiolarian faunal change was caused by cooling of surface waters. Benthic $\delta^{18}\text{O}$ does not exhibit a significant positive shift until the E-O boundary. This surface water cooling event postdates the Middle Eocene cooling trend

reported by Bijl et al. (2013) at the Early-Middle Eocene boundary (~48 Ma) and predates the reorganization of the Southern Ocean inferred by Houben et al. (2013) to have occurred in the earliest Oligocene (33.9 Ma). The event is consistent with other evidence from siliceous microfossils and opal accumulation that indicates long-term cooling of the Southern Ocean began in the middle Late Eocene (Lazarus et al., 2008) and predated large scale ice sheet growth by ~2 million years.

REFERENCES

- Bijl P.K., Bendle J.A., Bohaty S.M., Pross J., Schouten S., Tauxe L., Stickley C.E., McKay R.M., Röhl U. & Olney, M. (2013) - Eocene cooling linked to early flow across the Tasmanian Gateway. *P. Natl. Acad. Sci. USA*, 110(24), 9645-9650.
- Bijl P.K., Houben A.J., Schouten S., Bohaty S.M., Sluijs A., Reichert G.-J., Damsté J.S.S. & Brinkhuis H. (2010) - Transient Middle Eocene atmospheric CO₂ and temperature variations. *Science*, 330(6005), 819-821.
- Hollis C.J., Waghorn D.B. Strong C.P., & Crouch E.M. (1997) - Integrated Paleogene Biostratigraphy of DSDP Site 277 (Leg 29): Foraminifera, Calcareous Nannofossils, Radiolaria, and Palynomorphs: Institute of Geological & Nuclear Sciences Science Report 97/07, 87 p.
- Houben A.J., Bijl P.K., Pross J., Bohaty S.M., Passchier S., Stickley C.E., Röhl U., Sugisaki S., Tauxe L., & van de Flierdt T. (2013) - Reorganization of Southern Ocean Plankton Ecosystem at the Onset of Antarctic Glaciation. *Science*, 340(6130), 341-344.
- Lazarus D., Hollis C.J., & Apel M. (2008) - Patterns of opal and radiolarian change in the Antarctic mid-Paleogene: Clues to the origin of the Southern Ocean. *Micropaleontol.*, 41-48.
- Liu Z., Pagani M., Zinniker D., DeConto R., Huber M., Brinkhuis H., Shah S. R., Leckie R.M., & Pearson A. (2009) - Global cooling during the Eocene-Oligocene climate transition. *Science*, 323(5918), 1187-1190.

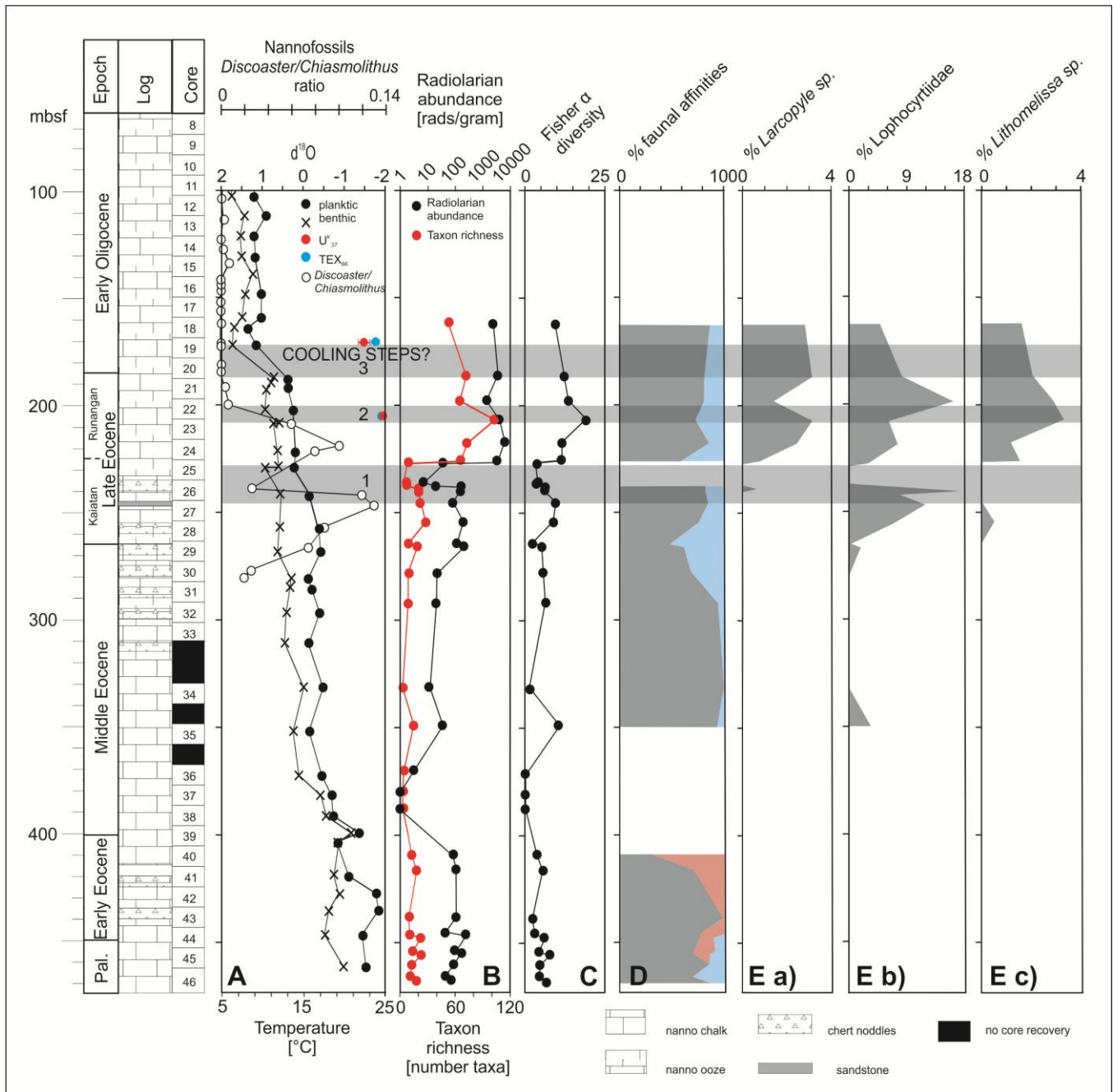


Fig. 1 - **A**: Summary of trends in paleotemperature: *Discoaster/Chiasmolithus* ratio (Hollis et al., 1997), stable planktic and benthic oxygen isotopes (Shackleton & Kennett, 1975), and U^{K}_{37} and TEX_{86} calculated SSTs (Liu et al., 2009); **B**: radiolarian abundance and taxon richness; **C**: Fisher α diversity index; **D**: relative abundance of low-latitude (red), high-latitude (blue) and cosmopolitan+undifferentiated taxa (grey); **E**: relative abundance of selected taxa: **a**) *Larcopyle* sp. (*L. polyacantha*, *L. hayesi*, *L. tetrapila*, *L. cf. titan*); **b**) Lophocyrtiidae (*Aphetocyrtis gnomabax*, *A. bianulus*, *A. rossi*, *Lophocyrtis aspera*, *L. kersaspera*, *L. longiventer*, *L. dunitricai*, *L. hadra*); **c**) *Lithomelissa* sp. (*L. cheni*, *L. sphaerocephalis*, *L. ehrenbergi*, *L. gelasinus*, *L. cf. haeckeli*, *L. robusta*, *L. cf. thoracites*, *L. tricomis*).

Shackleton N.J. & Kennett J. (1975) - Paleotemperature history of the Cenozoic and the initiation of Antarctic glaciation: oxygen and carbon isotope analyses in DSDP Sites 277,

279, and 281. Initial Reports of the Deep Sea Drilling Project, 29, 743-755.

Astronomically driven short-term climate change, a factor controlling Eocene turbidite accumulation

Aitor Payros ^(a) & Naroa Martinez-Braceras ^(a)

^(a) Dept. Stratigraphy and Paleontology, Faculty of Science and Technology, University of the Basque Country (UPV/EHU), Ap. 644, E48080 Bilbao, Spain. E-mail: a.payros@ehu.es

Document type: Short note.

Manuscript history: received 15 May 2014; accepted 30 May 2014; editorial responsibility and handling by Gerald R. Dickens & Valeria Luciani.

KEY WORDS: climate, Eocene, Milankovitch, Pyrenees, turbidite.

The influence of astronomically driven short-term climate change (Milankovitch cycles) on deep-marine turbidite systems is not well known, particularly in the case of long-term greenhouse intervals with no significant glacio-eustatic sea-level fluctuations. The aim of our study was to fill in some of the gaps.

To this end, we studied part of the western Pyrenean Gorrondatxe section, which is the Global Stratotype Section and Point for the base of the Middle Eocene Lutetian Stage (Molina et al., 2011). The Gorrondatxe deposits accumulated in an epoch characterized by high concentrations of greenhouse gases, which produced the warmest global temperature recorded over the last 100 million years (Zachos et al., 2001). The succession is composed of alternating pelagic limestones and marls interspersed with thin-bedded turbidites (<35 cm, but mainly just a few centimetres thick), which accumulated in submarine fan fringe or basin plain environments at approximately 1500 m water depth and 35°N palaeolatitude (Payros et al., 2007, 2009). These deposits form recurrent tripartite sequences, commonly less than 10 cm thick, each of which consists of a basal thin-bedded sandy turbidite, its capping clay (division Te of the Bouma sequence) and a pelagic mudstone.

Light grey limy and dark grey marly pelagic mudstones alternate cyclically, defining 45 limestone-marl couplets. In addition, ten cyclic bundles composed of four to six couplets occur, along which the carbonate content first increases and then decreases. The supra-regional significance of the Gorrondatxe pelagic cycles was demonstrated by bed-by-bed correlation with coeval sections from other sedimentary basins (Payros et al., 2011, 2012). On the basis of a precise biomagnetostratigraphy, it was concluded that the limestone-marl couplets represent 21 kyr-long precession cycles and the bundles represent 100 kyr-long eccentricity cycles. The astronomically driven short-term climate change cycles determined the rate of terrigenous sediment input into the sea. Thus, terrigenous sediment contribution to pelagic sedimentation fluctuated by a factor of five during opposite

precessional situations at maximum eccentricity, whereas there was almost no fluctuation at minimum eccentricity.

An in-depth analysis of the Gorrondatxe fan-fringe/basin-plain turbidites demonstrated that their characteristics also varied in line with orbitally-forced fluctuations in seasonal rainfall, runoff and terrigenous input to the sea (Payros & Martinez-Braceras, 2014). Reduced turbiditic activity during the formation of the limy precessional hemicouplets indicates subdued seasonality and low terrigenous input. Conversely, turbidity currents were more frequent, had greater energy and were more voluminous during the formation of pelagic marly hemicouplets, suggesting precessional hemicycles with strong seasonality and heavy summer rainfall.

These differences at precessional timescales were enhanced at maximum eccentricity, as turbiditic activity was most intense when boreal summer occurred at perihelion (i.e., maximum seasonality) but declined when it occurred at aphelion. At minimum eccentricity, with relatively weak seasonality throughout one (or more than one) precessional cycle (>21 kyr), turbiditic activity remained relatively low.

The pattern observed at the Gorrondatxe fan-fringe/basin-plain succession implies that the orbitally forced environmental changes must also have affected the inner and middle parts of the submarine fan. In particular, the long-term reduction in turbiditic activity at minimum eccentricity was followed by major re-arrangements of the turbidite system, which could have been related to channel abandonment and/or shifts in the location of depositional lobes. However, it remains unclear whether the turbiditic successions accumulated in the inner and middle fan can reliably record Milankovitch cycles, as these environments are frequently traversed by erosive sediment gravity flows that may lead to incomplete sedimentary successions, unsuitable for cyclostratigraphic analyses.

ACKNOWLEDGEMENTS

Research funded by the Spanish Government FEDER project CGL 2011-23770 and by the Basque Government project GIC07/122-IT-215-07.

REFERENCES

- Molina E., Alegret L., Apellaniz E., Bernaola G., Caballero F., Dinarès-Turell J., Hardenbol J., Heilmann-Clausen C., Larrasoña J.C., Luterbacher H., Monechi S., Ortiz S., Orue-Etxebarria X., Payros A., Pujalte V., Rodríguez-Tovar F.J., Tori F., Tosquella J. & Uchman, A. (2011) - The Global Stratotype Section and Point (GSSP) for the base of the Lutetian Stage at the Gorrondatxe section, Spain. *Episodes*, 34, 86-108.
- Payros A. & Martínez-Braceras N. (2014) - Orbital forcing in turbidite accumulation during the Eocene greenhouse interval. *Sedimentology*, doi:10.1111/sed.12113.
- Payros A., Bernaola G., Orue-Etxebarria X., Dinarès-Turell J., Tosquella J. & Apellaniz E. (2007) - Reassessment of the Early-Middle Eocene biomagnetostratigraphy based on evidence from the Gorrondatxe section (Basque Country, western Pyrenees). *Lethaia*, 40, 183-195.
- Payros A., Orue-Etxebarria X., Bernaola G., Apellaniz E., Dinarès-Turell J., Tosquella J. & Caballero F. (2009) - Characterization and astronomically calibrated age of the first occurrence of *Turborotalia frontosa* in the Gorrondatxe section, a prospective Lutetian GSSP: implications for the Eocene time scale. *Lethaia*, 42, 255-264.
- Payros A., Dinarès-Turell J., Bernaola G., Orue-Etxebarria X., Apellaniz E. & Tosquella J. (2011) - On the age of the Early/Middle Eocene boundary and other related events: cyclostratigraphic refinements from the Pyrenean Otsakar section and the Lutetian GSSP. *Geol. Mag.*, 148, 442-460.
- Payros A., Ortiz S., Alegret L., Orue-Etxebarria X., Apellaniz E. & Molina E. (2012) - An early Lutetian carbon-cycle perturbation: insights from the Gorrondatxe section (western Pyrenees, Bay of Biscay). *Paleoceanography*, 27, PA2213.
- Zachos J., Pagani M., Sloan L., Thomas E. & Billups K. (2001) - Trends, rhythms, and aberrations in global climate 65 Ma to Present. *Science*, 292, 686-693.

Testing the metabolic hypothesis: temperature-dependent carbon cycling in the Eocene oceans

Paul N. Pearson ^(a), Eleanor H. John ^(a), Jamie D. Wilson ^(a) & Andy Ridgwell ^(c)

^(a) School of Earth and Ocean Sciences, Cardiff University, Park Place, Cardiff, CF10 3AT, UK. E-mail: pearsonp@cardiff.ac.uk

^(b) School of Geographical Sciences, University of Bristol, University Road, Clifton, Bristol, BS8 1SS, UK

Document type: Short note.

Manuscript history: received 15 May 2014; accepted 30 May 2014; editorial responsibility and handling by Gerald R. Dickens & Valeria Luciani.

KEY WORDS: carbon isotopes, foraminifera, GENIE, metabolic hypothesis, remineralization, respiration.

Temperature-dependency of metabolic rates including photosynthesis and respiration could mean that large-scale ecosystem processes operated differently in past warm climate states, and may do so again under anthropogenic global warming. It is well known that sinking of organic matter in the ocean transfers carbon from the surface layer to the deep ocean reservoir causing a replacement flux of CO₂ from the atmosphere (the biological pump). The efficiency of this process may be temperature-dependent because metabolic rates in heterotrophic bacteria and other respiring organisms are much more sensitive to temperature than are rates of primary production. Faster respiration rates in the warmer Eocene ocean may have resulted in more rapid remineralization of sinking organic matter higher in the water column, and hence a less efficient biological pump, with implications for carbon and nutrient cycling, rates of organic matter burial, and potential feedbacks on global temperature via the CO₂ greenhouse effect (Olivarez-Lyle & Lyle, 2006).

We tested this hypothesis by reconstructing a series of water column carbon isotope-depth profiles using well-preserved planktonic foraminifera assemblages from the Eocene of Tanzania and Mexico (John et al., 2013, unpublished data). The profiles were constructed based on rules developed in the modern ocean for excluding various types of vital effect fractionation in the foraminifera (Birch et al., 2013). Species and size fractions were assigned calcification depths based on their oxygen isotope paleotemperatures fitted to modeled seawater temperature profiles as extracted from Eocene GCM simulations. The results indicate relatively sharp carbon isotope gradients of dissolved inorganic carbon in the upper water column, supporting the hypothesis that high metabolic rates led to faster recycling of organic matter (John et al., 2013).

Shallower remineralization depths would have caused an upward displacement and intensification of oxygen depletion in the water column and reduced food supply at depth. This may

be why pelagic ecosystem seems to have been focused over a narrower depth range nearer the surface than the modern, especially in the early Eocene. Global cooling in the middle Eocene may have been linked to less hostile conditions at depth and the development of deep planktonic niches such as that exploited by the *Hantkenina* lineage of planktonic foraminifera (Pearson & Coxall, 2014).

We incorporated temperature-dependence of respiration rates into the Earth system model GENIE to illustrate the potential effects particulate organic carbon fluxes and vertical carbon isotope gradients (John et al., in press). The modeled carbon isotope profiles agree well with the reconstructed Eocene profiles. The implications for Eocene and future carbon cycling are discussed.

REFERENCES

- Birch H., Coxall H.K., Pearson P.N., Kroon D. & O'Regan M. (2013) - Planktonic foraminifera stable isotopes and water column structure: Disentangling ecological signals. *Mar. Micropaleont.*, 101, 127-145.
- John E.H., Pearson P.N., Coxall H.K., Birch H., Wade B.S. & Foster G.L. (2013) - Warm ocean processes and carbon cycling in the Eocene. *Phil. Trans. R. Soc. A*, 371, 20130099.
- John E.H., Wilson J.D., Pearson P.N. & Ridgwell A. (in press) - Temperature-dependent remineralization and carbon cycling in the warm Eocene oceans. *Palaeogeogr. Palaeoclimatol. Palaeoecol.*
- Olivarez-Lyle A. & Lyle M.W. (2006) - Missing organic carbon in Eocene marine sediments: Is metabolism the biological feedback that maintains end-member climates?. *Paleoceanography*, 21, PA2007, 2005PA001230.
- Pearson P.N. & Coxall H.K. (2014) - Origin of the Eocene planktonic foraminifer *Hantkenina* by gradual evolution. *Palaeontology*, 57, 243-267.

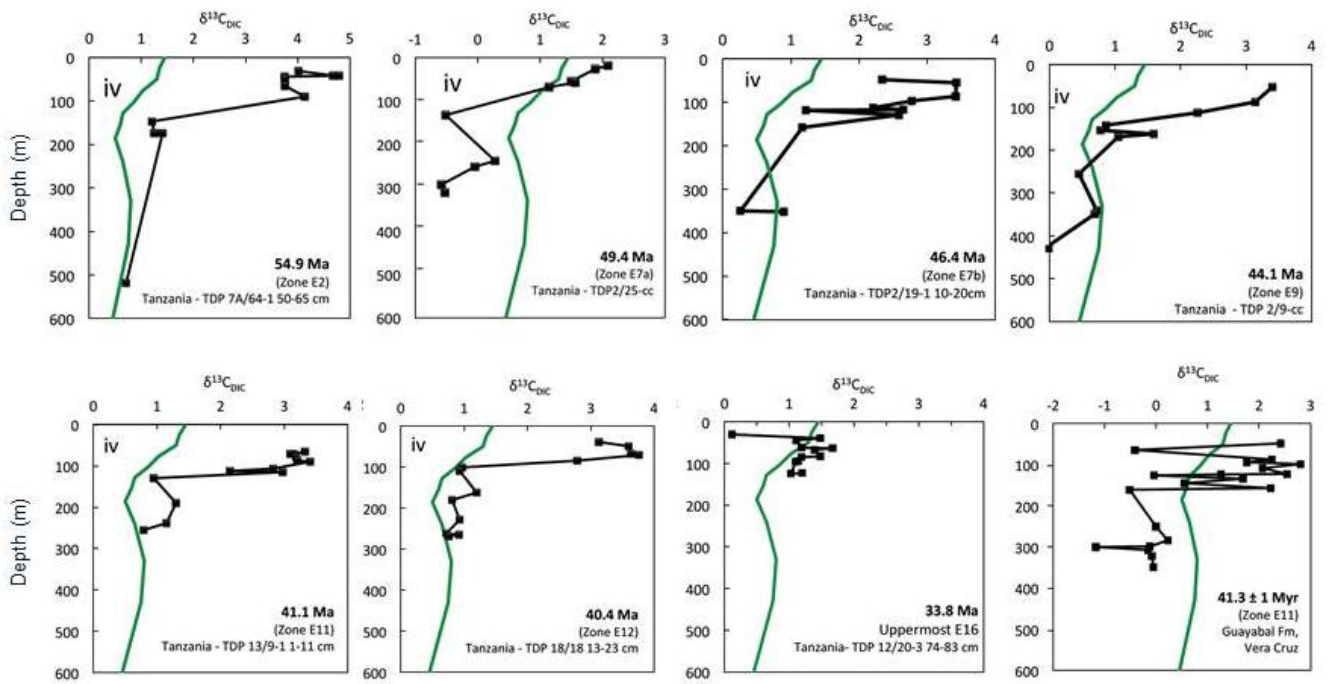


Fig. 1 – Carbon isotope / depth profiles. Black squares are measured planktonic foraminifer data which have been assigned depths by fitting their corresponding oxygen isotope paleotemperatures to a modelled water column temperature profile as extracted from a General Circulation Model. The green line is the modern carbon isotope / depth profile for the offshore Tanzania. Modified from John et al. (2013).

Boron proxy constraints on the magnitude of surface ocean acidification during the Paleocene-Eocene Thermal Maximum

Donald E. Penman^(a), Barbel Hönlisch^(b), Ellen Thomas^(c), Richard E. Zeebe^(d), D. Clay Kelly^(e) & James C. Zachos^(a)

^(a) Dept. of Earth and Planetary Sciences, University of California Santa Cruz, 1156 High Street, Santa Cruz, CA 95064, USA. E-mail: dpenman@ucsc.edu

^(b) Dept. of Earth and Environmental Sciences and Lamont-Doherty Earth Observatory of Columbia University, Palisades, NY USA

^(c) Dept. of Geology and Geophysics, Yale University, New Haven, CT 06520-8109 USA

^(d) Dept. of Oceanography, SOEST, University of Hawai'i at Mānoa, Honolulu, HI, USA

^(e) Dept. of Geoscience, Lewis G. Weeks Hall for Geological Sciences, University of Wisconsin-Madison, WI, 53706-1692, USA

Document type: Short note.

Manuscript history: received 15 May 2014; accepted 30 May 2014; editorial responsibility and handling by Gerald R. Dickens & Valeria Luciani.

KEY WORDS: Boron Isotopes, B/Ca, ocean acidification, PETM.

On the basis of a globally observed carbon isotope excursion, widespread dissolution of deep sea carbonates, and warming, the Paleocene-Eocene Thermal Maximum (PETM) has been associated with the release of several thousands of petagrams of carbon as methane and/or carbon dioxide into the ocean-atmosphere system within ~10 thousand years (kyr) (Dickens et al., 1997; Panchuk et al., 2008; Zeebe et al., 2009). In theory, dissolution of excess carbon in seawater should have caused ocean acidification, direct evidence of which comes from the deep sea (e.g., Thomas et al., 1999; Zachos et al., 2005), but has only recently been documented for the surface ocean. Here, using the B/Ca ratio and boron isotopic composition ($\delta^{11}\text{B}$) of planktic foraminifera, we present the first geochemical evidence for a significant drop in surface and thermocline pH during the PETM (Penman et al., 2014). These two techniques compliment each other in that the more complete understanding of the $\delta^{11}\text{B}$ proxy allows a more quantitative interpretation, while the small sample size requirement of B/Ca analyses allows generation of a much higher resolution record, so that timing and structure can be resolved more precisely. Analyses of planktic foraminifera from multiple, globally distributed marine sediment cores (ODP Sites 689, 690, 865, 1209, and 1263) show a 30-40% reduction in shell B/Ca at the onset of the event, coincident with a 0.8‰ decrease in $\delta^{11}\text{B}$. This observation is consistent with a significant acidification event of a duration approximately equal to that of the peak carbon isotope excursion (~50 kyr), followed by a recovery to pre-event conditions. Using calibrations of modern foraminifera (Allen & Hönlisch, 2012; Hönlisch and Hemming 2004; Henehan et al., 2013) and a numerical model, the B data are applied to derive pH anomalies. Timing of the onset and duration of these geochemical anomalies compares favourably with model simulations based on other constraints, but the magnitude of the B/Ca and $\delta^{11}\text{B}$ excursions suggests a carbon release consistent with the higher end of available estimates. Quantification of the pH change recorded by $\delta^{11}\text{B}$ and B/Ca

relies on a number of assumptions, including the $\delta^{11}\text{B}$ of ancient seawater and carbonate chemistry conditions prior to the event, as well as the possible influence of symbiont bleaching, dissolution, diagenesis, and changing temperature and salinity on our records. Considering the uncertainty of these constraints, our data suggest an average pH drop of ~0.3 units. At these levels the surface ocean likely did not become corrosive to calcite, consistent with the general lack of major extinctions among planktic calcifiers.

REFERENCES

- Allen K. A. & B. Hönlisch (2012) - The planktic foraminiferal B/Ca proxy for seawater carbonate chemistry: A critical evaluation. *Earth Planet. Sci. Lett.*, 345–348, 203-211.
- Dickens G., Castillo M.M. & J. Walker C.G. (1997) - A blast of gas in the latest Paleocene: Simulating first-order effects of massive dissociation of oceanic methane hydrate. *Geology*, 25(3), 259-262.
- Henehan M.J., Rae J.W.B., Foster G.L., Erez J., Prentice K.C., Kucera, M., Bostock, H.C., Martínez-Botí M.A., Milton J.A., Wilson P.A., Marshall B.J. & Elliott T. (2013) - Calibration of the boron isotope proxy in the planktonic foraminifera *Globigerinoides ruber* for use in palaeo-CO₂ reconstruction. *Earth Planet. Sci. Lett.*, 364, 111-122.
- Hönlisch B. & Hemming N.G. (2004) - Ground-truthing the boron isotope paleo-pH proxy in planktonic foraminifera shells: Partial dissolution and shell size effects. *Paleoceanography*, 19, PA1016, doi:10.1029/2004PA001026.
- Panchuk K., Ridgwell A. & Kump L.R. (2008) -, Sedimentary response to Paleocene-Eocene Thermal Maximum carbon release: A model-data comparison. *Geology*, 36(4), 315-318.
- Penman D.E., Hönlisch B., Zeebe R.E., Thomas E. & Zachos, J.C. (2014) - Rapid and sustained surface ocean acidification during the Paleocene-Eocene Thermal Maximum. *Paleoceanography*, 29, PA2621, doi:10.1002/2014PA002621.

- Thomas D., Bralower T.J. & Zachos J.C. (1999)- New evidence for subtropical warming during the Late Paleocene Thermal Maximum: Stable isotope evidence from DSDP Site 527, Walvis Ridge. *Paleoceanography*, 14, 561-570.
- Zachos J.C., Röhl U., Schellenberg S.A., Sluijs A., Hodell D.A., Kelly D.C., Thomas E., Nicolo M., Raffi I., Lourens L.J., McCarren H. & Kroon D. (2005) - Rapid Acidification of the Ocean During the Paleocene-Eocene Thermal Maximum. *Science*, 308 (5728), 1611-1615, doi: 10.1126/science.1109004
- Zeebe, R.E., Zachos J.C. & Dickens G.R. (2009) - Carbon dioxide forcing alone insufficient to explain Palaeocene-Eocene Thermal Maximum warming, *Nat. Geosci.*, 2(8), 576-580.

Extremely bad early Eocene weather: Evidence for extreme precipitation from rived deposits

Piret Plink-Björklund ^(a), Lauren Birgeneier ^(b) & Evan Jones ^(a)

^(a) Department of Geology and Geological Engineering, Colorado School of Mines, Golden, CO 80401, USA. E-mail: pplink@mines.edu

^(b) Department of Geology and Geophysics, University of Utah, FASB 323, UT, USA

Document type: Short note.

Manuscript history: received 15 May 2014; accepted 30 May 2014; editorial responsibility and handling by Gerald R. Dickens & Valeria Luciani.

KEY WORDS: chemical weathering, drought, early Eocene hydrological cycle, extreme precipitation, flashy rivers, fluvial facies, global warming, high deposition rate, hyperthermals, upper flow regime.

Here we document the effects of early Eocene global warming events on the hydrological cycle. We present results of detailed stratigraphic, sedimentologic, $\delta^{13}\text{C}$, ichnological and palaeosol study of early Eocene river sediments from Uinta Basin, UT, USA. We compare to literature data globally, and present modern analogues. We show that increased precipitation peakedness rather than increased mean annual precipitation was the response of the hydrological cycle to the early Eocene hyperthermals in subtropics and mid-latitudes. An increase in precipitation peakedness or extreme precipitation is a condition where an increased amount of annual precipitation falls during a few high-intensity rainfall events, resulting in intermittent droughts.

Our dataset indicates a significant increase in extreme precipitation in the Western Interior during the Palaeocene-Eocene Thermal Maximum (PETM) and the consecutive Early Eocene Climatic Optimum (EECO) hyperthermals. This increase in extreme precipitation is evidenced by changes in the early Eocene river form and function, and the nature of paleosols and terrestrial bioturbation.

Extreme precipitation causes terrestrial flooding with intermittent droughts. The high discharge flooding events removed large quantities of sediment from the drainage basin, due to stream erosion and landslide initiation. The initiation of landslides was especially significant, due to a high gradient drainage basin, and vegetation decline that accompanied the extreme precipitation intensification due to the intermittent droughts. These large discharge floods laden with sediment caused rapid deposition from high-velocity currents. Thus, the resultant river deposits resemble megaflood or flash flood deposits, rather than existing river facies models, in that they are dominated by Froude trans- and supercritical or upper flow regime and high deposition rate sedimentary structures (Fig. 1). The upper flow regime structures include planar laminations, convex-up low-angle bedforms and scour and fill features. The

latter two indicate extremely high flow velocities in antidune or chute and pool regimes. The high deposition rates are indicated

by gradational nature of laminations and by climbing and aggradational bedforms. In contrast, perennial sandy river deposits are dominated by cross strata (Fig. 1). Thus, facies in rivers with highly variable discharge are distinct, and can be readily recognized in outcrop and core. They are unique for extreme precipitation forcing, and can accordingly be used as direct evidence for recognizing precipitation pattern changes. Moreover, the proportion of high-magnitude flood deposition can be quantified, in comparison to low-magnitude flood or non-flood discharge deposition, using the percentage of upper flow regime and high deposition rate deposits (Fig. 1).

Comparison to modern river deposits with similar facies proportions, allows for estimation of annual precipitation amounts and specific precipitation peakedness. This analysis shows that channel fills with more than 80% of upper flow regime and high deposition rate sedimentary structures, and thus at least 80% of high-magnitude flood deposition (uniform channels in Fig 1), occur where annual precipitation amounts vary from substantial with 750 mm (e.g., Billi, 2007) to less than 100 mm (e.g., Sneh, 1983; Stear, 1985), but this annual precipitation falls in a few downpours that last from hours to a few days. In contrast, channel fills with less than 40-50% of upper flow regime and high deposition rate sedimentary structures, and thus with a significant proportion of low-magnitude flood and non-flood discharge deposition (highly variable channels in Fig. 1), occur where mean annual precipitation of 1000-1200 mm (e.g., Fielding et al., 2009) to 100 mm (e.g., Abdullatif, 1989) is distributed over weeks to months. Thus, precipitation peakedness or extreme precipitation, rather than mean annual rainfall, controls the nature of the river facies.

Other effects of the high deposition rates include local rapid channel bed aggradation and deposition of extremely thick (more than 10 m in places), simple downstream accretion sets (Fig. 1C). Sediment was rapidly deposited as the flow expanded downstream of previous accumulations. Another effect of local rapid deposition is increased frequency of

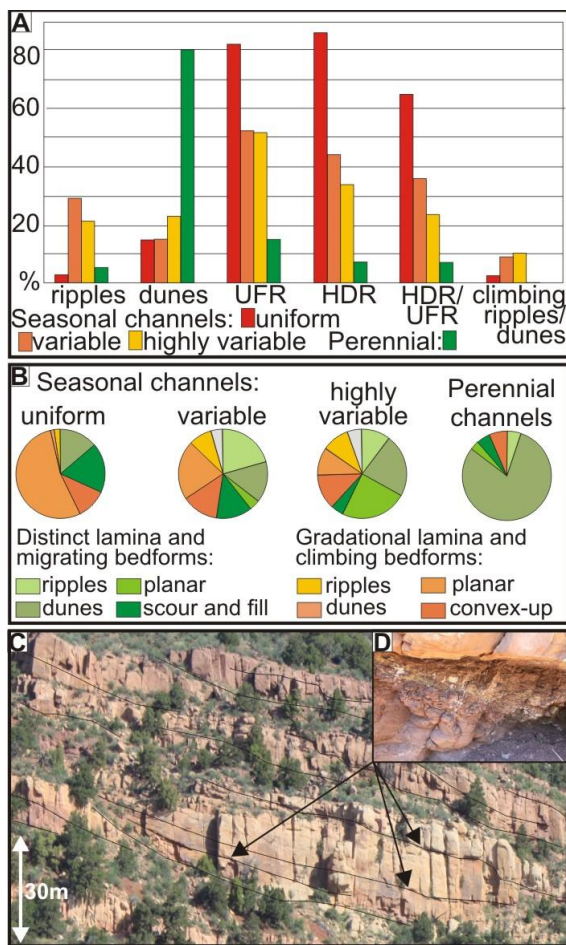


Fig. 1 – Comparison of facies in flashy and perennial rivers (A) by channel types and (B) by specific sedimentary structures. UFR – upper flow regime, HDR – high deposition rate. Some channel fills have a vary uniform appearance due to thick, simple downstream accreting bars (C). In-channel terrestrial bioturbation and pedogenic modification indicates that channels were dry at times (D).

channel avulsions, in places producing highly amalgamated channel packages.

In addition to the sparse vegetation, the intermittent droughts are evidenced by the occurrence of in-channel terrestrial bioturbation and, in places pedogenic modification, on bar accretion surfaces. This implies that the river channels were dry for sustained periods of time and transmitted discharge only during the extreme precipitation triggered flooding events. Moreover, the terrestrial burrows, such as simple vertical burrows and insect nests are in many places several meters long, indicating highly variable water tables.

On larger scale, development of fluvial megafan systems, similar to those, e.g. in the Himalayan foreland, was the response of the rivers to the extreme precipitation. Correlation to the available absolute age dates and biostratigraphy, and our new $\delta^{13}\text{C}$ record, shows that these fluvial megafan systems expanded in direct response to the PETM and the consequent EECO hyperthermals. We conclude that extreme precipitation intensification was a recurring response to early Eocene transient global warming events.

Comparison to literature reveals that extreme precipitation events were not unique for the Uinta Basin, but occurred

widely across the Western Interior of US, and in Europe (e.g., McInerney & Wing, 2011 and references therein). In contrast to the modern climate conditions, where climates with peaked precipitation distribution occur only in the sub-tropical zone, many early Eocene examples come from paleo mid-latitudes. Thus, increase in precipitation peakedness and occurrence of extreme precipitation, rather than increase in humidity was the effect of early Eocene global warming on the hydrological cycle, at least in sub-tropics and mid-latitudes. This is in contrast to the existing global early Eocene climate models that predict increased average humidity.

Moreover, our data on river sediment petrography from the Uinta Basin does not indicate loss of unstable minerals, such as feldspar or lithic fragments during the PETM. In contrast to what has been predicted by existing models, where increase in humidity has been assumed to cause increased chemical weathering rates of silicate minerals. We conclude that increased precipitation peakedness restrained chemical weathering, due to the sustained intermittent droughts and the increased physical erosion during extreme precipitation events.

Comparison to Cretaceous, Jurassic and Triassic river systems shows that intensification of precipitation extremes was not unique for the early Eocene climate system, but also occurred during other past greenhouse times. Thus intensification of extreme precipitation may be a principal, long-term response to global warming. Moreover, IPCC Extreme Weather Report states that there is currently a statistically significant increase in extreme precipitation and more increase predicted for the 21st century. Thus precipitation peakedness needs to be considered as one of the important parameters in understanding the climate systems, rather than just the mean annual precipitation.

REFERENCES

- Abdullatif O.M. (1989) - Channel-fill and sheet-flood facies sequence in the ephemeral terminal River Gash, Kassala, Sudan. *Sedimentary Geology*, 63, 171–184.
- Billi P. (2007) - Morphology and sediment dynamics of ephemeral stream terminal distributary systems in the Kobo Basin (northern Welo, Ethiopia). *Geomorphology*, 85, 98–113.
- Fielding C.R., Allen J.P., Alexander J. & Gibling M.R. (2009) - A facies model for fluvial systems in the seasonal tropics and subtropics. *Geology*, 37, 623–626.
- McInerney F.A. & Wing, S.L. (2011) - The Paleocene-Eocene Thermal Maximum: A perturbation of carbon cycle, climate, and biosphere with implications for the future. *Annu. Rev. Earth Planet. Sci.*, 39, 489–516.
- Sneh, A. (1983) - Desert stream sequences in the Sinai Peninsula. *J. Sediment. Petrol.*, 53, 1271–1280.
- Stear, W.M. (1985) - Comparison of the bedform distribution and dynamics of modern and ancient sandy ephemeral flood deposits in the southwestern Karoo region, South Africa. *Sediment. Geol.*, 45, 209–230.

Input of coarse-grained siliciclastics into the Pyrenean Basin during the PETM (1): overview

Victoriano Pujalte ^(a), Juan Ignacio Baceta ^(a) & Birger Schmitz ^(c)

^(a) Dpt. of Stratigraphy and Paleontology, Faculty of Science and Technology, University of the Basque Country UPV/EHU, Ap. 644, 48080 Bilbao, Spain; E-mail: victoriano.pujalte@ehu.es

^(b) Division of Nuclear Physics, Department of Physics, University of Lund, P.O. Box 118 SE-221 00 Lund, Sweden

Document type: Short note.

Manuscript history: received 15 May 2014; accepted 30 May 2014; editorial responsibility and handling by Gerald R. Dickens & Valeria Luciani.

KEY WORDS: hydrological cycle, siliciclastic deposition, PETM, Spanish Pyrenees.

The PETM is represented in shallow and deep marine sections of the central and western Pyrenees by a 1–4 m thick unit (locally ca. 20 m) of clays or marly clays intercalated into a carbonate-dominated succession (e.g., Baceta, 1996; Schmitz et al., 2001). This unit signifies a massive input of fine-grained terrestrial siliciclastics into the Pyrenean Gulf, which has been attributed to an abrupt and large increase in seasonal rain during the PETM (Schmitz et al., 2001; Schmitz & Pujalte 2007). However, if the hydrodynamic cycle was greatly enhanced during the PETM, terrigenous sediments of a wide range of grain size should be expected to be delivered to the marine basin, which begs the question: where is the coarse-grained fraction? Here we show that coarse-grained siliciclastics were indeed brought into the basin, but that their accumulation mainly occurred in three areally restricted settings: incised valleys, deltas and a deep-sea channel (Fig. 1). The occurrence of these coarse-grained deposits have been known for some time, but evidence of their correlation with the PETM is reported here for the first time.

Incised valley deposits are mainly represented by cross-bedded sands and pebbly sands, almost exclusively made of quartz, and currently being actively quarried for glassware. Proof that these quartz sands pertain to the PETM includes: (1) their stratigraphic position, sandwiched between upper Thanetian and lower Ilerdian marine carbonates (Baceta et al., 1994; Baceta, 1996); (2) organic carbon isotope data, and (3) the fact that clay minerals from the sand matrix are almost 100% kaolinite. The incised valleys, which were excavated during a sea-level lowstand preceding the PETM (Pujalte et al., 2014), funneled coarse siliciclastic deposits towards the sea, a fraction of which accumulated in fluvial-dominated deltas (Fig. 1; Pujalte et al., this volume).

An axially-flowing deep-sea channel existed throughout Paleocene times in the Pyrenean Basin (Fig. 1), within which coarse-grained calciclastic deposits, and lesser volumes of siliciclastic sands, accumulated (Baceta, 1996; Pujalte et al.,

1998). However, these Paleocene deposits are abruptly overlain by coarse-grained quartz sandstone and cm-sized conglomerates, which can be assigned to the PETM based on clay mineral and organic carbon isotopic data, and their position just below marly limestones of the NP10 calcareous nannoplankton biozone (Bernaola et al., 1998).

There have been suggestions that the near absence of carbonates during the PETM in deep marine settings of the Pyrenean Basin was due to dissolution after a rise of the lysocline. The data above, however, reinforce the alternative proposal: the main reason for the carbonate decrease in these hemipelagic sections was dilution by siliciclastics, both coarse- and fine-grained, linked to a dramatic enhancement of riverine discharge.

ACKNOWLEDGEMENTS

Funds to VP and JIB provided by Research Project CLG2011-23770 (Ministerio de Economía y Competitividad, Spanish Government) and Research Group of the Basque University System, Basque Government, IT-631-13, and to BS by the Swedish Research Council (Linné Grant).

REFERENCES

- Baceta J.I. (1996) - El Maastrichtiense superior, Paleoceno e Ilerdiense inferior de la Región Vasco-Cantábrica: secuencias deposicionales, facies y evolución paleogeográfica. Unpublished PhD thesis, University of the Basque Country, 372 pp.
- Baceta J. I., Pujalte V. & Payros A. (1994) - Rellenos de valles encajados en el Maastrichtiense superior y Paleógeno inferior de Alava (Plataforma Noribérica, Cuenca Vasca). *Geogaceta*, 16, 86–89.
- Bernaola G., Nuño-Arana Y. & Payros A. (1998) - Análisis biostratigráfico del Eoceno inferior de la sección de Barinatxe (Pirineos Occidentales) mediante nanofósiles calcáreos. *Geogaceta*, 40, 175–178.
- Pujalte V., Robador A., Payros A. & Samsó J.M. (this volume) - Input of coarse-grained siliciclastics into the Pyrenean

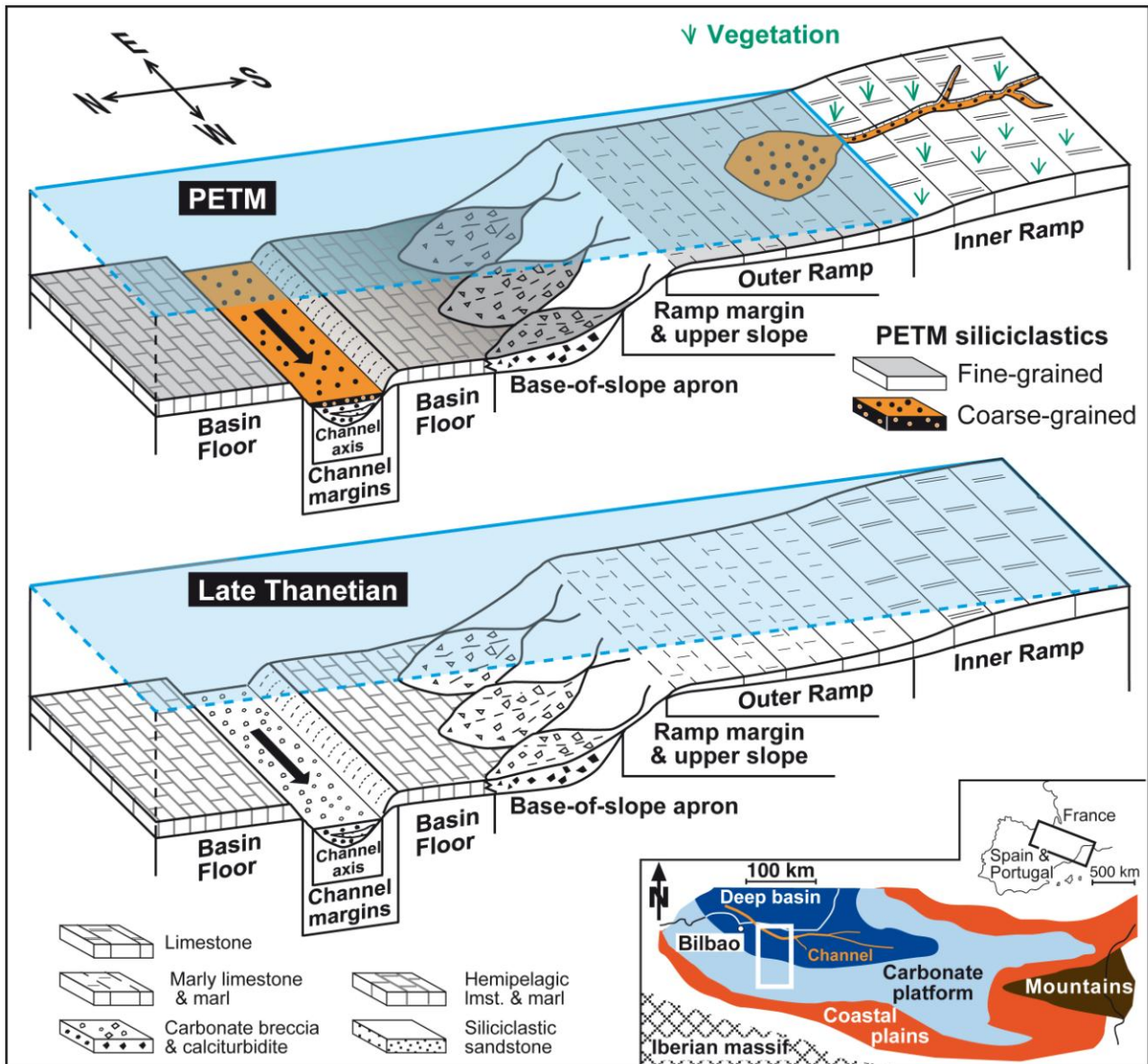


Fig.1 – Reconstructed S-N transects of the southwestern margin of the early Paleogene Pyrenean Basin (inset). Sedimentation was dominantly of a carbonate nature during late Thanetian times in the shallow-marine ramp and in the base-of-slope apron and, in part, also in the axial-flowing deep-sea channel. After a sea-level fall in the latest Thanetian the shallow part of the carbonate ramp became emergent and incised by valleys, through which coarse- and fine-grained siliclastic sediments were funnelled towards the basin during the PETM: coarse-grained sands were accumulated within the incised channels and in delta system, while fine-grained siliclastics mantled most of the basin. An important increase in the grain size of siliclastic deposits is also recorded in the deep-sea channel succession.

Basin during the PETM (2): a river-dominated fandelta within a carbonate platform system.

Pujalte V., Baceta, J.I., Orue-Etxebarria X. & Payros A. (1998) - Paleocene Strata of the Basque Country, W Pyrenees, N Spain: Facies and Sequence Development in a Deep-water, Starved Basin": In: de Graciansky, P.C., Hardenbol, J., Jacquin, T. & Vail, P.R. (eds.), Mesozoic and Cenozoic Sequence Stratigraphy of European basins, SEPM Special Publication, 60, 311–325

Pujalte V., Schmitz B. & Baceta J.I. (2014) - Sea-level changes across the Paleocene–Eocene interval in the Spanish Pyrenees, and their possible relationship with North

Atlantic magmatism. *Palaeogeogr. Palaeoclimatol. Palaeoecol.*, 393, 45–60.

Schmitz B., Pujalte V. & Núñez-Betelu K. (2001) - Climate and sea-level perturbations during the Initial Eocene Thermal Maximum: Evidence from siliclastic units in the Basque Basin (Ermua, Zumaya and Trabakua Pass), northern Spain. *Palaeogeogr. Palaeoecol. Palaeoclimatol.*, 165, 299–320.

Schmitz B. & Pujalte V. (2007) - Abrupt increase in seasonal extreme precipitation at the Paleocene-Eocene boundary. *Geology*, 35, 215–218.

Input of coarse-grained siliciclastics into the Pyrenean Basin during the PETM (2): a river-dominated fan delta within a carbonate platform system

Victoriano Pujalte^(a), Alejandro Robador^(b), Aitor Payros^(a) & Josep María Samsó^(c)

^(a) Dpt. of Stratigraphy and Paleontology, Faculty of Science and Technology, University of the Basque Country UPV/EHU, Ap. 644, 48080 Bilbao, Spain. E-Mail: victoriano.pujalte@ehu.es

^(b) Área de Cartografía Geocientífica, Instituto Geológico y Minero de España (IGME), La Calera 1, Tres Cantos, Madrid, Spain

^(c) Consulting Geologist, C/ Mayor 30, 1º, Jaca, Huesca, Spain

Document type: Short note.

Manuscript history: received 15 May 2014; accepted 30 May 2014; editorial responsibility and handling by Gerald R. Dickens & Valeria Luciani.

KEY WORDS: fluvial-dominated fan delta, hydrological cycle, Ordesa-Monte Perdido National Park, PETM, Spanish Pyrenees.

The Danian–early Ilerdian interval is represented in most of the south-central and south-western Pyrenees by a laterally extensive accumulation of shallow marine carbonates ca. 300 m thick. In the Ordesa-Monte Perdido National Park of Spain, however, a siliciclastic-dominated unit up to 25 m thick, La Pardina Formation, occurs intercalated within this carbonate succession (Fig. 1).

Two major interdigitated lithofacies are recognized within La Pardina Formation, siliciclastic and calcareous. The former makes up the bulk of the unit in the National Park; the latter is secondary in the Park but widespread throughout most of the southern Pyrenees. The calcareous lithofacies includes nummulites-rich sandy marls and marly or sandy limestones and, based on biostratigraphic and isotopic evidence, is confidently ascribed to the PETM. Neither fossil nor isotopic information could be obtained from the siliciclastic lithofacies, but it can be assigned to the PETM on account of its lateral interfingering with the calcareous lithofacies.

La Pardina Formation accumulated in a river-dominated fan delta system, now exposed in the impressive large-scale and laterally continuous vertical cliffs of the National Park, probably near the mouth of a river draining the Iberian Massif (Pujalte et al., this volume). Seaward from the river mouth four intergradational depositional zones are recognized: proximal, middle, distal and prodelta.

Three main subfacies are recognized within the siliciclastic lithofacies, all of them mainly or exclusively composed of quartz sandstones, occasionally pebbly. Siliciclastic subfacies (Ssf) 1 is arranged in fining-up sequences interpreted as delta plain distributary channel fills. In the proximal zone, Ssf1 abruptly overlies an irregular erosional surface carved into upper Thanetian marine carbonates, locally with subaerial exposure features. This is clear proof of a pre-PETM sea-level fall. Ssf2, interpreted as an upper delta front accumulation, it is developed in the middle zone of the system. It is characterized by an overall thickening-coarsening-up trend, being usually

capped by Ssf1. In favourable exposures, large-scale low-angle foresets or clinofolds can be clearly perceived, which attest to a rapid and near continuous progradation and explains the vertical trend. Ssf3 have a massive appearance probably due to bioturbation. It occurs in the distal zone and is attributed to the lower delta front. Deposits of Ssf1 and 2 are unfossiliferous and quartz-cemented, whereas those of Ssf3 have variable proportions of carbonate cement and locally larger foraminifera, often included within tempestite beds. Ssf3 evolves gradually up from, and passes laterally into, the sandy marls and marly limestones of the calcareous lithofacies, interpreted as prodelta deposits.

Clearly, a dramatic sedimentological change took place in the southern Pyrenean shallow-marine setting during the PETM, recorded by a massive input of both coarse- and fine-grained siliciclastics. This input temporarily halted a long-lasting period of carbonate-dominated sedimentation, which resumed after the termination of the thermal event (Fig. 1). Coarse-grained siliciclastics were trapped within the La Pardina fan delta, whereas the prodelta marls and fine-grained siliciclastics became widely redistributed and can now be found in many shallow-marine sections of the southern Pyrenees. This massive but temporary terrigenous supply to the sea can only be explained by a coeval increase in continental runoff and stream power of rivers draining the Iberian Massif, an increase readily attributable to an intensification of the hydrological cycle during the PETM. The occurrence of tempestite beds in the distal delta front further suggests occasional stormy weather episodes.

ACKNOWLEDGEMENTS

This is a contribution to Research Project CLG2011-23770 (Ministerio de Economía y Competitividad, Spanish Government) and Research Group of the Basque University System, Basque Government, IT-631-13.

REFERENCES

Pujalte V., Baceta J. I. & Schmitz B. (This volume) - Input of coarse-grained siliciclastics into the Pyrenean Basin during the PETM (1): overview.



Fig.1 – General view of part of the lower Paleogene succession of the Ordesa and Monte Perdido National Park, southern Pyrenees, Spain. The Mondarruego Formation (lower Thanetian) is composed of limestones with subordinate dolomites. The San Urbez Formation (upper Thanetian) consists of sandy limestones. The bulk of La Pardina Formation (PETM) is comprised of quartz sandstones and pebbly sandstones, except the lowest part, which is formed by marly clays very rich in nummulites of the lowest Ilerdian (= basal Ypresian). The Góriz Formation (Ilerdian) is again entirely composed of limestones rich in *Alveolina* (“*Alveolina* Limestone”). For scale, La Pardina Formation at this location is approximately 25 m thick.

A prospective Early Late Paleocene event (ELPE) from the expanded Río Gor hemipelagic section (Betic Cordillera, southern Spain): foraminifera, nannofossil and isotopic data

Victoriano Pujalte^(a), Xabier Orue-Etxebarria^(a), Estibaliz Apellaniz^(a), Fernando Caballero^(a), Simonetta Monechi^(b), Silvia Ortiz^(c), & Birger Schmitz^(d)

^(a) Dpt. of Stratigraphy and Paleontology, Fac. of Science and Technology, Univ. of the Basque Country UPV/EHU, Ap. 644, 48080 Bilbao, Spain. E-mail: victoriano.pujalte@ehu.es

^(b) Dipartimento di Scienze della Terra, Università di Firenze, Via La Pira 4, I-50121 Firenze, Italy

^(c) PetroStrat Ltd, Tan-y-Graig, Parc Caer Seion, Conwy, LL32 8FA, Wales, UK.

^(d) Division of Nuclear Physics, Department of Physics, University of Lund, P.O. Box 118 SE-221 00 Lund, Sweden

Document type: Short note.

Manuscript history: received 15 May 2014; accepted 30 May 2014; editorial responsibility and handling by Gerald R. Dickens & Valeria Luciani.

KEY WORDS: Betic Cordillera, ELPE hyperthermal, hemipelagic succession, Paleocene, southern Spain.

The Río Gor section (Pujalte et al., 2012) is far more expanded and complete than Alamedilla, so far the most studied lower Paleogene hemipelagic section of the Betic Cordillera (e.g., Arenillas & Molina, 1996). This fact is especially striking in the Paleocene succession, which in Río Gor is about 250 metres thick and probably continuous (Fig. 1A) while in Alamedilla is less than 20 metres thick (Fig. 1B), with an important hiatus comprising most of the Danian, the entire Selandian and the lower part of the Thanetian (Pujalte et al., 2012). The probability of locating Paleocene hyperthermals is, therefore, far greater in Río Gor than in Alamedilla.

The Paleocene is mainly represented at Río Gor by grey-coloured lithologies, the lower part of the section being formed by alternating calcarenites and marls, the remainder by marls and marly limestones. However, intercalated within these grey marly lithologies, there occurs an interval ca. 10 m thick of a prominent red colour (Figs. 1A, C) that, on a preliminary survey, was tentatively assigned to the PETM (Pujalte et al., 2012). The more detailed study herein presented, based on analyses of foraminifera, calcareous nannofossil and carbon isotope composition of dispersed organic matter of 26 samples, leads to a different interpretation.

In effect, the planktonic foraminiferal assemblage includes *I. albeardi*, *I. pusilla*, *I. laevigata*, *Gl. pseudomenardii*, *Gl. ehrenbergi*, *M. occlusa*, *M. velascoensis*, *M. angulata*, *M. conicotruncata*, *M. acutispira*, *S. velascoensis* and *A. subsphaerica*, which suggests a mid-Paleocene age. The calcareous nannofossil assemblage reinforces this conclusion, as it comprises, among others, *F. tympaniformis*, *T. eminens*, *T. pertusus*, *C. pelagicus*, *E. subpertusa*, *S. moriformis*, *E. macellus* and the appearance of the genera *Discoasteroides* and *Heliolithus*, indicative of the upper part of Zone NP5 and Zone NP6.

The studied interval has been subdivided into five parts based on its foraminiferal associations (Fig. 1C). Planktonic specimens in parts 1 and 5 account for more than 95% of the total foraminiferal assemblage. The planktonic foraminifera are still dominant in parts 2 and 4, but their sizes are always notably smaller than in parts 1 and 5. Finally, in part 3 benthic foraminifera account for ca. 50% of the total foraminiferal population, their assemblages being moderately diverse but low in evenness, as they are characterized by the dominance of small abyssaminids known to peak after the PETM and other Eocene hyperthermals (e.g., Thomas, 2007). The Lowest occurrence (LO) of *H. kleinpellii*, marker of the base of NP6 and CP5 (Martini, 1971; Okada & Bukry, 1980), was found at the bottom of part 3, which is characterized by the occurrence of *D. bramlettei*, *S. anarrhopus* and *Sphenolithus sp.1* of Agnini et al. 2007.

Although the isotopic values show significant scatter, with $\delta^{13}\text{C}_{\text{toc}}$ values ranging between -22.2 and -27.5‰ , the typical early to mid Paleocene gradual rise in $\delta^{13}\text{C}_{\text{toc}}$ can be seen. The $\delta^{13}\text{C}_{\text{toc}}$ values in the lower part of the section are generally a few per mil lower than in the upper part. However, very negative values (-27.5‰) occur also around parts 3 and 4, indicating some environmental stress.

It is concluded that the studied interval contains what is probably the most expanded record of the ELPE reported to date, with part 2 recording a comparatively long period of stressed oceanic conditions, part 3 the climax of the event and part 4 the recovery to normal background conditions indicated by part 5.

In the stratotypic Zumaia section (western Pyrenees) the core of the ELPE was found to occur eight precession cycles below the GSSP of the Thanetian Stage, situated at the base of magnetochron C26n (Bernaola et al., 2007; Schmitz et al., 2011). It is thus a good criterion to approximate the Selandian/Thanetian boundary, its utility being reinforced by its finding in the Betic Cordillera.

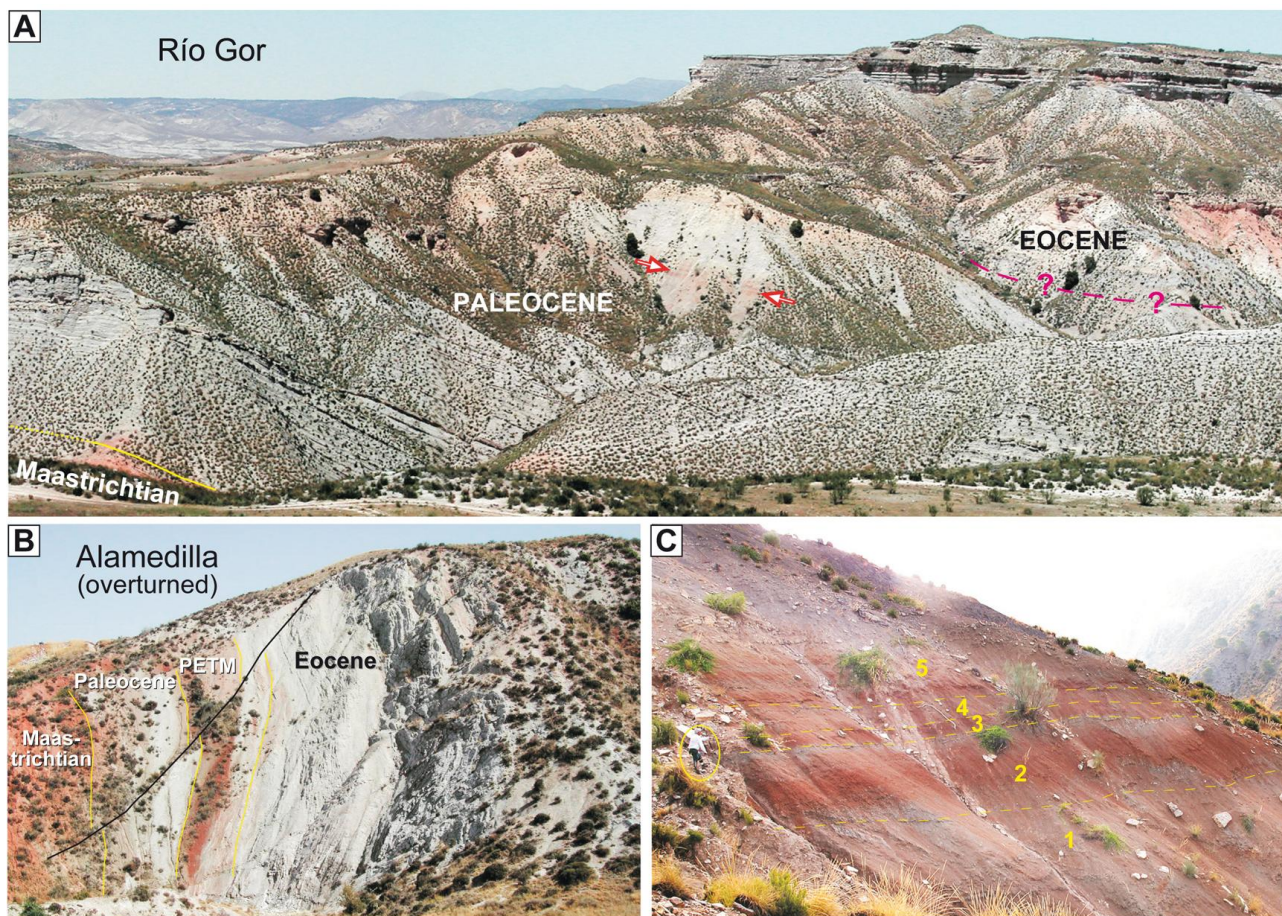


Fig. 1. A and B, Field view of the expanded (ca. 250 m) Río Gor section and of the lower Paleogene segment of the Alamedilla section, both from the Betic Cordillera, southern Spain. C, Close-up of the interval analyzed in this study (arrowed in Fig. 1A), with indication of the 5 parts differentiated (encircled geologist in the left gives scale).

ACKNOWLEDGEMENTS

This study is a contribution to Research Project CLG2011-23770 (Ministerio de Economía y Competitividad, Spanish Government) and Research Group of the Basque University System, Basque Government, IT-631-13.

REFERENCES

- Agnini C., Fornaciari E., Raffi I., Rio D., Röhl U. & Westerhold T. (2007) - High-resolution nannofossil biochronology of middle Paleocene to early Eocene at ODP Site 1262: Implications for calcareous nannoplankton evolution. *Mar. Micropaleontol.*, 64, 215–248.
- Arenillas I & Molina E. (1996) - Biostratigrafía y evolución de las asociaciones de foraminíferos planctónicos del tránsito Paleoceno-Eoceno en Alamedilla (Cordilleras Béticas). *Revista Española de Micropaleontología*, 18, 85–98.
- Bernaola G., Baceta J. I., Orue-Etxebarria X., Alegret L., Martín-Rubio M., Arostegui J. & Dinarès-Turell J., (2007) - Evidence of an abrupt environmental disruption during the mid-Paleocene biotic event (Zumaia section, western Pyrenees). *Geol. Soc. Am. Bull.*, 119, 785–795.
- Pujalte V., Orue-Etxebarria X., Apellaniz E., Caballero F. & Robles S. (2012) - Río Gor, comarca de Guadix, provincia de Granada: una nueva sección de referencia del Paleógeno inferior Subbético. *Geogaceta*, 52, 53–56.
- Schmitz B., Pujalte V., Molina E., Monechi S., Orue-Etxebarria X., Speijer R. P., Alegret L., Apellaniz E., Arenillas I., Aubry M. P., Baceta J. I., Berggren W. A., Bernaola G., Caballero F., Clemmensen A., Dinarès-Turell J., Dupuis C., Heilmann-Clausen C., Hilario, A., Knox R., Martín-Rubio M., Ortiz S., Payros A., Petrizzo M.R., von Salis K., Sprong J., Steurbaut E., & Thomsen, E. (2011) - The Global Stratotype Sections and Points for the bases of the Selandian (Middle Paleocene) and Thanetian (Upper Paleocene) stages at Zumaia, Spain. *Episodes*, 34, 220–243.
- Thomas, E., 2007. Cenozoic mass extinctions in the deep sea; what disturbs the largest habitat on Earth?. In: Monechi S., Coccioni R. & Rampino M. (Eds.), *Large Ecosystem Perturbations: Causes and Consequences*, Geological Society of America Special Paper 424: Boulder, Colorado, 1-24.

An unexpected record of the PETM in terrestrial and organic sediments of Avesnois, between the Paris and Belgian Basins, NW Europe

Florence Quesnel ^(a,b), Jean-Yves Storme ^(c), Emile Roche ^(c), Alina Iakovleva ^(d), Pieter Missiaen ^(e), Thierry Smith ^(f), Chantal Bourdillon ^(g), Jean-Marc Baele ^(h), Johan Yans ⁽ⁱ⁾, Johann Schnyder ^(j), Paola Iacumin ^(k), Christine Fléhoc ^(l) & Christian Dupuis ^(h)

^(a) BRGM (French Geological Survey), Georesources Division, Land Use Geology Unit, 3, Avenue Cl. Guillemin, 45060 Orléans Cedex 2, France. E-mail: f.quesnel@brgm.fr

^(b) UMR 7327 of the CNRS/INSU, Orléans University & BRGM, 1A, rue de la Férollerie, 45071 Orléans, France

^(c) Geology Dept, Palaeobiogeology-Palaeobotany-Palaeopalynology, Liège University, Allée du 6 Août, 17, 4000 Liège Sart-Tilman, Belgium

^(d) Geological Institute, Russian Academy of Sciences, Pyzhevsky pereulok 7, 119017 Moscow, Russia

^(e) Research Unit Palaeontology, Ghent University, Krijgslaan 281, S8, B-9000 Ghent, Belgium

^(f) O.D. Earth & History of Life, Royal Belgian Institute of Natural Sciences, Vautierstraat 29, 1000 Brussels, Belgium

^(g) ERADATA, 170, Avenue Félix Gesnelay, 72100 Le Mans, France

^(h) Geology and Applied Geology, Faculty of Engineering, University of Mons, 20, Place du Parc, 7000 Mons, Belgium

⁽ⁱ⁾ University of Namur, Department of Geology, Rue de Bruxelles, 61, 5000 Namur, Belgium

^(j) ISTeP, Pierre & Marie Curie University-Paris 6, 4, Place Jussieu, 75252 Paris cedex 05, France

^(k) Earth Sciences Department, Parma University, Viale G.P. Usberti, 157/A, 43100 Parma, Italy

^(l) BRGM (French Geological Survey), Laboratory Division, Isotopes Unit, 3, Avenue Cl. Guillemin, 45060 Orléans Cedex 2, France

Document type: Short note.

Manuscript history: received 15 May 2014; accepted 30 May 2014; editorial responsibility and handling by Gerald R. Dickens & Valeria Luciani.

KEY WORDS: Avesnois, Belgian & Paris Basins, Carbon Isotope Excursion, faunal & floral changes, palynology, PETM, stratigraphy.

The stratigraphy of the Late Paleocene-Early Eocene has been revised in Avesnois thanks to drillings supporting a geological mapping project. Detailed sampling and analyses were performed along selected drillings, among which sedimentological, mineralogical, chemostratigraphic ($\delta^{13}\text{C}_{\text{org}}$), biostratigraphic and palynological data have been obtained. New members/formations (Mbs/Fms) are defined around the Paleocene-Eocene boundary (PEb, PETM) and compared to the lithostratigraphic nomenclatures of the Belgian and Paris Basins (Steurbaut, 1998; Aubry et al., 2005). Biostratigraphy based on the study of foraminifera and mammal fauna, palynological content and chemostratigraphy enable correlation to be established between adjacent basins as well as sea level and landscape evolutions to be refined during this critical interval.

Upper Thanetian marine units

In the AVE 007-drilling (Mormal Forest, Locquignol, between Englefontaine, Landrecies and Maroilles villages), the Coniacian chalk is overlain by a flint conglomerate, whose sandy-clayey matrix contains Thanetian pollen and dinocysts. Widespread in Avesnois and containing often reworked Upper Cretaceous foraminifera and occasionally glauconite, this unit constitutes the Vervins Mb (cf. ‘Argile à silex de Vervins’ interpreted as a marine conglomerate by Gosselet, 1879). It is often overlain by the Mondrepuis-Bettrechies Sand Mb (cf. ‘Sable verts de l’Avesnois’), a thin sandy glauconiferous unit, more clayey and silty westward (cf. ‘Tuffeau de Valenciennes’ Mb). The three Mbs constitute the Hainaut-Valenciennois Fm and can be correlated to the Belgian Grandglise Mb (upper part of the Hannut Fm) and Bois-Gilles Fm, and to the Paris Basin

Châlons-sur-Vesles and Bracheux Fms, all Thanetian in age.

Uppermost Paleocene to lowermost Eocene terrestrial units

In AVE 007 the Vervins Mb is unconformably overlain by flint gravels (Mormal Mb), then a pyritic sand (Le Quesnoy Sand Mb, cf. ‘Sables et Grès du Quesnoy’ of Gosselet, 1890), and a lignitic clay (Locquignol Mb), silty and ochreous at the top. All but the top ochreous paleosol contain spores and pollen grains and are devoid of dinocysts, they were thus probably deposited in terrestrial environments. The Carbon Isotope Excursion (CIE) of the PEb begins below the top of the sandy unit and continues in the lignitic clay. The palynological study confirms the Locquignol Mb’s earliest Eocene age and allows correlation with the base of the Tienen Fm.

To the East of AVE 007 along the Belgium-France border, fluvial fossiliferous gravels and sands have been studied in past sand quarries (Erquelinnes Sand Mb). Above a sharp unconformity, they i) overly Upper Thanetian marine sands (Bois-Gilles Fm, NP9a, then Grandglise Mb, NP8), ii) contain a mammal fauna referred as MP7 in the Mammalian biochronological scale for the European Paleogene (Missiaen et al., 2013) and iii) record the first part of the CIE onset in the basal fossiliferous gravel and marl beds.

Three km west of Erquelinnes and toward AVE 007 a few drillings have recognized a sandy and pyritic unit containing resinite fragments, lignite and peat beds (Vieux Reng Mb), overlying a thin basal flint gravel bed (Mormal Mb).

These five Mormal, Le Quesnoy, Locquignol, Vieux-Reng and Erquelinnes Sand Mbs form the Sambre Fm. Such fluvial gravels and sands, more or less lignitic, clayey or marly are widespread in northern France and southeastern Belgium. They belong to the so-called Upper “Landenian” and are correlated to the Tienen Fm. In AVE 007, they record the CIE onset marking the PEb and 2.5 m of Upper Paleocene fluvial units, in contrast with Belgian drillings such as Doel and Kallo where a hiatus is present at the PEb.

Lower Ypresian hiatus and marine units

In AVE 007, a laminated silty unit overlies the Locquignol Mb, contains dinocysts *Wetzeliella sp.* and agglutinated foraminifera similar to those of the base of the Orchies Clay Mb. Widespread in Avesnois-Valenciennois that marine unit is named Avesnois Mb, it is locally richer in very fine sand, and correlated to the base of the Kortrijk Clay Fm (Ieper Gp).

In Avesnois, Sparnacian lagoonal units are absent upon the terrestrial ones described above, again marking a reverse trend when compared with the Belgian and adjacent Basins. This may result from restricted terrestrial environments coinciding with Variscan accidents and structural highs between the Artois anticline and Ardenne Massif, or to their deposition followed by subsequent erosion prior to the Lower Ypresian marine transgression (cf. sea level drop 2 of Dupuis et al., 2011).

Correlations and PETM impact on land

All terrestrial units here described fill fluvial channels incised in marine Thanetian and older units such as the Cretaceous or the Variscan basement in Avesnois and Belgium, as already reported elsewhere in northern France (cf. sea level drop 1 of Dupuis et al., 2011). They exhibit locally cross stratification, lignite, flora or vertebrate fauna, for example at Leval, Hoegaarden and Dormaal, and/or are intensively silicified with scarce root or leaf casts.

Similar fluvial sediments and silcretes are recognized in the first Sparnacian units and paleogeography of the Paris, Dieppe-Hampshire and London Basins, where the PEb is also present, the CIE being recorded on thicknesses between 3 m (as in AVE 007) to >20 m (as in Sinceny). These features may be regarded now as constant in those Sparnacian landscapes recording the PETM, with very rapid lateral and vertical facies shift, particular paleosols, a few fossiliferous fluvial to lacustrine units and variable deposition rates/sediments preservation.

Terrestrial sediments, flora and fauna have been described there before the CIE onset as well, for example at Cobham, Vasterival or Rivecourt (e.g. Smith et al., 2014). Lihons, an intermediate outlier situated between AVE 007 and Sparnacian sites of those basins has further been investigated: marine Thanetian sands are overlain by thin fluvial, lacustrine then lagoonal sediments, the two latter recording the CIE of the PETM on an interval 4 m thick. Here again the basal terrestrial sediments have been deposited before the PEb.

In AVE 007, depositional environments are fluvial for the Mormal and Le Quesnoy Mbs, and evolve toward flood plain then palustrine ones for the Locquignol Mb, probably here after the river bed migration, but still recording sporo-pollen fluvial inputs from the hinterland, the whole indicating a rather humid subtropical climate. Compared to the Locquignol Mb, the sporopollinic assemblage of the Mormal and Le Quesnoy Mbs (below the CIE onset) is different, particularly regarding the *Normapolles* distribution, the Tricolpates, Tricolporates and Monocolpates relative pollen abundances and the pollen ratio of *Plicapollis pseudoexcelsus*/Juglandaceae.

In the three Mbs, rapid vertical variations characterize pollen and fern spores assemblages, with peaks of particular taxa reaching 25% of the total counts, such as for *P.*

pseudoexcelsus, *T. platycaryoides*, *C. dorogensis*, *P. mcgregorii*, *T. robustus*. They suggest rapid floral changes in the catchment and/or sources changes in the surrounding landscapes compartments for the rivers supplying the fluvial sediments. Resinite particles are irregularly abundant as well as microcharcoals are occasionally abundant, notably slightly before the CIE onset and 1.5 m above it, still within the CIE.

The clay mineral assemblage is homogeneous along marine Thanetian units and strongly dominated by Illite-Smectite (IS) mixed layers, whatever the facies, while it is more variable in the marine Ypresian silts (abundant IS, followed by Kaolinite, Illite, Chlorite and Vermiculite). In contrast terrestrial units are dominated by IS followed by Kaolinite, Illite and very rare Chlorite, and no variation is observed across the PEb.

Those data would suggest that major environmental changes have regionally begun before the PETM, at the very end of the Paleocene, when terrestrial realm has settled, in relation with a regional uplift. Clay minerals reflect constant reworking of preexisting weathering profiles established upon Cretaceous strata and Variscan basement, while vegetation modifications are subtle and more likely attributable to changes of depositional environments.

REFERENCES

- Aubry M.P., Thiry M., Dupuis Ch. & Berggren W.A. (2005) - The Sparnacian deposits of the Paris Basin: A lithostratigraphic classification. *Stratigraphy*, 2 (1), 65-100.
- Dupuis C., Quesnel P., Iakovleva A.I., Storme J.Y., Yans J. & Magioncalda R. (2011) - Sea level changes in the Paleocene-Eocene interval in the NW France: Evidence of two major drops encompassing the PETM. In: Egger H. (ed.), CBEP 2011, Conference Program and Abstracts, 5-8 June 2011, Salzburg, Austria. *Berichte der Geologischen Bundesanstalt*, 85, 68.
- Gosselet J. (1879) - L'Argile à silex de Vervins, *Annales de la Société Géologique du Nord*, VI, 317-339, 1 planche.
- Gosselet J. (1890) - Relations entre les sables de l'Eocène Inférieur dans le Nord de la France et dans le Bassin de Paris, *Bull. Serv. Carte Géol. de la France et des topographies souterraines*, 8, janvier 1890, 1-16.
- Missiaen P., Quesnel F., Dupuis C., Storme J.-Y. & Smith T. (2013) - The earliest Eocene mammal fauna of the Erquelinnes Sand Member near the French-Belgian border. *Geologica Belgica*, 16/4, 262-273.
- Smith T., Quesnel F., De Ploëg G., De Franceschi D., Métais G., De Bast E., Solé F., Folie A., Boura A., Claude J., Dupuis C., Gagnaison C., Iakovleva A.I., Martin J., Maubert M., Prieur J., Roche E., Storme J.-Y., Thomas T., Tong H., Yans J. & Buffetaut E. (2014) - First Clarkforkian equivalent Land Mammal Age in the latest Paleocene basal Sparnacian facies of Europe: fauna, Flora, paleoenvironment and (bio)stratigraphy. *PLoS ONE* 9(1): e86229, 20 p, doi:10.1371/journal.pone.0086229.
- Sturbaut E. (1998) - High resolution holostratigraphy of Middle Paleocene to Early Eocene strata in Belgium and adjacent area. *Palaeontographica*, A 247, 91-15.

A Paleocene Pre-onset Carbon Isotope Excursion Recorded in the Shallow Marine Environment of Southern Maryland (USA)

Marci M. Robinson ^(a), Jean M. Self-Trail ^(a), Gregory A. Wandless ^(b) & Debra A. Willard ^(a)

^(a)Eastern Geology and Paleoclimate Science Center, United States Geological Survey, Reston, Virginia 20192, USA. E-mail: mmrobinson@usgs.gov

^(b)Eastern Mineral and Environmental Resources Science Center, United States Geological Survey, Reston, Virginia 20192, USA

Document type: Short note.

Manuscript history: received 15 May 2014; accepted 30 May 2014; editorial responsibility and handling by Gerald R. Dickens & Valeria Luciani.

KEY WORDS: calcareous nannofossils, foraminifera, PETM, pre-onset excursion, South Dover Bridge.

The Paleocene-Eocene Thermal Maximum (PETM) is marked by a carbon isotope excursion (CIE) at 55.8 Ma that appears dramatic and geologically instantaneous in deep-sea cores where accumulation rates are low and the CIE onset is often truncated. Shallow marine sections are thought to provide a more detailed and complete record of the event as well as the response of shallow marine ecosystems. In a shallow water core from South Dover Bridge in southern Maryland (USA), the CIE onset is recorded as a change of -4 per mil over 4m of sediment (Self-Trail et al., 2012) and is preceded by a pre-onset excursion (POE) of -2 per mil over 0.8m of sediment (Fig. 1). A POE is not recorded in other shallow marine cores from this region. Does this early, minor excursion represent an initial step toward the CIE, or is it an unrelated local event? We will examine the sedimentologic and biotic response to this event and to the CIE to help determine the nature of the POE.

The CIE onset at South Dover Bridge is roughly coincident with a lithologic change at ~204m from the glauconitic sand of the Aquia Formation below to the massive, kaolinite-dominated Marlboro Clay above. Based on benthic foraminifera, both formations were deposited under inner to middle neritic conditions, and this transition is interpreted as an increase in influx from the continent (Kopp et al., 2009). Pollen data support this interpretation as pollen productivity remains very low throughout the Aquia Formation and begins to increase at 204.7m. The lithologic change may also indicate a sea level rise, as planktic to benthic foraminifer ratios increase across the contact.

Carbon isotope data show the CIE onset at ~204m and the earlier, smaller POE of -2 per mil in the Aquia Formation beginning at 206.7m and ending at 205.9m (~2m beneath the CIE). Both the CIE and the POE are characterized by changes in grain size as well as in microfossil assemblages, abundance and preservation.

The majority of the Marlboro Clay is composed of <3% sand by weight. Most of the Aquia Formation is ~60% sand by weight, but during the POE, sand weight percent falls to 40%

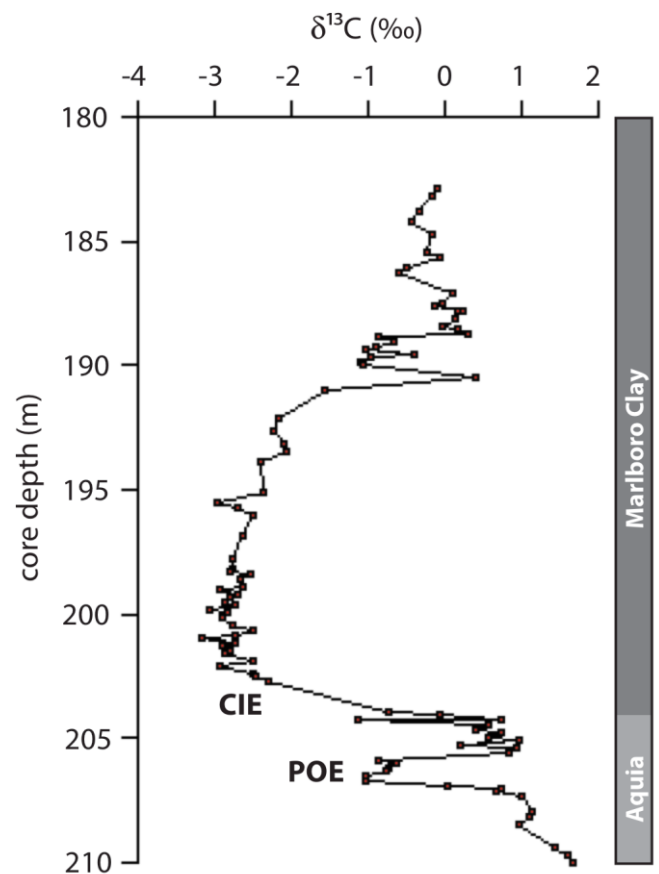


Fig.1 – Carbon isotope (bulk) changes with depth across the PETM, highlighting the carbon isotope excursion (CIE) and the pre-onset excursion (POE) in the South Dover Bridge core from Maryland, USA.

then rebounds to 80% before returning to baseline values. The clayey layer within the POE is visible in the core. The uppermost Aquia Formation, just below the Marlboro Clay contact, is also clayey and ~40% sand.

A dissolution zone exists at the CIE onset (204.0m to 202.7m) in which no calcareous nannofossils are present. Planktic and benthic foraminifers decrease in abundance and species richness during this dissolution zone and show obvious signs of dissolution. The planktic foraminifers that remain are visibly recrystallized due to diagenetic alteration. This pattern of dissolution coupled with decreases in abundance and species richness is repeated in the POE, to a lesser degree, marking a second, less severe dissolution zone.

Calcareous nannofossils also decrease in species richness during the POE. Although many of the species present during the POE are dissolution resistant (i.e., the Fasciculiths), others with delicate central areas such as *Calciosolenia aperta* show little or no increase in dissolution. Additionally, *Chiasmolithus bidens*, *Ellipsolithus distichus* and *Placozygus sigmoides* show a decrease in relative abundance during the POE while other species (*C. aperta*, *Prinsius bisulcus*, *Toweius tovae*) show a marked increase in abundance. This suggests that at least some of the changes in the calcareous nannofossil assemblage are caused by a process or response other than ocean acidification. Immediately following the POE, *Hornibrookina arca*, a species possibly indicative of high fertility, increases to >70% relative abundance, possibly due to an increase in continental runoff.

The lithologic and biotic changes recorded at SDB during the POE may represent a precursor event related to the global CIE onset, one that is not recorded in deep-sea records. If so, these data highlight the necessity to study shallow records from sites with high accumulation rates to fully understand the PETM causation and ocean acidification processes. It is also possible that the South Dover Bridge POE event may record a local response. Carbon isotopic data based on n-alkanes and benthic foraminifers are currently being collected and will be used to decouple any local signal from the bulk carbon isotopic signal.

REFERENCES

- Kopp R.E., Schumann D., Raub T.D., Powars D.S., Godfrey L.V., Swanson-Hysell N.L., Maloof A.C. & Vali, H. (2009) - An Appalachian Amazon? Magnetofossil evidence for the development of a tropical river-like system in the mid-Atlantic United States during the Paleocene–Eocene thermal maximum. *Paleoceanography*, 24, 1–17.
- Self-Trail J.M., Powars D.S., Watkins D.K. & Wandless, G.A. (2012) - Calcareous nannofossil assemblage changes across the Paleocene-Eocene Thermal Maximum: Evidence from a Shelf Setting. *Mar. Micropaleontol.*, 92-93, 61-80.

A record of fire through the Early Eocene

Brittany E. Robson ^(a), Margaret E. Collinson ^(a), Walter Riegel ^(b), Volker Wilde ^(c),
Andrew C. Scott ^(a) & Richard D. Pancost ^(d)

^(a) Department of Earth Sciences, Royal Holloway University of London, Egham, Surrey, TW20 0EX, UK. E-mail: Brittany.Robson.2008@live.rhul.ac.uk

^(b) Geowissenschaftliches Zentrum Göttingen, Geobiologie, Goldschmidtstrasse 3, D-37077, Göttingen, Germany

^(c) Sektion Palaeobotanik, Senckenberg Forschungsinstitut und Naturmuseum, Senckenberganlage 25, 60325 Frankfurt am Main; Germany

^(d) The Cabot Institute and the Organic Geochemistry Unit, School of Chemistry, University of Bristol, Cantocks Close, Bristol, BS8 1TS, UK

Document type: Short note.

Manuscript history: received 15 May 2014; accepted 30 May 2014; editorial responsibility and handling by Gerald R. Dickens & Valeria Luciani.

KEY WORDS: charcoal, Early Eocene, EECO, fire, inertinite, lignite, Schöningen.

One of the key sources of evidence for ancient wildfires is the presence of charcoal (usually termed inertinite in coals) in the fossil record (Scott et al., 2014). A 400 million year record of charcoal in coals (Glasspool & Scott, 2010) showed low amounts of charcoal in the Eocene. However, the time interval covered in that study inevitably meant that the temporal resolution was insufficient to determine any link between charcoal abundance and Paleogene hyperthermal events such as the Early Eocene Climatic Optimum (EECO). Riegel et al. (2012) have undertaken a long term stratigraphic, sedimentological and palaeoenvironmental project on the Early Eocene lignite and interbed sequence in the Schöningen mine in Germany that they considered to be unique worldwide. Their qualitative field evidence suggested that wildfire activity in the Early Eocene might have been higher than implied by the Glasspool and Scott study. Paleogene hyperthermals, such as the EECO, are important partial analogues for future warming trends in the current climate system. Consequently, better understanding of Early Eocene wildfire may contribute to better predictions of future wildfire activity.

The Schöningen mine exposes a sequence of 170m that includes 11 lignite seams spanning the Early Eocene. The lignites are rooted, indicative of autochthonous peat accumulation. One clastic interbed contains palm stumps, whilst others show features of intertidal and nearshore marine influence (including clay/sand alternations, cross-bedding and *Ophiomorpha* burrows). One of the interbeds contains rooted herbaceous plants, which were clearly tolerant of some marine influence. The sequence, therefore, is ideal for investigating the temporal variations in charcoal occurrence through the Early Eocene in a low-lying coastal setting. The lignites are chosen for study for several reasons: (i) the peat-forming depositional environments were not affected by the multiple variables of fluvial charcoal transport (concentration, floatation, size sorting, fragmentation etc.), (ii) being autochthonous these

lignites can provide a record of local fire and (iii) results can be compared with previous work on coals.

Stratigraphically oriented lignite pillars were excavated in the field and tightly wrapped in extra strong aluminium foil to prevent breakage. In the laboratory these were dried, embedded in resin, cut and polished (following the method in Collinson et al., 2007) to produce an “in situ pillar” suitable for study using a reflectance microscope (under oil). As can be seen from Figure 1 (c. 2 mm thickness of lignite) this method provides high-resolution information and an *in situ* record of charcoal in original temporal and spatial context. Not only can charcoal be quantified but also minimum particle sizes can be measured (particles could be larger than seen in this single plane of section), and charcoal distribution can be assessed (e.g. banded, clumped or irregular).

Previous work has quantified charcoal in polished blocks using eyepiece graticule grids (e.g. Belcher et al., 2005, Collinson et al., 2007; Hudspith et al., 2012), but there is no standard quantification method and those studies were very time intensive. In this study a new line transect method, counting three transects of 500 points each, was devised and tested to quantify inertinite (=fossil charcoal) as defined by the International Committee for Coal and Organic Petrology’s (ICCP) standard classification system. The new method is least time-consuming allowing for more samples to be studied, it accounts for variation in charcoal distribution through the oriented block and the point count is comparable with industry standards and previous work. Using this method *in situ* inertinite percentages have been obtained from 10 of the 11 lignite seams at Schöningen spanning the Early Eocene.

Charcoal occurs in all seams indicating that fires occurred in the area throughout the Early Eocene. Charcoal is present in a range of particle sizes indicating that local fires occurred in the peat forming environment and suggesting that there may also have been regional fire activity with some small charcoal blown in. The charcoal shows no distinctive distribution pattern unlike the repeated, multiple scale banding that characterises immediately pre PETM fires at Cobham, UK (Collinson et al., 2007; 2009). Early Eocene fires were not,

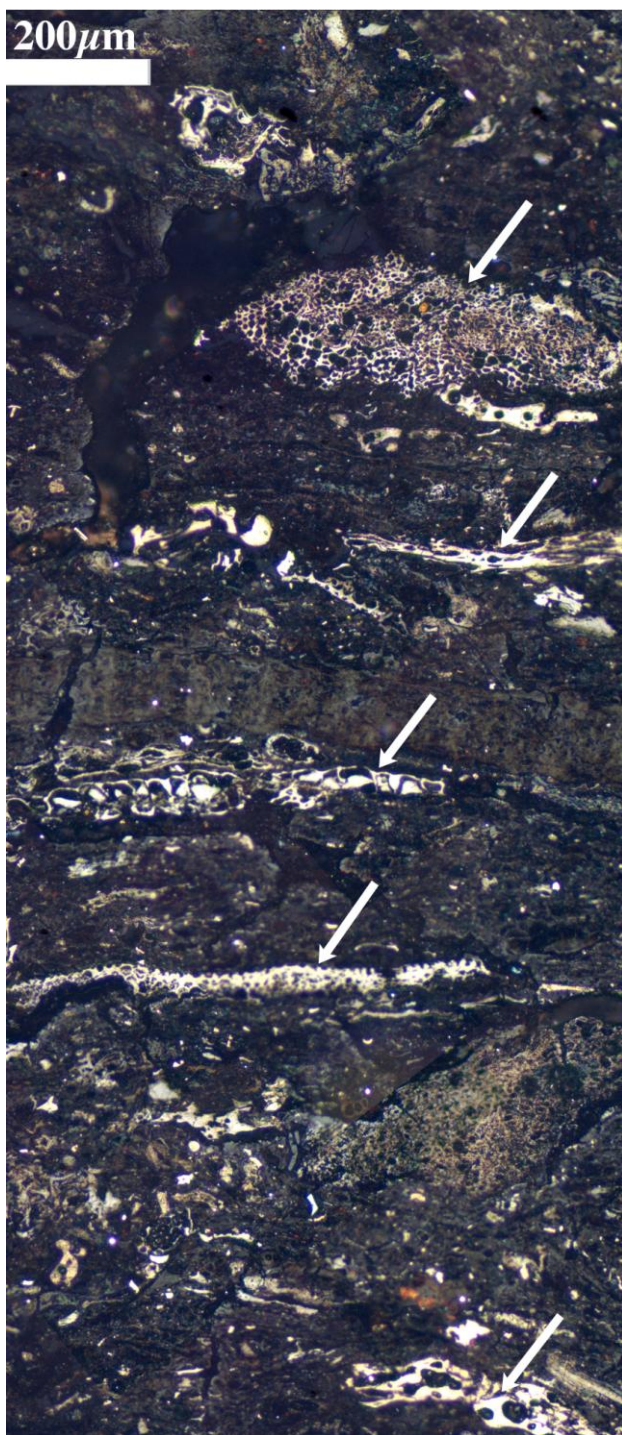


Fig. 1 – A small portion of a polished block of lignite, from the top of Seam 1 at Schöningen, comprising a montage of images seen in reflected light under oil. Inertinite (charcoal, white arrows) is recognized by the high reflectance (light grey to white) compared to surrounding material. (From Seam 1, bed 10, base of block 0).

therefore, episodic or periodic events. Charcoal percentages through the Early Eocene of Schöningen do not indicate any increase in fire activity during the EECO.

ACKNOWLEDGEMENTS

We gratefully acknowledge funding to Collinson, Robson and Scott from NERC grant NE/J008656/1 and to Pancost from NERC grant NE/J008591/1. We thank Neil Holloway (Earth Sciences, Royal Holloway University of London) for production of polished blocks and Karin Schmidt (Senckenberg Forschungsinstitut und Naturmuseum, Frankfurt) for extensive logistical support. Marcus Badger & Gordon Inglis (University of Bristol), Olaf Lenz (TU Darmstadt) and Karin Schmidt are thanked for help with fieldwork at Schöningen. We are grateful to the mine management for access to the mine and to the mine staff for technical support.

REFERENCES

- Belcher C.M., Collinson M.E. & Scott A.C. (2005) - Constraints on the thermal energy released from the Chicxulub impactor: new evidence from multi-method charcoal analysis. *J. Geol. Soc. London*, 162, 591–602.
- Collinson M.E., Steart D.C., Scott A.C., Glasspool I.J. & Hooker J.J. (2007) - Episodic fire, runoff and deposition at the Palaeocene-Eocene boundary. *J. Geol. Soc. London*, 164, 87–97.
- Collinson M.E., Steart D.C., Harrington G.J., Hooker J.J., Scott A.C., Allen L.O., Glasspool I.J. & Gibbons S.J. (2009) - Palynological evidence of vegetation dynamics in response to palaeoenvironmental change across the onset of the Paleocene-Eocene Thermal maximum at Cobham, Southern England. *Grana*, 48, 38–66.
- Glasspool I.J. & Scott A.C. (2010) - Phanerozoic concentrations of atmospheric oxygen reconstructed from sedimentary charcoal. *Nature Geosci.*, 3, 627–630
- Hudspeth V., Scott A.C., Collinson M.E., Pronina N. & Beeley T. (2012) - Evaluating the extent to which wildfire history can be interpreted from inertinite distribution in coal pillars: An example from the Late Permian, Kuznetsk Basin, Russia. *International Journal of Coal Geology*, 89, 13–25.
- Riegel W., Wilde V. & Lenz O.K. (2012) - The early Eocene of Schöningen (N-Germany) – an interim report. *Austrian J. Earth Sci.*, 105, 88–109.
- Scott A.C., Bowman D.M.J.S., Bond W.J., Pyne S.J. & Alexander M.E. (2014) - *Fire on Earth: An Introduction*. Wiley and Sons. 413pp.

An organic geochemical investigation of organic matter sources and carbon cycling within Eocene Lake Uinta, Parachute Creek Member, Green River Formation, Uinta Basin

Megan Rohrsen ^(a), Alice Charteris ^(a), Gordon N. Inglis ^(a), Danielle Grogan ^(b), Richard D. Pancost ^(a) & Jessica H. Whiteside ^(c)

^(a) Organic Geochemistry Unit, School of Chemistry, The Cabot Institute, University of Bristol, Cantock's Close, Bristol BS8 1TS, U.K.: E-mail: megan.rohrsens@bristol.ac.uk

^(b) Institute for the Study of Earth, Oceans, and Space, University of New Hampshire, USA

^(c) Ocean and Earth Science, National Oceanography Centre Southampton, University of Southampton, European Way, Southampton SO14 3ZH, UK.

Document type: Short note.

Manuscript history: received 15 May 2014; accepted 30 May 2014; editorial responsibility and handling by Gerald R. Dickens & Valeria Luciani.

KEY WORDS: carbon isotopes, compound-specific Early Eocene Climatic Optimum, Green River Formation, lipid biomarker.

The Green River Formation of western North America provides an exceptional archive of lacustrine sediments deposited during the Early Eocene Climatic Optimum. Rhythmic lamination in Green River Formation rocks with high organic carbon content has been demonstrated to reflect expression of Milankovitch periodicities (e.g., Bradley, 1929; Machlus et al., 2008) through climatic influences on lake ecosystems (Whiteside & Van Keuren, 2009). Here we present a high-resolution, lipid biomarker record of organic matter sources and carbon cycling in paleo-Lake Uinta during the Early Eocene Climatic Optimum, using a drill core from the Parachute Creek Member of the Green River Formation centered on the organic carbon-rich Mahogany Zone. We demonstrate that productivity in the lake rose and fell on longer (400 kyr) timescales, while primary producer community composition and recycling of organic matter, including *via* methanogenesis and methanotrophy, changed on more variable (10s to 100s of kyr) timescales.

Compound specific carbon isotope analyses reveal the same two main groups of geolipids previously identified (Collister et al., 1991; Ruble et al., 1994): 1. pristane, phytane, steranes, and gammacerane with heavier and more stable values; and 2. hopanes with lighter and more variable $\delta^{13}\text{C}$ compositions reflecting methanotrophic inputs.

The carbon isotope compositions of pristane and phytane show gradual, long-term variation, increasing from around -33 to -34 permil at the base of the section to around -30 per mil in the interval of 735 to 705 feet core depth, and then returning to values of around -33 to -34 permil at the top. This pattern spans a timescale longer than either the 20 kyr or 100 kyr cycles identified by Whiteside & Van Keuren (2009). We attribute this to long-term change in growth rate or nutrient levels. Sterane carbon isotope compositions follow a similar trend to pristane and phytane but that trend is superimposed by shorter-term variability that parallels the carbon isotope composition of

total organic carbon. Sterane carbon isotope patterns are accompanied by shifts in algal community composition, suggesting additional environmental impacts to those reflected in the isotopic compositions of pristane and phytane. This could well be the case on a range of timescales, given that the Green River lacustrine system was likely quite sensitive to climatic influences on local hydrological balance (e.g., Frantz et al., 2014) and temperature in addition to more stochastic impacts of active local tectonics (Smith et al., 2008).

Contrary to of the expected greater ^{13}C -depletion and elevated abundances of methanotrophic bacterial biomarkers at higher total organic carbon contents, preliminary results indicate a substantial methanotroph contribution throughout the majority of the study interval.

REFERENCES

- Bradley W.C. (1929) - The varves and climate of the Green River Epoch. U.S.G.S. Professional Paper, 158-E, 87-110.
- Collister J., Summons R.E., Lichtfouse E. & Hayes J.M. (1991) - An isotopic biogeochemical study of the Green River oil shale. *Adv. Org. Geochem.*, 19, 265-276.
- Frantz C.M., Petryshyn V.A., Marengo P.J., Tripathi A., Berelson W.M. & Corsetti F.A. (2014) - Dramatic local environmental change during the Early Eocene Climatic Optimum detected using high resolution chemical analyses of Green River Formation stromatolites. *Palaeogeogr. Palaeoclimat. Palaeoecol.*, 405, 1-15.
- Machlus M., Olsen P.E., Christie-Blick N., Hemming S.R. (2008) - Spectral analysis of the Lower Eocene Wilkins Peak Member, Green River Formation, Wyoming: Support for Milankovitch Cyclicity. *Earth Planet. Sci. Lett.*, 268, 64-75.
- Ruble T.E., Bakel A.J. & Philip R.P. (1994) - Compound specific isotopic variability in Uinta Basin native bitumens: paleoenvironmental implications. *Org. Geochem.*, 21, 661-671.

Smith M.E., Carroll A.R. & Singer B.S. (2008) - Synoptic reconstruction of a major ancient lake system: Eocene Green River Formation, western United States. *Geol. Soc. Am. Bull.*, 120, 54-84.

Whiteside J.H. & Van Keuren M.A. (2009) - Multiproxy environmental characterization of lake level cycles in the Green River Formation of Utah and Colorado. *Open-File Report 544*, Utah Geological Survey, Salt Lake City, 22 pp.

Stacking PEAT; A stacked Nd isotope record for the Paleogene equatorial Pacific

Howie Scher ^(^a)

^(^a) Department of Earth and Ocean Sciences, University of South Carolina, Columbia, SC 29205, USA. E-mail: hscher@geol.sc.edu

Document type: Short note.

Manuscript history: received 15 May 2014; accepted 30 May 2014; editorial responsibility and handling by Gerald R. Dickens & Valeria Luciani.

KEY WORDS: deep water circulation, fossil fish teeth, neodymium isotopes, Paleogene equatorial age transect (PEAT)

Deep ocean circulation and water mass mixing in the Paleogene Pacific has been reconstructed with neodymium (Nd) isotopes from ferromanganese (FeMn) crusts (Frank, 2002 and references therein) and deep-sea sediment cores (Thomas, 2004; Thomas et al., 2014; Thomas et al., 2008), and are generally low resolution compared to other paleoclimate/paleoceanographic records. Temporal and spatial Nd isotope patterns have been proposed as evidence for a bimodal mode of deep ocean circulation during the Paleogene. This hypothesis suggests that a North Pacific Deep Water (NPDW) mass with radiogenic (i.e., more positive) ϵ_{Nd} values occupied the North Pacific, and a less radiogenic Southern Component Water (SCW) mass the southern Pacific (Thomas, 2004; Thomas et al., 2014; Thomas et al., 2008).

New drilling of exceptionally preserved Paleogene sections in the equatorial Pacific provides an opportunity to test the bimodal Pacific circulation hypothesis based on previously published Nd isotope records. The Pacific Equatorial Age Transect (PEAT) consisted of two consecutive IODP Expeditions, IODP Exp. 320/321, with the aim of recovering a complete sequence of sediment deposited at or near the equator through the Cenozoic. Due to the northward motion of the Pacific plate over time, successive crustal ages were drilled (between 53 and 18 Ma) to obtain sediment that was deposited near the past position of the equator. The age/depth relationship of the seafloor resulting from lithospheric subsidence results in vertical offsets between Paleogene sequences of equal or overlapping age. The vertical offset of the PEAT cores has been exploited to reconstruct, and thereby significantly revise, the history of the carbonate compensation depth (CCD) in the equatorial Pacific (Pälike et al., 2012).

The goal of this study is to utilize the depth transect formed by the PEAT cores to reconstruct the water mass composition in the Pacific. Five of the PEAT cores (U1331 to U1335) contain Paleogene sequences, and are the focus of this study. Over the study interval (*ca.* 45 to 20 Ma) sediment was deposited between 2800 and 4500 m water depth and in an 8°

latitude band (from 1°S to 6°N). The deep equatorial Pacific was the interface where NPDW and SCW mixed during the Paleogene (Thomas et al., 2014), making the paleo-positions of the PEAT cores ideal to investigate changes in ocean circulation in the Pacific. The relative proportion of these end members in the deep equatorial Pacific is expected to have responded to changes in global climate; NPDW is believed to form during very warm climate states while SCW export becomes greater during intervals of high-latitude cooling. Moreover the water mass composition of the deep equatorial Pacific may have influenced carbonate deposition and influenced the fluctuation of the equatorial Pacific CCD.

Using shipboard physical property samples from Paleogene sections of the PEAT cores, Nd isotope records were generated from fossil fish teeth handpicked from the >125 μm fraction of washed samples. All Nd isotope data reported here were produced on a Neptune multi-collector inductively coupled plasma mass spectrometer at the University of South Carolina, following the methodology reported in Scher et al. (2011). Long-term uncertainty based on replicate analysis of the JNdi-1 standard is $\pm 0.2 \epsilon_{Nd}$. The age models applied to the records from U1331 to U1334 are from (Westerhold et al., 2011) and the shipboard age model was used for U1335 (Pälike et al., 2010).

The Nd isotope records from the Paleogene section of the PEAT cores are very similar. With the exception of a short high-resolution interval in the U1333 record, the average time step in the records is around 250 kyr. In general the range of ϵ_{Nd} values for a given 250-kyr interval is equal to or slightly greater than analytical uncertainty (Figure 1a), suggesting that the sites were under the influence of a common water mass. The basic structure of the records is that of an overall decrease from more radiogenic to less radiogenic values, with the main transition phase occurring in the late Eocene, between 37 and 36 Ma. Samples from the middle Eocene have ϵ_{Nd} values around -3.5 to -4.0. Starting around 37 Ma ϵ_{Nd} values begin to decrease and by the early Oligocene fall to between -4.5 and -5.0. During the Oligocene ϵ_{Nd} values average -4.5, though significant maxima are observed around 30, 26, and 22 Ma.

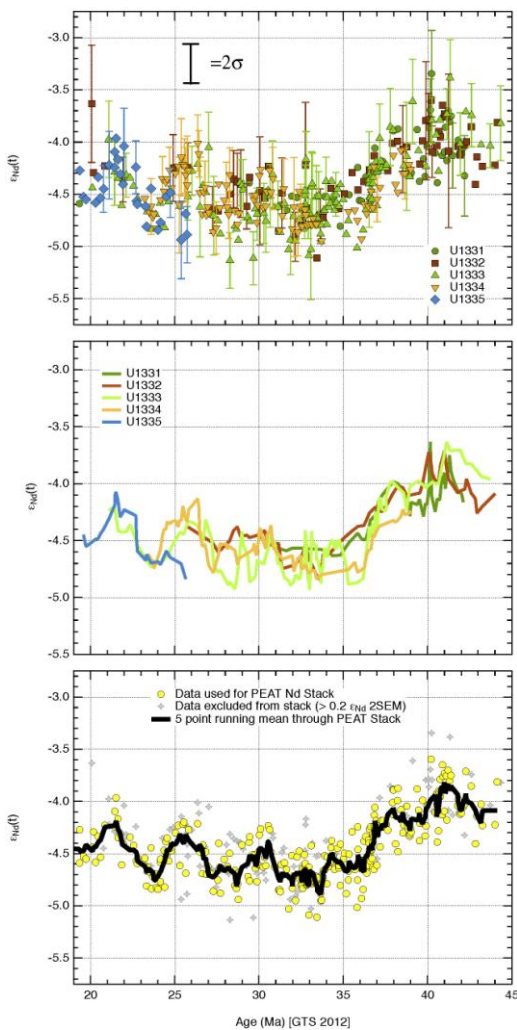


Fig. 1 – Nd isotope data from PEAT sediment cores. Top panel shows all data, with error bars for data where measurement error exceeds 2σ instrumental uncertainty of $\pm 0.2 \epsilon_{Nd}$ units, usually due small sample size. Black error bar at top left shows 2σ instrumental uncertainty based on replicate analyses of the JNdi-1 standard. Middle panel shows PEAT Nd records smoothed with a 3-point running mean, using all data for each record. Bottom panel shows data used for the PEAT stack, which was limited to samples having 2σ measurement errors of $\pm 0.2 \epsilon_{Nd}$ units or less (yellow circles). The thick dark line is a 5-point running mean through the yellow circles. Data with 2σ measurement errors exceeding $\pm 0.2 \epsilon_{Nd}$ units are shown as gray diamonds.

To determine if the PEAT sites are significantly correlated, the Nd isotope records were smoothed using a three point running mean (Figure 1b) and resampled to a common age scale at a 250 kyr time step over an age range suitable for each record. Using the software package *analyseries* (Paillard et al., 1996), correlation tests were carried out on various pairings of Nd isotope records. Results of these tests indicate a strong correlation between the Nd isotope records. The preliminary conclusion from these results is that the PEAT sites were bathed by a common water mass.

A stacked Nd isotope record was generated using these cores in which several features are apparent (Figure 1c). The

radiogenic water mass occupying the deep equatorial Pacific in the middle Eocene gave way to a less radiogenic water mass around 37 Ma. This timing coincides with initial cooling in the Southern Ocean, and the formation of a small ice sheet on East Antarctica (Scher et al., submitted). A shift toward less radiogenic values at 34 Ma may reflect either a decrease in the ϵ_{Nd} of SCW due to the surge of erosion resulting from Antarctic glaciation (Scher et al., 2011) or increased export of SCW due to cooling. In the Oligocene ϵ_{Nd} values fluctuate between -4.0 and -5.0, with prominent maxima at 26 and 22 Ma, and a less significant maxima at 30 Ma. It is speculated that this fluctuation represents the response of the equatorial Pacific water mass to climate driven changes in the export of SCW.

REFERENCES

- Frank M. (2002) - Radiogenic isotopes: tracers of past ocean circulation and erosional input. *Rev. Geophys.*, 40, 1001.
- Pälike H., Nishi H., Lyle M. et al. (2010) - Expedition 320/321 summary. In: H. Pälike, M. Lyle, H. Nishi, I. Raffi, K. Gamage, A. Klaus and E. Scientists. (Eds.), *Proc. IODP. Integrated Ocean Drilling Program Management International, Inc.*, 1-95.
- Pälike H., Lyle M.W., Nishi H. et al. (2012) - A Cenozoic record of the equatorial Pacific carbonate compensation depth. *Nature*, 488, 609-614.
- Paillard D., Labeyrie L. & Yiou P. (1996) - Macintosh program performs time-series analysis. *Eos Trans. AGU*, 77, 379.
- Scher H.D., Bohaty, S.M., Smith B. et al. (submitted) - Isotopic interogation of a suspected late Eocene glaciation. *Paleoceanography*, manuscript number 2014PA002648.
- Scher H.D., Bohaty S.M., Zachos J.C. et al. (2011) - Two-stepping into the icehouse: East Antarctic weathering during progressive ice-sheet expansion at the Eocene-Oligocene Transition. *Geology*, 39, 383-386.
- Thomas D.J. (2004) - Evidence for deep-water production in the North Pacific Ocean during the early Cenozoic warm interval. *Nature*, 430, 65-68.
- Thomas D.J., Kory R., Huber M. et al. (2014) - Nd Isotopic Structure of the Pacific Ocean 70-30 Ma and Numerical Evidence for Vigorous Ocean Circulation and Ocean Heat Transport in a Greenhouse World. *Paleoceanography*, 2013PA002535.
- Thomas D.J., Lyle M., Moore T.C. et al. (2008) - Paleogene deepwater mass composition of the tropical Pacific and implications for thermohaline circulation in a greenhouse world. *Geochem. Geophys. Geosyst.*, 9, Q02002.
- Westerhold T., Röhl U., Wilkens R. et al. (2011) - Revised composite depth scales and integration of IODP Sites U1331–U1334 and ODP Sites 1218–1220. In: Pälike H., Lyle M., Nishi H., Raffi I., Gamage K., Klaus A. (Eds.), *Proc. IODP. (Integrated Ocean Drilling Program Management International, Inc.)*, 240-360.

Deep water composition and water mass mixing in the Paleogene North Atlantic; Results from the Newfoundland ridges

Howie D. Scher ^(a)

^(a) Department of Earth and Ocean Sciences, University of South Carolina, Columbia, SC, USA Department of Earth Sciences, E-mail: hscher@geol.sc.edu

Document type: Short note.

Manuscript history: received 15 May 2014; accepted 30 May 2014; editorial responsibility and handling by Gerald R. Dickens & Valeria Luciani.

KEY WORDS: Fossil fish teeth, neodymium isotopes, North Atlantic, thermohaline circulation.

The water mass composition of deep waters in the North Atlantic during the Paleogene is known only from a few low-resolution neodymium (Nd) isotope records in the North Atlantic (Frank, 2002). Understanding the onset of export of the Northern Component Water (NCW) mass from the North Atlantic is of fundamental importance for reconstructions of Paleogene climate due to the strong link between deep-water formation in the North Atlantic and climate change on Pleistocene time scales. The onset of NCW export from the North Atlantic during the Eocene and Oligocene has been linked to connections with Arctic seas (Abelson et al., 2008; Wright and Miller, 1996) southern hemisphere gateway evolution (Mikolajewicz et al., 1993; Toggweiler and Samuels, 1995) and the deposition of drift deposits in the North Atlantic (Davies et al., 2001). Several Nd isotope records from the Southern Ocean document a shift to less radiogenic ϵ_{Nd} values starting in the earliest Oligocene (Scher and Martin, 2008; Via and Thomas, 2006), which have been interpreted with respect to the influx of NCW.

New drilling on the Newfoundland Ridges during IODP Expedition 342 recovered exceptionally preserved Paleogene sequences, each with a robust magneto- bio-stratigraphy. The drill sites span approximately 2000 to 4500 meters water depth during the Paleogene. In this study the Nd isotopic composition of fossil fish teeth have been measured from early Eocene to early Oligocene sections of Sites U1403, U1406, U1409, and U1411 to reconstruct bottom water circulation and water mass mixing in the North Atlantic during the Paleogene. Here, the principle results and preliminary interpretations are presented.

Nd isotope records were generated from fossil fish teeth handpicked from the $>125 \mu\text{m}$ fraction of washed samples. All of the Nd isotope data reported here was produced on a Neptune multi-collector inductively coupled plasma mass spectrometer at the University of South Carolina, following the methodology reported in Scher and Delaney (2010). Long-term

uncertainty based on replicate analysis of the JNdi-1 standard is $\pm 0.2 \epsilon_{Nd}$.

Site U1403 (lower J anomaly ridge) was drilled at a depth of 4949 m, the deepest on the J anomaly ridge. Late Paleocene ϵ_{Nd} values average -8.3. At a depth in the core that corresponds with the presumed position of Eocene Thermal Maximum 2 (ETM2), the water mass bathing the lower J-anomaly ridge became more radiogenic, increasing in ϵ_{Nd} to -6.6. The shift to radiogenic values is short-lived as ϵ_{Nd} values decrease to -8.6 in the early Eocene following ETM2. Middle Eocene ϵ_{Nd} values are less radiogenic compared to the early Eocene, reaching a minimum of -10 around 42 Ma. A gradual shift to more radiogenic ϵ_{Nd} values appears to culminate around the time of the Middle Eocene Climatic Optimum (MECO) when values reached -8.8. Following this maximum, ϵ_{Nd} values during the late Eocene and Oligocene show a long-term decline reaching -10.5 in the late Oligocene.

Site U1406 (upper J anomaly ridge) was drilled at a depth of 3799 m, the shallowest on the J anomaly ridge. Middle Eocene ϵ_{Nd} values average -9.5, which overlap with the ϵ_{Nd} values on lower J anomaly ridge. During the late Eocene ϵ_{Nd} values increase to reach a maximum of -9.0 at the onset of the Eocene Oligocene Transition (EOT). A decrease of 0.7 ϵ_{Nd} accompanies the EOT at upper J anomaly ridge. Values vary between -9 and -10 during the early Oligocene.

Site U1409 (southeast Newfoundland Ridge) was drilled at a depth of 3500 m. A low resolution record from the Paleocene and early Eocene illustrates a shift from more radiogenic values (-6 to -7) to less radiogenic values (-11).

Site U1411 (southeast Newfoundland Ridge) was drilled at a depth of 3300 m. The late Eocene to early Oligocene was sampled at a resolution of 50 kyr. The ϵ_{Nd} values fluctuate between -9.8 and -10.8 over the sampled interval. In the early Oligocene the resolution increased to about 10 kyr and a saw tooth pattern of ϵ_{Nd} variability emerges; large rapid shifts toward radiogenic ϵ_{Nd} values followed by more gradual shifts to less radiogenic values.

Today, overflow waters from the Labrador and Greenland-Norwegian Seas spill over shallow sills and cascade into the

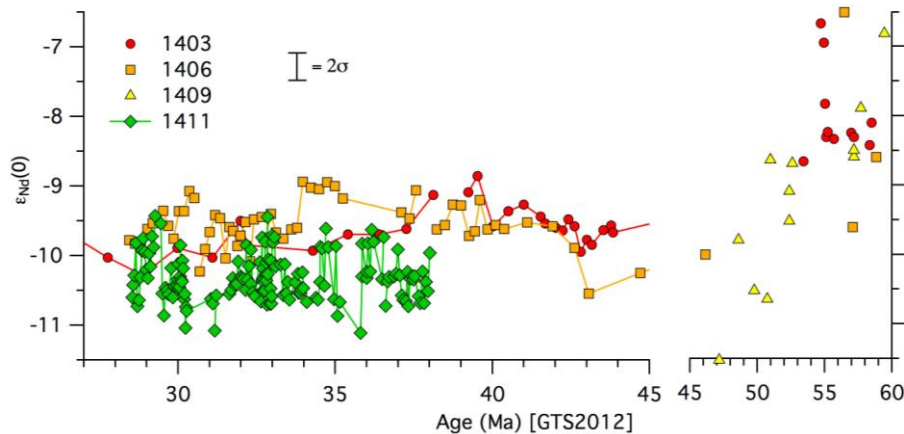


Fig.1 – Fossil fish tooth Nd isotope records from Newfoundland Ridge sediment cores. Note the axis break at 45 Ma. The error bar represents instrumental uncertainty based on replicate analysis of the JNdi-1 Nd isotope standard. Error on data points are smaller than instrumental uncertainty ($< \pm 0.2 \epsilon_{Nd}$).

deep North Atlantic. These overflow waters contribute to the relatively unradiogenic ϵ_{Nd} value of North Atlantic Deep Water (NADW; $\epsilon_{Nd} \sim -13$) that is ultimately transported southward in the deep western boundary current (DWBC) that flows past the study area. It is thus interesting that the largest Nd isotope shifts are observed in the deepest sites investigated in this study. This observation points to the importance of dense overflow waters from emergent polar seas, which by analogy to the present-day, would have a greater influence in the deepest part of the water column. At U1403 the most radiogenic ϵ_{Nd} values appear to be associated with warm climate intervals (e.g., ETM2 and MECO), while conversely at U1406 there is a significant shift to less radiogenic values at the EOT, which is associated with the onset of globally cooler conditions. It is noteworthy that the Nd isotope records generated from the Newfoundland Ridges do not strongly co-vary with one another; which is in stark contrast to the equatorial Pacific Nd isotope records covering a similar age and depth range (see Scher, 2014, this volume). This comparison illustrates that the North Atlantic had a more complex vertical water mass structure, possibly indicating proximity to deep-water source regions.

Over the course of the Paleogene there was an overall shift towards less radiogenic values on the Newfoundland Ridges. The prevailing water mass in the warm Paleogene ocean was Southern Component Water (SCW) (Thomas et al., 2003), which had a relatively radiogenic ϵ_{Nd} composition. The trend to less radiogenic ϵ_{Nd} values observed on the Newfoundland ridges may reflect cooling and enhanced cascading of overflow waters spilling into the North Atlantic. This interpretation is supported by temporary reversals in the decreasing ϵ_{Nd} trend during warm climate intervals (e.g., ETM2 and MECO), and the pronounced ϵ_{Nd} decrease at U1406 across the EOT. This interpretation opens two possibilities; one that overflow waters significantly increased at the EOT and/or two the isotopic composition of overflow waters decreased resulting from enhanced weathering of ancient continental rocks at the EOT.

REFERENCES

- Abelson M., Agnon A. & Almogi-Labin A, (2008) - Indications for control of the Iceland plume on the Eocene-Oligocene "greenhouse-icehouse" climate transition. *Earth Planet. Sci. Lett.*, 265, 33-48.
- Davies R., Cartwright J., Pike J. et al. (2001) - Early Oligocene initiation of North Atlantic Deep Water formation. *Nature*, 410, 917-920.
- Frank M., (2002) - Radiogenic isotopes: tracers of past ocean circulation and erosional input. *Rev. Geophys.*, 40, 1001.
- Mikolajewicz U., Maier-Reimer E., Crowley T. J. et al. (1993) - Effect of Drake and Panamanian Gateways on the circulation of an ocean model. *Paleoceanography*, 8, 409-426.
- Scher H.D. & Martin E.E. (2008) - Oligocene deep water export from the North Atlantic and the development of the Antarctic Circumpolar Current examined with neodymium isotopes. *Paleoceanography*, 23, PA1205.
- Scher H.D. & Delaney, M.L. (2010) – Breaking the glass ceiling for high resolution Nd isotope analyses. *Chem. Geol.*, 269, 329-338.
- Toggweiler J.R. & Samuels B. (1995) - Effect of Drake Passage on the global thermohaline circulation. *Deep Sea Research*, 42, 477-500.
- Thomas D.J., Bralower T.J. & Jones C.E., (2003) - Neodymium isotopic reconstruction of late Paleocene-early Eocene thermohaline circulation. *Earth Planet. Sci. Lett.*, 209, 309-322.
- Via R.K. & Thomas D.J. (2006) - Evolution of Atlantic thermohaline circulation; early Oligocene onset of deep-water production in the North Atlantic. *Geology*, 34, 441-444.
- Wright J.D. & Miller K.G. (1996) - Control of North Atlantic deep water circulation by the Greenland-Scotland Ridge. *Paleoceanography*, 11, 157-170.

Comparison between two middle to outer neritic PETM sections: South Dover Bridge and Mattawoman Creek Billingsley Road cores, Mid-Atlantic Coastal Plain, USA

Jean M. Self-Trail ^(a), Marci M. Robinson ^(a), Debra A. Willard ^(a), Timothy J. Bralower ^(b), Lucy E. Edwards ^(a), David S. Powars ^(a), Greg A. Wandless ^(c), Katherine H. Freeman ^(b) & Elizabeth Denis ^(b)

^(a) U.S. Geological Survey, MS926A, Reston, VA, 20192, USA. E-mail: jstrail@usgs.gov

^(b) Pennsylvania State University, State College, PA, 16801, USA

^(c) U.S. Geological Survey, MS951, Reston, VA, 20192, USA

Document type: Short note.

Manuscript history: received 15 May 2014; accepted 30 May 2014; editorial responsibility and handling by Gerald R. Dickens & Valeria Luciani.

KEY WORDS: calcareous nannofossils, CIE, foraminifera, palynomorphs, PETM.

Detailed analyses of Paleocene-Eocene Thermal Maximum (PETM) sediments from two cores in the Mid-Atlantic Coastal Plain, (Maryland, USA) highlight the differences between sections over relatively short distances and emphasize the inherent problems related to study of shallow marine environments. The Mattawoman Creek Billingsley Road (MCBR) and the South Dover Bridge (SDB) cores are ~85 km apart along a shallow (middle neritic) to deeper (outer neritic) water transect. Biostratigraphic and paleoenvironmental analyses of the SDB (Self-Trail, 2011; Self-Trail et al., 2012) and MCBR (Self-Trail et al., 2013) cores document sedimentologic, isotopic, biostratigraphic, and environmental differences between them that are most likely related to varying degrees of sediment and fresh water influx from the continent.

Relative to deep-ocean sites, the carbon isotope excursion (CIE) at SDB and MCBR is greatly expanded (Fig. 1). At MCBR, which is closer to the sediment source, bulk $\delta^{13}\text{C}$ records an approximate negative 23 per mil shift and there is no dissolution zone associated with the CIE onset. At SDB, which is deeper in the basin, bulk $\delta^{13}\text{C}$ isotopes record a negative 4 per mil shift and a thin (<2 m) dissolution zone (red in color) is present at and above the CIE onset. Increased sedimentation (Kopp et al., 2009) and proximity to sediment source clearly play a role in characterization of the CIE. Preliminary analyses confirm the presence of leaf waxes (long-chain alkanes), which are being analyzed for ^{13}C abundances. Biomarker isotopes can potentially distinguish the global CIE from local processes that influenced the carbonate isotopic record, such as increased flux in inorganic carbon from terrestrial sources. At MCBR, prominent color changes occur within the PETM interval: gray at the bottom, to pink and gray, to red-brown and gray, to red-brown at the top. Sandy silt beds are tan to light-gray throughout the section, and clays are dark to light gray to pink in the lower part and various

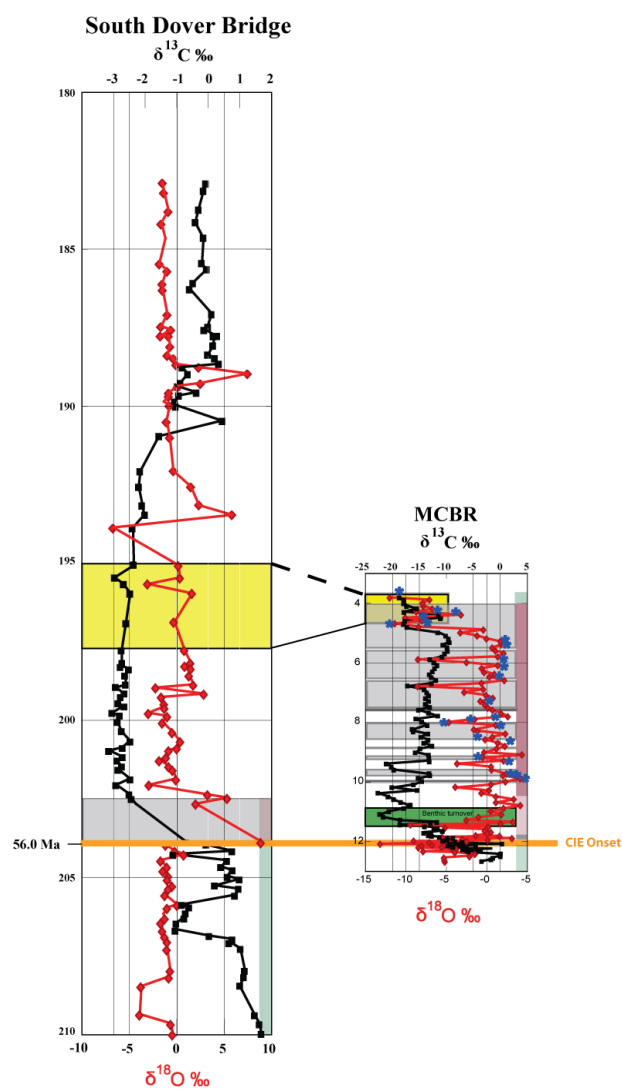


Fig.1 – Comparison between the PETM sections of the South Dover Bridge and Mattawoman Creek cores. Gray shaded areas represent zones of dissolution. Blue stars represent the presence of foraminifera in CaCO_3 poor, or barren, sediments. Yellow shading is the dinoflagellate overlap zone.

shades of red-brown in the upper part. The benthic foraminifera turnover (11.5-10.8 m) occurs where colors are pink and gray. Above this, brief increases in percent abundance of benthic and planktic foraminifera correspond to a positive shift in carbon isotope values. Calcareous material is absent in the upper third of the core. Color changes reflect both dissolution and changes in primary source material.

Biotic response to changing paleoceanographic conditions is unique to each location. At MCBR, fern spores are common throughout the entire PETM interval, varying from 30% to >70%. In SDB, fern spores double in abundance from 30% to >70% at 203.6 m before dropping back to ~30% at 202.8 m. Overall terrestrial pollen concentrations decrease dramatically above 202.8 m. The benthic foraminifera *Bulimina virginiana* dominates the assemblage above the CIE onset at MCBR, but in SDB an assemblage of planktic and benthic foraminifera representative of normal shelf conditions is present. Species turnover following the CIE onset occurs at both sites. Species richness of calcareous nannoplankton above the dissolution zone in SDB average 35 species per sample, but average less than 15 in MCBR for the same interval. The calcareous nannofossil assemblage becomes increasingly affected by dissolution above 11.2 m at MCBR. The absence of *Rhomboaster* spp. and *Discoaster anartios*, an assemblage typical of the PETM, in this core is most likely caused by this. The overlap of the dinoflagellate species *Phthanoperidinium*

crenulatum and *Apectodinium augustum* at both sites may prove to be a useful regional biostratigraphic marker within the PETM.

REFERENCES

- Kopp R.E., Schumann D., Raub T.D., Powars D.S., Godfrey L.V., Swanson-Hysell N.L., Maloor A.C., & Vali H. (2009) - An Appalachian Amazon? Magnetofossil evidence for the development of a tropical river-like system in the mid-Atlantic United States during the Paleocene-Eocene Thermal Maximum. *Paleoceanography*, doi: 10.1029/2009PA001783.
- Self-Trail J.M. (2011) - Paleogene calcareous nannofossils of Southern Maryland, South Dover Bridge Core, USA. *Journal of Nannoplankton Research*, 32 (1), 1-28.
- Self-Trail J.M., Powars D.S., Watkins D.K., & Wandless G. (2012) - Calcareous nannofossil assemblage changes across the Paleocene-Eocene thermal maximum: Evidence from a shelf setting. *Mar. Micropaleontol.*, 92-93, 61-80.
- Self-Trail J.M., Robinson M.M., Edwards L.E., Powars D.S., Wandless G.A. & Willard D.A. (2013) - Integrated stratigraphy of a shallow marine Paleocene-Eocene boundary section, MCBR cores, Maryland (USA). Abstract, American Geophysical Union (AGU) Fall Meeting, San Francisco, CA, 2013, PP23B-1968.

Eocene nannofossil biostratigraphy of the mid-Waipara river section, Canterbury Basin, New Zealand: preliminary results

Claire L. Shepherd ^(a,b), Denise K. Kulhanek ^(c) & Christopher J. Hollis ^(b)

^(a) School of Geography, Environment and Earth Sciences, Victoria University of Wellington, PO Box 600, Wellington 6140, New Zealand. E-mail: C.Shepherd@gns.cri.nz

^(b) GNS Science, PO Box 30-368, Lower Hutt 5040, New Zealand

^(c) Integrated Ocean Drilling Program, Texas A&M University, College Station, Texas, USA

Document type: Short note.

Manuscript history: received 15 May 2014; accepted 30 May 2014; editorial responsibility and handling by Gerald R. Dickens & Valeria Luciani.

KEY WORDS: biostratigraphy, calcareous nannofossils, Eocene, mid-Waipara, paleobiogeography, paleoclimate, New Zealand.

Earth's climate underwent extreme change during the Eocene, transitioning from greenhouse conditions in the early Eocene, to icehouse conditions by late Eocene-early Oligocene. This long term shift to cooler conditions was punctuated by brief episodes of warmth, during which global sea-surface temperatures (SST) increased by almost 5°C above background. These transient periods of warmth had a significant effect on oceanic planktonic biota, and changes in geographic distribution and species turnover can be used to elucidate changes in sea-surface temperature and productivity.

The mid-Waipara River section, northern Canterbury Basin, provides an important climatic record for the New Zealand region across the early to middle Eocene (Hollis et al., 2009; Hollis et al., 2012). A recent study by Dallanave et al. (in press) presents new paleomagnetic data from the mid-Waipara River section that provides an integrated magneto-biostratigraphic chronology for the early-middle Eocene. Samples collected in association with this paleomagnetic study have been analysed in this study for nannofossil content and the data are used to better elucidate climatic changes within the section.

Biostratigraphic analysis indicates that the sampled section spans the lower to uppermost middle Eocene (nannofossil Zone NP12 to NP16/17; Mangaorapan to Bortonian local stage) with a hiatus in the middle Eocene (NP15, Porangan local stage). Preservation of nannofossils is variable throughout the section but is generally poor and worsens in the upper middle Eocene (Heretaungan local stage). Key index fossils present include *Tribrachiatum orthostylus*, *Discoaster lodoensis*, *Reticulofenestra umbilicus*, and *Reticulofenestra reticulata*.

Recent SST reconstructions using TEX₈₆^L (Hollis et al., 2012) indicate peak temperatures in the Mangaorapan, which corresponds with the early Eocene Climatic Optimum (EECO), with stepped cooling in the middle Eocene (Fig.1). However, early nannofossil results from mid-Waipara suggest more pronounced cooling followed the EECO (Fig.1). The *Discoaster/Chiasmolithus* ratio shows a significant decline in

the upper Mangaorapan, which continues into the Heretaungan and signals a shift from warm water to cooler conditions. Taxonomic richness shows a similar trend, with values declining steadily after the EECO, although this may be an artefact of deteriorating preservation.

Previous studies have identified a shift in the background assemblage during the EECO from a *Toweius* dominated assemblage to one dominated by *Reticulofenestra*, separated by an acme in *Discoaster* at the EECO. (Agnini et al., 2006; Shamrock & Watkins, 2012). These features are evident in nannofossil assemblages in the mid-Waipara section (Fig.1).

The next phase of this study will focus on a high-resolution record of well-preserved nannofossil assemblages in the coeval Eocene section at Hampden Beach, south Canterbury (Morgans, 2009).

REFERENCES

- Agnini C., Muttoni G., Kent D. V. & Rio D. (2006). Eocene biostratigraphy and magnetic stratigraphy from Possagno, Italy: The calcareous nannofossil response to climate variability. *Earth Planet. Sci. Lett.*, 241, 815-830, doi: 10.1016/j.epsl.2005.11.005.
- Dallanave, E., Tauxe, L., Bachtadse, V., Sugisaki, S., Morgans, H. E. G., Hines, B. R., et al. (in press) - The magneto-biochronology of the early Eocene climatic optimum in the Southwest Pacific and Southern Ocean. *Earth Planet. Sci. Lett.*
- Hollis C.J., Handley L., Crouch E.M., Morgans H.E.G., Baker J.A., Creech J., Collins K.S., Gibbs S.J., Huber M., Schouten S., Zachos J.C. & Pancost R.D. (2009) - Tropical sea temperatures in the high-latitude South Pacific during the Eocene. *Geology*, 37(2), 99-102, doi: 10.1130/G25200A.
- Hollis C.J., Taylor K.W.R., Handley L., Pancost R.D., Huber M., Creech J.B., Hines B.R., Crouch E.M.; Morgans H.E.G., Crampton J.S., Gibbs S.J., Pearson P.N. & Zachos J.C. (2012) - Early Paleogene temperature history of the Southwest Pacific Ocean: Reconciling proxies and models. *Earth Planet. Sci. Lett.*, 349-350, 53-66, doi: 10.1016/j.epsl.2012.06.024.

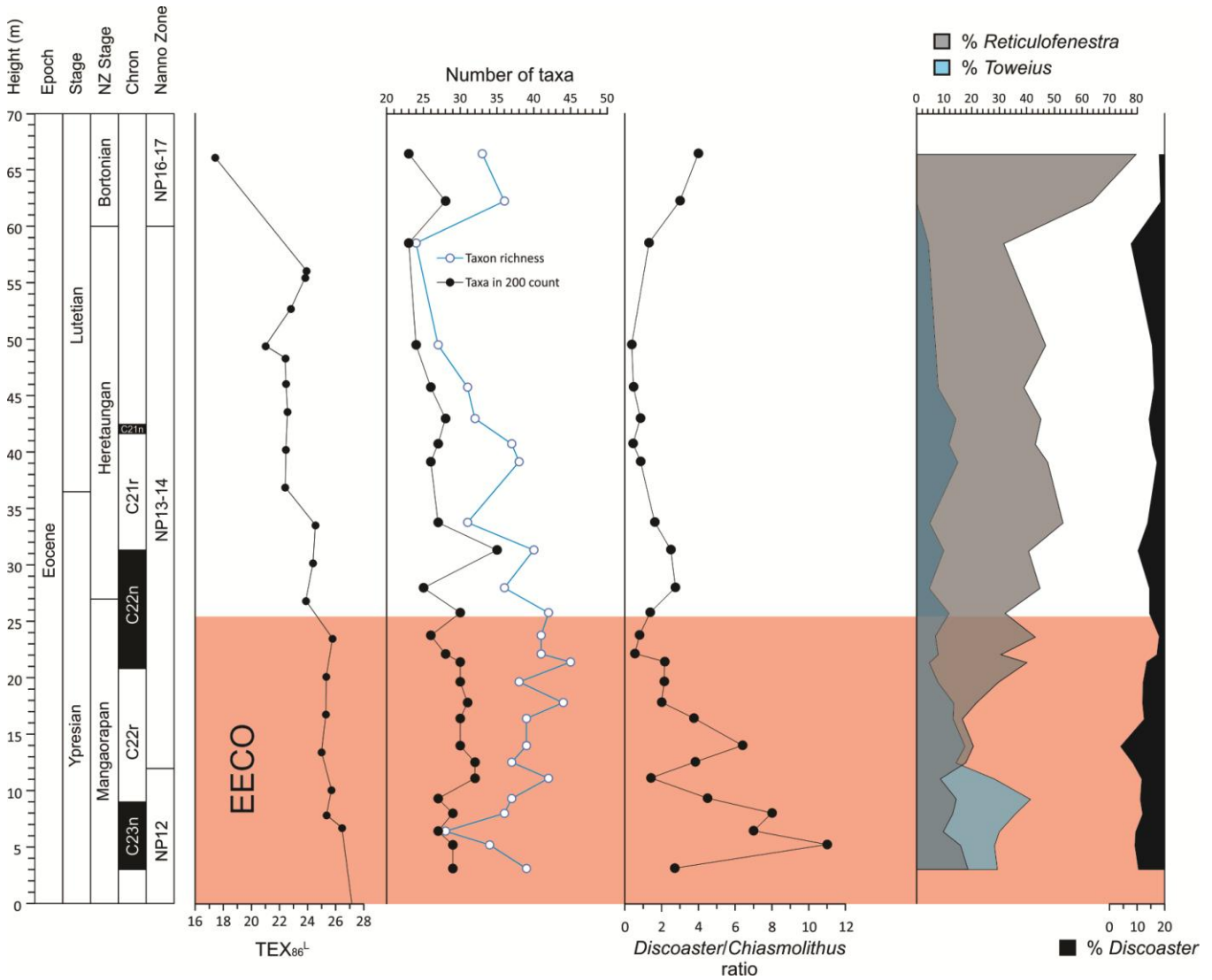


Fig. 1 – Trends in calcareous nannofossil assemblages in the Eocene section at mid-Waipara River compared with sea surface temperatures derived from the TEX_{86}^L proxy (Hollis et al., 2012). Magnetostratigraphy and correlation to international and local stages based on Dallanave et al. (in press).

Morgans H.E.G. (2009) - Late Paleocene to middle Eocene foraminiferal biostratigraphy of the Hampden Beach section, eastern South Island, New Zealand. *New Zealand Journal of Geology and Geophysics*, 52(4), 273-320, doi: 10.1080/00288306.2009.9518460.

Shamrock J.L. & Watkins D.K. (2012) - Eocene calcareous nannofossil biostratigraphy and community structure from Exmouth Plateau, Eastern Indian Ocean (ODP Site 762). *Stratigraphy*, 9(1), 1-54.

Cell geometry records the physiological responses of coccolithophores to Paleogene climate change

Rosie M. Sheward ^(a), Samantha J. Gibbs ^(a), Paul R. Bown ^(b), Alex J. Poulton ^(c), Chris J. Daniels ^(a),
David Higgins ^(a) & Paul A. Wilson ^(a)

^(a) Ocean and Earth Science, National Oceanography Centre, Southampton, University of Southampton, Southampton, SO14 3ZH, UK E-mail: rosie.sheward@noc.soton.ac.uk

^(b) Department of Earth Sciences, University College London, Gower Street, London, WC1E 6BT, UK

^(c) Ocean Biogeochemistry and Ecosystems, National Oceanography Centre, Waterfront Campus, Southampton, SO14 3ZH, UK

Document type: Short note.

Manuscript history: received 15 May 2014; accepted 30 May 2014; editorial responsibility and handling by Gerald R. Dickens & Valeria Luciani.

KEY WORDS: cell geometry, coccolithophores, Paleogene, phytoplankton.

The physiology and ecology of the calcifying marine phytoplankton group coccolithophores are expected to be susceptible to future changes in environmental conditions forced by increasing atmospheric carbon dioxide and temperature (e.g., Fabry et al., 2008). A key trait of the physiological state of a phytoplankton cell is cell size (e.g., Finkel et al., 2007), which we have captured from exquisitely preserved fossil coccospheres in biometric measurements of coccolith length, coccosphere size and number of coccoliths per coccosphere (Fig. 1).

Our exquisitely preserved calcareous microfossils are obtained from sites where post-depositional alteration of the calcite is virtually absent. Typically these sites contain hemipelagic, clay-rich lithologies with high sedimentation rates that rapidly encapsulate calcareous microfossils, isolating them within an impermeable matrix (Bown et al., 2008). These sediments contain a remarkably high diversity of fossil coccolithophores and an unusually high abundance of intact coccospheres, where the original spherical-sub-spherical cell covering of coccoliths is completely preserved, instead of the typical disarticulation into loose coccoliths. The pristine preservation of fragile and taxonomically important central-area structures in coccoliths combined with the preservation of very small (<3µm) coccoliths enables us to study coccosphere geometry across a wide variety of Paleogene taxa at species level.

We present material from Tanzania (Nicholas et al., 2006), New Jersey (Miller et al., 1998) and Californian (John et al., 2008) continental shelf environments, where the shallow water depth minimized water-column disaggregation and dissolution and the shelf setting promoted high sedimentation rates. The thick sequence of clay-rich oozes at deep-sea Labrador Sea site ODP 647A (Firth, 1989) has also yielded diverse coccospheres that illustrate a high-latitude North Atlantic Eocene assemblage.

Intact fossil coccospheres can be interpreted on a cellular level through analogy with the cellular geometry of their modern counterparts (Gibbs et al., 2013). This facilitates an unprecedented insight into the cellular physiology of cells that are millions of years old and its link to population-level responses to climate change.

Our biometric data (following Fig. 1; Gibbs et al., 2013 and Henderiks, 2008) reveals the cellular growth and calcification response of more than 30 coccolithophore species to long-term variability in sea-surface conditions during the Paleogene greenhouse interval, between 66 and 34 million years ago. Cell geometry from abundant coccospheres of the common Paleogene genera *Coccolithus*, *Reticulofenestra*, *Cyclicargolithus* and *Toweius* have been documented, as well as coccosphere measurements of less common *Chiasmolithus*, *Cruciplacolithus*, *Claussicoccus* and *Markalius* genera and rare taxa such as *Braarudosphaera*, *Coronocyclus*, *Campylosphaera*, *Kilwalithus* and *Goniolithus*.

We find that there is a high degree of within- and between-genera variability in coccosphere geometry, driven by both species-specific characteristics in coccosphere architecture and long-term shifts in environmental growth controls. Although larger cells typically have larger coccoliths forming the cell covering, the large number of species included in this study reveals that some genera, particularly *Cruciplacolithus* and *Kilwalithus*, exhibit cells with a characteristic covering of many smaller coccoliths (Fig. 1).

Accurate interpretation of cell size change through time, based solely on coccolith length data, must therefore consider the number of coccoliths per cell and coccolith length, specific to each genus. Observations from culture experiments of extant *Coccolithus pelagicus* and *Emiliania huxleyi* suggest that cell geometry is also variable within species and particularly related to cellular growth phase. Typically, nutrient depleted cells unable to maintain exponential growth show an increase in the number of coccoliths per cell (Gibbs et al., 2013). We can use this 'framework' to recognize trends in growth phase in related fossil taxa, such as *Coccolithus* and *Reticulofenestra*. Paleogene cell geometry and cell size data for these taxa

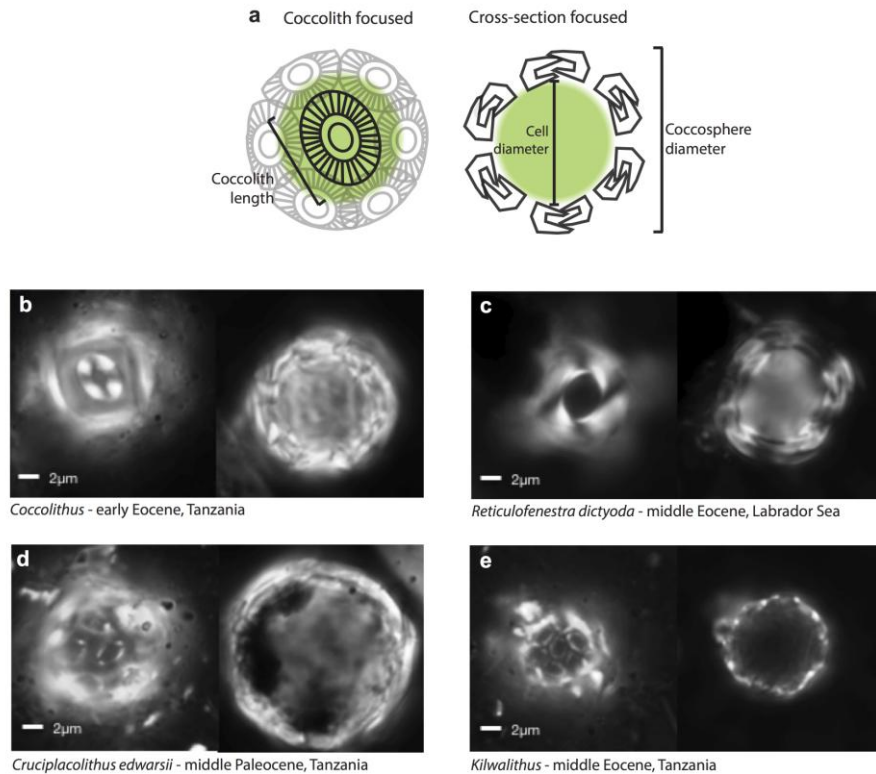


Fig.1 – Coccosphere geometry of four Paleogene species. a. Diagram illustrating terminology and measurements of coccolith length, cell diameter and coccosphere diameter from individual coccospheres used in this study. b.-e. Polarised light microscope images of representative individual coccospheres of two key Paleogene lineages *Coccolithus* and *Reticulofenestra*, and two genera that typically have a high number of coccoliths per cell – *Cruciplacolithus edwardsii* and *Kilwalithus*.

suggest that each genus responded differently to the significant changes in climate through this time interval, with *Coccolithus* showing remarkable conservatism in biometry and *Reticulofenestra* revealing rapid morphological turnover during its rise to dominance.

We emphasize the advantage of considering the whole coccosphere geometry, not just coccolith size, in determining the growth phase and calcification of individual cells and its importance in interpreting the size evolution of genera during the warming and cooling intervals of the Paleogene.

REFERENCES

- Bown P.R., Dunkley Jones T., Lees J.A., Randell R.D., Mizzi J.A., Pearson P.N., Coxall H.K., Young J.R., Nicholas C.J., Karega A., Singano J. & Wade B.S. (2008) - A Paleogene calcareous microfossil Konservat-Lagerstätte from the Kilwa Group of coastal Tanzania. *Geol. Soc. Am. Bull.*, 120, 3-12.
- Fabry V.J., Seibel B.A., Feely R.A. & Orr J.C. (2008) - Impacts of ocean acidification on marine fauna and ecosystem processes. *ICES J. Mar. Sci.*, 65, 414-432.
- Finkel Z.V., Sebbo J., Feist-Burkhardt S., Irwin A.J., Katz M.E., Schofield O.M.E., Young J.R. & Falkowski P.G. (2007) - A universal driver of macroevolutionary change in the size of marine phytoplankton over the Cenozoic. *P. Natl. Acad. Sci. USA*, 104, 51, 20416-20420.
- Firth J.V. (1989) - Eocene and Oligocene calcareous annofossils from the Labrador Sea, ODP Leg 105. In: Srivastava S.P., Arthur M., Clement B. et al. (Eds.), *Proc. ODP, Sci. Res. Ocean Drilling Program, 105*, Texas A&M University, 263-286.
- Gibbs S.J., Poulton A.J., Bown P.R., Daniels C.J., Hopkins J., Young J.R., Jones H.L., Thiemann G.J., O’Dea S.A. & Newman C. (2013) - Species-specific growth response of coccolithophores to Palaeocene-Eocene environmental change. *Nature Geosci.*, 6, 218-222.
- John C.M., Bohaty S.M., Zachos J.C., Sluijs A., Gibbs S.J., Brinkhuis H. & Bralower T.J. (2008) - North American continental margin records of the Paleocene-Eocene thermal maximum: Implications for global carbon and hydrological cycling. *Paleoceanography*, 23, PA2217.
- Miller K.G., Sugarman P.J., Browning J.V., Olsson R.K., Pekar S.F., Reilly T.J., Cramer B.S., Aubry M.-P., Lawrence R.P., Curran J., Stewart M., Metzger J.M., Uptegrove J., Bukry D., Burckle L.H., Wright J.D., Feigenson M.D., Brenner G.J. & Dalton R.F. (1998) - Bass River Site. In: Miller K.G., Sugarman P.J., Browning J.V. et al. (Eds.), *Proc. ODP, Init. Rep.. Ocean Drilling Program, 174AX*, Texas A&M University, 5-43.
- Nicholas C.J., Pearson P.N., Bown P.R., Dunkley Jones T., Huber B.T., Karega A., Lees J.A., McMillan I.K., O’Halloran A., Singano J.M. & Wade B.S. (2006) - Stratigraphy and sedimentology of the Upper Cretaceous to Paleogene Kilwa Group, southern coastal Tanzania. *J. Afr. Earth. Sci.*, 45, 431-466.

Extending lithologic and stable carbon isotope records at Mead Stream (New Zealand) through the Middle Eocene

Benjamin S. Slotnick ^(a), Gerald R. Dickens ^(a), Chris J. Hollis ^(b), James S. Crampton ^(b),
C. Percy Strong ^(b) & James C. Zachos ^(c)

^(a) Department of Earth Sciences, Rice University, Houston, TX 77005, USA E-mail: bss2@rice.edu

^(b) GNS Science, Lower Hutt, New Zealand

^(c) Earth and Planetary Sciences Department, University of California, Santa Cruz, Santa Cruz, CA, USA

Document type: Short note.

Manuscript history: received 15 May 2014; accepted 30 May 2014; editorial responsibility and handling by Gerald R. Dickens & Valeria Luciani.

KEY WORDS: Middle Eocene, New Zealand, stable carbon isotopes.

The early Paleogene was characterized by prominent variations in climate and global carbon cycling, which operated on both long ($>10^6$) and short ($<10^5$) time scales (e.g.; Zachos et al., 2008). The carbon cycle changes are evident in records of $\delta^{13}\text{C}$ and deep-sea carbonate accumulation, which indicate times of greater and lesser net fluxes of organic carbon from the ocean and atmosphere (Dickens et al., 1997; Komar et al., 2013). Detailed $\delta^{13}\text{C}$ records have been constructed at multiple sites for the interval spanning about 58 to 52 Ma (Zachos et al., 2010; Slotnick et al., 2012). In a general sense, $\delta^{13}\text{C}$ dropped significantly and the CCD deepened by several hundred meters. Superimposed on these long-term trends were a series of rapid global warming events, so-called 'hyperthermals', each associated with a rapid drop in global exogenic $\delta^{13}\text{C}$ and a CCD shoaling, and strongly suggestive of massive carbon input to the ocean and atmosphere (Dickens et al., 1997). A current issue is whether such events, which were likely paced by orbital variations, occurred during the Late Paleocene [before the Paleocene Eocene Thermal Maximum (PETM)] or during the middle Eocene [after the start of Early Eocene Climatic Optimum (EECO)]. This line of inquiry arises in part because the CCD was relatively shallow prior to 58 Ma and after 52 Ma, such that well-resolved, single-site deep-sea records spanning the entire early Paleogene are rare.

Tributaries along the northwest margin of Clarence Valley, New Zealand, expose dm-scale bedded, calcareous-rich sedimentary rocks originally emplaced on the ancient continental margin during the late Cretaceous and early Paleogene. The sections generally become thicker and more continuous to the northeast, where the paleo-environment was most distal from land (Crampton et al., 2003). Mead Stream exposes a ~650-m-thick sequence deposited on an upper continental slope. Initial work at this location (Strong et al. 1995) provided a robust but coarsely resolved stratigraphy. Subsequent studies (Hollis et al. 2005; Nicolo et al. 2007; Slotnick et al., 2012) have focused on two units (Figure 1):

Lower Limestone, exposed from 116 to 204 m above the K/Pg Boundary, and Lower Marl, a unit exposed from 204 to 327 m. The first contains the PETM, H and I events (Nicolo et al., 2007), and the latter contains the J, K/X, and L events, as well as several lesser CIEs (Slotnick et al., 2012). This work also has shown that known hyperthermals are marked by clay-rich horizons (marls), and many marls span EECO. Notably, this is caused by excess terrigenous dilution, presumably related to enhanced seasonality in precipitation.

Two additional units at Mead Stream have not been examined in detail: Upper Limestone and Upper Marl, which span from 327 to 523 m. A total of 623 new rock samples were chiseled from outcrops along Mead Stream, generally at a resolution of one sample per bed. These were analyzed for lithology, carbonate content, and bulk carbonate carbon isotopes. Most samples came from 265 to 523 m, or from the uppermost Lower Marl, Upper Limestone, and Upper Marl. The remaining samples came from intervals of Lower Limestone and Lower Marl where previous coverage was limited (e.g., below PETM, between PETM and H-1). In summary, the new samples greatly increase the resolution and temporal scope of existing data sets from Mead Stream.

These new preliminary data (Figure 1) complement previous work, such that detailed records now extend from 58 to 38 Ma. The long-term drop in $\delta^{13}\text{C}$, from 58-52 Ma, was followed by a long-term rise in $\delta^{13}\text{C}$. Numerous geologically-brief (<0.2 Myr) but relatively minor ($<1.0\%$) carbon isotope excursions (CIEs) occur through the interval from 52 to 38 Ma, although it is not clear if any of them are hyperthermals. Notably, none of these CIEs are as extreme as those across the PETM, H and K/X events. Particularly low carbonate contents span strata in the late Early Eocene and across Middle Eocene Climatic Optimum (MECO). This may indicate increased flux of siliciclastic material, but perhaps also a decreased flux of carbonate to the seafloor. Overall, the Mead Stream section provides a single location to construct a detailed carbon isotope template for the early Paleogene, and to link such changes to lithology.

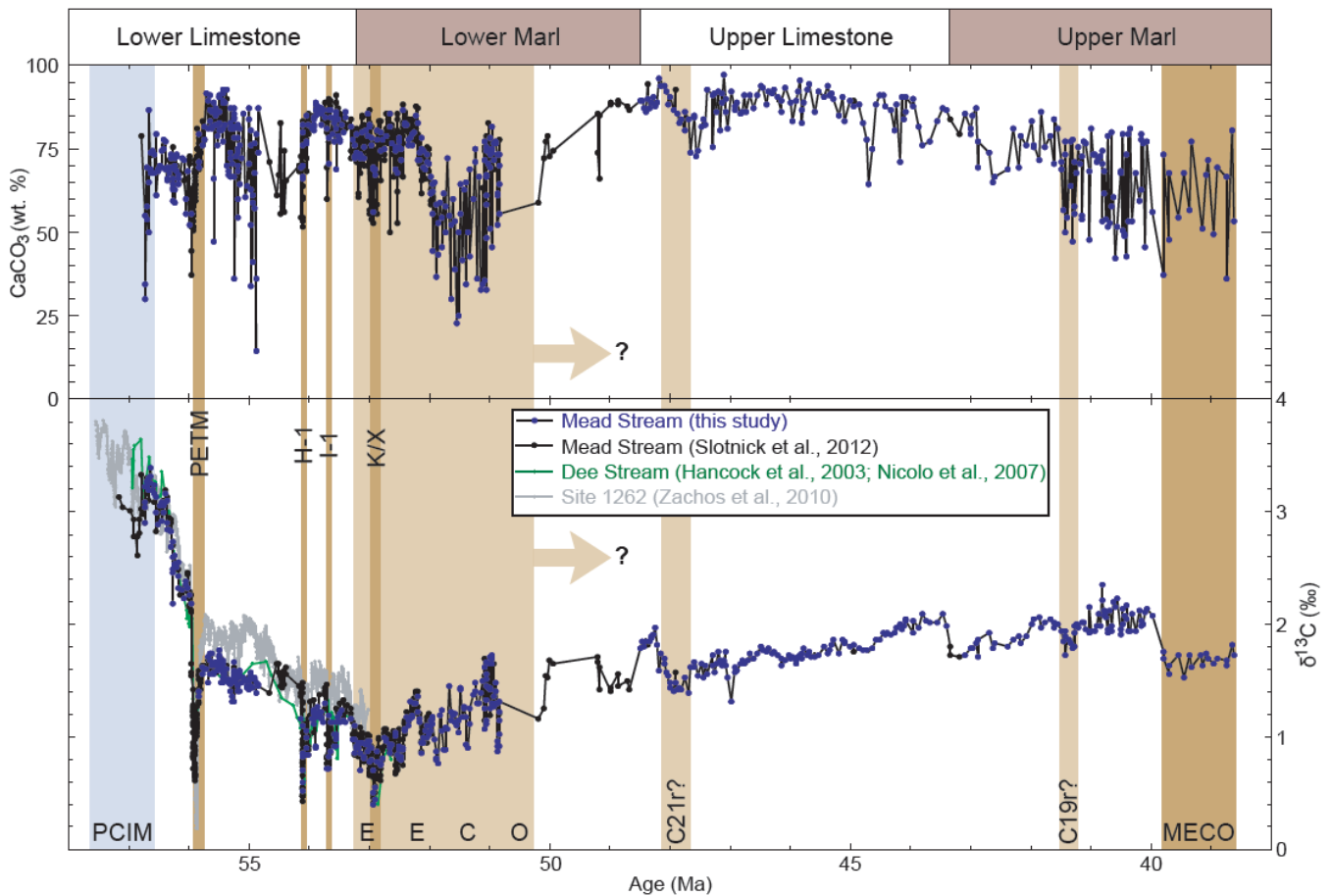


Fig.1 – Late Paleocene to early Late Eocene carbonate content and $\delta^{13}\text{C}$ records generated to date at Mead Stream. Formation names are from Hollis et al. (2005). The total data set comprises new data [blue circles; $n = 623$] and information in previous papers (black circles; Hollis et al., 2005, $n = 79$; Nicolo et al., 2007, $n = 108$; Nicolo et al., 2010, $n = 49$; Slotnick et al., 2012, $n = 308$). Also shown are carbon isotope data from Dee Stream (Hancock et al., 2003; Nicolo et al., 2007) and Site 1262 (Zachos et al., 2010). The preliminary age model integrates carbon isotope stratigraphic datums to Site 1262 (Zachos et al., 2010) and chron boundaries from Mead Stream (Dallanave et al., *in prep*). The end of the EECO remains poorly defined.

REFERENCES

- Crampton J.S., Laird M., Nicol A., Townsend D. & Van Dissen R. (2003) - Palinspastic reconstructions of southeastern Marlborough, New Zealand, for late Cretaceous to Eocene times. *New Zeal. J. Geol. Geop.*, 46, 153–175.
- Dickens G.R., Castillo M.M. & Walker J.C.G. (1997) - A blast of gas in the latest Paleocene: Simulating first-order effects of massive dissociation of oceanic methane hydrate, *Geology*, 25, 259–262.
- Hollis C.J., Dickens G.R., Field B.D., Jones C.M. & Strong C.P. (2005) - The Paleocene-Eocene transition at Mead Stream, New Zealand: a southern Pacific record of early Cenozoic global change. *Palaeogeogr. Palaeoclimatol. Palaeoecol.*, 215, 313–343.
- Komar N., Zeebe R.E. & Dickens G.R. (2013) - Understanding long-term carbon cycle trends: The late Paleocene through the early Eocene. *Paleoceanography*, 28, 1–13.
- Nicolo M.J., Dickens G.R. & Hollis C.J. (2010) - South Pacific intermediate water oxygen depletion at the onset of the Paleocene-Eocene thermal maximum as depicted in New Zealand margin sections. *Paleoceanography*, 25, PA4210.
- Nicolo M. J., Dickens G. R., Hollis C.J. & Zachos, J.C. (2007) – Multiple early Eocene Hyperthermals: Their sedimentary expression on the New Zealand continental margin and in the deep sea. *Geology*, 35, 699–702.
- Slotnick B.S., Dickens G.R., Nicolo M.J., Hollis C.J., Crampton J.S., Zachos J.C. & Sluijs A. (2012) - Numerous large amplitude variations in carbon cycling and terrestrial weathering throughout the latest Paleocene and earliest Eocene. *J. Geol.*, 120, 487–505.
- Strong C.P., Hollis C.J. & Wilson G.J. (1995) - Foraminiferal, radiolarian, and dinoflagellate biostratigraphy of Late Cretaceous to Middle Eocene pelagic sediments (Muzzle Group), Mead Stream, Marlborough, New Zealand. *New Zeal. J. Geol. Geop.*, 28, 171–212.
- Zachos J.C., McCarren H., Murphy B., Röhl U., & Westerhold T., (2010) - Tempo and scale of late Paleocene and early Eocene carbon isotope cycles. *Earth Planet. Sci. Lett.*, 299, 242–249.
- Zachos J.C., Dickens G.R., & Zeebe R.E., (2008) – An early Cenozoic perspective on greenhouse warming and carbon-cycle dynamics. *Nature*, 451, 279–283.

Sub-orbital climate variability in the Late Oligocene North Atlantic Ocean

Richard E. Smith ^(a), Ursula Röhl ^(b), Thomas Westerhold ^(b), Steve M. Bohaty ^(a) & Paul A. Wilson ^(a)

^(a) National Oceanography Centre, University of Southampton, Southampton SO14 3ZH, UK. E-mail: res1e13@soton.ac.uk

^(b) MARUM, University of Bremen, Leobener Strasse, Bremen, Germany

Document type: Abstract.

Manuscript history: received 15 May 2014; accepted 30 May 2014; editorial responsibility and handling by Gerald R. Dickens & Valeria Luciani.

KEY WORDS: Arctic glaciation, IODP, Oligocene-Miocene boundary, sub-orbital climate variability

The beginning and end of the Oligocene were marked by major glaciation events. While the Eocene-Oligocene transition is known to have initiated sustained major ice sheets on Antarctica, the intensification of glaciation associated with the Oligocene-Miocene transition appears to have been ephemeral. The inference of a rapid growth and then retreat of large Antarctic ice sheets on orbital time scales is difficult to reconcile with the strong hysteresis seen in the results of numerical ice sheet model experiments and the modest variability seen in reconstructions of atmospheric CO₂ levels.

Furthermore, we know very little about the contemporaneous behaviour of the cryosphere in the high northern latitudes and virtually nothing about climate variability at sub-orbital timescales, in sharp contrast to the Pleistocene.

IODP Expedition 342 (Newfoundland Sediment Drifts) recovered a number of highly expanded intervals, including from the Oligocene at Site 1405 (NW Atlantic, 40°N). This presents an exciting opportunity to break new ground and develop an understanding of Oligocene climate dynamics at unparalleled temporal resolution in the North Atlantic Ocean, a key site for ocean circulation. We present data from the latest Oligocene at Site 1405, where sedimentation rates are high (>10cm/kyr) to provide the first indications of sub-orbital ocean climate cyclicity in the Paleogene.

Large temperature changes on land during Early Eocene hyperthermals

Kathryn E. Snell ^(a), Henry C. Fricke ^(b), William C. Clyde ^(c) & John M. Eiler ^(a)

^(a) Division of Geological and Planetary Sciences, California Institute of Technology, 1200 E. California Blvd, Pasadena, CA 91125. E-mail: ksnell@caltech.edu

^(b) Department of Geology, Colorado College, 14 E. Cache La Poudre, Colorado Springs, CO 80903; USA

^(c) Department of Earth Sciences, 56 College Road, University of New Hampshire, Durham, NH 03824, USA

Document type: Short note.

Manuscript history: received 15 May 2014; accepted 30 May 2014; editorial responsibility and handling by Gerald R. Dickens & Valeria Luciani.

KEY WORDS: hyperthermals, paleothermometry, terrestrial, stable isotopes.

Numerous rapid global warming events termed 'hyperthermals' occurred during the Early Paleogene. These events coincided with negative carbon isotope excursions (CIEs) indicative of perturbations to the global carbon cycle that are thought to reflect large additions of carbon to the ocean/atmosphere system. As a result of the suggested link between rapid warming and increased pCO₂ in the atmosphere, these hyperthermals have been researched as potential analogs for present-day changes in climate and carbon cycle.

The largest of these events, the Paleocene-Eocene Thermal Maximum (PETM), had pronounced impacts across marine and terrestrial environments, although it is currently uncertain whether other hyperthermals (e.g. ETM2 and H2) were associated with similar changes, particularly in terrestrial environments. In addition, it remains unclear whether all of the hyperthermals share a common, underlying cause, or whether the PETM, as the largest of the events, was somehow driven by a different mechanism, or combination of mechanisms. Temperature records through multiple hyperthermals from terrestrial basins are necessary to identify similarities and differences in the terrestrial response to these hyperthermals, which can provide insight into whether there is a common underlying cause to all the events or not. For example, if all hyperthermals share a common, underlying cause, then we might expect the magnitude of temperature change to vary proportionally with the magnitude of the CIEs. To date, however, the PETM is the only hyperthermal for which there are estimates of terrestrial temperatures (Fricke & Wing, 2004; Snell et al., 2013; VanDeVelde et al., 2013; Wing et al., 2005; 2000).

To help address these issues, we generated high-resolution carbon isotope ratios ($\delta^{13}\text{C}$) and paleotemperature estimates using carbonate clumped isotope (Δ_{47}) thermometry (Ghosh et al. 2006) of paleosol carbonate nodules. Our samples are from the McCullough Peaks region of the Bighorn Basin in NW Wyoming and span a ~500 kyr interval that includes the ETM2

and H2 hyperthermals, based on lithologic correlation, magnetostratigraphy and biostratigraphy. Our high-resolution $\delta^{13}\text{C}$ record is similar in pattern and magnitude of change to the $\delta^{13}\text{C}$ record from the Deer Creek section of McCullough peaks region (Abels et al., 2012) and confirms that our section preserves both ETM2 and H2 hyperthermals.

The Δ_{47} paleotemperature estimates were generated from a subset of the samples (n=38) and binned according to whether they were relatively shallow (< 100 cm depth) or deep (> 100 cm depth) in the soil profile. Based on their depth, and the interpretation that Paleogene paleosol carbonates from the Bighorn Basin formed during summer (Snell et al. 2013), we interpret our data as a record of summer temperatures. The Δ_{47} paleotemperatures range from 23-42°C (Fig. 1), and show regularly spaced variability that cannot be attributed to differences in soil depth. The variability includes the temperature change across ETM2 and H2 and occurs on ~67-104 kyr intervals, given uncertainties in sediment accumulation rate. Thus this pacing plausibly reflects the 100 kyr eccentricity cycle, though not with certainty.

The Δ_{47} paleotemperature estimates negatively and non-linearly correlate with $\delta^{13}\text{C}$ values. An intriguing possibility is that this non-linearity reflects the non-linear relationship of temperature change with increasing pCO₂; according to our understanding of climate sensitivity, progressively larger amounts of additional CO₂ are required to effect the same amount of temperature change as pCO₂ levels increase. If this is true, then it may help explain why peak Δ_{47} paleotemperature for the PETM, ETM2 and H2 are all roughly the same (~39°C) in the Bighorn Basin. This result also implies that temperatures during peak hyperthermal conditions exhibit a narrower range of variability than during non-hyperthermal times, which has implications for associated impacts on biological systems. It is important to note, however, that there are processes besides just changes in pCO₂ levels that may influence our $\delta^{13}\text{C}$ values and contribute to this non-linear relationship.

Finally, our data indicate that average summer soil temperatures during ETM2 and H2 are ~8-9°C (\pm 3°C) higher than during non-hyperthermal periods; this is similar to the

$\sim 7^{\circ}\text{C}$ ($\pm 2^{\circ}\text{C}$) temperature change during the PETM in the Bighorn Basin. However, given that the PETM CIE is roughly twice as large as the CIEs for ETM2 and H2, we would expect the temperature response during the PETM to be substantially greater than during ETM2 and H2 if the hyperthermals shared a common, underlying cause, and if other factors such as climate sensitivity and background $p\text{CO}_2$ levels were the same for all events. These data instead appear to support previous studies that suggest the PETM may be unique relative to the other hyperthermals, and driven by a different mechanism or combination of mechanisms (Sexton et al., 2011; Zachos et al., 2010).

Notably, this interpretation differs from those based on marine records that suggest the temperature response scales proportionally with CIE magnitude for the PETM, ETM2 and H2 events (Stap et al., 2010). This is largely a function of the fact that the magnitude of temperature change on land during ETM2 and H2 implied by our data is larger than marine temperature changes during these events, while temperature change during the PETM was similar for the land and ocean ($\sim 5\text{-}7^{\circ}\text{C}$).

Together, these data provide critical insight into the terrestrial temperature response during Early Eocene hyperthermals and raise intriguing questions about the differences between the marine and terrestrial responses during PETM, ETM2 and H2. More paleotemperature estimates from terrestrial settings are required to confirm these conclusions.

REFERENCES

- Abels H.A., Clyde W.C., Gingerich P.D., Hilgen F.J., Fricke H.C., Bowen G.J. & Lourens L.J. (2012) - Terrestrial carbon isotope excursions and biotic change during Palaeogene hyperthermals. *Nature Geosci.*, 5(5),326-329.
- Fricke H. & Wing S. (2004) - Oxygen isotope and paleobotanical estimates of temperature and delta(18) O-latitude gradients over North America during the early Eocene. *Am. J. Sci.*, 304(7),612-635.
- Ghosh P., Adkins J., Affek H., Balta B., Guo W., Schauble E.A., Schrag D. & Eiler J.M. (2006) - C-13-O-18 bonds in carbonate minerals: A new kind of paleothermometer. *Geochim. Cosmochim. Acta*, 70(6):1439-1456.
- Sexton P.F., Norris R.D., Wilson P.A., Palike H., Westerhold T., Röhl, U., Bolton C.T. & Gibbs S.J. (2011) - Eocene global warming events driven by ventilation of oceanic dissolved organic carbon. *Nature*, 471(7338), 349-52.
- Snell K.E., Thrasher B.L., Eiler J.M., Koch P.L., Sloan L.C. & Tabor N.J. (2013) - Hot summers in the Bighorn Basin during the early Paleogene. *Geology*, 41(1), 55-58.
- Stap L., Lourens L.J., Thomas E., Sluijs A., Bohaty S.M. & Zachos J.C. (2010) - High-resolution deep-sea carbon and oxygen isotope records of Eocene Thermal Maximum 2 and H2. *Geology*, 38(7), 607-610.
- VanDeVelde J.H., Bowen G.J., Passey B.H. & Bowen B.B. (2013) - Climatic and diagenetic signals in the stable isotope geochemistry of dolomitic paleosols spanning the Paleocene-Eocene boundary. *Geochim. Cosmochim. Acta*, 109, 254-267.
- Wing S.L., Bao H. & Koch, P.L. (2000) - An early Eocene cool period? Evidence for continental cooling during the warmest part of the Cenozoic. In: Huber B.T., MacLeod K. & Wing S.L. (Eds.), *Warm Climates in Earth History*. Cambridge University Press, Cambridge, 197-237.
- Wing S., Harrington G., Smith F., Bloch J., Boyer D. & Freeman K. (2005) - Transient floral change and rapid global warming at the Paleocene-Eocene boundary. *Science*, 310(5750), 993-996.
- Zachos J.C., McCarren H., Murphy B., Rohl U. & Westerhold T. (2010) - Tempo and scale of late Paleocene and early Eocene carbon isotope cycles: Implications for the origin of hyperthermals. *Earth Planet. Sci. Lett.*, 299(1), 242-249.

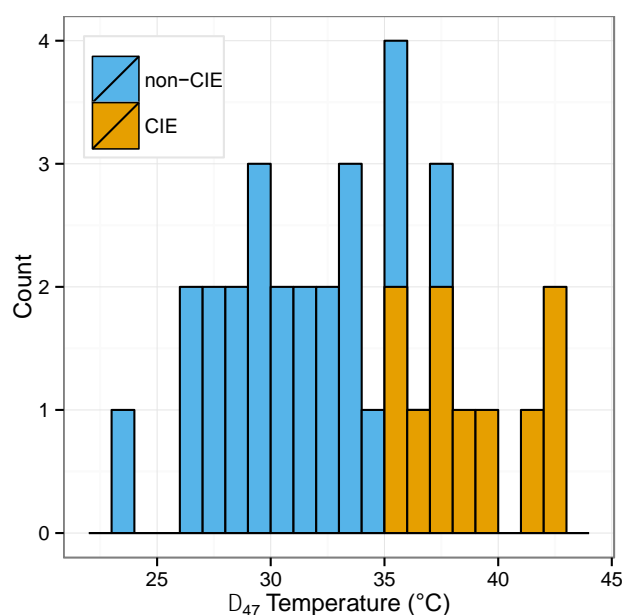


Fig.1 – Histogram of Δ_{47} paleotemperature estimates for Early Eocene samples from the Bighorn Basin. CIE samples are the samples with peak CIE $\delta^{13}\text{C}$ values for ETM2 and H2. Non-CIE samples include the samples from the onset and recovery intervals of ETM2 and H2, as well as all of the samples that are not a part of ETM2 and H2.

Scrutinizing data on climatic and biotic events of the Paleogene

Robert P. Speijer ^(a)

^(a) Department of Earth and Environmental Sciences, KU Leuven, Celestijnenlaan 200E, 3001, Heverlee, Belgium. E-mail: robert.speijer@ees.kuleuven.be

Document type: Short note.

Manuscript history: received 15 May 2014; accepted 30 May 2014; editorial responsibility and handling by Gerald R. Dickens & Valeria Luciani.

KEY WORDS: data quality, marine micropaleontology, Paleogene

Reviewing a manuscript dealing with climatic and biotic events of the Paleogene normally starts as a joy, but often ends in disappointment. One of the main causes for disappointment is the lack of basic quality control of the data. This can range from stable isotopic - or other geochemical - records without an explicit preservation assessment of the microfossils used, to quantitative faunal analyses based on too limited numbers of microfossils, to ignoring destructive taphonomic effects on fossil assemblages. This problem is not limited to unpublished manuscripts. Occasionally, papers that made it through the review process also appear fundamentally flawed with respect to the quality of the data.

Paleoenvironmental interpretations can only be as reliable and accurate as the quality of the proxies used to determine them. For instance, it is well-established and acknowledged by Quaternary researchers that a reliable stable isotope record depends on well preserved microfossils. In this respect, cores through non-lithified marine sediments provide relatively few problems. However, lithified, deep-time, pre-Quaternary rocks with a long history of burial and diagenesis are quite another issue. Generating reliable data from such rocks requires more scrutiny, especially when exposed on land and under the influence of ground water.

For the above reasons, studying geochemical proxies based on Paleogene outcrops may be more challenging than generally appreciated. Excellent tools used to analyze deep-sea cores cannot be simply copied to outcrop studies. For instance, marly sequences in North Africa commonly yield foraminifera that appear quite well preserved from the outside, but virtually all are fully infilled by secondary calcite. Such foraminifera cannot and should not be used for geochemical analyses, not even for a standard stable isotope analysis (O, C). This problem can partly be overcome by using only thick-shelled foraminifera, such as nodosarians and lenticulinids from which the secondary calcite can be separated relatively easily (Schmitz et al., 1996). Unfortunately, using these taxa leads to another problem: their stable isotopic values appear rather variable even within a single sample (e.g., Wendler et al.,

2013). Consequently, in these marly sequences, the planktic and thin-shelled benthic foraminifera cannot be used for isotope analysis (infillings) and nodosarians-lenticulinids provide a relatively large scatter, so that multiple specimen averaging is required to obtain more or less robust isotopic profiles (e.g., Bornemann et al., 2009).

Another example of the need for more scrutiny: only consistent selection of a certain species can yield a reliable monospecific stable isotopic record. This is less obvious than it seems, since few geochemists received extensive training in micropaleontology. *Nuttallides truempyi* and *Gavelinella beccariiformis* are frequently used species in Paleocene-Eocene deep-sea records. These can hardly be misidentified, even by non-experts. However, in continental margin sequences these deep-sea taxa are mostly absent and in order to obtain isotopic records species of *Cibicidoides* or *Anomalinoidea* are used (Stassen et al., 2009). Individual species of these taxa are often notoriously difficult to distinguish. This matters, because different species within these genera may yield different isotopic signatures with offsets of up to 0.5 per mille. This offset is in the same range as the numerous early Paleogene carbon isotopic excursions (CIEs), some of which are linked to hyperthermals (Cramer et al., 2003). Mistaking or lumping different species in a stable isotopic sequence may lead to erroneous identifications of minor CIEs and hyperthermals relative to the background signal.

Other recurrent and often neglected problems arise when foraminiferal (and other calcareous microfossil) assemblages are interpreted at face value, without assessment of the quality of the material. Allochthony (reworking), winnowing, and dissolution may all interfere with the composition of the assemblage. The consequences of partial dissolution remain widely underestimated in quantitative micropaleontology, notably in the Paleogene. Fluids saturated with carbon dioxide (e.g., at the seafloor, during early diagenesis, or by outcrop weathering) are corrosive for calcareous sediments and their microfossils. Consequently, at various stages during and after generation of the death assemblage, the composition of this assemblage will change by differential dissolution: susceptible components will be preferentially removed and robust

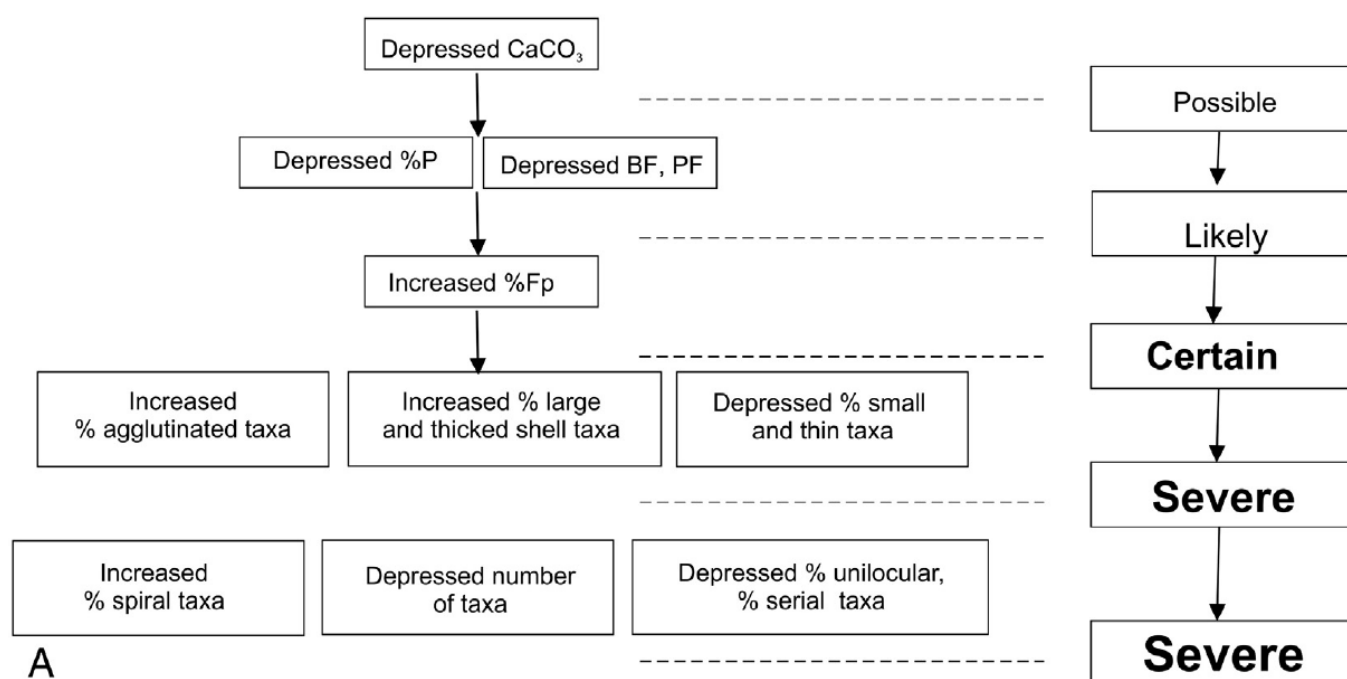


Fig.1 – Outline of the procedure to evaluate dissolution. A: Combined procedure for both benthic and planktic assemblages. On the left of the graph dissolution indicators are listed and arranged following the procedure while on the right, the certainty of each step of the procedure is indicated, in correlation with the indicators on the left. Note that all of the criteria mentioned here have to be judged in relation to the surrounding beds. (Reproduced from Nguyen & Speijer, 2014)

components will be relatively enriched. Strong dissolution leads to strongly altered and relatively impoverished calcareous microfossil assemblages, but minor dissolution may leave much more subtle traces. Whereas this is relevant to any study involving the study of calcareous assemblages, it is particularly relevant in studies aiming at sea-level reconstructions using planktic/benthic (P/B) ratios. The reason for this is, that the tests of planktic foraminifera are generally more susceptible than benthic ones. Variations in P/B values resulting from dissolution may thus be misinterpreted as variations in water depth and/or sea-level. Nguyen & Speijer (2014) proposed a new procedure to evaluate the quality of foraminiferal assemblages from lithified and non-lithified rocks based on a number of criteria, such as P/B ratio, fragmentation ratio (%F), foraminiferal numbers, abundance of agglutinated taxa, etc. (Fig. 1). Such a procedure is needed in order to avoid the 'garbage in garbage out' principle in paleoenvironmental research.

In conclusion, progress in climatic and biotic events of the Paleogene depends not only on creativity, the evaluation of new ideas, development of analytical tools and the exploration of new areas. Maintenance of high standards of classical analytical skills (e.g., fossil identifications, quantitative methods) and a critical scientific attitude are equally important to improve our understanding of Earth's past and future.

REFERENCES

- Bornemann A., Schulte P., Sprong J., Steurbau, E., Youssef M. & Speijer R.P. (2009) - Latest Danian carbon isotope anomaly and associated environmental change in the Southern Tethys (Nile Basin, Egypt). *J. Geol. Soc. London*, 166, 1135-1142.
- Nguyen T.M.P. & Speijer R.P. (2014) - A new procedure to assess dissolution based on experiments on Pliocene - Quaternary foraminifera (ODP Leg 160, Eratosthenes Seamount, Eastern Mediterranean). *Mar. Micropaleontol.*, 106, 22-39.
- Schmitz B., Speijer R.P. & Aubry M.-P. (1996) - Latest Paleocene benthic extinction event on the southern Tethyan shelf (Egypt): Foraminiferal stable isotopic ($\delta^{13}\text{C}$, $\delta^{18}\text{O}$) records. *Geology*, 24, 347-350.
- Stassen P., Thomas E. & Speijer R.P. (2009) - Benthic foraminiferal isotope records across the PETM from the New Jersey coastal plain. *GNS Science Miscellaneous Series 18*, 135-137.
- Wendler I., Huber B.T., MacLeod K.G. & Wendler, J.E. (2013) - Stable oxygen and carbon isotope systematics of exquisitely preserved Turonian foraminifera from Tanzania - understanding isotopic signatures in fossils. *Mar. Micropaleontol.*, 102, 1-33.

Possible evidence of ice-rafting in the North Atlantic across the Eocene-Oligocene Transition: Preliminary findings from the Newfoundland Margin

James F. Spray ^(a), Paul A. Wilson ^(a), Steve M. Bohaty ^(a) & Ian Bailey ^(b)

^(a) Department of Ocean and Earth Sciences, University of Southampton, National Oceanography Center, Southampton SO14 3ZH, UK. E-mail: jfs1g12@soton.ac.uk

^(b) Camborne School of Mines, College of Engineering, Mathematics & Physical Sciences, University of Exeter, Cornwall TR10 9FE, UK

Document type: Abstract.

Manuscript history: received 15 May 2014; accepted 30 May 2014; editorial responsibility and handling by Gerald R. Dickens & Valeria Luciani.

KEY WORDS: Eocene-Oligocene Transition, ice-rafted debris, IODP Expedition 342, North Atlantic.

The initiation and development of glacial conditions on Antarctica is relatively well understood through the Palaeogene, with a small ice cap forming by the late Eocene, followed by a rapid expansion of ice across the Eocene Oligocene Transition (EOT). Much less is known, however, about the development of glacial conditions in the Northern Hemisphere.

Previous work in the Arctic (IODP Exp. 302), and in the Norwegian- Greenland Sea (ODP Leg 151), has highlighted the

likelihood of the existence of perennial Arctic sea-ice and coastal mountain outlet glaciers on Greenland from the Middle Eocene. Little more is known, however, about the temporal or spatial extent of Palaeogene glacial conditions in the high northern latitudes.

IODP expedition 342 to the Newfoundland Margin recovered an exceptionally high-resolution record of the EOT, one of the key intervals of Palaeogene climate change. The drift sediments recovered at Site U1411 contain angular grains of silt and fine sand that were tentatively interpreted shipboard as being ice-rafted in origin. Here we report preliminary results of an investigation of these grains, with the aim of determining their composition, origin, abundance, and provenance.

Eocene hyperthermals in the North Sea Basin: a Belgian Ypresian perspective.

Peter Stassen ^(a,b), Robert P. Speijer ^(a), Xavier Devleeschouwer ^(b), Hemmo A. Abels ^(c), Chris King ^(d),
Willy Willems ^(e,†) & Etienne Steurbaut ^(a,b)

^(a) Department of Earth and Environmental Sciences, KU Leuven, B-3001 Leuven, Belgium. E-mail: Peter.Stassen@ees.kuleuven.be

^(b) Directorate Earth and History of Life, Royal Belgian Institute of Natural Sciences, B-1000 Brussels, Belgium

^(c) Department of Earth Sciences, Utrecht University, 3584 CD Utrecht, The Netherlands

^(d) 16A Park Road, Bridport DT6 5DA, UK

^(e,†) Department Geology and Soil Sciences, UGent, Belgium

Document type: Short note.

Manuscript history: received 15 May 2014; accepted 30 May 2014; editorial responsibility and handling by Gerald R. Dickens & Valeria Luciani.

KEY WORDS: Belgium, Hyperthermals, North Sea Basin, Ypresian.

Abrupt climate changes, involving threshold crossings towards new regimes, frequently occurred in the past with the early Eocene rapid global warming events (so-called hyperthermals) as the most conspicuous. The early Eocene greenhouse world is characterized by a succession of orbitally-controlled global stable carbon isotope excursions (CIE), of which some have been shown to be associated with abrupt climate change and biotic perturbations. The impact of these isotopic excursions has been primarily studied in deep-sea sections under comparably stable conditions, while their impact on shallow marine ecosystems is unexplored, specifically for the smaller hyperthermals that occur after the Paleocene-Eocene Thermal Maximum (PETM). Preliminary investigations however indicate a significant biotic disruption during ETM-2 in the southern Tethyan shelf (Stassen et al., 2012) showing their potential importance.

In order to understand the impact on the biosphere of these Eocene hyperthermals, identification and analysis is needed in additional shallow shelf sequences. Here we aim at deciphering the lithologic, biotic, and geochemical signature of the successive hyperthermals in the Ypresian shallow marine context at the southern edge of the North Sea Basin (Fig. 1). The PETM has already been recorded in the lagoonal Tienen Formation, representing the earliest Eocene of Belgium (Sturbaut et al., 2003). The Belgian Basin also contains a relatively complete, rather fossiliferous and well-studied marine lower Eocene succession (the classical Belgian Ypresian clays). The thickness of these heterogeneous Ypresian silts and clays reaches 116 meters in the Belgian Geological Survey Kallo core (Fig. 1), which is used for a regional stratigraphic framework (Sturbaut, 2006).

Calcareous nannofossil biostratigraphy positions this sedimentary sequence within nannoplankton zones NP11-12 with a partially decalcified lower part (NP10?). This implies a

time span of about 3.6-3.7 Myr and overall sedimentation rates of about 5 cm/kyr, allowing potential high-resolution studies of hyperthermal events. Foraminiferal bioevents (I-events; King, 1991) and benthic foraminiferal associations (Willems, 1980; Willems & Moorkens, 1991) have been used for regional correlations, but their paleoecologic meaning remained unresolved and may be related to global warming events.

Isotope data ($\delta^{13}C_{org}$) and magnetic susceptibility indicate the presence of distinct lithologic events and a succession of CIE's in the Belgian Ypresian deposits, which may represent the H1, H2, I1, I2, J?, K and L? isotope events (Fig. 1). These levels are biostratigraphically correlated with coeval isotope excursions at DSDP site 550 (Gulf of Biscay) and Albæk Hoved (Denmark) using a mid-latitude nannoplankton subzonation (e.g., Steurbaut, 1998; 2011). Major regional foraminiferal faunal changes seem to relate to these events. During H1 (Elmo/ETM-2) a lowermost incursion of nannoplankton species occurs, coincident with the establishment of calcareous benthic foraminiferal faunas, at I1 consistent occurrences of nannofossils occurs and establishment of a well-diversified benthic foraminiferal fauna, and during K (X-event / ETM-3) a temporary influx of characteristic planktic foraminifera (*Subbotina patagonica* acme) and an acme of *Asterigerina bartoniana kaasschieteri* (I5 event) are seen. The latter is considered indicative of deposition in a shallow tropical sea and may thus represent a basin-wide zonal expansion of its life habitat.

Although Early Eocene hyperthermals in shallow water sequences still need to be fully characterized relative to regional background conditions, our results seem to indicate that also these lesser hyperthermal events had short- and potentially long-term impacts on the development of regional shallow marine ecosystems. Furthermore, these lithologic and biotic expressions of the hyperthermals may reflect environmental changes constrained by specific climate thresholds, in addition to regional tectonics, triggering transient reorganizations of the hydrologic cycle, and deep-water

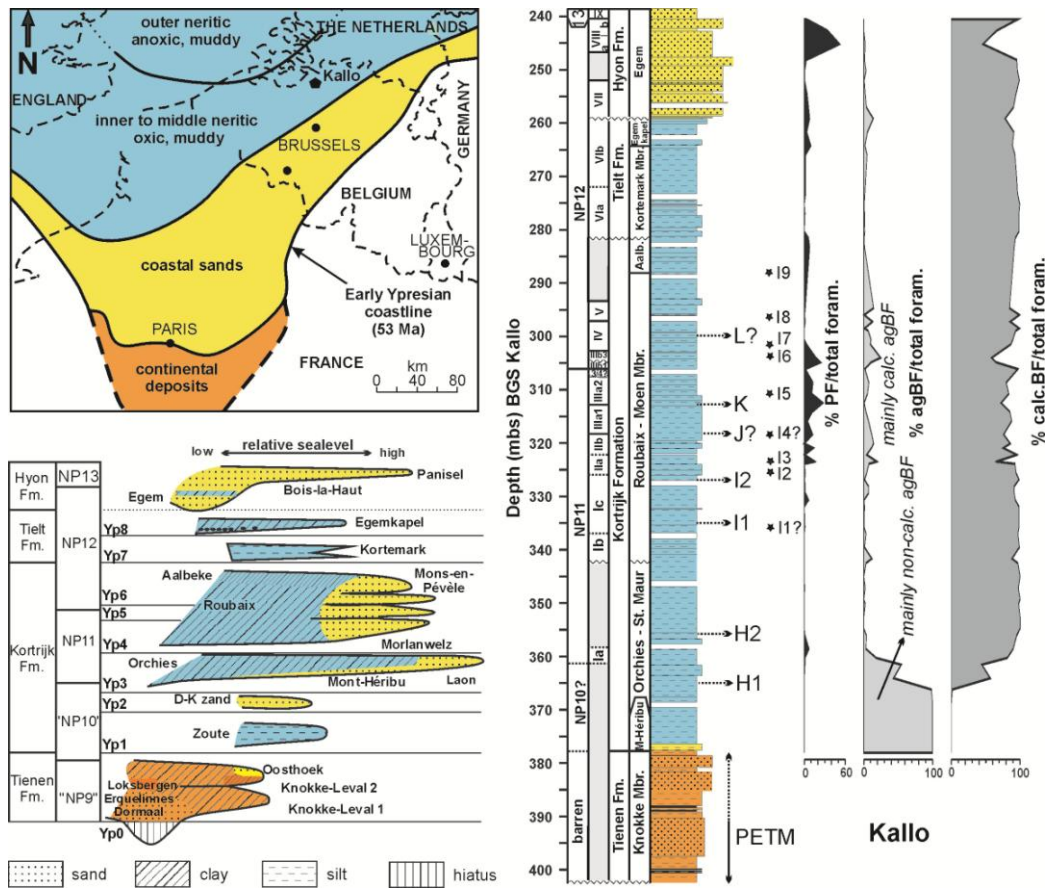


Fig.1 – Early Ypresian paleogeography and lithofacies distribution at the southern North Sea Basin at 53 Ma (modified after Steurbaut, 2011), and biotic and CIE events within the Kallo reference core (data of Willems, 1980; King, 1991; Steurbaut, 1991)

circulation in the Northern Atlantic region (e.g., D'haenens et al., 2014). Our datasets emphasize the potential application of hyperthermal event stratigraphy to correlate over a wide range of different environmental settings in the North Atlantic Ocean and adjacent basins, and to understand the spatial heterogeneity of climate changes in these shallow-water settings.

REFERENCES

- D'haenens S., Bornemann A., Claeys P., Röhl U., Steurbaut E. & Speijer R.P. (2014) - A transient deep-sea circulation switch during Eocene Thermal Maximum 2 (ETM2). *Paleoceanography*, PA002567.
- King C. (1991) - Stratigraphy of the Ieper Formation and Argile de Flandres (Early Eocene) in Western Belgium and Northern France. In: C. Dupuis, J. De Coninck and E. Steurbaut (Eds.), *The Ypresian stratotype*. *B Soc. Belg. Géol.*, 97, 349-372.
- Stassen P., Steurbaut E., Morsi A.-M.M., Schulte P. & Speijer, R.P. (2012) - The biotic impact of Eocene thermal maximum 2 in a shelf setting (Dababiya, Egypt). *Austrian J. Earth Sci.*, 105, 154-160.
- Sturbaut E. (1991) - Ypresian calcareous nannoplankton biostratigraphy and paleogeography of the Belgian Basin. In: C. Dupuis, J. De Coninck and E. Steurbaut (Eds.), *The Ypresian Stratotype*. *B Soc. Belg. Géol.*, 97, 251-285.
- Sturbaut E. (1998) - High-resolution holostratigraphy of Middle Paleocene to Early Eocene strata of Belgium and adjacent areas. *Palaeontogr. Abt. A.*, 247, 91-156.
- Sturbaut, E. (2006) - Ypresian. In: L. Dejonghe (Editor), *Current status of chronostratigraphic units named from Belgium and adjacent areas*. *Geol. Belg.*, 9, 73-93.
- Sturbaut E. (2011) - New Calcareous nannofossil taxa from the Ypresian (Early Eocene) of the North Sea Basin and the Turan Platform in West Kazakhstan. *Bulletin de l'Institut royal des Sciences naturelles de Belgique*, 81, 247-277.
- Sturbaut E., Magioncalda R., Dupuis C., Van Simaey S., Roche E. & Roche M. (2003) - Palynology, paleoenvironments and organic carbon isotope evolution in lagoonal Paleocene/Eocene boundary settings in North Belgium. In: S.L. Wing, P.D. Gingerich, B. Schmitz and E. Thomas (Eds.), *Causes and consequences of Globally Warm Climates in the Early Paleogene*. *GSA Special Paper*, 369, 291-317.
- Willems W. (1980) - Foraminifera of the Ieper Formation (Early Eocene) in the southern North Sea Basin (biostratigraphy, paleoecology and systematic). Unpublished PhD thesis, Gent University, 364 pp.
- Willems, W. and Moorkens, T. (1991) - The Ypresian Stage in the Belgian Basin. In: C. Dupuis, J. De Coninck and E. Steurbaut (Eds.), *The Ypresian Stratotype*. *B Soc. Belg. Géol.*, 97, 231-249.

Implacement and fluctuations of the Antarctic Ice Sheet across the Eocene-Oligocene transition

Paolo Stocchi ^(a), Simone Galeotti ^(b), Jean-Baptiste Ladant ^(c), Edward Gasson ^(d), Robert M. DeConto ^(d), David Pollard ^(e), Maria Rugenstein ^(f), Bert L.A. Vermeersen ^(a) & Henk Brinkhuis ^(a)

^(a) NIOZ Royal Netherlands Institute for Sea Research, 1797 TA, Texel, The Netherlands. E-mail: Paolo.Stocchi@nioz.nl

^(b) Dipartimento di Scienze della Terra, della Vita e dell' Ambiente, University of Urbino, Urbino, Italy

^(c) Laboratoire des Sciences du Climat et de l' Environnement, CEA-CNRS-UVSQ, CEA Saclay, Orme des Merisiers, FR-91191 Gif-sur-Yvette, France

^(d) Climate System Research Center, University of Massachusetts, Amherst, USA

^(e) Earth and Environmental Systems Institute, Pennsylvania State University, State College, USA

^(f) IMAU Institute for Marine and Atmospheric Research, Utrecht University, Utrecht, The Netherlands

Document type: Short note.

Manuscript history: received 15 May 2014; accepted 30 May 2014; editorial responsibility and handling by Gerald R. Dickens & Valeria Luciani.

KEY WORDS: Antarctica, Antarctic ice sheet, Glacial Isostatic Adjustment, numerical modeling, rheology, sea level change).

Climate cooling across the late Eocene (48 - 34 Million years ago, Ma) eventually put an end to the ice-free hot-house world and triggered the establishment of ice-house conditions. In particular, the Eocene-Oligocene transition (EOT; ~34 Ma) is marked by a ~1.5% positive increase in deep-sea oxygen isotopic values that is commonly related to the establishment of a persistent continental-scale Antarctic Ice Sheet (DeConto & Pollard, 2003). Regardless of the geographical configuration of Southern Ocean gateways, geochemical data and ice-sheet modeling show that AIS glaciation initiated as atmospheric CO₂ fell below 2.5 times pre-industrial values (DeConto & Pollard, 2003). Quantifying the magnitude and timing of AIS volume variations by means of $\delta^{18}\text{O}$ records is hampered by the fact that the latter reflect a coupled signal of temperature and ice-sheet volume. Besides, bathymetric variations based on marine geologic sections are affected by large uncertainties and, most importantly, reflect the local response of relative sea level (rsl) to ice volume fluctuations rather than the global eustatic signal. AIS proximal and Northern Hemisphere (NH) shallow marine settings show an opposite trend of rsl change across the EOT. In particular, low-latitude Northern Hemisphere shallow marine sequences record a $60 \pm 20\text{m}$ rsl fall (Houben et al., 2012), suggesting that AIS volume could have expanded to either near modern dimensions or as much as 25% larger than present day (Pearson et al., 2009). On the other hand, sedimentary facies from shallow marine shelfal areas around East Antarctica and in the proximity of the AIS margins show that local rsl rose by ~150 m during the EOT glaciation (Stocchi et al., 2013). Accounting for ice-load-induced crustal and geoidal deformations and for the mutual gravitational attraction between the growing AIS and the ocean water is a necessary requirement to reconcile near- and far-field rsl sites, regardless of tectonics and of any other possible local contamination. In this work we investigate the AIS inception

and variability across the EOT by combining the observed rsl changes with predictions based on numerical modeling of Glacial Isostatic Adjustment (GIA). We solve the gravitationally self-consistent Sea Level Equation (Spada and Stocchi, 2007; Stocchi et al., 2013) for two different and independent AIS models (Ladant et al., 2014; Stocchi et al., 2013) both driven by atmospheric CO₂ variations and evolving on different Antarctic topographies (Ladant et al., 2014; Wilson et al., 2012, 2013). In particular, minimum and maximum AIS volumes, respectively of ~57m and ~70m equivalent sea level (esl), stem from a smaller and a larger Antarctic topography. Minimum and maximum GIA predictions at the NH rsl sites respectively correspond to the lower limit and central value of the EOT rsl drop inferred from geological data.

For both GIA models, the departures from the eustatic trend significantly increase southward toward Antarctica, where the AIS growth is accompanied by a rsl rise. Accordingly, the cyclochronological record of sedimentary cycles retrieved from Cape Roberts Project Drillcore CRP-3 witness a deepening across the EOT (Galeotti et al, 2012; Stocchi et al., 2013), which is in line with the predicted rsl changes. However, CRP-3 record shows that full glacial conditions consistent with the maximum AIS model dimensions were reached only at 32.0 Ma, i.e. ~1 Ma after the Oi-1 event, while AIS volume fluctuations around the minimum AIS model volume persisted during the first million years of glaciation.

The strong gradients of GIA-induced rsl change around Antarctica are maintained by the lithospheric flexure and result in regionally-varying bathymetric variations that affect the circumpolar ocean flow (Rugenstein et al., 2014). In particular, we find along-meridian shifts of frontal patterns of the order of several degrees. Also, differences in velocity are locally more than 100%, and the zonal transport decreases in mean and variability. Our modeling results therefore suggest that GIA-induced ocean flow variations alone could have significant impacts on local nutrient variability as well as on erosion and sedimentation rates and ocean heat transport. Hence, these so

far overlooked effects should be considered when interpreting sediments cores.

REFERENCES

- DeConto R.M. & Pollard D. (2003) - Rapid Cenozoic glaciation of Antarctica induced by declining atmospheric CO₂. *Nature*, 421, 245.
- Galeotti S, Lanci L., Florindo F., Naish T.R., Sagnotti L., Sandroni S. & Talarico F.M. - Cyclochronology of the Eocene-Oligocene transition from the Cape Roberts Project-3 core, Victoria Land basin, Antarctica. *Palaeogeogr. Palaeoclimatol. Palaeoecol.*, 335-336, 84-94.
- Houben A.J.P., van Mourik C.A., Montanari A., Coccioni R. & Brinkhuis H. (2012) - The Eocene–Oligocene transition: Changes in sea level, temperature or both?, *Palaeogeogr. Palaeoclimatol. Palaeoecol.*, 335-336, 75-83.
- Ladant J.-B., Donnadiou Y., Lefebvre V. & Dumas C. (2014) - Consistent ice sheet evolution at the Eocene-Oligocene transition under the influence of atmospheric carbon dioxide and orbital parameters. *Clim. Past*, Under review.
- Pearson P.N., Foster G.L. & Wade B. S. (2009) - Atmospheric carbon dioxide through the Eocene-Oligocene climate transition. *Nature*, 461, 1110-1113.
- Rugenstein M., Stocchi P., Von der Heyght A., Deekstra H. & Brinkhuis H. (2014) - Emplacement of Antarctic ice sheet mass affects circumpolar ocean flow. *Global Planet. Changes*, 118, 16-24.
- Spada G. & Stocchi P. (2007) - SELEN a fortran 90 program for solving the sea level equation. *Computers and Geoscience*, 33 (4), 538 – 562.
- Stocchi P., Escutia C., Houben A.J.P., Vermeersen B.L.A., Bijl P.K., Brinkhuis H., DeConto R.M., Galeotti S., Passchier S., Pollard D., Klaus A., Fehr A., Williams T., Bendle J.A.P., Bohaty S.M., Carr S.A., Dunbar R.B., Flores J.A., González J.J., Hayden T.G., Iwai M., Jimenez-Espejo F.J., Katsuki K., Kong G.S., McKay R.M., Nakai M., Olney M.P., Pekar S.F., Pross J., Riesselman C., Röhl U., Sakai T., Shrivastava P.K., Stickley C.E., Sugisaki S., Tauxe L., Tuo S., Van De Flierdt T., Welsh K. & Yamane M. (2013) - Relative sea-level rise around East Antarctica during Oligocene glaciation. *Nat. Geosci.*, 6, 380-384.
- Wilson D.S., Jamieson S.S.R., Barrett P.J., Leitchkov G., Gohl K. & Larter R.D. (2012) - Antarctic topography at the Eocene–Oligocene boundary. *Palaeogeogr., Palaeoclimatol., Palaeoecol.*, 335-336, 24-34.
- Wilson, D.S., Pollard D., DeConto R.M., Jamieson S.R.S. & Luyendyk B.P. (2013) - Initiation of the West Antarctic Ice Sheet and estimates of total Antarctic ice volume in the earliest Oligocene. *Geophys. Res. Lett.*, 40, 4305-4309.

The Paleocene-Eocene transition in Bulgaria: inference from calcareous nannofossils

Kristalina Stoykova (a)

(a) Department of Paleontology, Stratigraphy and Sedimentology, Geological Institute Bulgarian Academy of Sciences, 24 Acad. G. Bonchev Str., 1113 Sofia, Bulgaria. E-mail: stoykova@geology.bas.bg

Document type: Short note.

Manuscript history: received 15 May 2014; accepted 30 May 2014; editorial responsibility and handling by Gerald R. Dickens & Valeria Luciani.

KEY WORDS: Bulgaria, calcareous nannofossils, PETM.

The first biostratigraphic data identifying the Paleocene-Eocene Thermal Maximum (PETM) in Bulgaria are published by Stoykova and Ivanov (2005). The succession of calcareous nannofossil bioevents in the transient interval and the substantial changes in the nannofloral composition within NP9-NP10 Zones served as key evidence in identifying this prominent global warming event in Bulgaria. Following the biostratigraphic confirmation of PETM, bulk rock samples of these sections have been analyzed for $\delta^{13}\text{C}$ content. They proved the presence of clear negative carbon isotope excursion (CIE) (Sprovieri in Stoykova et al., 2005).

In the present study, these three land sections (Kladorub, Riben and Bozhuritsa) and one offshore site (Yurii Shimanov well in the Bulgarian Black Sea shelf) have been re-investigated in order to document the composition of the nannofossil assemblages during the PETM and to provide insight into the biotic response of nanoplankton communities to the extreme global warming. High-resolution cm-scale sampling, approximately every 20 cm, has been performed in the entire PETM interval (72 samples analyzed). Calcareous nannofossil associations before, during and after the PETM are examined to infer the biotic response of abrupt warming. The sedimentology of the studied successions suggests that deposition likely took place in a middle to outer shelf setting.

The pre-PETM nannofossil associations are rich and diversified, comprising abundant *Discoaster protomultiradiatus*, *D. multiradiatus*, *D. elegans*, *Fasciculithus mitreus*, *F. siderius*, *F. fenestrellatus*, *F. tonii*, *F. thomasi*, *F. bobii*, *F. involutus*, *Chiasmolithus bidens*, *Toweius eminens*, *T. tovae*, *Neochiastozygus junctus*, *Ellipsolithus distichus*.

The onset of the climatic event in all studied sections is lithologically marked by a drop of the carbonate content and deposition of Carbonate Dissolution Interval (CDI). The thickness of the dissolution zone, where calcareous nannofossils are completely absent, varies between 0.6 - 2.5 m in different sections. At the top of the dissolution zone,

fragments of dissolution-resistant species such as *Discoaster multiradiatus*, *D. elegans* and *Fasciculithus* spp. are spotted. The association is very poor, with poor preservation and signs of dissolution. All sections reveal the drastic decrease to complete extinction of *Fasciculithus* species following the offset of the PETM.

The Paleocene-Eocene boundary is recognized by the first occurrence of the representatives of *Rhomboaster* (*Rhomboaster* spp., *R. bramlettei*, *R. cuspis*). It is everywhere positioned above the onset of the climatic event.

Upwards in the Eocene portion of the PETM, a specific warm-water nannofossil association has been identified. Khan & Aubry (2004) defined it as a specific "*Rhomboaster* spp. – *Discoaster araneus* (RD) association", whereas Self-Trail et al. (2012) called it "CIE-taxa", restricted entirely to the PETM interval. In Bulgaria, the excursion taxa assemblage includes *Toweius serotinus*, *Rhomboaster* spp., *Discoaster araneus*, *D. sp. aff. anartios*. The last two species have a very sporadic occurrence and never become abundant in the overall nannofossil association, as noted by Self-Trail et al. (2012). The vertical distribution of CIE-association entirely coincides and reflects the negative $\delta^{13}\text{C}$ excursion interval. However, in Bulgarian localities the RD association occurs slightly higher than the CIE-onset, as previously pointed out by Angori et al. (2007) and Self-Trail et al. (2012).

By the time that carbon isotope values are beginning to recover, the *Rhomboaster*-lineage quickly flourished, rapidly increasing in abundance up sections with successive, almost simultaneous occurrence of *R. bramlettei*, *R. cuspis*, *R. calcitrapa*. *Toweius* and *Discoaster* representatives also recover in the upper portion of PETM - *T. callosus*, *T. occultatus*, *T. pertusus*, *D. multiradiatus*, *D. falcatus*, *D. limbatus*. Other Lazarus taxa include *Zygrhablithus bijugatus*, *Chiasmolithus bidens* and *C. consuetus*. Bulgarian data indicate that the first occurrence of *Discoaster diastypus* is rather later in the Early Eocene, beyond the climatic event interval. Some of the key bioevents in the calcareous nanoplankton (first and last occurrence), as well as stratigraphically important nannofossil species are shown on Fig. 1.

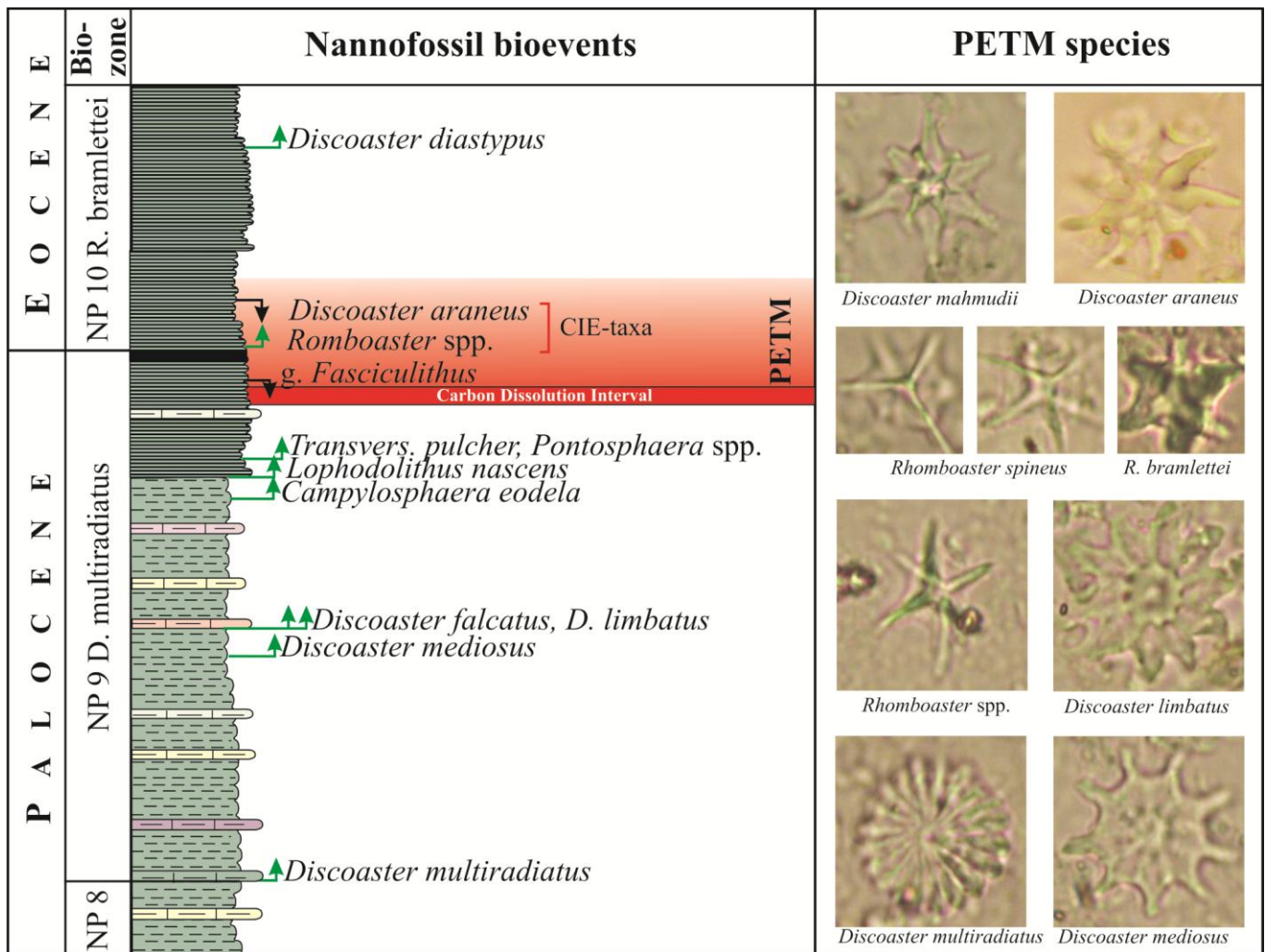


Fig.1 – Nannofossil bioevents and key stratigraphic taxa across the Paleocene-Eocene transition interval in Bulgaria.

REFERENCES

- Angori E., Bernaola G. & Monechi S. (2007) - Calcareous nannofossil assemblages and their response to the Paleocene-Eocene Thermal Maximum event at different latitudes: ODP Site 690 and Tethyan sections. In: Monechi, S., Coccioni, R., Rampino, M. R. (Eds.), Large ecosystem perturbations: causes and consequences. Geol. Soc. of America Spec. Paper, 424, 69-85.
- Khan A. & Aubry M.-P. (2004) - Provincialism associated with the Paleocene/Eocene thermal maximum: temporal constraint. Mar. Micropaleontol., 52, 117-131.
- Self-Trail J. M., Powars D.S., Watkins D. K. & Wandless G.A. (2012) - Calcareous nannofossil assemblage changes across the Paleocene-Eocene Thermal Maximum: Evidence from a shelf setting. Mar. Micropaleontol., 92-93, 61-80.
- Stoykova K. & Ivanov M. (2005) - First data on the presence of the Paleocene-Eocene Thermal Maximum in Bulgaria. C. R. Acad. bulg. Sci, 58, 3, 297-302.
- Stoykova K., Ivanov M., Dinares-Turell J. & Sprovieri M. (2005) - Paleocene-Eocene Thermal Maximum – biostratigraphic and stable isotope data in Bulgarian sections. Proc. Jubilee Intern. Conference Bulg. Geol. Society, 80-th Anniversary, 21-23 (in Bulgarian).

Early Paleogene Pacific Deep-water Lead Isotope Variations – Implications for the Evolution of Water Mass Composition

Deborah J. Thomas ^(a)

^(a) Department of Oceanography, Texas A&M University, College Station, Texas 77843 United States. E-mail: dthomas@ocean.tamu.edu

Document type: Short note.

Manuscript history: received 15 May 2014; accepted 30 May 2014; editorial responsibility and handling by Gerald R. Dickens & Valeria Luciani.

KEY WORDS: International Ocean Discovery Program, meridional overturning circulation, radiogenic isotopes.

A growing body of water mass proxy data and numerical simulations indicates a Late Cretaceous through early Paleogene reconstruction of meridional overturning circulation (MOC) characterized by convection in the South and North Pacific. Fully coupled GCM simulations indicate that the “age” of deep waters in the Pacific increased from high to low latitudes in both the South and North Pacific (Hague et al., 2012). Nd isotope data also suggest that the MOC in the Pacific was distinct and separate from that in the Atlantic (Thomas et al., 2014).

In this study we pair new seawater Pb isotope data with previously published seawater Nd isotopes to assess and refine the current reconstruction of Early Paleogene MOC and qualitatively estimate rates of deep-water circulation. Based on what is known of the marine geochemical cycling of Nd and Pb, the dominant influence on the dissolved Pb isotopic composition at the seafloor in regions proximal to water mass convection likely was weathering inputs to the surface waters (e.g., fluvial). Variations in the seafloor dissolved Pb isotopic composition should be coupled to those of Nd. In contrast, the seafloor dissolved Pb isotopic composition in regions far from the water mass formation region should also bear the imprint of dust or ash dissolution, particularly in regions remote from any continental margin. In such regions, the dissolved Nd and Pb isotope records likely would not covary – the Nd in dust and ash is less susceptible to mobilization in seawater than the corresponding Pb (e.g., Jones et al., 1994; Jones et al., 2000).

Dissolved Pb isotope values reconstructed from analyses of authigenic oxide minerals at DSDP and ODP Sites 464, 596 and 883 generally fluctuate consistently. The three Pb isotope ratios ($^{206,207,208}\text{Pb}/^{204}\text{Pb}$) recorded at North Pacific Site 883 exhibit generally coincident maxima and minima in each of the three tracers. The coherent variations in all three Pb systems might track the overall variations in dissolved Pb in the deep-water formation region. At Site 464, all three Pb isotope systems also behave similarly. However, at Site 596, all three isotopes record maxima at ~66 and 40 Ma, while $^{207,208}\text{Pb}/^{204}\text{Pb}$ values show additional peaks at ~60 and from ~56 to 50 Ma

that do not occur in the $^{206}\text{Pb}/^{204}\text{Pb}$. One potential explanation for the variations in $^{207,208}\text{Pb}/^{204}\text{Pb}$ without concomitant changes in $^{206}\text{Pb}/^{204}\text{Pb}$ is the contribution of Pb from the dissolution of detrital silicate dust. Dissolution of silicate dust could have produced the increases in $^{207,208}\text{Pb}/^{204}\text{Pb}$ without impacting the corresponding $^{206}\text{Pb}/^{204}\text{Pb}$ values.

We potentially can assess the contribution of detrital silicate dust to the seawater value through comparison of the dissolved Pb isotopic composition derived from the oxide fraction with that recorded by the detrital sediment fraction. Two fine-grained detrital samples from Site 596 (~56 and 60 Ma, respectively) record $^{206}\text{Pb}/^{204}\text{Pb}$ nearly identical to the seawater ratios. However, the corresponding detrital $^{207,208}\text{Pb}/^{204}\text{Pb}$ values were 0.1 to 0.3 lower than the contemporaneous seawater values. The relatively low detrital $^{207,208}\text{Pb}/^{204}\text{Pb}$ values likely reflect contributions of volcanic ash, and release of Pb from the ash at the seafloor may impact the dissolved seawater value recorded by the leached oxides.

In the North Pacific, at Site 883, the detrital $^{206}\text{Pb}/^{204}\text{Pb}$ and $^{208}\text{Pb}/^{204}\text{Pb}$ values were 0.2 to 0.4 higher than their corresponding seawater values, while the seawater and detrital $^{207}\text{Pb}/^{204}\text{Pb}$ were the same. At Site 464, the difference between detrital and seawater Pb isotope values increased up-section with similar detrital and seawater values recorded at ~42 and 62 Ma (except the seawater $^{208}\text{Pb}/^{204}\text{Pb}$ value was 0.3 lower than the detrital value in the ~42 Ma sample), but detrital values recorded at ~33 Ma were 0.2 to 0.3 higher than the associated seawater values.

Paired Pb and Nd isotope data derived from authigenic oxide minerals from DSDP and ODP Sites 464, 596 and 883 allow us to assess potential variations in the coupling of dissolved Pb and Nd in North Pacific Deep Water (NPDW) and South Pacific Deep Water (SPDW) as these waters advected toward the tropical Pacific (Figure 1). Variations in the dissolved $^{206}\text{Pb}/^{204}\text{Pb}$, $^{207}\text{Pb}/^{204}\text{Pb}$, and $^{208}\text{Pb}/^{204}\text{Pb}$ values recorded at ODP Site 883 (the site located furthest north in this study) mirror $\epsilon_{\text{Nd}}(t)$ variations. Relatively high Pb isotope values correspond to relatively low $\epsilon_{\text{Nd}}(t)$, suggesting that variations in both systems resulted from a common process. However there is little apparent relationship between Pb and Nd in cross-plots of the three Pb systems with $\epsilon_{\text{Nd}}(t)$.

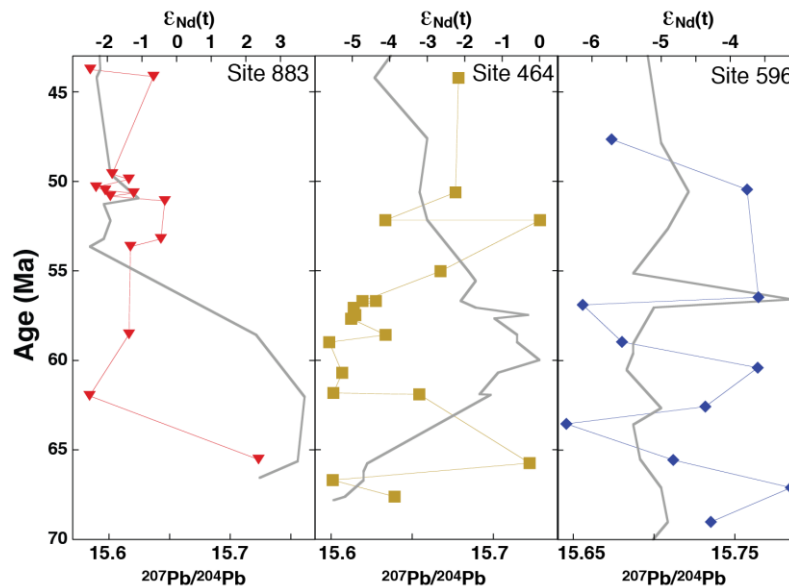


Fig.1. - Comparison of new Pb isotope data ($^{207}\text{Pb}/^{204}\text{Pb}$ shown here) with previously published Nd isotope data (Hague et al., 2012; Thomas et al., accepted).

DSDP Site 464 was located to the south of Site 883 in the subtropical North Pacific, however Nd isotope reconstructions suggest it was bathed by the same water mass (NPDW). Comparison of the new Pb data to the existing Nd isotope record suggests a relatively weak relationship. For example, maximum Nd isotope values recorded between ~61 to 50 Ma correspond with relatively low Pb isotope values in all three systems. In fact, the Pb and Nd values from ~66 to 50 Ma show an inverse relationship, much like that at Sites 883. After ~50 Ma, Pb and Nd tend to co-vary (e.g., Nd and Pb both decrease to the top of the study interval). This change in the relationship between Nd and Pb could reflect a change in the dominant source of dissolved Pb to the central North Pacific region. From ~61 to 50 Ma, the dissolved Pb composition was likely controlled by water mass composition. This is consistent with Nd isotope evidence for a strong contribution of North Pacific Deep Water (NPDW) to the region over the time period (Hague et al., 2012). Subsequently, as convection of NPDW waned and the contribution of deep waters from the South Pacific increased (SPDW), the Nd isotope composition decreased.

DSDP Site 596 in the subtropical South Pacific exhibits the greatest degree of decoupling. At Site 596, dissolved $\epsilon_{\text{Nd}}(t)$ isotope values remain nearly constant at ~-5.5 for nearly 30 million years, while dissolved Pb varies significantly (Figure 1). $^{207}\text{Pb}/^{204}\text{Pb}$ values vary between ~15.65 and 15.75 and $^{208}\text{Pb}/^{204}\text{Pb}$ values vary between ~38.7 and 39.1. This strong and consistent decoupling is somewhat unexpected given the persistent Nd isotope signature of SPDW recorded at Site 596 for the entire Paleogene. The likely explanation is that the proposed formation region of SPDW in the Ross Sea region (Thomas et al., accepted) was sufficiently far from Site 596 to permit dust and ash dissolution en route to obscure the original water mass Pb signature. Coupled and ocean-only GCM results suggest that the convection of SPDW was the dominant water mass in the Pacific basin. The simulated age of deep

waters in the region of Site 596 was between ~150–450 years (Hague et al., 2012). The new Pb isotope data suggest that the age of SPDW in the subtropical South Pacific likely was at the higher end of that range, essentially “exceeding” the residence time of Pb in the water mass.

REFERENCES

- Erel Y., Harlavan Y. & Blum J.D. (1994) - Lead isotope systematics of granitoid weathering. *Geochim. Cosmoch. Acta*, 58(23), 5299-5306.
- Hague A.M., Thomas D.J., Huber M., Kory R., Woodard S. & Jones L.B. (2012) - Convection of North Pacific Deep Water During the Early Cenozoic. *Geology*, doi:10.1130/G32886.1.
- Jones C.E., Halliday A.N., Rea D.K. & Owen R.M. (1994) - Neodymium isotopic variations in North Pacific modern silicate sediment and the insignificance of detrital REE contributions to seawater. *Earth Planet. Sci. Lett.*, 127(1-4), 55-66.
- Jones C.E., Halliday A.N., Rea D.K. & Owen R.M. (2000) - Eolian inputs of lead to the North Pacific. *Geochim. Cosmoch. Acta*, 64(8), 1405-1416.
- Pettke T., Halliday A.N. & Rea D.K. (2002) - Cenozoic evolution of Asian climate and sources of Pacific seawater Pb and Nd derived from eolian dust of sediment core LL44-GPC3. *Paleoceanography*, 17(3), 1031.
- Thomas D.J., Kory R., Huber M., Schubert J.A. & Haines B. (2014) - Nd Isotopic Structure of the Pacific Ocean 70-30 Ma and Numerical Evidence for Vigorous Ocean Circulation and Ocean Heat Transport in a Greenhouse World. *Paleoceanography*, doi: 10.1002/2013PA002535.
- von Blanckenburg F. & Nägler T.F. (2001) - Weathering versus circulation-controlled changes in radiogenic isotope tracer composition of the Labrador Sea and North Atlantic Deep Water. *Paleoceanography*, 16(4), 424-434.

Temperature, seasonality and salinity history of the early Eocene North Sea Basin inferred from fish otoliths and mollusks

Daan Vanhove^(a,b), Robert P. Speijer^(a), Etienne Steurbaut^(a,b), Philippe Claeys^(c) & Linda Ivany^(d)

^(a) Department of Earth and Environmental Sciences, University of Leuven, Celestijnenlaan, 200E box 2410, 3001, Heverlee, Belgium. E-mail: daan.vanhove@ees.kuleuven.be

^(b) OD Earth and History of Life, Royal Belgian Institute of Natural Sciences, Vautierstraat, 29, 1000, Brussels, Belgium

^(c) Earth System Science, Vrije Universiteit Brussel, Pleinlaan, 2, 1050, Elsene, Belgium

^(d) Department of Earth Sciences, Syracuse University, Heroy Geology Building, 204, 13244-1070 Syracuse, NY, USA

Document type: Short note.

Manuscript history: received 15 May 2014; accepted 30 May 2014; editorial responsibility and handling by Gerald R. Dickens & Valeria Luciani.

KEY WORDS: early Eocene, North Sea Basin, otolith, oxygen isotopes, paleotemperature, salinity, seasonality.

Shelf settings comprise invaluable information on the impact of paleoenvironmental change on shallow marine ecosystems. We measured $\delta^{18}\text{O}$ ratios in fossil fish otoliths (fish ear stones) and mollusks to assess temperature, seasonality and salinity variability in the Ypresian (56.0-47.8 Ma) southern North Sea Basin (sNSB). This interval is characterized by a long-term trend of globally increasing temperatures towards the early Eocene climatic optimum (EECO), on which transient intervals of abrupt global warming are superimposed (Zachos et al., 2008). Much like today, during the Ypresian the sNSB was a shallow shelf (0-200 m paleodepth), presenting an ideal test case to reveal interactions between biota and regional temperature variability, changing water chemistry and sea-level change.

Otoliths were selected from the Natural History Museum in London and the Royal Belgian Institute of Natural Sciences, Brussels, representing a series of levels mainly within the following formations (Fms.): Hannut Fm. (Thanetian); Tienen, Blackheath and Harwich Fms. (lower Ypresian); London Clay and Kortrijk Fms. (middle Ypresian); Wittering, Tielt and Aalter Fms. (upper Ypresian) (see Steurbaut, 1998, fig. 12 for correlation). Thirteen species were selected, of which 8 belong to demersal and probably non-migratory fish such as ophidiids, bythitids and congrid. Additional otolith and mollusk stable isotope data were incorporated from previous studies (Moorkens et al., 2000; Vanhove et al., 2011; 2012). Powders for bulk (mean annual temperature, MAT) and incremental (seasonality) paleotemperature analyses were generated by micromilling the sagittal plane of embedded and polished otoliths. Stable isotope analyses were run at the University of Michigan and the Vrije Universiteit Brussel.

Results are shown on figure 1. Oxygen isotope values range between 0 and -8 ‰, largely covering the three environmental phases (facies groups A, B, C) recorded in the sNSB during the Ypresian.

Paleotemperatures are determined from phase B, covering Division B to D of the London Clay Fm. and the Roubaix Clay Member of the Kortrijk Fm. (~54-52 Ma), as these units are interpreted to be fully marine in character. This phase is represented by fine silts and clay units deposited in an outer neritic realm (+/- 100 km from coast, 100-200 m water depth), of which the lower parts of the water column are unlikely to be influenced by freshwater lids. The presence of planktonic foraminifera indicates that the basin was well-connected with the Atlantic at that time (e.g., King, 1991). Mean bulk per-taxon $\delta^{18}\text{O}$ values reveal within-horizon consistency among different co-occurring taxa. These means through the sampled interval, including all taxa, range between -1.9 and -3.4 ‰. Using the Patterson et al. (1993) equation for otoliths, this translates to high MAT for shelf bottom waters of ~25 °C during this interval. A paleowater composition of -1 ‰ is assumed, based on latitudinal correction and an open scenario for the Greenland-Norway Seaway (Roberts et al., 2009). Incremental sampling reveals low seasonality of 3-6 °C (about 1 to 1.5 ‰). This contrasts with a 10 °C seasonality calculated from the inner neritic Mons-en-Pévèle Sand Fm (lateral to Roubaix Clay Mb.). The lower seasonal range in the outer neritic setting is mainly due to reduced summer temperatures, probably caused by summer stratification in deeper and less ventilated parts of the basin and attenuation of the seasonal signal with increasing water depth (e.g., Ivany, 2012).

By contrast, mean bulk $\delta^{18}\text{O}$ otolith and mollusk values from the Tienen, Harwich and Blackheath Fms. (phase A, ~55.5-55.0 Ma) are very negative, ranging from -4 to -8 ‰. The marine character of the Harwich Fm. is indicated by the presence of glauconite, but euryhaline otoliths and mollusks demonstrate that inner neritic (and probably basin-wide) waters were reduced in salinity, lowering $\delta^{18}\text{O}_w$ by probably 3-4 ‰. Restricted connection of the sNSB with the North Atlantic and an intense regional humidity cycle in the mid-latitudes shortly after the PETM may both contribute to lower values. Paleocene values predating this interval are much more positive (0-1.4 ‰).

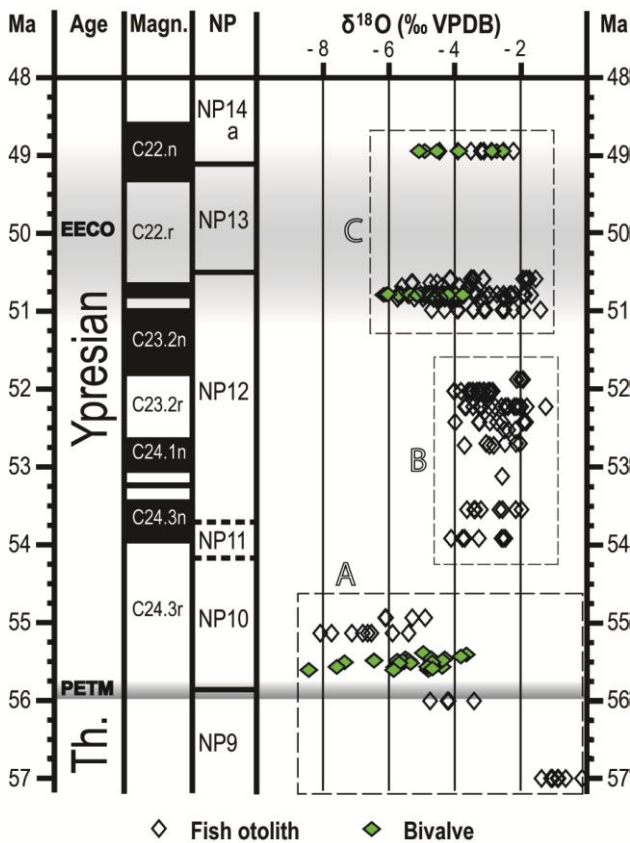


Fig.1 – Otolith and mollusk stable oxygen isotope results for the early Eocene southern North Sea Basin, plotted against the 2012 geological time scale (Gradstein et al., 2012). Dashed line boxes represent three successive environmental phases / facies: A) late Paleocene – early Eocene restriction of the basin / marginal sands and silts, B) sea level rise and connection to the Atlantic / silts and clays, C) semi-connected basin probably influenced by seasonal riverine input / shallow sands.

Samples from phase C, covering the EECO interval and represented by the inner neritic sandy Wittering, Tielt and Aalter Fms. (~51-49 Ma), bear values between -2 and -6 ‰. Congrids and platycephalids bear the most negative values of this range and congrid are characterized by a high intra-annual range of 3-4 ‰. Probably these taxa were tolerant for seasonally paced freshwater influx in summer. Ophidiid data do not exhibit this large range and are thought to have preferred fully marine conditions and therefore reliably represent paleotemperatures. Average bulk temperatures for the latter translate to a MAT for shelf bottom waters of ~27 °C, suggesting a ~2 °C increase in mean temperature towards the EECO interval.

In summary, Stable oxygen isotope analysis of early

Eocene otoliths and mollusks of the SNSB reveal a MAT for the deep shelf of ~25 °C in the mid-Ypresian, with an increase of ~2 °C with the peak EECO interval. Summer temperatures in the deeper parts of the basin were probably reduced in the mid-Ypresian. Salinity decreased in inner neritic settings and probably basin wide around the Paleocene-Eocene interval, suggesting an intense humidity cycle.

REFERENCES

- Gradstein F.M., Ogg J.G., Schmitz M. & Ogg G. (2012) - The geologic time scale 2012. Volume 2, pp. 1144. Elsevier.
- Ivany L.C. (2012) - Reconstructing paleoseasonality from accretionary skeletal carbonates - challenges and opportunities. In Reconstructing Earth's deep-time climate. The state of the art in 2012, Paleontological Society Short Course, November 3, 2012. The Paleontological Society Papers, Volume 18 (Eds. L. C. Ivany & B. T. Huber), pp. 133-165.
- King C. (1991) - Stratigraphy of the Ieper Formation and Argile de Flandres (Early Eocene) in western Belgium and northern France. In: Dupuis, C., De Coninck, J. & Steurbaut, E. (eds.) (1991) The Ypresian Stratotype. Bulletin de la Société belge de Géologie, 97(3-4), 349-372.
- Moorkens T.L., Steurbaut E., Jutson D. & Dupuis C. (2000) - The Knokke borehole of northwestern Belgium re-analysed: new data on the Paleocene-Eocene transitional strata in the southern North Sea Basin. GFF, 122, 111-114.
- Patterson W.P., Smith G.R. & Lohmann K.C. (1993) - Continental paleothermometry and seasonality using the isotopic composition of aragonitic otoliths of freshwater fishes. Geophysical Monographs, 78, 191-202.
- Roberts C.D., Legrande A.N. & Tripathi A.K. (2009) - Climate sensitivity to Arctic seaway restriction during the early Paleogene. Earth Planet. Sci. Lett., 286(3-4), 576-585.
- Steurbaud E. (1998) - High-resolution holostratigraphy of middle Paleocene to early Eocene strata in Belgium and adjacent areas. Palaeontographica Abt. A 247(5-6), 91-156.
- Vanhove D., Stassen P., Speijer R.P., Claeys P. & Steurbaut E. (2012) - Intra- and intertaxon stable O and C isotope variability of fossil fish otoliths: an early Eocene test case. Austrian J. Earth Sci., 105(1), 200-207.
- Vanhove D., Stassen P., Speijer R.P. & Steurbaut E. (2011) - Assessing paleotemperature and seasonality during the early Eocene climatic optimum (EECO) in the Belgian Basin by means of fish otolith stable O and C isotopes. Geologica Belgica 14(3-4), 143-158.
- Zachos J.C., Dickens G.R. & Zeebe R.E. (2008) - An early Cenozoic perspective on greenhouse warming and carbon-cycle dynamics. Nature, 451(7176), 279-283.

Unravelling volcanism and impact related environmental change in the latest Maastrichtian and early Danian

Johan Vellekoop ^(a), Jan Smit, ^(b); Selen Esmeray ^(c); Kenneth G. Miller ^(c), James V. Browning ^(c),
Bas Van De Schootbrugge ^(a), Jaap S. Sinnighe-Damsté, J.S. ^(d,e) & Henk Brinkhuis ^(a)

^(a) Marine Palynology & Palaeoceanography, Department of Earth Sciences, Utrecht University, Budapestlaan 4, 3584CD, Utrecht, The Netherlands. E-mail: j.vellekoop@uu.nl

^(b) Eventstratigraphy, Department of Sedimentology and Marine geology, VU University Amsterdam, De Boelelaan 1085, 1018HV, Amsterdam, The Netherlands

^(c) Department of Earth and Planetary Sciences, Rutgers University, 610 Taylor Road, Piscataway, NJ, USA

^(d) Marine Organic Biogeochemistry, Royal Netherlands Institute for Sea Research (NIOZ), Landsdiep 4, 1797 SZ, 't Horntje, Texel, The Netherlands

^(e) Geochemistry, Department of Earth Sciences, Utrecht University, Budapestlaan 4, 3584CD, Utrecht, The Netherlands.

Document type: Short note.

Manuscript history: received 15 May 2014; accepted 30 May 2014; editorial responsibility and handling by Gerald R. Dickens & Valeria Luciani.

Key words: K-Pg, Chixculub, volcanism, dinoflagellates, TEX₈₆

The Cretaceous-Paleogene (K-Pg) boundary mass extinction is related to the impact of a large extraterrestrial body, one of the most devastating events in the history of life (Schulte et al., 2010). This impact caused a major perturbation of the global carbon cycle and significant global climate change (Kring, 2007; Vellekoop et al., 2014). It is nevertheless unclear how the environmental perturbations at the K-Pg boundary are related to this background of ongoing, long-term environmental changes. Planktic and benthic foraminiferal distributions and $\delta^{18}\text{O}$ records show a strong warming phase between 500 and 20 kyr before the K-Pg boundary (Kucera & Malmgren, 1998; Olsson et al., 2002). This warming event is most likely related to extensive volcanism of the Deccan Traps Large Igneous Province in India (Olsson et al., 2002). Strikingly, although geochemical proxy data indicates that this outpouring phase of the Deccan Traps resulted in major global climate change, benthic and planktic foraminiferal communities at well studied normal marine sites at lower latitudes, such as El Kef, Tunisia, Agost, Spain and Brazos River, Texas appear to be relatively stable up to the K-Pg boundary (Speijer & Van der Zwaan, 1996; Culvier et al., 2003). At some shallower marine sites, ecological changes are recorded in the Late Maastrichtian, but these are likely related to enigmatic coeval sea level changes (Culvier et al., 2003; Keller & Abramovich, 2009). Hence, there is an interesting conundrum in the latest Maastrichtian, with global climate changes that are apparently not matched by global biological responses.

Being able to both disentangle these biological responses and record the enigmatic sea level changes calls for a shelf site with a depositional environment shallow enough to record (minor) sea level changes, but deep enough to be stratigraphically complete. The New Jersey shelf provides such a shelf site. In 2008 and 2009, eight new, shallow (<25m) cores were drilled across the K-Pg boundary deposits in New Jersey (Miller et al., 2010), presenting ideal records that could be used to unravel biological responses of the Deccan Traps volcanism,

the K-Pg boundary impact and ongoing sea level changes. Organic-walled dinocysts assemblages have proven to be very successful in reconstructing environmental changes and as a biostratigraphic tool in such shallow marine sites (Sluijs et al., 2005). Therefore, the eight shallow cores from New Jersey were analyzed using the TEX₈₆ sea surface temperature (SST) proxy to quantitatively assess regional climatic responses to the Deccan Traps volcanism and K-Pg boundary impact and for organic-walled dinoflagellate cysts to (1) provide a biostratigraphic framework, and (2) unravel regional biological responses to these changes in climate and sea level.

Our TEX₈₆ SST records clearly portray the latest Maastrichtian warming event and subsequent cooling across the K-Pg boundary. In addition, a short, transient cooling is observed directly at the boundary, likely representing a brief 'impact winter' phase. The dinocyst record of the New Jersey shelf comprises a high diversity assemblage typical for Northern Hemisphere mid-latitudes, showing strong responses to changes in relative sea level. In addition, at the peak warmth of the uppermost Maastrichtian warm event, the dinocyst record shows incursions of typical lower latitude taxa and morphological forms that might be related to stress. Approximately 50 kyr before the boundary, SSTs decrease again, whilst the dinocyst record shows a bloom of the taxon *Palynodinium grallator*. Before the K-Pg boundary the community had recovered again. These results indicate that the latest Maastrichtian warming event and the K-Pg boundary impact are two separate events with distinctly different signatures in the biological record.

REFERENCES

- Culvier S.J. (2003) - Benthic foraminifera across the Cretaceous-Tertiary (K-T) boundary: a review. *Mar. Micropaleontol.*, 47, 177-226.
- Keller G. & Abramovich S. (2009) - Lilliput effect in late Maastrichtian planktic foraminifera: Response to environmental stress. *Palaeogeogr. Palaeoclimatol. Palaeoecol.*, 284, 47-62.

- Kring D.A. (2007) - The Chicxulub impact event and its environmental consequences at the Cretaceous-Tertiary boundary. *Palaeogeogr. Palaeoclimatol. Palaeoecol.*, 255, 4-21.
- Kucera M. & Malmgren B.A. (1998) - Terminal Cretaceous warming event in the mid-latitude South Atlantic Ocean: evidence from poleward migration of *Contusotruncana contuse* (planktonic foraminifera) morphotypes. *Palaeogeogr. Palaeoclimatol. Palaeoecol.*, 138, 1-15.
- Miller K.G., Sherrell R.M., Browning J.V., Paul Field M., Gallagher W., Olsson R.K., Sugarman P.J., Tuorto S. & Wahyudi H. (2010) - Relationship between mass extinction and iridium across the Cretaceous-Paleogene boundary in New Jersey. *Geology*, 38, 10, 867-870.
- Olsson R.K., Miller K.G., Browning J.V., Wright J.D. & Cramer, B.S. (2002) - Sequence stratigraphy and sea-level change across the Cretaceous-Tertiary boundary on the New Jersey passive margin. *GSA Special Paper*, 356, 97-108.
- Schulte P., Alegret L., Arenillas I. et al. (2010) - The Chicxulub asteroid impact and mass extinction at the Cretaceous-Paleogene boundary. *Science*, 327, 1214-1218.
- Sluijs A., Pross J. & Brinkhuis H. (2005) - From greenhouse to icehouse; organic-walled dinoflagellate cysts as paleoenvironmental indicators in the Paleogene. *Earth-Sci. Rev.*, 68, 281-315.
- Speijer R.P. & Van der Zwaan G.J. (1996) - Extinction and survivorship of southern Tethyan Benthic foraminifera across the Cretaceous/Paleogene boundary. *Geological Society, London, Special Publications*, 102, 343-371.
- Vellekoop J., Sluijs A., Smit J., Schouten S., Weijers J.W.H., Sinninghe Damsté J.S., Brinkhuis H. (2014) - Rapid short-term cooling following the Chicxulub impact at the Cretaceous-Paleogene boundary. *Proceedings of the National Academy of Sciences of the United States of America* [accepted manuscript].

Antarctic glacial history and Southern Ocean productivity during the Middle Eocene - Late Oligocene

Giuliana Villa ^(a), Chiara Fioroni ^(b), Davide Persico ^(a), Andrew P. Roberts ^(c) & Fabio Florindo ^(d)

^(a) Università degli Studi di Parma, Dipartimento di Fisica e Scienze della Terra, Parco Area delle Scienze, 157 a, 78, 43100 Parma, Italy. E-mail: giuliana.villa@unipr.it

^(b) Università degli Studi di Modena e Reggio Emilia, Dipartimento di Scienze Chimiche e Geologiche, L.go S. Eufemia, 19, 41100 Modena, Italy

^(c) Research School of Earth Sciences, The Australian National University, Canberra, ACT 0200, Australia

^(d) Istituto Nazionale di Geofisica e Vulcanologia, Via di Vigna Murata 605, 00143 Rome, Italy

Document type: Short note.

Manuscript history: received 15 May 2014; accepted 30 May 2014; editorial responsibility and handling by Gerald R. Dickens & Valeria Luciani.

KEY WORDS: biostratigraphy, Eocene, magnetotactic bacteria, nannofossils, Oligocene, paleoceanography

Calcareous nannofossil assemblages from five Ocean Drilling Program (ODP) sites (Kerguelen Plateau and Maud Rise), provide excellent age control along a continuous record from the Middle Eocene (~42.5 Ma) to the Late Oligocene (~24 Ma) and allow evaluation of paleoceanographic response to Antarctic ice sheet evolution. Through quantitative analyses and correlation to multivariate analyses we differentiated groups of taxa with similar paleoecological preferences, as compared with previous paleoecological assignments (e.g. Bralower, 2002; Villa et al., 2008). This procedure allowed assignment of species preference in response to changes in SST and trophic conditions. The correlation of nannofossil data with $\delta^{18}\text{O}$ and $\delta^{13}\text{C}$ records allowed identifying different paleoceanographic conditions through time (Fig.1). Nannofossil paleoecology enables identification of several steps in the paleoceanographic evolution of the Southern Ocean (SO) that reflect changes in sea surface temperature and trophic state in Subantarctic water masses. We recognized a cooling trend which started in the Middle Eocene with a short cooling episode (cooling A), approximately coincident with a positive $\delta^{18}\text{O}$ shift which is likely connected to global cooling rather than to ice sheet growth (Pagani et al., 2005). The trend was interrupted by a transient warming episode, the Middle Eocene Climatic Optimum (MECO), characterized by eutrophic warm-water taxa. Just after MECO, from 39.6 to 39.1 Ma, pronounced peaks in cool-water taxa indicate a cooling event previously documented as cooling B (Villa et al., 2008). From ~39.1 to ~36.2 Ma, oligotrophic nannofossil assemblages dominated. We suggest that these oligotrophic conditions were associated with increased water mass stratification, low nutrient contents, and high efficiency of the oceanic biological pump that, in turn, promoted sequestration of carbon from surface waters, which favored cooling. After 36.2 Ma, we document a large synchronous surface water productivity turnover with a dominant eutrophic nannofossil assemblage that was accompanied by a pronounced increase in abundance

of magnetotactic bacteria. The presence of magnetotactic bacteria in marine sediments is related to a complex interplay between nutrient limitations, organic carbon flux, paleoproductivity, paleoclimate, iron bioavailability and redox conditions (e.g., Roberts et al., 2011). Increased hematite concentrations are ascribed to a major Late Eocene influx of eolian dust, which likely delivered limiting micronutrients to surface waters that gave rise to eutrophication. This iron fertilization would have stimulated increased primary productivity that would have also enhanced delivery of organic carbon to the seafloor. The rise of eutrophic taxa from ~36.2 Ma is related to augmented nutrient contents, which could be linked to a partial retreat of a transient Antarctic ice sheet (Katz et al., 2008). The eutrophication could have been driven/enhanced by iron delivered as eolian dust. Increased glacial flour and other glaciofluvial outwash with fine grain sizes, which are commonly iron coated, are likely to have been easily deflated by wind from an ice-free Antarctic land surface.

Tectonic activity may have also influenced paleoproductivity. Water flow from the Pacific Ocean through Drake Passage began immediately after the MECO event (Livermore et al., 2007) and rapid Late Eocene deepening of the Antarctic Circumpolar Current (ACC) (Livermore et al., 2007) facilitated interoceanic seawater exchange, which could have contributed to increased upwelling, which in turn, would have induced high SO productivity.

The interval encompassing the Eocene-Oligocene boundary witnessed an abrupt cooling event that culminated in build up of a large-scale Antarctic ice sheet (e.g. Coxall et al., 2005; Lear et al., 2008). Nannofossil assemblages reveal a response to this climatic change, which corresponds to maximum $\delta^{18}\text{O}$ values during the Oi-1 event. In all the studied sites, nannofossil assemblages underwent an abrupt turnover, with a decrease in species diversity, a strong increase in cool-water taxa, a decrease of temperate-water taxa, and a collapse of warm-water taxa. Our results provide evidence that interactions between calcareous nannofossil plankton, primary productivity, the global carbon cycle, and atmospheric CO_2 levels resulted from inter-related causes and effects and feedback mechanisms

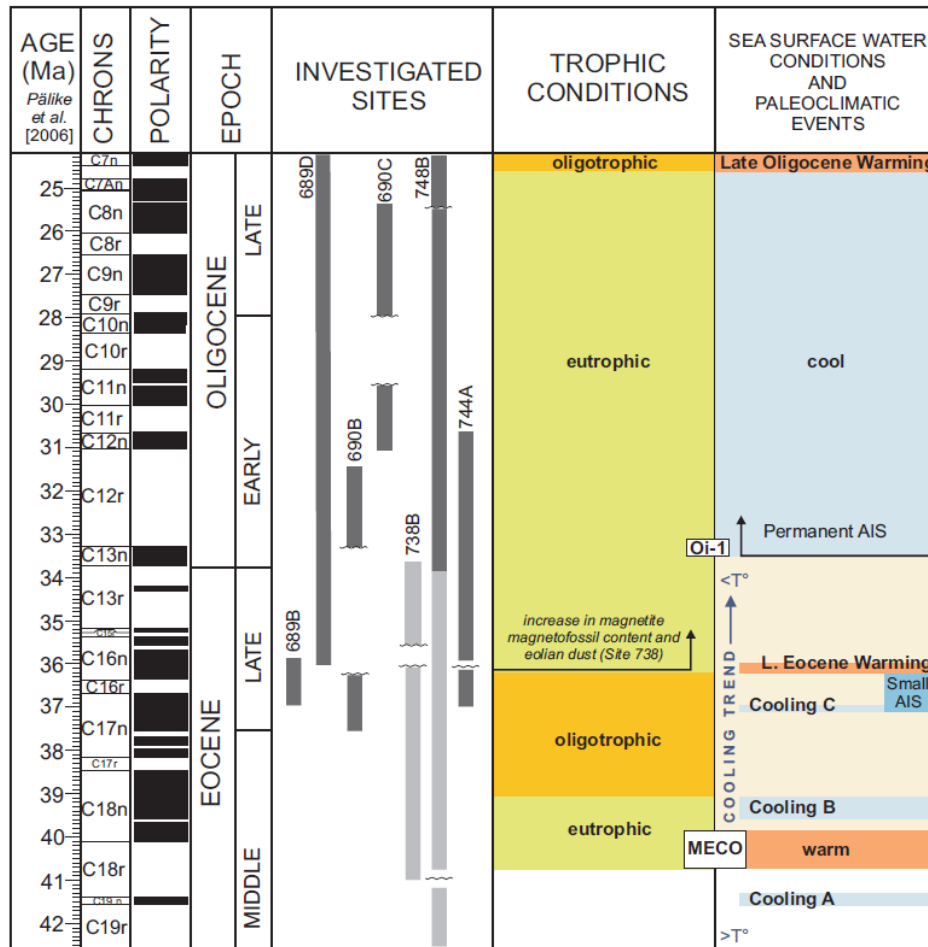


Fig.1: Paleoclimatic and paleoceanographic summary of the investigated sites plotted against the geomagnetic polarity time scale (age calibration from Pälike et al., 2006). Site logs in dark grey indicate that magnetostratigraphy is available; light grey indicates that magnetostratigraphy is not reliable/available. Identified hiatuses are indicated by wavy lines. Coloured bands indicate paleoceanographic conditions. AIS = Antarctic Ice Sheet.

rather than to a single factor that led to change in the global climate system.

REFERENCES

- Bralower T. J. (2002) - Evidence of surface water oligotrophy during the Paleocene–Eocene thermal maximum: Nannofossil assemblage data from Ocean Drilling Program Site 690, Maud Rise, Weddell Sea. *Paleoceanography*, 17(2), 1023, doi:10.1029/2001PA000662.
- Coxall H.K., Wilson P.A., Pälike H., Lear C.H. & Backman J. (2005) - Rapid stepwise onset of Antarctic glaciation and deeper calcite compensation in the Pacific Ocean. *Nature*, 433, 53–57, doi:10.1038/nature03135.
- Katz M.E., Miller K.G., Wright J.D., Wade B.S, Browning J.V. Cramer B.S. & Rosenthal Y. (2008) - Stepwise transition from the Eocene greenhouse to the Oligocene icehouse. *Nat. Geosci.*, 1, 329–333
- Lear C.H., Bailey T.R., Pearson P.N., Coxall H.K. & Rosenthal Y. (2008) - Cooling and ice growth across the Eocene–Oligocene transition. *Geology*, 36, 251–254, doi: 10.1130/G24584A.1.
- Livermore R., Hillenbrand C.-D. Meredith M. & Eagles G. (2007) - Drake Passage and Cenozoic climate: An open and shut case?. *Geochem. Geophys. Geosyst.*, 8, Q01005, doi:10.1029/2005GC001224.
- Pagani M., Zachos J.C., Freeman K. H., Tipple B. & Bohaty S.M. (2005) - Marked decline in atmospheric carbon dioxide concentrations during the Paleogene. *Science*, 309, 600–603, doi:10.1126/science.1110063.
- Pälike H., Norris R.D., Herrle J. O., Wilson P.A., Coxall H.K., Lear C.H., Shackleton N.J., Tripathi A.K. & Wade B.S. (2006) - The heartbeat of the Oligocene climate system. *Science*, 314, 1894–1898, doi:10.1126/science.1133822.
- Roberts A.P., Florindo F., Villa G., Chang L., Jovane L., Bohaty S.M., Larrasoana J.C., Heslop D. & Fitz Gerald J.D. (2011) - Magnetotactic bacterial abundance in pelagic marine environments is limited by organic carbon flux and availability of dissolved iron. *Earth Planet. Sci. Lett.*, 310, 441–452, doi:10.1016/j.epsl.2011.08.011.
- Villa G., Fioroni C., Pea L., Bohaty S.M. & Persico D. (2008) - Middle Eocene–late Oligocene climate variability: Calcareous nannofossil response at Kerguelen Plateau, Site 748. *Mar. Micropaleont.*, 69, 173–192, doi:10.1016/j.marmicro.2008.07.006.

Ypresian isopod crustaceans from Monte Bolca and Monte Postale (Italy)

Ronald Vonk ^(*)

^(*) Department of Marine Zoology, Naturalis Biodiversity Center, Darwinweg 2, 2333 CR Leiden, The Netherlands. E-mail: ronald.vonk@naturalis.nl

Document type: Short note.

Manuscript history: received 15 May 2014; accepted 30 May 2014; editorial responsibility and handling by Gerald R. Dickens & Valeria Luciani.

KEY WORDS: coral reef association, Eocene, estuarine, lagoon.

In this study fossil specimens of the flabelliferan isopod *Palaega acuticauda* and the sphaeromatid *Heterosphaeroma veronensis* are investigated. Additional museum material was used that came in at a later date than the original material on which the first descriptions were based. An outline of new features is made from material that came from Monte Bolca and Monte Postale marine fish and terrestrial plant bearing layers. The results point in the direction of low salinity affinities and add to the understanding of environmental details concerning the microhabitat of these fossil isopods.

The Lower Eocene isopod fossils from the Pesciara of Bolca have been described by Secretan as part of her very well documented and complete work on ‘Les Crustacés du Monte Bolca’ (Secretan, 1975). There was very little isopod material at her disposal at that time. She placed one specimen in the popular fossil genus *Palaega* Woodward, 1870, and some other four specimens in *Heterosphaeroma* Munier-Chalmas 1872, an undiagnosed genus with one representative from lacustrine deposits of late Paleocene age of the Champagne region in France (Munier-Chalmas, 1872; Van Straelen, 1928). With additional material, on which the body somites are clearly visible (Figs. A), coming into the palaeontological collections of the Museo Civico di Storia Naturale of Verona from Monte Bolca and Monte Postale it will be possible to re-investigate the systematic position of the fossils.

Next to that also recent paleo-environmental data on the biostratigraphy have revealed a more detailed picture of the situation in which the organisms have lived (Trevisani et al, 2005; Papazzoni et al, 2006; Schwark et al, 2009). Benthic crustaceans such as the isopods studied here form a minor part of the fossils that mainly consist of the famous “Pesciara di Bolca” fishes. Their environmental requirements as they are perceived today by studying related taxa may help elucidate microhabitat conditions at the time of burial.

The suborder Flabellifera is present in the fossil record from Triassic to Pliocene, with fossils in the families of Cirolanidae, Serolidae, Sphaeromatidae and Aegidae. These

fossils vary greatly in length, from 2 mm to over a 100 mm. Juvenile specimens have not been recognized so far. Frequent fossil remains consist mainly of moult stages; entire animals are rare. Secretan (1975) commented on the possibility of parasitism as the main mode of living for the isopods found in

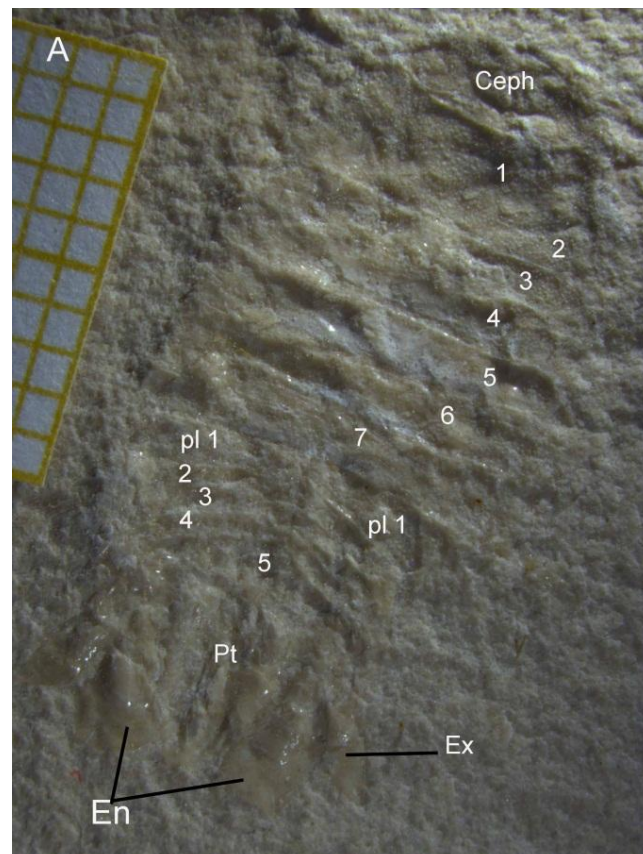


Fig. A - *Palaega acuticauda* Secretan 1975, additional material. VR 27.476, positive; Ceph = cephalon; numbers 1-7 placed in pereonites; pl 1 = pleonite 1, 2-5 remaining pleonites; pt = pleotelson; Ex = exopod of uropod; En = endopod of uropod. Scale = 10 mm

the Bolca layers because they are so scarce. Parasites are less probable to be buried in sediment as they cling to their hosts

and do not frequently walk on stretches of the bottom. For the sphaeromatids she concludes that all forms found until the Miocene come from lacustrine environments and that the Pesciara di Bolca isopods may have lived in waters of low salinity.

In confirmation of Secretan's hypothesis, more recent paleoenvironmental reconstructions suggest that the Pesciara di Bolca in the late Ypresian age (between 49 and 50 Ma) was a basin or a subtropical lagoon floor. Pieces of amber in the lowest fish-bearing level contained bryophytes and pteridophytes as well as conifer pollen from Araucariaceae, and specimens from angiosperms (Trevisani et al., 2005). The fish bearing levels contain, next to marine reef fishes, also brackish genera such as the perch *Cyclopoma* (Trevisani et al., 2005) confirming the estuarine features of the environment.

Contrary to the lacustrine hypothesis are the discoveries, after 1975, of fossil sphaeromatids and other flabelliferans in Italy that are all reported from marine deposits (De Angeli & Rossi, 2006; De Angeli & Lovato, 2009; Passini & Garassino, 2012a; b). It remains uncertain if the Bolca isopods lived in true marine and shallow reef like conditions or had a supratidal and fluvial-terrestrial habitat.

ACKNOWLEDGMENTS

I gratefully acknowledge the help of Anna Vaccari, Roberta Salmaso, Leonardo Latella, and Roberto Zorzin (Museo Civico di Storia Naturale of Verona) in enabling the work in the collections. Antonio de Angeli (Museum "G. Zannato", Vicenza), Alessandro Garassino (Natural History Museum of Milan) and Cesare Papazzoni (University of Modena and Reggio Emilia) are thanked for sending literature.

REFERENCES

De Angeli A. & Lovato A. (2009) - *Sphaeroma gasparellai* n. sp. (Isopoda, Flabellifera, Sphaeromatidae), nuova specie di isopode dell'Eocene superiore dei Monti Berici (Italia settentrionale). *Lavori Società Veneziana di Scienze Naturali*, 34, 101-104.

De Angeli A. & Rossi A. (2006) - Crostacei oligocenici di Perarolo (Vicenza – Italia settentrionale), con la descrizione di una nuova specie di Mysida e di Isopoda. *Lavori Società Veneziana di Scienze Naturali*, 31, 85-93.

Munier-Chalmas Ch. (1872) - Sur des Crustacés, des Fleurs et des Insectes découverts dans les Travertins lacustres de Sézanne. *Bulletin de la Société Géologique de France*, 2^{eme} série, Tome XXIX, 166.

Papazzoni C.A. & Trevisani E. (2006) - Facies analysis, palaeoenvironmental reconstruction, and biostratigraphy of the "Pesciara di Bolca" (Verona, northern Italy): An early Eocene Fossil-Lagerstätte. *Palaeogeography, Palaeoclimatology, Palaeoecology* 242, 21–35.

Passini G. & Garassino A. (2012a) - *Palaega pisana* n. sp. (Crustacea, Isopoda, Cirolanidae) from the Pliocene of Orciano Pisano, Pisa (Toscana, Central Italy). *Atti della Società Italiana di Scienze Naturali e del Museo Civico di Storia Naturale di Milano*, 153, 3-11.

Passini G. & Garassino A. (2012b) - *Palaega picena* n. sp. (Crustacea, Isopoda, Cirolanidae) from the Miocene of Arcevia, Ancona (Marche, Central Italy). *Atti della Società Italiana di Scienze Naturali e del Museo Civico di Storia Naturale di Milano*, 153, 21-26.

Schwark L., Ferretti A., Papazzoni C.A. & Trevisani E. (2009) - Organic geochemistry and paleoenvironment of the Early Eocene "Pesciara di Bolca" Konservat-Lagerstätte, Italy. *Palaeogeography, Palaeoclimatology, Palaeoecology* 273, 272–285.

Secretan S. (1975) - Les Crustacés du Monte Bolca. In: *Studi e ricerche sui giacimenti Terziari di Bolca, II*, Museo Civico di Storia Naturale di Verona, 315-424.

Trevisani E., Papazzoni C.A., Ragazzi E. & Roghi G. (2005) - Early Eocene amber from the 'Pesciara di Bolca' (Lessini Mountains, Northern Italy). *Palaeogeogr. Palaeoclimatol. Palaeoecol.*, 223, 260–274.

Van Straelen V. (1928) - Contribution a l'étude des Isopodes Méso- et Cénozoïques. *Mémoires de l'Académie royale des sciences, des lettres et des beaux-arts de Belgique* 4, Série 2, 9(5), 68 pp.

Status and perspectives integrating marine and terrestrial archives

Thomas Westerhold ^(a), Ursula Röhl ^(a), James C. Zachos ^(b) & Jaume Dinarès-Turell ^(c)

^(a) MARUM, University of Bremen, Leobener Strasse, Bremen, Germany. e-mail: twesterhold@marum.de

^(b) Department of Earth and Planetary Sciences, University of California Santa Cruz, CA 4, USA

^(c) Istituto Nazionale di Geofisica e Vulcanologia, Rome, Italy

Document type: Short note.

Manuscript history: received 15 May 2014; accepted 30 May 2014; editorial responsibility and handling by Gerald R. Dickens & Valeria Luciani.

KEY WORDS: chronostratigraphy (cyclostratigraphy, stable isotopes), age models, marine - terrestrial correlation.

Understanding Earth's climate evolution in detail, especially carbon cycle dynamic, is a key to sharpen Earth system models predicting the future climate development of our planet. Deep-sea sediments recovered by ocean drilling in combination with newly developed proxies have provided a remarkable archive recording Earth's climate evolution in the Paleogene.

Congruent to the efforts in ocean drilling important new information has been obtained from marine as well as terrestrial successions on land. Combining marine and terrestrial records provides a vibrant picture of the overall climate state on land and in the ocean. Of highest interest is this connection to study causal relationships and interactions both for long-term evolution of environmental changes and in more detail for hyperthermal events like the Paleocene Eocene Thermal Maximum (PETM).

Basis for efficacious linkage of marine and land records are precise correlation and highly accurate age models. To integrate records an integration of bio-, magneto-, cyclo-, and isotope-stratigraphy is anticipated.

More than four decades of scientific ocean drilling successfully provided unique sample material to develop accurate astronomically calibrated timescales including high-resolution stable isotope records for the past 34 million years. For the Eocene, the coverage and resolution of bulk and benthic stable isotope data is still sparse, composed of numerous sites from several oceans, and dominated by records from the Southern Ocean. For the Paleocene the situation is similar although a single site, high-resolution benthic stable isotope record from the Pacific is now available. Strong orbital influence on early Paleogene sedimentation has been documented, but only floating orbital time scales have been established for early Eocene and Paleocene intervals until now.

With the recovery of new high-quality, multiple-hole cored sedimentary successions from the Atlantic (Leg 207, Demerara Rise; Leg 208, Walvis Ridge) and the Pacific (Leg 198, Shatsky Rise; Leg 199 and Exp. 320/321, both East Equatorial Pacific) the situation improved dramatically, but the

established cyclostratigraphies for the early Paleogene are still floating in the context of absolute time. However, high-resolution studies from these sites revealed a spectacular new insight into climate dynamics of the Paleocene, early to middle Eocene, and Eocene/Oligocene Transition (EOT). Several bulk and benthic stable isotope records have been published from these sedimentary records at variable resolution indicating that a detailed reconstructed climate history requires a sampling resolution of 5 kyr and less to capture short live transient events and the full climate dynamics of the early Paleogene greenhouse world.

Efforts to anchor the floating astronomically calibrated Paleogene time scale to the astronomically tuned Neogene time scale (ATNS) has been hampered by fundamental problems related to the mid Eocene "cyclostratigraphic gap" an interval that still is not completely covered by cyclostratigraphic studies in pelagic sediments, by the uncertainties and limits of astronomical calculations, and by uncertainties in radio-isotopic age constraints. A cyclostratigraphic framework based on the stable long (405-kyr) eccentricity cycle in deep-sea sections has been established for the Paleocene, the early to middle Eocene and recently the late middle Eocene to early Oligocene.

Main focus of several on-going marine studies is the closure of the mid Eocene "cyclostratigraphic gap". Integration of bio-, magneto-, cyclo-, and isotope-stratigraphy from deep-sea sediments as well as land-based marine successions will form the backbone for climate reconstructions. However, to establish a full picture of global and regional climate change in the Paleogene terrestrial records need to be tied to the stratigraphic framework of the deep-sea records. Combining soil-carbonate isotope records, cyclo- and magnetostratigraphy from terrestrial deposits in the Eocene Bighorn Basin over the recent years now provides a powerful approach to integrate marine and terrestrial records at the desired precision.

The presentation will review history, status, milestones and challenges integrating marine and terrestrial records and will also discuss potential key areas for future research. Examples involve the legacy of Robert W.O'B. Knox as well as both accomplished and ongoing research in the Bighorn Basin (WY, USA), Basque Basin (e.g. Zumaia, Spain), and ocean drilling (DSDP, ODP, IODP²).

Climate and oceanography of the Tasmanian Gateway during the Middle Eocene Climatic Optimum (MECO)

Lineke Woelders ^(a), Appy Sluijs ^(b) & Peter Bijl ^(b)

^(a) Department of Earth and Environmental Sciences, division of Geology, KU Leuven, Celestijnenlaan 200E, B-3001 Leuven-Heverlee, Belgium. E-mail: lineke.woelders@ees.kuleuven.be

^(b) Earth Sciences Department, Marine Palynology Group, Utrecht University, Budapestlaan 4, 3584 CD Utrecht, the Netherlands

Document type: Short note.

Manuscript history: received 15 May 2014; accepted 30 May 2014; editorial responsibility and handling by Gerald R. Dickens & Valeria Luciani.

KEY WORDS: paleoceanography, paleoclimate, Tasmanian Gateway, Eocene, Middle Eocene Climatic Optimum, MECO, dinoflagellates, TEX₈₆.

Observations by Villa et al. (2008) and Bijl et al. (2011) suggest a relationship between sea water temperatures and endemism in the Southern Ocean around the Tasmanian Gateway during the Middle Eocene Climatic Optimum (MECO). Their research does however not clarify if and to what extent the currents on both sides of the Tasmanian Gateway may have changed or even mixed during the MECO, which also could have influenced dinocyst assemblages. Neither does their research provide information on changing sea levels during the MECO, although sea levels are likely to have increased (Dawber et al., 2011) which may have affected oceanography. As changing oceanography may have had an impact on regional climate (Sijp et al., 2011), it is of importance to gain more insight in possibly changing oceanography and climate during the MECO in the Tasmanian Gateway. ODP Site 1170 is located at the midpoint of the Tasmanian Gateway and is thus a key location in understanding changing paleocurrents and regional climate of the Tasmanian region during the MECO.

Based on improved biostratigraphic control of Cores 9R to 38R from ODP Hole 1170D, the material is dated between ~43 and ~35 Ma. Sea surface temperatures (SSTs) generally decreased from ~25°C to ~21°C during this period according to TEX₈₆ based SST reconstruction. This temperature decline is within the order of magnitude of what would be expected (e.g. Bijl et al., 2009) although TEX₈₆ based SSTs may be skewed towards summer temperatures (e.g., Sluijs et al., 2011). Biostratigraphy indicates furthermore that the MECO is present at ~600 mbsf in the investigated material, which is supported by the occurrence of a sea surface temperature peak of ~4°C, from ~21.5°C to ~25.5°C, between ~600 and 575 mbsf in the investigated material. This peak is within the expected order of magnitude (e.g. Bohaty et al., 2009). Stable oxygen and carbon isotope records of the investigated material unfortunately do not show a clear signal throughout the investigated material.

Endemism in the Tasmanian Gateway seems to have been influenced more by paleoceanography than by SST directly. Biogeography of dinocyst taxa suggests ODP Site 1170 to have been under direct influence of the Tasman Current (located east from the Tasmanian Gateway), like ODP Site 1172, until the MECO. During and after the MECO, the different dinocyst assemblages at both sites suggest ODP Site 1170 was located in a more isolated position, out of direct reach of any current. This enabled high latitude dinocyst taxa to thrive at ODP Site 1170 during and after the MECO. It is uncertain if water masses exchanged through the Tasmanian Gateway during the MECO.

The shift of the Tasman Current away from ODP Site 1170 could be somehow related to sea level changes during the MECO. During the MECO, sea level appears to have increased. This is in line with what was found at other Sites (e.g. Dawber et al., 2011). After the MECO, sea levels seem to decline.

According to P cyst abundances, paleoproductivity levels were low during the MECO. Absolute abundances however suggest high paleoproductivity during the MECO. Both P cyst percentages as well as absolute abundance could have been influenced by both paleoproductivity as well as by sediment and dinocyst reallocation. It is therefore not possible to draw conclusions on paleoproductivity during the MECO based on these variables only. It remains unclear why general absolute dinocyst abundances in ODP Hole 1170D are relatively high compared to other Sites in the Southern Ocean, and why in particular *Enneadocysta dictyostila* thrived during the MECO.

REFERENCES

- Bijl P.K., Pross J., Warnaar J., Stickley C.E., Huber M., Guerstein R., Houben A.J.P., Sluijs A., Visscher H. & Brinkhuis H. (2011) - Environmental Forcings of Paleogene Southern Ocean Dinoflagellate Biogeography. *Paleoceanography*, PA001905.

- Bohaty S.M., Zachos J.C., Florindo F. & Delaney M.L. (2009) - Coupled greenhouse warming and deep-sea acidification in the Middle Eocene. *Paleoceanography*, 24, PA2207.
- Dawber C.F., Tripathi A.K., Gale A.S., MacNiocail C. & Hesselbo S.P. (2011) - Glacioeustasy during the middle Eocene? Insights from the stratigraphy of the Hampshire Basin, UK. *Palaeogeogr. Palaeoclimatol. Palaeoecol.*, 300, 84–100.
- Sijp W.P., England M.H. & Huber M. (2011) - Effect of the deepening of the Tasman Gateway on the global ocean. *Paleoceanography* 26 PA4207.
- Sluijs A., Bijl P.K., Schouten s., Röhl U., Reichert G.-J. & Brinkhuis H. (2011) - Southern ocean warming, sea level and hydrological change during the Paleocene-Eocene thermal maximum. *Clim. Past*, 7(1), 47-61, doi:10.5194/cp-7-47-201.
- Villa, G., Fioroni C., Pea L., Bohaty S. & Persico D. (2008) - Middle Eocene-late Oligocene climate variability: Calcareous nannofossil response at Kerguelen Plateau, Site 748. *Mar. Micropaleontol.*, 69, 173-192.

Benthic foraminiferal, sea level and climate change across the Cretaceous/Paleogene boundary at Brazos River, Texas

Lineke Woelders ^(a), Robert Speijer ^(a) & Philippe Claeys ^(b)

^(a) Department of Earth and Environmental Sciences, division of Geology, KU Leuven, Celestijnenlaan 200E, B-3001 Leuven-Heverlee, Belgium. E-mail: lineke.woelders@ees.kuleuven.be

^(b) Vrije Universiteit Brussel, Department Geology, Pleinlaan 2, B-1050 Brussels, Belgium

Document type: Short note.

Manuscript history: received 15 May 2014; accepted 30 May 2014; editorial responsibility and handling by Gerald R. Dickens & Valeria Luciani.

KEY WORDS: benthic foraminifera, Cretaceous/Paleogene boundary, paleoclimate, sea level change, turnover.

The Cretaceous/Paleogene (K/Pg) boundary marks one of the largest extinctions in the Phanerozoic. About 50% of all marine genera went extinct at this boundary (Sepkoski, 1996). Environmental deterioration, for instance caused by sea level and climatic changes, is suggested by some to have contributed to biotic turnover at or even before the K/Pg boundary (e.g. O’Dea et al., 2011). In addition, changes in food supply and oxygenation directly after the K/Pg boundary could have contributed to the major extinction (e.g. Coccioni & Galeotti, 1994; Alegret et al., 2003).

Foraminifera are excellently suited to reveal sea level (e.g. Olsson & Nyong, 1984) and climate changes, and changes in food supply and oxygenation (e.g. Corliss & Chen, 1988; Widmark & Speijer, 1997). Most studies on benthic foraminiferal assemblages around the K/Pg boundary however focus on deep-sea environments. The study of benthic foraminiferal assemblages from a shallow-sea environment may therefore provide crucial additional information to elucidate changes in oceanic environments around the K/Pg boundary. In this study, we therefore analyzed benthic foraminifera from a continuous shallow sea K/Pg transition from the Brazos River area, Texas.

Two cores drilled close to the shallow shelf Brazos River outcrops are investigated. Together they constitute an expanded succession of 14.5 m of the uppermost Maastrichtian (Biozones CF2 to CF1) and lower Danian (Biozone P0 to P1a). Benthic foraminiferal assemblages are used to reconstruct changes in water depth through time. Percentages of buliminids and an oxygen index based on infaunal taxa (Kaiho, 1994) are used to unravel food supply and oxygenation conditions across the K/Pg boundary. In addition, stable isotope analysis of benthic taxa *Anomalinoides midwayensis*, *Gavelinella dumblei* and *Anomalinoides acutus* and planktic taxon *Heterohelix globulosa* allow for climate and environmental reconstruction.

The quantitative benthic foraminiferal record shows a succession of three distinct assemblages. The late

Maastrichtian assemblage is very stable and dominated by a few species (*Clavulinoides trilatera*, *Gavelinella dumblei*, *Cibicidoides harperi*, *Gyroidina pontoni* and *Bulimina kickapooensis*). The stable fauna indicates a constant middle to outer neritic paleodepth of ~100 to 150 m during the latest Maastrichtian. Stable, low percentages of buliminids (~5%) and a high oxygen index (~95) suggest well oxygenated, low food conditions throughout this interval. Stable isotope analysis of both benthic and planktic foraminifera also indicates very stable late Maastrichtian conditions, except for one significant isotopic excursion indicating a major warming event just before the K/Pg boundary. This warming event was also observed in other records (e.g. Li & Keller, 1999) and is most likely related to the Deccan traps. Interestingly, the benthic assemblage including the percentage of buliminids was not influenced by this warming event, although the number of foraminifera per gram of sediment increased during this interval.

The K/Pg event bed marks an abrupt faunal change in the benthic foraminiferal assemblage. Out of the 16 dominant late Maastrichtian taxa (>2% of the assemblage at least once in the record), 10 disappear from the record during P0 and P α (~63%). In addition, P/B ratios in this interval gradually drop from a peak value of 80% just above the event bed to 0% during Zone P0. This suggests that a proportion of both foraminifera groups is probably reworked within this interval. Paleobathymetric estimates within this interval are therefore uncertain. However, the dominance of coastal taxa *Eponides elevatus* and *Anomalinoides umboniferus* in combination with coarser grained sediments (Schulte et al., 2006) suggest a sea level shallowing during this interval. Buliminid percentages and the oxygen index do not change significantly during this interval, indicating well oxygenated conditions and no significant quantitative change in food supply. The sudden appearance of certain taxa (*Pseudovigierina naheolensis* and trochospiral agglutinants) however do suggest an unstable qualitative food supply, different from the late Maastrichtian.

During Zone P α -P1a, 10 new dominant taxa emerged and a typical benthic Midway fauna was established, dominated by

Anomalinoidea midwayensis, *Alabamina midwayensis*, *Anomalinoidea acutus*, *Gyroidina subangulata* and *Bulimina quadrata*. The Midway fauna typifies deposition in a middle to outer shelf setting (~100 to 150 m). The depositional environment at Brazos during Biozone Pa-P1a thus appears to have been similar to the latest Maastrichtian. Stable isotope analysis indicates two consequent warming events in zone P1a, which could indicate the Danian-C2 event. Again, neither the benthic assemblage, percentage of buliminids, nor the oxygen index were not directly influenced by this warming event, although the number of foraminifera per gram increased.

In conclusion, there is no indication of sea-level change prior to the K/Pg boundary at Brazos River. At the boundary, sea-level seems to have shallowed, although reworking could have influenced the benthic foraminiferal assemblages. The early Danian record suggests a gradual deepening. The Brazos River data thus indicates that sea-level change could possibly be a controlling parameter in the global biotic turnover after the K/Pg boundary, but is not likely to have influenced ecosystem stability prior to the boundary. The major warming event in the otherwise stable late Maastrichtian, on the other hand, could have had an effect on global ecosystem stability before the K/Pg boundary, although it did not affect the benthic foraminiferal assemblage. Climate seems to have become less stable after the K/Pg boundary, which could have played a role in the global biotic turnover after the boundary. Finally, organic flux and sea floor oxygenation at Brazos River remained stable throughout the investigated interval. Anoxia and quantitative changes in organic carbon flux are thus unlikely to have contributed to extinction events around the K/Pg boundary in this area. Only directly after the K/Pg boundary, organic carbon flux may have been qualitatively unstable, which may have influenced extinction at this location.

REFERENCES

- Alegret L., Molina, E. & Thomas, E. (2003) – Benthic foraminiferal turnover across the Cretaceous/Paleogene boundary at Agost (southeastern Spain): paleoenvironmental inferences. *Mar. Micropaleontol.*, 48, 251-279
- Coccioni R. & Galeotti S. (1994) – K-T boundary extinction: geologically instantaneous or gradual event? Evidence from deep-sea benthic foraminifera. *Geology*, 22, 779-782.
- Corliss B.H. & Chen C. (1988) - Morphotype patterns of Norwegian Sea deep-sea benthic foraminifera and ecological implications. *Geology*, 16, 716-719.
- Kaiho K. (1994) - Benthic foraminiferal dissolved oxygen index and dissolved oxygen levels in the modern ocean. *Geology*, 22, 719-722.
- O'Dea A., Håkansson E., Taylor P.D. & Okamura B. (2011) – Environmental change prior to the K-T boundary inferred from temporal variation in the morphology of cheilostome bryozoans. *Palaeogeogr. Palaeoclimatol. Palaeoecol.*, 308(3-4), 502-512
- Olsson R.K. & Nyong E.E. (1984) - A paleoslope model for Campanian-lower Maastrichtian foraminifera of New Jersey and Delaware. *J. Foramin. Res.*, 14, 50-68.
- Sepkoski J.J. (1996) - Patterns of Phanerozoic Extinction: a Perspective from Global Data Bases. In: Walliser O.H. (ed), *Global Events and Event Stratigraphy in the Phanerozoic*. Springer, 35-51.
- Schulte P., Speijer R., Mai H. & Kontny A. (2006) The Cretaceous-Paleogene (K-P) boundary at Brazos, Texas: sequence stratigraphy, depositional events and the Chicxulub impact. *Sediment. Geol.*, 184, 77-109
- Widmark J.G.V. & Speijer R.P. (1997) - Benthic foraminiferal ecomarker species of the terminal Cretaceous (late Maastrichtian) deep-sea Tethys. *Mar. Micropaleontol.*, 31, 135-155.

Chemostratigraphy ($\delta^{13}\text{C}_{\text{org}}$, $\delta^{13}\text{C}_{\text{inorg}}$, $\delta^{18}\text{O}_{\text{PO}_4}$) of the phosphate series from the Ouled Abdoun Basin, Morocco: constraints and significance for earliest known African placental mammals

Johan Yans^(a), László Kocsis^(b), Emmanuel Gheerbrant^(c), M'Barek Amaghazaz^(d), Baadi Bouya^(d), Henri Cappetta^(e), Paola Iacumin^(f), Mustapha Mouflih^(g), Omar Selloum^(d), Sevket Sen^(c), Corentin Noiret^(a) & Jean-Yves Storme^(a,h)

^(a) University of Namur, Department of Geology, NaGRIDD, 61 rue de Bruxelles, 5000 Namur, Belgium. E-mail: johan.yans@unamur.be

^(b) University of Lausanne, Faculty of Geoscience and Environment, Institute of Earth Sciences, UNIL - Geopolis, CH-1015 Lausanne, Switzerland

^(c) UMR-CNRS 7207, Centre de Recherches sur la Paléobiodiversité et les Paléoenvironnements, MNHN, CP38, 8 rue Buffon, 75005 Paris, France

^(d) Groupe Office Chérifien des Phosphates (OCP), Centre Minier de Khouribga, Service Géologique, Khouribga, Morocco

^(e) Université Montpellier II, UMR 5554, France

^(f) Parma University, Earth Sciences, Parco Area delle Scienze, 157, 43100 Parma, Italy

^(g) University Hassan II-Mohammedia, Faculty of Sciences Ben M'sik, Casablanca, Morocco

^(h) University of Liège, Geology Department, Palaeobiogeology-Palaeobotany-Palaeopalynology, allée du 6 Août, 17, B18, 4000 Liège Sart-Tilman, Belgium

Document type: Short note.

Manuscript history: received 15 May 2014; accepted 30 May 2014; editorial responsibility and handling by Gerald R. Dickens & Valeria Luciani.

KEY WORDS: EECO, isotopes, mammals, Morocco, PETM, phosphate.

Correlate the fossil mammal-bearing localities with the standard marine stratigraphy remains challenging. During the Paleogene, distinctive land mammal faunas are recognized in various areas. Correlations at wide scale between these faunas are problematic due to effects of endemism, lack of refined dating of the continental and marine proximal mammalian localities, variations in the tempo of evolution of different lineages, preservation biases, etc. The famous Maastrichtian-Ypresian phosphate series, in the Ouled Abdoun Basin (Morocco), that has yielded the earliest known placentals from Africa, is classically dated using regional selachian biostratigraphy zonation (e.g. Arambourg 1952; Cappetta, 2012).

Matching 1) carbon isotopes on dispersed organic matter of bulk sediments ($\delta^{13}\text{C}_{\text{org}}$), 2) carbon isotopes on shark tooth enameloid and dentine ($\delta^{13}\text{C}_{\text{inorg}}$), and 3) oxygen isotopes on shark teeth ($\delta^{18}\text{O}_{\text{PO}_4}$), we propose a refined chronostratigraphic framework of the Ouled Abdoun mammal-bearing phosphate series, by correlations with worldwide reference sections. We propose the following stratigraphy, from the base to the top of the series.

The condensed Cretaceous beds in the Ouled Abdoun Basin are probably latest Maastrichtian (upper Bed III).

The uppermost part of the Paleocene series (Bed IIa) is dated late Selandian–early Thanetian. The base, just above the *Eritherium* Bone Bed, would be correlated with the Early Late Paleocene Event (ELPE). This provides a late Selandian minimum age of the earliest known placentals mammals (*Eritherium azzouzorom*, *Ocepeia daouiensis*, *Abdounodus hamdii*, *Lahimia selloumi*).

The isotope data suggest a local sedimentary hiatus around the Paleocene–Eocene boundary, where the ETM1 (Eocene

Thermal Maximum 1 or PETM - Paleocene Eocene Thermal Maximum) event and the latest Thanetian most likely lack. The *Otodus obliquus* and *Phosphatherium escuilliei* Bone Bed, within the Intercalary BII/I, is earliest Ypresian in age.

The middle part of the series (from Intercalary Bed I/0' to Sillon A) shows minimal $\delta^{13}\text{C}_{\text{org}}$ values, in good agreement with the ETM2-ETM3 interval, dated upper NP11-lower NP12. This includes the phosphorite Bed 0, from which probably came *Daouitherium rebouli*, the first large mammal known in Africa (Gheerbrant et al., 2002). Possible role of paleoenvironmental changes in the evolution of the large size in African mammals such as *Daouitherium* seems to be related to early–middle Ypresian ETM2 and ETM3 hyperthermal events (called ETM2-ETM3 interval), instead of the PETM.

The top of the series, with chert-enriched facies, should correlate with the Early Eocene Climatic Optimum. The isotopic values support the lack of Lutetian in the studied area.

Our chemostratigraphic conclusions might be limited by 1) the ecological control of the different species of sharks that are sampled for analysis, 2) the origin and the potential oxidation of the organics, and 3) phosphate diagenesis.

The large variation in $\delta^{18}\text{O}_{\text{PO}_4}$ values of the shark teeth corresponds to different species habitats. The average $\delta^{18}\text{O}_{\text{PO}_4}$ values for the studied beds however show important sequential trends, correlating with the $\delta^{13}\text{C}$ values.

In sedimentary phosphate deposits, phosphatic intraclasts, made of francolite (carbonate fluoroapatite), are biogenic debris such as bone, coprolites, invertebrate fragments and microorganisms (Lucas & Prévôt-Lucas, 1995).

Phosphatogenesis involve organic matter recycling and might thus affect the primary isotopic signal of organics. The origin of the carbon in the apatite structure could derive from several sources and are often modified by post-depositional processes (Iacumin et al., 1996). The upwelling zones supply nutrients to surface waters, resulting in high primary productivities, and high organic carbon fluxes to the seafloor. It

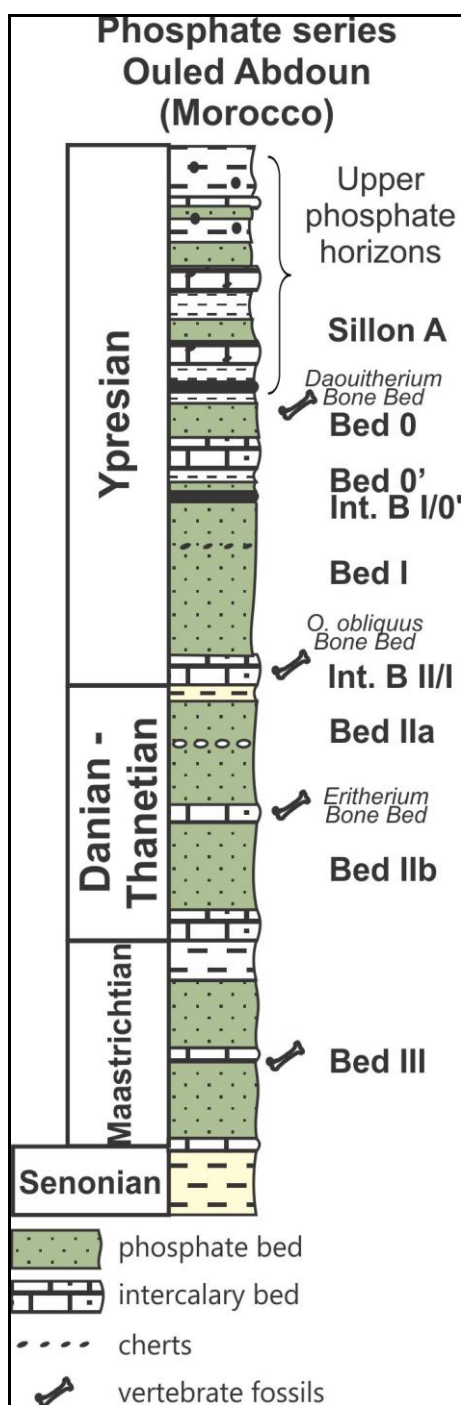


Fig.1 – Phosphate series of Ouled Abdoun (Morocco).

is the source of differences in dissolved CO_2 content between surface and bottom waters, and the finally distinctive $\delta^{13}\text{C}$ signatures. Surface waters CO_2 are depleted in ^{12}C , because the latter is assimilated by phytoplankton, whereas bottom waters CO_2 are depleted in ^{13}C due to oxidation of organics (e.g., Föllmi, 1996). Primary organic material is most probably incorporated into phosphates and may be altered during phosphatogenesis.

However, little is known about potential isotopic fractionation of organic carbon during phosphatogenesis and deposition of phosphate grains. Moreover, later phosphatogenesis may also generate depleted $\delta^{13}\text{C}$ values, due

to potential bacterial activity. In the Ouled Abdoun phosphate series, the very low $\delta^{13}\text{C}_{\text{inorg}}$ isotopic compositions of coprolites reflect depositional conditions with intensive organic matter recycling.

Therefore, at the current state of knowledge (i.e. without precise understanding of the effects of the phosphatogenesis on carbon isotopes), we recommend the use of repeated and consistent isotopic trends, performed on relatively numerous samples from several sections, of various materials with good preservation state (organics, inorganics, enamel/enameloid, dentine) to provide reliable results for chemostratigraphy in such phosphate series, as proposed by Yans et al. (2014) and Kocsis et al. (2014) for Late Cretaceous-Early Eocene sediments in the Ouled Abdoun (Morocco) and by Ounis et al. (2008) around the Paleocene/Eocene boundary in Tunisia.

REFERENCES

- Arambourg C. (1952) - Vertébrés fossiles des Phosphates d'Afrique du Nord (Maroc, Algérie, Tunisie). Notes et Mémoires du Service Géologique du Maroc (Rabat), 92, 1-372.
- Cappetta H. (2012) - Chondrichthyes (Mesozoic and Cenozoic Elasmobranchii: teeth). In: Schultze, H.-P. (Ed.), Handbook of Paleichthyology. Chondrichthyes, 3E., Verlag F. Pfeil, 1-512.
- Föllmi K.B. (1996) - The phosphorus cycle, phosphogenesis and marine phosphate-rich deposits. Earth-Sci. Rev., 40, 55-124.
- Gheerbrant E., Sudre J., Cappetta H., Iarochène M., Amaghaz M. & Bouya B. (2002) - A new large mammal from the Ypresian of Morocco: evidence of surprising diversity of early proboscideans. Acta Palaeont. Polonica, 47 (3), 493-506.
- Iacumin P., Bocherens H., Mariotti A. & Longinelli A. (1996) - Oxygen isotope analyses of co-existing carbonate and phosphate in biogenic apatite; a way to monitor diagenetic alteration of bone phosphate? Earth Planet. Sci. Lett., 142, 1-6.
- Kocsis L., Gheerbrant E., Mouflih M., Cappetta H., Yans J. & Amaghaz M. (2014) - Comprehensive stable isotope investigation of marine biogenic apatite from the late Cretaceous-early Eocene phosphate series of Morocco. Palaeogeogr. Palaeoclimatol. Palaeoecol. 394, 74-88.
- Lucas J. & Prevôt-Lucas L. (1995) - Tethyan phosphates and bioproductites. In: Nairn, A.E., et al. (Eds.), The Ocean Basins and Margins: The Tethys Ocean, 8. Plenum Press, 367-391.
- Ounis A., Kocsis L., Chaabani F. & Pfeifer H.-R. (2008) - Rare earth element and stable isotope geochemistry ($\delta^{13}\text{C}$ and $\delta^{18}\text{O}$) of phosphorite deposits in the Gafsa Basin, Tunisia. Palaeogeogr. Palaeoclimatol. Palaeoecol. 268, 1-18.
- Yans J., Amaghaz M., Bouya B., Cappetta H., Iacumin P., Kocsis L., Mouflih M., Selloum O., Sen S., Storme J.-Y. & Gheerbrant E. (2014) - First carbon isotope chemostratigraphy of the Ouled Abdoun phosphate Basin, Morocco: implications for dating and evolution of earliest African placental mammals. Gondwana Research, 25, 257-269.

Paleogene Climate, Biota, and the Carbon Cycle: Progress and Promise

James C. Zachos ^(a)

^(a) Dept. of Earth and Planetary Sciences, University of California Santa Cruz, 1156 High Street, Santa Cruz, CA 95064, USA; E-mail: jzachos@ucsc.edu

Document type: Short note.

Manuscript history: received 15 May 2014; accepted 30 May 2014; editorial responsibility and handling by Gerald R. Dickens & Valeria Luciani.

KEY WORDS: carbon isotopes, global warming, greenhouse gases, Paleocene-Eocene

Over the last 25 years substantial progress has been made in defining the major patterns of climate change over the Paleogene, and linking these patterns to changes in the carbon cycle as well as the evolution of biota. This includes the timing and scale of long-term warming and cooling, onset of continental glaciation, the occurrence of transient thermal maxima and ocean acidification events, and the relative timing of changes in atmospheric CO₂. These achievements can be attributed to a number of factors including advances in high resolution (i.e., orbital) stratigraphy, and in the reconstruction of key climate and carbon cycle parameters (e.g., T, pCO₂) in both marine and terrestrial settings, facilitated in part by the development and refinement of new and existing proxies. The advances in climate archives have been paralleled by additional developments with general circulation climate models (GCM's), and the development of Earth system models of intermediate complexity (EMIC's), which can simulate the coupling of climate and biogeochemical processes, and on the long time scales relevant to studying Paleo-events.

Arguably, one of most important developments was the discovery of an intense focus on fast, large climatic excursions or transitions, which, because of the scale and rate of change, often provide a clear set of testable hypotheses regarding the coupling of climate and the carbon cycle, and impacts on ecosystems. These events, the PETM, ELMO, MECO, and EOT, all represent geologic case studies of the climate system responding to relatively rapid and/or large changes in GHG. Such case studies are far more suitable for model/data comparisons in part because our ability to reconstruct Δ of parameters exceeds that of reconstructing absolute values. More importantly, for model/data comparisons, many of the non-greenhouse boundary conditions of climate can essentially be considered fixed on the brief time scales of these events. Some of these excursions and transitions also appear to involve the action of non-linear carbon cycle feedbacks that might have amplified the initial changes in climate. Indeed, the Paleogene offers natural experiments of how earth system sensitivity to a

wide range of GHG levels. As a consequence, various intervals of the Paleogene have been targeted for assessing climate or earth system sensitivity to GHG forcing.

Given the scale of climate change, one of the more popular case studies for model/data comparisons is the PETM. The pattern of warming has been fairly well established and (see review by Dunkley-Jones et al., 2013), with constraints using the CCD and other constraints, the mass of carbon released and Δ pCO₂ is being narrowed (Panchuk et al., 2008; Zeebe et al., 2009; Penman et al., 2014). Because of the fast rate of change, the event is particularly suitable as a natural case study of the climate response to GHG forcing. All other boundary conditions, with the exception of orbital forcing, can be treated as fixed, thus enabling a more complete analysis of sensitivity to greenhouse forcing, to the extent that Δ pCO₂ can be quantified.

With 5 to 6°C of global warming, and peak SST in excess of 35°C in the tropics, and >20°C in the Arctic and southern Oceans, the PETM also offers an opportunity to assess the sensitivity of the hydrologic cycle to warming. Dramatic changes in global precipitation patterns and intensity have been inferred from proxies, the general character of which is consistent with a highly energetic hydrologic cycle (e.g., Wing et al., 2006; Zachos et al., 2006; Puljate and Schmitz, 2007; Nicolo et al., 2007). Sections with multi-proxies show good agreement on Δ SST, which if coupled with $\delta^{18}\text{O}$, can be used to estimate Δ SSS. The latter is critical as it affords an opportunity to evaluate regional changes in precipitation patterns and intensity (i.e., E-P). For example, a number of marine localities show shifts in local salinity, typically higher SSS in low to mid-latitudes, and lower in high latitudes suggesting increased meridional vapor transport. In fact, most paleohydrologic indicators in coastal and continental sections (e.g. Wing et al., 2006; Foreman et al., 2012), support a global shift toward a more energetic hydrologic cycle with enhanced seasonality. In general, AOGCM's simulations under high greenhouse gas levels also exhibit enhanced E-P (Kiehl & Shields, 2013), with intensification of aridity in lower latitudes and amplification of the seasonal cycle of precipitation (i.e., weather extremes). In this regard, the PETM might be the best analogue for assessing the sensitivity of the global hydrologic

cycle to extreme greenhouse warming. For the Paleogene community, one key challenge will be to develop quantitative reconstructions of precipitation, particularly in defining changes in the seasonal cycle.

REFERENCES

- Dunkley-Jones T., Lunt D.J., Schmidt D.N., Ridgwell A., Sluijs A., Valdes P. J. & Maslin M. (2013) - Climate model and proxy data constraints on ocean warming across the Paleocene-Eocene Thermal Maximum. *Earth-Sci. Rev.*, 125, 123-145.
- Kiehl J.T. & Shields C.A. (2013) - Sensitivity of the Paleocene-Eocene Thermal Maximum climate to cloud properties. *Philos. T. Roy. Soc. A*, 371, 20130093
- Lunt D.J., Valdes P.J., Dunkley Jones T., Ridgwell A., Haywood A.M., Schmidt D.N., Marsh R., Maslin M. (2010) - CO₂-driven ocean circulation changes as an amplifier of Paleocene–Eocene thermal maximum hydrate destabilization. *Geology*, 38, 875–878.
- Nicolo M.J., Dickens G.R., Hollis C.J. & Zachos J.C. (2007) - Multiple Early Eocene hyperthermals: Their sedimentary expression on the New Zealand continental margin and in the deep-sea. *Geology*, 35, 699–702.
- Panchuk K., Ridgwell A. Kump L.R. (2008) - Sedimentary response to Paleocene-Eocene Thermal Maximum carbon release: A model-data comparison. *Geology*, 36(4), 315-318.
- Penman D.E., Hönisch B., Zeebe R.E., Thomas E. & Zachos J.C. (2014) - Rapid and sustained surface ocean acidification during the Paleocene-Eocene Thermal Maximum. *Paleoceanography*, 29, doi:10.1002/2014PA002621.
- Schmitz B. & Pujalte V. (2003) - Sea-level, humidity, and land-erosion records across the initial Eocene thermal maximum from a continental-marine transect in northern Spain. *Geology* 31, 689–692.
- Wing S.L., Harrington G.J., Smith F.A., Bloch J.I., Boyer D.M. & Freeman K.H. (2005) - Transient floral change and rapid global warming at the Paleocene–Eocene boundary. *Science*, 310, 993–996.
- Zachos J.C., Schouten S., Bohaty S.M., Sluijs A., Brinkhuis H., Gibbs S.J., Bralower T.J. & Quattlebaum T. (2006) - Extreme warming of mid-latitude coastal ocean during the Paleocene-Eocene Thermal Maximum: Inferences from TEX₈₆ and Isotope Data. *Geology*, 34, 737–740.
- Zeebe R.E., Zachos J.C. & Dickens G.R. (2009) - Carbon dioxide forcing alone insufficient to explain Palaeocene-Eocene Thermal Maximum warming, *Nature Geosci.*, 2(8), 576-580.

Stepped carbon isotope excursion during the Paleocene-Eocene Thermal Maximum triggered initially by volcanic CO₂ emission

Qinghai Zhang ^(a,b), Xiaoxia Xu ^(a), Helmut Willems ^(a), Lin Ding ^(b), Xiaolei Liu ^(c) & Kai-Uwe Hinrichs ^(c)

^(a) Department of Geosciences, University of Bremen, Klagenfurter Straße, 28359 Bremen, Germany. E-mail: zhang@uni-bremen.de

^(b) Key Laboratory of Continental Collision and Plateau Uplift, Institute of Tibetan Plateau Research, Chinese Academy of Sciences, 100101 Beijing, China

^(c) MARUM Center for Marine Environmental Sciences, University of Bremen, Leobener Straße, 28359 Bremen, Germany

Document type: Short note.

Manuscript history: received 15 May 2014; accepted 30 May 2014; editorial responsibility and handling by Gerald R. Dickens & Valeria Luciani.

KEY WORDS: nodular limestone, paired $\delta^{13}\text{C}_{\text{bulk}}$ and $\delta^{13}\text{C}_{\text{TOC}}$, PETM, shallow marine, stepped CIE patterns, Tibet, volcanic CO₂ emission

The Carbon Isotope Excursion (CIE) during the Paleocene-Eocene Thermal Maximum (PETM) reflects a strong perturbation of carbon cycle about 56 Ma ago. It caused a ~4-5 °C global warming and dramatic changes in the environmental and biotic realm (Zachos et al., 2003; Gibbs et al., 2006). However, the magnitude (Bains et al., 1999; Pagani et al., 2006) and duration (Röhl et al., 2007; Cui et al., 2011) of the CIE from previous studies are highly variable, and the exact patterns of the CIE are still unknown. All those are key to understanding mechanisms causing the PETM-CIE event. Comparatively, the CIE patterns have more significant implications, because (1) the full magnitude and duration of the CIE can only be acquired on the basis of complete CIE records, which, theoretically, should manifest the true patterns of the CIE; (2) the patterns contain the details of carbon isotope variations within the CIE and thus can reveal more information about light carbon emissions.

A great amount of knowledge about this event was obtained from sections in deep Oceans, where diagenesis usually had a negligible effect on carbon and oxygen isotopes of sediments and fossils. However, low sedimentation rates and possible dissolutions owing to ocean acidification usually form very thin (<1m), incomplete records. By contrast, sections from shallow marine environments could be formed at higher sedimentation rates and without effects of ocean acidification, whereas diagenetic overprints on the isotopes are usually thought to be stronger.

In this study, we have investigated a shallow marine limestone section in the Tingri area of south Tibet. Trace elements concentrations, strontium isotope ($^{87}\text{Sr}/^{86}\text{Sr}$), paired carbon isotopes from bulk carbonate ($\delta^{13}\text{C}_{\text{bulk}}$) and total organic carbon ($\delta^{13}\text{C}_{\text{TOC}}$), weight percent of calcium carbonate (CaCO₃ wt%) and total organic carbon (TOC wt%), and C:N ratios of TOC have been analyzed.

To evaluate diagenetic effects on the $\delta^{13}\text{C}_{\text{bulk}}$ values, some traditional geochemical methods, such as concentrations of Mn and Sr, Mn/Sr ratio, and Sr isotope, have been used. Low Mn

(<100 ppm), high Sr (~800-1000 ppm), low Mn/Sr (<0.15) and $^{87}\text{Sr}/^{86}\text{Sr}$ values (~0.7078) support an insignificant influence of diagenesis on $\delta^{13}\text{C}_{\text{bulk}}$ values.

The $\delta^{13}\text{C}_{\text{bulk}}$ data show an extended CIE record (~11m for the main CIE) in a homogeneous nodular limestone. Since some nodular limestones can be formed by allochthonous redeposition, thus, variations of $\delta^{13}\text{C}_{\text{bulk}}$ values cannot be used to indicate changes of carbon isotope compositions in the ocean. In order to test whether the nodular limestone at Tingri was formed allochthonously or autochthonously, we made another sampling from a laterally different outcrop and measured $\delta^{13}\text{C}_{\text{bulk}}$. The $\delta^{13}\text{C}_{\text{bulk}}$ variations from two outcrops are roughly identical, which demonstrates that the nodular limestone was formed by 'in-situ' processes and the $\delta^{13}\text{C}_{\text{bulk}}$ variations can represent changes of carbon isotope in the ocean.

For the main CIE, the $\delta^{13}\text{C}_{\text{bulk}}$ curve at Tingri shows stepped patterns similar with those (phase c, d, e, f, g) from Ocean Drilling Program (ODP) Site 690 (Bains et al., 1999), but the magnitude of the negative CIE in the former (~7‰) is much larger than that in the latter (~2.2‰). During the PETM, the section at Tingri was formed in a carbonate ramp environment near the equator. The nodular limestone is rich in larger benthic foraminifera, and the larger foraminiferal assemblage of *Lockhartia-Miscellanea-Kathina-Operculina-Ranikothalia* indicates a water depth of ~40-80 m. By contrast, ODP 690 section was situated in a deep ocean environment at high latitude. The similarity of the CIE patterns from two palaeogeographically distant and different locations implies that $\delta^{13}\text{C}$ variations during the PETM followed these particular patterns in the entire ocean. The magnitude of ~7‰ at Tingri is quite similar to those from many terrestrial records, but much larger than those from deep oceans. It implies that carbon reservoirs of atmosphere and surface ocean were well mixed whereas those of surface ocean and deep ocean didn't reach equilibrium during the PETM.

The $\delta^{13}\text{C}_{\text{bulk}}$ and $\delta^{13}\text{C}_{\text{TOC}}$ don't covary with each other before 'phase e'. Immediately before the onset of the CIE (uppermost phase b), $\delta^{13}\text{C}_{\text{TOC}}$ was gradually decreasing ~2‰, whereas $\delta^{13}\text{C}_{\text{bulk}}$ was increasing ~0.2‰. These changes can be caused by an increased volcanic (or metamorphic) CO₂

emission to the atmosphere-ocean system (Kump & Arthur, 1999). If so, the CO₂ emission, probably originating from circum-Caribbean volcanism (Bralower et al., 1997) and/or Northeast Atlantic opening (Storey et al., 2007), can lead to the pre-CIE warming (Sluijs et al., 2007), acting as the first trigger for the subsequent PETM-CIE event.

REFERENCES

- Bains S., Corfield R.M. & Norris R.D. (1999) - Mechanisms of climate warming at the end of the Paleocene. *Science*, 285, 724-727.
- Bralower T.J., Thomas D.J., Zachos J.C., Hirschmann M.M., Röhl U., Sigurdsson H., Thomas E. & Whitney D.L. (1997) - High-resolution records of the late Paleocene thermal maximum and circum-Caribbean volcanism: Is there a causal link?. *Geology*, 25, 963-966.
- Cui Y., Kump L.R., Ridgwell A.J., Charles A.J., Junium C.K., Diefendorf A.F., Freeman K.H., Urban N.M. & Harding I.C. (2011) - Slow release of fossil carbon during the Palaeocene-Eocene Thermal Maximum. *Nature Geosci.*, 4, 481-485.
- Gibbs S.J., Bown P.R., Sessa J.A., Bralower T.J. & Wilson P.A. (2006) - Nannoplankton extinction and origination across the Paleocene-Eocene Thermal Maximum. *Science*, 314, 1770-1773.
- Kump L.R. & Arthur M.A. (1999) - Interpreting carbon-isotope excursions: carbonates and organic matter. *Chem. Geol.*, 161, 181-198.
- Pagani M., Pedentchouk N., Huber M., Sluijs A., Schouten S., Brinkhuis H., Sinninghe Damste J.S., Dickens G.R. & Expedition Scientists (2006) - Arctic hydrology during global warming at the Palaeocene/Eocene thermal maximum. *Nature*, 442, 671-675.
- Röhl U., Westerhold T., Bralower T.J. & Zachos J.C. (2007) - On the duration of the Paleocene-Eocene thermal maximum (PETM). *Geochem. Geophys. Geosyst.* 8, Q12002, doi:10.1029/2007gc001784.
- Sluijs A., Brinkhuis H., Schouten S., Bohaty S.M., John C.M., Zachos J.C., Reichert G.-J., Sinninghe Damste J.S., Crouch E.M. & Dickens G.R. (2007) - Environmental precursors to rapid light carbon injection at the Palaeocene/Eocene boundary. *Nature*, 450, 1218-1221.
- Storey M., Duncan R.A. & Swisher III C.C. (2007) - Paleocene-Eocene Thermal Maximum and the opening of the northeast Atlantic. *Science*, 316, 587-589.
- Zachos J.C., Wara M.W., Bohaty S., Delaney M.L., Petrizzo M.R., Brill A., Bralower T.J. & Premoli-Silva I. (2003) - A transient rise in tropical sea surface temperature during the Paleocene-Eocene Thermal Maximum. *Science*, 302, 1551-1554.

I/Ca in Planktic Foraminifera: Evidence for upper ocean deoxygenation during the Paleocene/Eocene Thermal Maximum

Xiaoli Zhou ^(a), Ellen Thomas ^(b,c), Rosalind E.M. Rickaby ^(d), Arne Winguth ^(e) & Zunli Lu ^(a)

^(a) Department of Earth Sciences, Syracuse University, Syracuse NY 13244, USA

^(b) Department of Geology and Geophysics, Yale University, New Haven, CT 06511, USA. E-mail: ellen.thomas@yale.edu

^(c) Department of Earth & Environmental Sciences, Wesleyan University, Middletown, CT 06459, USA

^(d) Department of Earth Sciences, University of Oxford, South Parks Road, Oxford OX13AN, UK

^(e) Department of Earth and Environmental Sciences, University of Texas at Arlington, Arlington TX 76029, USA

Document type: Short note.

Manuscript history: received 15 May 2014; accepted 30 May 2014; editorial responsibility and handling by Gerald R. Dickens & Valeria Luciani.

KEY WORDS: deoxygenation, PETM, planktic foraminifera, ocean stratification

Anthropogenic global warming affects marine ecosystems in complex ways, and declining ocean oxygenation is a growing concern. Forecasting the geographical and bathymetric extent, rate and intensity of future deoxygenation and its effects on oceanic biota, however, remains highly challenging because of the complex feedbacks in the earth-ocean-biota system. Information on past global warming events such as the Paleocene Eocene Thermal Maximum (PETM, ~55.5 Ma), a potential analog for present and future global warming, may help in such forecasting, but documenting past ocean deoxygenation is hampered by the lack of sensitive proxies for oceanic oxygen levels throughout the water column. During the PETM, bottom waters and pore waters along continental margins and in epicontinental basins may have been suboxic to anoxic (Thomas, 1998). Bottom waters at bathyal depths in the Atlantic and Southern Ocean, but not in the equatorial Pacific, may have been suboxic (Pälike et al., 2014), but as yet no evidence has been presented for pervasive deoxygenation in the upper water column through expansion of Oxygen Minimum Zones (OMZs). We apply a novel proxy for paleo-redox conditions, the iodine to calcium ratio (I/Ca), based on the fact that only the oxidized form of iodine (iodate, IO_3^-), but not the reduced form (iodide), can be incorporated in the calcite structure. I/Ca in bulk sediment was used to study deoxygenation during Mesozoic anoxic events (Lu et al., 2010), and we use I/Ca in bulk coarse fraction sediment as well as planktic foraminiferal tests from pelagic sites in different oceans, then compare our reconstruction with modeled oxygen levels.

The I/Ca proxy is based on knowledge about iodine speciation in the modern oceans, where total iodine (sum of iodate and iodide) is uniformly around $0.45 \mu\text{mol/L}$. The iodate concentration is thus inversely correlated to the iodide concentration, and high primary productivity and decomposition of organic matter cause iodate loss and iodide production. Under hypoxic conditions, >75% of iodate is converted to iodide, the dominant species below the

oxygenated surface water in anoxic basins. Iodine occurs mostly as iodate in oxic bottom waters.

The vertical iodate concentration profile in the oceans is thus influenced by productivity and the presence/absence of an oxygen minimum zone (OMZ). Primary productivity is negatively correlated with the iodate concentration in surface waters, thus I/Ca is expected to be lower in mixed-layer dwelling planktic foraminifera at higher productivity (M in Fig. 1). We observed that the average I/Ca in Paleocene mixed-layer planktics is indeed negatively correlated with the modeled export productivity (CCSM3, Winguth et al., 2012), suggesting that productivity was lower at Sites 1209, 865 and 1262 than at 690, 738 and 762.

If there is no OMZ (Fig. 1A), the iodate concentration increases downwards from the mixed layer where primary productivity occurs to greater depths. In contrast, if there is a shallow OMZ (Fig. 1B), the iodate concentration decreases from the mixed layer down to the upper OMZ. When the top of

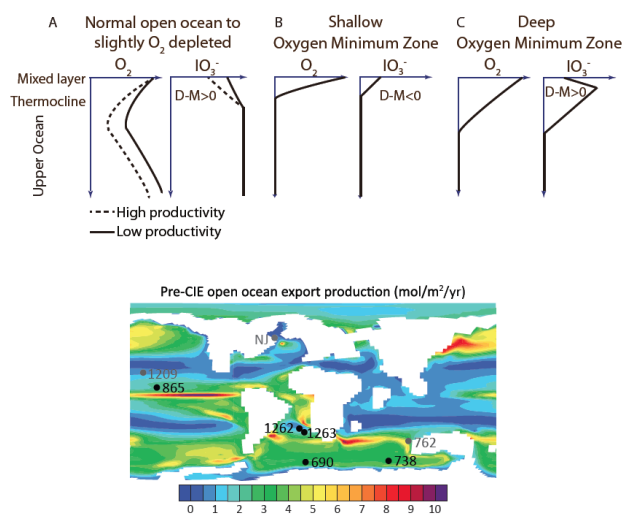


Fig. 1 – Schematic seawater iodate and oxygen concentration profiles. D-M stands for the difference between I/Ca of deep- and mixed layer calcifiers, and study sites plotted on the paleo-map of the modeled export productivity during the late Paleocene at open ocean sites (Winguth et al., 2012).

the OMZ is at deeper levels, the iodate concentration may increase downwards from the mixed layer, then decrease further down to zero in the OMZ (Fig. 1C). Shallowing of OMZs should have caused an overall decrease in planktic foraminiferal I/Ca, with lower values in thermocline (D; *Subbotina* spp.) than in mixed layer calcifiers (M; *Acarinina* spp. and *Morozovella* spp.). Changes in I/Ca in mixed-layer (M) as compared to deep dwelling (D) planktic foraminifera reflect changes in the iodate depth gradient, related to the vertical extent of OMZs (Fig. 1).

Records from the open ocean Pacific (865), Weddell Sea (690), SE Atlantic (1262, 1263) and Indian (738, 762) sites, generally show decreased I/Ca values in monogeneric mixed layer and thermocline dwelling planktic foraminiferal records over the CIE, with minimum values around the peak CIE. We argue that decrease is probably indicative of widespread deoxygenation in the upper ocean waters. Ocean stratification induced by warming may be the mechanism for lowering oxygen levels (Norris et al., 2013). The deoxygenation likely was stronger in the Atlantic and Indian Oceans, than in the Pacific Ocean.

The difference in I/Ca values of deep dwellers and mixed-layer dwellers (D-M) was used to reconstruct the iodate gradient and detect whether an OMZ was present, and compared with dissolved oxygen profiles modeled with CCSM3 at 4xCO₂ (Winguth et al., 2012). The average D-M through the studied interval and the minimum oxygen levels in the water column estimated from the model at the sites are positively correlated. The D-M values vary geographically, with different sites showing different patterns of presence and changes in depth of OMZs across the PETM.

Overall, we speculate that a widespread (possibly global) upward extension of OMZs might have influenced pelagic ecosystems, as predicted for the future (Norris et al., 2013). Vertical compression of the zone above the OMZ may have contributed to the observed changes in planktic foraminiferal assemblages during hyperthermal events, which have commonly been attributed to changes in ocean stratification (Kelly, 2002; Petrizzo 2007). The enrichment in fish debris in CIE sediment at Shatsky Rise sites (Colosimo et al., 2006) could be not just concentration due to carbonate dissolution, but might reflect a mortality event due to vertical expansion of the OMZ.

In conclusion, the reconstructed iodate gradients indicate that deoxygenation occurred in the upper water column in the Pacific, Atlantic and Indian Oceans during the PETM, due to vertical and potentially lateral expansion of Oxygen Minimum Zones.

REFERENCES

- Colosimo A.B., Bralower T. J. & Zachos J.C. (2006) - Evidence for lysocline shoaling at the Paleocene Eocene Thermal Maximum on Shatsky Rise, Northwest Pacific, Proceedings of the Ocean Drilling Program, Scientific Results, 198, doi:10.2973/odp.proc.sr.198.112.2006
- Kelly D. C. (2002) - Response of Antarctic (ODP Site 690) planktonic foraminifera to the Paleocene-Eocene thermal maximum: Faunal evidence for ocean/climate change. *Paleoceanography*, 17(4), 1071.
- Lu Z., Jenkyns, H.C. & Rickaby R.E.M. (2010) - Iodine to calcium ratios in marine carbonate as a paleo-redox proxy during oceanic anoxic events. *Geology*, 38, 1107–1110.
- Norris R.D., Turner S.K., Hull P.M. & Ridgwell A. (2013) - Marine Ecosystem Responses to Cenozoic Global Change. *Science*, 341, 492-498
- Pälike C., Delaney M.L. & Zachos J.C. (2014) - Deep-sea redox across the Paleocene-Eocene thermal maximum, *Geochem. Geophys. Geosyst.*, 15, doi: 10.1002/2013GC005074.
- Petrizzo M. R. (2007) - The onset of the Paleocene-Eocene Thermal Maximum (PETM) at Sites 1209 and 1210 (Shatsky Rise, Pacific Ocean) as recorded by planktonic foraminifera. *Mar. Micropaleontol.*, 63, 187-200.
- Thomas E. (1998) - The biogeography of the late Paleocene benthic foraminiferal extinction, In: M.-P. Aubry, S. Lucas, & W. A. Berggren (eds.), *Late Paleocene-early Eocene Biotic and Climatic Events in the Marine and Terrestrial Records*, Columbia University Press, 214-243.
- Winguth A., Thomas E. & Winguth C. (2012) - Global decline in ocean ventilation, oxygenation and productivity during the Paleocene-Eocene Thermal Maximum - Implications for the benthic extinction. *Geology*, 40, 263-266.

RENDICONTI *Online*
della Società Geologica Italiana

Instructions for authors

The “Rendiconti Online della Società Geologica Italiana” are published in quarterly volumes. The size of each volume is 21 × 29,7 cm (A4) and the printed portion is 18,5 × 24,4 cm, in two columns of 9 × 24,4 cm.

All Authors may submit to the journal original scientific contributions, both in Italian and English, concerning all aspects of geosciences. The instructions described below should be strictly followed by the authors. The non-compliance with these instructions may delay or prevent publication. Text and figures accepted for publication are copyright of the journal.

Types of contributions published in the Rendiconti Online della Società Geologica Italiana

The Rendiconti Online host three types of contributions: “abstracts”, “short notes”, and “articles”.

Abstracts - These are very short contributions (up to 3000 characters, without figures or tables) submitted to national or international conferences. Abstracts will be included in supplements to ordinary volumes.

Short notes - These are short reports (up to 3-4 pages, plus three figures or tables and no more than 15 references). Short notes, if accepted following a peer-reviewing process, will be published faster than articles.

Articles - These are original research peer-reviewed papers. They should not exceed 15 printed pages, including references and figure captions. There are no limits for the number of figures, even if it should be in due proportion with the length of the text.

Manuscript formatting

Manuscripts must be submitted in digital format, using the ROL template.

The text may be in English or Italian. It is, however, recommended to adopt English language to enable and promote a wider dissemination of the articles. Title of the manuscript, abstract, key words and figure captions must be bilingual. Manuscripts written in English should have an extended abstract in Italian and viceversa.

The manuscript, including references and figure captions, must be double spaced.

Submit the text in the following order: Title, authors' names and addresses, telephone, fax and e-mail of the corresponding author. Below abstract/riassunto, key words/parole chiave, text, acknowledgements, references. Figures, captions and tables should be inserted using the format provided by the editorial office.

References and quotations in the text

References should be inserted in parentheses in the text in full for single- and dual-authored papers (e.g. Lyell & Bertrand, 1987), but using first author and “et al.” for multiple authored papers (e.g. Lyell et al., 1988). Authors should be written with uppercase initials. The order in the text should be chronological, then alphabetical. List all references cited in alphabetical order at the end of the article in the following standard form:

Journal article

Baker V.R. (2006) - Water and the evolutionary geological history of Mars. *Boll. Soc. Geol. It.*, 125, 357-369.

Article in volume

Martini I.P., Sagri M. & Colella A. (2001) - Neogene-Quaternary basins of the inner Apennines and Calabrian arc. In: Vai G.B. & Martini I.P. (eds.), *Anatomy of an Orogen: The Apennines and Adjacent Mediterranean Basins*. Kluwer Academic Publisher, 375-400.

Volume

Ramsay J.G. & Huber M. (1987) - *The techniques of Modern Structural geology*. Volume 2: *Folds and Fractures*. Academic Press, London, 500 pp.

Thesis

Ghinassi M. (2000) - Il passaggio tra la prima e la seconda fase fluvio-lacustre del bacino del Valdarno Superiore nei pressi di S. Giovanni Valdarno. Unpublished Master thesis, University of Florence, 110 pp.

Headings

Please use a maximum of three levels of headings, hierarchically arranged as outlined below.

FIRST ORDER HEADINGS

Capital letters, centered, bold.

The first sentence after the heading begins after a blank line.

SECOND ORDER HEADINGS

Capital letters, left margin.

The first sentence after the heading begins after a blank line.

Third order headings

Italic, left margin. The first sentence after the heading begins after a blank line.

Footnotes

Footnotes are not allowed.

Abbreviations

All abbreviations used in the text must be clearly explained the first time they appear.

Illustrations

The maximum available space for an illustration is 185×244 mm (full page) or 90×244 mm (column). Figures should be prepared with lettering and symbols of sufficient size and clarity to be reduced (Arial, 6-8 pt. minimum). After reduction the smallest lettering should be a minimum of 2 mm high. Figures should be provided as .tif or .jpg format (at least with a resolution of 500dpi). Tables can be submitted as .xls or .doc files. Figures in the text must be quoted as fig. or figs., plates as pl. and tables as tab. (tabs). It is the responsibility of the authors to ensure that permission is granted for reproduction of any copyright material (reproduced figures, tables, text passages) and that this permission is acknowledged in their articles.

Proofs

The corresponding author will receive a single copy of the proof in PDF format. PDF proofs can be annotated using Adobe Reader version 11. The proof must be sent after correction to the Editors within five days. Text or figure changes can be also listed in a .doc file.

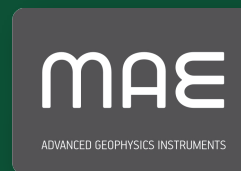
Manuscript submission

Manuscripts must be sent to the Editorial Board of the “Rendiconti Online della Società Geologica Italiana”, to the following e-mail addresses: domcalca@unina.it and fabio.petti@socgeol.it.

RENDICONTI *Online* della Società Geologica Italiana

Volume 31 - Luglio 2014

main partner



Cover: The Castello Estense ('Este castle') at Ferrara. (Photo: Marco Stefani).

RENDICONTI ONLINE DELLA SOCIETÀ GEOLOGICA ITALIANA

Direttore responsabile: DOMENICO CALCATERRA

Iscrizione ROC 18414.

Publicato online il 1 Luglio 2014.